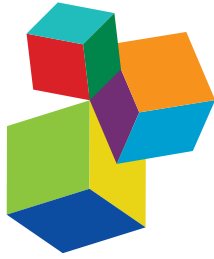


# VIRAL ENCEPHALITIS

EDITED BY: Mei-Ling LI, Bo-Shiun Chen and Shin-Ru Shih

PUBLISHED IN: Frontiers in Microbiology and

Frontiers in Cellular and Infection Microbiology



# frontiers

## Frontiers eBook Copyright Statement

The copyright in the text of individual articles in this eBook is the property of their respective authors or their respective institutions or funders. The copyright in graphics and images within each article may be subject to copyright of other parties. In both cases this is subject to a license granted to Frontiers.

The compilation of articles constituting this eBook is the property of Frontiers.

Each article within this eBook, and the eBook itself, are published under the most recent version of the Creative Commons CC-BY licence.

The version current at the date of publication of this eBook is CC-BY 4.0. If the CC-BY licence is updated, the licence granted by Frontiers is automatically updated to the new version.

When exercising any right under the CC-BY licence, Frontiers must be attributed as the original publisher of the article or eBook, as applicable.

Authors have the responsibility of ensuring that any graphics or other materials which are the property of others may be included in the CC-BY licence, but this should be checked before relying on the CC-BY licence to reproduce those materials. Any copyright notices relating to those materials must be complied with.

Copyright and source acknowledgement notices may not be removed and must be displayed in any copy, derivative work or partial copy which includes the elements in question.

All copyright, and all rights therein, are protected by national and international copyright laws. The above represents a summary only. For further information please read Frontiers' Conditions for Website Use and Copyright Statement, and the applicable CC-BY licence.

ISSN 1664-8714

ISBN 978-2-88966-317-0

DOI 10.3389/978-2-88966-317-0

## About Frontiers

Frontiers is more than just an open-access publisher of scholarly articles: it is a pioneering approach to the world of academia, radically improving the way scholarly research is managed. The grand vision of Frontiers is a world where all people have an equal opportunity to seek, share and generate knowledge. Frontiers provides immediate and permanent online open access to all its publications, but this alone is not enough to realize our grand goals.

## Frontiers Journal Series

The Frontiers Journal Series is a multi-tier and interdisciplinary set of open-access, online journals, promising a paradigm shift from the current review, selection and dissemination processes in academic publishing. All Frontiers journals are driven by researchers for researchers; therefore, they constitute a service to the scholarly community. At the same time, the Frontiers Journal Series operates on a revolutionary invention, the tiered publishing system, initially addressing specific communities of scholars, and gradually climbing up to broader public understanding, thus serving the interests of the lay society, too.

## Dedication to Quality

Each Frontiers article is a landmark of the highest quality, thanks to genuinely collaborative interactions between authors and review editors, who include some of the world's best academicians. Research must be certified by peers before entering a stream of knowledge that may eventually reach the public - and shape society; therefore, Frontiers only applies the most rigorous and unbiased reviews. Frontiers revolutionizes research publishing by freely delivering the most outstanding research, evaluated with no bias from both the academic and social point of view. By applying the most advanced information technologies, Frontiers is catapulting scholarly publishing into a new generation.

## What are Frontiers Research Topics?

Frontiers Research Topics are very popular trademarks of the Frontiers Journals Series: they are collections of at least ten articles, all centered on a particular subject. With their unique mix of varied contributions from Original Research to Review Articles, Frontiers Research Topics unify the most influential researchers, the latest key findings and historical advances in a hot research area! Find out more on how to host your own Frontiers Research Topic or contribute to one as an author by contacting the Frontiers Editorial Office: [researchtopics@frontiersin.org](mailto:researchtopics@frontiersin.org)

# VIRAL ENCEPHALITIS

Topic Editors:

**Mei-Ling LI**, The State University of New Jersey, United States

**Bo-Shiun Chen**, Augusta University, United States

**Shin-Ru Shih**, Chang Gung University, Taiwan

**Citation:** LI, M.-L., Chen, B.-S., Shih, S.-R., eds. (2021). Viral Encephalitis. Lausanne: Frontiers Media SA. doi: 10.3389/978-2-88966-317-0

# Table of Contents

- 04 Editorial: Viral Encephalitis**  
Mei-Ling Li, Bo-Shiun Chen and Shin-Ru Shih
- 06 The First Case of Bovine Astrovirus-Associated Encephalitis in the Southern Hemisphere (Uruguay), Uncovers Evidence of Viral Introduction to the Americas From Europe**  
Federico Giannitti, Rubén Darío Caffarena, Patricia Pesavento, Francisco Alejandro Uzal, Leticia Maya, Martín Fraga, Rodney Colina and Matías Castells
- 14 Z-DNA-Binding Protein 1 is Critical for Controlling Virus Replication and Survival in West Nile Virus Encephalitis**  
Hussin A. Rothan, Komal Arora, Janhavi P. Natekar, Philip G. Strate, Margo A. Brinton and Mukesh Kumar
- 24 EHV-1: A Constant Threat to the Horse Industry**  
Fatai S. Oladunni, David W. Horohov and Thomas M. Chambers
- 49 Enterovirus and Encephalitis**  
Bo-Shiun Chen, Hou-Chen Lee, Kuo-Ming Lee, Yu-Nong Gong and Shin-Ru Shih
- 64 The Mechanism of the Zika Virus Crossing the Placental Barrier and the Blood-Brain Barrier**  
Chi-Fen Chiu, Li-Wei Chu, I-Chen Liao, Yogy Simanjuntak, Yi-Ling Lin, Chi-Chang Juan and Yueh-Hsin Ping
- 79 RIPK3 Promotes JEV Replication in Neurons via Downregulation of IFI44L**  
Peiyu Bian, Chuantao Ye, Xuyang Zheng, Chuanyu Luo, Jiali Yang, Mengyuan Li, Yuan Wang, Jing Yang, Yun Zhou, Fanglin Zhang, Jianqi Lian, Ying Zhang, Zhansheng Jia and Yingfeng Lei
- 94 Molecular Pathogenicity of Enteroviruses Causing Neurological Disease**  
Anna Majer, Alan McGreevy and Timothy F. Booth
- 116 A Large-Scale Outbreak of Echovirus 30 in Gansu Province of China in 2015 and Its Phylodynamic Characterization**  
Jianhua Chen, Zhenzhi Han, Haizhuo Wu, Wenbo Xu, Deshan Yu and Yong Zhang
- 128 Establishment of a Fosmid Library for Pseudorabies Virus SC Strain and Application in Viral Neuronal Tracing**  
Hansong Qi, Hongxia Wu, Muhammad Abid, Hua-Ji Qiu and Yuan Sun
- 141 Polymerase Spiral Reaction Assay for Rapid and Real Time Detection of West Nile Virus From Clinical Samples**  
Priyanka Singh Tomar, Jyoti S. Kumar, Sapan Patel and Shashi Sharma



# Editorial: Viral Encephalitis

Mei-Ling Li<sup>1\*</sup>, Bo-Shiun Chen<sup>2,3</sup> and Shin-Ru Shih<sup>2,4,5,6,7,8</sup>

<sup>1</sup> Department of Biochemistry and Molecular Biology, Rutgers-Robert Wood Johnson Medical School, Piscataway, NJ, United States, <sup>2</sup> Research Center for Emerging Viral Infections, College of Medicine, Chang Gung University, Taoyuan, Taiwan, <sup>3</sup> Department of Neuroscience and Regenerative Medicine, Medical College of Georgia, Augusta University, Augusta, GA, United States, <sup>4</sup> Department of Laboratory Medicine, Linkou Chang Gung Memorial Hospital, Taoyuan, Taiwan, <sup>5</sup> Department of Medical Biotechnology and Laboratory Science, College of Medicine, Chang Gung University, Taoyuan, Taiwan, <sup>6</sup> Research Center for Chinese Herbal Medicine, College of Human Ecology, Chang Gung University of Science and Technology, Taoyuan, Taiwan, <sup>7</sup> Research Center for Food and Cosmetic Safety, College of Human Ecology, Chang Gung University of Science and Technology, Taoyuan, Taiwan, <sup>8</sup> Graduate Institute of Health Industry Technology, College of Human Ecology, Chang Gung University of Science and Technology, Taoyuan, Taiwan

**Keywords:** viral encephalitis, antiviral and vaccine, epidemiology and diagnosis, enterovirus, Flavivirus, herpes virus, astrovirus, Pseudorabies virus (PRV)

## Editorial on the Research Topic

### Viral Encephalitis

Viral encephalitis, an inflammation of the brain parenchyma caused by virus infection, poses a serious threat to global public health. The major causal agents worldwide are herpes viruses and arboviruses. HSV-1 is the leading cause of adult encephalitis in developed countries. While Japanese encephalitis is the most common encephalitis worldwide, West Nile virus is the most widespread virus. Recently, Zika virus, chikungunya virus, and Dengue virus have co-circulated in many regions of the Americas (Silva, 2013; Acevedo et al., 2017; Venkatesan and Murphy, 2018).

Despite the advance in studying the complex interplay between viruses and infected cells, the pathogenesis of viral encephalitis is largely unknown. For example, the regulation of blood brain barrier (BBB) permeability and the regulation of immune responses to virus infection in the CNS remain to be explored.

This Research Topic combines 10 publications from 64 authors, including 3 review articles and 7 research articles, covering many aspects of RNA and DNA virus-associated encephalitis.

The two in-depth reviews by Chen B-S et al. and Majer et al. provide readers a convenient way to understand the most up-to-date knowledge of non-polio, enterovirus-associated encephalitis. These two articles cover all aspects of recent advances in enterovirus-induced encephalitis including the routes of CNS infection, tropism, virulence, immune response, and molecular pathogenesis. These two reviews provide insightful information for the development of effective antiviral strategies and vaccines.

Chen J. et al. described the epidemiological and phylogenetic analysis of the very first large-scale Echovirus 30 (E-30, genus Enterovirus) outbreak in northwest China in 2015. The study shows children aged 6–15 years are more susceptible to E-30 infection. The highly similar E-30 genomes in this outbreak suggested an aggregate outbreak of E-30. The dominant lineage has a complex genetic transmission that indicates the infection initiated from coastal provinces of China and then spread to other parts of the country. The study provides valuable information for future surveillance.

Globalization promotes virus transmission and disease spreading among continents. The ongoing COVID-19 pandemic is a devastating example (Harapan et al., 2020; Yuki et al., 2020). Astrovirus-associated encephalitis cases have been reported in Asia, North American, and Europe. Giannitti et al. characterized the first case of bovine astrovirus-associated encephalitis in Uruguay (South America). Phylogeographic analysis suggests the virus was introduced to South America from Europe and later spread to North American and Japan. The study advances the understanding of the geographic distribution and genetic diversity of astroviruses.

## OPEN ACCESS

### Edited by:

Akio Adachi,  
Kansai Medical University, Japan

### Reviewed by:

Bo Zhang,  
Wuhan Institute of Virology  
(CAS), China  
Ping Qian,  
Huazhong Agricultural  
University, China

### \*Correspondence:

Mei-Ling Li  
lime@rwjms.rutgers.edu

### Specialty section:

This article was submitted to  
Virology,  
a section of the journal  
Frontiers in Microbiology

**Received:** 26 August 2020

**Accepted:** 22 October 2020

**Published:** 11 November 2020

### Citation:

Li M-L, Chen B-S and Shih S-R (2020)  
Editorial: Viral Encephalitis.  
*Front. Microbiol.* 11:599257.  
doi: 10.3389/fmicb.2020.599257

The vast majority of papers in this Research Topic are related to Flavivirus-associated encephalitis with distant emphasis on different viruses. Rothan et al. described expression of Z-DNA-binding protein 1 (ZBP1) restricting virus replication in West Nile virus (WNV)-induced encephalitis. WNV is the leading cause of viral encephalitis in the United States. ZBP1 plays an essential role in triggering robust immune responses. WNV infection dramatically up-regulates ZBP1 expression in mouse brain and primary mouse cells. Deletion of ZBP1 results in higher morbidity and mortality after WNV infection in mice. Infection of ZBP1<sup>-/-</sup> mice with the virus is lethal, indicating that ZBP1 is required for survival after WNV infection.

Tomar et al. reported the development of a polymerase spiral reaction assay for real time detection of WNV from clinical samples. As there is no FDA-approved vaccine or antiviral against WNV, early diagnosis of WNV infection is critical for clinical management and disease control. The reverse transcription polymerase spiral reaction (RT-PSR) assay rapidly and accurately detects the envelope gene of WNV using real-time turbidimeter or visual detection by the addition of SYBR Green I dye. The assay is validated and is able to detect as low as one copy of RNA, which is 100-fold higher than conventional RT-PCR. The assay has a potential to be used for rapid testing of a large number of clinical samples.

Zika virus (ZIKV) is another important member in the Flavivirus family that causes severe neurological complications such as meningoencephalitis in adults and microcephaly in fetus (Musso and Gubler, 2016). To better understand how ZIKV crosses the placental barrier and the blood brain barrier (BBB) to cause microcephaly in a fetus, Chiu et al. used human placenta trophoblasts cells (JEG-3) and human brain-derived endothelial cells (hCMEC/D3) as *in vitro* models to study the mechanisms ZIKV uses to cross the physiological barriers. The study shows ZIKV infection changes the permeability of JEG-3 cells by disrupting the tight junction and by transcytosis. ZIKV crosses the BBB by transcytosis.

Japanese encephalitis virus (JEV) is the major cause of viral encephalitis worldwide. JEV infection targets neurons and receptor interacting serine/threonine-protein kinase 3 (RIPK3), which contributes to neuron inflammation and death. Bian et al. found that RIPK3 plays multiple roles in JEV infection. The progression of JEV was inhibited in RIPK3-knockout (RIPK3<sup>-/-</sup>)

mice and in RIPK3-knockdown neuro2a cells with a significantly increased level of interferon (IFN)-induced protein 44-like gene (IFI44L). Over-expression of IFI44L decreases JEV replication in neuro2a cells and double knockdown of RIPK3 and IFI44L promotes virus replication. On the other hand, RIPK3 inhibits IFI44L expression to promote JEV propagation in neurons.

DNA virus infection can induce encephalitis as well. Equine herpesvirus-1 (EHV-1) is one of the most important pathogens of horse and causes a constant threat to the equine industry worldwide. There are increasing numbers of devastating equine herpesviral myeloencephalopathy outbreaks. Oladunni et al. reviewed the discovery of the virus, the latest developments of treatment and disease control, and summarizes recent advances in the research of EHV-1 pathogenesis. The information presented is useful for development of strategies to limit the spread of EHV-1 in equine populations.

Pseudorabies virus (PRV) is a member of the Herpesvirus family. Qi et al. used a fosmid library as a platform and Red/ET recombination technology to generate recombinant PRV fused with EGFP. The rescued recombinant virus is used to monitor retrograde and anterograde moving in the axon, making it a powerful tool for neuronal circuit analysis. The study is helpful for development of vaccines against PRV and other herpesviruses.

We hope that this Research Topic provides readers a better understanding of virus-associated encephalitis. A deeper understanding of viral encephalitis will facilitate the development of innovative antiviral approaches.

## AUTHOR CONTRIBUTIONS

All authors listed have made a substantial, direct and intellectual contribution to the work, and approved it for publication.

## FUNDING

This work was financially supported by the Research Center for Emerging Viral Infections from The Featured Areas Research Center Program within the framework of the Higher Education Sprout Project by the Ministry of Education in Taiwan and the Ministry of Science and Technology, Taiwan (MOST 108-3017-F-182-001).

## REFERENCES

- Acevedo, N., Waggoner, J., Rodriguez, M., Rivera, L., Landivar, J., Pinsky, B., et al. (2017). Zika Virus, Chikungunya Virus, and Dengue Virus in Cerebrospinal Fluid from Adults with Neurological Manifestations, Guayaquil, Ecuador. *Front. Microbiol.* 8:42. doi: 10.3389/fmicb.2017.00042
- Harapan, H., Itoh, N., Yufika, A., Winardi, W., Keam, S., Te, H., et al. (2020). Coronavirus disease 2019 (COVID-19): a literature review. *J. Infect. Public Health* 13, 667–673. doi: 10.1016/j.jiph.2020.03.019
- Musso, D., and Gubler, D. J. (2016). Zika virus. *Clin. Microbiol. Rev.* 29, 487–524. doi: 10.1128/CMR.00072-15
- Silva, M. T. (2013). Viral encephalitis. *Arq. Neuropsiquiatr.* 71, 703–709. doi: 10.1590/0004-282X20130155
- Venkatesan, A., and Murphy, O. C. (2018). Viral encephalitis. *Neurol. Clin.* 36, 705–724. doi: 10.1016/j.ncl.2018.07.001
- Yuki, K., Fujiogi, M., and Koutsogiannaki, S. (2020). COVID-19 pathophysiology: a review. *Clin. Immunol.* 215:108427. doi: 10.1016/j.clim.2020.108427

**Conflict of Interest:** The authors declare that the research was conducted in the absence of any commercial or financial relationships that could be construed as a potential conflict of interest.

Copyright © 2020 Li, Chen and Shih. This is an open-access article distributed under the terms of the Creative Commons Attribution License (CC BY). The use, distribution or reproduction in other forums is permitted, provided the original author(s) and the copyright owner(s) are credited and that the original publication in this journal is cited, in accordance with accepted academic practice. No use, distribution or reproduction is permitted which does not comply with these terms.



# The First Case of Bovine Astrovirus-Associated Encephalitis in the Southern Hemisphere (Uruguay), Uncovers Evidence of Viral Introduction to the Americas From Europe

## OPEN ACCESS

### Edited by:

Mei-Ling Li,

Rutgers, The State University  
of New Jersey, United States

### Reviewed by:

Marta Canuti,

Memorial University of Newfoundland,  
Canada

Torsten Seuberlich,

University of Bern, Switzerland

### \*Correspondence:

Federico Giannitti

fgiannitti@inia.org.uy

Matias Castells

matiascastellsbauer@gmail.com

### Specialty section:

This article was submitted to

Virology,

a section of the journal

Frontiers in Microbiology

**Received:** 22 March 2019

**Accepted:** 17 May 2019

**Published:** 04 June 2019

### Citation:

Giannitti F, Caffarena RD,

Pesavento P, Uzal FA, Maya L,

Fraga M, Colina R and Castells M

(2019) The First Case of Bovine

Astrovirus-Associated Encephalitis

in the Southern Hemisphere

(Uruguay), Uncovers Evidence of Viral

Introduction to the Americas From

Europe. *Front. Microbiol.* 10:1240.

doi: 10.3389/fmicb.2019.01240

**Federico Giannitti<sup>1\*</sup>, Rubén Darío Caffarena<sup>1,2</sup>, Patricia Pesavento<sup>3</sup>,  
Francisco Alejandro Uzal<sup>3</sup>, Leticia Maya<sup>4</sup>, Martín Fraga<sup>1</sup>, Rodney Colina<sup>4</sup> and  
Matias Castells<sup>1,4\*</sup>**

<sup>1</sup> Instituto Nacional de Investigación Agropecuaria (INIA), Plataforma de Investigación en Salud Animal, Estación Experimental INIA La Estanzuela, Colonia, Uruguay, <sup>2</sup> Facultad de Veterinaria, Universidad de la República, Montevideo, Uruguay, <sup>3</sup> Pathology, Microbiology and Immunology Department, School of Veterinary Medicine, University of California, Davis, Davis, CA, United States, <sup>4</sup> Laboratorio de Virología Molecular, Centro Universitario Regional (CENUR) Litoral Norte, Universidad de la República, Salto, Uruguay

Astrovirus species members of the *Mamastrovirus* genus (family *Astroviridae*) have been increasingly recognized as neuroinvasive pathogens in various mammals, including humans, mink, cattle, sheep, and pigs. While cases of astrovirus-associated encephalitis have been reported in North America, Europe, and Asia, their presence has never been documented in the Southern hemisphere. This paper describes a case of astrovirus-associated encephalitis in cattle in Uruguay that broadens the geographic distribution and genetic diversity of neuroinvasive astroviruses and provides phylogeographic evidence of viral introduction to the Americas from Europe. A 22-month-old Holstein steer from a farm in Colonia Department, Uruguay developed progressive neurological signs over a 3-days period before dying. Histopathological examination of the brain and proximal cervical spinal cord revealed disseminated, moderate to severe lymphocytic, histiocytic, and plasmacytic poliomeningoencephalomyelitis with neuronal necrosis. A *Mamastrovirus* strain in the CH13/NeuroS1 clade, that we called bovine astrovirus (BoAstV)-Neuro-Uy, was identified by reverse transcriptase PCR followed by nearly complete genome sequencing. Additionally, BoAstV was detected intralésionally in the brain by chromogenic RNA *in situ* hybridization within neuronal perikarya, axons and dendrites. Phylogenetic analysis of BoAstV-Neuro-Uy revealed a close relationship to neurotropic BoAstVs within the Virginia/Human-Mink-Ovine clade, which contains a growing cadre of neuroinvasive astroviruses. Analyzing the complete coding region of neuroinvasive BoAstVs sequences available in GenBank, we estimated an evolutionary

rate of  $4.27 \times 10^{-4}$  (95% HPD  $2.19\text{--}6.46 \times 10^{-4}$ ) nucleotide substitutions/site/year. Phylogeographic analysis suggests that the common viral ancestor circulated in Europe between 1794–1940, and was introduced in Uruguay between 1849–1967, to later spread to North America and Japan.

**Keywords:** bovine astrovirus, cattle, encephalitis, infectious diseases, *Mamastrovirus*, phylogeography, South America, Uruguay

## INTRODUCTION

The *Astroviridae* family contains non-enveloped, positive-sense, single-stranded RNA viruses within two genera, *Mamastrovirus* and *Avastrovirus*, which infect mammals and birds, respectively. Currently, the International Committee on Taxonomy of Viruses (International Committee on Taxonomy of Viruses [ICTV], 2018) recognizes 19 species, namely *Mamastrovirus-1* through *-19*, within the *Mamastrovirus* genus; however, there are numerous strains awaiting classification, some of which are tentatively considered new species (Donato and Vijaykrishna, 2017).

Since 2010, several astroviruses have increasingly been recognized as neuroinvasive in various mammalian species, including humans (Quan et al., 2010; Naccache et al., 2015), mink (Blomström et al., 2010), cattle (Li et al., 2013), sheep (Pfaff et al., 2017), and pigs (Boros et al., 2017). After initial recognition of bovine astrovirus-associated encephalitis in United States cattle (Li et al., 2013), a retrospective study in cases of sporadic bovine encephalitis of undetermined etiology from Switzerland revealed that this neuroinvasive astrovirus had gone undetected for decades (Selimovic-Hamza et al., 2016). Although the epidemiology and transmission routes of these astroviruses are unknown, cross-species transmission has been suggested based on the high level of identity (>98%), shared between bovine and ovine neuroinvasive astroviruses at the nucleotide and amino acid levels (Boujon et al., 2017).

Bovine astroviruses (BoAstVs), named BoAstV-NeuroS1 (Li et al., 2013) and BoAstV-CH13 (Bouzalas et al., 2014), were initially found in the brain of cattle with non-suppurative encephalitis in the United States and Switzerland, respectively. Despite the different nomenclature, both viruses represent the same genotype species (Bouzalas et al., 2016; Selimovic-Hamza et al., 2017a) that is still awaiting official classification by the ICTV. In 2015, a previously unknown BoAstV strain, named BoAstV-CH15, was identified in the brain of cows with encephalitis in Switzerland. Full genome phylogenetic comparison revealed a closer relationship of BoAstV-CH15 with an ovine astrovirus (OvAstV) than with BoAstV-CH13 (Seuberlich et al., 2016). Coinfection with BoAstV-CH13 and BoAstV-CH15 was also documented in one case (Seuberlich et al., 2016). The same year in Germany, Schlottau et al. (2016) reported a novel astrovirus, namely BoAstV-BH89/14, in a cow with encephalitis, that was most closely related to OvAstV and BoAstV-CH15. Subsequently, BoAstV-CH13/NeuroS1 was identified in 2017 in cases of bovine encephalitis in eastern and western Canada (Spinato et al., 2017; Selimovic-Hamza et al., 2017b). In 2018, a novel neuroinvasive

BoAstV closely related with North American and European BoAstV-NeuroS1/BoAstV-CH13, was identified in a steer with non-suppurative encephalomyelitis in Japan, and the occurrence of intra-genotypic recombination between the North American and European strains was suggested (Hirashima et al., 2018).

While cases of astrovirus-associated encephalitis have been reported in North America, Europe, and Asia, their presence has never been documented in the Southern hemisphere. Here we describe a case of astrovirus-associated encephalitis in cattle in Uruguay, which broadens the geographic distribution and genetic diversity of neuroinvasive astroviruses and provide phylogeographic evidence that suggests that this virus was introduced into the Americas from Europe and later spread to Asia.

## MATERIALS AND METHODS

### History and Signalment

In June 2018, a 22-month-old Holstein steer in a group of 37 steers in a ~300-hectare farm in Colonia, Uruguay, developed progressive neurological signs including unusual behavior, aimless walking, circling, ataxia, repetitive and uncoordinated tongue movements, and recumbency. The herd grazed on an annual oat pasture and was supplemented with corn silage. A presumptive clinical diagnosis of cerebral listeriosis by the veterinary practitioner prompted treatment with penicillin and streptomycin, however the animal died spontaneously after a clinical course lasting 3 days.

### Pathologic Examination, *in situ* Hybridization (ISH) and Immunohistochemistry (IHC)

The head of the steer was removed from the carcass and submitted to INIA's Veterinary Diagnostic Laboratory (Animal Health Platform) for diagnostic work-up. Half of the brain, a short segment of proximal cervical spinal cord (C1), trigeminal ganglion and root of the trigeminal nerve, salivary gland, retropharyngeal lymph node, oropharynx, esophagus, tongue and skeletal muscle, were immersion-fixed in 10% neutral buffered formalin for 48–72 h. Tissues were routinely processed for histology, embedded in paraffin, microtome-sectioned at 4–5  $\mu\text{m}$  and stained with hematoxylin and eosin (H&E) and Gram stains.

Chromogenic ISH was performed manually on 5  $\mu\text{m}$  sections of formalin-fixed, paraffin-embedded (FFPE) brainstem, cerebrum and cerebellum on Superfrost Plus slides (Thermo Fisher Scientific, Pittsburgh, PA, United States) using the

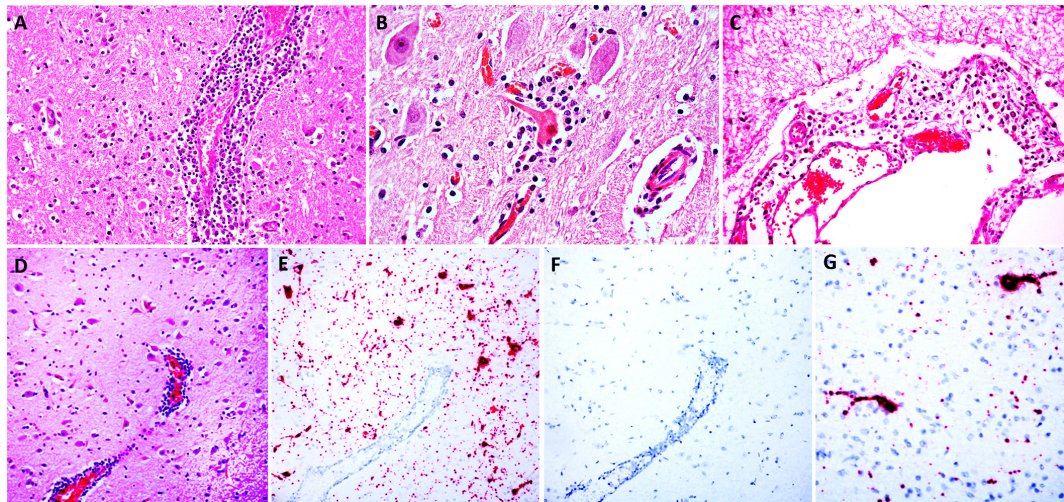


**FIGURE 1 |** Histologic lesions in the brainstem (**A,B**) and cerebral cortex (**C,D**) and detection of BoAstV RNA in the cerebral cortex (**E,G**). Images (**A–D**) are sections of brain stained with H&E; images **E** and **G** are sections of cerebral cortex demonstrating hybridization using chromogenic ISH using the BoAstV specific probe, counterstained with hematoxylin; image **F** is a serial section of cerebral cortex DapB probe (negative control), counterstained with hematoxylin. (**A**) A perivascular space is markedly expanded by inflammatory cells (mostly lymphocytes and histiocytes) that also infiltrate the adjacent neuropil. (**B**) The neuron in the center has hypereosinophilic perikaryon and karyorrhexis (necrosis) and the neuronal body is surrounded by increased numbers of glial (satellitosis) and inflammatory cells. (**C**) The leptomeninge is infiltrated by lymphocytes and histiocytes. (**D**) A region of cerebral cortex with multiple hypereosinophilic (necrotic) neurons and a large vessel with perivascular lymphocytic cuffs. (**E**) In a serial section of cerebral cortex, the abundant intracytoplasmic BoAstV RNA labeling is depicted by strong, granular red chromogen deposition within neuronal cytoplasm of the soma and neuronal extensions (**E,G**), that is not present with hybridization using the negative control probe (**F**).

RNAscope 2.5 Red assay kit (Cat #322360, Advanced Cell Diagnostics, Hayward, CA, United States) and the BoAstV probe Cat. #406921. The probe is composed of 20ZZ pairs targeting region 5232–6180 of the virus (GenBank KF233994.1). Each 5  $\mu\text{m}$  section of tissue was pretreated with heat and protease prior to probe hybridization for 2 h at 40°C and processed as per the manufacturers' recommendations. Negative controls used for validation of signal included an unrelated (GC-content matched) probe run on serial sections and probing tissue from uninfected animals. Slides were counterstained with hematoxylin and mounted with EcoMount (Biocare Medical, Concord, CA, United States).

Additionally, IHC was performed in FFPE sections of brainstem, cerebrum and cerebellum, as previously described, for the identification of West Nile virus (WNV, *Flavivirus*) (Palmieri et al., 2011), rabies virus (*Lyssavirus*) (Stein et al., 2010), and *Chlamydia* spp. (Giannitti et al., 2016) antigens.

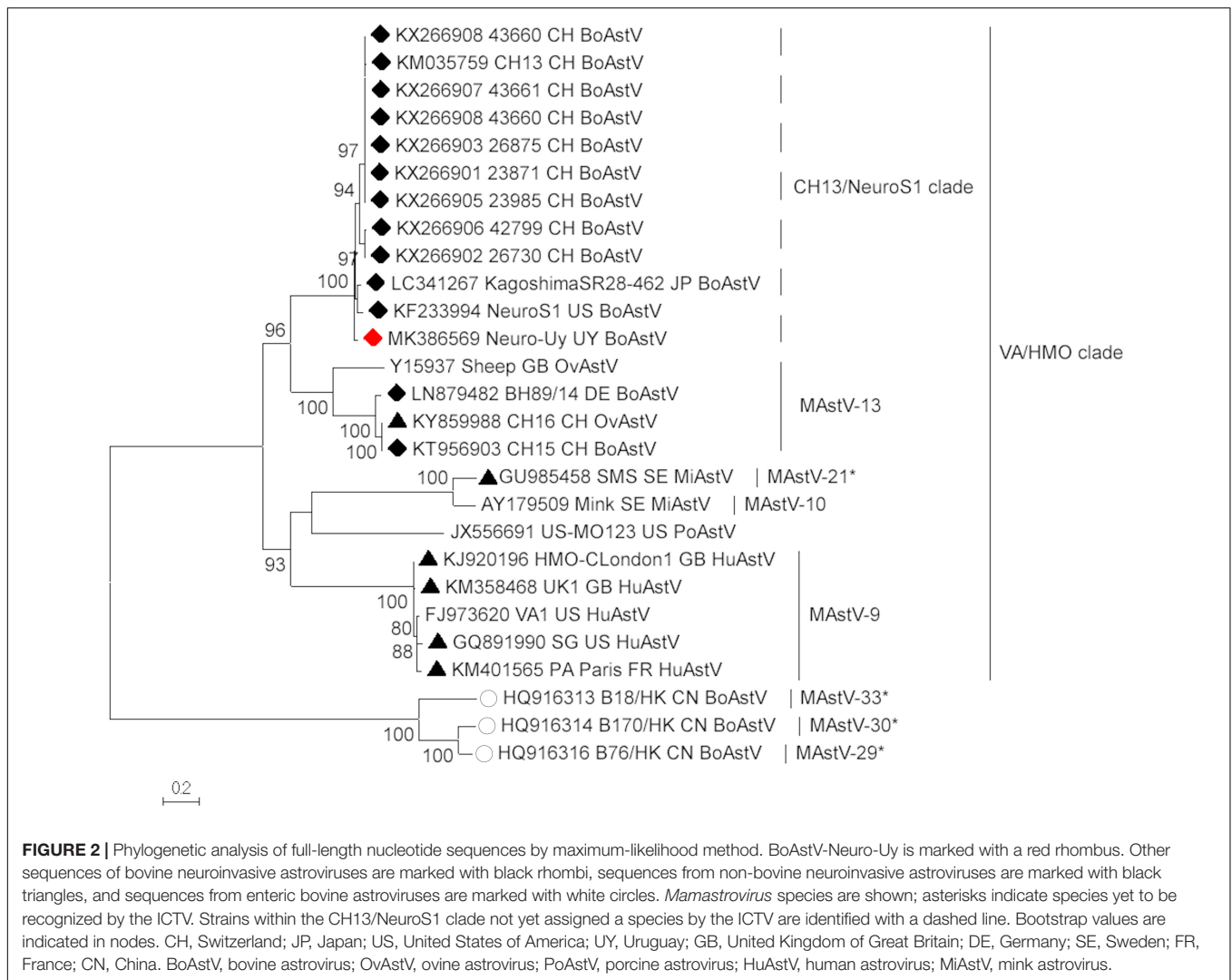
## Molecular Virology

Nucleic acid extraction was accomplished from a pooled sample of frozen (–20°C) brain using MagMAX Nucleic Acid Isolation Kit® (Thermo Fisher Scientific). For astrovirus detection, reverse transcription (RT) was performed with RevertAid Reverse Transcriptase® (Thermo Fisher Scientific) and random hexamer primers (Qiagen). PCR was performed from cDNA using MangoMix® (Bioline) and primers that amplify a 432-nucleotide fragment of the astrovirus polymerase gene (Tse et al., 2011). The PCR product was visualized in 2% agarose gel, purified using PureLink® Quick Gel Extraction

and PCR Purification Combo Kit (Invitrogen), and sequenced at Macrogen Inc. (Seoul, South Korea). For astrovirus whole genome amplification, Maxima H Minus Reverse Transcriptase (Thermo Fisher Scientific) and oligo(dT)18 for obtention of cDNA, and MangoMix® (Bioline) or Ranger DNA Polymerase (Bioline) with primers described by Hirashima et al., 2018, were used. The PCR products were visualized in 1–2% agarose gel, purified and sequenced as mentioned above. Sequence assembly was conducted with SeqMan (Lasergene 8, DNASTAR). Twenty-six complete genome sequences of neuroinvasive astrovirus from cattle, sheep, pigs, humans and mink, and enteric bovine astrovirus available in GenBank were downloaded and aligned using Clustal W in MEGA 7 software (Kumar et al., 2016). W-IQ-TREE<sup>1</sup> (Trifinopoulos et al., 2016) was used to determine the best-fit model of sequence evolution (SYM+I+G4) and to construct a maximum-likelihood phylogenetic tree with the nearly complete sequences of the BoAstV detected in this case, and those complete sequences downloaded from GenBank, using bootstrap as the statistical method to assess clades robustness. Similarity plot was performed with SimPlot software (Lole et al., 1999). *P*-distances at amino acid level of the ORF2 were estimated with MEGA 7 software (Kumar et al., 2016).

Additionally, a Bayesian phylogeographic analysis was performed with the BEAST v1.8.4 package (Drummond et al., 2012), using: the complete coding region of BoAstV CH13/NeuroS1 lineage, ORF1ab (non-structural genes), ORF2 (structural gene), ORF1a (protease) and a partial ORF1b

<sup>1</sup><http://iqtree.cibiv.univie.ac.at>



(polymerase genomic region, for which Canadian strains were available), with all the sequences available in GenBank (last accession April 18, 2019), to determine the evolutionary rate, the ages/years of the common ancestors, and the most probable route of viral circulation by country (Switzerland, Uruguay, United States, Canada, and Japan). Lack of recombination in the dataset was determined using Recombination Detection Program 4. The substitution model that best fit each alignment was determined using MEGA 7 software through Bayesian information criterion (BIC) values, and the temporal structure of each dataset was evaluated using TempEst (Rambaut et al., 2016). The lognormal relaxed molecular clock with Bayesian Skyline analysis was selected by Bayes Factor among the different combinations of molecular clocks and coalescent tree priors used. The country of detection was used as trait. The Markov chain Monte Carlo length was 100 million generations, ensuring the convergence of the analysis, evaluated in Tracer v1.6.0, and the posterior probability was used to evaluate clades. The maximum clade credibility tree (MCCT) was obtained using TreeAnnotator software from BEAST and visualized in FigTree v1.4.3.

Lastly, DNA extracted from frozen brain was processed by PCR for the detection of bovine herpesviruses 1 and 5 (BHV-1 and -5), as previously described (Ashbaugh et al., 1997).

## Bacteriology

Fresh samples of cerebrum and brainstem were routinely processed for aerobic bacterial cultures in blood and MacConkey agars, and selective culture for *Listeria monocytogenes* (Al-Zoreky and Sandine, 1990).

## RESULTS AND DISCUSSION

The clinical signs and epidemiological findings in the case described herein, albeit non-specific, were similar to those described in other cases of bovine astrovirus-associated encephalitis, which is usually described as sporadic (Selimovic-Hamza et al., 2016), with a variety of neurological deficits (Deiss et al., 2017), with a duration of clinical signs that typically ranges from 1 day to 3 weeks

**TABLE 1** | Estimates of evolutionary divergence at the amino acid level of the complete ORF2 region between sequences of bovine and ovine Mamastrovirus-13 and strains within the CH13/NeuroS1 clade not yet assigned to a species by the International Committee on Taxonomy of Viruses (ICTV).

Sequences and GenBank accession numbers	1	2	3	4	5	6	7	8	9	10	11	12	13	14	15	16
1- KY859988_OvAstV_CH16	-	-	-	-	-	-	-	-	-	-	-	-	-	-	-	-
2- Y15937_OvAstV_OvAstV-1	0.263	-	-	-	-	-	-	-	-	-	-	-	-	-	-	-
3- LC341267_BoAstV_KagoshimaSR28-462	0.343	0.317	-	-	-	-	-	-	-	-	-	-	-	-	-	-
4- KM035759_BoAstV_CH13	0.341	0.321	0.012	-	-	-	-	-	-	-	-	-	-	-	-	-
5- KF233994_BoAstV_NeuroS1	0.348	0.327	0.016	0.015	-	-	-	-	-	-	-	-	-	-	-	-
6- KY266902_BoAstV_26730	0.341	0.321	0.012	0.005	0.015	-	-	-	-	-	-	-	-	-	-	-
7- KY266903_BoAstV_26875	0.344	0.320	0.012	0.005	0.015	0.005	-	-	-	-	-	-	-	-	-	-
8- KY266907_BoAstV_43661	0.341	0.320	0.009	0.003	0.012	0.003	0.003	-	-	-	-	-	-	-	-	-
9- KY266901_BoAstV_23871	0.343	0.321	0.012	0.005	0.012	0.005	0.005	0.003	-	-	-	-	-	-	-	-
10- KY266906_BoAstV_42799	0.341	0.320	0.011	0.004	0.013	0.004	0.004	0.001	0.004	-	-	-	-	-	-	-
11- KY266908_BoAstV_43660	0.341	0.320	0.011	0.004	0.013	0.004	0.004	0.001	0.004	0.003	-	-	-	-	-	-
12- KY266905_BoAstV_23985	0.341	0.318	0.012	0.005	0.015	0.005	0.005	0.003	0.005	0.004	0.004	-	-	-	-	-
13- KY266904_BoAstV_36716	0.341	0.320	0.008	0.004	0.013	0.004	0.004	0.001	0.004	0.003	0.003	0.004	-	-	-	-
14- MK386569_BoAstV_Neuro-Uy	0.342	0.323	0.016	0.013	0.019	0.013	0.013	0.011	0.013	0.012	0.012	0.013	0.012	-	-	-
15- KT956903_BoAstV_CH15	0.007	0.266	0.347	0.345	0.352	0.345	0.347	0.345	0.347	0.345	0.345	0.345	0.345	0.346	-	-
16- LN879482_BoAstV_BH89/14	0.007	0.260	0.344	0.343	0.349	0.343	0.344	0.343	0.344	0.343	0.343	0.343	0.343	0.344	0.011	-

Based on current ICTV criteria, strains with  $p$ -distances  $< 0.35$  should be considered within the same genotype species. The number of amino acid differences per site between sequences are shown. The analysis involved 16 amino acid sequences. All ambiguous positions were removed for each sequence pair. There was a total of 773 positions in the final dataset. OvAstV, ovine astrovirus; BoAstV, bovine astrovirus.

(Schlottau et al., 2016; Deiss et al., 2017; Spinato et al., 2017; Hirashima et al., 2018).

Macroscopic examination of the brain, the C1 segment of the spinal cord, and other tissues of the head did not reveal significant gross anatomic lesions. Histologically, there was moderate to severe, lymphocytic, histiocytic and plasmacytic meningoencephalomyelitis affecting the telencephalon (including the cerebral hemisphere and hippocampus), brainstem, and the only examined segment of spinal cord. Lesions were predominantly distributed in the gray matter and limiting areas of white matter. In affected areas there was perivascular cuffing and lymphoplasmacytic and histiocytic inflammation and neuronal necrosis/neuronophagia with gliosis in the adjacent neuropil. There was satellitosis of affected, necrotic neurons (Figures 1A–D). The lesions were much less frequent and severe in the cerebellar parenchyma, although there was multifocal moderate cerebellar leptomeningitis. No intralosomal bacteria were found with H&E and Gram stains. No significant histologic changes were found in the other examined tissues.

A neuroinvasive viral infection was suspected upon histologic examination of the central nervous system. Cattle with encephalitis are of concern because many ruminant neuropathogens are zoonotic (Cantile and Youssef, 2016); thus, a diagnosis of encephalitis should prompt extensive laboratory testing to screen for infectious agents when possible. In the case described herein, IHCs for WNV, rabies virus and *Chlamydia* spp., and PCR for BHV-1 and -5 were all negative, and no pathogenic bacteria were cultured from brain tissue. Because the steer was  $< 2$  years old and no spongiform changes were observed in the brainstem, the animal was not tested for bovine spongiform encephalopathy (BSE), which is an exotic disease of adult cattle that has never been reported in Uruguay. Moreover, BSE is not inflammatory (Cantile and Youssef, 2016).

*In situ* hybridization was performed using a probe generated from BoAstV-NeuroS1, and there was probe hybridization abundant within, and limited to the cytoplasm of neurons in the cerebral hemisphere and hippocampus (Figures 1E–G). In these areas the probe hybridization colocalized with necrotic neurons and regions of gliosis, with no probe hybridization detectable in the glial cells, or inflammatory cells of the perivascular cuffs. No viral nucleic acid was detected by ISH in the cerebellum, which had only minimal inflammatory lesions in the parenchyma but moderate leptomeningitis, or the brainstem, including sections with severe inflammation. This means that, topographically, detection of viral distribution by ISH was more limited than encephalitis in the sections examined, which has occasionally been described in cases of BoAstV-CH13/NeuroS1-associated encephalitis in cattle (Selimovic-Hamza et al., 2017a,b). A reason for this occasional lack of viral RNA detection in lesioned areas of brain might be the detection limit of the ISH, or the clearance of the virus in inflamed areas of the brain by the time of death, as previously suggested (Selimovic-Hamza et al., 2017b). As expected, no probe hybridization was detected by ISH in the brain tissue used as negative control.

Astrovirus was detected in brain by RT-PCR. Nearly complete genome sequence analysis revealed a Mamastrovirus strain within



estimated using the complete coding region was  $4.27 \times 10^{-4}$  (95% highest probability density -HPD-,  $2.19\text{--}6.46 \times 10^{-4}$ ) nucleotide substitutions/site/year, which is expected for an RNA virus (Jenkins et al., 2002), but lower than that estimated for enteric human astroviruses (Babkin et al., 2012, 2014). The ORF1ab region showed a similar evolutionary rate ( $4.20 \times 10^{-4}$ , 95% HPD  $1.66\text{--}6.46 \times 10^{-4}$  substitutions/site/year) as the complete coding region, while the ORF1a ( $2.92 \times 10^{-4}$ , 95% HPD  $1.19 \times 10^{-6}\text{--}6.46 \times 10^{-4}$  substitutions/site/year) and ORF2 ( $2.86 \times 10^{-4}$ , 95% HPD  $4.13 \times 10^{-6}\text{--}5.79 \times 10^{-4}$  substitutions/site/year) showed a slightly faster evolutionary rate, and the partial polymerase genomic region (ORF1b) showed a slightly slower evolutionary rate ( $5.39 \times 10^{-4}$ , 95% HPD  $6.41 \times 10^{-7}\text{--}1.10 \times 10^{-3}$  substitutions/site/year).

As determined by the phylogeographic analysis with the complete coding region, and shown in the MCTT (Figure 3), there are two sub-lineages (CH13 and NeuroS1) based on reference strains, that have a common ancestor. The most recent common ancestor of these sub-lineages (lineage CH13/NeuroS1) arose in Europe approximately in 1885 (95% HPD, 1794–1940). At the beginning of the 1900's, the two sub-lineages diverged, the CH13 sub-lineage stayed circulating in Europe, while the NeuroS1 sub-lineage spread to America and Asia. The most likely scenario is that the NeuroS1 sub-lineage was introduced in Uruguay from Europe around the year 1921 (95% HPD, 1849–1967), presumably through livestock trade, then spread to North America, and later to Japan (Figure 3). Due to the limitation in the number of sequences available in GenBank, which could have biased the analysis, the results obtained using the complete coding region were compared with those obtained with other genomic regions (ORF1ab, ORF2, ORF1a, and ORF1b) available for a larger number of strains (i.e., Canadian strains). In all the analyses the most likely scenario is that the introduction of the virus to Uruguay occurred from Europe (Supplementary Figures S1A–D). In addition, the estimated date for this introduction, obtained with the ORF1ab and partial polymerase genomic region (ORF1b) (Supplementary Figures S1A,D), was similar to that obtained with the complete coding region, whereas the estimated date of introduction obtained with ORF2 and ORF1a was earlier but with wider 95% HPD interval (Supplementary Figures S1B,C). An introduction of the sub-lineage NeuroS1 directly to Canada from Europe, with subsequent spread to United States and Japan, is also plausible, as shown in Supplementary Figure S1D.

Further investigations are needed to assess the geographic distribution, pathogenic mechanisms (particularly mechanisms of transmission and entry), molecular epidemiology, and potential interspecies transmission of neuroinvasive astroviruses.

## REFERENCES

Al-Zoreky, N., and Sandine, W. E. (1990). Highly selective medium for the isolation of *Listeria monocytogenes* from food. *Appl. Environ. Microbiol.* 56, 3154–3157.

## DATA AVAILABILITY

The datasets generated for this study can be found in GenBank, MK386569.

## AUTHOR CONTRIBUTIONS

FG, RDC, and MC contributed with the conception of the study. FG and RDC performed the pathological examination and sampling. PP performed the *in situ* hybridization. FU performed the immunohistochemistry. LM, RC, and MC performed molecular virology testing. MC performed the sequence and phylogeographic analyses and associated figures. FG and PP obtained the histologic images. MF performed the bacterial cultures. FG and MC wrote the first draft of the manuscript. RDC, PP, FU, LM, MF, and RC wrote sections of the manuscript. All authors contributed to manuscript revision, read and approved the submitted version.

## FUNDING

This work was funded by Grants PL-015 N-15156 from INIA and 158 from the “Programa de Iniciación a la Investigación 2017” from “Comisión Sectorial de Investigación Científica” (CSIC). MC and RDC acknowledge support from the “Agencia Nacional de Investigación e Innovación” (ANII) and INIA, respectively, through Ph.D. scholarships. FG acknowledges support from ANII through mobility grant MOV\_CA\_2018\_1\_150021.

## ACKNOWLEDGMENTS

The authors thank Yisell Perdomo and Cecilia Monesiglio from INIA, and Karen Sverlow and Juliann Beingesser from CAHFS for technical assistance.

## SUPPLEMENTARY MATERIAL

The Supplementary Material for this article can be found online at: <https://www.frontiersin.org/articles/10.3389/fmicb.2019.01240/full#supplementary-material>

**FIGURE S1** | Maximum clade credibility trees (MCCTs) obtained by analysis of the full-length ORF1ab (A), full-length ORF2 (B), full-length ORF1a (C), and partial ORF1b (D). The color of the branches represents the most likely country where the ancestors circulated, posterior probability values are shown in the branches, and the numbers in each node represent the years of origin for each clade with the 95% HPD interval. Sub-lineages are indicated with labels.

Ashbaugh, S. E., Thompson, K. E., Belknap, E. B., Schultheiss, P. C., Chowdhury, S., and Collins, J. K. (1997). Specific detection of shedding and latency of bovine herpesvirus 1 and 5 using a nested polymerase chain reaction. *J. Vet. Diagn. Invest.* 9, 387–394. doi: 10.1177/104063879700900408

- Babkin, I. V., Tikunov, A. Y., Sedelnikova, D. A., Zhirakovskaia, E. V., and Tikunova, N. V. (2014). Recombination analysis based on the HAstV-2 and HAstV-4 complete genomes. *Infect. Genet. Evol.* 22, 94–102. doi: 10.1016/j.meegid.2014.01.010
- Babkin, I. V., Tikunov, A. Y., Zhirakovskaia, E. V., Netesov, S. V., and Tikunova, N. V. (2012). High evolutionary rate of human astrovirus. *Infect. Genet. Evol.* 12, 435–442. doi: 10.1016/j.meegid.2012.01.019
- Blomström, A. L., Widén, F., Hammer, A. S., Belák, S., and Berg, M. (2010). Detection of a novel astrovirus in brain tissue of mink suffering from shaking mink syndrome by use of viral metagenomics. *J. Clin. Microbiol.* 48, 4392–4396. doi: 10.1128/JCM.01040-10
- Boros, Á., Albert, M., Pankovics, P., Bíró, H., Pesavento, P. A., Phan, T. G., et al. (2017). Outbreaks of neuroinvasive astrovirus associated with encephalomyelitis, weakness, and paralysis among weaned pigs, Hungary. *Emerg. Infect. Dis.* 23, 1982–1993. doi: 10.3201/eid2312.170804
- Boujon, C. L., Koch, M. C., Wüthrich, D., Werder, S., Jakupovic, D., Bruggmann, R., et al. (2017). Indication of cross-species transmission of astrovirus associated with encephalitis in sheep and cattle. *Emerg. Infect. Dis.* 23, 1604–1608. doi: 10.3201/eid2309.170168
- Bouzalas, I. G., Wüthrich, D., Selimovic-Hamza, S., Drögemüller, C., Bruggmann, R., and Seuberlich, T. (2016). Full-genome based molecular characterization of encephalitis-associated bovine astroviruses. *Infect. Genet. Evol.* 44, 162–168. doi: 10.1016/j.meegid.2016.06.052
- Bouzalas, I. G., Wüthrich, D., Walland, J., Drögemüller, C., Zurbriggen, A., Vandeveld, M., et al. (2014). Neurotropic astrovirus in cattle with nonsuppurative encephalitis in Europe. *J. Clin. Microbiol.* 52, 3318–3324. doi: 10.1128/JCM.01195-14
- Cantile, C., and Youssef, S. (2016). “Nervous System,” in *Jubb, Kennedy, and Palmer’s Pathology of Domestic Animals*, 6th Edn, ed. M. G. Maxie (Saint Louis, MO: Elsevier), 205–406.
- Deiss, R., Selimovic-Hamza, S., Seuberlich, T., and Meylan, M. (2017). Neurologic clinical signs in cattle with astrovirus-associated encephalitis. *J. Vet. Intern. Med.* 31, 1209–1214. doi: 10.1111/jvim.14728
- Donato, C., and Vijaykrishna, D. (2017). The broad host range and genetic diversity of mammalian and avian astroviruses. *Viruses* 9:E102. doi: 10.3390/v9051012
- Drummond, A. J., Suchard, M. A., Xie, D., and Rambaut, A. (2012). Bayesian phylogenetics with BEAUti and the BEAST 1.7. *Mol. Biol. Evol.* 29, 1969–1973. doi: 10.1093/molbev/mss075
- Giannitti, F., Anderson, M., Miller, M., Rowe, J., Sverlow, K., Vasquez, M., et al. (2016). *Chlamydia pecorum*: fetal and placental lesions in sporadic caprine abortion. *J. Vet. Diagn. Invest.* 28, 184–189. doi: 10.1177/1040638715625729
- Hirashima, Y., Okada, D., Shibata, S., Yoshida, S., Fujisono, S., Omatsu, T., et al. (2018). Whole genome analysis of a novel neurotropic bovine astrovirus detected in a Japanese black steer with non-suppurative encephalomyelitis in Japan. *Arch. Virol.* 163, 2805–2810. doi: 10.1007/s00705-018-3898-3
- International Committee on Taxonomy of Viruses [ICTV] (2018). *Master Species List (MSL32), Version 1*. Available at: <https://talk.ictvonline.org/files/master-species-lists/m/msl/7185> (accessed March, 2019).
- Jenkins, G. M., Rambaut, A., Pybus, O. G., and Holmes, E. C. (2002). Rates of the molecular evolution in RNA viruses: a quantitative phylogenetic analysis. *J. Mol. Evol.* 54, 156–165. doi: 10.1007/s00239-001-0064-3
- Kumar, S., Stecher, G., and Tamura, K. (2016). MEGA7: molecular evolutionary genetics analysis version 7.0 for bigger datasets. *Mol. Biol. Evol.* 33, 1870–1874. doi: 10.1093/molbev/msw054
- Li, L., Diab, S., McGraw, S., Barr, B., Traslavina, R., Higgins, R., et al. (2013). Divergent astrovirus associated with neurologic disease in cattle. *Emerg. Infect. Dis.* 19, 1385–1392. doi: 10.3201/eid1909.130682
- Lole, K. S., Bollinger, R. C., Paranjape, R. S., Gadkari, D., Kulkarni, S. S., Novak, N. G., et al. (1999). Full-length human immunodeficiency virus type 1 genomes from subtype C-infected seroconverters in India, with evidence of intersubtype recombination. *J. Virol.* 73, 152–160.
- Naccache, S. N., Peggs, K. S., Mattes, F. M., Phadke, R., Garson, J. A., Grant, P., et al. (2015). Diagnosis of neuroinvasive astrovirus infection in an immunocompromised adult with encephalitis by unbiased next-generation sequencing. *Clin. Infect. Dis.* 60, 919–923. doi: 10.1093/cid/ciu912
- Palmieri, C., Franca, M., Uzal, F., Anderson, M., Barr, B., Woods, L., et al. (2011). Pathology and immunohistochemical findings of West Nile virus infection in psittaciformes. *Vet. Pathol.* 48, 975–984. doi: 10.1177/0300985810391112
- Pfaff, F., Schlottau, K., Scholes, S., Courtenay, A., Hoffmann, B., Höper, D., et al. (2017). A novel astrovirus associated with encephalitis and ganglioneuritis in domestic sheep. *Transbound. Emerg. Dis.* 64, 677–682. doi: 10.1111/tbed.12623
- Quan, P. L., Wagner, T. A., Bries, T., Torgerson, T. R., Hornig, M., Tashmukhamedova, A., et al. (2010). Astrovirus encephalitis in boy with X-linked agammaglobulinemia. *Emerg. Infect. Dis.* 16, 918–925. doi: 10.3201/eid1606.091536
- Rambaut, A., Lam, T. T., Max Carvalho, L., and Pybus, O. G. (2016). Exploring the temporal structure of heterochronous sequences using TempEst (formerly Path-O-Gen). *Virus Evol.* 2:vev007. doi: 10.1093/ve/vev007
- Reuter, G., Pankovics, P., and Boros, A. (2018). Nonsuppurative (aseptic) meningoencephalomyelitis associated with neurovirulent astrovirus infections in humans and animals. *Clin. Microbiol. Rev.* 31, e00040-18. doi: 10.1128/CMR.00040-18
- Schlottau, K., Schulze, C., Bilk, S., Hanke, D., Höper, D., Beer, M., et al. (2016). Detection of a novel bovine astrovirus in a cow with encephalitis. *Transbound. Emerg. Dis.* 63, 253–259. doi: 10.1111/tbed.12493
- Selimovic-Hamza, S., Boujon, C. L., Hilbe, M., Oevermann, A., and Seuberlich, T. (2017a). Frequency and pathological phenotype of bovine astrovirus CH13/NeuroS1 infection in neurologically-diseased cattle: towards assessment of causality. *Viruses* 9:E12. doi: 10.3390/v9010012
- Selimovic-Hamza, S., Sanchez, S., Philibert, H., Clark, E. G., and Seuberlich, T. (2017b). Bovine astrovirus infection in feedlot cattle with neurological disease in western Canada. *Can. Vet. J.* 58, 601–603.
- Selimovic-Hamza, S., Bouzalas, I. G., Vandeveld, M., Oevermann, A., and Seuberlich, T. (2016). Detection of astrovirus in historical cases of European sporadic bovine encephalitis, Switzerland 1958–1976. *Front. Vet. Sci.* 3:91. doi: 10.3389/fvets.2016.00091
- Seuberlich, T., Wüthrich, D., Selimovic-Hamza, S., Drögemüller, C., Oevermann, A., Bruggmann, R., et al. (2016). Identification of a second encephalitis-associated astrovirus in cattle. *Emerg. Microbes Infect.* 5:e5. doi: 10.1038/emi.2016.5
- Spinato, M. T., Vince, A., Cai, H., and Ojckic, D. (2017). Identification of bovine astrovirus in cases of bovine non-suppurative encephalitis in eastern Canada. *Can. Vet. J.* 58, 607–609.
- Stein, L. T., Rech, R. R., Harrison, L., and Brown, C. C. (2010). Immunohistochemical study of rabies virus within the central nervous system of domestic and wildlife species. *Vet. Pathol.* 47, 630–633. doi: 10.1177/0300985810370013
- Trifinopoulos, J., Nguyen, L. T., von Haeseler, A., and Minh, B. Q. (2016). W-IQ-TREE: a fast online phylogenetic tool for maximum likelihood analysis. *Nucleic Acids Res.* 44, W232–W235. doi: 10.1093/nar/gk w256
- Tse, H., Chan, W. M., Tsoi, H. W., Fan, R. Y., Lau, C. C., Lau, S. K., et al. (2011). Rediscovery and genomic characterization of bovine astroviruses. *J. Gen. Virol.* 92(Pt 8), 1888–1998. doi: 10.1099/vir.0.030817-0

**Conflict of Interest Statement:** The authors declare that the research was conducted in the absence of any commercial or financial relationships that could be construed as a potential conflict of interest.

The reviewer TS declared a past co-authorship with one of the authors PP to the handling editor.

Copyright © 2019 Giannitti, Caffarena, Pesavento, Uzal, Maya, Fraga, Colina and Castells. This is an open-access article distributed under the terms of the Creative Commons Attribution License (CC BY). The use, distribution or reproduction in other forums is permitted, provided the original author(s) and the copyright owner(s) are credited and that the original publication in this journal is cited, in accordance with accepted academic practice. No use, distribution or reproduction is permitted which does not comply with these terms.



# Z-DNA-Binding Protein 1 Is Critical for Controlling Virus Replication and Survival in West Nile Virus Encephalitis

Hussin A. Rothan<sup>†</sup>, Komal Arora<sup>†</sup>, Janhavi P. Natekar, Philip G. Strate, Margo A. Brinton and Mukesh Kumar\*

Department of Biology, College of Arts and Sciences, Georgia State University, Atlanta, GA, United States

## OPEN ACCESS

### Edited by:

Mei-Ling Li,  
Rutgers University, United States

### Reviewed by:

Yueh-Hsin Ping,  
National Yang-Ming University,  
Taiwan  
Victor R. DeFilippis,  
Oregon Health & Science University,  
United States

### \*Correspondence:

Mukesh Kumar  
mkumar8@gsu.edu

<sup>†</sup>These authors have contributed  
equally to this work

### Specialty section:

This article was submitted to  
Virology,  
a section of the journal  
Frontiers in Microbiology

Received: 04 June 2019

Accepted: 26 August 2019

Published: 11 September 2019

### Citation:

Rothan HA, Arora K, Natekar JP,  
Strate PG, Brinton MA and Kumar M  
(2019) Z-DNA-Binding Protein 1 Is  
Critical for Controlling Virus  
Replication and Survival in West Nile  
Virus Encephalitis.  
*Front. Microbiol.* 10:2089.  
doi: 10.3389/fmicb.2019.02089

West Nile virus (WNV), a neurotropic flavivirus, is the leading cause of viral encephalitis in the United States. Recently, Zika virus (ZIKV) infections have caused serious neurological diseases and birth defects, specifically Guillain-Barré syndrome and microcephaly. Z-DNA binding protein 1 (ZBP1) is a cytoplasmic sensor that has been shown to play a significant role in initiating a robust immune response. We previously reported that WNV and ZIKV infections induce dramatic up-regulation of ZBP1 in mouse brains as well as in infected primary mouse cells. Herein, we show the critical role of ZBP1 in restricting the pathogenesis of WNV and ZIKV infections. Deletion of ZBP1 resulted in significantly higher morbidity and mortality after infection with a pathogenic WNV NY99 strain in mice. No mortality was observed in wild-type (WT) mice infected with the non-pathogenic WNV strain, Eg101. Interestingly, infection of ZBP1<sup>-/-</sup> mice with WNV Eg101 was lethal resulting in 100% mortality, suggesting that ZBP1 is required for survival after WNV infection. Viremia and brain viral load were significantly higher in ZBP1<sup>-/-</sup> mice compared to WT mice. In addition, protein levels of interferon (IFN)- $\alpha$ , and inflammatory cytokines and chemokines were significantly higher in the serum and brains of infected ZBP1<sup>-/-</sup> mice compared to the WT mice. Primary mouse cortical neurons and mouse embryonic fibroblasts (MEFs) derived from ZBP1<sup>-/-</sup> mice produced higher virus titers compared to WT cells after infection with WNV NY99 and WNV Eg101. Similarly, neurons and MEFs lacking ZBP1 exhibited significantly enhanced replication of PRVABC59 (Asian) and MR766 (African) ZIKV compared to WT cells. The knockout of ZBP1 function in MEFs inhibited ZBP1-dependent virus-induced cell death. In conclusion, these data reveal that ZBP1 restricts WNV and ZIKV production in mouse cells and is required for survival of a peripheral WNV infection in mice.

**Keywords:** West Nile virus, flavivirus, Zika virus, Z-DNA-binding protein 1, DNA-dependent activator of IFN-regulatory factors, host-pathogen interaction, virus replication

## INTRODUCTION

Members of the genus *flavivirus* are the most important arthropod-borne viruses causing disease in humans. West Nile virus (WNV) is a neurotropic flavivirus that infects humans, birds, and horses resulting in complex neurological sequelae (Brinton, 2013). WNV infection in humans is usually asymptomatic, but can cause severe neurological disease including meningitis,

encephalitis, paralysis, and death (Brinton, 2013; Donadieu et al., 2013). Zika virus (ZIKV) infection can cause fever, headache, fatigue, and neurological symptoms. ZIKV infection is also associated with microcephaly in newborns and Guillain-Barré syndrome in adults (Coyne and Lazear, 2016; Costa and Ko, 2018; Hygino da Cruz et al., 2018; Mehta et al., 2018; Rothan et al., 2018a,b). No anti-viral drugs currently exist for treating patients infected with WNV or ZIKV infection.

Z-DNA binding protein 1 (ZBP1), also called DAI, is one of the cytoplasmic DNA sensors that has been shown to play a significant role in initiating a robust immune response (Schwartz et al., 2001; Ha et al., 2006; Takaoka et al., 2007; Wang et al., 2008). Recent reports demonstrate that ZBP1 senses accumulation of RNA rather than DNA to initiate receptor-interacting protein homotypic interaction motif (RHIM)-dependent activation of receptor-interacting kinase-3 (RIPK3)-dependent necroptosis during HSV-1, murine cytomegalovirus virus (MCMV), influenza virus, and vaccinia virus infections (Kim et al., 2003; Upton et al., 2012; Pham et al., 2013; Wang et al., 2014; Kuriakose et al., 2016; Thapa et al., 2016; Kesavardhana et al., 2017; Koehler et al., 2017). Necroptosis is a form of cell death triggered by RIPK3 phosphorylation that activates the pseudo-kinase MLKL, which upon oligomerization ruptures the plasma membrane, leading to cell death (Wallach et al., 2016). Thus, necroptosis represents a host defense mechanism that combats virus replication in host tissues (Orozco and Oberst, 2017). In addition, recent work has implicated additional roles for ZBP1 and RIPK3 in promoting inflammation, independent of cell death (Daniels et al., 2017, 2019). ZBP1 also regulates NLRP3 inflammasome-mediated production of IL-1 $\beta$  in response to influenza virus infection (Kuriakose et al., 2016). In addition, ZBP1 has been shown to be involved in interferon (IFN) induction in response to HSV-1 (Wang et al., 2008) and human CMV infection (DeFilippis et al., 2010).

We previously reported that WNV and ZIKV infections induce dramatic up-regulation of ZBP1 in mouse brains as well as in infected primary mouse cells (Kumar et al., 2016; Azouz et al., 2019). In the present study, we show the critical role of ZBP1 in restricting the pathogenesis of WNV and ZIKV infections. The ZBP1<sup>-/-</sup> mice exhibited higher morbidity and mortality after infection with lethal and non-lethal WNV strains compared to wild-type (WT) mice. Primary neuronal cultures and mouse embryonic fibroblasts (MEFs) lacking ZBP1 produced higher virus titers after infection with WNV and ZIKV compared to cells derived from WT mice. Collectively, these data provide the first evidence of the requirement for ZBP1 to restrict WNV and ZIKV production and demonstrate that ZBP1-dependent signaling is required to effectively control WNV infection in mice.

## MATERIALS AND METHODS

### Animals

Wild-type (WT) C57BL/6J mice were purchased from the Jackson Laboratory (Bar Harbor, ME), and ZBP1<sup>-/-</sup> mice (nbio155) were obtained from the JCRB Laboratory Animal Resource Bank of the National Institutes of Biomedical Innovation, Health and

Nutrition (Osaka, Japan). All mice were bred and genotyped in the animal facility at Georgia State University. The WNV infection experiments were conducted in the animal biosafety level-3 laboratory. This study was carried out following the guidelines of the National Institutes of Health and the Institutional Animal Care and Use Committee (IACUC). The protocol was approved by the Georgia State University IACUC (Protocol number A19006).

### Animal Infection Experiments and Plaque Assay

Eight-week-old WT and ZBP1<sup>-/-</sup> mice were inoculated subcutaneously with 100 plaque-forming units (PFU) of WNV NY99, or 1,000 PFU of WNV Eg101, and the disease symptoms were observed twice daily (Kumar et al., 2013, 2014a,b; Krause et al., 2019). On specific days after inoculation, blood was collected from the tail vein, and serum was separated. In independent experiments, mice were inoculated with PBS (Mock) or WNV NY99 or WNV Eg101 subcutaneously, and on day 8 after inoculation, mice were anesthetized, extensively perfused with PBS, and the brains were harvested. WNV titers in the serum and brain homogenates were measured by plaque assay as described previously (Krause et al., 2019).

### West Nile Virus and Zika Virus Infection of Neuronal Cultures and Mouse Embryonic Fibroblast

Mouse cortical neuron cultures and mouse embryonic fibroblasts (MEFs) were prepared from 1-day-old pups obtained from established colonies of C57/B6J WT and ZBP1<sup>-/-</sup> mice as described previously (Durkin et al., 2013; Forest et al., 2018; Azouz et al., 2019). The neurons were plated onto poly-D-lysine-coated 6-well or 24-well plates in serum Neurobasal-A medium (Gibco). The cultures were maintained in serum-free Neurobasal A medium supplemented with B27 (Gibco) for 7 days prior to infection. MEFs were grown in DMEM (Gibco) supplemented with 10% heat-inactivated fetal bovine serum and 10  $\mu$ g/ml gentamicin (Gibco).

Primary neuronal cultures were infected with WNV NY99 at a multiplicity of infection (MOI) of 0.01 and MEFs were infected at a MOI of 1. Both primary neuronal cultures and MEFs were infected with WNV Eg101 at a MOI of 1. For ZIKV infection experiments, neuronal cultures and MEFs were infected at a MOI of 1 with a ZIKV strain, PRVABC59 (Asian strain) or MR766 (prototype African strain). After infection, supernatants and cell lysates were harvested at 24, 48, and 72 h after infection. Virus titers were measured in cell supernatants by plaque assay (Kumar et al., 2013; Kim et al., 2018; Azouz et al., 2019).

### Enzyme-Linked Immunosorbent Assay and Multiplex Immunoassay

Protein levels of IFN- $\alpha$  were measured in the serum and brain homogenates using the VeriKine™ Mouse Interferon- $\alpha$  enzyme-linked immunosorbent assay (ELISA) Kit (PBL Interferon Source) as described previously (Kumar et al., 2012). Multiplex immunoassay kit (MILLIPLEX MAP Mouse Cytokine/Chemokine

Kit, Millipore) was used to measure protein levels of inflammatory cytokines and chemokines in the serum (Kumar et al., 2012).

### Quantitative Reverse Transcription-Polymerase Chain Reaction

Virus RNA levels were analyzed in the mouse brains and primary mouse cultures by quantitative reverse transcription-polymerase chain reaction (qRT-PCR). Briefly, total RNA was extracted from homogenized mice brains or cell lysates using a RNeasy Mini Kit (Qiagen) and a iScript™ cDNA Synthesis Kit (Bio-Rad) was used to prepare cDNA samples. Quantitative RT-PCR was used to measure viral RNA levels using primers and probes specific for the WNV or ZIKV as described previously (Kumar et al., 2013, 2017).

### Cell Viability Assay

Neuronal cultures and MEFs seeded in 96-well plates (1 × 10<sup>4</sup> cells/well) were mock-infected with PBS or infected with WNV NY99. Neuronal cultures were infected at a MOI of 0.01, while MEFs were infected at a MOI of 1. Cell viability was assessed at days 1–3 after infection using a CellTiter 96<sub>AQueous</sub> One Solution Cell Proliferation Assay (Promega) as described previously (Kumar et al., 2010).

### Statistical Analysis

GraphPad Prism 7.0 was used to perform a Kaplan Meier log-rank test to compare survival curves. Unpaired Student's

*t*-test using GraphPad was used to calculate values of *p* for the clinical scores and plaque assay titers in mouse brains and serum. For plaque assay titers in cell culture supernatants and intracellular viral RNA copies in the cell lysates, two-way analysis of variance (ANOVA) with the *post hoc* Bonferroni test was used to calculate values of *p*. Differences with *p*'s of <0.05 were considered significant.

## RESULTS

### Z-DNA-Binding Protein 1 Signaling Controls West Nile Virus Pathogenesis in Mice Following Peripheral Infection

To determine the role of ZBP1 in WNV pathogenesis, we evaluated morbidity of WT and ZBP1<sup>-/-</sup> mice after WNV infection. Mice were inoculated subcutaneously with either the lethal WNV, strain NY99 (100 PFU) or the non-lethal WNV, strain Eg101 (1,000 PFU). While the infectious dose of 100 PFU of WNV NY99 (Figure 1A) resulted in 40% mortality in WT mice, mortality in ZBP1<sup>-/-</sup> mice was 100%. The median survival time of infected ZBP1<sup>-/-</sup> mice was also shorter than in the WT mice. As expected, no mortality was observed in WT mice infected with 1,000 PFU of WNV Eg101 (Figure 1B). Interestingly, infection of ZBP1<sup>-/-</sup> mice with WNV Eg101 was highly lethal and resulted in 100% mortality. The median survival times observed in WNV Eg101-infected ZBP1<sup>-/-</sup> mice was similar to the WNV NY99-infected ZBP1<sup>-/-</sup> mice.

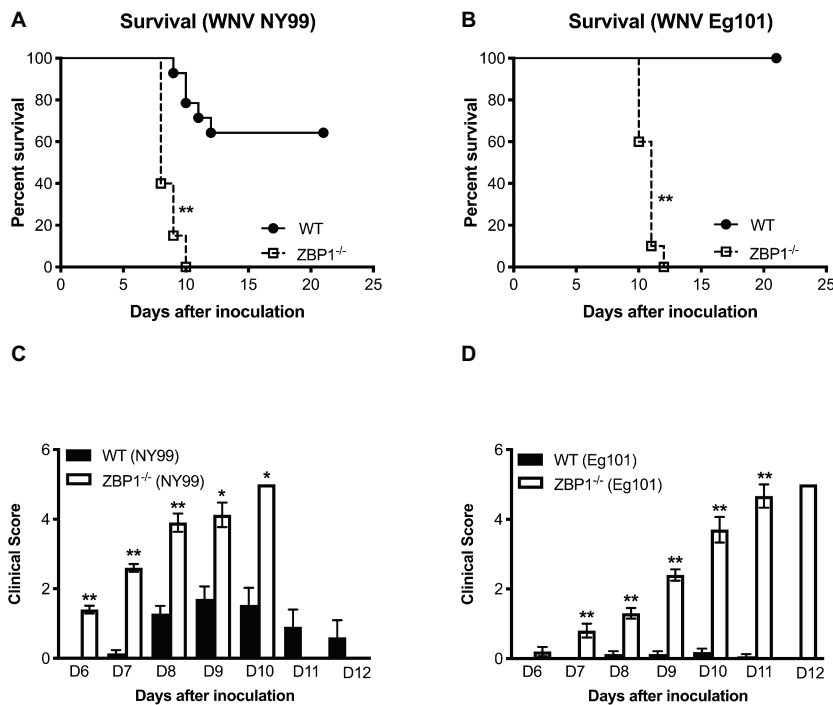


**FIGURE 1 |** Analysis of survival and clinical score in WT and ZBP1<sup>-/-</sup> mice following WNV infection. WT and ZBP1<sup>-/-</sup> mice were inoculated subcutaneously *via* footpad with (A) WNV NY99 (100 PFU) or (B) WNV Eg101 (1,000 PFU). The difference in the survival of WT and ZBP1<sup>-/-</sup> mice was statistically significant for both WNV NY99 and WNV Eg101 (*n* = 12–22 mice per group). (C,D) Animals were monitored twice daily for clinical signs. The designation for the clinical scores is as follows: 1, ruffled fur/hunched back; 2, paresis/difficulty walking; 3, paralysis; 4, moribund/euthanized; and 5, dead. Error bars represent SEM, \**p* < 0.05, \*\**p* < 0.001.

All ZBP1<sup>-/-</sup> mice developed severe neurological signs after inoculation with WNV NY99 or WNV Eg101 (Figures 1C,D). These clinical signs include ruffled fur, hunched posture, paralysis, tremors, and ataxic gait. WT mice infected with WNV NY99 developed moderate clinical signs while the WT mice infected with Eg101 demonstrated no significant clinical signs. The observation of high morbidity and mortality in ZBP1<sup>-/-</sup> mice inoculated with WNV Eg101 suggested that ZBP1 is required for survival after WNV infection in mice.

### Z-DNA-Binding Protein 1 Is Required for Control of West Nile Virus Load in the Periphery and Brain

We next measured the viral titers in the serum of WT and ZBP1<sup>-/-</sup> mice at different time-points after subcutaneous WNV NY99 or WNV Eg101 infection. The WNV replication kinetics in the serum of WT and ZBP1<sup>-/-</sup> mice as measured by plaque assay demonstrated higher viremia in ZBP1<sup>-/-</sup> mice. WNV titers were significantly higher in ZBP1<sup>-/-</sup> mice as compared to WT mice at day 3 after WNV NY99 (Figure 2A) or WNV Eg101 infection (Figure 2B). At day 6 post-infection, WNV levels decreased in WT mice, while they remained significantly high in ZBP1<sup>-/-</sup> mice infected with WNV NY99.

In separate experiments, mice were inoculated with WNV NY99 or WNV Eg101 subcutaneously, and brains were harvested at day 8 after inoculation. It is known that WNV is first detected in the mouse brain around day 6 after subcutaneous

inoculation and peak virus load is observed at day 8 after infection. Therefore, we examined viral load in the brains at day 8 after infection. WNV titers in the brain homogenates were measured by plaque assay. WNV load in the brains of ZBP1<sup>-/-</sup> mice was significantly higher than the WT mice infected with WNV NY99 or WNV Eg101 (Figure 2C). We next measured the WNV RNA copies in the brains of WT and ZBP1<sup>-/-</sup> mice infected subcutaneously with WNV NY99 or WNV Eg101. WNV RNA copies in the brains of ZBP1<sup>-/-</sup> mice were significantly higher than the WT mice at day 8 after infection with WNV NY99 (Figure 2D). Very low levels of WNV RNA were detected in the brains of the WT mice infected with WNV Eg101. Nonetheless, significantly higher WNV RNA levels were detected in the brains of ZBP1<sup>-/-</sup> mice at day 8 after infection (Figure 2D). These data suggest that ZBP1-dependent signaling plays a significant role in controlling WNV load in both the periphery and in the brain.

### Anti-Viral Immune Responses in Wild-Type and ZBP1<sup>-/-</sup> Mice

IFN- $\alpha$  is essential for the WNV clearance from the periphery and in the brain (Suthar et al., 2013). ZBP1 has also been shown to be involved in IFN induction after virus infection (Wang et al., 2008; DeFilippis et al., 2010). Therefore, we measured the protein levels of IFN- $\alpha$  in the serum (day 3 after infection) and brain homogenates (day 8 after infection) of WT and ZBP1<sup>-/-</sup> mice using ELISA. Our data demonstrate

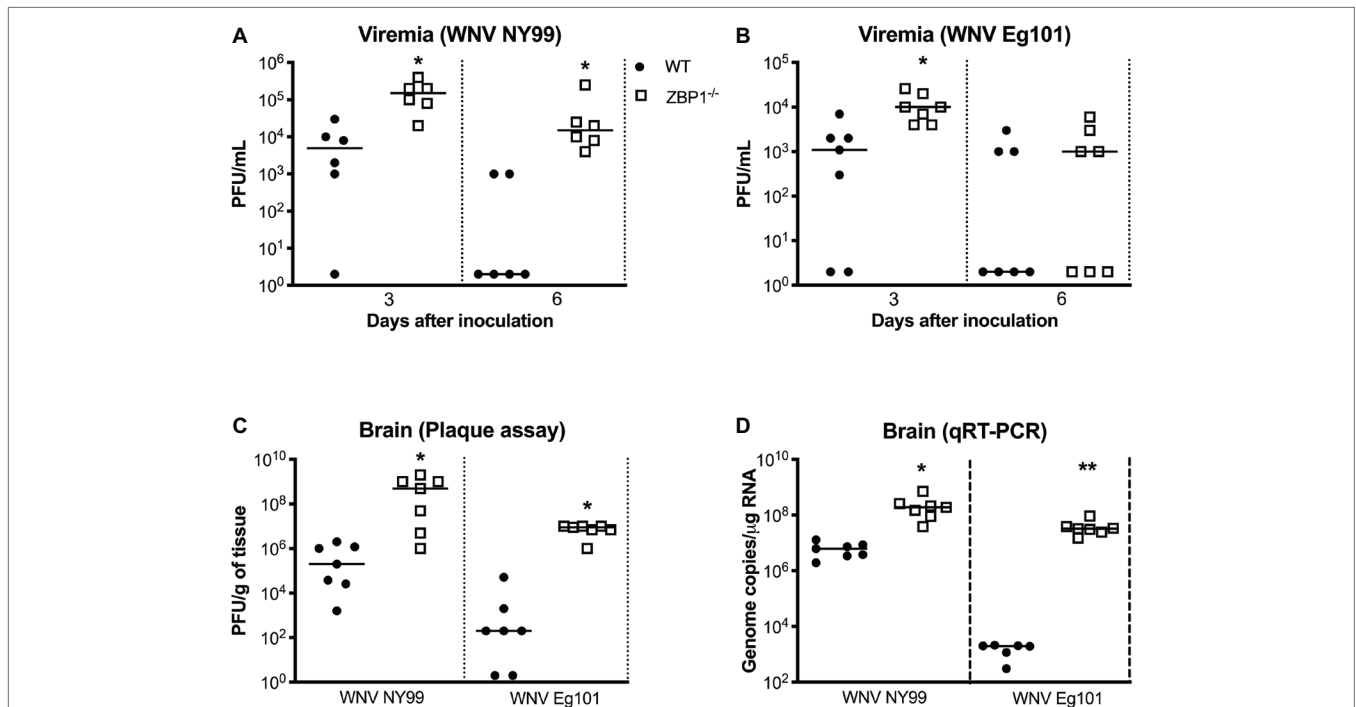
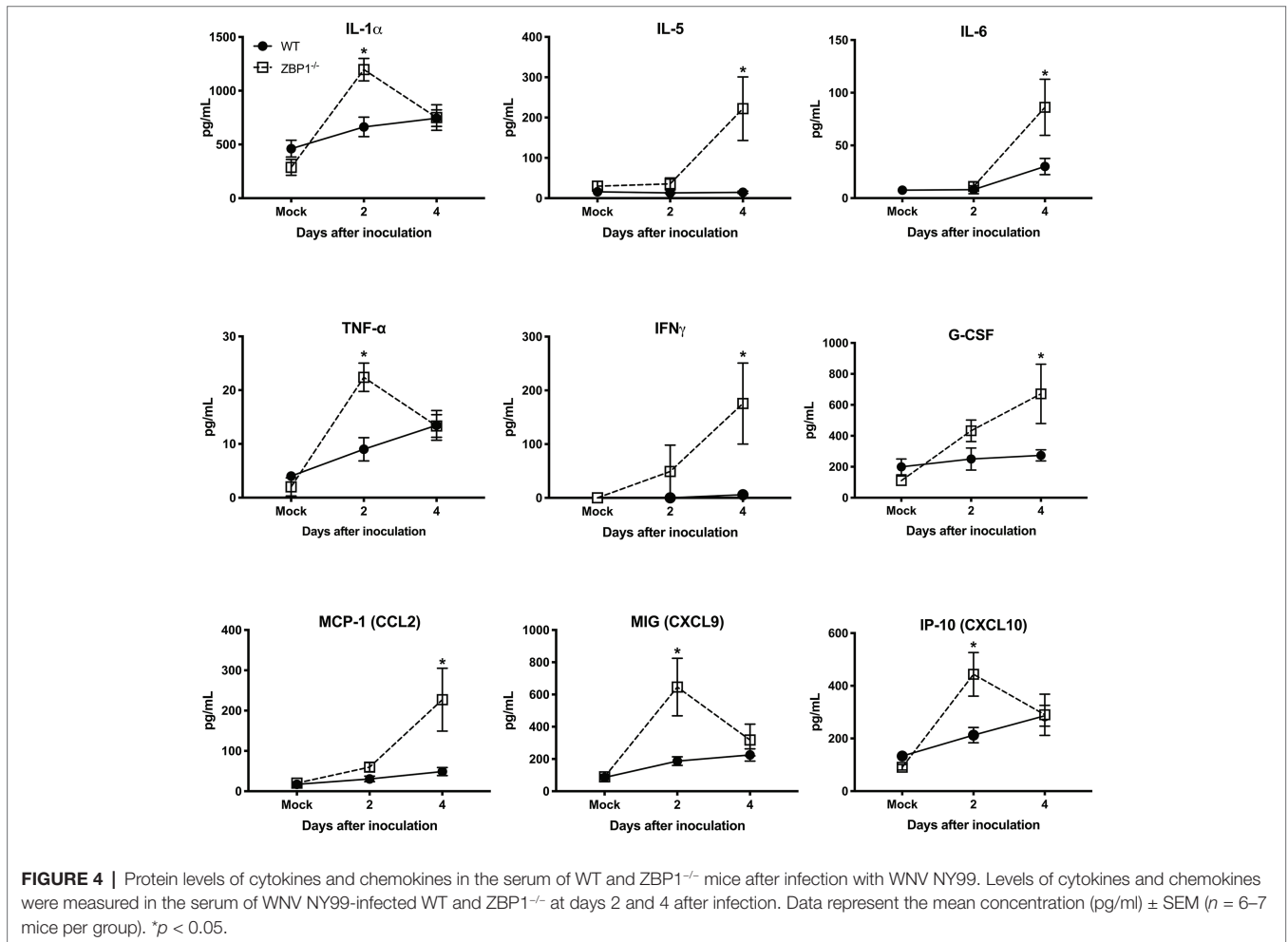
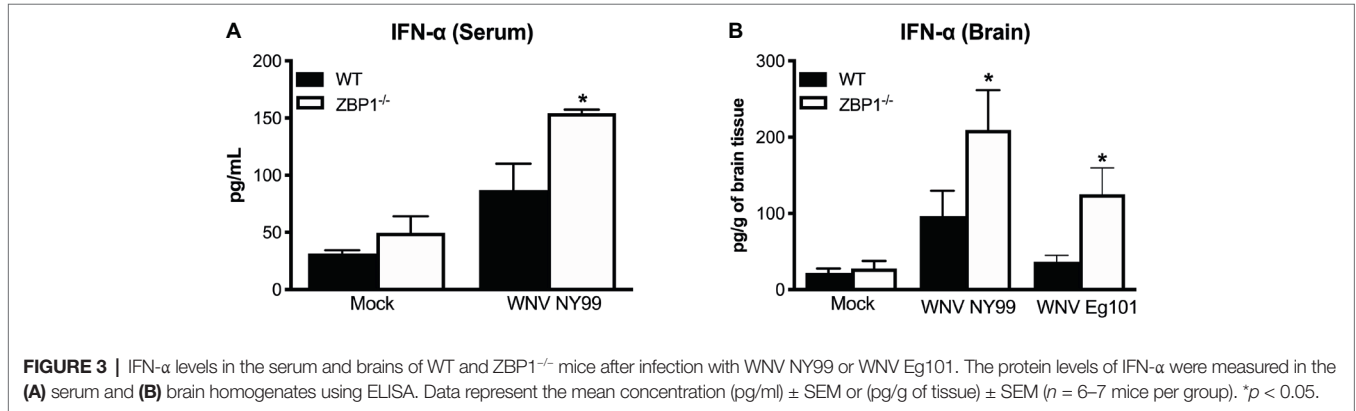


**FIGURE 2 |** Analysis of virus titers in WT and ZBP1<sup>-/-</sup> mice. Virus titers were measured in the serum at days 3 and 6 after (A) WNV NY99 or (B) WNV Eg101 infection by plaque assay and expressed as PFU/mL. (C) Virus titers were measured in brain homogenates (day 8 after infection with WNV NY99 or WNV Eg101) and expressed as PFU/g of tissue. (D) The WNV RNA copy number in the brain was determined by qRT-PCR and expressed as genome copies/μg of RNA (day 8 after infection with WNV NY99 or WNV Eg101). Each data point represents an individual mouse. The solid horizontal lines signify the median (n = 6–7 mice per group). \*p < 0.05, \*\*p < 0.001.

that protein levels of IFN- $\alpha$  in the serum and brain homogenates were significantly higher in ZBP1<sup>-/-</sup> mice compared to the WT mice (Figure 3).

Recent work has implicated a role for ZBP1 in promoting protective inflammation (Daniels et al., 2019). It is known that WNV infection induces a strong up-regulation of multiple cytokines and chemokines. WNV-induced pro-inflammatory mediators are also known to protect mice from lethal WNV

disease (Suthar et al., 2013). Therefore, we next assessed the protein levels of key cytokines and chemokines in the serum using a multiplex immunoassay. Protein levels of key antiviral cytokines and chemokines were significantly higher in the serum of ZBP1<sup>-/-</sup> mice compared to the WT mice. The protein levels of interleukin (IL)-1 $\alpha$ , TNF $\alpha$ , MIG (CXCL9), and IP-10 (CXCL10) were significantly higher in ZBP1<sup>-/-</sup> mice compared to the WT mice at day 2 after infection (Figure 4).



The protein levels of IL-5, IL-6, IFN $\gamma$ , G-CSF, and MCP-1 (CXCL2) were significantly higher in ZBP1<sup>-/-</sup> mice compared to the WT mice at day 4 after infection (Figure 4). It is possible that high virus replication in ZBP1<sup>-/-</sup> mice resulted in a higher inflammatory response. Collectively, these data indicate that ZBP1-mediated restriction of peripheral WNV infection is independent of IFN- $\alpha$ , and anti-viral cytokines and chemokines.

### Z-DNA-Binding Protein 1 Restricts West Nile Virus and Zika Virus Replication in Mouse Cells

To further define the role of ZBP1 during WNV infection, we performed a multistep virus growth analysis in cortical neurons and MEFs isolated from WT and ZBP1<sup>-/-</sup> mice. Cells were infected with WNV NY99 or WNV Eg101, and supernatants and cell lysates were harvested at 24, 48, and 72 h after infection. Virus titers were measured in cell supernatants by plaque assay. WNV infection of MEFs and neuronal cultures from ZBP1<sup>-/-</sup> mice resulted in significantly higher virus titers compared to those from WT mice (Figure 5). Total RNA was extracted from the cell lysates and WNV RNA copies were measured using qRT-PCR. Intracellular WNV RNA levels were also significantly higher in cell cultures from ZBP1<sup>-/-</sup> mice compared to those from WT mice (Figure 6).

We next examined the role of ZBP1 in ZIKV replication. Similar to WNV, MEFs and neuronal cultures from ZBP1<sup>-/-</sup> mice produced significantly enhanced virus yields compared to those from WT mice after infection with the Asian or African strains of ZIKV (Figure 7). ZIKV RNA levels were also significantly higher in cell cultures from ZBP1<sup>-/-</sup> mice compared to those from WT mice (Figure 8). The difference in both WNV and ZIKV titers between WT and ZBP1<sup>-/-</sup> cells was consistently more dramatic in MEFs (2–3 logs) compared to cortical neurons (1 log). These results correlate with the increased virus titers observed in the serum and brains of ZBP1<sup>-/-</sup> mice compared to the WT mice after WNV infection.

### Z-DNA-Binding Protein 1-Dependent Cell Death in Primary Mouse Cells Following Infection With West Nile Virus NY99

MEF and neuronal cultures from WT and ZBP1<sup>-/-</sup> mice were infected with WNV NY99 and cell viability was measured at 24, 48, and 72 h after infection. Our data demonstrate that the cell viability of infected ZBP1<sup>-/-</sup> MEFs was significantly higher than that of the WT MEFs at both 48 and 72 h after infection (Figure 9A). However, we did not observe this trend in neuronal cultures as the decrease in WNV-induced cell death was similar in both WT and ZBP1<sup>-/-</sup> neuronal cultures (Figure 9B).

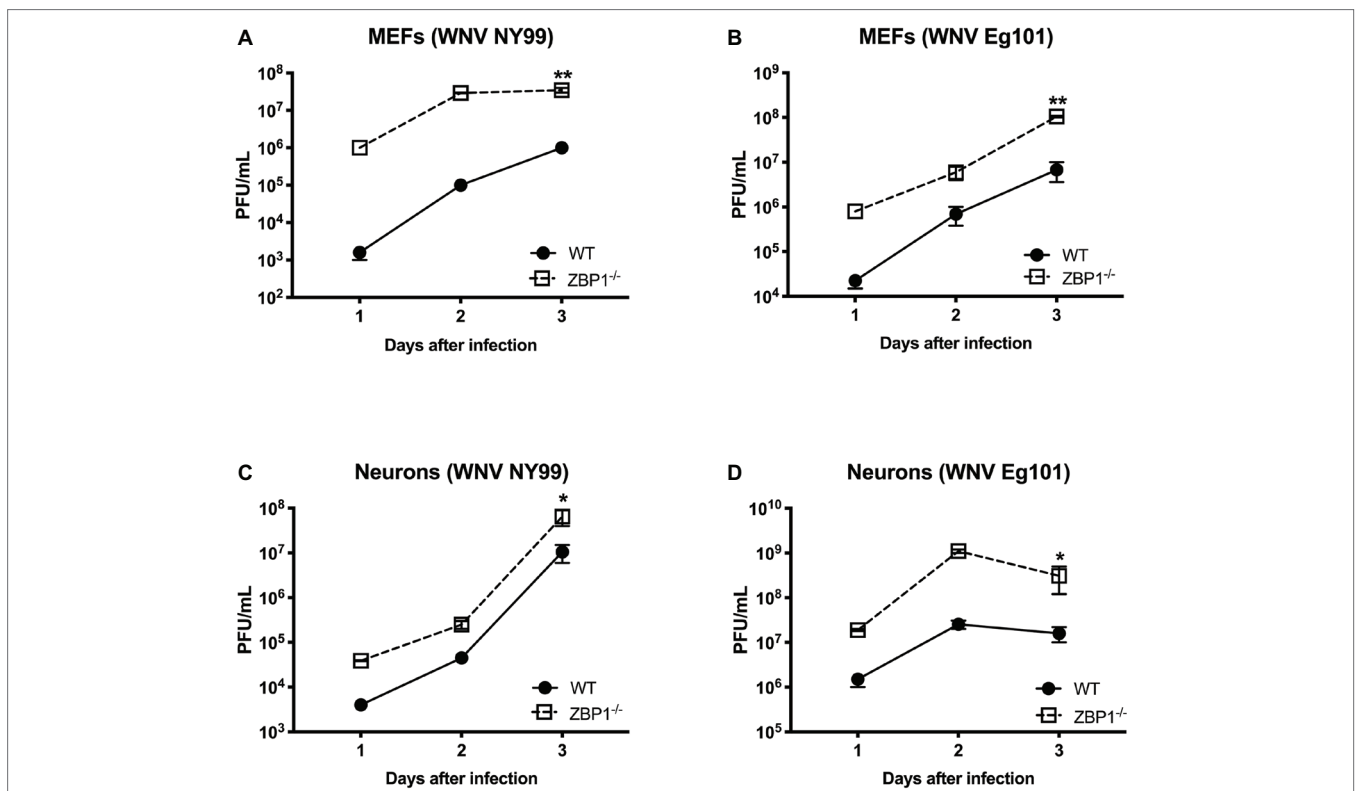


**FIGURE 5 |** Analysis of virus titers produced by primary cells isolated from WT and ZBP1<sup>-/-</sup> mice. (A–D) MEFs and neuronal cultures were infected with WNV NY99 or WNV Eg101 (as described in Materials and Methods) and virus titers in the cell culture supernatants were measured by plaque assay. Results are expressed as PFU/ml  $\pm$  SEM from at least three independent experiments conducted in duplicate. \**p* < 0.05, \*\**p* < 0.001.

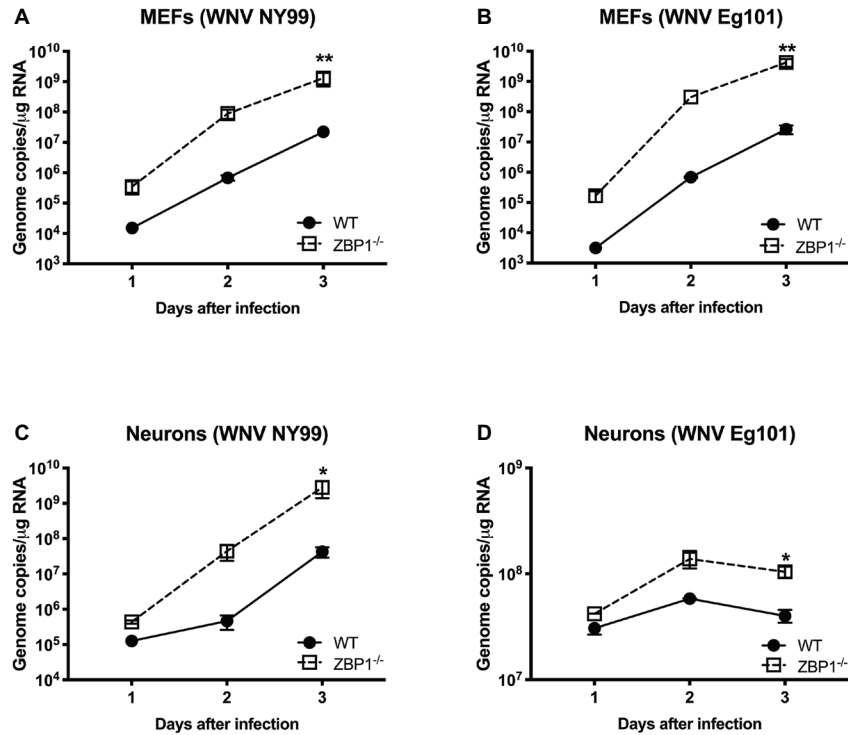


**FIGURE 6 |** Analysis of viral RNA levels in the primary cells isolated from WT and ZBP1<sup>-/-</sup> mice. (A–D) Cells were infected with WNV NY99 or Eg101 and total RNA extracted from cell lysates was used to conduct qRT-PCR to measure WNV RNA (expressed as genome copies/μg of RNA). Error bars represent SEM (three independent experiments conducted in duplicate), \**p* < 0.05, \*\**p* < 0.001.

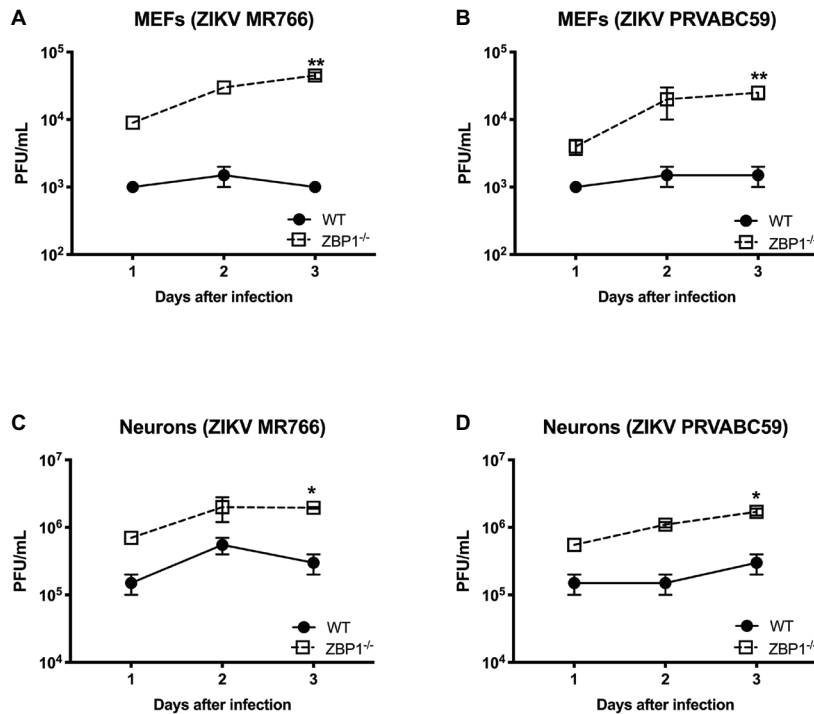


**FIGURE 7 |** Analysis of ZIKV yields produced by primary mouse cells. (A–D) MEFs and neuronal cultures derived from WT and ZBP1<sup>-/-</sup> were infected with ZIKV MR766 or ZIKV PRVABC59 at a MOI of 1 and virus titers in the cell culture supernatants were measured by plaque assay. Results are expressed as PFU/mL ± SEM from at least three independent experiments conducted in duplicate. \**p* < 0.05, \*\**p* < 0.001.

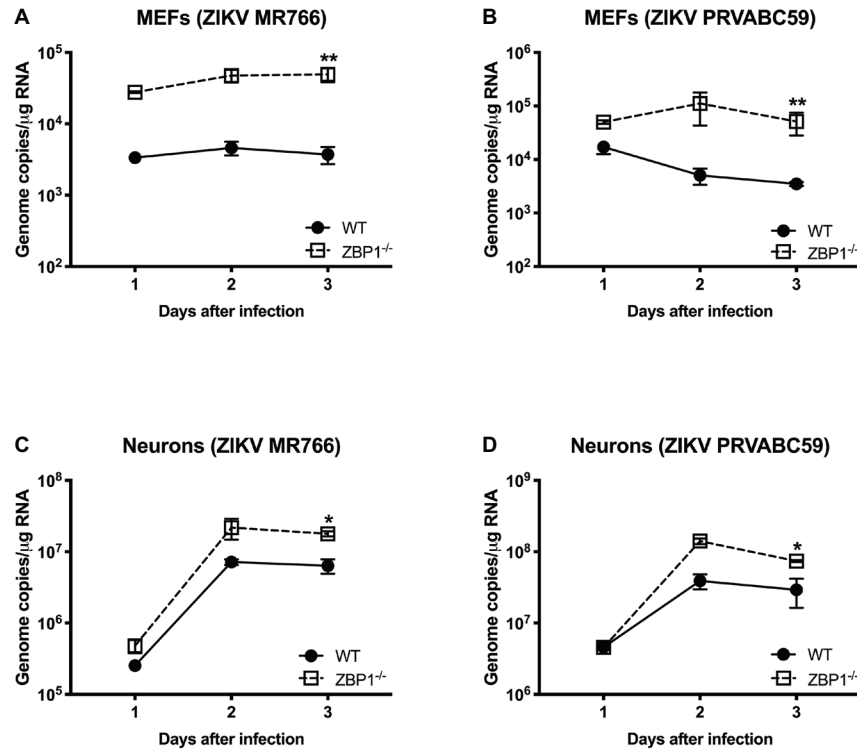


**FIGURE 8 |** ZIKV RNA levels in the MEFs and neurons isolated from WT and ZBP1<sup>-/-</sup> mice. (A–D) Cells were infected with ZIKV MR766 or ZIKV PRVABC59 at a MOI of 1. Total RNA was extracted from cell lysates and ZIKV RNA was measured by qRT-PCR (expressed as genome copies/μg of RNA). Error bars represent SEM (three independent experiments conducted in duplicate), \**p* < 0.05, \*\**p* < 0.001.

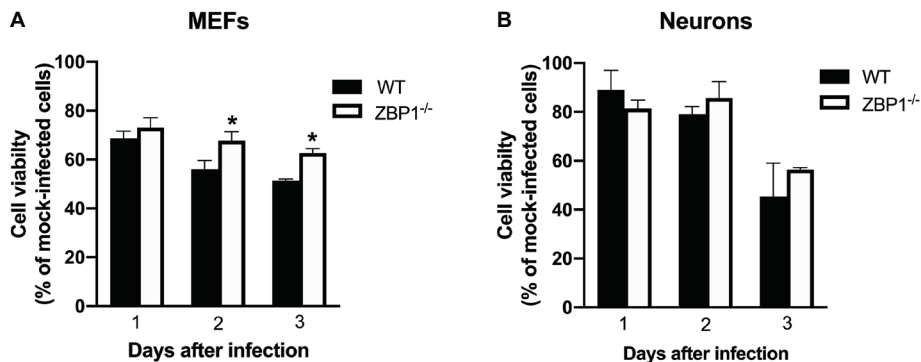


**FIGURE 9 |** Assay of primary mouse cell viability following WNV infection. (A) MEFs and (B) neuronal cultures from WT and ZBP1<sup>-/-</sup> mice were infected with WNV NY99. Cell toxicity on days 1, 2, and 3 after infection was evaluated by cell proliferation assay and the percentage of cell viability was calculated by comparing values to those from mock-infected cells at the corresponding time points. The data are expressed as the mean ± SEM for two independent experiments conducted in triplicate. Error bars represent SEM, \**p* < 0.05.

## DISCUSSION

Our data for the first time demonstrate the critical role of ZBP1 in restricting WNV-induced pathogenesis in mice. ZBP1 reduces WNV and ZIKV production in primary mouse cells and is crucial for survival in the mouse model of WNV disease.

It is known that WNV Eg101 is largely non-pathogenic in adult mice after subcutaneous inoculation (Shirato et al., 2004;

Kumar et al., 2014a). However, adult ZBP1<sup>-/-</sup> mice exhibited 100% mortality after subcutaneous inoculation of WNV Eg101. These data suggest a critical role for ZBP1 in controlling the pathogenic effects of a WNV infection. Viral loads were also significantly higher in the serum and brains of WNV-infected ZBP1<sup>-/-</sup> mice compared to those of the WT mice. Several previous studies have reported increased virus titers and disease severity in ZBP1<sup>-/-</sup> mice after infection with influenza virus

(Kuriakose et al., 2016; Thapa et al., 2016), HSV-1 (Guo et al., 2018), and MCMV (Upton et al., 2012; Sridharan et al., 2017). One recent study published while this manuscript was in preparation suggests that ZBP1 senses ZIKV infection and restricts disease pathogenesis after intracranial inoculation of ZIKV in mice (Daniels et al., 2019). Another study from the same group previously reported that neuronal RIPK3 signaling is required for survival after subcutaneous WNV infection in mice (Daniels et al., 2017). Our data are in agreement with these observations demonstrating that ZBP1 reduces ZIKV production in primary mouse cells. However, our data for the first time also demonstrate that ZBP1 restricts replication of WNV in mouse cells and is required for survival of a peripheral WNV infection in mice.

Recent work has implicated a role for ZBP1 in promoting protective inflammation. Daniels et al. reported that ZBP1-mediated protective neuroinflammation is required for the protection against intracranial ZIKV infection (Daniels et al., 2019). In the present study, we showed that high virus titers in the serum of ZBP1<sup>-/-</sup> mice were associated with elevated levels of anti-viral cytokines and chemokines after subcutaneous infection with WNV. Our results are in agreement with previous studies demonstrating high levels of pro-inflammatory cytokines and chemokines in ZBP1<sup>-/-</sup> mice after infection with *Toxoplasma gondii* and influenza virus (Kuriakose et al., 2016; Pittman et al., 2016). It is known that IFN- $\alpha$  is essential for the WNV clearance from the periphery and in the brain (Suthar et al., 2013). ZBP1 has also been shown to be involved in IFN induction after virus infection (DeFilippis et al., 2010). Our data demonstrate that protein levels of IFN- $\alpha$  in the serum and brain homogenates were significantly higher in ZBP1<sup>-/-</sup> mice compared to the WT mice. Collectively, these data indicate that ZBP1-mediated restriction of peripheral WNV infection is independent of IFN- $\alpha$ , and anti-viral cytokines and chemokines.

One interesting finding of our study was that we observed a dramatic difference in WNV or ZIKV virus replication in MEFs in the absence of ZBP1. In contrast, deletion of ZBP1 resulted in a modest increase in virus replication in neurons. In addition, we found that the viability of ZBP1<sup>-/-</sup> MEFs infected with WNV was significantly higher than that of infected WT MEFs. However, the viability of ZBP1<sup>-/-</sup> neurons was similar to that of WT neurons after WNV infection. These data are in agreement with previous observations demonstrating that ZIKV did not induce ZBP1-dependent cell death in primary neuronal cultures (Daniels et al., 2017,

2019). However, ZBP1-dependent cell death in virus-infected MEFs had never been examined. It is known that activation of the ZBP1-RIPK3 pathway requires high levels of ZBP1 expression and therefore a cell-specific difference in the levels of ZBP1 expression may determine the outcome (Guo et al., 2018). Interestingly, it has been reported that the expression level of ZBP1 is strongly up-regulated in MEFs when stimulated with a synthetic DNA and therefore evokes a stronger innate immune response (Ishii et al., 2006). It could be possible that the ZBP1 and RIPK3 activation is more effective in MEFs compared to neurons. However, more studies are warranted to further understand the cell-specific role of ZBP1 in virus replication.

To our knowledge, our study for the first time revealed a critical role of ZBP1 during peripheral WNV infection in mice. There is need for further mechanistic studies to understand how ZBP1 restricts peripheral WNV and ZIKV infection.

## DATA AVAILABILITY

All datasets generated for this study are included in the manuscript and/or the supplementary files.

## ETHICS STATEMENT

The animal study was reviewed and approved by Georgia State University Institutional Animal Care and Use Committee (Protocol number A19006).

## AUTHOR CONTRIBUTIONS

MK, HR, KA, and MB designed the experiments, analyzed the data, and wrote the manuscript. MK, HR, KA, JN, and PS conducted the experiments. All authors have read and approved the final version of the manuscript.

## FUNDING

This work was supported by a grant (R21NS099838) from National Institute of Neurological Disorders and Stroke and a grant (R21OD024896) from the Office of the Director, National Institutes of Health and Institutional funds.

## REFERENCES

- Azouz, F., Arora, K., Krause, K., Nerurkar, V. R., and Kumar, M. (2019). Integrated MicroRNA and mRNA profiling in Zika virus-infected neurons. *Viruses* 11:162. doi: 10.3390/v11020162
- Brinton, M. A. (2013). Replication cycle and molecular biology of the West Nile virus. *Viruses* 6, 13–53. doi: 10.3390/v6010013
- Costa, F., and Ko, A. I. (2018). Zika virus and microcephaly: where do we go from here? *Lancet Infect. Dis.* 18, 236–237. doi: 10.1016/S1473-3099(17)30697-7
- Coyne, C. B., and Lazear, H. M. (2016). Zika virus - reigniting the TORCH. *Nat. Rev. Microbiol.* 14, 707–715. doi: 10.1038/nrmicro.2016.125
- Daniels, B. P., Kofman, S. B., Smith, J. R., Norris, G. T., Snyder, A. G., Kolb, J. P., et al. (2019). The nucleotide sensor ZBP1 and kinase RIPK3 induce the enzyme IRG1 to promote an antiviral metabolic state in neurons. *Immunity* 50, 64–76.e4. doi: 10.1016/j.immuni.2018.11.017
- Daniels, B. P., Snyder, A. G., Olsen, T. M., Orozco, S., Oguin, T. H. III, Tait, S. W. G., et al. (2017). RIPK3 restricts viral pathogenesis via cell death-independent neuroinflammation. *Cell* 169, 301–313.e11. doi: 10.1016/j.cell.2017.03.011
- DeFilippis, V. R., Alvarado, D., Sali, T., Rothenburg, S., and Fruh, K. (2010). Human cytomegalovirus induces the interferon response via the DNA sensor ZBP1. *J. Virol.* 84, 585–598. doi: 10.1128/jvi.01748-09

- Donadieu, E., Bahuon, C., Lowenski, S., Zientara, S., Couplier, M., and Lecollinet, S. (2013). Differential virulence and pathogenesis of West Nile viruses. *Viruses* 5, 2856–2880. doi: 10.3390/v5112856
- Durkin, M. E., Qian, X., Popescu, N. C., and Lowy, D. R. (2013). Isolation of mouse embryo fibroblasts. *Bio. Protoc.* 3:e908. doi: 10.21769/BioProtoc.908
- Forest, K. H., Alfulajj, N., Arora, K., Taketa, R., Sherrin, T., Todorovic, C., et al. (2018). Protection against beta-amyloid neurotoxicity by a non-toxic endogenous N-terminal beta-amyloid fragment and its active hexapeptide core sequence. *J. Neurochem.* 144, 201–217. doi: 10.1111/jnc.14257
- Guo, H., Gilley, R. P., Fisher, A., Lane, R., Landsteiner, V. J., Ragan, K. B., et al. (2018). Species-independent contribution of ZBP1/DAI/DLM-1-triggered necroptosis in host defense against HSV1. *Cell Death Dis.* 9:816. doi: 10.1038/s41419-018-0868-3
- Ha, S. C., Van Quyen, D., Hwang, H. Y., Oh, D. B., Brown, B. A. II, Lee, S. M., et al. (2006). Biochemical characterization and preliminary X-ray crystallographic study of the domains of human ZBP1 bound to left-handed Z-DNA. *Biochim. Biophys. Acta* 1764, 320–323. doi: 10.1016/j.bbapap.2005.12.012
- Hygino da Cruz, L. C. Jr., Nascimento, O. J. M., Lopes, E., and Da Silva, I. R. F. (2018). Neuroimaging findings of Zika virus-associated neurologic complications in adults. *AJNR Am. J. Neuroradiol.* 39, 1967–1974. doi: 10.3174/ajnr.a5649
- Ishii, K. J., Coban, C., Kato, H., Takahashi, K., Torii, Y., Takeshita, F., et al. (2006). A toll-like receptor-independent antiviral response induced by double-stranded B-form DNA. *Nat. Immunol.* 7, 40–48. doi: 10.1038/ni1282
- Kesavardhana, S., Kuriakose, T., Guy, C. S., Samir, P., Malireddi, R. K. S., Mishra, A., et al. (2017). ZBP1/DAI ubiquitination and sensing of influenza vRNPs activate programmed cell death. *J. Exp. Med.* 214, 2217–2229. doi: 10.1084/jem.20170550
- Kim, Y. G., Muralinath, M., Brandt, T., Percy, M., Hauns, K., Lowenhaupt, K., et al. (2003). A role for Z-DNA binding in vaccinia virus pathogenesis. *Proc. Natl. Acad. Sci. USA* 100, 6974–6979. doi: 10.1073/pnas.0431131100
- Kim, J. A., Seong, R. K., Kumar, M., and Shin, O. S. (2018). Favipiravir and ribavirin inhibit replication of Asian and African strains of Zika virus in different cell models. *Viruses* 10:72. doi: 10.3390/v10020072
- Koehler, H., Cotsmire, S., Langland, J., Kibler, K. V., Kalman, D., Upton, J. W., et al. (2017). Inhibition of DAI-dependent necroptosis by the Z-DNA binding domain of the vaccinia virus innate immune evasion protein, E3. *Proc. Natl. Acad. Sci. USA* 114, 11506–11511. doi: 10.1073/pnas.1700999114
- Krause, K., Azouz, F., Nakano, E., Nerurkar, V. R., and Kumar, M. (2019). Deletion of pregnancy zone protein and murinoglobulin-1 restricts the pathogenesis of West Nile virus infection in mice. *Front. Microbiol.* 10:259. doi: 10.3389/fmicb.2019.00259
- Kumar, M., Belcaid, M., and Nerurkar, V. R. (2016). Identification of host genes leading to West Nile virus encephalitis in mice brain using RNA-seq analysis. *Sci. Rep.* 6:26350. doi: 10.1038/srep38916
- Kumar, M., Krause, K. K., Azouz, F., Nakano, E., and Nerurkar, V. R. (2017). A guinea pig model of Zika virus infection. *Viol. J.* 14:75. doi: 10.1186/s12985-017-0750-4
- Kumar, M., O'connell, M., Namekar, M., and Nerurkar, V. R. (2014a). Infection with non-lethal West Nile virus Eg101 strain induces immunity that protects mice against the lethal West Nile virus NY99 strain. *Viruses* 6, 2328–2339. doi: 10.3390/v6062328
- Kumar, M., Roe, K., Nerurkar, P. V., Namekar, M., Orillo, B., Verma, S., et al. (2012). Impaired virus clearance, compromised immune response and increased mortality in type 2 diabetic mice infected with West Nile virus. *PLoS One* 7:e44682. doi: 10.1371/journal.pone.0044682
- Kumar, M., Roe, K., Nerurkar, P. V., Orillo, B., Thompson, K. S., Verma, S., et al. (2014b). Reduced immune cell infiltration and increased pro-inflammatory mediators in the brain of type 2 diabetic mouse model infected with West Nile virus. *J. Neuroinflammation* 11:80. doi: 10.1186/1742-2094-11-80
- Kumar, M., Roe, K., Orillo, B., Muruve, D. A., Nerurkar, V. R., Gale, M. Jr., et al. (2013). Inflammasome adaptor protein apoptosis-associated speck-like protein containing CARD (ASC) is critical for the immune response and survival in West Nile virus encephalitis. *J. Virol.* 87, 3655–3667. doi: 10.1128/JVI.02667-12
- Kumar, M., Verma, S., and Nerurkar, V. R. (2010). Pro-inflammatory cytokines derived from West Nile virus (WNV)-infected SK-N-SH cells mediate neuroinflammatory markers and neuronal death. *J. Neuroinflammation* 7:73. doi: 10.1186/1742-2094-7-73
- Kuriakose, T., Man, S. M., Malireddi, R. K., Karki, R., Kesavardhana, S., Place, D. E., et al. (2016). ZBP1/DAI is an innate sensor of influenza virus triggering the NLRP3 inflammasome and programmed cell death pathways. *Sci. Immunol.* 1:aag2045. doi: 10.1126/sciimmunol.aag2045
- Mehta, R., Soares, C. N., Medialdea-Carrera, R., Ellul, M., Da Silva, M. T. T., Rosala-Hallas, A., et al. (2018). The spectrum of neurological disease associated with Zika and chikungunya viruses in adults in Rio de Janeiro, Brazil: a case series. *PLoS Negl. Trop. Dis.* 12:e0006212. doi: 10.1371/journal.pntd.0006212
- Orozco, S., and Oberst, A. (2017). RIPK3 in cell death and inflammation: the good, the bad, and the ugly. *Immunol. Rev.* 277, 102–112. doi: 10.1111/imr.12536
- Pham, T. H., Kwon, K. M., Kim, Y. E., Kim, K. K., and Ahn, J. H. (2013). DNA sensing-independent inhibition of herpes simplex virus 1 replication by DAI/ZBP1. *J. Virol.* 87, 3076–3086. doi: 10.1128/JVI.02860-12
- Pittman, K. J., Cervantes, P. W., and Knoll, L. J. (2016). Z-DNA binding protein mediates host control of toxoplasma gondii infection. *Infect. Immun.* 84, 3063–3070. doi: 10.1128/IAI.00511-16
- Rothan, H. A., Bidokhti, M. R. M., and Byrareddy, S. N. (2018a). Current concerns and perspectives on Zika virus co-infection with arboviruses and HIV. *J. Autoimmun.* 89, 11–20. doi: 10.1016/j.jaut.2018.01.002
- Rothan, H. A., Fang, S., Mahesh, M., and Byrareddy, S. N. (2018b). Zika virus and the metabolism of neuronal cells. *Mol. Neurobiol.* 56, 2551–2557. doi: 10.1007/s12035-018-1263-x
- Schwartz, T., Behlke, J., Lowenhaupt, K., Heinemann, U., and Rich, A. (2001). Structure of the DLM-1-Z-DNA complex reveals a conserved family of Z-DNA-binding proteins. *Nat. Struct. Biol.* 8, 761–765. doi: 10.1038/nsb0901-761
- Shirato, K., Kimura, T., Mizutani, T., Kariwa, H., and Takashima, I. (2004). Different chemokine expression in lethal and non-lethal murine West Nile virus infection. *J. Med. Virol.* 74, 507–513. doi: 10.1002/jmv.20205
- Sridharan, H., Ragan, K. B., Guo, H., Gilley, R. P., Landsteiner, V. J., Kaiser, W. J., et al. (2017). Murine cytomegalovirus IE3-dependent transcription is required for DAI/ZBP1-mediated necroptosis. *EMBO Rep.* 18, 1429–1441. doi: 10.15252/embr.201743947
- Suthar, M. S., Diamond, M. S., and Gale, M. Jr. (2013). West Nile virus infection and immunity. *Nat. Rev. Microbiol.* 11, 115–128. doi: 10.1038/nrmicro2950
- Takaoka, A., Wang, Z., Choi, M. K., Yanai, H., Negishi, H., Ban, T., et al. (2007). DAI (DLM-1/ZBP1) is a cytosolic DNA sensor and an activator of innate immune response. *Nature* 448, 501–505. doi: 10.1038/nature06013
- Thapa, R. J., Ingram, J. P., Ragan, K. B., Nogusa, S., Boyd, D. F., Benitez, A. A., et al. (2016). DAI senses influenza A virus genomic RNA and activates RIPK3-dependent cell death. *Cell Host Microbe* 20, 674–681. doi: 10.1016/j.chom.2016.09.014
- Upton, J. W., Kaiser, W. J., and Mocarski, E. S. (2012). DAI/ZBP1/DLM-1 complexes with RIP3 to mediate virus-induced programmed necrosis that is targeted by murine cytomegalovirus vIRA. *Cell Host Microbe* 11, 290–297. doi: 10.1016/j.chom.2012.01.016
- Wallach, D., Kang, T. B., Dillon, C. P., and Green, D. R. (2016). Programmed necrosis in inflammation: toward identification of the effector molecules. *Science* 352:aaf2154. doi: 10.1126/science.aaf2154
- Wang, Z., Choi, M. K., Ban, T., Yanai, H., Negishi, H., Lu, Y., et al. (2008). Regulation of innate immune responses by DAI (DLM-1/ZBP1) and other DNA-sensing molecules. *Proc. Natl. Acad. Sci. USA* 105, 5477–5482. doi: 10.1073/pnas.0801295105
- Wang, X., Li, Y., Liu, S., Yu, X., Li, L., Shi, C., et al. (2014). Direct activation of RIP3/MLKL-dependent necrosis by herpes simplex virus 1 (HSV-1) protein ICP6 triggers host antiviral defense. *Proc. Natl. Acad. Sci. USA* 111, 15438–15443. doi: 10.1073/pnas.1412767111

**Conflict of Interest Statement:** The authors declare that the research was conducted in the absence of any commercial or financial relationships that could be construed as a potential conflict of interest.

Copyright © 2019 Rothan, Arora, Natekar, Strate, Brinton and Kumar. This is an open-access article distributed under the terms of the Creative Commons Attribution License (CC BY). The use, distribution or reproduction in other forums is permitted, provided the original author(s) and the copyright owner(s) are credited and that the original publication in this journal is cited, in accordance with accepted academic practice. No use, distribution or reproduction is permitted which does not comply with these terms.



# EHV-1: A Constant Threat to the Horse Industry

Fatai S. Oladunni<sup>1,2\*</sup>, David W. Horohov<sup>1</sup> and Thomas M. Chambers<sup>1</sup>

<sup>1</sup> Maxwell H. Gluck Equine Research Center, Department of Veterinary Science, University of Kentucky, Lexington, KY, United States, <sup>2</sup> Department of Veterinary Microbiology, University of Ilorin, Ilorin, Nigeria

## OPEN ACCESS

### Edited by:

Mei-Ling Li,  
Rutgers, The State University  
of New Jersey, United States

### Reviewed by:

Sylvie Lecollinet,  
National Agency for Sanitary Safety  
of Food, Environment and Labor  
(ANSES), France  
Joel D. Baines,  
Louisiana State University,  
United States

### \*Correspondence:

Fatai S. Oladunni  
kanmi01@gmail.com

### Specialty section:

This article was submitted to  
Virology,  
a section of the journal  
Frontiers in Microbiology

**Received:** 02 September 2019

**Accepted:** 01 November 2019

**Published:** 03 December 2019

### Citation:

Oladunni FS, Horohov DW and  
Chambers TM (2019) EHV-1:  
A Constant Threat to the Horse  
Industry. *Front. Microbiol.* 10:2668.  
doi: 10.3389/fmicb.2019.02668

Equine herpesvirus-1 (EHV-1) is one of the most important and prevalent viral pathogens of horses and a major threat to the equine industry throughout most of the world. EHV-1 primarily causes respiratory disease but viral spread to distant organs enables the development of more severe sequelae; abortion and neurologic disease. The virus can also undergo latency during which viral genes are minimally expressed, and reactivate to produce lytic infection at any time. Recently, there has been a trend of increasing numbers of outbreaks of a devastating form of EHV-1, equine herpesviral myeloencephalopathy. This review presents detailed information on EHV-1, from the discovery of the virus to latest developments on treatment and control of the diseases it causes. We also provide updates on recent EHV-1 research with particular emphasis on viral biology which enables pathogenesis in the natural host. The information presented herein will be useful in understanding EHV-1 and formulating policies that would help limit the spread of EHV-1 within horse populations.

**Keywords:** EHV-1, abortion, myeloencephalopathy, latency, horse

## EHV-1 INFECTION OF HORSES: HOW IT ALL BEGAN

After the discovery of the first virus (Ivanovsky, 1882), 50 years passed before Dimock and Edwards in 1932 first showed that a different kind of microorganism, other than bacteria, was causing contagious epizootic abortion in mares (Dimock and Edwards, 1932). Around the same time, the disease was reproduced by experimental infection of mares with materials from aborted fetuses. Their research indicated that a filterable viral agent was causing abortions in pregnant mares, and they coined the term “viral abortion” to refer to the syndrome (Dimock and Edwards, 1933). They further identified the gross pathological changes in the aborted fetuses, including intranuclear inclusion bodies in fetal pneumocytes and hepatocytes, and established the term ‘equine viral abortions’ to describe the disease (Dimock, 1940). Subsequently, the ‘equine abortion virus’ (EAV) was grown *in vivo* and *in vitro* (Anderson and Goodpasture, 1942; Doll et al., 1953; Randall et al., 1953), and detailed pathological findings were published (Westerfield and Dimock, 1946).

Around the same period, Manninger and Csontos in Hungary also documented the same symptoms of viral abortions as in Kentucky, along with signs of respiratory disease including mild fever (Manninger and Csontos, 1941). They observed the development of symptoms resembling that of mild influenza when bacteriological sterile filtrate from the aborted fetuses with lesions of viral abortion was inoculated into pregnant mares (Manninger and Csontos, 1941). Salyi (1942) also demonstrated that the observed gross and microscopic lesions in fetal abortion material were identical with those reported in Kentucky. In fact, Kress (1941) indicated that the abortion virus is pneumotropic due to the prevalence of bronchopneumonia in horses in contact with aborted

materials. This prompted Manning (1949) to infer that the viral abortion was caused by infection with equine influenza virus in pregnant mares.

Doll et al. (1954b) first studied the respiratory infection associated with EAV, and the symptomatology developed in young inoculated horses was again similar to that described as equine influenza, the cause of which had not yet been identified. The evidence from their research showed that EAV is the etiological agent of epizootic respiratory disease of young horses (Doll et al., 1954b). It remained for Doll and co-workers to show that several putative isolates of the influenza virus were the same as EAV (Doll and Kintner, 1954a; Doll et al., 1954a; Doll and Wallace, 1954b). In another study, Bryans et al. (1957) suggested that the causative agent previously known as EAV should be considered a respiratory virus because of the prominence of the major histological lesions in the respiratory tract of young and aborted foals. The authors, therefore, referred to the virus-induced disease as viral pneumonitis and the agent as an equine viral pneumonitis virus. In 1963, electron microscopy revealed that the virus was a member of the herpes group (Plummer and Waterson, 1963).

## CLASSIFICATION OF HERPESVIRUSES

Herpesviruses have undergone significant diversification in terms of virion morphology, biological properties, and antigenic properties (Roizman, 1982). The Herpesviridae family members are classified into three subfamilies: *Alphaherpesvirinae*, *Betaherpesvirinae*, and *Gammaherpesvirinae* (Roizman et al., 1981) based on their morphology and biological properties.

Alphaherpesviruses are found in a wide range of host species. They undergo an efficient and relatively short replicative cycle, and they establish latency in the sensory neurons or lymphocytes of their hosts (Pellet, 2007). They spread well from cell to cell, but are also easily released from infected cells where they replicate, causing cytopathic effects and the development of intranuclear eosinophilic inclusion bodies (Rajcani and Durmanova, 2001). *In vitro*, they are often able to infect cells from different animal species. Although *in vivo* the alphaherpesviruses can infect various host species, there is always a species to which each virus has been adapted (Rajcani and Durmanova, 2001). In such a host, they have the propensity to undergo latency, during which viral pathogenicity is absent. It is suspected that the alphaherpesviruses spread best in the host along the nerves, where intra-axonal transmission predominates (Rajcani and Durmanova, 2001). Members of *Alphaherpesvirinae* subfamily include four different genera; *Simplexvirus*, *Varicellovirus*, *Mardivirus*, and *Iltovirus* (Davison, 2007). EHV-1 is a member of the genus *Varicellovirus*.

Unlike alphaherpesviruses, betaherpesviruses have a limited host range and a long cycle of replication (Riaz et al., 2017). *In vitro*, members of the *Betaherpesvirinae* only replicate in cells derived from their specific host, further underscoring their narrow host range (Rajcani and Durmanova, 2001). They have a slow replication cycle (running for several days), and their release from infected cells is ineffective (Rajcani and Durmanova, 2001). Betaherpesvirus infection slowly progresses in tissue culture and

the infected cells become larger rather than lyse and contain intranuclear inclusion bodies (Roizmann et al., 1992; Rajcani and Durmanova, 2001). Latent infection is established predominantly in monocytes or macrophages (Riaz et al., 2017). Since they do not exhibit preferential neural expansion, they typically exist in leukocytes, reticuloendothelial cells, as well as in renal tubular epithelial cells and the salivary gland ducts (Rajcani and Durmanova, 2001). The viruses in this subfamily are further classified into four genera namely *Roseolovirus*, *Proboscivirus*, *Cytomegalovirus*, and *Muromegalovirus* (Davison et al., 2009).

The members of the subfamily *Gammaherpesvirinae* are slow replicating viruses with lymphotropic properties and limited host range (Rajcani and Durmanova, 2001). Unlike alpha- and betaherpesviruses, gammaherpesviruses initially seem to favor the development of latency in either T or B cells, whereas only a subset of cells supports lytic replication (Ackermann, 2006). There are more homolog genes conserved within members of the subfamily *Gammaherpesvirinae* than members of the other two subfamilies (Riaz et al., 2017). In addition to the genes conserved between herpesviruses, each gammaherpesvirus also contains a set of unique genes which are usually present at the terminal regions of the genome and which are important for viral pathogenesis (Riaz et al., 2017). This subfamily consists of four genera: *Percavirus*, *Macavirus*, *Rhadinovirus*, and *Lymphocryptovirus* (Davison et al., 2009).

## EQUINE HERPESVIRUSES

To date, all the nine equid herpesviruses isolated belong to either the *alphaherpesvirinae* or *gammaherpesvirinae* subfamilies (Table 1). The members of the subfamily of alphaherpesviruses include EHV-1, EHV-3, EHV-4, EHV-6, EHV-8, and EHV-9 (Davison, 2007). The members of the gammaherpesviruses include EHV-2, EHV-5, and EHV-7. Only five of the nine herpesviruses (*viz.* EHV-1, 2, 3, 4, and 5) can produce disease in horses (Allen et al., 2004). EHV-6 to 8 produce diseases in donkeys and are also known as asinine herpesvirus (AHV, AHV-1 to 3), while EHV-9 or gazelle herpesvirus (GHV) is a pathogen of Thomson's gazelles (Ostlund, 1993; Crabb and Studdert, 1995; Taniguchi et al., 2000).

## EPIDEMIOLOGY AND TRANSMISSION OF EHV-1

Exposure of horses to either EHV-1 or its close relative EHV-4 occurs very early in life. It has been reported that between 80 to 90% of horses are infected, with either pathogen, by the time they are 2 years of age (Allen, 2002). The great level of antigenic relatedness between EHV-1 and EHV-4 often complicates seroepidemiological findings as a result of a lack of type-specific antibodies and extensive antigenic cross-reactivity that exists in natural infection (Patel and Heldens, 2005). In the early 1990s, evidence became available that the envelope glycoprotein, gG, of EHV-4 elicits a type-specific antibody response, which enabled the differentiation between antibodies

**TABLE 1** | Known equine herpesviruses.

Subfamily of <i>Herpesviridae</i>	<i>Equus</i> species				<i>Gazella thomsoni</i>
	Domestic horse ( <i>Equus caballus</i> )	Donkey ( <i>Equus asinus</i> )	Zebra ( <i>Equus grevyi</i> )	Onager ( <i>Equus hemionus onager</i> )	
<i>Alphaherpesvirinae</i> :	Equine herpesvirus 1 <sup>a</sup> ( <i>Equid herpesvirus 1</i> ) <sup>b</sup>	Asinine herpesvirus 3 ( <i>Equid herpesvirus 8</i> )	Zebra herpesvirus isolates	Onager herpesvirus isolates	Gazelle herpesvirus 1 ( <i>Equid herpesvirus 9</i> )
(a) Viscerotropic subgroup	Equine herpesvirus 4 ( <i>Equid herpesvirus 4</i> )				
(b) Dermatotropic subgroup	Equine herpesvirus 3 ( <i>Equid herpesvirus 3</i> )	Asinine herpesvirus 1 ( <i>Equid herpesvirus 6</i> )			
<i>Gammaherpesvirinae</i>	Equine herpesvirus 2 ( <i>Equid herpesvirus 2</i> )	Asinine herpesvirus 2 ( <i>Equid herpesvirus 7</i> )			
	Equine herpesvirus 5 ( <i>Equid herpesvirus 5</i> )				

Table adapted from Allen et al. (2004). <sup>a</sup>Viruses in the same horizontal row of the table are closely related equid herpesviruses with minor antigenic and genetic variation imposed by natural selection for specific host species. <sup>b</sup>Virus nomenclatures in parentheses are assigned by the Herpesvirus Study Group of the International Committee on Taxonomy and Nomenclature of Viruses (ICTV) (Roizman et al., 1995; Davison et al., 2000). At this time, the study group has not given ICTV designations to zebra or onager herpesviruses (Davison et al., 2000). A neurotropic herpesvirus isolate from captive gazelle has provisionally been designated *Equid herpesvirus 9* (Fukushi et al., 1997; Davison et al., 2000; Taniguchi et al., 2000).

present in polyclonal sera from mixed cases of infection involving both EHV-1 and EHV-4 (Crabb et al., 1992). The antigenic determinants in the carboxyl domain of the gG's of EHV-1 and EHV-4 have been described as useful tools for differentiating between these viruses based on distinct humoral responses that they elicit in their natural hosts (Crabb et al., 1992; Crabb and Studdert, 1993). The annual incidence of EHV-1 is not well defined, as a result of mixed infection with EHV-4 and the ability of both viruses to undergo latency. Latency is an important survival strategy employed by alphaherpesviruses for continuous persistence and dissemination within their natural host population (Whitley and Gnann, 1993). Virus reactivation in an infected host, following latency, could occur at any time to promote a clinical course of the disease and virus shedding.

EHV-1 infection is highly contagious and can easily be acquired by contact with infectious materials, including fomites and aerosols (Lunn et al., 2009). Transmission of the virus to susceptible horses is facilitated by contact with an acutely infected horse or a reactivated virus-shedding horse, or from contact with an aborted fetus or placenta which is rich in infectious virus particles (Allen et al., 2004). Extensive work investigating the transmission cycle of EHV-1 has identified mare and foal populations as important reservoirs enabling virus transmission before and after weaning, with infection in foals occurring within the first 30 days of life (Gilkerson et al., 1999). In a different report, viral shedding was detected in 22 day-old foals even after a widespread vaccination of mares (Foote et al., 2004). Evidence suggests that infected mares, especially those incubating latent EHV-1, serve as a continuous source of viral exposure to foals by horizontal transmission when contact is established between foals and the nursing dam. Broodmares may undergo recrudescence of latent viral infection as a result of stress resulting from pregnancy/parturition, which may expose young foals to EHV-1 infections from mares that are actively shedding the virus (Paillot et al., 2008). Overall, available data suggest a cyclic but mostly quiet epidemiologic

pattern of EHV-1 infection with an infected dam serving as a continuous source of infectious virus particles to its foals between breeding seasons.

## GENOMIC STRUCTURE AND GENE FUNCTIONS OF EHV-1

The full genome sequence of EHV-1 has been published (Telford et al., 1992, 1998) making information regarding the genomic organization of the virus available. EHV-1 has a linear dsDNA genome of about 150.2 kbp in size with base composition of about 56.7% G+C content (Roizmann et al., 1992). The entire genome is composed of a long unique region (U<sub>L</sub>, 112,870 bp) flanked by a small inverted repeat sequence (TR<sub>L</sub>/IR<sub>L</sub>, 32 bp), and a short unique region (U<sub>S</sub>, 11,861 bp) that is flanked by a large inverted repeat (TR<sub>S</sub>/IR<sub>S</sub>, 12,714 bp) (Roizmann et al., 1992). The genome contains 80 open reading frames (ORFs) encoding 76 different genes, with four duplicated ORFs present in the terminal repeat sequence (TRS) (Telford et al., 1992; Crabb and Studdert, 1996). The four duplicated ORFs in the EHV-1 genome are ORF 64, 65, 66, and 67 which are present in the sequences flanking the unique short segment (Allen et al., 2004). The inverted repeats allow the short components to give rise to virion populations which exist in two orientations, generating two isomeric DNA molecules (Henry et al., 1981; O'Callaghan et al., 1981, 1983; Whalley et al., 1981; Ruyechan et al., 1982). The gene layout of EHV-1 reveals tightly arranged ORFs with little intervening sequence, the absence of extensive ORF overlap, and few instances of exon splicing (Allen et al., 2004). Generally, this gene arrangement of EHV-1 is similar to other sequenced herpesviruses with the only difference being that EHV-1 encodes five genes (ORF1, 2, 67, 71, and 75) which have no structural homolog when compared to all other herpesviruses sequenced to date (Allen et al., 2004). Some

of these genes' functions remain unknown but have been predicted to exert major influence in the unique biology of EHV-1 enabling them to adapt to the horse as their natural host (Allen et al., 2004). The genomic details of EHV-1 ORFs including the functions of individual genes are listed in **Table 2**.

## BIOLOGICAL FUNCTIONS OF EHV-1 PROTEINS

The structural architecture of a typical EHV-1 particle (**Figure 1**) is made up of about 30 discrete kinds of polypeptides (Perdue et al., 1974; Turtinen et al., 1981; Turtinen and Allen, 1982; Turtinen, 1984; Meredith et al., 1989). It consists of a genomic core made up of a linear double-stranded DNA neatly packed within an icosahedral capsid of  $T = 16$  with an approximate diameter of 100–110 nm (Riaz et al., 2017). The nucleocapsid, which houses the viral genome, is in itself made up of six proteins encoded by ORFs 22, 25, 35, 42, 43, and 56 (Perdue et al., 1974; Allen et al., 2004). The capsids of all herpesviruses are similar, comprising 162 capsomers (12 pentons and 150 hexons) (Paillot et al., 2008). The nucleocapsid contains a ring structure made up of 12 portal proteins which enables viral DNA to enter into the capsid (Newcomb et al., 1989; Baker et al., 1990). Although their names differ between herpesvirus families, capsid protein structure and arrangement are preserved across all herpesviruses (Baines, 2011; Brown and Newcomb, 2011).

The amorphous tegument layer, which corresponds to the area between the nucleocapsid and the envelope, comprises about twelve different proteins encoded by ORFs 11, 12, 13, 14, 15, 23, 24, 40, 46, 49, 51, and 76 (Allen et al., 2004). These tegument proteins and enzymes are critically involved in very early events during infection which are required for initiating viral replication (Batterson et al., 1983; Coulter et al., 1993; Paillot et al., 2008). The large tegument protein, UL36, interacts with the capsid's pentons (VP5), which gives an icosahedral symmetry to the innermost portion of the tegument (Machtiger et al., 1980; Newcomb et al., 1996; Zhou et al., 1999). The outermost part of the tegument engages with the envelope membrane of the virus and may sometimes associate with the intravirion part of the integral membrane proteins.

Surrounding the nucleocapsid and the tegument is the viral envelope derived from patches of an altered host-derived cell membrane (Riaz et al., 2017). Embedded in the EHV-1 envelope are eleven glycoproteins which are functional homologs of those found in HSV-1. The eleven EHV-1 glycoproteins (i.e., gB-gp14, gC-gp13, gD-gp18, gE, gG, gH, gI, gK, gL, gM, and gN) are preserved across all alphaherpesviruses and are therefore named according to the HSV-1 nomenclature (Paillot et al., 2008). As with other herpesviruses, the envelope glycoproteins of EHV-1 are critical determinants of virus entry into a susceptible host cell, host range, virus cell-to-cell spread, pathogenicity, and immunologic responses to infection. EHV-1 encodes an extra gp2 that has homologs only in AHV-3 and EHV-4 (Paillot et al., 2008). The inclusion of tegument and viral envelope enables the virion size to

markedly increase from 120 nm to approximately 300 nm (Roizmann et al., 1992).

## CELL INFECTION AND VIRUS REPLICATION

The lytic replication cycle of EHV-1 can be summarized as follows: entry into a permissive host cell, viral nucleocapsid uncoating, viral gene expression, viral DNA replication, virion assembly, and virion particle egress (**Figure 2**). In horses, EHV-1 can infect a diverse range of cell types, including endothelial cells of inner organs, epithelial cells of the respiratory tract, and mononuclear cells in lymphoid organs and the peripheral blood (PBMCs) (Osterrieder and Van de Walle, 2010). Cells are either infected by direct contact with an infectious EHV-1 particle or by cell-to-cell spread following contact with an infected cell (Paillot et al., 2008). Like HSV-1 and most other alphaherpesviruses, including EHV-1, efficient infection is initiated by a relatively unstable attachment to heparan sulfate molecules on the proteoglycan cell surface, mediated by gC and gB, followed by binding of gD to one of the specific receptors on the cell surface (Osterrieder, 1999; Spear, 2004; Azab et al., 2010). The changes in conformation as a result of receptor engagement with gD enables intricate interactions between gB and gH/gL (Spear, 2004). However, for virus entry into host cells, EHV-1 also utilizes a unique receptor that is different from those described for other alphaherpesviruses (Frampton et al., 2005). It has been shown that the Major Histocompatibility Complex I (MHC-I) molecules on some equine cells serve as entry receptors for EHV-1 by binding directly to gD on the viral envelope membrane (Kurtz et al., 2010; Sasaki et al., 2011).

EHV-1 can enter permissive cells either by direct fusion with the host cell membrane or by cell-mediated endocytosis, producing a productive infection in both cases (Frampton et al., 2007). Both entry pathways facilitate the release of viral nucleocapsid and tegument proteins into the infected host cell. As with other alphaherpesviruses, once the virus is released inside the host cell, the tegument proteins dissociate from the nucleocapsid and the capsid is transported along microtubules via dynein, a minus-end-director motor protein, to the nucleus of the cell (Paillot et al., 2008). This mechanism of capsid transport is important especially in the infection of cells such as neurons where the virus may have to travel a long distance away from the site of infection to reach the nucleus (Paillot et al., 2008; Kukhanova et al., 2014). Following the arrival of the capsid at the nucleus, the capsid directly binds to the nuclear pore complex (NPC) and extrudes its content into the nucleus leaving the capsid behind in the cytoplasm (Whittaker and Helenius, 1998; Ojala et al., 2000). For HSV-1, the inner tegument protein UL36 (ICP1/2) which bears a nuclear localization signal (Ojala et al., 2000), together with nucleoporins Nup358 and Nup214 which both bind either directly or indirectly to the capsid, facilitate this process (Kukhanova et al., 2014). Seemingly, all these associations and interactions are necessary for the nuclear import of the viral DNA by importin  $\beta$  (Copeland et al., 2009).

**TABLE 2** | EHV-1 gene products and their functions.

EHV-1 ORF #	Start	Stop	Functional class of HSV homolog (core genes)	Gene products and proposed functions
<b>Capsid protein assembly</b>				
43 <sup>†</sup>	82083	83027	UL18	VP23, involved in intercapsomeric formation with VP19c
42 <sup>†</sup>	77703	81832	UL19	VP5, major capsid protein
35 <sup>†</sup>	67093	65153	UL26	VP24 and VP21 are products of self-cleavage of UL26, serine protease
35.5 <sup>†</sup>	66142	65153	UL26.5	VP22a, scaffolding protein
25 <sup>†</sup>	47311	46952	UL35*	VP26, capsid protein
22 <sup>†</sup>	32916	31519	UL38	VP19c, a component of intercapsomeric complex
<b>DNA replication</b>				
57 <sup>†</sup>	102375	105020	UL5	DNA helicase-primase, DNA replication
54 <sup>†</sup>	97069	99324	UL8	DNA helicase-primase, DNA replication
31 <sup>†</sup>	55453	59082	UL29	ICP8, Single stranded DNA-binding protein
30 <sup>†</sup>	55184	51522	UL30	DNA polymerase, DNA replication
18	25696	24479	UL42	Double-stranded DNA binding protein, DNA polymerase subunit
7 <sup>†</sup>	10301	7056	UL52	DNA primase, DNA helicase-primase subunit
<b>DNA cleavage/packaging</b>				
56 <sup>†</sup>	102391	100130	UL6	Associated with capsids, a subunit of portal complex
44 <sup>†</sup>	84320	83148	UL15	DNA terminase activity, involved in DNA packaging
45 <sup>†</sup>	84480	86600	UL17	Associated with B and C capsids, DNA encapsidation
36 <sup>†</sup>	68975	67212	UL25	Capsid protein, involved in packaging of cleaved viral DNA
32 <sup>†</sup>	59243	61570	UL28	ICP18.5, pac motif-specific DNA binding activity, DNA packaging protein
28 <sup>†</sup>	48763	50625	UL32	Cytoplasmic/nuclear protein involved in DNA cleavage/packaging
27 <sup>†</sup>	48791	48369	UL33	DNA packaging protein involved in capsid assembly
<b>Nucleic acid metabolism</b>				
61 <sup>†</sup>	108144	107206	UL2*	Uracil-DNA glycosylase
50 <sup>†</sup>	91135	92832	UL12*	Alkaline nuclease, involved in viral DNA processing
21 <sup>†</sup>	31276	28904	UL39*	ICP6, ribonucleotide reductase large subunit involved with protein kinase activity
9 <sup>†</sup>	12115	11135	UL50*	Deoxyuridine triphosphate
<b>Envelope glycoprotein</b>				
62 <sup>†</sup>	108843	108147	UL1	gL, forms complex with gH to direct viral entry, egress and cell-to-cell spread
52 <sup>†</sup>	94472	93120	UL10*	gM, involved in viral cell-to-cell spread
39 <sup>†</sup>	71192	73738	UL22	gH, forms complex with gL to direct viral entry, egress and cell-to-cell spread
33 <sup>†</sup>	61432	64374	UL27	gB, VP7, required for viral entry into a cell, forms a dimer and induces neutralization antibody
<b>Others</b>				
55 <sup>†</sup>	100332	99421	UL7*	Associated with intracellular capsids, involved in DNA packaging?
51 <sup>†</sup>	92784	93008	UL11*	Myristoylated viral protein involved in efficient capsid envelopment and egress
49 <sup>†</sup>	89369	91153	UL13*	UL13 PK, tegument protein with protein kinase activity
48 <sup>†</sup>	88947	89900	UL14*	Tegument protein with molecular chaperone function
46 <sup>†</sup>	86620	87732	UL16*	Tegument protein, located within the intron of UL15, involved in DNA packaging?
37 <sup>†</sup>	69897	69079	UL24*	Non-glycosylated membrane-associated protein, neuropathogenic virulence factor?
29 <sup>†</sup>	50618	51598	UL31*	Nuclear matrix binding protein, interacts with UL34
26 <sup>†</sup>	48230	47403	UL34*	Associate with inner nuclear membrane, required for nuclear egress
24 <sup>†</sup>	36588	46853	UL36	ICP1/2, largest tegument protein, involved in both uncoating and egress

(Continued)

TABLE 2 | (Continued)

EHV-1 ORF #	Start	Stop	Functional class of HSV homolog (core genes)	Gene products and proposed functions
23 <sup>†</sup>	33292	36354	UL37	ICP32, Tegument protein with nuclear export signal, involved in egress and virion maturation
NA			UL49.5*	Small membrane-associated protein
8 <sup>†</sup>	10300	11037	UL51*	Palmitoylated virion protein, associated with the Golgi
5 <sup>†</sup>	5874	4462	UL54	ICP27, regulation of gene expression at the post-transcriptional level
<b>Non-core essential genes</b>				
53	94390	97053	UL9	Replication origin-binding protein
12	13595	14944	UL48	VP16, tegument protein involved in (immediate early) IE gene expression
64	118591	114128	RS1	ICP4, major regulatory protein
	144569	149032		
72	131583	132791	US6	gD, required for virus entry
<b>Non-core accessory genes</b>				
NA			RL1*	ICP34.5, protein synthesis regulator
63	111985	110387	RL2*	ICP0, promiscuous transactivator with E3 ubiquitin ligase domains involved in gene regulation
60	107116	106478	UL3*	Nuclear phosphoprotein, involved in nucleolar localization
58	105070	105747	UL4*	Nuclear protein, co-localized with UL3 and ICP22
41	76793	77512	UL20*	Virion protein, essential for viral exocytosis
40	76224	74632	UL21*	Tegument protein, associated with microtubules
38	69910	70968	UL23*	ICP36, thymidine kinase (TK) required for nucleotide metabolism
20	28859	27894	UL40*	Ribonucleotide reductase small subunit, involved in nucleotide metabolism
19	26262	27755	UL41*	vhs, virion host shut-off protein, causes non-specific cellular mRNA degradation
17	24234	23029	UL43*	Membrane-associated protein
16	22851	21445	UL44*	gC, VP7.5, involved in cell attachment and adsorption, C3b-binding activity
15	21170	20487	UL45*	Virion protein, type-II membrane protein involved in virus egress
14	18083	20326	UL46*	VP11/12, tegument protein, interacts with UL48 (VP16)
13	15317	17932	UL47*	VP13/14, tegument protein, enhances immediate early gene expression
11	12549	13463	UL49*	VP22, tegument protein with intercellular trafficking activity
6	7042	6011	UL53*	gK, required for efficient viral exocytosis
4	4249	3647	UL55*	Nuclear protein, nuclear matrix-binding protein
NA			UL56*	Type-II membrane protein, associated with intercellular trafficking
65	121368	122249	US1*	ICP22, regulatory protein involved in the expression of late genes
	141792	140911		
68	126275	125019	US2*	Virion protein, interacts with cytokeratin
69	126411	127559	US3*	US3 PK, has anti-apoptotic activity
70	127681	128916	US4*	gG, involved in viral entry and egress
71	129097	131490	US5*	gJ, protects from Fas-mediated apoptosis
73	132899	134173	US7*	gI, interacts with gE, involved in cell-to-cell spread
74	134406	136058	US8*	gE, forms complex with gI, Fc receptor activity, cell-to-cell spread
NA			US8.5*	Localized in nucleoli of infected cells
76	136783	137442	US9*	Type-II membrane protein, involved in anterograde transport of envelope glycoprotein?
66	122862	123572	US10*	Tegument protein, tightly associated with capsids
	140298	139588		

(Continued)

**TABLE 2 |** (Continued)

EHV-1 ORF #	Start	Stop	Functional class of HSV homolog (core genes)	Gene products and proposed functions
NA			US11*	Tegument protein, RNA-binding activity, and intercellular trafficking
NA			US12*	TAP-binding protein, involved in MHC class I downregulation
1	1298	1906	NA	Downregulates MHC class I
2	2562	1945	NA	Virion virulence factor
3	2841	3614	NA	Unknown
34	64578	65060	NA	Unknown
47 <sup>†</sup>	88917	87886	NA	Unknown
10 <sup>†</sup>	12084	12386	UL49A	gN, Envelope protein
59	106416	105877	NA	V57, virion morphogenesis?
67	125194	124376	NA	VP67, co-localizes with nuclear lamin
	137966	138784		
75	136055	136447	NA	US8A, unknown function

Table was prepared according to available data published in Allen et al. (2004); Nishiyama (2004), Davison (2010), Sarkar (2014), Roizman (1996); Kasem et al. (2010), Telford et al. (1998), and Ma et al. (2012). \*Indicates that the gene is dispensable for replication in cell culture; NA, not available; <sup>†</sup>indicates conserved genes across all mammalian herpesviruses.

Once in the nucleus, the virus can transcribe and replicate its genome, which is a critical step toward virus progeny assembly (Kukhanova et al., 2014). These events lead to the reorganization of the nucleus resulting in increased nucleus size, nucleolus and nuclear domain-10 (ND-10) disruption, chromatin condensation and eventual degradation along with nuclear lamina destruction in late infection (Everett et al., 1998; Simpson-Holley et al., 2005; Callé et al., 2008). Six regulatory proteins expressed as one IE protein (IEP), four early proteins (EICP0, EICP22, EICP27, and IR2) and the late EHV-1  $\alpha$ -gene trans-inducing factor (ETIF or VP16) control the coordinated transcription of EHV-1 genes (Caughman et al., 1985; Gray et al., 1987a; Bowles et al., 1997, 2000; Buczynski et al., 1999; Derbigny et al., 2002). This cascade starts with the tegument VP16 (HSV) homolog protein of EHV-1 acting as a transactivator of an IE ( $\alpha$ ) gene expression (Purewal et al., 1994). During viral entry, VP16 is carried into the infected cell as a tegument protein and is required for efficient initiation of the lytic replicative cycle of the virus (Lewis et al., 1997; Paillot et al., 2008). The IEP of EHV-1 is encoded by ORF64 and synthesized by host cell RNA polymerase II (Gray et al., 1987a,b). The IEP, a polypeptide of 1487-amino acids (aa), is encoded in each of the two inverted repeats (Grundy et al., 1989) and is essential for virus replication (Garko-Buczynski et al., 1998). It stimulates the expression of heterologous viral promoters during the initial stages of infection, self-regulates its own expression, and acts synergistically with EICP22 and EICP27 to activate the expression of early (E or  $\beta$ ) and late (L or  $\gamma$ ) viral genes (Smith R.H. et al., 1992; Matsumura et al., 1993; Holden et al., 1995; Zhao et al., 1995). For the transcription of IE genes of HSV-1, the cellular transcription factor Oct-1 binds to a unique canonical sequence: 5'-GyATGnTAATGARATTCyTTGnGGG-3' (where r is a purine base, y is a pyrimidine base, and n is any base) that overlaps the transcription initiation site of the IE promoter (Mackem and Roizman, 1982; Kukhanova et al., 2014). The VP16 protein then interacts with Oct-1 and forms a complex along with the HCFC1 protein which then activates IE gene

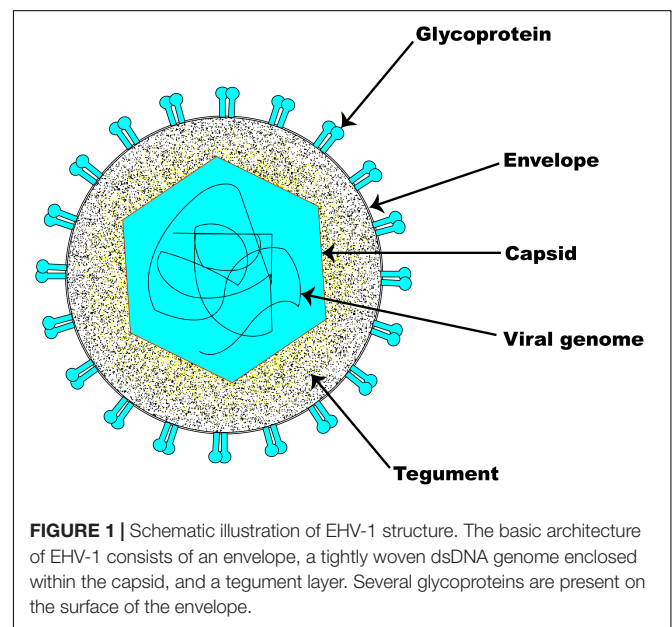


**FIGURE 1 |** Schematic illustration of EHV-1 structure. The basic architecture of EHV-1 consists of an envelope, a tightly woven dsDNA genome enclosed within the capsid, and a tegument layer. Several glycoproteins are present on the surface of the envelope.

transcription (Kukhanova et al., 2014). As with HSV-1, EHV-1 also encodes a similar consensus sequence within its IE promoter region (Purewal et al., 1992), however, other octamers within EHV-1 IE promoter seem to participate in ETIF/Oct-1 complex formation which directs the transactivation of EHV-1 IE genes (Elliott and O'hare, 1995).

The E genes of EHV-1, encoding additional regulatory proteins (EICP27, EICP22, and EICP0) along with proteins involved in viral genome replication, are then transcribed (Caughman et al., 1985; Holden et al., 1992, 1995; Zhao et al., 1992; Bowles et al., 1997). Transcription of the EHV-1 E genes occurs before viral DNA synthesis is initiated and is tightly regulated by IEP (Bowles et al., 2000). The IR2 gene is located in the IE gene and encodes an early protein that

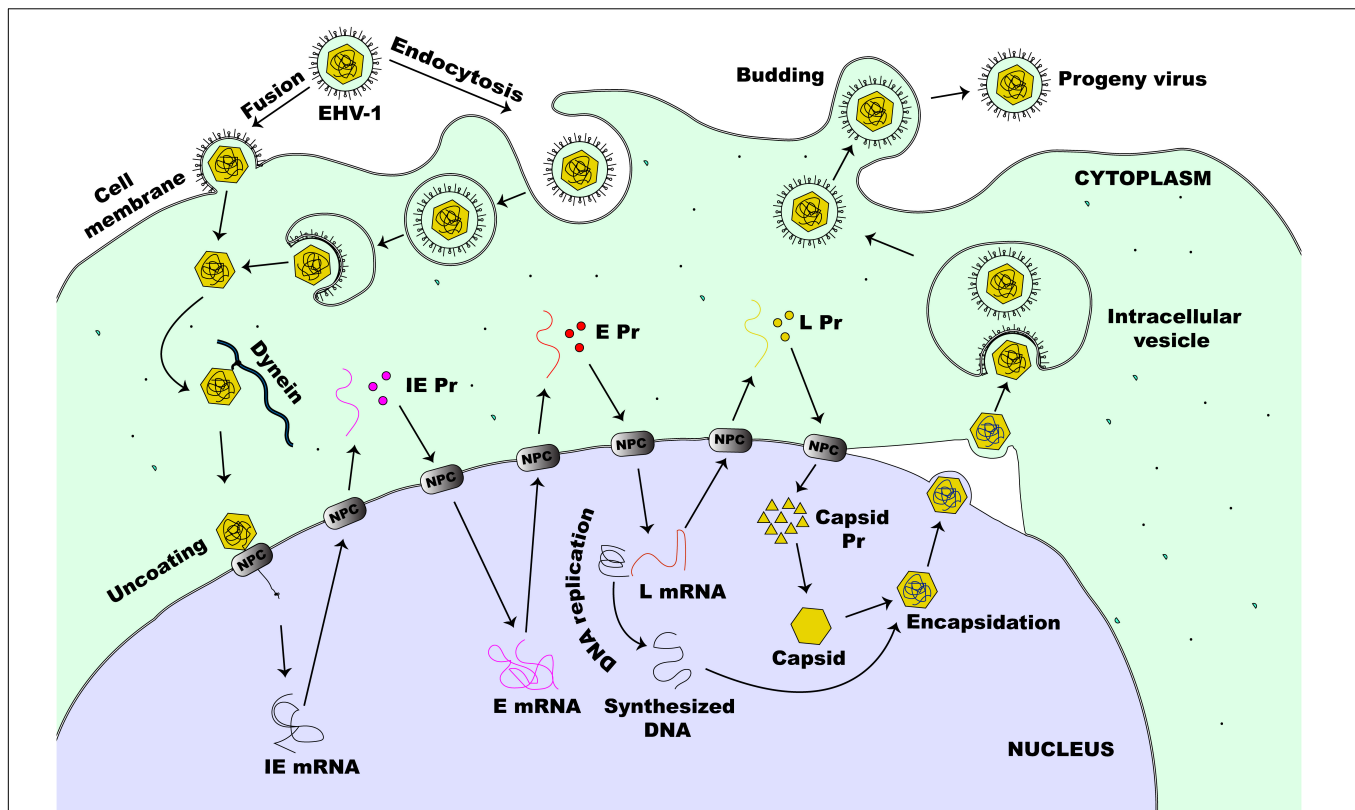


**FIGURE 2 |** Lytic life cycle of EHV-1. The virus enters susceptible cells either by fusion at the cell membrane or by the non-classical endocytosis pathway. This is followed by the release of nucleocapsid into the cytoplasm of an infected cell. The nucleocapsid, which is transported to the nucleus via dynein, docks at the NPC and extrudes the viral DNA directly into the nucleus. This initiates viral gene expression beginning with the transcription of IE ( $\alpha$ ) gene. Immediate early proteins are then synthesized in the cytoplasm and migrate to the nucleus where they direct the transcription of E ( $\beta$ ) genes. Early proteins, synthesized in the cytoplasm, translocate to the nucleus to initiate virus DNA replication and virus L ( $\gamma$ ) gene expression. Next, some of the L proteins synthesized in the cytoplasm, migrate to the nucleus to form the capsid before encapsidation of the new virus DNA. The newly assembled virion then migrates through the nucleus and the cytoplasmic membranes before it is eventually released outside of the cell.

is a shortened version (aa 323–1,487) of the IEP (Harty and O’Callaghan, 1991). While IR2 protein can trans-repress the IE gene expression, E and L gene expression cannot be trans-activated due to the lack of an IEP *trans*-activation domain encoded by amino acid residues 3–89 (Smith et al., 1994). An early nuclear phosphoprotein, about 419 bp, encoded by the EICP0 gene, can trans-activate all types of EHV-1 promoters (Bowles et al., 1997, 2000). Toward its N terminus, the EICP0 contains a conserved cysteine-rich zinc RING finger domain (C3HC4 type) that is important for the activation of the promoters of E ( $\beta$ ) and L ( $\gamma$ 1 and  $\gamma$ 2) genes (Bowles et al., 2000). Although both the IE and the EICP0 proteins of EHV-1 can *trans*-activate the promoters of EHV-1, their relationship is antagonistic rather than being synergistic (Kim et al., 1999; Bowles et al., 2000). The E genes of EHV-1 encode proteins that are critical for its replication, while the L genes encode the viral structural proteins (Paillot et al., 2008). Following the model of HSV-1 replication, it is now known that once the E proteins are synthesized, viral DNA replication will be started. This involves the interplay of at least seven early proteins including the gene products of UL5, UL8, UL9, UL29,

UL30, UL42, and UL52 (Rixon et al., 1996; Davison, 2010; Muylaert et al., 2011). The initial step of replication of HSV DNA involves the separation of the double-stranded helical structure by ICP8 (UL29) or UL9 proteins in the AT-rich domains of the oriL or oriS origin of replication (Kukhanova et al., 2014). The latter has a copy in the  $U_L$  region and two copies in the  $U_S$  region of the herpesviral genome respectively (Kukhanova et al., 2014). ICP8 and UL9 bind specifically to ssDNA fragments and the oriS, respectively. This interaction enables the unwinding of the double-stranded helical structure, which then allows for the loading of the helicase-primase complex (UL52, UL8, and UL5) (Kukhanova et al., 2014). Following unwinding of the dsDNA, a complex of processivity factor UL42 and viral DNA polymerase (UL30) synthesize the leading and the lagging strand of the DNA (Kukhanova et al., 2014). This replication occurs in a rolling circle form termed ‘theta form of replication,’ the mechanism of which has not yet been identified. Such replication ensures the formation of long head-to-tail viral DNA concatemers, which are then cut into separate units when viral DNA is packaged into capsids (Roizman and Knipe, 2001).

In addition to the viral factors, other cellular components involved in the replication of the viral genome include DNA ligase, topoisomerase II, and various DNA repair and homologous recombination systems (Weller and Coen, 2012). Another important factor for viral DNA replication is cellular chaperone protein Hsp90 which is essential for intranuclear localization of viral DNA polymerase (Burch and Weller, 2005). Some viral proteins such as uracil *N*-glycosylase (UL2), deoxyuridine triphosphatase (UL50), thymidine kinase (UL23), alkaline nuclease (UL12), and ribonucleotide reductase (UL39, UL40) participate in nucleotide metabolism, viral DNA synthesis, and DNA repair (Kukhanova et al., 2014).

The production of late ( $\gamma$ ) viral genes peaks only after replication of viral DNA has commenced and requires ICP27, ICP8, and ICP4 for an optimal transcription efficiency (Rybachuk, 2009).  $\gamma$ 1 (leaky-late) genes such as ICP5 (major capsid protein), ICP34.5, gD, and gB are expressed throughout infection, increasing in transcription only a few fold after replication of DNA has commenced while expression of  $\gamma$ 2 (true-late) genes such as UL41 (VHS), UL38, UL36, UL20, gC, and gK, does not occur in significant amounts until after replication of DNA (Rybachuk, 2009). The increase in the expression levels of the late genes, especially those encoding for viral capsids, just after DNA replication has been initiated enables the assembly of progeny virion particles (Kukhanova et al., 2014).

**Figure 3** illustrates the pathway involved in herpesviral capsid formation. The assembly of the herpesviral nucleocapsid occurs in the nucleus first as a DNA-free precursor capsid in the presence of scaffolding proteins just before viral DNA encapsidation (Perdue et al., 1976; Lee et al., 1988; Rixon et al., 1988; Paillot et al., 2008). The first step in the capsid formation involves the auto-catalytic assembly of a procapsid following the association of pUL6 and pUL19 with a scaffold made up of conserved pUL26 and pUL26.5 proteins (Mettenleiter et al., 2006). The interaction of these proteins produces an angular portion of the spherical procapsid enhanced by scaffold-scaffold complex formation and triplexes connected to VP5 molecules (Brown and Newcomb, 2011). This is then followed by progressive enlargement of the angular segments, called partial procapsids, to form an enclosed spherical procapsid (Newcomb et al., 1996). Although the procapsid appears to be spherical rather than being polyhedral, it has similar diameter (125 nm) and symmetry ( $T = 16$ ) as the mature capsid (Brown and Newcomb, 2011). In a similar fashion as the major capsid protein VP5, the portal is incorporated into the developing procapsid by interacting with scaffold proteins to form a complex (Newcomb et al., 2003; Singer et al., 2005; Huffman et al., 2008; Yang and Baines, 2008).

Following the formation of the procapsid, the viral dsDNA genome is then packaged into the capsid (encapsidation) regulated by a three subunit protein known as terminase (Yang et al., 2007). The transport of the virion genome into the capsid marks the exit of the scaffold proteins from the procapsid creating the polyhedral shape of the mature capsid.

The first step in the egress of herpesviruses from the nucleus is the budding phase. During this stage, the capsid, which is surrounded by tegument proteins, acquires an envelope from the nuclear membrane's inner leaflet (Mettenleiter, 2002). After the

viral genome has been packaged and assembled, the nucleocapsid travels within the nucleus with the aid of actin filament (Forest et al., 2005) to establish contact with the inner membrane of the nucleus before primary envelopment (**Figure 4**). Two viral proteins (pUL31 and pUL34) that are structurally and functionally conserved across herpesviruses (Mettenleiter et al., 2006) are required for the partial dissolution of the nuclear lamina enabling the nucleocapsid to interact with the inner leaflet of the nuclear membrane (Reynolds et al., 2004). Complex formation between these two proteins is essential for the process of primary envelopment, and the lack of either protein stalls the process of nuclear egress tremendously (Chang et al., 1997; Klupp et al., 2000; Roller et al., 2000; Reynolds et al., 2001; Fuchs et al., 2002b). The association of the pUL31-pUL34 complex with nuclear lamins A/C or B (Reynolds et al., 2004; Gonnella et al., 2005) leads to the recruitment of cellular protein kinase C (PKC) which then activates intranuclear lamins A/C and/or B (Muranyi et al., 2002). This complex interaction leads to the breakdown of the nuclear lamin network and the underlying structures (Reynolds et al., 2004; Simpson-Holley et al., 2005), enabling the nucleocapsid to interact with the inner nuclear membrane (Mettenleiter et al., 2006). Although the nucleocapsid acquires its primary envelope through the process of budding from the inner nuclear membrane, there is a striking difference in morphology and protein content when compared to the mature virus (Granzow et al., 2001; Miranda-Saksena et al., 2002). While the primary envelope contains both pUL31 and pUL34 proteins (Fuchs et al., 2002b; Reynolds et al., 2004), the mature virus particle lacks these two proteins demonstrating the differences in composition between primary and matured virions (Mettenleiter et al., 2006). The underlying mechanism by which the enveloped nucleocapsid gain access into the cytoplasm is not well understood. However, it has been shown that entry into the cytoplasm is by direct fusion of the enveloped nucleocapsid with the outer nuclear membrane (Mettenleiter et al., 2006) rather than exit through the nuclear pore. This eventually leads to loss of envelope (de-envelopment) enabling the naked nucleocapsid to acquire tegument proteins once inside the cytoplasm (Mettenleiter, 2002). The phosphorylation-mediated activation of a portion of primary-enveloped virions achieved by the kinase activity of pUS3, a component of these particles in itself, is required for a successful de-envelopment process (Klupp et al., 2001; Reynolds et al., 2002; Schumacher et al., 2005).

Final tegumentation and secondary envelopment occur in the cytoplasmic compartments and require a highly coordinated network of protein-protein interactions (Mettenleiter et al., 2006). The herpesviral proteins interact on one side with the capsid and on the other side with the cytoplasmic tails of the envelope glycoproteins, enabling the structural integrity of the matured virus particle (Mettenleiter, 2002). Two subassemblies, the capsid and the future envelope, are distinct sites where final tegumentation takes place and they efficiently combine to produce the mature virion (Mettenleiter et al., 2006). The capsid proximal proteins consist of conserved pUL36 and pUL37 that contribute to the physical structure of the tegument, the conserved pUL25, and pUS3 which remains closely associated with the capsid (Mettenleiter et al., 2006). Except for pUS3, the

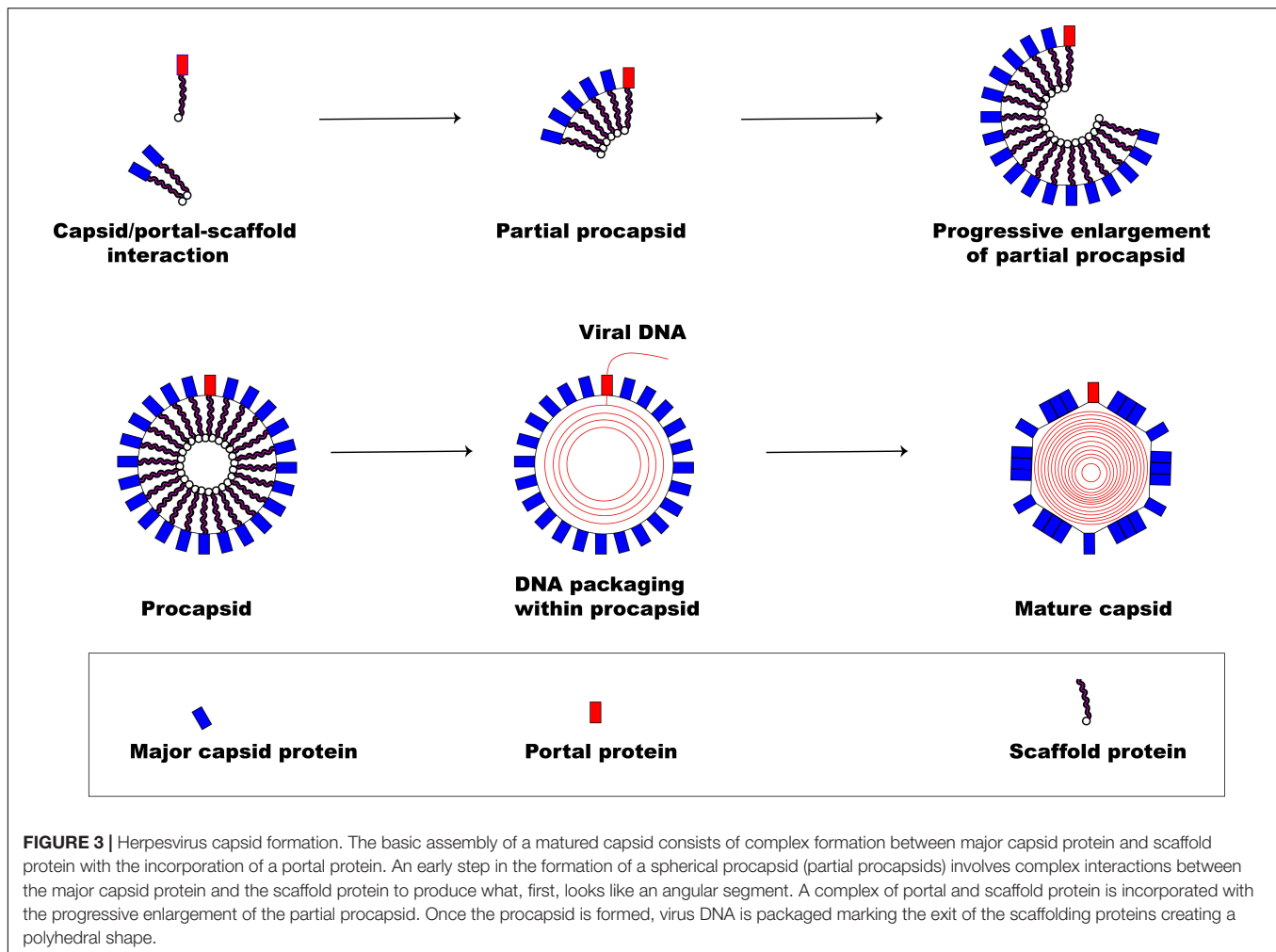


**FIGURE 3 |** Herpesvirus capsid formation. The basic assembly of a matured capsid consists of complex formation between major capsid protein and scaffold protein with the incorporation of a portal protein. An early step in the formation of a spherical procapsid (partial procapsids) involves complex interactions between the major capsid protein and the scaffold protein to produce what, first, looks like an angular segment. A complex of portal and scaffold protein is incorporated with the progressive enlargement of the partial procapsid. Once the procapsid is formed, virus DNA is packaged marking the exit of the scaffolding proteins creating a polyhedral shape.

other known components of the inner tegument are preserved across all herpesviruses. Both pUL36 and pUL37 remain closely linked to the capsid until they reach the nuclear pore (Granzow et al., 2005; Luxton et al., 2005) and also serve as a vehicle for intracytoplasmic transport of the capsid during entry and exit of the cytoplasm (Luxton et al., 2006; Wolfstein et al., 2006). Apart from these conserved components, other non-conserved proteins may associate with the inner tegument (Mettenleiter et al., 2006). Strikingly, the abundance of both pUL36 and pUL37 inner tegument proteins in the virion is tightly controlled, unlike those of the outer tegument which vary widely (Michael et al., 2006). Once the outer tegument is added, the virion acquires its secondary envelope. This process of final envelopment occurs within the trans-Golgi network, where glycoproteins together with a subset of tegument proteins (Turcotte et al., 2005), like pUL46, pUL47, and pUL49 for the alphaherpesviruses, are incorporated (Mettenleiter et al., 2006). Two conserved proteins, glycoprotein M and pUL11, that are important for this process have been identified. Glycoprotein M, an envelope protein of the matured virion, helps in retrieving envelope glycoproteins from the cell surface and retaining them at the envelopment site (Crump et al., 2004), while pUL11, a small myristoylated protein,

directs envelope protein to future envelope sites (Bowzard et al., 2000; Loomis et al., 2003). At this stage, complex associations between many different proteins are required for the ultimate assembly of a mature herpes virion (Fuchs et al., 2002a; Chi et al., 2005; Mettenleiter, 2006). Following the development of a secondary envelope, a mature herpesvirial particle enclosed within an intracellular vesicle is formed and transported to the cell membrane (Mettenleiter et al., 2006), by anterograde cellular microtubule-dependent molecular motor kinesin (Guo et al., 2010). The fusion between this intracellular vesicle and cell membrane enables the release of the newly produced virion particles outside of the cell (Mettenleiter et al., 2009).

## ESTABLISHMENT OF LATENCY

EHV-1, like other herpesviruses, can establish a lifelong presence within cells of a susceptible host following primary infection. The initial stages of EHV-1 infection of the epithelial upper respiratory tract (URT) are accompanied by progression into a stage of latency in which infected horses show no clinical signs of the disease, virus shedding, or cell-associated viremia (Allen

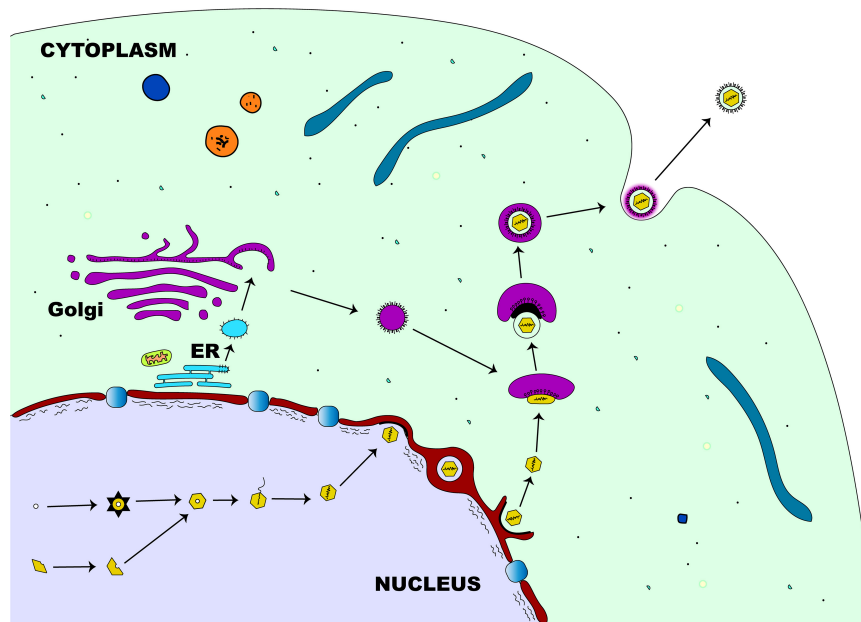


**FIGURE 4 |** Herpesvirus egress pathway. Following intranuclear encapsidation of the virus genome, the herpesviral nucleocapsid will bud through the inner nuclear membrane resulting in perinuclear localization of an enveloped primary virion. This primary envelope becomes lost (de-envelopment) as the virus translocates into the cytosol where the nucleocapsid acquires tegument proteins. Final (secondary) envelopment then occurs in the cytoplasm derived from the *trans*-Golgi network and the enveloped virion is transported in a vesicle to the plasma membrane for release.

et al., 2004; Paillot et al., 2008). While productive infection by EHV-1 leads to active viral gene expression in a well-coordinated manner as described above, the hallmark of latency is the restriction of viral gene expression which culminates in failure to synthesize viral factors and absence of infectious virus particles. The primary site of latency establishment by EHV-1 in the horse has been a subject of debate. While some studies have demonstrated that latency of EHV-1 occurs in lymphocytes, both circulating and those in draining lymph nodes (Welch et al., 1992; Edington et al., 1994; Chesters et al., 1997), others have shown that the sensory nerve cell bodies within the trigeminal ganglia are the preferred primary site of latency for EHV-1 (Slater et al., 1994b; Baxi et al., 1995). While about 80% of CD5+/CD8+ T- lymphocytes have been demonstrated as the major lymphoid cell population enabling latency of EHV-1, a smaller sub-population of 20% CD5+/CD8-/CD4- cells have also been found to support latency (Smith et al., 1998). Regardless of the site of establishment, it appears that the ability of EHV-1 to pass into a latency stage is a deliberate biological behavior that the virus utilizes to perpetuate itself in the host and this enables viral spread to susceptible horses upon reactivation. During latency, the expression of the EHV-1 genome is suppressed and only the latency-associated transcripts (LATs) antisense to either the immediate-early viral gene (ORF 64) or a regulatory early gene (ORF 63) are present in infected cells (Baxi et al., 1995; Chesters et al., 1997; Paillot et al., 2008). The exact molecular and physiological mechanisms that direct latency in EHV-1 infected horses are poorly understood. However, latency has been much better studied in HSV-1

and findings reveal that the major detectable transcript lies within an 8.6-kb sequence antisense to and overlapping the immediate-early (IE) gene IE-1 (ICP0) (Chesters et al., 1997). The LAT itself is a 2.0 kb transcript lacking a polyadenylation site and found mostly in the nuclei of infected neurons (Chesters et al., 1997). In HSV, LAT can promote latency but is dispensable for maintenance or viral reactivation from latency (Efstathiou and Preston, 2005).

It has been shown that reactivation of latent EHV-1 is possible following exposure to stressful conditions such as transportation, handling, re-housing, and weaning or following the administration of corticosteroids (Burrows and Goodridge, 1984; Edington et al., 1985; Slater et al., 1994a). The fact that EHV-1 has been experimentally reactivated from cases of both natural and experimental infection following administration of immunosuppressant (Edington et al., 1985, 1994; Slater et al., 1994b) suggests that horses harboring latent EHV-1 could periodically shed the virus following exposure to stressors. Viral factors, such as the thymidine kinase, have been shown to modulate EHV-1 virulence and latency (Xie et al., 2019).

As a result, the cycle of persistent latent infection followed by reactivation of the virus with shedding into nasal mucus may enable virus propagation and disease spread to susceptible uninfected horses. In certain instances, the characteristic respiratory illness followed by nasal shedding is absent following EHV-1 reactivation and such horses are therefore silent virus shedders (Edington et al., 1985). It has been reported that during the reactivation process a small fraction of lymphocytes carrying the latent EHV-1 genome can progress toward active

transcription resulting in DNA revival and fusogenic viral glycoprotein expression on their cell surfaces ultimately leading to active virus replication (Edington et al., 1985; Slater et al., 1994a). The fine details of the molecular mechanism underlying reactivation of EHV-1 from its quiescent state to a lytic productive infection remain elusive. However, it has been suggested that the IE gene promoter of a latent EHV-1 can be trans-activated by the presence of another equine herpesvirus, EHV-2, in a mixed infection (Purewal et al., 1992).

## THE ECONOMIC IMPORTANCE OF EHV-1 TO THE US HORSE INDUSTRY

About 10 million of the world horse population reside in the United States (Smith R.H. et al., 1992. FAOSTAT: Livestock 2017). The horse industry is a large and economically diverse industry which accommodates a wide array of economic activities. It has been reported that in the US, the horse industry generates annually an income of about \$102 billion when considering both direct and indirect spending (Anonymous, 2005). With such enormous revenue generated from the horse industry in the US, an outbreak of any disease affecting its horse population is likely to perturb the economic health of the industry. The relevant effects of EHV-1 on the equine industry have been summarized (Lunn et al., 2009). Firstly, EHV-1 outbreaks may result in cases of subclinical to mild respiratory illness especially with young athletic horses developing pyrexia and thus lead to interruptions of training schedules. This can be considered as the least significant economic effect of EHV-1 on the horse industry. Secondly, the incidence of abortion in pregnant mares during the third trimester of gestation results in major losses to the growth of the industry. Thirdly, neurologic outbreaks of the disease, equine herpesviral myeloencephalopathy (EHM), are very severe and may lead to deaths of horses, disruption of breeding or training schedules, cancelation of horse events, and extensive movement restrictions with consequent management difficulties at racetracks, training facilities, and other horse shows. Even though horses may recover from the disease, their productivity is usually compromised, and the money expended in the care and management of horses infected with EHV-1 may run into several thousands of dollars depending on the farm size.

## PATHOGENESIS AND DISEASE MANIFESTATIONS

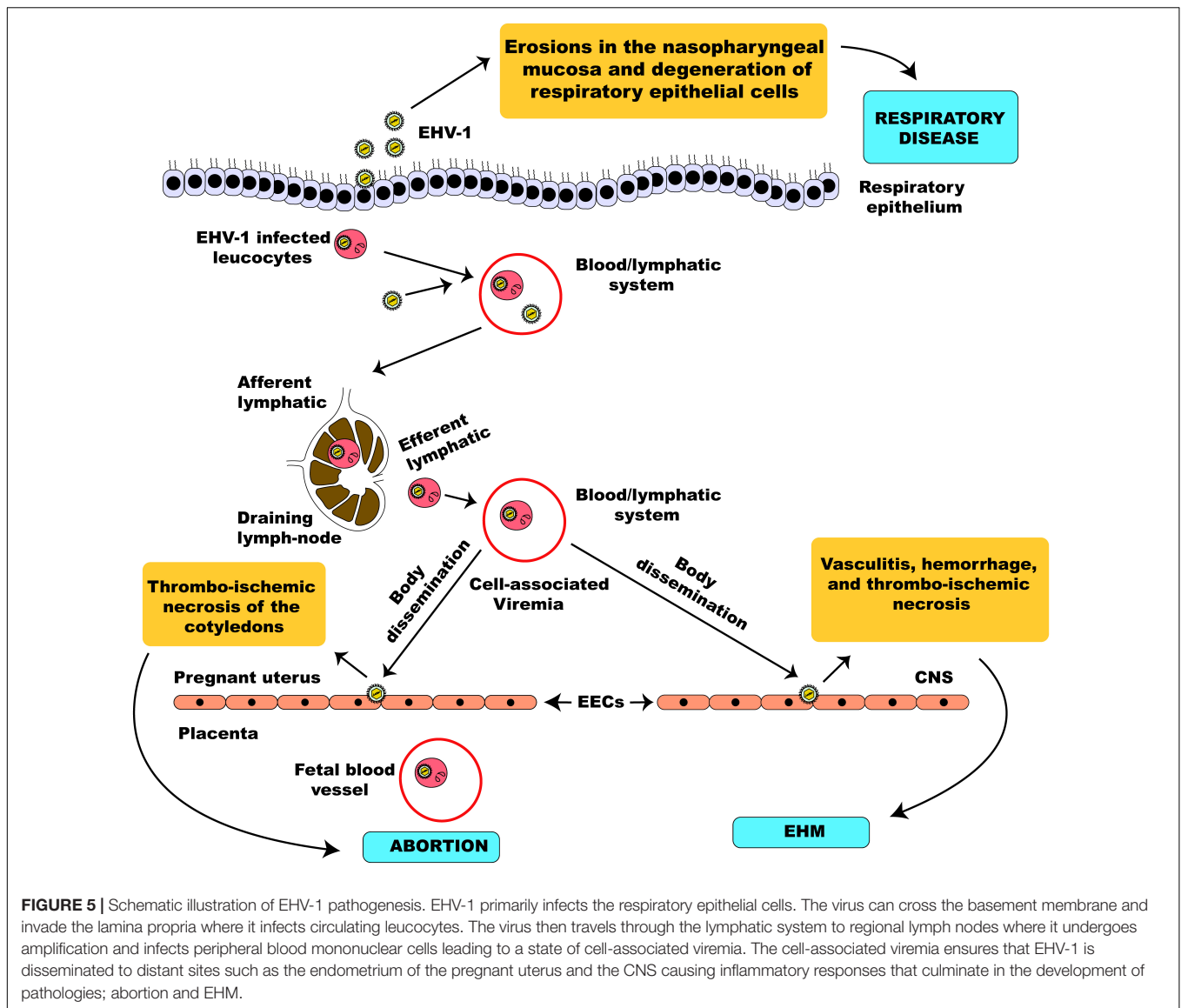
The pathogenesis of EHV-1 infection has been described by the study of an experimental model of infection using the EHV-1 strain, AB4 (Paillot et al., 2008). EHV-1 is a highly contagious viral pathogen of horses usually transmitted following direct contact with infectious materials such as nasal discharges and materials from aborted fetuses or indirectly by fomites (Allen et al., 2004). In horses lacking protective mucosal immunity, nasal and mucosal epithelial cells are the primary sites of replication of EHV-1 (Patel et al., 1982; Kydd et al., 1994a; Rusli et al., 2014). Subsequently, virus replication is quickly

followed by erosions of epithelial cells of the URT due to necrosis and inflammatory cellular responses which ultimately lead to nasal shedding of infectious virus (Paillot et al., 2008). Once in the URT, EHV-1 can spread quickly utilizing and hijacking infected mucosal monocytes to invade the deeper connective tissues (Gryspeerd et al., 2010; Vandekerckhove et al., 2010). Consequently, EHV-1 can cross the basement membrane, invading the reticuloendothelial system and the lymphatics to infect circulating leucocytes and endothelial cells of blood vessels (Gryspeerd et al., 2010). Within 24 h of infection, infected mononuclear leucocytes could be found present in the sinuses and parenchyma of respiratory tract-associated lymphoid organs (Kydd et al., 1994a). Here, EHV-1 undergoes a second round of replication and viral particles are significantly amplified culminating in infected leucocytes escaping, via the efferent lymph, into the blood-vascular circulation leading to a state of cell-associated viremia (Patel et al., 1982; Dutta and Myrup, 1983; Scott et al., 1983; Edington et al., 1986). The ability to establish viremia is key and defines the outcome of EHV-1 pathogenesis produced from the second round of replication. Viremia facilitates the spread of the virus to tertiary replication sites in the endothelium of the pregnant uterus or the central nervous system (Allen et al., 2004) leading to two clinically important sequelae of EHV-1 respiratory infection, namely abortion or a neurological syndrome (Mumford et al., 1994; Slater et al., 1994a).

## Respiratory Disease

EHV-1 is a leading etiological agent of respiratory disease in horses, producing upper airway infection primarily in young horses. The virus is highly ubiquitous among horse populations causing an epidemic disease in young horses and having an estimated prevalence rate of 80 – 90% in horses below 2 years of age (Allen, 2002). Following contact with an infectious viral particle, the mucosal epithelial cells of the URT of an infected horse are the prime target of EHV-1 where the virus undergoes its first round of replication (Figure 5). Within 12 h post-infection, progeny virus and viral antigen are detectable in the respiratory epithelium of an infected horse (Paillot et al., 2008) and the virus can quickly spread to the respiratory endothelium within 24 h of infection (Kydd et al., 1994b). Besides, circulating mononuclear cells and endothelial cells of blood vessels are also infected as a result of viral cell-to-cell spread, thus facilitating viral dissemination throughout the body (Paillot et al., 2008; Vandekerckhove et al., 2011).

Subsequently, there is erosion and necrosis of the respiratory epithelium, release of proinflammatory cytokines, and shedding of infectious virus particles within the first week of the respiratory disease (Paillot et al., 2008). Depending on the pathogenicity of the EHV-1 strain, the incubation period of infection may either be short (1–3 days) (Gibson et al., 1992a,b,c) or prolonged (up to 10 days) (Ostlund, 1993). EHV-1 primarily results in respiratory tract disease (rhino-pharyngitis and tracheo-bronchitis) (Allen, 2002) presenting a clinical picture similar to other viral pathogens of the respiratory tract of the horse (e.g., equine arteritis virus, influenza virus, adenovirus, or rhinovirus) (Allen, 2002). Although most of these respiratory



infections are subclinical or mild, and a large number of foals seroconvert without clinical signs, some young naively exposed horses may show visible signs of nasal discharge and coughing (Allen, 2002; Allen et al., 2004). Previously exposed horses have immune memory that helps reduce the clinical severity of the disease and are infected for only a short duration (Kydd et al., 1994a,b; Allen, 2002). Based on the age and the level of immunity in the infected horse, the respiratory infection may be mild in older horses, pregnant mares, and previously exposed horses, even following virus reactivation from latency (Allen et al., 2004). Experimental infection using the virulent Ab4 strain of EHV-1 revealed a biphasic pattern of pyrexia which may last for up to 10 days (Gibson et al., 1992a,b,c). The clinical picture of the disease includes moderate depression and anorexia, conjunctivitis and serous ocular discharge, and notably a serous nasal discharge which rapidly progresses to mucoid and mucopurulent discharge (Allen et al., 2004). The presence

of mucopurulent discharge can be associated with a secondary bacterial infection which may exacerbate the disease. There is progressive lymphadenopathy mainly affecting submandibular lymph nodes (LN) (Allen et al., 2004) and evidence of leukopenia (both lymphopenia and neutropenia) have also been reported (Doll et al., 1954b; Lunn et al., 1991; McCulloch et al., 1993). Occasionally, retropharyngeal LN may also be enlarged and become palpable for some days (Allen et al., 2004). LN may reach maximum size between 3 to 10 days and may remain enlarged for several weeks following infection (Allen et al., 2004). In some infected foals, EHV-1 may reach the lungs inducing bronchopneumonia as a result (Crabb and Studdert, 1996).

While infected horses may occasionally cough, the severity and duration of clinical signs of the disease in a horse are influenced by proper hygiene and rest from exercise or training (Mumford and Rossdale, 1980). Generally, the upper respiratory tract disease (URTD) associated with EHV-1 infection

is short-lived and of acute course with clinical symptoms and nasal shedding of the virus manifesting for the first few days following infection (Allen, 2002). Although the prognosis of URTD from EHV-1 is good with spontaneous recovery by the end of the second week of onset of infection, severe bacterial co/secondary infection can prolong the disease and undermine the prognostic chances of survival (Allen, 2002). Upon recovery from URTD caused by EHV-1, some horses may develop non-specific bronchial hypersensitivity, resembling chronic obstructive pulmonary disease, which may hinder their performance and lead to poor performance syndrome (Mumford and Rosedale, 1980).

### Abortion, Neonatal and Perinatal Disease

The associated health implications of EHV-1 extend beyond causing URTD since the virus may invade other organs causing more pronounced disease manifestations (Allen, 2002). One of the sequelae of EHV-1 URTD is abortion in which the virus travels to distant sites such as the reproductive tract by cell-associated viremia or latent viral reactivation (Allen et al., 1999) thereby inducing premature detachment of the fetus from the placenta, stillbirth, or weak neonatal foals (Reed and Toribio, 2004). Pregnant mares infected with the virus may abort spontaneously without prior signs of primary URTD by EHV-1 (Dimock, 1940; Dimock et al., 1942; Bryans and Allen, 1986; Smith K. et al., 1992; Mumford et al., 1994). The important roles exerted by host immune and inflammatory responses, and vascular coagulation cascades mediating EHV-1-induced abortion have not been fully elucidated (Allen et al., 2004). However, infection of the endothelium of a pregnant uterus by EHV-1 results in vasculitis particularly affecting the small vascular networks of the glandular endothelia of microcotyledons (Jackson et al., 1977; Edington et al., 1991; Smith K. et al., 1992; Smith et al., 1993). Within 9–13 days post-infection, endothelial cell infection becomes widespread resulting in multifocal vasculitis of the affected blood vessels (Allen et al., 2004). The appearance of microthrombosis within blood vessels may sometimes promote thrombo-ischemic necrosis of the cotyledons and intercotyledonary stroma causing the fetus to detach from the placenta (Smith et al., 1993). The aborted fetus dies of anoxia following a rapidly progressive separation of the placenta-endometrium immediately before fetal expulsion (Allen, 2002). Widespread vascular endothelial damage may cause the fetus to be aborted even before any detectable level of virus is transferred via the placenta to the fetus (Smith K. et al., 1992).

Experimentally induced abortions by EHV-1 in which virus was not recovered from the aborted fetus have been reported to be as a result of either maternal stress or pyrexia (Gleeson and Coggins, 1980; Carrigan et al., 1991). In another experimental study, the extent of uterine vasculitis and intercotyledonary necrosis corresponds to reduced viral burden in the aborted fetus with fewer lesions found in mares aborting virus-positive fetuses (Smith et al., 1993, 1997). The severity of disease leading to abortion is usually dependent on certain factors including the virulence of the EHV-1 strain involved, the level and magnitude of viremia, and the hormonal state of the pregnant mare. More

virulent strains of EHV-1 such as Ab4 have been reported to produce more pathologies including abortion at a higher rate in pregnant mares than the less virulent strains like V592 (Mumford et al., 1994). The pathogenesis of EHV-1-induced abortion by the less virulent strains of EHV-1 is not clear but it appears that those strains have reduced affinity for endothelial cell invasion (Allen et al., 2004). It has also been reported that the magnitude rather than the duration of viremia is a significant correlate of abortion induced by EHV-1 during an experimental challenge (Mumford et al., 1994). Similarly, hormones such as prostaglandin and chorionic gonadotrophin (CG) released by the placenta have been reported to exert some roles in reactivating the virus and initiating abortion (Allen et al., 2004; Paillet et al., 2008). EHV-1 may be transferred by the placenta to the fetus thereby inducing multi-organ pathologies. EHV-1-infected fetuses that are born alive become sick either at conception or within 1–2 days of birth (Bryans et al., 1977; Dixon et al., 1978; Hartley and Dixon, 1979; McCartan et al., 1995). However, such foals rapidly deteriorate and soon die. Infected foals develop severe respiratory distress, which increases the risk of viral pneumonia or bacterial co/secondary infection, leading to respiratory failure within a few days (Crabb and Studdert, 1996; Allen et al., 1999). Foals infected with EHV-1 can also show signs of gastrointestinal disorder (manifested in diarrhetic excretion) and neurological deficiencies such as visual and vestibular defects (Dixon et al., 1978). Prognosis is grave and no treatment is available to stop the fatal clinical deterioration of health in infected foals. It has been suggested that congenital defects resulting from EHV-1 infection may be epizootic, especially during sporadic outbreaks of EHV-1-induced abortion (Allen, 2002).

### Myeloencephalopathy

Another clinical sequel of EHV-1 respiratory disease is the neurological form of the disease termed EHM, sometimes appearing after 1 week of infection (Crabb and Studdert, 1996; Donaldson and Sweeney, 1997; Wilson, 1997; Pusterla et al., 2009). Neurologic symptoms may be simultaneously present with or without respiratory disease or abortion (Timoney, 1992; Hahn et al., 1999). Fundamentally important in the spread of EHV-1 is cell-associated viremia which effectively disseminates the virus to the vascular network of the CNS. The intracellular localization of EHV-1 during infection protects it from the neutralizing effect of circulating antibody, enabling an efficient spread of the virus throughout the body, including to the CNS, even when high levels of antibodies are present (Bryans, 1969). Like other members of *Herpesviridae*, EHV-1 can be transmitted directly from cell to cell independent of an extracellular phase (Allen, 1986). The vascular endothelium of the CNS serves as the preferred site for EHV-1 replication following the transfer of the virus from circulating mononuclear cells (Wilson, 1997). Endothelial cell invasion and the accompanying inflammation of the vasculature of the CNS is central to the neurological syndrome caused by EHV-1 (Jackson and Kendrick, 1971; Jackson et al., 1977; Patel et al., 1982; Edington et al., 1986). The vasculitis of the endothelium resulting from EHV-1 infection may be as a result of two different events; first, direct damage of the vascular endothelium during EHV-1 replication, and second, immune complex formation between

EHV-1 and antibody (Arthus-type reaction) (Reed and Toribio, 2004). Common hallmarks of the neurological form of EHV-1 are the development of vasculitis with or without hemorrhage, and thrombo-ischemic necrosis of the microvasculature of the brain or CNS (Allen et al., 2004). The observed clinical signs in infected horses are a culmination of the vasculitis, edema, hemorrhage, ischemia, and necrosis resulting from the viral predilection for vascular endothelium (Reed and Toribio, 2004). Indeed, the ability of certain EHV-1 strains to inflict damage on the CNS is not reflective of their neurotropic trait but instead an endotheliotropic attribute (Jackson and Kendrick, 1971; Jackson et al., 1977; Edington et al., 1986, 1991; Nowotny et al., 1987). However, the observation of neural lesions and chorioretinopathy during experimental infection of specific pathogen-free ponies indicates that at least some EHV-1 strains may be neurotropic (Slater et al., 1992). There seems to be no satisfactory scientific explanation for the variable incidence of EHM and different clinical manifestations observed during outbreaks of EHV-1 (Whitwell and Blunden, 1992; McCartan et al., 1995). Several factors including sex, age, immune status of the horse, the reproductive status of the mare (including the stage of gestation), the severity of infection, the type of strain, and perhaps the route of transmission determine the clinical picture of EHV-1 infection (Studdert et al., 1984; Whitwell and Blunden, 1992; McCartan et al., 1995).

Clinical signs of the neurologic disease may become apparent within 2 weeks of URTD or may occur without any antecedent sign of the disease (Wilson, 1997). The clinical presentations are highly variable and widespread depending on the site of neurologic impact and usually peak between 2 and 3 days of onset (Allen et al., 2004). Generally, there is anorexia, pyrexia, edema of the distal limb, abortion, fetal death, or neurologic syndrome, and these are variable in different horses (McCartan et al., 1995). The extent of neurological dysfunction ranges from temporary ataxia with an abnormal gait to complete paralysis. Conscious proprioceptive deficits have also been observed (Allen et al., 2004). The neurological disorders affect mainly the hind limbs, although complete recumbency or tetraplegia have also been observed (Kohn and Fenner, 1987; McCartan et al., 1995; Allen et al., 2004). In some cases, there are signs of bladder dysfunction with accompanying urinary incontinence and scalding of the perineal area or urinary retention which may lead to colic (Franklin et al., 1985). Horses that are non-recumbent have a good prognosis unlike recumbent horses that may suffer additional complications such as pneumonia, colic or bladder rupture (George, 1990; McCartan et al., 1995; Allen et al., 2004) and are generally euthanized.

### Recent Outbreaks of EHM

Outbreaks of disease resembling EHM, among domestic horse populations, have been recorded for centuries. Today, a resurgence in the number of EHM cases across the world has necessitated the classification of this syndrome as an emerging disease of the horse. According to the Center for Emerging Issues report of 2007, EHM satisfies the requirement for an emerging viral disease premised on (1) the more virulent nature of the circulating EHV-1 strains than previously reported and

(2) increased incidence of the disease with a heightened case fatality rate (APHIS and USDA, 2008). Increased outbreaks of EHM were reported not only in North America and Europe, but also in Africa, Oceania, and Asia (Henninger et al., 2007; Gryspeerdt et al., 2011; Tsujimura et al., 2011; Burgess et al., 2012; Pronost et al., 2012; Traub-Dargatz et al., 2013; Walter et al., 2013; Estell et al., 2015; van Galen et al., 2015; McFadden et al., 2016; Negussie et al., 2017). The recent increased incidence of EHM during EHV-1 outbreaks supports the observation that the currently circulating neuropathogenic EHV-1 strain has evolved into a more pathogenic strain producing a higher rate of morbidity and mortality than previously (APHIS and USDA, 2007). EHM has been associated with an A<sub>2254</sub>→G<sub>2254</sub> mutation in ORF 30 encoding the DNA polymerase of EHV-1. Generally, non-neuropathogenic strains possess asparagine at position 752 of DNA polymerase which is substituted by aspartic acid in neuropathogenic strains (Nugent et al., 2006; Goodman et al., 2007). This relationship is strong but not always true in field outbreaks, and other factors may contribute to neuropathogenicity (Lunn et al., 2009; Pronost et al., 2010). Approximately, 14 percent to 24 percent of EHV-1 strains from horses displaying clinical signs of EHM lack this genetic indicator suggesting that the so-called non-neuropathogenic genotype of EHV-1 can also cause EHM (Nugent et al., 2006; Perkins et al., 2008). This disease condition is a major concern for the horse industry considering its negative impact on the economic health of the industry.

The associated risk factors for this increased incidence of EHM are still poorly defined. However, outbreaks have been reported mostly at places such as racetracks, riding schools, and veterinary hospitals where horses from different origins congregate (Kohn et al., 2006; Henninger et al., 2007; Traub-Dargatz et al., 2013). The high stocking density of stabled horses during events such as horse racing may facilitate the quick spread of EHM by direct contact when outbreaks occur. International movement of horses has also played a role in some recent outbreaks of EHM (APHIS and USDA, 2007; Barbić et al., 2012). Other factors that have been reported to facilitate increased incidence of EHM include poor biosecurity measures and presence of stressors (Traub-Dargatz et al., 2013; Pusterla and Hussey, 2014) along with other ill-defined environmental and host factors (Perkins et al., 2009). Importantly, the mutant EHV-1 (G<sub>2254</sub>) is now widely distributed within horse populations which implies a tendency toward the increased incidence and severity of recent EHM outbreaks.

### Ocular Disease

Occasionally and particularly in foals, respiratory tract infection with highly pathogenic EHV-1 strains is associated with severe ocular lesions such as chorioretinitis or uveitis (Del Piero and Wilkins, 2001). Within 3–5 weeks of URTD by EHV-1, foals may develop three distinct types of chorioretinal lesions (focal, multifocal or diffuse) without uveitis (Slater et al., 1992). Although the first report of EHV-1 associated chorioretinitis was in llamas and alpacas (Rebhun et al., 1988; House et al., 1991), this condition has also been documented in natural outbreaks of paralytic EHV-1 infection involving a mare and foal (Whitwell and Blunden, 1992). More recently, an incidence rate

of 50–90% of horses was shown to develop chorioretinal lesions during an experimental challenge with EHV-1 (Hussey et al., 2013). Like the pathogenesis of EHV-1 induced abortion and neurologic syndromes, replication of EHV-1 in the vasculature of the chorioretina may result in ischemic necrosis resulting in visual impairment (Slater et al., 1995). Apart from chorioretinitis, uveitis is another ocular condition seen in some foals following outbreaks of EHM in mares and stallions (McCartan et al., 1995). Young foals that come in close contact with EHM-infected mares and stallions are at high risk of developing ocular disease associated with EHV-1 (McCartan et al., 1995).

## EHV-1 INTERACTIONS WITH THE HOST IMMUNE SYSTEM

Several efforts over the decades have been channeled toward understanding and characterizing the protective host immune response against EHV-1 which could be exploited to advance diagnostic approaches and vaccine development. However, despite over 80 years since EHV-1 was first recognized, we do not yet fully understand how the virus' interaction with the host immune response can be harnessed for the development of more effective immunotherapy.

Following experimental infection of horses with a virulent strain of EHV-1, viral components were immediately detected in the regional LN of the respiratory tract within 12 hpi (Kydd et al., 1994a,b). This indicates that the virus has close interaction with the host immune system during early infection, and triggers an immediate host response consisting predominantly of inflammatory cytokines. Johnstone et al. (2016) recently reported the upregulation of pro-inflammatory cytokines in an equine endothelial cell (EEC) model at 10 hpi with either neurovirulent or non-neurovirulent strain of EHV-1. Similarly, studies from our laboratory have shown the ability of EHV-1 to produce type-I IFN induction in EECs as early as 3 hpi which is subsequently followed by a progressive decline by 6 and 12 hpi (Sarkar et al., 2015, 2016a,b; Oladunni et al., 2018, 2019). The initial upregulation of inflammatory cytokines during early EHV-1 infection helps to activate the adaptive arm of the host immune response toward eliminating the viral antigen. However, there is a concern that this response may be a double-edged sword: induced proinflammatory cytokines and activated coagulative responses that follow may also induce pathology that could negate their antiviral benefits.

It has also been reported that the host humoral immunity toward EHV-1 infection is temporary (van der Meulen et al., 2006) making horses susceptible to re-infection even after vaccination. EHV-1 infected horses usually display virus-neutralizing (VN) and complement-fixing (CF) antibodies within 2 weeks of infection (Hannant et al., 1993). This has proved important for early diagnosis of EHV-1 which is critical to quickly forestall the spread of infection to naïve, unexposed horses. While VN antibodies are type-specific and give longer protection (up to a year), there is cross-reactivity between CF antibodies of EHV-1 and EHV-4; however, CF antibodies only last for about

3 months. The host humoral immunity is usually targeted to recognize epitopes on the surface of envelope glycoproteins of EHV-1 (Allen and Yeargan, 1987; Crabb et al., 1991; Packiarajah et al., 1998; Perkins et al., 2019), and IgG<sub>a</sub>, IgG<sub>b</sub>, IgG<sub>c</sub>, IgG<sub>d</sub>, IgM, and IgG(T) antibody isotypes have all been detected in EHV-1-infected horses (Paillot et al., 2008; Wagner et al., 2015; Perkins et al., 2019). The protective effect of circulating antibodies during infection with EHV-1 is limited once a state of cell-associated viremia is established. However, local protection from freely circulating EHV-1 in the URT can be achieved with the help of mucosal antibody, particularly the IgA isotype. As a result, VN antibodies are helpful during the initial respiratory infection produced by EHV-1 but incompetent to provide protective immunity against the more severe sequelae: abortion and neurologic diseases which are enabled by the establishment of cell-associated viremia.

As with other intracellular pathogens, successful elimination of EHV-1 following the establishment of cell-associated viremia is dependent on an activated cytotoxic T lymphocyte (CTL) response. An upregulated CTL response has been reported following experimental EHV-1 infection (Breathnach et al., 2006) with IFN- $\gamma$  playing a critical role in activating antigen-presenting cells and enhancing the antiviral effects of the circulating cytotoxic CD8 T cells. There is a relationship between the level/frequency of circulating CTL and protection from clinical signs of the diseases caused by EHV-1. Adult ponies with a previous history of exposure to EHV-1 produce high levels of EHV-1 specific circulating CTL and show fewer signs of clinical disease when compared to young ponies with low EHV-1 specific circulating CTL (O'Neill et al., 1999). This highlights the important role played by CTL precursor or memory cells during EHV-1 re-infection which may prove useful for testing the efficiency of EHV-1 vaccines in horses. The gene product of EHV-1 IEP encoded by ORF 64 has been reported to have epitopes specifically targeted by CTL from horses expressing the MHC class 1 A3/B2 serological haplotype (Soboll et al., 2003; Kydd et al., 2006). While this finding looks exciting for the development of vaccines for the immunodominant 95% population of Thoroughbred horses that express these serological haplotypes, further research is warranted to identify EHV-1 gene products expressed by other MHC class I haplotypes present in outbred horse populations.

## LABORATORY DIAGNOSIS

A rapid diagnosis of URTD associated with EHV-1 within a group of horses is highly desirable to aid therapeutic decisions and shape future control strategies to prevent an epidemic outbreak of the disease (Allen, 2002). Usually, the presenting clinical sign alone is not sufficient to reach a precise diagnosis as the initial clinical presentation may also resemble that of equine influenza, adenovirus, etc. As a result, laboratory diagnostic confirmation of EHV-1 induced URTD is predicated on the ability to detect the virus in submitted clinical materials. Polymerase chain reaction (PCR) is a useful diagnostic tool for an immediate identification/detection of genomic materials of

EHV-1 in submitted clinical or pathological samples such as aborted fetus, placenta, nasal swabs, nasal discharges, brain and spinal cord, paraffin-embedded archival tissues, and infected cell cultures (Ballagi-Pordany et al., 1990; Borchers and Slater, 1993; Kirisawa et al., 1993; Lawrence et al., 1994; Mackie et al., 1996). Perhaps the most sensitive diagnostic tool for EHM is the real-time PCR which can discriminate isolates possessing the single point mutation in the ORF30 gene associated with the neurologic phenotype of the disease (Smith et al., 2012). Evaluation of this newly improved real-time PCR revealed that it is more specific, besides being capable of discriminating an A<sub>2254</sub> from a G<sub>2254</sub>, than an old assay (Allen, 2007) that produces false dual positive results in detecting viral components in clinical samples. Allelic discrimination of viral nucleic acid during field outbreaks of EHV-1 is a useful epidemiological tool that allows for a rapid diagnosis and timely imposition of appropriate control measures required to prevent viral spread. It does not, of course, definitely diagnose EHM as the genetic correlation is not absolute as discussed above. One major caveat to the use of PCR is that it is not able to distinguish nucleic acid from a viable virus from that of a non-viable virus. It has been reported that the agreement between PCR and virus isolation is about 85–90 percent (Allen et al., 2004). This may be a particular concern when interpreting the presence of extremely low levels of viral DNA in clinical samples.

Direct detection of viral antigen from clinical samples using immunofluorescence staining also provides for rapid diagnosis of EHV-1. Detection of viral antigen in impression smears from nasopharyngeal swabs following fluorescent antibody staining can be used to demonstrate a positive EHV-1 infection (Allen, 2002; Allen et al., 2004). Immunohistochemically, EHV-1 antigens can be detected in paraffin-embedded tissues from infected horses using immunoperoxidase staining (Allen et al., 2004). Histopathological examination of paraffin-embedded tissue sections can also be employed to identify pathognomonic lesions typical of EHV-1 infections. However, these findings should also be verified by virus isolation from submitted clinical specimens.

Differential diagnosis of EHV-1 from cases of EHV-4 infection is difficult by serology. Using type-specific antigen, serological diagnostic tests such as enzyme-linked immunosorbent assay (ELISA), complement fixation (CF), and virus neutralization (VN) can be employed on paired serum samples to differentiate between EHV-1 and EHV-4. Serum samples that were taken during the acute and convalescent phases of infection can be screened to determine their titer; i.e., the highest dilution of sera with detectable binding/neutralization for either EHV-1/EHV-4. A type-specific ELISA assay, which detects distinct humoral response to a unique EHV-1/EHV-4 peptide antigen, has been developed and shown to be a valuable tool for a more accurate diagnosis (Lang et al., 2013).

The gold standard technique for a definitive diagnosis of EHV-1 is virus inoculation of cell cultures for isolation of the virus. EHV-1 can be isolated from various cell lines including those from the horse (EEC), rabbit (RK-13), monkey (Vero), and cattle (MDBK) (Allen et al., 2004; Rybachuk, 2009). The cytopathic effect (CPE), develops rapidly in cell

cultures as clusters of rapidly enlarging, rounded, and detached cells which are characteristically herpetic in appearance (Allen et al., 2004). The application of a quick diagnostic technique such as PCR in conjunction with virus culture and isolation is useful to characterize the virus for further epidemiological investigation. Confirmatory diagnosis of EHV-1 should rule out other differentials such as equine arteritis virus, influenza virus, adenovirus, rhinovirus, EHV-4, and *Sarcocystis neurona* infection, which may all present disease phenotypes that mimic EHV-1 infection.

## CURRENT TREATMENT AND CONTROL RECOMMENDATIONS

There is no specific drug effective against EHV-1 disease conditions. However, good hygiene and management practices together with symptomatic treatment of infected horses may help curtail the spread of the viral infection. The current recommendations for treatment of recumbent horses include offering supportive care, nutritional care and rehydration, frequent bladder and rectal evacuation to prevent colic, and reduction of CNS inflammation (Wilson and Erickson, 1991; Goehring and Lunn, 2008). Symptomatic treatment with non-steroidal anti-inflammatory agents as an adjunct therapy may be helpful (Reed and Toribio, 2004; Lunn et al., 2009). Similarly, corticosteroids and immunomodulatory agents may be used to symptomatically treat early signs in cases of EHM. However, there is no evidence-based study to support the effectiveness of either drug class and caution must be applied not to reactivate virus shedding in latently infected horses (Lunn et al., 2009; Rybachuk, 2009). Corticosteroids are suggested to be protective against the cellular response to CNS infection thereby preventing the development of hemorrhage, edema, vasculitis, and thrombosis that are common early signs of EHM, and their use should be reserved for severe cases of EHM (Lunn et al., 2009).

Similarly, the administration of immunostimulants before horses are exposed to stressors could help prevent viral reactivation and replication but their value for treating EHV-1 infection is yet to be ascertained (Lunn et al., 2009). Antiviral drugs, especially virustatic agents like acyclovir derivatives, are theoretically beneficial for EHV-1 infection (Garré et al., 2007). Beside acyclovir, prophylactic administration of valacyclovir hydrochloride has been tried in experimentally infected horses with demonstrable benefits (Maxwell et al., 2017). Ganciclovir has been demonstrated to be the most potent inhibitor of EHV-1 infection in an *in vitro* study that investigated the efficacy of many antivirals against EHV-1 (Garré et al., 2007), and in a more recent study, it also offers a much-improved bioavailability, *in vivo* (Carmichael et al., 2013) compared to acyclovir.

Like other herpesviruses, EHV-1 infection is more complicated than most other viral infections; the establishment of persistent latent infection ensures that EHV-1 is naturally maintained in horse populations all year-round. Also, EHV-1 has evolved a vast array of strategies to avoid many components of the host innate and adaptive immune responses

(van der Meulen et al., 2006). As a result, an efficient EHV-1 vaccine must be able to invoke strong and sustained levels of humoral and cell-mediated immunity against the virus. In addition, since the establishment of cell-associated viremia is required for the development of abortion as well as EHM, an effective vaccine candidate must, also, be able to stimulate those immune responses needed to block the development of cell-associated viremia. The currently available commercial vaccines against EHV-1 in North America are in the form of inactivated whole virus vaccine and modified live vaccine (MLV). In a recent study, three groups of horses were either administered with a saline placebo or vaccinated with Rhinomune (Boehringer Ingelheim), derived from *Rac-H* strain (Mayr et al., 1968), or Pneumabort K-1B (Zoetis), which contains EHV-1 1P and 1B strains (Allen et al., 1985). The efficacy of either vaccine was then evaluated following an EHV-1 challenge experiment with the Findlay OH03 strain. Observed clinical signs of disease following infection with EHV-1 in the saline control group included pyrexia, depression, anorexia, coughing, nasal discharge, and dyspnea. Both the Rhinomune (Boehringer Ingelheim), an MLV, and Pneumabort K-1B (Zoetis), an inactivated vaccine, reduced the clinical incidence of disease with the former offering better protection (Goehring et al., 2010). However, the effectiveness of either vaccine in preventing EHV-1 induced abortion or EHM is still far from proven. EHV-1 antigen is also incorporated in some multivalent vaccines marketed across the US in their inactivated forms. Recombinant vaccine models expressing EHV-1 gB, gC, and gD reduced the initial nasal viral shedding in vaccinates but offered less protection against cell-associated viremia and clinical signs of disease (Minke et al., 2006; Soboll et al., 2006). Intriguingly, a recombinant vaccine expressing an EHV-1 IE gene, encoded by ORF 64, significantly reduced cell-associated viremia in vaccinated ponies, however, its effect on EHV-1 induced abortion and EHM remain inconclusive (Soboll et al., 2010). There is currently no available vaccine that completely prevents EHV-1 infection, or EHV-1-induced cell-associated viremia or latency, and EHV-1 myeloencephalopathy has been reported in vaccinated horses (Kohn and Fenner, 1987; Wilson and Erickson, 1991; Friday et al., 2000; Henninger et al., 2007). Nonetheless, it is recommended to vaccinate every horse that is at risk of exposure to EHV-1 to help reduce the severity of EHV-1-related clinical manifestations. The updated version of American Association of Equine Practitioners (AAEP) guidelines for vaccination of adult horses provides a detailed recommendation for vaccinating against EHV-1 (Anonymous, 2015).

Control measures for curtailing EHV-1 infection are aimed at reducing viral dissemination to susceptible horses and also at preventing the reactivation of the virus in latently infected horses (Allen, 1986; Ostlund et al., 1990; Ostlund, 1993). Infected sick horses are primary sources of infectious EHV-1, and as such, should be quarantined to prevent direct contact with uninfected horses. Also, infected materials such as aborted fetus or uterine contents, including placenta, should be disposed of appropriately to curtail the spread of EHV-1 (Reed and Toribio, 2004). High-level biosecurity measures should be put in place in farms and all visitors should be encouraged to use a footbath and wash their hands before entering or leaving horse farms. Infected

equipment must be disinfected and disposed of, and different equipment and workers must operate on affected and unaffected horses to prevent horizontal transmission of the disease (Allen, 1986). Movement of horses and visitors should be restricted onto and off the infected farm premises until laboratory tests indicate negative results for EHV-1 infection. Newly acquired horses should be quarantined from the rest of the herd for at least 3 weeks and must be certified negative for EHV-1 before being allowed to join the resident population. Horse owners and horse farmers should immediately report EHM outbreaks to relevant government agencies to contain the spread of the disease and to help formulate policies against future outbreaks.

## CONCLUDING REMARKS

EHV-1 is still persistent among domesticated horses around the world and the vaccines currently available are not completely protective, especially against EHM. As a result, EHV-1 still poses a huge threat to the horse industry and efforts geared toward preventing the outbreak of the disease are strongly encouraged. Detailed information on both the host and certain environmental factors that enable the recent incidence of EHV-1 myeloencephalopathy are still elusive. Further research is required to determine robust epidemiological factors that promote the disease. Most research on how EHV-1 modulates host immune responses have been carried out *in vitro* with only a few studies investigating the immunomodulatory effects of EHV-1 *in vivo*. More *in vivo* studies focusing on viral properties that are important for the evasion of host immunity will help to expose putative therapeutic targets of EHV-1. Future progress in treatment and control of EHV-1 hinges on the combined application of detailed epidemiological data and in-depth knowledge of how the sophisticated viral biology promotes pathogenesis.

## AUTHOR CONTRIBUTIONS

FO wrote the manuscript while both DH and TC edited it.

## FUNDING

FO was supported by grant from the American Quarter Horse Association Young Investigator Award and by a fellowship from the Geoffrey C. Hughes Foundation. This work was supported in part by a grant from the Equine Drug Research Council of the Kentucky Horse Racing Commission. This work is a project of the Kentucky Agricultural Experiment Station (KY014053), supported by the National Institute of Food and Agriculture, U.S. Department of Agriculture, Animal Health Program.

## ACKNOWLEDGMENTS

We thank Mr. Jamie Norris for his technical expertise with the use of Adobe Illustrator.

## REFERENCES

- Ackermann, M. (2006). Pathogenesis of gammaherpesvirus infections. *Vet. Microbiol.* 113, 211–222.
- Allen, G. (1986). Molecular epizootiology, pathogenesis, and prophylaxis of equine herpesvirus-1 infections. *Prog. Vet. Microbiol. Immunol.* 2, 78–144.
- Allen, G. (2002). “Respiratory infections by equine herpesvirus types 1 and 4,” in *Equine Respiratory Diseases*, ed. P. Lekeux, (Ithaca, NY: International Veterinary Information Service).
- Allen, G., Kydd, J., Slater, J., and Smith, K. (1999). “Advances in understanding the pathogenesis, epidemiology and immunological control of equid herpes-1 (EHV-1) abortion,” in *Proceedings of the Eighth International Conference on Equine Infectious Diseases*, eds U. Wernery, J. F. Wade, J. A. Mumford, and O. R. Kaaden, (Newmarket: R&W Publications Limited), 129–146.
- Allen, G., Kydd, J., Slater, J., and Smith, K. (2004). Equid herpesvirus 1 and equid herpesvirus 4 infections. *Infect. Dis. Livest.* 2, 829–859.
- Allen, G., Yeargan, M., Turtinen, L., and Bryans, J. (1985). A new field strain of equine abortion virus (equine herpesvirus-1) among Kentucky horses. *Am. J. Vet. Res.* 46, 138–140.
- Allen, G. P. (2007). Development of a real-time polymerase chain reaction assay for rapid diagnosis of neuropathogenic strains of equine herpesvirus-1. *J. Vet. Diagn. Invest.* 19, 69–72.
- Allen, G. P., and Yeargan, M. R. (1987). Use of lambda gt11 and monoclonal antibodies to map the genes for the six major glycoproteins of equine herpesvirus 1. *J. Virol.* 61, 2454–2461.
- Anderson, K., and Goodpasture, E. W. (1942). Infection of newborn Syrian hamsters with the virus of mare abortion (Dimock and Edwards). *Am. J. Pathol.* 18, 555.
- Anonymous (2005). *National Economic Impact of the U.S. Horse Industry*. Washington, DC: The American Horse Council.
- Anonymous (2015). *Vaccination for Adult Horses*. Available at: <https://aaep.org/sites/default/files/Guidelines/AdultVaccinationChart81216.pdf> (accessed August 25, 2019).
- APHIS, and USDA (2007). *Equine Herpesvirus Myeloencephalopathy: a Potentially Emerging Disease*. Riverdale Park, MD: APHIS.
- APHIS, and USDA (2008). *Equine Herpesvirus Myeloencephalopathy: Mitigation Experiences, Lessons Learned, and Future Needs*. Riverdale Park, MD: APHIS.
- Azab, W., Tsujimura, K., Maeda, K., Kobayashi, K., Mohamed, Y. M., Kato, K., et al. (2010). Glycoprotein C of equine herpesvirus 4 plays a role in viral binding to cell surface heparan sulfate. *Virus Res.* 151, 1–9. doi: 10.1016/j.virusres.2010.03.003
- Baines, J. D. (2011). Herpes simplex virus capsid assembly and DNA packaging: a present and future antiviral drug target. *Trends Microbiol.* 19, 606–613. doi: 10.1016/j.tim.2011.09.001
- Baker, T., Newcomb, W., Booy, F., Brown, J., and Steven, A. (1990). Three-dimensional structures of maturable and abortive capsids of equine herpesvirus 1 from cryoelectron microscopy. *J. Virol.* 64, 563–573.
- Ballagi-Pordany, A., Klingeborn, B., Flensburg, J., and Belak, S. (1990). Equine herpesvirus type 1: detection of viral DNA sequences in aborted fetuses with the polymerase chain reaction. *Vet. Microbiol.* 22, 373–381.
- Barbić, L., Ljokić, I., Stevanović, V., Bedeković, T., Starešina, V., Lemo, N., et al. (2012). Two outbreaks of neuropathogenic equine herpesvirus type 1 with breed-dependent clinical signs. *Vet. Rec.* 170, 227. doi: 10.1136/vr.100150
- Batterson, W., Furlong, D., and Roizman, B. (1983). Molecular genetics of herpes simplex virus. VIII. further characterization of a temperature-sensitive mutant defective in release of viral DNA and in other stages of the viral reproductive cycle. *J. Virol.* 45, 397–407.
- Baxi, M., Efstathiou, S., Lawrence, G., Whalley, J., Slater, J., and Field, H. (1995). The detection of latency-associated transcripts of equine herpesvirus 1 in ganglionic neurons. *J. Gen. Virol.* 76, 3113–3118.
- Borchers, K., and Slater, J. (1993). A nested PCR for the detection and differentiation of EHV-1 and EHV-4. *J. Virol. Methods* 45, 331–336.
- Bowles, D. E., Holden, V. R., Zhao, Y., and O’Callaghan, D. J. (1997). The ICP0 protein of equine herpesvirus 1 is an early protein that independently transactivates expression of all classes of viral promoters. *J. Virol.* 71, 4904–4914.
- Bowles, D. E., Kim, S. K., and O’callaghan, D. J. (2000). Characterization of the trans-activation properties of equine herpesvirus 1 ICP0 protein. *J. Virol.* 74, 1200–1208.
- Bowzard, J. B., Visalli, R. J., Wilson, C. B., Loomis, J. S., Callahan, E. M., Courtney, R. J., et al. (2000). Membrane targeting properties of a herpesvirus tegument protein-retrovirus Gag chimera. *J. Virol.* 74, 8692–8699.
- Breathnach, C., Yeargan, M., Timoney, J., and Allen, G. (2006). Detection of equine herpesvirus-specific effector and memory cytotoxic immunity in the equine upper respiratory tract. *Vet. Immunol. Immunopathol.* 111, 117–125.
- Brown, J. C., and Newcomb, W. W. (2011). Herpesvirus capsid assembly: insights from structural analysis. *Curr. Opin. Virol.* 1, 142–149. doi: 10.1016/j.coviro.2011.06.003
- Bryans, J. (1969). On immunity to disease caused by equine herpesvirus 1. *J. Am. Vet. Med. Assoc.* 155, 294–300.
- Bryans, J., Crowe, M., Doll, E., and McCollum, W. (1957). Isolation of a filterable agent causing arteritis of horses and abortion by mares; its differentiation from the equine abortion (influenza) virus. *Cor. Vet.* 47, 3–41.
- Bryans, J., Swerczek, T., Darlington, R., and Crowe, M. (1977). Neonatal foal disease associated with perinatal infection by equine herpesvirus I. *Equine Med. Surg.* 1, 20–26. doi: 10.1016/j.vetmic.2016.04.004
- Bryans, J. T., and Allen, G. P. (1986). Equine viral rhinopneumonitis. *Rev. Sci. Tech.* 5, 837–847.
- Buczynski, K. A., Kim, S. K., and O’Callaghan, D. J. (1999). Characterization of the transactivation domain of the equine herpesvirus type 1 immediate-early protein. *Virus Res.* 65, 131–140.
- Burch, A. D., and Weller, S. K. (2005). Herpes simplex virus type 1 DNA polymerase requires the mammalian chaperone hsp90 for proper localization to the nucleus. *J. Virol.* 79, 10740–10749.
- Burgess, B., Tokatloff, N., Manning, S., Lohmann, K., Lunn, D., Hussey, S., et al. (2012). Nasal shedding of equine Herpesvirus-1 from horses in an outbreak of equine herpes myeloencephalopathy in Western Canada. *J. Vet. Intern. Med.* 26, 384–392.
- Burrows, R., and Goodridge, D. (1984). “Studies of persistent and latent equid herpesvirus 1 and herpesvirus 3 infections in the Pirbright pony herd,” in *Latent Herpes Virus Infections in Veterinary Medicine*, eds G. Wittmann, R. M. Gaskell, and H. J. Rziha, (Dordrecht: Springer), 307–319.
- Callé, A., Ugrinova, I., Epstein, A. L., Bouvet, P., Diaz, J.-J., and Greco, A. (2008). Nucleolin is required for an efficient herpes simplex virus type 1 infection. *J. Virol.* 82, 4762–4773. doi: 10.1128/JVI.00077-08
- Carmichael, R., Whitfield, C., and Maxwell, L. J. (2013). Pharmacokinetics of ganciclovir and valganciclovir in the adult horse. *J. Vet. Pharmacol. Ther.* 36, 441–449. doi: 10.1111/jvp.12029
- Carrigan, M., Cosgrove, P., Kirkland, P., and Sabine, M. (1991). An outbreak of equid herpesvirus abortion in New South Wales. *Equine Vet. J.* 23, 108–110.
- Caughman, G. B., Staczek, J., and O’Callaghan, D. J. (1985). Equine herpesvirus type 1 infected cell polypeptides: evidence for immediate early/early/late regulation of viral gene expression. *Virology* 145, 49–61.
- Chang, Y. E., Van Sant, C., Krug, P. W., Sears, A. E., and Roizman, B. (1997). The null mutant of the U (L) 31 gene of herpes simplex virus 1: construction and phenotype in infected cells. *J. Virol.* 71, 8307–8315.
- Chesters, P., Allsop, R., Purewal, A., and Edington, N. (1997). Detection of latency-associated transcripts of equid herpesvirus 1 in equine leukocytes but not in trigeminal ganglia. *J. Virol.* 71, 3437–3443.
- Chi, J. H. I., Harley, C. A., Mukhopadhyay, A., and Wilson, D. W. (2005). The cytoplasmic tail of herpes simplex virus envelope glycoprotein D binds to the tegument protein VP22 and to capsids. *J. Gen. Virol.* 86, 253–261.
- Copeland, A. M., Newcomb, W. W., and Brown, J. C. (2009). Herpes simplex virus replication: roles of viral proteins and nucleoporins in capsid-nucleus attachment. *J. Virol.* 83, 1660–1668. doi: 10.1128/JVI.01139-08
- Coulter, L., Moss, H., Lang, J., and McGeoch, D. (1993). A mutant of herpes simplex virus type 1 in which the UL13 protein kinase gene is disrupted. *J. Gen. Virol.* 74, 387–395.
- Crabb, B. S., and Studdert, M. J. (1996). “Equine rhinopneumonitis (equine herpesvirus 4) and equine abortion (equine herpesvirus 1),” in *Virus Infections of Equines*, ed M. J. Studdert (Amsterdam: Elsevier Science BV), 11–37.
- Crabb, B. S., Allen, G. P., and Studdert, M. J. (1991). Characterization of the major glycoproteins of equine herpesviruses 4 and 1 and asinine herpesvirus 3 using monoclonal antibodies. *J. Gen. Virol.* 72, 2075–2082.
- Crabb, B. S., Nagesha, H. S., and Studdert, M. J. (1992). Identification of equine herpesvirus 4 glycoprotein G: a type-specific, secreted glycoprotein. *Virology* 190, 143–154.

- Crabb, B. S., and Studdert, M. J. (1993). Epitopes of glycoprotein G of equine herpesviruses 4 and 1 located near the C termini elicit type-specific antibody responses in the natural host. *J. Virol.* 67, 6332–6338.
- Crabb, B. S., and Studdert, M. J. (1995). Equine herpesviruses 4 (equine rhinopneumonitis virus) and 1 (equine abortion virus). *Adv. Virus Res.* 45, 153–190.
- Crump, C. M., Bruun, B., Bell, S., Pomeranz, L. E., Minson, T., and Browne, H. M. (2004). Alphaherpesvirus glycoprotein M causes the relocalization of plasma membrane proteins. *J. Gen. Virol.* 85, 3517–3527.
- Davison, A., Eberle, R., Desrosiers, R. C., Fleckenstein, B., McGeoch, D. J., Pellet, P. E., et al. (2000). “Herpesviridae,” in *Proceeding of the Seventh Report of the International Committee on Taxonomy of Viruses*, eds M. H. V. Van Regenmortel, et al. (Orlando, FL: Academic Press), 114–127.
- Davison, A. J. (2007). “Overview of classification,” in *Human Herpesviruses: Biology, Therapy, and Immunoprophylaxis*, eds A. Arvin, G. Campadelli-Fiume, E. Mocarski, P. S. Moore, B. Roizman, R. Whitley, et al. (Cambridge: Cambridge University Press).
- Davison, A. J. (2010). Herpesvirus systematics. *Vet. Microbiol.* 143, 52–69. doi: 10.1016/j.vetmic.2010.02.014
- Davison, A. J., Eberle, R., Ehlers, B., Hayward, G. S., McGeoch, D. J., Minson, A. C., et al. (2009). The order herpesvirales. *Arch. Virol.* 154, 171–177. doi: 10.1007/s00705-008-0278-4
- Del Piero, F., and Wilkins, P. A. (2001). Pulmonary vasculotropic EHV-1 infection in equids. *Vet. Pathol.* 38, 474.
- Derbigny, W. A., Kim, S. K., Jang, H. K., and O’Callaghan, D. J. (2002). EHV-1 EICP22 protein sequences that mediate its physical interaction with the immediate-early protein are not sufficient to enhance the trans-activation activity of the IE protein. *Virus Res.* 84, 1–15.
- Dimock, W. (1940). The diagnosis of virus abortion in mares. *J. Am. Vet. Med. Assoc.* 96, 665–666.
- Dimock, W., and Edwards, P. (1933). Is there a filterable virus of abortion in mares. *Bull. Kentucky Agriculture Experiment Station* 333, 291–301.
- Dimock, W. W., Bruner, D. W., and Edwards, P. R. (1942). Equine virus abortion. *Bull. Kentucky Agriculture Experiment Station* 426, 3–20.
- Dimock, W. W., and Edwards, P. R. (1932). *Infections of Fetuses and Foals*. Lexington: Kentucky Agricultural Experiment Station, 291–339.
- Dixon, R., Hartley, W., Hutchins, D., Lephed, E., Feilen, C., Jones, R., et al. (1978). Perinatal foal mortality associated with a herpesvirus. *Aust. Vet. J.* 54, 103–105.
- Doll, E., and Kintner, J. (1954a). A comparative study of the equine abortion and equine influenza viruses. *Cor. Vet.* 44, 355.
- Doll, E., Richards, M. G., and Wallace, M. (1954a). Cultivation of the equine influenza virus in suckling Syrian hamsters. Its similarity to the equine abortion virus. *Cor. Vet.* 44, 133–138.
- Doll, E., Wallace, E., and Richards, M. (1954b). Thermal, hematological, and serological responses of weanling horses following inoculation with equine abortion virus: its similarity to equine influenza. *Cor. Vet.* 44, 181–190.
- Doll, E., and Wallace, M. (1954b). Cultivation of equine abortion and equine influenza viruses on the chorioallantoic membrane of chicken embryos. *Cor. Vet.* 44, 453–461.
- Doll, E., Wallace, M., Bryans, J., and Richards, M. (1953). Complement-fixation antibody response following administration of equine virus abortion vaccine. *Am. J. Vet. Res.* 14, 46–48.
- Donaldson, M. T., and Sweeney, C. R. (1997). Equine herpes myeloencephalopathy. *Compend. Contin. Educ. Pract. Vet.* 19, 864–871.
- Dutta, S., and Myrup, A. (1983). Infectious center assay of intracellular virus and infective virus titer for equine mononuclear cells infected in vivo and in vitro with equine herpesviruses. *Can. J. Comp. Med.* 47, 64–69.
- Edington, N., Bridges, C., and Huckle, A. (1985). Experimental reactivation of equid herpesvirus 1 (EHV 1) following the administration of corticosteroids. *Equ. Vet. J.* 17, 369–372.
- Edington, N., Bridges, C., and Patel, J. (1986). Endothelial cell infection and thrombosis in paralysis caused by equid herpesvirus-1: equine stroke. *Arch. Virol.* 90, 111–124.
- Edington, N., Smyth, B., and Griffiths, L. (1991). The role of endothelial cell infection in the endometrium, placenta and foetus of equid herpesvirus 1 (EHV-1) abortions. *J. Comp. Pathol.* 104, 379–387.
- Edington, N., Welch, H., and Griffiths, L. (1994). The prevalence of latent equid herpesviruses in the tissues of 40 abattoir horses. *Equ. Vet. J.* 26, 140–142.
- Efstathiou, S., and Preston, C. (2005). Towards an understanding of the molecular basis of herpes simplex virus latency. *Virus Res.* 111, 108–119.
- Elliott, G., and O’hare, P. J. V. (1995). Equine herpesvirus 1 Gene 12, the functional homologue of herpes simplex virus VP16, transactivates via octamer sequences in the equine herpesvirus IE Gene promoter. *Virology* 213, 258–262.
- Estell, K., Dawson, D., Magdesian, K., Swain, E., Laing, S., Siso, S., et al. (2015). Quantitative molecular viral loads in 7 horses with naturally occurring equine herpesvirus-1 infection. *Equ. Vet. J.* 47, 689–693. doi: 10.1111/evj.12351
- Everett, R. D., Freemont, P., Saitoh, H., Dasso, M., Orr, A., Kathoria, M., et al. (1998). The disruption of ND10 during herpes simplex virus infection correlates with the Vmw110-and proteasome-dependent loss of several PML isoforms. *J. Virol.* 72, 6581–6591.
- Food and Agriculture Organization of the United Nations [FAOSTAT] (2017). *Livestock, 2017*. Rome: FAOSTAT.
- Footo, C., Love, D., Gilkerson, J., and Whalley, J. (2004). Detection of EHV-1 and EHV-4 DNA in unweaned thoroughbred foals from vaccinated mares on a large stud farm. *Equine Vet. J.* 36, 341–345.
- Forest, T., Barnard, S., and Baines, J. D. (2005). Active intranuclear movement of herpesvirus capsids. *Nat. Cell Biol.* 7, 429–431.
- Frampton, A. R., Goins, W. F., Cohen, J. B., Von Einem, J., Osterrieder, N., O’Callaghan, D. J., et al. (2005). Equine herpesvirus 1 utilizes a novel herpesvirus entry receptor. *J. Virol.* 79, 3169–3173.
- Frampton, A. R., Stolz, D. B., Uchida, H., Goins, W. F., Cohen, J. B., and Glorioso, J. C. (2007). Equine herpesvirus 1 enters cells by two different pathways, and infection requires the activation of the cellular kinase ROCK1. *J. Virol.* 81, 10879–10889.
- Franklin, T., Daft, B., Silverman, V., Powers, E., and Weidenbach, S. (1985). Serological titers and clinical observations in equines suspected of being infected with EHV-1. *Calif. Vet.* 39, 22–24.
- Friday, P. A., Scarratt, W. K., Elvinger, F., Timoney, P. J., and Bonda, A. (2000). Ataxia and paresis with equine herpesvirus type 1 infection in a herd of riding school horses. *J. Vet. Intern. Med.* 14, 197–201.
- Fuchs, W., Klupp, B. G., Granzow, H., Hengartner, C., Brack, A., Mundt, A., et al. (2002a). Physical interaction between envelope glycoproteins E and M of pseudorabies virus and the major tegument protein UL49. *J. Virol.* 76, 8208–8217.
- Fuchs, W., Klupp, B. G., Granzow, H., Osterrieder, N., and Mettenleiter, T. C. (2002b). The interacting UL31 and UL34 gene products of pseudorabies virus are involved in egress from the host-cell nucleus and represent components of primary enveloped but not mature virions. *J. Virol.* 76, 364–378.
- Fukushi, H., Tomita, T., Taniguchi, A., Ochiai, Y., Kirisawa, R., Matsumura, T., et al. (1997). Gazelle herpesvirus 1: a new neurotropic herpesvirus immunologically related to equine herpesvirus 1. *Virology* 227, 34–44.
- Garko-Buczynski, K. A., Smith, R. H., Kim, S. K., and O’Callaghan, D. J. (1998). Complementation of a replication-defective mutant of equine herpesvirus type 1 by a cell line expressing the immediate-early protein. *Virology* 248, 83–94.
- Garré, B., Van Der Meulen, K., Nugent, J., Neyts, J., Croubels, S., De Backer, P., et al. (2007). In vitro susceptibility of six isolates of equine herpesvirus 1 to acyclovir, ganciclovir, cidofovir, adefovir, PMEDAP and foscarnet. *Vet. Microbiol.* 122, 43–51.
- George, L. W. (1990). “Equine herpesvirus 1 myeloencephalitis (rhinopneumonitis myelitis),” in *Large Animal Internal Medicine*, ed. B. P. Smith, (St Louis, MO: CV Mosby), 913.
- Gibson, J., O’Neill, T., Thackray, A., Hannant, D., and Field, H. (1992a). Serological responses of specific pathogen-free foals to equine herpesvirus-1: primary and secondary infection, and reactivation. *Vet. Microbiol.* 32, 199–214.
- Gibson, J., Slater, J., Awan, A., and Field, H. (1992b). Pathogenesis of equine herpesvirus-1 in specific pathogen-free foals: primary and secondary infections and reactivation. *Arch. Virol.* 123, 351–366.
- Gibson, J., Slater, J., and Field, H. (1992c). The pathogenicity of Ab4p, the sequenced strain of equine herpesvirus-1, in specific pathogen-free foals. *Virology* 189, 317–319.
- Gilkerson, J., Whalley, J., Drummer, H., Studdert, M., and Love, D. (1999). Epidemiological studies of equine herpesvirus 1 (EHV-1) in thoroughbred foals: a review of studies conducted in the Hunter Valley of New South Wales between 1995 and 1997. *Vet. Microbiol.* 68, 15–25.
- Gleeson, L., and Coggins, L. (1980). Response of pregnant mares to equine herpesvirus 1 (EHV1). *Cor. Vet.* 70, 391–400.

- Goehring, L., Wagner, B., Bigbie, R., Hussey, S., Rao, S., Morley, P., et al. (2010). Control of EHV-1 viremia and nasal shedding by commercial vaccines. *Vaccine* 28, 5203–5211. doi: 10.1016/j.vaccine.2010.05.065
- Goehring, L. S., and Lunn, D. P. (2008). “Equine herpesvirus myeloencephalopathy,” in *Current Therapy in Equine Medicine*, 6th Edn, eds N. E. Robinson, and K. Sprayberry, (St Louis, MO: Saunders), 77–181.
- Gonnella, R., Farina, A., Santarelli, R., Raffa, S., Feederle, R., Bei, R., et al. (2005). Characterization and intracellular localization of the Epstein-Barr virus protein BFLF2: interactions with BFRF1 and with the nuclear lamina. *J. Virol.* 79, 3713–3727.
- Goodman, L. B., Loregian, A., Perkins, G. A., Nugent, J., Buckles, E. L., Mercorelli, B., et al. (2007). A point mutation in a herpesvirus polymerase determines neuropathogenicity. *PLoS Pathog.* 3:e160. doi: 10.1371/journal.ppat.0030160
- Granzow, H., Klupp, B. G., Fuchs, W., Veits, J., Osterrieder, N., and Mettenleiter, T. C. (2001). Egress of alphaherpesviruses: comparative ultrastructural study. *J. Virol.* 75, 3675–3684.
- Granzow, H., Klupp, B. G., and Mettenleiter, T. C. (2005). Entry of pseudorabies virus: an immunogold-labeling study. *J. Virol.* 79, 3200–3205.
- Gray, W. L., Baumann, R. P., Robertson, A. T., Caughman, G. B., O’Callaghan, D. J., and Staccek, J. (1987a). Regulation of equine herpesvirus type 1 gene expression: characterization of immediate early, early, and late transcription. *Virology* 158, 79–87.
- Gray, W. L., Baumann, R. P., Robertson, A. T., O’Callaghan, D. J., and Staccek, J. (1987b). Characterization and mapping of equine herpesvirus type 1 immediate early, early, and late transcripts. *Virus Res.* 8, 233–244.
- Grundy, F. J., Baumann, R. P., and O’Callaghan, D. J. (1989). DNA sequence and comparative analyses of the equine herpesvirus type 1 immediate early gene. *Virology* 172, 223–236.
- Gryspeerd, A., Vandekerckhove, A., Van Doorselaere, J., Van de Walle, G., and Nauwynck, H. (2011). Description of an unusually large outbreak of nervous system disorders caused by equine herpesvirus 1 (EHV1) in 2009 in Belgium. *Vlaams Diergeneeskundig Tijdschrift* 80, 147–153.
- Gryspeerd, A. C., Vandekerckhove, A., Garré, B., Barbé, F., Van de Walle, G., and Nauwynck, H. (2010). Differences in replication kinetics and cell tropism between neurovirulent and non-neurovirulent EHV1 strains during the acute phase of infection in horses. *Vet. Microbiol.* 142, 242–253. doi: 10.1016/j.vetmic.2009.10.015
- Guo, H., Shen, S., Wang, L., and Deng, H. (2010). Role of tegument proteins in herpesvirus assembly and egress. *Protein Cell* 1, 987–998. doi: 10.1007/s13238-010-0120-0
- Hahn, C., Mayhew, I., and MacKay, R. (1999). Diseases of multiple or unknown sites. *Equ. Med. Surg.* 2, 884–903.
- Hannant, D., Jessett, D., O’Neill, T., Dolby, C., Cook, R., and Mumford, J. A. (1993). Responses of ponies to equid herpesvirus-1 ISCOM vaccination and challenge with virus of the homologous strain. *Res. Vet. Sci.* 54, 299–305.
- Hartley, W., and Dixon, R. (1979). An outbreak of foal perinatal mortality due to equid herpesvirus type 1: pathological observations. *Equ. Vet. J.* 11, 215–218.
- Harty, R. N., and O’Callaghan, D. J. (1991). An early gene maps within and is 3’coterminal with the immediate-early gene of equine herpesvirus 1. *J. Virol.* 65, 3829–3838.
- Henninger, R. W., Reed, S. M., Saville, W. J., Allen, G. P., Hass, G. F., Kohn, C. W., et al. (2007). Outbreak of neurologic disease caused by equine herpesvirus-1 at a university equestrian center. *J. Vet. Intern. Med.* 21, 157–165.
- Henry, B. E., Robinson, R. A., Dauenhauer, S. A., Atherton, S. S., Hayward, G. S., and O’Callaghan, D. J. (1981). Structure of the genome of equine herpesvirus type 1. *Virology* 115, 97–114.
- Holden, V. R., Yalamanchili, R. R., Harty, R. N., and O’Callaghan, D. (1992). ICP22 homolog of equine herpesvirus 1: expression from early and late promoters. *J. Virol.* 66, 664–673.
- Holden, V. R., Zhao, Y., Thompson, Y., Caughman, G. B., Smith, R. H., and O’Callaghan, D. J. (1995). Characterization of the regulatory function of the ICP22 protein of equine herpesvirus type 1. *Virology* 210, 273–282.
- House, J. A., Gregg, D. A., Lubroth, J., Dubovi, E. J., and Torres, A. (1991). Experimental equine herpesvirus-1 infection in llamas (*Lama glama*). *J. Vet. Diagn. Invest.* 3, 137–143.
- Huang, T., Ma, G., and Osterrieder, N. (2015). Equine herpesvirus 1 multiply inserted transmembrane protein pUL43 cooperates with pUL56 in downregulation of cell surface major histocompatibility complex class I. *J. Virol.* 89, 6251–6263. doi: 10.1128/JVI.00032-15
- Huffman, J. B., Newcomb, W. W., Brown, J. C., and Homa, F. L. (2008). Amino acids 143 to 150 of the herpes simplex virus type 1 scaffold protein are required for the formation of portal-containing capsids. *J. Virol.* 82, 6778–6781. doi: 10.1128/JVI.00473-08
- Hussey, G. S., Goehring, L. S., Lunn, D. P., Hussey, S. B., Huang, T., Osterrieder, N., et al. (2013). Experimental infection with equine herpesvirus type 1 (EHV-1) induces chorioretinal lesions. *Vet. Res.* 44:118. doi: 10.1186/1297-9716-44-118
- Ivanovsky, D. (1882). Concerning the mosaic disease of the tobacco plant. *St. Petersburg Acad. Imp. Sci. Bul.* 35, 67–70. doi: 10.1016/j.jprot.2015.09.030
- Jackson, T., and Kendrick, J. (1971). Paralysis of horses associated with equine herpesvirus 1 infection. *Am. Vet. Med. Ass. J.* 158, 1351–1357.
- Jackson, T., Osburn, B., Cordy, D., and Kendrick, J. (1977). Equine herpesvirus 1 infection of horses: studies on the experimentally induced neurologic disease. *Am. J. Vet. Res.* 38, 709–719.
- Johnstone, S., Barsova, J., Campos, I., and Frampton, A. R. (2016). Equine herpesvirus type 1 modulates inflammatory host immune response genes in equine endothelial cells. *Vet. Microbiol.* 192, 52–59. doi: 10.1016/j.vetmic.2016.06.012
- Kasem, S., Yu, M. H. H., Yamada, S., Kodaira, A., Matsumura, T., Tsujimura, K., et al. (2010). The ORF37 (UL24) is a neuropathogenicity determinant of equine herpesvirus 1 (EHV-1) in the mouse encephalitis model. *Virology* 400, 259–270. doi: 10.1016/j.virol.2010.02.012
- Kim, S. K., Bowles, D. E., and O’Callaghan, D. J. (1999). The  $\gamma$ 2 late glycoprotein K promoter of equine herpesvirus 1 is differentially regulated by the IE and EICP0 proteins. *Virology* 256, 173–179.
- Kirisawa, R., Endo, A., Iwai, H., and Kawakami, Y. (1993). Detection and identification of equine herpesvirus-1 and-4 by polymerase chain reaction. *Vet. Microbiol.* 36, 57–67.
- Klupp, B. G., Granzow, H., and Mettenleiter, T. C. (2000). Primary envelopment of pseudorabies virus at the nuclear membrane requires the UL34 gene product. *J. Virol.* 74, 10063–10073.
- Klupp, B. G., Granzow, H., and Mettenleiter, T. C. (2001). Effect of the pseudorabies virus US3 protein on nuclear membrane localization of the UL34 protein and virus egress from the nucleus. *J. Gen. Virol.* 82, 2363–2371.
- Kohn, C. W., and Fenner, W. R. (1987). Equine herpes myeloencephalopathy. *Vet. Clin. North Am.* 3, 405–419.
- Kohn, C. W., Reed, S. M., Sofaly, C. D., Henninger, R. W., Saville, W. J., Allen, G. P., et al. (2006). Transmission of EHV-1 by horses with EHV-1 myeloencephalopathy: implications for biosecurity and review. *Clin. Tech. Equ. Pract.* 5, 60–66.
- Kress, F. (1941). Virus abortus bei der Stute, Wien. *Tieraerztl. Wochenschr.* 28:320.
- Kukhanova, M., Korovina, A., and Kochetkov, S. (2014). Human herpes simplex virus: life cycle and development of inhibitors. *Biochemistry* 79, 1635–1652. doi: 10.1134/S0006297914130124
- Kurtz, B. M., Singletary, L. B., Kelly, S. D., and Frampton, A. R. (2010). Equus caballus major histocompatibility complex class I is an entry receptor for equine herpesvirus type 1. *J. Virol.* 84, 9027–9034. doi: 10.1128/JVI.00287-10
- Kydd, J. H., Davis-Poynter, N., Birch, J., Hannant, D., Minke, J., Audonnet, J.-C., et al. (2006). A molecular approach to the identification of cytotoxic T-lymphocyte epitopes within equine herpesvirus 1. *J. Gen. Virol.* 87, 2507–2515.
- Kydd, J. H., Smith, K., Hannant, D., Livesay, G. J., and Mumford, J. A. (1994a). Distribution of equid herpesvirus-1 (EHV-1) in respiratory tract associated lymphoid tissue: implications for cellular immunity. *Equ. Vet. J.* 26, 470–473.
- Kydd, J. H., Smith, K., Hannant, D., Livesay, G. J., and Mumford, J. A. (1994b). Distribution of Equid herpesvirus-1 (EHV-1) in the respiratory tract of ponies: implications for vaccination strategies. *Equ. Vet. J.* 26, 466–469.
- Lang, A., de Vries, M., Feineis, S., Müller, E., Osterrieder, N., and Damiani, A. M. (2013). Development of a peptide ELISA for discrimination between serological responses to equine herpesvirus type 1 and 4. *J. Virol. Methods* 193, 667–673. doi: 10.1016/j.jviromet.2013.07.044
- Lawrence, G., Gilkerson, J., Love, D., Sabine, M., and Whalley, J. (1994). Rapid, single-step differentiation of equid herpesviruses 1 and 4 from clinical material using the polymerase chain reaction and virus-specific primers. *J. Virol. Methods* 47, 59–72.

- Lee, J. Y., Irmieri, A., and Gibson, W. (1988). Primate cytomegalovirus assembly: evidence that DNA packaging occurs subsequent to B capsid assembly. *Virology* 167, 87–96.
- Lewis, J. B., Thompson, Y. G., Feng, X., Holden, V. R., O'callaghan, D., and Caughman, G. B. (1997). Structural and antigenic identification of the ORF12 protein ( $\alpha$ TIF) of equine herpesvirus 1. *Virology* 230, 369–375.
- Loomis, J. S., Courtney, R. J., and Wills, J. W. (2003). Binding partners for the UL11 tegument protein of herpes simplex virus type 1. *J. Virol.* 77, 11417–11424.
- Lunn, D., Davis-Poynter, N., Flaminio, M., Horohov, D., Osterrieder, K., Pusterla, N., et al. (2009). Equine herpesvirus-1 consensus statement. *J. Vet. Intern. Med.* 23, 450–461. doi: 10.1111/j.1939-1676.2009.0304.x
- Lunn, D., Holmes, M., Gibson, J., Field, H., Kydd, J. H., and Duffus, W. (1991). Haematological changes and equine lymphocyte subpopulation kinetics during primary infection and attempted re-infection of specific pathogen free foals with EHV-1. *Equ. Vet. J.* 23, 35–40.
- Luxton, G. G., Haverlock, S., Coller, K. E., Antinone, S. E., Pincetic, A., and Smith, G. A. (2005). Targeting of herpesvirus capsid transport in axons is coupled to association with specific sets of tegument proteins. *Proc. Natl. Acad. Sci. U.S.A.* 102, 5832–5837.
- Luxton, G. G., Joy, I., Lee, H., Haverlock-Moyns, S., Schober, J. M., and Smith, G. A. (2006). The pseudorabies virus VP1/2 tegument protein is required for intracellular capsid transport. *J. Virol.* 80, 201–209.
- Ma, G., Feineis, S., Osterrieder, N., and Van de Walle, G. R. (2012). Identification and characterization of equine herpesvirus type 1 pUL56 and its role in virus-induced downregulation of major histocompatibility complex class I. *J. Virol.* 86, 3554–3563. doi: 10.1128/JVI.06994-11
- Machtiger, N., Pancake, B., Eberle, R., Courtney, R., Tevethia, S., and Schaffer, P. (1980). Herpes simplex virus glycoproteins: isolation of mutants resistant to immune cytolysis. *J. Virol.* 34, 336–346.
- Mackem, S., and Roizman, B. (1982). Structural features of the herpes simplex virus alpha gene 4, 0, and 27 promoter-regulatory sequences which confer alpha regulation on chimeric thymidine kinase genes. *J. Virol.* 44, 939–949.
- Mackie, J., Macleod, G., Reubel, G., and Studdert, M. (1996). Diagnosis of equine herpesvirus 1 abortion using polymerase chain reaction. *Aust. Vet. J.* 74, 390–391.
- Manninger, R. (1949). Studies on infectious abortion in mares due to a filterable virus. *Acta Vet. Acad. Sci. Hungaricae* 1, 62–69.
- Manninger, R., and Csontos, J. (1941). Virusabortus der Stuten. *Dtsch Tierarztl Wschr* 49, 105–111.
- Matsumura, T., Smith, R. H., and O'Callaghan, D. J. (1993). DNA sequence and transcriptional analyses of the region of the equine herpesvirus type 1 Kentucky A strain genome encoding glycoprotein C. *Virology* 193, 910–923.
- Maxwell, L. K., Bentz, B. G., Gilliam, L. L., Ritchey, J. W., Pusterla, N., Eberle, R., et al. (2017). Efficacy of the early administration of valacyclovir hydrochloride for the treatment of neuropathogenic equine herpesvirus type-1 infection in horses. *Am. J. Vet. Res.* 78, 1126–1139. doi: 10.2460/ajvr.78.10.1126
- Mayr, A., Pette, J., Petzoldt, K., and Wagener, K. (1968). Studies on the development of a live vaccine against rhinopneumonitis (mare abortion) of horses. *Zentralbl Veterinarmed B* 15, 406–418.
- McCartan, C., Russell, M., Wood, J., and Mumford, J. (1995). Clinical, serological and virological characteristics of an outbreak of paresis and neonatal foal disease due to equine herpesvirus-1 on a stud farm. *Vet. Rec.* 136, 7–12.
- McCulloch, J., Williamson, S. A., Powis, S. J., and Edington, N. (1993). The effect of EHV-1 infection upon circulating leucocyte populations in the natural equine host. *Vet. Microbiol.* 37, 147–161.
- McFadden, A., Hanlon, D., McKenzie, R., Gibson, I., Bueno, I., Pulford, D., et al. (2016). The first reported outbreak of equine herpesvirus myeloencephalopathy in New Zealand. *N. Z. Vet. J.* 64, 125–134. doi: 10.1080/00480169.2015.1096853
- Meredith, D. M., Stocks, J.-M., Whittaker, G. R., Halliburton, I. W., Snowden, B. W., and Killington, R. A. (1989). Identification of the gB homologues of equine herpesvirus types 1 and 4 as disulphide-linked heterodimers and their characterization using monoclonal antibodies. *J. Gen. Virol.* 70, 1161–1172.
- Mettenleiter, T. C. (2002). Herpesvirus assembly and egress. *J. Virol.* 76, 1537–1547.
- Mettenleiter, T. C. (2006). Intriguing interplay between viral proteins during herpesvirus assembly or: the herpesvirus assembly puzzle. *Vet. Microbiol.* 113, 163–169.
- Mettenleiter, T. C., Klupp, B. G., and Granzow, H. (2006). Herpesvirus assembly: a tale of two membranes. *Curr. Opin. Microbiol.* 9, 423–429.
- Mettenleiter, T. C., Klupp, B. G., and Granzow, H. (2009). Herpesvirus assembly: an update. *Virus Res.* 143, 222–234. doi: 10.1016/j.virusres.2009.03.018
- Michael, K., Klupp, B. G., Mettenleiter, T. C., and Karger, A. (2006). Composition of pseudorabies virus particles lacking tegument protein US3, UL47, or UL49 or envelope glycoprotein E. *J. Virol.* 80, 1332–1339.
- Minke, J., Fischer, L., Baudu, P., Guigal, P., Sindle, T., Mumford, J., et al. (2006). Use of DNA and recombinant canarypox viral (ALVAC) vectors for equine herpes virus vaccination. *Vet. Immunol. Immunopathol.* 111, 47–57.
- Miranda-Saksena, M., Boadle, R. A., Armati, P., and Cunningham, A. L. (2002). In rat dorsal root ganglion neurons, herpes simplex virus type 1 tegument forms in the cytoplasm of the cell body. *J. Virol.* 76, 9934–9951.
- Mumford, J. A., Hannant, D., Jessett, D. M., O'Neil, T., Smith, K. C., and Ostlund, E. N. (1994). "Equine infectious diseases VII," in *Proceedings of the Seventh International Conference on Equine Infectious Diseases*, eds Abortigenic, et al. (New market: R&W Publications), 261–275.
- Mumford, J. A., and Rosedale, P. (1980). Virus and its relationship to the "poor performance" syndrome. *Equ. Vet. J.* 12, 3–9.
- Muranyi, W., Haas, J., Wagner, M., Krohne, G., and Koszinowski, U. H. (2002). Cytomegalovirus recruitment of cellular kinases to dissolve the nuclear lamina. *Science* 297, 854–857.
- Muylaert, I., Tang, K.-W., and Elias, P. (2011). Replication and recombination of herpes simplex virus DNA. *J. Biol. Chem.* 286, 15619–15624.
- Negussie, H., Gizaw, D., Tessema, T. S., and Nauwynck, H. (2017). Equine herpesvirus-1 myeloencephalopathy, an emerging threat of working equids in ethiopia. *Transbound Emerg. Dis.* 64, 389–397. doi: 10.1111/tbed.12377
- Newcomb, W., Brown, J., Booy, F., and Steven, A. (1989). Nucleocapsid mass and capsomer protein stoichiometry in equine herpesvirus 1: scanning transmission electron microscopic study. *J. Virol.* 63, 3777–3783.
- Newcomb, W. W., Homa, F. L., Thomsen, D. R., Booy, F. P., Trus, B. L., Steven, A. C., et al. (1996). Assembly of the herpes simplex virus capsid: characterization of intermediates observed during cell-free capsid formation. *J. Mol. Biol.* 263, 432–446.
- Newcomb, W. W., Thomsen, D. R., Homa, F. L., and Brown, J. C. (2003). Assembly of the herpes simplex virus capsid: identification of soluble scaffold-portal complexes and their role in formation of portal-containing capsids. *J. Virol.* 77, 9862–9871.
- Nishiyama, Y. (2004). Herpes simplex virus gene products: the accessories reflect her lifestyle well. *Rev. Med. Virol.* 14, 33–46.
- Nowotny, N., Burtscher, H., and Bürki, F. (1987). Neuropathogenicity for suckling mice of equine herpesvirus 1 from the Lipizzan outbreak 1983 and of selected other EHV 1 strains. *J. Vet. Med. Ser. B* 34, 441–448.
- Nugent, J., Birch-Machin, I., Smith, K. C., Mumford, J. A., Swann, Z., Newton, J. R., et al. (2006). Analysis of equid herpesvirus 1 strain variation reveals a point mutation of the DNA polymerase strongly associated with neuropathogenic versus nonneuropathogenic disease outbreaks. *J. Virol.* 80, 4047–4060.
- O'Callaghan, D. J., Gentry, G. A., and Randall, C. C. (1983). "The equine herpesviruses," in *The Herpesviruses*, ed. B. Roizman, (Boston, MA: Springer), 215–318.
- O'Callaghan, D. J., Henry, B. E., Wharton, J. H., Dauenhauer, S. A., Vance, R. B., Staczek, J., et al. (1981). "Equine herpesviruses: biochemical studies on genomic structure, DI particles, oncogenic transformation and persistent infection," in *Herpesvirus DNA*, ed. Y. Becker, (Dordrecht: Springer), 387–418.
- Ojala, P. M., Sodeik, B., Ebersold, M. W., Kutay, U., and Helenius, A. (2000). Herpes simplex virus type 1 entry into host cells: reconstitution of capsid binding and uncoating at the nuclear pore complex in vitro. *Mol. Cell. Biol.* 20, 4922–4931.
- Oladunni, F. S., Sarkar, S., Reedy, S., Balasuriya, U. B., Horohov, D. W., and Chambers, T. M. (2018). Absence of relationship between type-I interferon suppression and neuropathogenicity of EHV-1. *Vet. Immunol. Immunopathol.* 197, 24–30. doi: 10.1016/j.vetimm.2018.01.007
- Oladunni, F. S., Sarkar, S., Reedy, S., Balasuriya, U. B., Horohov, D. W., and Chambers, T. M. (2019). Equine herpesvirus type 1 targets the sensitization and induction steps to inhibit type-I interferon response in equine endothelial cells. *J. Virol.* 93:e01342-19. doi: 10.1128/JVI.01342-19

- O'Neill, T., Kydd, J., Allen, G., Watrang, E., Mumford, J., and Hannant, D. (1999). Determination of equid herpesvirus 1-specific, CD8+, cytotoxic T lymphocyte precursor frequencies in ponies. *Vet. Immunol. Immunopathol.* 70, 43–54.
- Osterrieder, N. (1999). Construction and characterization of an equine herpesvirus 1 glycoprotein C negative mutant. *Virus Res.* 59, 165–177.
- Osterrieder, N., and Van de Walle, G. R. (2010). Pathogenic potential of equine alphaherpesviruses: the importance of the mononuclear cell compartment in disease outcome. *Vet. Microbiol.* 143, 21–28. doi: 10.1016/j.vetmic.2010.02.010
- Ostlund, E. (1993). The equine herpesviruses. *Vet. Clin. North Am. Equ. Pract.* 9, 283–294.
- Ostlund, E. N., Powell, D., and Bryans, J. T. (1990). Equine herpesvirus 1: a review. *Annu. Conv. Am. Assoc. Equ. Pract.* 36, 387–395.
- Packiarajah, P., Walker, C., Gilkerson, J., Whalley, J. M., and Love, D. N. (1998). Immune responses and protective efficacy of recombinant baculovirus-expressed glycoproteins of equine herpesvirus 1 (EHV-1) gB, gC and gD alone or in combinations in BALB/c mice. *Vet. Microbiol.* 61, 261–278.
- Paillet, R., Case, R., Ross, J., Newton, R., and Nugent, J. (2008). Equine herpes virus-1: virus, immunity and vaccines. *Open Vet. Sci. J.* 2, 68–91.
- Patel, J., Edington, N., and Mumford, J. (1982). Variation in cellular tropism between isolates of equine herpesvirus-1 in foals. *Arch. Virol.* 74, 41–51.
- Patel, J., and Heldens, J. (2005). Equine herpesviruses 1 (EHV-1) and 4 (EHV-4)—epidemiology, disease and immunoprophylaxis: a brief review. *Vet. J.* 170, 14–23.
- Pellet, P. (2007). The family Herpesviridae: a brief introduction. *Fields Virol.* 5, 3137–3166.
- Perdue, M. L., Cohen, J. C., Randall, C. C., and O'Callaghan, D. J. (1976). Biochemical studies of the maturation of herpesvirus nucleocapsid species. *Virology* 74, 194–208.
- Perdue, M. L., Kemp, M. C., Randall, C. C., and O'Callaghan, D. J. (1974). Studies of the molecular anatomy of the LM cell strain of equine herpes virus type 1: proteins of the nucleocapsid and intact virion. *Virology* 59, 201–216.
- Perkins, G., Babasyan, S., Stout, A. E., Freer, H., Rollins, A., Wimer, C. L., et al. (2019). Intranasal IgG4/7 antibody responses protect horses against equid herpesvirus-1 (EHV-1) infection including nasal virus shedding and cell-associated viremia. *Virology* 531, 219–232. doi: 10.1016/j.virol.2019.03.014
- Perkins, G., Goodman, L., Tsujimura, K., Van de Walle, G., Kim, S., Dubovi, E., et al. (2008). Investigation of neurologic equine herpes virus 1 epidemiology from 1984–2007. *J. Vet. Internal Med.* 22, 819–820. doi: 10.1016/j.vetmic.2009.06.033
- Perkins, G. A., Goodman, L. B., Tsujimura, K., Van de Walle, G. R., Kim, S. G., Dubovi, E. J., et al. (2009). Investigation of the prevalence of neurologic equine herpes virus type 1 (EHV-1) in a 23-year retrospective analysis (1984–2007). *Vet. Microbiol.* 139, 375–378.
- Plummer, G., and Waterson, A. (1963). Equine herpes viruses. *Virology* 19, 412–416.
- Pronost, S., Cook, R. F., Fortier, G., Timoney, P. J., and Balasuriya, U. B. (2010). Relationship between equine herpesvirus-1 myeloencephalopathy and viral genotype. *Equ. Vet. J.* 42, 672–674.
- Pronost, S., Legrand, L., Pitel, P. H., Wegge, B., Lissens, J., Freymuth, F., et al. (2012). Outbreak of equine herpesvirus myeloencephalopathy in France: a clinical and molecular investigation. *Transbound Emerg. Dis.* 59, 256–263. doi: 10.1111/j.1865-1682.2011.01263.x
- Purewal, A., Allsopp, R., Riggio, M., Telford, E., Azam, S., Davison, A., et al. (1994). Equid herpesviruses 1 and 4 encode functional homologs of the herpes simplex virus type 1 virion transactivator protein, VP16. *Virology* 198, 385–389.
- Purewal, A., Smallwood, A., Kaushal, A., Adegboye, D., and Edington, N. (1992). Identification and control of the cis-acting elements of the immediate early gene of equid herpesvirus type 1. *J. Gen. Virol.* 73, 513–519.
- Pusterla, N., and Hussey, G. S. (2014). Equine herpesvirus 1 myeloencephalopathy. *Vet. Clin. North Am. Equ. Pract.* 13, 53–72.
- Pusterla, N., Wilson, W. D., Madigan, J. E., and Ferraro, G. L. (2009). Equine herpesvirus-1 myeloencephalopathy: a review of recent developments. *Vet. J.* 180, 279–289.
- Rajcani, J., and Durmanova, V. (2001). Mechanisms of replication of alpha- and betaherpesviruses and their pathogenesis. *Bratisl. Lek. Listy* 102, 505–514.
- Randall, C. C., Ryden, F. W., Doll, E., and Schell, F. S. (1953). Cultivation of equine abortion virus in fetal horse tissue in vitro. *Am. J. Pathol.* 29, 139–153.
- Rebhun, W. C., Jenkins, D. H., Riis, R. C., Dill, S., Dubovi, E., and Torres, A. (1988). An epizootic of blindness and encephalitis associated with a herpesvirus indistinguishable from equine herpesvirus 1 in a herd of alpacas and llamas. *J. Am. Vet. Med. Assoc.* 192, 953–956.
- Reed, S. M., and Toribio, R. E. (2004). Equine herpesvirus 1 and 4. *Vet. Clin. Equ. Pract.* 20, 631–642.
- Reynolds, A. E., Liang, L., and Baines, J. D. (2004). Conformational changes in the nuclear lamina induced by herpes simplex virus type 1 require genes UL31 and UL34. *J. Virol.* 78, 5564–5575.
- Reynolds, A. E., Ryckman, B. J., Baines, J. D., Zhou, Y., Liang, L., and Roller, R. J. (2001). UL31 and UL34 proteins of herpes simplex virus type 1 form a complex that accumulates at the nuclear rim and is required for envelopment of nucleocapsids. *J. Virol.* 75, 8803–8817.
- Reynolds, A. E., Wills, E. G., Roller, R. J., Ryckman, B. J., and Baines, J. D. (2002). Ultrastructural localization of the herpes simplex virus type 1 UL31, UL34, and US3 proteins suggests specific roles in primary envelopment and egress of nucleocapsids. *J. Virol.* 76, 8939–8952.
- Riaz, A., Murtaz-ul-Hasan, K., and Akhtar, N. (2017). Recent understanding of the classification and life cycle of herpesviruses: a review. *Sci. Lett.* 5, 195–207.
- Rixon, F. J., Addison, C., McGregor, A., Macnab, S. J., Nicholson, P., Preston, V. G., et al. (1996). Multiple interactions control the intracellular localization of the herpes simplex virus type 1 capsid proteins. *J. Gen. Virol.* 77, 2251–2260.
- Rixon, F. J., Cross, A. M., Addison, C., and Preston, V. G. (1988). The products of herpes simplex virus type 1 gene UL26 which are involved in DNA packaging are strongly associated with empty but not with full capsids. *J. Gen. Virol.* 69, 2879–2891.
- Roizman, B. (1982). “The family herpesviridae: general description, taxonomy, and classification,” in *The Herpesviruses*, ed. B. Roizman, (Boston, MA: Springer), 1–23.
- Roizman, B. (1996). The function of herpes simplex virus genes: a primer for genetic engineering of novel vectors. *Proc. Natl. Acad. Sci. U.S.A.* 93, 11307–11312.
- Roizman, B., Carmichael, L., and Deinhardt, F. (1981). Herpes-viridae. Definition, provisional nomenclature, and taxonomy. *Intervirology* 16, 201–217.
- Roizman, B., Desrosiers, R. C., Fleckenstein, B., Lopez, C., Minson, A. C., and Studdert, M. J. (1995). “Herpesviridae,” in *Virus Taxonomy. Report of the International Committee on Taxonomy of Viruses*, eds F. A. Murray, C. M. Fauquet, D. H. L. Bishop, et al. (New York, NY: Springer-Verlag), 114–127.
- Roizman, B., and Knipe, D. M. (2001). “Herpes simplex viruses and their replication,” in *Fields Virology*, eds D. M. Knipe, and P. M. Howley, (Philadelphia, PA: Lippincott Williams & Wilkins), 2399–2460.
- Roizmann, B., Desrosiers, R., Fleckenstein, B., Lopez, C., Minson, A., and Studdert, M. (1992). The family Herpesviridae: an update. *Arch. Virol.* 123, 425–449.
- Roller, R. J., Zhou, Y., Schnetzer, R., Ferguson, J., and DeSalvo, D. (2000). Herpes simplex virus type 1 UL34 gene product is required for viral envelopment. *J. Virol.* 74, 117–129.
- Rusli, N. D., Mat, K. B., and Harun, H. C. (2014). A review: interactions of equine herpesvirus-1 with immune system and equine lymphocyte. *Open J. Vet. Med.* 4, 294–307.
- Ruyechan, W., Dauenhauer, S., and O'Callaghan, D. (1982). Electron microscopic study of equine herpesvirus type 1 DNA. *J. Virol.* 42, 297–300.
- Rybachuk, G. V. (2009). *Antiviral Chemotherapeutic Agents Against Equine Herpesvirus Type 1: The Mechanism of Antiviral Effects of Porphyrin Derivatives*. Doctoral Dissertations. LSU: Baton Rouge, LA, 2545
- Salyi, J. (1942). Beitrag zur Pathohistologie des Virusabortus der Stuten. *Arch. Wiss. Prakt. Tierheilkd* 77, 244.
- Sarkar, S. (2014). Modulation of Type-I Interferon Mediated Immune Response: A Novel Innate Immune Evasion Strategy of Equine Herpesvirus. Available at: [https://uknowledge.uky.edu/gluck\\_etds/14](https://uknowledge.uky.edu/gluck_etds/14) (accessed December 5, 2017).
- Sarkar, S., Balasuriya, U. B., Horohov, D. W., and Chambers, T. M. (2015). Equine herpesvirus-1 suppresses type-I interferon induction in equine endothelial cells. *Vet. Immunol. Immunopathol.* 167, 122–129. doi: 10.1016/j.vetimm.2015.07.015
- Sarkar, S., Balasuriya, U. B., Horohov, D. W., and Chambers, T. M. (2016a). Equine herpesvirus-1 infection disrupts interferon regulatory factor-3 (IRF-3) signaling pathways in equine endothelial cells. *Vet. Immunol. Immunopathol.* 173, 1–9. doi: 10.1016/j.vetimm.2016.03.009
- Sarkar, S., Balasuriya, U. B., Horohov, D. W., and Chambers, T. M. (2016b). The neuropathogenic T953 strain of equine herpesvirus-1 inhibits type-I IFN

- mediated antiviral activity in equine endothelial cells. *Vet. Microbiol.* 183, 110–118. doi: 10.1016/j.vetmic.2015.12.011
- Sasaki, M., Hasebe, R., Makino, Y., Suzuki, T., Fukushi, H., Okamoto, M., et al. (2011). Equine major histocompatibility complex class I molecules act as entry receptors that bind to equine herpesvirus-1 glycoprotein D. *Genes Cells* 16, 343–357. doi: 10.1111/j.1365-2443.2011.01491.x
- Schumacher, D., Tischer, B. K., Trapp, S., and Osterrieder, N. (2005). The protein encoded by the US3 orthologue of Marek's disease virus is required for efficient de-envelopment of perinuclear virions and involved in actin stress fiber breakdown. *J. Virol.* 79, 3987–3997.
- Scott, J. C., Dutta, S., and Myrup, A. (1983). In vivo harboring of equine herpesvirus-1 in leukocyte populations and subpopulations and their quantitation from experimentally infected ponies. *Am. J. Vet. Res.* 44, 1344–1348.
- Simpson-Holley, M., Colgrove, R. C., Nalepa, G., Harper, J. W., and Knipe, D. M. (2005). Identification and functional evaluation of cellular and viral factors involved in the alteration of nuclear architecture during herpes simplex virus 1 infection. *J. Virol.* 79, 12840–12851.
- Singer, G. P., Newcomb, W. W., Thomsen, D. R., Homa, F. L., and Brown, J. C. (2005). Identification of a region in the herpes simplex virus scaffolding protein required for interaction with the portal. *J. Virol.* 79, 132–139.
- Slater, J., Arnold, J., Taylor, K., Baxi, S., and Field, H. (1995). Fluorescein angiographic appearance of the normal fundus and of focal chorioretinal lesions in the horse. *Investig. Ophthalmol. Vis. Sci.* 36:S779.
- Slater, J., Baxi, M., Tewari, D., Gibson, J., Field, H., Ludwig, H., et al. (1994a). "Experimental infection of specific pathogen-free ponies with equid herpesvirus-1: detection of infectious virus and viral DNA," in *Equine Infectious Diseases*, Vol. VII, eds W. Plowright, and H. Nakajima, (Newmarket: R&W Publications Ltd.), 255–260.
- Slater, J., Borchers, K., Thackray, A., and Field, H. (1994b). The trigeminal ganglion is a location for equine herpesvirus 1 latency and reactivation in the horse. *J. Gen. Virol.* 75, 2007–2016.
- Slater, J., Gibson, J., Barnett, K., and Field, H. (1992). Chorioretinopathy associated with neuropathology following infection with equine herpesvirus-1. *Vet. Rec.* 131, 237–239.
- Smith, D., Iqbal, J., Purewal, A., Hamblin, A., and Edington, N. (1998). In vitro reactivation of latent equid herpesvirus-1 from CD5+/CD8+ leukocytes indirectly by IL-2 or thionine gonadotrophin. *J. Gen. Virol.* 79, 2997–3004.
- Smith, K., McGladdery, A., Binns, M., and Mumford, J. (1997). Use of transabdominal ultrasound-guided amniocentesis for detection of equid herpesvirus 1-induced fetal infection in utero. *Am. J. Vet. Res.* 58, 997–1002.
- Smith, K., Whitwell, K. E., Binns, M., Dolby, C. A., Hannant, D., and Mumford, J. A. (1992). Abortion of virologically negative foetuses following experimental challenge of pregnant pony mares with equid herpesvirus 1. *Equ. Vet. J.* 24, 256–259.
- Smith, K., Whitwell, K. E., Mumford, J. A., Gower, S. M., Hannant, D., and Tearle, J. (1993). An immunohistological study of the uterus of mares following experimental infection by equid herpesvirus 1. *Equ. Vet. J.* 25, 36–40.
- Smith, K. L., Li, Y., Breheny, P., Cook, R. F., Henney, P. J., Sells, S., et al. (2012). New real-time PCR assay using allelic discrimination for detection and differentiation of equine herpesvirus-1 strains with A2254 and G2254 polymorphisms. *J. Clin. Microbiol.* 50, 1981–1988. doi: 10.1128/JCM.00135-12
- Smith, R. H., Caughman, G. B., and O'Callaghan, D. J. (1992). Characterization of the regulatory functions of the equine herpesvirus 1 immediate-early gene product. *J. Virol.* 66, 936–945.
- Smith, R. H., Zhao, Y., and O'Callaghan, D. J. (1994). The equine herpesvirus type 1 immediate-early gene product contains an acidic transcriptional activation domain. *Virology* 202, 760–770.
- Soboll, G., Breathnach, C., Kydd, J., Hussey, S., Mealey, R., and Lunn, D. (2010). Vaccination of ponies with the IE gene of EHV-1 in a recombinant modified live vaccinia vector protects against clinical and virological disease. *Vet. Immunol. Immunopathol.* 135, 108–117. doi: 10.1016/j.vetimm.2009.11.009
- Soboll, G., Hussey, S., Whalley, J., Allen, G., Koen, M., Santucci, N., et al. (2006). Antibody and cellular immune responses following DNA vaccination and EHV-1 infection of ponies. *Vet. Immunol. Immunopathol.* 111, 81–95.
- Soboll, G., Whalley, J. M., Koen, M. T., Allen, G. P., Fraser, D. G., Macklin, M. D., et al. (2003). Identification of equine herpesvirus-1 antigens recognized by cytotoxic T lymphocytes. *J. Gen. Virol.* 84(Pt 10), 2625–2634.
- Spear, P. G. (2004). Herpes simplex virus: receptors and ligands for cell entry. *Cell Microbiol.* 6, 401–410.
- Studdert, M., Fitzpatrick, D., Horner, G., Westbury, H., and Gleeson, L. (1984). Molecular epidemiology and pathogenesis of some equine herpesvirus type 1 (equine abortion virus) and type 4 (equine rhinopneumonitis virus) isolates. *Aust. Vet. J.* 61, 345–348.
- Taniguchi, A., Fukushi, H., Matsumura, T., Yanai, T., Masegi, T., and Hirai, K. (2000). Pathogenicity of a new neurotropic equine herpesvirus 9 (gazelle herpesvirus 1) in horses. *J. Vet. Med. Sci.* 62, 215–218.
- Telford, E., Watson, M. S., Perry, J., Cullinane, A. A., and Davison, A. J. (1998). The DNA sequence of equine herpesvirus-4. *J. Gen. Virol.* 79, 1197–1203.
- Telford, E. A., Watson, M. S., McBride, K., and Davison, A. J. (1992). The DNA sequence of equine herpesvirus-1. *Virology* 189, 304–316.
- Timoney, P. (1992). *Rhinopneumonitis and Viral Abortion. Veterinary Diagnostic Virology*. St Louis, MO: Mosby Year Book Inc, 173–177.
- Traub-Dargatz, J., Pelzel-McCluskey, A., Creekmore, L., Geiser-Novotny, S., Kasari, T., Wiedenheft, A., et al. (2013). Case-control study of a multistate equine herpesvirus myeloencephalopathy outbreak. *J. Vet. Intern. Med.* 27, 339–346. doi: 10.1111/jvim.12051
- Tsujimura, K., Oyama, T., Katayama, Y., Muranaka, M., Bannai, H., Nemoto, M., et al. (2011). Prevalence of equine herpesvirus type 1 strains of neuropathogenic genotype in a major breeding area of Japan. *J. Vet. Med. Sci.* 73, 1663–1667.
- Turcotte, S., Letellier, J., and Lippé, R. (2005). Herpes simplex virus type 1 capsids transit by the trans-Golgi network, where viral glycoproteins accumulate independently of capsid egress. *J. Virol.* 79, 8847–8860.
- Turtinen, L., Allen, G., Darlington, R., and Bryans, J. (1981). Serologic and molecular comparisons of several equine herpesvirus type 1 strains. *Am. J. Vet. Res.* 42, 2099–2104.
- Turtinen, L. W. (1984). *Studies on the Antigenic and Genetic Variation Between the Two Subtypes of Equine Herpesvirus 1*. Ph.D. thesis, University of Kentucky, Lexington. (accessed May 5, 2019).
- Turtinen, L. W., and Allen, G. P. (1982). Identification of the envelope surface glycoproteins of equine herpesvirus type 1. *J. Gen. Virol.* 63, 481–485.
- van der Meulen, K. M., Favoreel, H. W., Pensaert, M. B., and Nauwynck, H. J. (2006). Immune escape of equine herpesvirus 1 and other herpesviruses of veterinary importance. *Vet. Immunol. Immunopathol.* 111, 31–40.
- van Galen, G., Leblond, A., Tritz, P., Martinelle, L., Pronost, S., and Saegerman, C. (2015). A retrospective study on equine herpesvirus type-1 associated myeloencephalopathy in France (2008–2011). *Vet. Microbiol.* 179, 304–309.
- Vandekerckhove, A., Glorieux, S., Gryspeerdt, A., Steukers, L., Duchateau, L., Osterrieder, N., et al. (2010). Replication kinetics of neurovirulent versus non-neurovirulent equine herpesvirus type 1 strains in equine nasal mucosal explants. *J. Gen. Virol.* 91, 2019–2028. doi: 10.1099/vir.0.019257-0
- Vandekerckhove, A. P., Glorieux, S., Gryspeerdt, A., Steukers, L., Van Doorselaere, J., Osterrieder, N., et al. (2011). Equine alpha herpesviruses (EHV-1 and EHV-4) differ in their efficiency to infect mononuclear cells during early steps of infection in nasal mucosal explants. *Vet. Microbiol.* 152, 21–28. doi: 10.1016/j.vetmic.2011.03.038
- Wagner, B., Goodman, L. B., Babasyan, S., Freer, H., Torsteinsdottir, S., Svansson, V., et al. (2015). Antibody and cellular immune responses of naive mares to repeated vaccination with an inactivated equine herpesvirus vaccine. *Vaccine* 33, 5588–5597. doi: 10.1016/j.vaccine.2015.09.009
- Walter, J., Seeh, C., Fey, K., Bleul, U., and Osterrieder, N. (2013). Clinical observations and management of a severe equine herpesvirus type 1 outbreak with abortion and encephalomyelitis. *Acta Vet. Scand.* 55, 19. doi: 10.1186/1751-0147-55-19
- Welch, H. M., Bridges, C. G., Lyon, A. M., Griffiths, L., and Edington, N. (1992). Latent equid herpesviruses 1 and 4: detection and distinction using the polymerase chain reaction and co-cultivation from lymphoid tissues. *J. Gen. Virol.* 73, 261–268.
- Weller, S. K., and Coen, D. M. (2012). Herpes simplex viruses: mechanisms of DNA replication. *Cold Spring Harb. Perspect. Biol.* 4:a013011. doi: 10.1101/cshperspect.a013011
- Westerfield, C., and Dimock, W. (1946). The pathology of equine virus abortion. *J. Am. Vet. Med. Assoc.* 109, 101–111.

- Whalley, J. M., Robertson, G. R., and Davison, A. J. (1981). Analysis of the genome of equine herpesvirus type 1: arrangement of cleavage sites for restriction endonucleases EcoRI, BglII and BamHI. *J. Gen. Virol.* 57, 307–323.
- Whitley, R. J., and Gnann, J. W. (1993). “The epidemiology and clinical manifestation of herpes simplex virus infections,” in *The Human Herpesviruses*, eds B. Roizman, R. J. Whitley, and C. Lopaz, (New York, NY: Raven Press), 69–105.
- Whittaker, G. R., and Helenius, A. (1998). Nuclear import and export of viruses and virus genomes. *Virology* 246, 1–23.
- Whitwell, K. E., and Blunden, A. (1992). Pathological findings in horses dying during an outbreak of the paralytic form of Equid herpesvirus type 1 (EHV-1) infection. *Equ. Vet. J.* 24, 13–19.
- Wilson, J., and Erickson, D. (1991). Neurological syndrome of rhinopneumonitis. *Proc. Am. Coll. Vet. Intern. Med.* 9, 419–421.
- Wilson, W. D. (1997). Equine herpesvirus 1 myeloencephalopathy. *Vet. Clin. North Am. Equ. Pract.* 13, 53–72.
- Wolfstein, A., Nagel, C. H., Radtke, K., Döhner, K., Allan, V. J., and Sodeik, B. (2006). The inner tegument promotes herpes simplex virus capsid motility along microtubules in vitro. *Traffic* 7, 227–237.
- Xie, Y., Wu, L., Wang, M., Cheng, A., Yang, Q., Wu, Y., et al. (2019). Alpha-herpesvirus thymidine kinase genes mediate viral virulence and are potential therapeutic targets. *Front. Microbiol.* 10:941. doi: 10.3389/fmicb.2019.00941
- Yang, K., and Baines, J. D. (2008). Domain within herpes simplex virus 1 scaffold proteins required for interaction with portal protein in infected cells and incorporation of the portal vertex into capsids. *J. Virol.* 82, 5021–5030. doi: 10.1128/JVI.00150-08
- Yang, K., Homa, F., and Baines, J. D. (2007). Putative terminase subunits of herpes simplex virus 1 form a complex in the cytoplasm and interact with portal protein in the nucleus. *J. Virol.* 81, 6419–6433.
- Zhao, Y., Holden, V., Harty, R. N., and O’Callaghan, D. J. (1992). Identification and transcriptional analyses of the UL3 and UL4 genes of equine herpesvirus 1, homologs of the ICP27 and glycoprotein K genes of herpes simplex virus. *J. Virol.* 66, 5363–5372.
- Zhao, Y., Holden, V. R., Smith, R. H., and O’Callaghan, D. J. (1995). Regulatory function of the equine herpesvirus 1 ICP27 gene product. *J. Virol.* 69, 2786–2793.
- Zhou, Z. H., Chen, D. H., Jakana, J., Rixon, F. J., and Chiu, W. (1999). Visualization of tegument-capsid interactions and DNA in intact herpes simplex virus type 1 virions. *J. Virol.* 73, 3210–3218.

**Conflict of Interest:** The authors declare that the research was conducted in the absence of any commercial or financial relationships that could be construed as a potential conflict of interest.

Copyright © 2019 Oladunni, Horohov and Chambers. This is an open-access article distributed under the terms of the Creative Commons Attribution License (CC BY). The use, distribution or reproduction in other forums is permitted, provided the original author(s) and the copyright owner(s) are credited and that the original publication in this journal is cited, in accordance with accepted academic practice. No use, distribution or reproduction is permitted which does not comply with these terms.



# Enterovirus and Encephalitis

**Bo-Shiun Chen<sup>1,2</sup>, Hou-Chen Lee<sup>1</sup>, Kuo-Ming Lee<sup>1</sup>, Yu-Nong Gong<sup>1,3</sup> and Shin-Ru Shih<sup>1,3,4,5,6,7\*</sup>**

<sup>1</sup> Research Center for Emerging Viral Infections, College of Medicine, Chang Gung University, Taoyuan, Taiwan, <sup>2</sup> Department of Neuroscience and Regenerative Medicine, Medical College of Georgia, Augusta University, Augusta, GA, United States, <sup>3</sup> Department of Laboratory Medicine, Linkou Chang Gung Memorial Hospital, Taoyuan, Taiwan, <sup>4</sup> Department of Medical Biotechnology and Laboratory Science, College of Medicine, Chang Gung University, Taoyuan, Taiwan, <sup>5</sup> Research Center for Chinese Herbal Medicine, College of Human Ecology, Chang Gung University of Science and Technology, Taoyuan, Taiwan, <sup>6</sup> Research Center for Food and Cosmetic Safety, College of Human Ecology, Chang Gung University of Science and Technology, Taoyuan, Taiwan, <sup>7</sup> Graduate Institute of Health Industry Technology, College of Human Ecology, Chang Gung University of Science and Technology, Taoyuan, Taiwan

## OPEN ACCESS

### Edited by:

Erna Geessien Kroon,  
Federal University of Minas Gerais,  
Brazil

### Reviewed by:

Sara Louise Cosby,  
Agri-Food and Biosciences Institute  
(AFBI), United Kingdom  
Varpu Seija Marjomäki,  
University of Jyväskylä, Finland

### \*Correspondence:

Shin-Ru Shih  
srshih@mail.cgu.edu.tw

### Specialty section:

This article was submitted to  
Virology,  
a section of the journal  
Frontiers in Microbiology

**Received:** 06 November 2019

**Accepted:** 04 February 2020

**Published:** 20 February 2020

### Citation:

Chen B-S, Lee H-C, Lee K-M,  
Gong Y-N and Shih S-R (2020)  
Enterovirus and Encephalitis.  
*Front. Microbiol.* 11:261.  
doi: 10.3389/fmicb.2020.00261

Enterovirus-induced infection of the central nervous system (CNS) results in acute inflammation of the brain (encephalitis) and constitutes a significant global burden to human health. These viruses are thought to be highly cytolytic, therefore normal brain function could be greatly compromised following enteroviral infection of the CNS. A further layer of complexity is added by evidence showing that some enteroviruses may establish a persistent infection within the CNS and eventually lead to pathogenesis of certain neurodegenerative disorders. Interestingly, enterovirus encephalitis is particularly common among young children, suggesting a potential causal link between the development of the neuroimmune system and enteroviral neuroinvasion. Although the CNS involvement in enterovirus infections is a relatively rare complication, it represents a serious underlying cause of mortality. Here we review a selection of enteroviruses that infect the CNS and discuss recent advances in the characterization of these enteroviruses with regard to their routes of CNS infection, tropism, virulence, and immune responses.

**Keywords:** enterovirus, encephalitis, CNS, Picornaviridae, RNA virus

## INTRODUCTION

Enteroviruses belong to the family Picornaviridae, a highly diverse group of small, non-enveloped, icosahedral-shaped viruses with single positive-strand RNA genomes. Based on the sequence diversity, they have been divided into 15 species: enterovirus A to L and rhinovirus A to C. Human enteroviruses containing four enterovirus species (A to D) and three rhinovirus species (A to C) infect millions of people worldwide every year. Although infections are frequently asymptomatic, human enteroviruses can cause a variety of symptoms comprising fever, headache, respiratory illness, sore throat, and, occasionally, vomiting and diarrhea. Importantly, several members of human enteroviruses are neurotropic pathogens with a wide range of clinical disorders ranging from aseptic meningitis to more severe encephalitis. In the United States, enterovirus has been shown to be the most common etiology of meningitis/encephalitis (Hasbun et al., 2017; Balada-Llasat et al., 2019). About 58% of the infected infants and children and 52% of the infected adults diagnosed with meningitis/encephalitis is due to enterovirus. In addition, age is highly associated with the clinical presentation with severe infections including CNS disease, myocarditis and

sepsis-like illness occurring most frequently in neonates and infants. The best-known neurotropic enterovirus is the poliovirus (PV), which belongs to the species Enterovirus C and is believed to have almost been eradicated by vaccinations from circulation in human populations. Non-polio enteroviruses are also known to infect the CNS and account for the majority of recent enteroviral infections with neurological disorders. Among the non-polio enteroviruses, the species Enterovirus A like enterovirus 71 (EV-A71), coxsackievirus A6 (CV-A6), and CV-A16 (Goto et al., 2009; Xu et al., 2012; Huang Y. et al., 2015; Holmes et al., 2016; B'Krong et al., 2018; Suresh et al., 2018), the species Enterovirus B like CV-B1 (Sun et al., 2019), CV-B3 (Fan and Liu, 2019), CV-B5 (Mao et al., 2018), CV-A9, Echovirus 6 (E-6), E-7, E-11, and E-13 (Holmes et al., 2016; Chen et al., 2017; B'Krong et al., 2018; Suresh et al., 2018; Chen et al., 2019; Ramalho et al., 2019; Sun et al., 2019), the species Enterovirus C like CV-A24 (Tapparel et al., 2013; B'Krong et al., 2018; Suresh et al., 2018), and the species Enterovirus D like EV-D68 (Tapparel et al., 2013; Messacar et al., 2018) have been shown to involve the CNS and cause diverse neurological complications such as encephalitis, meningitis and acute flaccid paralysis (AFP) (Tapparel et al., 2013) (see **Table 1** for details).

## ENTEROVIRUS LIFE CYCLE

The enterovirus genome contains approximately 7.5 kb with a single open reading frame flanked by 5'- and 3'-untranslated regions (UTR) and is enclosed in a capsid. While the 5' end is covalently attached to a viral protein genome-linked (VPg) required for replication, the polyadenylated 3' terminus is important not only for the negative-stranded RNA synthesis but also for translation and RNA stability (Zoll et al., 2009; Kempf and Barton, 2015). The life cycle of enteroviruses begins with binding to one or more specific receptors on the cell surface. The cell receptors for enteroviruses are quite divergent. For example, the cell surface receptor for PV is cluster of differentiation 155 (CD155), whereas EV-A71 has nine cell surface receptors including human scavenger receptor class B member 2 (hSCARB2), human P-selectin glycoprotein ligand 1 (hPSGL1), annexin II (Anx2), heparan sulfate, sialylated glycan, dendritic cell-specific ICAM3-grabbing non-integrin, vimentin, nucleolin and human tryptophanyl-tRNA synthetase (hWARS) (Baggen et al., 2018; Yeung et al., 2018). Receptor binding allows viruses to enter host cells via receptor-mediated endocytosis. There are several endocytic pathways that can mediate the entry of receptor-bound enterovirus particles at the plasma membrane, including macropinocytosis, clathrin-dependent endocytosis and clathrin-independent uptake such as caveolae-dependent and non-caveolae-dependent endocytosis (Marjomaki et al., 2015). The specific endocytic pathways that virus exploits to enter the cells depend on the viral species and serotype, host cell type and local microenvironment (such as pH and temperature). For instance, EV-A71 enters rhabdomyosarcoma (RD) cells through the clathrin-dependent pathway, whereas the caveolae-mediated pathway is used to enter Jurkat cells. EV-A71 exhibits distinct endocytic pathways in different host cells, partly because of the

diversity of the EV-A71 surface receptors (Yamayoshi et al., 2014). Upon entry into host cells, virus uncoating releases its viral RNA genome into the cytoplasm and translation is initiated from an internal ribosome sequence in the 5' UTR, which is called internal ribosome entry site (IRES). An IRES is a *cis*-acting RNA element that forms secondary and tertiary structures to allow cap-independent initiation of translation (Shih et al., 2011; Lee et al., 2017). Translation of viral RNA yields a single polyprotein, which is proteolytically processed by viral proteases to produce four capsid proteins (VP4, VP2, VP3, and VP1) required for virion packaging, and seven non-structural proteins (2A-2B-2C and 3A-3B-3C-3D<sup>Pol</sup>) as well as some stable precursors, which function in virus replication and disrupting the host cellular immune system. Viral RNA replication is catalyzed by the virally encoded RNA-dependent RNA polymerases, 3D<sup>Pol</sup>, which utilizes Vpg as a protein primer to initiate the replication process. The synthesis of viral RNA takes place on the virus-induced remodeling of intracellular membranes that form replication organelles and leads to double-stranded RNA formation, which in turn will be transcribed into positive single-stranded RNA (Hsu et al., 2010; van der Schaar et al., 2016). Newly synthesized RNA may either serve as a template for translation and replication or be packaged into new infectious virions.

## CNS INVASION

Enteroviruses infect humans primarily through the fecal-oral route and replicate in the gastrointestinal tract with the exception of some enteroviruses, e.g., rhinovirus and EV-D68, which can cause respiratory infection and spread via respiratory secretion. After initial infection in the first exposed area, the enteroviruses can gain access to the CNS through multiple pathways, which are not mutually exclusive (**Figure 1**; Rhoades et al., 2011; Huang and Shih, 2015). First, most neurotropic viruses including enteroviruses spread through the bloodstream to reach the CNS. The spread of virus particles from the blood to the CNS is normally restricted by the blood brain barrier (BBB), which is a highly selective semipermeable barrier between the brain's blood vessels and the cells in the brain. However, BBB integrity can be compromised by direct infection of the brain microvascular endothelial cells (BMECs) that make up the BBB or by the cytokines that are produced locally in the CNS during viral infections. For example, PV has been shown to invade the CNS via BBB transmission (Yang et al., 1997). Recent evidence has further demonstrated that mouse transferrin receptor 1 is responsible for PV attachment to the cell surface of BMECs, allowing invasion into the CNS via the BBB (Mizutani et al., 2016). Secondly, enteroviruses can invade the CNS through the peripheral circulating immune cells, which carry intracellular viruses (Tabor-Godwin et al., 2010). This is known as the Trojan horse route. Although the brain has been considered a site of immune-privilege, it has an active immune surveillance system that involves the recruitment of non-specific leukocytes such as phagocytes and lymphocytes into the meninges and cerebrospinal fluid (CSF) (Forrester et al., 2018). Indeed, it has been shown that the CSF contains a trafficking population of mononuclear

**TABLE 1** | Neurological symptoms of non-polio enteroviruses that involve the CNS.

Species	Serotype	CNS symptoms	References	
A	EV-A71	E/M/AFP	Huang Y. et al., 2015; Mao et al., 2016; B'Krong et al., 2018; Suresh et al., 2018; Ramalho et al., 2019	
	EV-A76	AFP	Suresh et al., 2018	
	EV-A90	AFP	Suresh et al., 2018	
	CV-A2	M/AFP	Holmes et al., 2016; Suresh et al., 2018	
	CV-A3	AFP	Suresh et al., 2018	
	CV-A4	AFP	Suresh et al., 2018	
	CV-A5	AFP	Suresh et al., 2018	
	CV-A6	E/M/AFP	Huang Y. et al., 2015; Holmes et al., 2016; Suresh et al., 2018	
	CV-A7	AFP	Suresh et al., 2018	
	CV-A10	E/M/AFP	Huang Y. et al., 2015; Mao et al., 2016; B'Krong et al., 2018; Suresh et al., 2018	
	CV-A12	AFP	B'Krong et al., 2018; Suresh et al., 2018	
	CV-A14	AFP	Suresh et al., 2018	
	CV-A16	E/M/AFP	Goto et al., 2009; Xu et al., 2012; Huang Y. et al., 2015; Holmes et al., 2016; Suresh et al., 2018	
	B	CV-A9	E/M/AFP	Holmes et al., 2016; Chen et al., 2017; B'Krong et al., 2018; Suresh et al., 2018; Ramalho et al., 2019; Sun et al., 2019
		CV-B1	E/M/AFP	Holmes et al., 2016; B'Krong et al., 2018; Suresh et al., 2018; Fan and Liu, 2019; Ramalho et al., 2019; Sun et al., 2019
		CV-B2	E/M/AFP	Holmes et al., 2016; B'Krong et al., 2018; Suresh et al., 2018; Fan and Liu, 2019; Ramalho et al., 2019
CV-B3		E/M/AFP	Holmes et al., 2016; Mao et al., 2016; Mao et al., 2018; Suresh et al., 2018; Fan and Liu, 2019; Ramalho et al., 2019; Sun et al., 2019	
CV-B4		E/M/AFP	Holmes et al., 2016; Mao et al., 2016; B'Krong et al., 2018; Mao et al., 2018; Suresh et al., 2018; Sun et al., 2019	
CV-B5		E/M/AFP	Holmes et al., 2016; Mao et al., 2016; Chen et al., 2017; B'Krong et al., 2018; Mao et al., 2018; Suresh et al., 2018; Ramalho et al., 2019; Sun et al., 2019	
CV-B6		M/AFP	Tapparel et al., 2013; Suresh et al., 2018	
E-1		M/AFP	Tapparel et al., 2013; Suresh et al., 2018	
E-2		M/AFP	Tapparel et al., 2013; Suresh et al., 2018	
E-3		E/M/AFP	Tapparel et al., 2013; Suresh et al., 2018; Ramalho et al., 2019	
E-4		E/M/AFP	Tapparel et al., 2013; B'Krong et al., 2018; Suresh et al., 2018	
E-5		E/M/AFP	Tapparel et al., 2013; Holmes et al., 2016; Suresh et al., 2018	
E-6		E/M/AFP	Holmes et al., 2016; Chen et al., 2017; B'Krong et al., 2018; Suresh et al., 2018; Ramalho et al., 2019; Sun et al., 2019	
E-7		E/M/AFP	Tapparel et al., 2013; Holmes et al., 2016; Suresh et al., 2018; Ramalho et al., 2019	
E-9		E/M/AFP	Holmes et al., 2016; B'Krong et al., 2018; Suresh et al., 2018; Ramalho et al., 2019; Sun et al., 2019	
E-11		E/M/AFP	Holmes et al., 2016; Suresh et al., 2018; Ramalho et al., 2019; Sun et al., 2019	
E-12		M/AFP	Tapparel et al., 2013; B'Krong et al., 2018; Suresh et al., 2018	
E-13		E/M/AFP	Tapparel et al., 2013; Holmes et al., 2016; Suresh et al., 2018; Ramalho et al., 2019	
E-14		E/M/AFP	Chen et al., 2017; Suresh et al., 2018; Ramalho et al., 2019; Sun et al., 2019	
E-15		M/AFP	Suresh et al., 2018; Ramalho et al., 2019	
E-16		E/M/AFP	Holmes et al., 2016; B'Krong et al., 2018; Suresh et al., 2018; Sun et al., 2019	
E-17		E/M/AFP	Tapparel et al., 2013; Holmes et al., 2016; Suresh et al., 2018	
E-18		E/M/AFP	Holmes et al., 2016; Chen et al., 2017; B'Krong et al., 2018; Suresh et al., 2018; Chen et al., 2019; Ramalho et al., 2019; Sun et al., 2019	
E-19		E/M/AFP	Tapparel et al., 2013; B'Krong et al., 2018; Suresh et al., 2018	
E-20		M/AFP	Tapparel et al., 2013; Suresh et al., 2018	
E-21		E/M/AFP	Holmes et al., 2016; Suresh et al., 2018; Ramalho et al., 2019; Sun et al., 2019	
E-22		AFP	Suresh et al., 2018	
E-24		E/M/AFP	Tapparel et al., 2013; B'Krong et al., 2018; Suresh et al., 2018	
E-25		E/M/AFP	Holmes et al., 2016; B'Krong et al., 2018; Suresh et al., 2018; Ramalho et al., 2019; Sun et al., 2019	
E-26		AFP	Suresh et al., 2018	
E-27		E/M/AFP	Tapparel et al., 2013; B'Krong et al., 2018; Suresh et al., 2018	
E-29		M/AFP	Tapparel et al., 2013; Suresh et al., 2018	
E-30		E/M/AFP	Holmes et al., 2016; Mao et al., 2016; Chen et al., 2017; B'Krong et al., 2018; Suresh et al., 2018; Ramalho et al., 2019; Sun et al., 2019	
E-31	M/AFP	Tapparel et al., 2013; Suresh et al., 2018		
E-32	M/AFP	Tapparel et al., 2013; Suresh et al., 2018		
E-33	E/M/AFP	Tapparel et al., 2013; Suresh et al., 2018; Sun et al., 2019		
EV-B73	AFP	Suresh et al., 2018		

*(Continued)*

TABLE 1 | Continued

Species	Serotype	CNS symptoms	References
	EV-B74	AFP	Suresh et al., 2018
	EV-B75	AFP	Tapparel et al., 2013; Suresh et al., 2018
	EV-B77	AFP	Tapparel et al., 2013; Suresh et al., 2018
	EV-B79	AFP	Suresh et al., 2018
	EV-B80	AFP	Suresh et al., 2018
	EV-B81	AFP	Tapparel et al., 2013; Suresh et al., 2018
	EV-B85	AFP	Tapparel et al., 2013; Suresh et al., 2018
	EV-B86	AFP	Tapparel et al., 2013; Suresh et al., 2018
	EV-B87	AFP	Tapparel et al., 2013; Suresh et al., 2018
	EV-B88	AFP	Tapparel et al., 2013; Suresh et al., 2018
	EV-B93	AFP	Tapparel et al., 2013; Suresh et al., 2018
	EV-B97	AFP	Tapparel et al., 2013; Suresh et al., 2018
	EV-B100	AFP	Tapparel et al., 2013; Suresh et al., 2018
	EV-B106	AFP	Suresh et al., 2018
	EV-B107	AFP	Suresh et al., 2018
C	CV-A1	AFP	Tapparel et al., 2013
	CV-A11	E/M/AFP	Tapparel et al., 2013; Suresh et al., 2018
	CV-A13	E/M/AFP	Tapparel et al., 2013; Suresh et al., 2018
	CV-A17	M/AFP	Tapparel et al., 2013; Suresh et al., 2018
	CV-A20	AFP	Tapparel et al., 2013; Suresh et al., 2018
	CV-A21	AFP	Tapparel et al., 2013
	CV-A22	M/AFP	Suresh et al., 2018
	CV-A24	M/AFP	Tapparel et al., 2013; Suresh et al., 2018
	EV-C96	AFP	Tapparel et al., 2013; B'Krong et al., 2018; Suresh et al., 2018
	EV-C99	AFP	Suresh et al., 2018
	EV-C109	AFP	Tapparel et al., 2013
D	EV-D68	E/M/AFP	Tapparel et al., 2013; Messacar et al., 2018; Suresh et al., 2018
	EV-D70	E/M/AFP	Tapparel et al., 2013; Suresh et al., 2018
	EV-D94	AFP	Tapparel et al., 2013; Suresh et al., 2018

E, encephalitis; M, meningitis; AFP, acute flaccid paralysis.

cells, consisting of T cells (~90%), B cells (~5%), monocytes (~5%), and dendritic cells (<1%) (Ransohoff and Engelhardt, 2012). Once these leukocytes are infected, they can act as carriers to bring viruses into the CNS. For instance, CV-B3-infected myeloid cells have been shown to cross the blood-CSF barrier in the choroid plexus (Tabor-Godwin et al., 2010). Upon entry into the CNS, the virus is likely released from myeloid cells and subsequently infect neurons and/or glia in the brain. There is also evidence that EV-A71 can infect leukocytes through binding to hPSGL1, a sialomucin membrane protein primarily expressed on leukocytes (Nishimura et al., 2009). Whether EV-A71-infected leukocytes can bring viruses into the CNS is not clear. Thirdly, certain enteroviruses can enter the CNS through peripheral nerves via retrograde axonal transport and *trans-synaptic* propagation (Gromeier and Wimmer, 1998; Chen et al., 2007; Ong et al., 2008). Axonal transport is an essential cellular process in neurons required for the movement of synaptic vesicles, lipids, proteins, and organelles including mitochondria, lysosomes, autophagosomes, and endosomes, to and from the cell body. It is well known that some neurotropic viruses can hijack the retrograde axonal transport to invade the CNS. For example, studies have shown that intramuscularly inoculated

PV is taken up by endocytosis at the neuromuscular junctions (Ohka et al., 2004). The endocytosed viral particles in the axon terminal are moved in the retrograde direction toward the cell body via dynein-mediated vesicular transport without initiating uncoating (Ohka et al., 2009). The uncoating event takes place upon arrival at the cell body of the motor neuron. EV-A71 and EV-D68 can also enter and infect the CNS by retrograde axonal transport via peripheral spinal motor nerves (Chen et al., 2007; Ong et al., 2008; Hixon et al., 2019). Interestingly, a recent report has demonstrated that EV-A71 can directly infect the brainstem via cranial nerves, suggesting that the virus can use not only the motor components of spinal nerves but also cranial nerves to enter the CNS (Tan et al., 2014).

## TROPISM

Each enterovirus has a distinct tropism that is determined by a combination of host and virus factors (Figure 2; Lin and Shih, 2014). Although neurotropic enteroviruses can invade the CNS and are associated with neurological disorders, dissemination of the virus to the CNS seems to occur sporadically and it is not clear

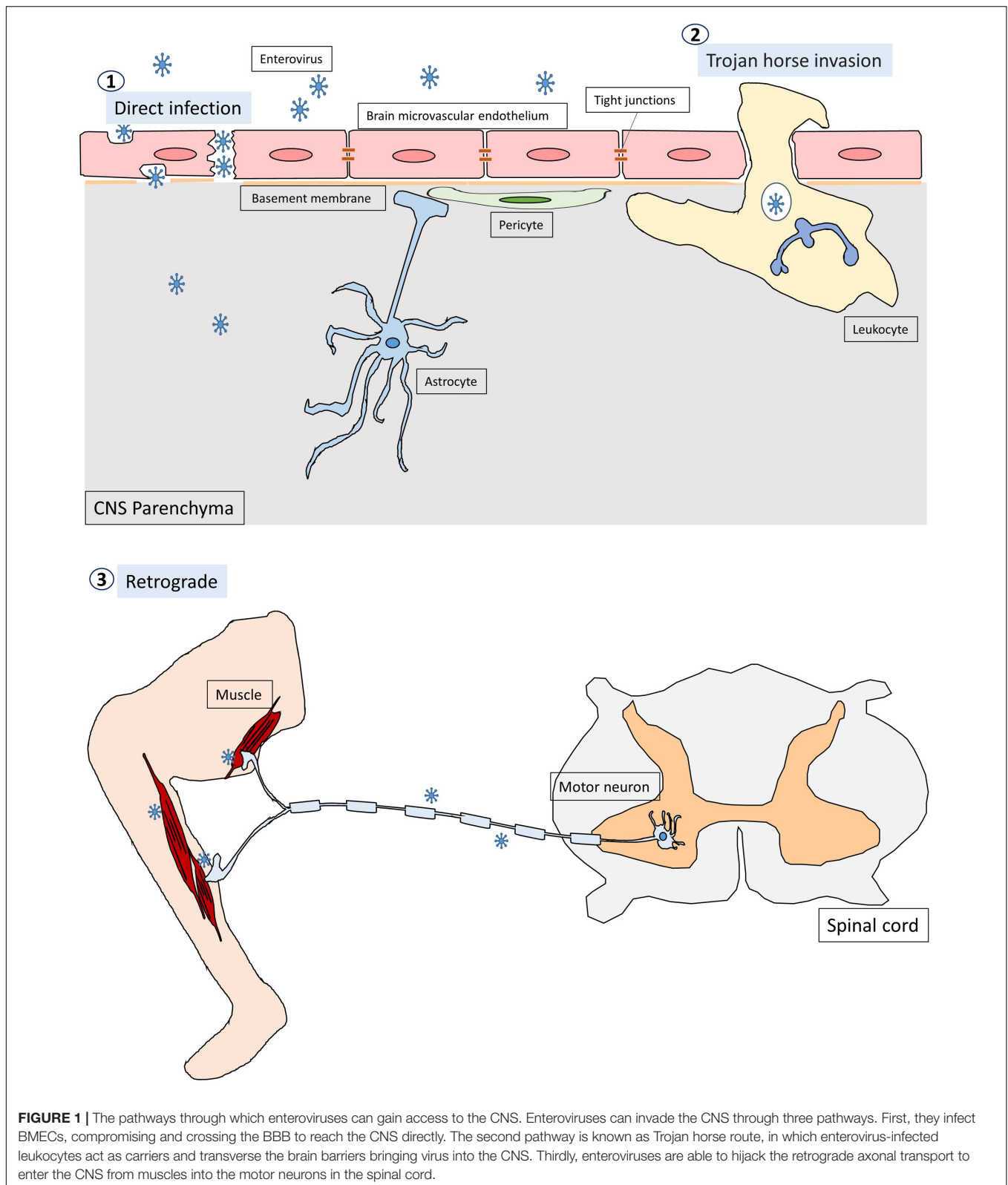
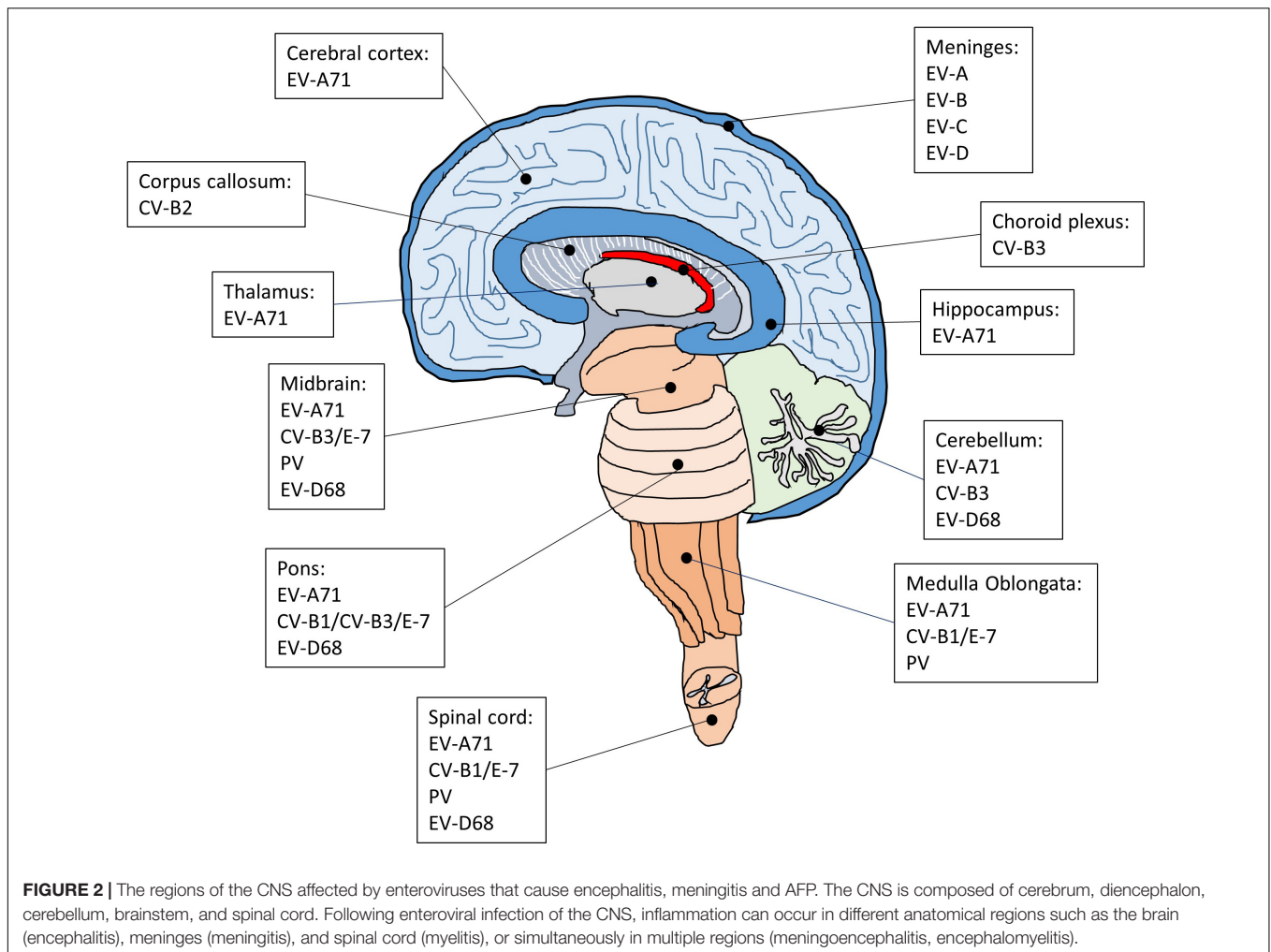


**FIGURE 1 |** The pathways through which enteroviruses can gain access to the CNS. Enteroviruses can invade the CNS through three pathways. First, they infect BMECs, compromising and crossing the BBB to reach the CNS directly. The second pathway is known as Trojan horse route, in which enterovirus-infected leukocytes act as carriers and transverse the brain barriers bringing virus into the CNS. Thirdly, enteroviruses are able to hijack the retrograde axonal transport to enter the CNS from muscles into the motor neurons in the spinal cord.

how enterovirus targets specific regions and cell types in the brain and spinal cord. Earlier studies on poliovirus have suggested that virus tropism is determined by the cellular receptor for virus

entry (Holland, 1961). However, the PV receptor CD155 is found in tissues that are not sites of PV infection (Mendelsohn et al., 1989; Freistadt et al., 1990; Koike et al., 1990), indicating that the



cellular receptor is required for susceptibility to PV infection but not the sole determinant for virus tropism. Subsequent studies have suggested that the tissue-specific activity of IRES on viral RNAs also plays an important role in determining virus tropism (Gromeier et al., 1996; Yanagiya et al., 2003). For example, a chimeric PV carrying the IRES of hepatitis C virus replicates well in the liver but not in the brain of a mouse model for poliomyelitis, whereas the control poliovirus replicates well both in the liver and brain (Yanagiya et al., 2003). There is also evidence that innate immune antiviral activities such as the interferon (IFN) response is critical for virus tropism (Wessely et al., 2001; Ida-Hosonuma et al., 2005). In transgenic mice containing human CD155, PV replicates and produces severe lesions in the brain and spinal cord, whereas other tissues did not show severe pathological changes. However, in the CD155 transgenic mice lacking alpha/beta IFN, severe lesions are detected in the liver, spleen, and pancreas in addition to the CNS, suggesting that the alpha/beta IFN system is an important determinant for the differential susceptibility of tissue to PV. Poliovirus invades the CNS, which leads to the development of a paralytic disease in about 1% of virus-infected people (Melnick, 1996). Therefore, it has been suggested that, in 99% of the infected cases, the

IFN response limits PV replication in extraneural tissues to prevent the invasion of the CNS (Racaniello, 2006). In the CNS, PV infects and replicates mainly in motor neurons in the anterior horn of the spinal cord, resulting in poliomyelitis (Nagata et al., 2004; Arita et al., 2006). In the most severe cases, PV attacks the neurons of the brainstem, causing bulbar poliomyelitis. In addition to neurons, the CNS contains three major types of non-neuronal cells called glial cells, including astrocytes, oligodendrocytes, and microglia. These glial cells play critical roles in maintaining homeostasis, myelin formation and providing support and protection for neurons. Interestingly, astrocytes and oligodendrocytes are also susceptible to PV infection in primary mouse culture prepared from the cerebral cortex of neonatal CD155 transgenic mice (Couderc et al., 2002). Whether these glial cells are targets for PV infection in the human brain is not known.

Although EV-A71 also invade the CNS, the infected areas are quite distinct compared with poliovirus. Brainstem encephalitis is the most common neurological presentation of EV-A71 infection. Consistently, viral lesions are mainly observed in the brainstem and predominantly located in the ventral, medial and caudal areas of the medulla oblongata (Kao et al., 2004). A few

lesions are also found in the cortex, cerebellum, and spinal cord. In severe cases of EV-A71 infection, the major histopathological changes in the CNS are characterized by inflammatory damage, which selectively leads to neurogenic pulmonary edema and cardiac failure. In agreement with the main CNS lesion locations of EV-A71 infection, the neurons in the medulla oblongata have been implicated in the onset of neurogenic pulmonary edema (Davison et al., 2012). In addition, several autopsy results have suggested that EV-A71 may infect neurons and cause neuronal degeneration, which would activate inflammatory responses in the lesion area and cause encephalitis (Yan et al., 2000; Khong et al., 2012; Yao et al., 2012). Indeed, studies have shown that neurons are susceptible to EV-A71 infection (Huang et al., 2014; Feng et al., 2016). Intriguingly, although neurons can be infected by EV-A71, neural progenitor cells and astrocytes appear to be the main targets for EV-A71 infection in the CNS (Huang et al., 2014; Feng et al., 2016). Both of these cell types are similar in that they are capable of mitosis, which may be critical for virus replication (Yu et al., 2015). Neural progenitor cells are the progenitor cells of the CNS that give rise to many, if not all, of the neuronal and glial cell types and are important for many brain functions including learning and memory and cognition. Thus, the loss of neural progenitor cells due to EV-A71 infection may cause long-term abnormalities of the CNS. This is supported by a long-term follow-up study showing that a large proportion of children after EV-A71 infection with severe CNS involvement and cardiopulmonary failure exhibited delayed neurodevelopment and reduced cognitive function (Chang et al., 2007). Astrocytes also perform many functions in the brain, such as contribution to the formation of the blood-brain barrier, maintenance of extracellular ionic and chemical homeostasis and involvement in the injury response. Since astrocytes are mitotic and localized in a much broader area in the brain than neural progenitor cells, the preferential infection of astrocytes over neurons may create a reservoir for viral proliferation and enable the viral progeny to quickly spread in the CNS and induce massive inflammatory responses. It would be of interest to understand how EV-A71 show a preference for neural progenitor cells and astrocytes.

Similar to EV-A71, coxsackievirus has also been shown to infect neural progenitor cells in addition to neurons (Feuer et al., 2005). Studies have revealed that CV-B3 can infect proliferating neural progenitor cells located in the neonatal subventricular zone and hippocampus. Interestingly, CV-B3 preferentially replicates and induces cytopathic effects in undifferentiated neural progenitor cells (Tsueng et al., 2011). CV-B3 mediated loss of neural progenitor cells leads to a rapid decline in neurogenesis and may eventually cause developmental defects and CNS dysfunction (Ruller et al., 2012). However, the determinants of CV-B3 tropism in the CNS remain unclear. CV-B3 binds to target cells through two main receptors: decay-accelerating factor (DAF) (Bergelson et al., 1995) and coxsackievirus and adenovirus receptor (CAR) (Bergelson, 2009), which has been found to be highly expressed in the developing brain (Xu and Crowell, 1996). There is evidence that immature neurons express relatively high levels of CAR compare to their fully differentiated counterparts (Ahn et al., 2008), suggesting that the level of virus

receptor is one of the critical determinants in preferential virus replication in undifferentiated neural progenitor cells. Besides, CAR exists as multiple isoforms and a specific isoform of CAR that is expressed at high levels in human pancreatic beta cells has been suggested to be prone to coxsackievirus infection (Ifie et al., 2018). Whether this specific isoform of CAR plays a role in coxsackievirus infection in the CNS is not known.

## PERSISTENT INFECTION

Though enteroviruses have been considered as cytolitic viruses and diseases caused by infection with enteroviruses are typically short-lived, several studies have indicated that some enteroviruses may be associated with lifelong disorders including post-polio syndrome (Muir et al., 1995; Julien et al., 1999), schizophrenia (Rantakallio et al., 1997; Suvisaari et al., 2003; Khandaker et al., 2012), amyotrophic lateral sclerosis (Woodall et al., 1994; Berger et al., 2000; Giraud et al., 2001), type 1 diabetes (Richardson and Morgan, 2018), and chronic viral cardiomyopathy (Chapman and Kim, 2008). The cause of these enterovirus-associated lifelong disorders is still not clear, but it has been hypothesized that persistent infection of enterovirus may occur based on the presence of enterovirus RNA and protein in the affected tissues at stages of disease after acute infection (Chapman and Kim, 2008). Consistently, the spread of enteroviruses within tissues is not always accompanied by cell death (Bird et al., 2014). Two major groups of persistent infection have been observed *in vitro* (Pinkert et al., 2011). One group, called steady-state infection, is characterized by infection of all cells, while the other group, named carrier-state infection, is characterized by a cytolitic infection of a small proportion of cells, which spares the majority of cells in culture from cytolysis. There is evidence that enteroviruses establish carrier-state infection *in vitro* (Heim et al., 1992; Heim et al., 1995; Pinkert et al., 2011). The carrier-state infection is thought to be induced by the selection of virus mutants that are less cytopathic and may involve the coevolution of both cells and viruses. For example, following CV-B3 infection, expression of the CV-B3 receptor CAR has evolved to be downregulated or eliminated in a subpopulation of cells (Pinkert et al., 2011), which is known to be associated with a decrease of CV-B3 infection and cell lysis (Werk et al., 2005; Fechner et al., 2007). As a result, these evolved cells are protected from virus infection and cell lysis and become dominant in the culture within several passages. In the meantime, the virus also adapts to persist by gaining a CAR-independent entry mechanism (Pinkert et al., 2011). Thus, during the development of persistent infection, viruses and cells have co-evolved such that cellular resistance to viral replication is balanced. In addition to the coevolution model, other viral genomic alterations that cause persistent infection have been reported in the highly conserved 5' UTR, which is critical for viral replication. For instance, CV-B mutants with deletions in the 5' end of the viral genome persist in host tissues, and RNA of the variants can be stably detected from heart tissue of mice experimentally inoculated with wild type CV-B3 and from human cases of

myocarditis (Kim et al., 2005; Chapman et al., 2008; Kim et al., 2008), suggesting that viral replication is important for persistent infection *in vivo*. Nonetheless, it has also been suggested that persistence of CV-B1 RNA in skeletal muscle or CV-B3 RNA in the CNS is not facilitated by genetic alterations that give rise to replication-defective forms, but occurs primarily through formation of stable and atypical double-stranded RNA complex (Tam and Messner, 1999; Feuer et al., 2009). Interestingly, besides the reduction of CAR, other cellular factors have also been shown to play an important role in persistent infection of CV-B3. In particular, CV-B3 replication is affected by the cell cycle status, suggesting that the persistence of CV-B3 may depend on infection of quiescent cells in which viral replication is lowered or suppressed (Feuer et al., 2002; Feuer et al., 2004). Therefore, the differences between these mechanisms are likely due to distinct patterns of virus-host interactions and there may be tissue- or cell-specific mechanisms for establishing a persistent infection.

Early viral infection of the CNS can cause severe physical and intellectual disability and, in some cases, results in unexpected neurological disorders years after acute infection. For example, approximately 30 percent of polio victims experience new symptoms (post-polio syndrome) about 50 years after the primary infection. Some studies have shown that post-polio syndrome is correlated with the presence of viral RNA in the CNS, suggesting that PV can persist and cause long-term damage in the CNS (Muir et al., 1995). In consistent with these findings, it has been shown that poliovirus strains are not fully lytic in neuroblastoma cell lines (Colbere-Garapin et al., 1989). Following PV infection, massive cytopathic effects are observed in cultured cells, but some cells survive infection without further observable cytopathic effects in spite of continuous viral production. During persistent infection, PV mutants are constantly selected, and many of the identified mutations occur at positions known to be involved in the binding of PV receptors, suggesting that the interactions of the virus with its receptor is critical for the establishment of persistent infections (Colbere-Garapin et al., 1998). Although there is not a single mechanism for establishing a persistent infection, it is believed that the virus must evade host's antiviral immune response. Because enteroviruses have high mutation rates due to the lack of proofreading ability in RNA polymerases, they can generate a variety of mutants not only to affect receptor binding and virus replication but also to evade the immune system. The CNS is relatively inaccessible to immune surveillance compared with other tissues, which makes it particularly vulnerable to persistent infection. Using *in vivo* imaging, a recent study has demonstrated that EV-A71 infection of AG129 mice, in which alpha/beta and gamma interferon receptors are deficient, shows rapid spread and long-term persistence of the virus in the brain of surviving animals (Caine and Osorio, 2017). Interestingly, high viral loads are maintained in the brain even at 6 weeks following infection, whereas viral loads in other tissues including heart, lung, liver, spleen and intestine are gradually reduced to a lower level. In agreement with these findings, *in vitro* studies have shown that in contrast to RD cells or neuroblastoma cell lines, motor neuron-like hybrid cell line (NSC-34) infected by EV-A71 does not display cytopathic effect and the viral particles adopt a non-lytic

exit pathway through autophagy (Too et al., 2016). Furthermore, there is evidence that EV-A71 RNA is present in stool weeks after initial infection (Han et al., 2010). Taken together, all these findings suggest that similar to PV and CV-B3, EV-A71 can also establish a persistent infection in the CNS, but the long-term impact of EV-A71 infection in the CNS remains elusive.

## NEUROVIRULENCE

Some enteroviruses can cause diseases within the nervous system. The most thoroughly studied neurovirulent enterovirus is PV. To eradicate global poliomyelitis, much effort has been made to develop polio vaccines including an inactivated PV given by injection and an attenuated PV given by mouth. Although both types of polio vaccines are effective, oral polio vaccines are superior not only in administration but also in providing longer-lasting immunity. The attenuated PV was developed based on the observation that the virus no longer caused disease after many passages in different animals and cell cultures, but replicated sufficiently to induce protective immunity. Genetic analysis of the attenuated PV has shown that a point mutation within the IRES of the vaccine strains is a critical determinant of the attenuation phenotype (Evans et al., 1985; Kawamura et al., 1989; Ren et al., 1991). For instance, the C472U mutation in the IRES of poliovirus type 3 causes a translation defect, which leads to reduced replication in the CNS and attenuation of neurovirulence (La Monica and Racaniello, 1989; Gutierrez et al., 1997; Ohka and Nomoto, 2001). Subsequent studies have shown that the C472U mutation reduces the efficiency of binding of the polypyrimidine-tract binding protein (PTB) to the IRES, which is required for initiation of translation (Guest et al., 2004). Sequence analysis has also identified additional mutations in the capsid region of the vaccine strains. These capsid mutations are likely to disrupt viral particle binding to host cells and reduce the capsid stability, which may contribute to and stabilize the attenuation phenotype. However, PV is notably adaptable and attenuated viruses can increase its virulence through mutation and/or recombination (Jorba et al., 2008; Minor, 2009). Thus, although unusual, immunization with the attenuated vaccine strains may cause vaccine-associated paralytic poliomyelitis, which could be due to the reversion of the mutations in the viral genome that confer the attenuation phenotype and/or acquisition of new mutations with enhanced virulence (Kew et al., 2005; Famulare et al., 2016). Moreover, these vaccine-derived polioviruses (VDPV) have caused outbreaks of poliomyelitis in areas with low routine immunization rates (Burki, 2019). Using approach combining phylogenetic analysis of sequence data from outbreaks of VDPV and an experimental evolution approach in cell culture, a recent study has provided a model describing the evolutionary steps sufficient for the vaccine strain to lose its attenuation and become virulent (Stern et al., 2017). In the first step, the critical mutations for the attenuation phenotype are reverted to increase the viral replication. This is followed by recombination events with co-circulating enterovirus strains, most often a coxsackievirus strain, but in some cases a circulating PV strain to optimize viral replication in the

human gut. In the final step, the virus continues to slowly revert to sequences that are conserved across wild-type PV to enhance the fitness of the virus. The information provides a powerful framework for developing safer vaccine strains and for forecasting virulence of viruses.

EV-A71 has emerged as a serious threat to public health across the Asia-Pacific region. EV-A71 causes hand, foot and mouth disease (HFMD) and herpangina, and occasionally severe neurological disorders. Unlike PV in which a point mutation within the IRES can attenuate neurovirulence, the association between EV-A71 neurovirulence and viral genome sequences remains largely unknown. So far, there are only a few reports showing that the neurovirulence can be weakened by mutations in the viral genome of EV-A71. For example, studies have shown that defined genetic manipulation of the EV-A71 genome based on the temperature-sensitive determinants of a poliovirus vaccine strain results in attenuated neurovirulence in monkeys (Arita et al., 2005). The generated EV-A71 mutant strain contains four mutations in the conserved regions of the enterovirus genome including one in the 5' UTR, two in the 3D polymerase gene and one in the 3' UTR, and all of them are required for substantial attenuation (Arita et al., 2008). Like PV, the capsid proteins also play an important role in EV-A71 virulence. For instance, the amino acid residue 145 of EV-A71 VP1, which affects receptor usage for cell surface attachment of the viral particles (Nishimura et al., 2013; Tan et al., 2017), has been shown to confer mouse adaptation with a G145E replacement (Arita et al., 2008; Chua et al., 2008) and influence the virulence in mice (Chua et al., 2008; Zaini and McMinn, 2012). Consistent with earlier results, a recent study has further demonstrated that the VP1-145 is a key determinant for EV-A71 neurovirulence in monkeys (Fujii et al., 2018). In addition, changes of nucleotides in the 5' UTR and an amino acid replacement in the 2A or 3C protein have been identified to play an important role for virulence determination of EV-A71 (Li et al., 2011; Yeh et al., 2011; Li et al., 2017). Whether they attenuate EV-A71 neurovirulence is unknown. Nonetheless, it is expected that all these findings would contribute to not only our understanding of EV-A71 but also the development of live attenuated EV-A71 vaccine in the future.

EV-D68 is another non-polio enterovirus that has an association with a polio-like neurological disorder known as acute flaccid myelitis (AFM) with symptoms such as dysnesia and muscle weakness although the most common clinical symptom of EV-D68 infection is respiratory illness (Holm-Hansen et al., 2016; Messacar et al., 2018). EV-D68 is quite unique among enteroviruses because it carries some characteristic features of respiratory enteroviruses (Rhinovirus A-C) including optimal growth temperature of 33°C allowing better replication in the nasal cavity and inability to survive in the stomach due to acid sensitivity, but is genetically more closely related to enteric enteroviruses based on phylogenetic analysis. EV-D68 has become an emerging pathogen since an outbreak occurred in 2014 in the United States. Studies have shown that six mutations including M291T, V341A, T860N, D297N, S1108G, and R2005K are associated with neurovirulence of the outbreak EV-D68 strains causing AFM in 2014 (Greninger et al., 2015). Interestingly, another study has identified 3 nucleotide variables,

C1817T, C3277A, and A4020G, in the 2014 outbreak strains, which differ significantly from previously identified EV-D68 strains (Huang W. et al., 2015). Among these three variables, C3277A causes amino acid substitution T860N in the protease 2A cleavage site between VP1 and 2A, whereas A4020G results in amino acid substitution S1108G in a protease 3C cleavage site between 2B and 2C, suggesting that mutation of these two sites may alter the cleavage efficiency and increase replication and transmission rates. However, using a mouse model of paralytic myelitis caused by EV-D68, a recent study has shown that the 2014 outbreak EV-D68 strains isolated from patients without AFM can also produce paralysis in neonatal mice (Hixon et al., 2017). Thus, further comparative analyses using infectious clones containing different combinations of previously identified mutations will be needed to establish the determinants of EV-D68 neurovirulence.

## IMMUNE RESPONSES IN THE CNS

About 3% of enterovirus infected people will develop encephalitis while most people never show evidence of CNS infection (Koskiniemi et al., 1991). Since encephalitis only occurs in a small percentage of infected people, it is thought that host-pathogen interactions and immune responses in peripheral sites prevent viruses from gaining access to and causing infection within the CNS. Patients with enterovirus encephalitis may present symptoms that range in severity from mild cognitive impairment and memory loss to permanent CNS damage and death. The symptoms are mainly caused by virus-induced inflammatory responses in the brain. Inflammation is the body's protective immune response against infection, but the brain was thought to be immune-privileged based on two predominant beliefs. First, the BBB prevents the entry of circulating immune cells and antibodies into the brain. Secondly, there is no lymphatic drainage to alert the immune system to the presence of CNS antigens. However, these two beliefs have been questioned by the detection of small numbers of leukocytes in the CSF and the newly identified lymphatics that allow leukocyte egress (Engelhardt et al., 2017). In addition to the BBB, two other brain barrier structures have been described: (1) blood – CSF barrier to the choroid plexus, which is located at the ventricles of the brain, and (2) blood – CSF barrier to the pia arachnoid, which is located at the surface of the brain. It is important to note that CSF spaces in these two brain barriers do not exhibit the same immune privilege as the CNS parenchyma and contain diverse immune cells to monitor the CSF for the presence of immune signals in response to viral pathogens. Therefore, the immune privilege of the brain is not absolute but instead is relative to other organs.

Enterovirus encephalitis is reported to occur more frequently in younger children. Although the exact cause remains unknown, it has been suggested that a compromised or immature immune system may be involved in the observed effect. Studies have shown that expression of CD40-ligand on activated T cells and interleukin 4 (IL-4) production are significantly lower in EV-A71 infected children with meningoencephalitis than those without it (Yang et al., 2001). CD40-ligand plays a pivotal role

in co-stimulation and regulation of the immune responses. It binds to the CD40 receptor on antigen-presenting cells including B cells and macrophages to facilitate cell-cell communication and modulate adaptive immunity. Interleukin-4 (IL-4) is also a key regulator in adaptive immunity. It is a cytokine that has many functions including the stimulation of activated B cell and T cell proliferation and the differentiation of naïve helper T cells and B cells into Th2 cells and plasma cells, respectively. Thus, a reduction in CD40-ligand and IL-4 may indicate that adaptive immunity is compromised. In addition, differences in the polymorphism of the cytotoxic T lymphocyte antigen-4 (CTLA-4) have been noted between children with and without meningoencephalitis in the same study (Yang et al., 2001). CTLA-4 is a surface receptor on T cells, which functions to downregulate T cell activity and polymorphism of CTLA-4 has been shown to be associated with certain autoimmune diseases (Marron et al., 1997). Interestingly, a recent study has reported a correlation between human leukocyte antigen (HLA) genotype and enterovirus infectivity in young children (Sioofy-Khojine et al., 2018). Consistently, there is evidence that genetic differences between individuals may affect the immune response to infection (Kim-Hellmuth et al., 2017). Taken together, these results suggest that genetic factors may confer susceptibility to neurological complications following enterovirus infection.

Although genetic susceptibility may provide clues to why enterovirus encephalitis only occurs in some children but not in others, it cannot explain why younger children infected with enteroviruses are at higher risk for developing encephalitis. It has been suggested that the immaturity of the BBB in early development may account, at least in part, for the age-related difference in viral neuroinvasion (Saunders et al., 2014). The development of the BBB is a multistep process that starts with the growth of new vessels into the embryonic neuroectoderm from pre-existing vessels (Blanchette and Daneman, 2015). This is followed by the expression of tight junction proteins and nutrient transporter in BMECs that lines blood vessels in the brain. The BBB becomes mature as nascent vessels come into close contact with pericytes and astrocytes, which provide structural and functional support to the BBB. In addition, the other cell types present at the BBB, including neurons, microglia, and perivascular macrophages also contribute to the properties of the BBB (Banerjee and Bhat, 2007). Interestingly, it has been shown that the BBB is capable of restricting entry of proteins and small molecules during embryogenesis prior to postnatal astrocyte generation and ensheathment of the vessels (Daneman et al., 2010; Saunders et al., 2014), suggesting that the BBB is functionally mature even without astrocytes in early development. Although astrocytes are not required for initial BBB formation, there is strong evidence that astrocytes play an important role in regulating the function of the BBB during postnatal development (Haseloff et al., 2005). For example, astrocytes secrete trophic factors that lead to tighter tight junctions between BMECs (Dehouck et al., 1990; Rubin et al., 1991). In addition to its role in regulating the BBB, astrocytes receive signals from neighboring neurons and responding to them with the release of neuroactive substances to modulate synaptic strength in the CNS (Santello et al., 2019). Moreover,

there is also evidence that astrocytes convey signals from neurons to the vasculature, leading to arteriolar dilation and an increase in local blood flow (Anderson and Nedergaard, 2003; Zonta et al., 2003). Thus, astrocytes link neuronal activity to functional properties of the BBB. Given that astrocytes are critical for structural support and the maintenance of the BBB, the developing brain containing immature astrocytes may have higher BBB permeability compared to that in the adult brain and is likely to be more vulnerable to viral neuroinvasion.

The CNS immune system may also be involved in the age-related difference in developing enterovirus encephalitis. Microglia, the primary resident immune cells of the brain, play a key role in regulating signaling pathways during CNS inflammation (Rivest, 2009). Although microglia are phenotypically and developmentally different from peripheral macrophages, they use phagocytic and cytotoxic mechanisms to destroy foreign pathogens and act as antigen-presenting cells to initiate T cell-mediated adaptive immune responses similar to macrophages. In addition, microglia have been shown to induce the recruitment of monocytes into the brain during viral infection (Fekete et al., 2018). However, whether microglia are fully functional during early development is not clear. Microglia in the early postnatal brain exhibit different morphologies compared to the adult brain (Cuadros and Navascues, 1998). They are largely non-ramified and take on an amoeboid shape during early development, and gradually differentiate into mature/ramified microglia as the brain matures. Consistently, distinct sets of genes are expressed in microglia during different phases of development (Bennett et al., 2016; Matcovitch-Natan et al., 2016). The amoeboid morphology observed in developing microglia is similar to activated phagocytic microglia from the adult brain, suggesting that microglia are in a constitutively “activated” state in the developing brain (Lenz and Nelson, 2018). Interestingly, it has been shown that activated microglia produce inflammatory cytokines such as TNF $\alpha$  and IL-1 $\beta$  (Nishioku et al., 2010; Yang et al., 2015), that increase BBB permeability and downregulate tight-junction proteins between BMECs (Gu et al., 2015; Almutairi et al., 2016). Taken together, these results suggest that developing microglia may increase BBB permeability by releasing inflammatory cytokines. Intriguingly, another study has shown that gene expression profiles are distinct between activated microglia from the adult brain and microglia from a control neonatal brain (Włodarczyk et al., 2017). Therefore, developing microglia are not the same as adult “activated” microglia even both of them exhibit a remarkable similarity in morphology. Nonetheless, this may provide a logical explanation of why younger children infected with enteroviruses are at higher risk for developing encephalitis.

## CONCLUSION

Enterovirus infection is a major public health concern considering the increase in outbreaks of serious neurological complications. Although there has been considerable progress in studying the complex interplay between enteroviruses and the infected cell in a culture dish, more complicated interaction

between virus and host *in vivo* is largely unknown and how enteroviruses gain access to and spread in the well-protected CNS remains to be explored. For example, a common feature of enteroviral encephalitis is the involvement of brainstem (Wasserstrom et al., 1992; Huang et al., 1999; Shen et al., 1999; Lum et al., 2002; Brecht et al., 2010; Fan and Liu, 2019), but some studies have revealed cerebral white matter lesions without brainstem involvement in neonatal enteroviral encephalitis (Verboon-Macielek et al., 2006; Hirata et al., 2011; Wu et al., 2014; Correia et al., 2016), suggesting that age and brain maturation may play an important role in the pathogenesis of enteroviral encephalitis. In the current review, we propose that there is a causal link between the development of the neuroimmune system and enteroviral neuroinvasion and have suggested that the age-related difference in developing enterovirus encephalitis may be associated with the development of neuroimmune system such as maturation of astrocytes and/or microglia. Future work will need to include the further characterization of the complex interactions between host and enteroviruses using appropriate animal models and the developmental roles of astrocytes and microglia in

regulating BBB permeability. We also need to better understand the regulation of immune responses in the CNS caused by enteroviruses.

## AUTHOR CONTRIBUTIONS

All authors contributed to the writing and discussion of this review article and approved the final version of the manuscript. H-CL made the figure and table.

## FUNDING

This work was financially supported by the Research Center for Emerging Viral Infections from the Featured Areas Research Center Program within the framework of the Higher Education Sprout Project by the Ministry of Education (MOE) in Taiwan, the Ministry of Science and Technology (MOST), Taiwan (MOST 108-3017-F-182-001) and the Chang Gung Memorial Hospital (CORPD1J0061).

## REFERENCES

- Ahn, J., Jee, Y., Seo, I., Yoon, S. Y., Kim, D., Kim, Y. K., et al. (2008). Primary neurons become less susceptible to coxsackievirus B5 following maturation: the correlation with the decreased level of CAR expression on cell surface. *J. Med. Virol.* 80, 434–440. doi: 10.1002/jmv.21100
- Almutairi, M. M., Gong, C., Xu, Y. G., Chang, Y., and Shi, H. (2016). Factors controlling permeability of the blood-brain barrier. *Cell. Mol. Life Sci.* 73, 57–77. doi: 10.1007/s00018-015-2050-8
- Anderson, C. M., and Nedergaard, M. (2003). Astrocyte-mediated control of cerebral microcirculation. *Trends Neurosci.* 26, 340–344; author reply 344–345.
- Arita, M., Ami, Y., Wakita, T., and Shimizu, H. (2008). Cooperative effect of the attenuation determinants derived from poliovirus sabin 1 strain is essential for attenuation of Enterovirus 71 in the NOD/SCID mouse infection model. *J. Virol.* 82, 1787–1797. doi: 10.1128/jvi.01798-07
- Arita, M., Nagata, N., Sata, T., Miyamura, T., and Shimizu, H. (2006). Quantitative analysis of poliomyelitis-like paralysis in mice induced by a poliovirus replicon. *J. Gen. Virol.* 87, 3317–3327. doi: 10.1099/vir.0.82172-0
- Arita, M., Shimizu, H., Nagata, N., Ami, Y., Suzuki, Y., Sata, T., et al. (2005). Temperature-sensitive mutants of Enterovirus 71 show attenuation in cynomolgus monkeys. *J. Gen. Virol.* 86, 1391–1401. doi: 10.1099/vir.0.80784-0
- Baggen, J., Thibaut, H. J., Strating, J., and Van Kuppeveld, F. J. M. (2018). The life cycle of non-polio Enteroviruses and how to target it. *Nat. Rev. Microbiol.* 16, 368–381. doi: 10.1038/s41579-018-0005-4
- Balada-Llasat, J. M., Rosenthal, N., Hasbun, R., Zimmer, L., Bozzette, S., Duff, S., et al. (2019). Cost of managing meningitis and encephalitis among infants and children in the United States. *Diagn. Microbiol. Infect. Dis.* 93, 349–354. doi: 10.1016/j.diagmicrobio.2018.10.012
- Banerjee, S., and Bhat, M. A. (2007). Neuron-glia interactions in blood-brain barrier formation. *Annu. Rev. Neurosci.* 30, 235–258. doi: 10.1146/annurev.neuro.30.051606.094345
- Bennett, M. L., Bennett, F. C., Liddelow, S. A., Ajami, B., Zamanian, J. L., Fernhoff, N. B., et al. (2016). New tools for studying microglia in the mouse and human CNS. *Proc. Natl. Acad. Sci. U.S.A.* 113, E1738–E1746. doi: 10.1073/pnas.1525528113
- Bergelson, J. M. (2009). Intercellular junctional proteins as receptors and barriers to virus infection and spread. *Cell Host Microbe* 5, 517–521. doi: 10.1016/j.chom.2009.05.009
- Bergelson, J. M., Mohanty, J. G., Crowell, R. L., St John, N. F., Lublin, D. M., and Finberg, R. W. (1995). Coxsackievirus B3 adapted to growth in RD cells binds to decay-accelerating factor (CD55). *J. Virol.* 69, 1903–1906. doi: 10.1128/jvi.69.3.1903-1906.1995
- Berger, M. M., Kopp, N., Vital, C., Redl, B., Aymard, M., and Lina, B. (2000). Detection and cellular localization of Enterovirus RNA sequences in spinal cord of patients with ALS. *Neurology* 54, 20–25.
- Bird, S. W., Maynard, N. D., Covert, M. W., and Kirkegaard, K. (2014). Nonlytic viral spread enhanced by autophagy components. *Proc. Natl. Acad. Sci. U.S.A.* 111, 13081–13086. doi: 10.1073/pnas.1401437111
- B'Krong, N., Minh, N. N. Q., Qui, P. T., Chau, T. T. H., Nghia, H. D. T., Do, L. A. H., et al. (2018). Enterovirus serotypes in patients with central nervous system and respiratory infections in Viet Nam 1997–2010. *Virol. J.* 15:69. doi: 10.1186/s12985-018-0980-0
- Blanchette, M., and Daneman, R. (2015). Formation and maintenance of the BBB. *Mech. Dev.* 138(Pt 1), 8–16. doi: 10.1016/j.mod.2015.07.007
- Brecht, M., Jyoti, R., Mcguire, W., and Chauhan, M. (2010). A case of neonatal coxsackie B virus brainstem encephalitis. *J. Paediatr. Child Health* 46, 699–701.
- Burki, T. (2019). Vaccine derived poliovirus cases exceed wild types. *Lancet Infect. Dis.* 19:140. doi: 10.1016/s1473-3099(19)30012-x
- Caine, E. A., and Osorio, J. E. (2017). In vivo imaging with bioluminescent Enterovirus 71 allows for real-time visualization of tissue tropism and viral spread. *J. Virol.* 91:e01759-16. doi: 10.1128/JVI.01759-16
- Chang, L. Y., Huang, L. M., Gau, S. S., Wu, Y. Y., Hsia, S. H., Fan, T. Y., et al. (2007). Neurodevelopment and cognition in children after Enterovirus 71 infection. *N. Engl. J. Med.* 356, 1226–1234. doi: 10.1056/nejmoa065954
- Chapman, N. M., and Kim, K. S. (2008). Persistent coxsackievirus infection: Enterovirus persistence in chronic myocarditis and dilated cardiomyopathy. *Curr. Top. Microbiol. Immunol.* 323, 275–292. doi: 10.1007/978-3-540-75546-3\_13
- Chapman, N. M., Kim, K. S., Drescher, K. M., Oka, K., and Tracy, S. (2008). 5' terminal deletions in the genome of a coxsackievirus B2 strain occurred naturally in human heart. *Virology* 375, 480–491. doi: 10.1016/j.virol.2008.02.030
- Chen, C. S., Yao, Y. C., Lin, S. C., Lee, Y. P., Wang, Y. F., Wang, J. R., et al. (2007). Retrograde axonal transport: a major transmission route of Enterovirus 71 in mice. *J. Virol.* 81, 8996–9003. doi: 10.1128/jvi.00236-07
- Chen, X., Ji, T., Guo, J., Wang, W., Xu, W., and Xie, Z. (2019). Molecular epidemiology of echovirus 18 circulating in mainland China from 2015 to 2016. *Virol. Sin.* 34, 50–58. doi: 10.1007/s12250-018-0080-8
- Chen, X., Li, J., Guo, J., Xu, W., Sun, S., and Xie, Z. (2017). An outbreak of echovirus 18 encephalitis/meningitis in children in Hebei Province, China, 2015. *Emerg. Microbes Infect.* 6:e54.

- Chua, B. H., Phuektes, P., Sanders, S. A., Nicholls, P. K., and Mcminn, P. C. (2008). The molecular basis of mouse adaptation by human Enterovirus 71. *J. Gen. Virol.* 89, 1622–1632. doi: 10.1099/vir.0.83676-0
- Colbere-Garapin, F., Christodoulou, C., Crainic, R., and Pelletier, I. (1989). Persistent poliovirus infection of human neuroblastoma cells. *Proc. Natl. Acad. Sci. U.S.A.* 86, 7590–7594. doi: 10.1073/pnas.86.19.7590
- Colbere-Garapin, F., Duncan, G., Pavo, N., Pelletier, I., and Petit, I. (1998). An approach to understanding the mechanisms of poliovirus persistence in infected cells of neural or non-neural origin. *Clin. Diagn. Virol.* 9, 107–113. doi: 10.1016/s0928-0197(98)00009-9
- Correia, J., Alves, J. E., Ferreira, P., Ferreira, M., Pires, P., and Garrido, C. (2016). Enterovirus 71 meningoencephalitis with extensive white matter damage. *Pediatr. Infect. Dis. J.* 35, 1277–1278. doi: 10.1097/inf.0000000000001292
- Couderc, T., Guivel-Benhassine, F., Calaora, V., Gosselin, A. S., and Blondel, B. (2002). An *ex vivo* murine model to study poliovirus-induced apoptosis in nerve cells. *J. Gen. Virol.* 83, 1925–1930. doi: 10.1099/0022-1317-83-8-1925
- Cuadros, M. A., and Navascues, J. (1998). The origin and differentiation of microglial cells during development. *Prog. Neurobiol.* 56, 173–189. doi: 10.1016/s0301-0082(98)00035-5
- Daneman, R., Zhou, L., Kebede, A. A., and Barres, B. A. (2010). Pericytes are required for blood-brain barrier integrity during embryogenesis. *Nature* 468, 562–566. doi: 10.1038/nature09513
- Davison, D. L., Terek, M., and Chawla, L. S. (2012). Neurogenic pulmonary edema. *Crit. Care* 16:212.
- Dehouck, M. P., Meresse, S., Delorme, P., Fruchart, J. C., and Cecchelli, R. (1990). An easier, reproducible, and mass-production method to study the blood-brain barrier in vitro. *J. Neurochem.* 54, 1798–1801. doi: 10.1111/j.1471-4159.1990.tb01236.x
- Engelhardt, B., Vajkoczy, P., and Weller, R. O. (2017). The movers and shapers in immune privilege of the CNS. *Nat. Immunol.* 18, 123–131. doi: 10.1038/ni.3666
- Evans, D. M., Dunn, G., Minor, P. D., Schild, G. C., Cann, A. J., Stanway, G., et al. (1985). Increased neurovirulence associated with a single nucleotide change in a noncoding region of the sabin type 3 poliovaccine genome. *Nature* 314, 548–550. doi: 10.1038/314548a0
- Famulare, M., Chang, S., Iber, J., Zhao, K., Adeniji, J. A., Bukbuk, D., et al. (2016). Sabin vaccine reversion in the field: a comprehensive analysis of sabin-like poliovirus isolates in Nigeria. *J. Virol.* 90, 317–331. doi: 10.1128/JVI.01532-15
- Fan, Y. K., and Liu, Y. P. (2019). Magnetic resonance imaging features of pediatric coxsackievirus encephalitis. *J. Belg. Soc. Radiol.* 103:6. doi: 10.5334/jbsr.1685
- Fechner, H., Pinkert, S., Wang, X., Sipo, I., Suckau, L., Kurreck, J., et al. (2007). Coxsackievirus B3 and adenovirus infections of cardiac cells are efficiently inhibited by vector-mediated RNA interference targeting their common receptor. *Gene Ther.* 14, 960–971. doi: 10.1038/sj.gt.3302948
- Fekete, R., Cserep, C., Lenart, N., Toth, K., Orsolits, B., Martinecz, B., et al. (2018). Microglia control the spread of neurotropic virus infection via P2Y12 signalling and recruit monocytes through P2Y12-independent mechanisms. *Acta Neuropathol.* 136, 461–482. doi: 10.1007/s00401-018-1885-0
- Feng, M., Guo, S., Fan, S., Zeng, X., Zhang, Y., Liao, Y., et al. (2016). The preferential infection of astrocytes by Enterovirus 71 plays a key role in the viral neurogenic pathogenesis. *Front. Cell. Infect. Microbiol.* 6:192. doi: 10.3389/fcimb.2016.00192
- Feuer, R., Mena, I., Pagarigan, R., Slifka, M. K., and Whitton, J. L. (2002). Cell cycle status affects coxsackievirus replication, persistence, and reactivation in vitro. *J. Virol.* 76, 4430–4440. doi: 10.1128/jvi.76.9.4430-4440.2002
- Feuer, R., Mena, I., Pagarigan, R. R., Hasset, D. E., and Whitton, J. L. (2004). Coxsackievirus replication and the cell cycle: a potential regulatory mechanism for viral persistence/latency. *Med. Microbiol. Immunol.* 193, 83–90. doi: 10.1007/s00430-003-0192-z
- Feuer, R., Pagarigan, R. R., Harkins, S., Liu, F., Hunziker, I. P., and Whitton, J. L. (2005). Coxsackievirus targets proliferating neuronal progenitor cells in the neonatal CNS. *J. Neurosci.* 25, 2434–2444. doi: 10.1523/jneurosci.4517-04.2005
- Feuer, R., Ruller, C. M., An, N., Tabor-Godwin, J. M., Rhoades, R. E., Maciejewski, S., et al. (2009). Viral persistence and chronic immunopathology in the adult central nervous system following Coxsackievirus infection during the neonatal period. *J. Virol.* 83, 9356–9369. doi: 10.1128/JVI.02382-07
- Forrester, J. V., Mcmenamin, P. G., and Dando, S. J. (2018). CNS infection and immune privilege. *Nat. Rev. Neurosci.* 19, 655–671. doi: 10.1038/s41583-018-0070-8
- Freistadt, M. S., Kaplan, G., and Racaniello, V. R. (1990). Heterogeneous expression of poliovirus receptor-related proteins in human cells and tissues. *Mol. Cell Biol.* 10, 5700–5706. doi: 10.1128/mcb.10.11.5700
- Fujii, K., Sudaka, Y., Takashino, A., Kobayashi, K., Kataoka, C., Suzuki, T., et al. (2018). VP1 amino acid residue 145 of Enterovirus 71 is a key residue for its receptor attachment and resistance to neutralizing antibody during cynomolgus monkey infection. *J. Virol.* 92:e00682-18. doi: 10.1128/JVI.00682-18
- Giraud, P., Beaulieux, F., Ono, S., Shimizu, N., Chazot, G., and Lina, B. (2001). Detection of enteroviral sequences from frozen spinal cord samples of Japanese ALS patients. *Neurology* 56, 1777–1778. doi: 10.1212/wnl.56.12.1777
- Goto, K., Sanefuji, M., Kusuha, K., Nishimura, Y., Shimizu, H., Kira, R., et al. (2009). Rhombencephalitis and coxsackievirus A16. *Emerg. Infect. Dis.* 15, 1689–1691. doi: 10.3201/eid1510.090594
- Greninger, A. L., Naccache, S. N., Messacar, K., Clayton, A., Yu, G., Somasekar, S., et al. (2015). A novel outbreak Enterovirus D68 strain associated with acute flaccid myelitis cases in the USA (2012–14): a retrospective cohort study. *Lancet Infect. Dis.* 15, 671–682. doi: 10.1016/S1473-3099(15)70093-9
- Gromeier, M., Alexander, L., and Wimmer, E. (1996). Internal ribosomal entry site substitution eliminates neurovirulence in intergeneric poliovirus recombinants. *Proc. Natl. Acad. Sci. U.S.A.* 93, 2370–2375. doi: 10.1073/pnas.93.6.2370
- Gromeier, M., and Wimmer, E. (1998). Mechanism of injury-provoked poliomyelitis. *J. Virol.* 72, 5056–5060. doi: 10.1128/jvi.72.6.5056-5060.1998
- Gu, X., Wei, Z. Z., Espinera, A., Lee, J. H., Ji, X., Wei, L., et al. (2015). Pharmacologically induced hypothermia attenuates traumatic brain injury in neonatal rats. *Exp. Neurol.* 267, 135–142. doi: 10.1016/j.expneurol.2015.02.029
- Guest, S., Pilipenko, E., Sharma, K., Chumakov, K., and Roos, R. P. (2004). Molecular mechanisms of attenuation of the Sabin strain of poliovirus type 3. *J. Virol.* 78, 11097–11107. doi: 10.1128/jvi.78.20.11097-11107.2004
- Gutierrez, A. L., Denova-Ocampo, M., Racaniello, V. R., and Del Angel, R. M. (1997). Attenuating mutations in the poliovirus 5' untranslated region alter its interaction with polypyrimidine tract-binding protein. *J. Virol.* 71, 3826–3833. doi: 10.1128/jvi.71.5.3826-3833.1997
- Han, J., Ma, X. J., Wan, J. F., Liu, Y. H., Han, Y. L., Chen, C., et al. (2010). Long persistence of EV71 specific nucleotides in respiratory and feces samples of the patients with Hand-Foot-Mouth Disease after recovery. *BMC Infect. Dis.* 10:178. doi: 10.1186/1471-2334-10-178
- Hasbun, R., Rosenthal, N., Balada-Llasat, J. M., Chung, J., Duff, S., Bozzette, S., et al. (2017). Epidemiology of meningitis and encephalitis in the United States, 2011–2014. *Clin. Infect. Dis.* 65, 359–363. doi: 10.1093/cid/cix319
- Haseloff, R. F., Blasig, I. E., Bauer, H. C., and Bauer, H. (2005). In search of the astrocytic factor(s) modulating blood-brain barrier functions in brain capillary endothelial cells in vitro. *Cell. Mol. Neurobiol.* 25, 25–39. doi: 10.1007/s10571-004-1375-x
- Heim, A., Brehm, C., Stille-Siegener, M., Muller, G., Hake, S., Kandolf, R., et al. (1995). Cultured human myocardial fibroblasts of pediatric origin: natural human interferon-alpha is more effective than recombinant interferon-alpha 2a in carrier-state coxsackievirus B3 replication. *J. Mol. Cell. Cardiol.* 27, 2199–2208. doi: 10.1016/s0022-2828(95)91515-x
- Heim, A., Canu, A., Kirschner, P., Simon, T., Mall, G., Hofschneider, P. H., et al. (1992). Synergistic interaction of interferon-beta and interferon-gamma in coxsackievirus B3-infected carrier cultures of human myocardial fibroblasts. *J. Infect. Dis.* 166, 958–965. doi: 10.1093/infdis/166.5.958
- Hirata, O., Ishikawa, N., Mizoguchi, Y., Nakamura, K., and Kobayashi, M. (2011). A case of neonatal coxsackie B2 meningo-encephalitis in which serial magnetic resonance imaging findings reveal the development of lesions. *Neuropediatrics* 42, 156–158. doi: 10.1055/s-0031-1285876
- Hixon, A. M., Clarke, P., and Tyler, K. L. (2019). Contemporary circulating Enterovirus D68 strains infect and undergo retrograde axonal transport in spinal motor neurons independent of sialic acid. *J. Virol.* 93:e00578-19. doi: 10.1128/JVI.00578-19
- Hixon, A. M., Yu, G., Leser, J. S., Yagi, S., Clarke, P., Chiu, C. Y., et al. (2017). A mouse model of paralytic myelitis caused by Enterovirus D68. *PLoS Pathog.* 13:e1006199. doi: 10.1371/journal.ppat.1006199
- Holland, J. J. (1961). Receptor affinities as major determinants of Enterovirus tissue tropisms in humans. *Virology* 15, 312–326. doi: 10.1016/0042-6822(61)90363-4
- Holmes, C. W., Koo, S. S., Osman, H., Wilson, S., Xerry, J., Gallimore, C. I., et al. (2016). Predominance of Enterovirus B and echovirus 30 as cause of viral

- meningitis in a UK population. *J. Clin. Virol.* 81, 90–93. doi: 10.1016/j.jcv.2016.06.007
- Holm-Hansen, C. C., Midgley, S. E., and Fischer, T. K. (2016). Global emergence of Enterovirus D68: a systematic review. *Lancet Infect. Dis.* 16, e64–e75. doi: 10.1016/S1473-3099(15)00543-5
- Hsu, N. Y., Ilnytska, O., Belov, G., Santiana, M., Chen, Y. H., Takvorian, P. M., et al. (2010). Viral reorganization of the secretory pathway generates distinct organelles for RNA replication. *Cell* 141, 799–811. doi: 10.1016/j.cell.2010.03.050
- Huang, C. C., Liu, C. C., Chang, Y. C., Chen, C. Y., Wang, S. T., and Yeh, T. F. (1999). Neurologic complications in children with Enterovirus 71 infection. *N. Engl. J. Med.* 341, 936–942. doi: 10.1056/nejm199909233411302
- Huang, H. I., Lin, J. Y., Chen, H. H., Yeh, S. B., Kuo, R. L., Weng, K. F., et al. (2014). Enterovirus 71 infects brain-derived neural progenitor cells. *Virology* 468–470, 592–600. doi: 10.1016/j.virol.2014.09.017
- Huang, H. I., and Shih, S. R. (2015). Neurotropic Enterovirus infections in the central nervous system. *Viruses* 7, 6051–6066. doi: 10.3390/v7112920
- Huang, W., Wang, G., Zhuge, J., Nolan, S. M., Dimitrova, N., and Fallon, J. T. (2015). Whole-genome sequence analysis reveals the Enterovirus D68 isolates during the United States 2014 outbreak mainly belong to a novel clade. *Sci. Rep.* 5:15223. doi: 10.1038/srep15223
- Huang, Y., Zhou, Y., Lu, H., Yang, H., Feng, Q., Dai, Y., et al. (2015). Characterization of severe hand, foot, and mouth disease in Shenzhen, China, 2009–2013. *J. Med. Virol.* 87, 1471–1479. doi: 10.1002/jmv.24200
- Ida-Hosonuma, M., Iwasaki, T., Yoshikawa, T., Nagata, N., Sato, Y., Sata, T., et al. (2005). The alpha/beta interferon response controls tissue tropism and pathogenicity of poliovirus. *J. Virol.* 79, 4460–4469. doi: 10.1128/jvi.79.7.4460-4469.2005
- Ifie, E., Russell, M. A., Dhayal, S., Leete, P., Sebastiani, G., Nigi, L., et al. (2018). Unexpected subcellular distribution of a specific isoform of the Coxsackie and adenovirus receptor, CAR-SIV, in human pancreatic beta cells. *Diabetologia* 61, 2344–2355. doi: 10.1007/s00125-018-4704-1
- Jorba, J., Campagnoli, R., De, L., and Kew, O. (2008). Calibration of multiple poliovirus molecular clocks covering an extended evolutionary range. *J. Virol.* 82, 4429–4440. doi: 10.1128/JVI.02354-07
- Julien, J., Leparac-Goffart, I., Lina, B., Fuchs, F., Foray, S., Janatova, I., et al. (1999). Postpolio syndrome: poliovirus persistence is involved in the pathogenesis. *J. Neurol.* 246, 472–476. doi: 10.1007/s004150050386
- Kao, S. J., Yang, F. L., Hsu, Y. H., and Chen, H. I. (2004). Mechanism of fulminant pulmonary edema caused by Enterovirus 71. *Clin. Infect. Dis.* 38, 1784–1788. doi: 10.1086/421021
- Kawamura, N., Kohara, M., Abe, S., Komatsu, T., Tago, K., Arita, M., et al. (1989). Determinants in the 5' noncoding region of poliovirus Sabin 1 RNA that influence the attenuation phenotype. *J. Virol.* 63, 1302–1309. doi: 10.1128/jvi.63.3.1302-1309.1989
- Kempf, B. J., and Barton, D. J. (2015). Picornavirus RNA polyadenylation by 3D(pol), the viral RNA-dependent RNA polymerase. *Virus Res.* 206, 3–11. doi: 10.1016/j.virusres.2014.12.030
- Kew, O. M., Sutter, R. W., De Gourville, E. M., Dowdle, W. R., and Pallansch, M. A. (2005). Vaccine-derived polioviruses and the endgame strategy for global polio eradication. *Annu. Rev. Microbiol.* 59, 587–635. doi: 10.1146/annurev.micro.58.030603.123625
- Khandaker, G. M., Zimbron, J., Dalman, C., Lewis, G., and Jones, P. B. (2012). Childhood infection and adult schizophrenia: a meta-analysis of population-based studies. *Schizophr. Res.* 139, 161–168. doi: 10.1016/j.schres.2012.05.023
- Khong, W. X., Yan, B., Yeo, H., Tan, E. L., Lee, J. J., Ng, J. K., et al. (2012). A non-mouse-adapted Enterovirus 71 (EV71) strain exhibits neurotropism, causing neurological manifestations in a novel mouse model of EV71 infection. *J. Virol.* 86, 2121–2131. doi: 10.1128/JVI.06103-11
- Kim, K. S., Chapman, N. M., and Tracy, S. (2008). Replication of coxsackievirus B3 in primary cell cultures generates novel viral genome deletions. *J. Virol.* 82, 2033–2037. doi: 10.1128/jvi.01774-07
- Kim, K. S., Tracy, S., Tappich, W., Bailey, J., Lee, C. K., Kim, K., et al. (2005). 5'-Terminal deletions occur in coxsackievirus B3 during replication in murine hearts and cardiac myocyte cultures and correlate with encapsidation of negative-strand viral RNA. *J. Virol.* 79, 7024–7041. doi: 10.1128/jvi.79.11.7024-7041.2005
- Kim-Hellmuth, S., Bechheim, M., Putz, B., Mohammadi, P., Nedelec, Y., Giangreco, N., et al. (2017). Genetic regulatory effects modified by immune activation contribute to autoimmune disease associations. *Nat. Commun.* 8:266. doi: 10.1038/s41467-017-00366-1
- Koike, S., Horie, H., Ise, I., Okitsu, A., Yoshida, M., Iizuka, N., et al. (1990). The poliovirus receptor protein is produced both as membrane-bound and secreted forms. *EMBO J.* 9, 3217–3224. doi: 10.1002/j.1460-2075.1990.tb07520.x
- Koskiniemi, M., Rautonen, J., Lehtokoski-Lehtiniemi, E., and Vaheri, A. (1991). Epidemiology of encephalitis in children: a 20-year survey. *Ann. Neurol.* 29, 492–497. doi: 10.1002/ana.410290508
- La Monica, N., and Racaniello, V. R. (1989). Differences in replication of attenuated and neurovirulent polioviruses in human neuroblastoma cell line SH-SY5Y. *J. Virol.* 63, 2357–2360. doi: 10.1128/jvi.63.5.2357-2360.1989
- Lee, K. M., Chen, C. J., and Shih, S. R. (2017). Regulation mechanisms of viral IRES-driven translation. *Trends Microbiol.* 25, 546–561. doi: 10.1016/j.tim.2017.01.010
- Lenz, K. M., and Nelson, L. H. (2018). Microglia and beyond: innate immune cells as regulators of brain development and behavioral function. *Front. Immunol.* 9:698. doi: 10.3389/fimmu.2018.00698
- Li, B., Yue, Y., Zhang, Y., Yuan, Z., Li, P., Song, N., et al. (2017). A novel Enterovirus 71 (EV71) virulence determinant: the 69th residue of 3C protease modulates pathogenicity. *Front. Cell. Infect. Microbiol.* 7:26. doi: 10.3389/fcimb.2017.00026
- Li, R., Zou, Q., Chen, L., Zhang, H., and Wang, Y. (2011). Molecular analysis of virulent determinants of Enterovirus 71. *PLoS One* 6:e26237. doi: 10.1371/journal.pone.0026237
- Lin, J. Y., and Shih, S. R. (2014). Cell and tissue tropism of Enterovirus 71 and other Enteroviruses infections. *J. Biomed. Sci.* 21:18. doi: 10.1186/1423-0127-21-18
- Lum, L. C., Chua, K. B., McMinn, P. C., Goh, A. Y., Muridan, R., Sarji, S. A., et al. (2002). Echovirus 7 associated encephalomyelitis. *J. Clin. Virol.* 23, 153–160. doi: 10.1016/s1386-6532(01)00214-1
- Mao, Q., Hao, X., Hu, Y., Du, R., Lang, S., Bian, L., et al. (2018). A neonatal mouse model of central nervous system infections caused by Coxsackievirus B5. *Emerg. Microbes Infect.* 7:185. doi: 10.1038/s41426-018-0186-y
- Mao, Q., Wang, Y., Bian, L., Xu, M., and Liang, Z. (2016). EV-A71 vaccine licensure: a first step for multivalent Enterovirus vaccine to control HFMD and other severe diseases. *Emerg. Microbes Infect.* 5:e75. doi: 10.1038/emi.2016.73
- Marjomaki, V., Turkki, P., and Huttunen, M. (2015). Infectious entry pathway of Enterovirus B species. *Viruses* 7, 6387–6399. doi: 10.3390/v7122945
- Marron, M. P., Raffel, L. J., Garchon, H. J., Jacob, C. O., Serrano-Rios, M., Martinez Larrad, M. T., et al. (1997). Insulin-dependent diabetes mellitus (IDDM) is associated with CTLA4 polymorphisms in multiple ethnic groups. *Hum. Mol. Genet.* 6, 1275–1282. doi: 10.1093/hmg/6.8.1275
- Matcovitch-Natan, O., Winter, D. R., Giladi, A., Vargas Aguilar, S., Spinrad, A., Sarrazin, S., et al. (2016). Microglia development follows a stepwise program to regulate brain homeostasis. *Science* 353:aad8670. doi: 10.1126/science.aad8670
- Melnick, J. L. (1996). Current status of poliovirus infections. *Clin. Microbiol. Rev.* 9, 293–300. doi: 10.1128/cmr.9.3.293-300.1996
- Mendelsohn, C. L., Wimmer, E., and Racaniello, V. R. (1989). Cellular receptor for poliovirus: molecular cloning, nucleotide sequence, and expression of a new member of the immunoglobulin superfamily. *Cell* 56, 855–865. doi: 10.1016/0092-8674(89)90690-9
- Messacar, K., Asturias, E. J., Hixon, A. M., Van Leer-Buter, C., Niesters, H. G. M., Tyler, K. L., et al. (2018). Enterovirus D68 and acute flaccid myelitis—evaluating the evidence for causality. *Lancet Infect. Dis.* 18, e239–e247. doi: 10.1016/S1473-3099(18)30094-X
- Minor, P. (2009). Vaccine-derived poliovirus (VDPV): impact on poliomyelitis eradication. *Vaccine* 27, 2649–2652. doi: 10.1016/j.vaccine.2009.02.071
- Mizutani, T., Ishizaka, A., and Nihei, C. (2016). Transferrin receptor 1 facilitates poliovirus permeation of mouse brain capillary endothelial cells. *J. Biol. Chem.* 291, 2829–2836. doi: 10.1074/jbc.M115.690941
- Muir, P., Nicholson, F., Sharief, M. K., Thompson, E. J., Cairns, N. J., Lantos, P., et al. (1995). Evidence for persistent Enterovirus infection of the central nervous system in patients with previous paralytic poliomyelitis. *Ann. N. Y. Acad. Sci.* 753, 219–232. doi: 10.1111/j.1749-6632.1995.tb27548.x
- Nagata, N., Iwasaki, T., Ami, Y., Sato, Y., Hatano, I., Harashima, A., et al. (2004). A poliomyelitis model through mucosal infection in transgenic mice bearing

- human poliovirus receptor, TgPVR21. *Virology* 321, 87–100. doi: 10.1016/j.virol.2003.12.008
- Nishimura, Y., Lee, H., Hafenstein, S., Kataoka, C., Wakita, T., Bergelson, J. M., et al. (2013). Enterovirus 71 binding to PSGL-1 on leukocytes: VP1-145 acts as a molecular switch to control receptor interaction. *PLoS Pathog.* 9:e1003511. doi: 10.1371/journal.ppat.1003511
- Nishimura, Y., Shimojima, M., Tano, Y., Miyamura, T., Wakita, T., and Shimizu, H. (2009). Human P-selectin glycoprotein ligand-1 is a functional receptor for Enterovirus 71. *Nat. Med.* 15, 794–797. doi: 10.1038/nm.1961
- Nishioku, T., Matsumoto, J., Dohgu, S., Sumi, N., Miyao, K., Takata, F., et al. (2010). Tumor necrosis factor- $\alpha$  mediates the blood-brain barrier dysfunction induced by activated microglia in mouse brain microvascular endothelial cells. *J. Pharmacol. Sci.* 112, 251–254. doi: 10.1254/jphs.09292sc
- Ohka, S., Matsuda, N., Tohyama, K., Oda, T., Morikawa, M., Kuge, S., et al. (2004). Receptor (CD155)-dependent endocytosis of poliovirus and retrograde axonal transport of the endosome. *J. Virol.* 78, 7186–7198. doi: 10.1128/jvi.78.13.7186-7198.2004
- Ohka, S., and Nomoto, A. (2001). The molecular basis of poliovirus neurovirulence. *Dev. Biol.* 105, 51–58.
- Ohka, S., Sakai, M., Bohnert, S., Igarashi, H., Deinhardt, K., Schiavo, G., et al. (2009). Receptor-dependent and -independent axonal retrograde transport of poliovirus in motor neurons. *J. Virol.* 83, 4995–5004. doi: 10.1128/JVI.02225-08
- Ong, K. C., Badmanathan, M., Devi, S., Leong, K. L., Cardosa, M. J., and Wong, K. T. (2008). Pathologic characterization of a murine model of human Enterovirus 71 encephalomyelitis. *J. Neuropathol. Exp. Neurol.* 67, 532–542. doi: 10.1097/NEN.0b013e31817713e7
- Pinkert, S., Klingel, K., Lindig, V., Dorner, A., Zeichhardt, H., Spiller, O. B., et al. (2011). Virus-host coevolution in a persistently coxsackievirus B3-infected cardiomyocyte cell line. *J. Virol.* 85, 13409–13419. doi: 10.1128/JVI.00621-11
- Racaniello, V. R. (2006). One hundred years of poliovirus pathogenesis. *Virology* 344, 9–16. doi: 10.1016/j.virol.2005.09.015
- Ramalho, E., Sousa, I. Jr., Burlandy, F., Costa, E., Dias, A., Serrano, R., et al. (2019). Identification and phylogenetic characterization of human Enteroviruses isolated from cases of aseptic meningitis in Brazil, 2013–2017. *Viruses* 11:E690. doi: 10.3390/v11080690
- Ransohoff, R. M., and Engelhardt, B. (2012). The anatomical and cellular basis of immune surveillance in the central nervous system. *Nat. Rev. Immunol.* 12, 623–635. doi: 10.1038/nri3265
- Rantakallio, P., Jones, P., Moring, J., and Von Wendt, L. (1997). Association between central nervous system infections during childhood and adult onset schizophrenia and other psychoses: a 28-year follow-up. *Int. J. Epidemiol.* 26, 837–843. doi: 10.1093/ije/26.4.837
- Ren, R. B., Moss, E. G., and Racaniello, V. R. (1991). Identification of two determinants that attenuate vaccine-related type 2 poliovirus. *J. Virol.* 65, 1377–1382. doi: 10.1128/jvi.65.3.1377-1382.1991
- Rhoades, R. E., Tabor-Godwin, J. M., Tsueng, G., and Feuer, R. (2011). Enterovirus infections of the central nervous system. *Virology* 411, 288–305. doi: 10.1016/j.virol.2010.12.014
- Richardson, S. J., and Morgan, N. G. (2018). Enteroviral infections in the pathogenesis of type 1 diabetes: new insights for therapeutic intervention. *Curr. Opin. Pharmacol.* 43, 11–19. doi: 10.1016/j.coph.2018.07.006
- Rivest, S. (2009). Regulation of innate immune responses in the brain. *Nat. Rev. Immunol.* 9, 429–439. doi: 10.1038/nri2565
- Rubin, L. L., Hall, D. E., Porter, S., Barbu, K., Cannon, C., Horner, H. C., et al. (1991). A cell culture model of the blood-brain barrier. *J. Cell Biol.* 115, 1725–1735.
- Ruller, C. M., Tabor-Godwin, J. M., Van Deren, D. A. Jr., Robinson, S. M., Maciejewski, S., Gluhm, S., et al. (2012). Neural stem cell depletion and CNS developmental defects after enteroviral infection. *Am. J. Pathol.* 180, 1107–1120. doi: 10.1016/j.ajpath.2011.11.016
- Santello, M., Toni, N., and Volterra, A. (2019). Astrocyte function from information processing to cognition and cognitive impairment. *Nat. Neurosci.* 22, 154–166. doi: 10.1038/s41593-018-0325-8
- Saunders, N. R., Dreifuss, J. J., Dziegielewska, K. M., Johansson, P. A., Habgood, M. D., Mollgard, K., et al. (2014). The rights and wrongs of blood-brain barrier permeability studies: a walk through 100 years of history. *Front. Neurosci.* 8:404. doi: 10.3389/fnins.2014.00404
- Shen, W. C., Chiu, H. H., Chow, K. C., and Tsai, C. H. (1999). MR imaging findings of enteroviral encephalomyelitis: an outbreak in Taiwan. *AJNR Am. J. Neuroradiol.* 20, 1889–1895.
- Shih, S. R., Stollar, V., and Li, M. L. (2011). Host factors in Enterovirus 71 replication. *J. Virol.* 85, 9658–9666. doi: 10.1128/JVI.05063-11
- Sioofy-Khojine, A. B., Oikarinen, S., Honkanen, H., Huhtala, H., Lehtonen, J. P., Briese, T., et al. (2018). Molecular epidemiology of Enteroviruses in young children at increased risk of type 1 diabetes. *PLoS One* 13:e0201959. doi: 10.1371/journal.pone.0201959
- Stern, A., Yeh, M. T., Zinger, T., Smith, M., Wright, C., Ling, G., et al. (2017). The evolutionary pathway to virulence of an RNA virus. *Cell* 169, 35–46.e19. doi: 10.1016/j.cell.2017.03.013
- Sun, Y., Miao, Z., Yan, J., Gong, L., Chen, Y., Chen, Y., et al. (2019). Seromolecular epidemiology of Enterovirus-associated encephalitis in Zhejiang Province, China, from 2014 to 2017. *Int. J. Infect. Dis.* 79, 58–64. doi: 10.1016/j.ijid.2018.11.002
- Suresh, S., Forgie, S., and Robinson, J. (2018). Non-polio Enterovirus detection with acute flaccid paralysis: a systematic review. *J. Med. Virol.* 90, 3–7. doi: 10.1002/jmv.24933
- Suvisaari, J., Mautemps, N., Haukka, J., Hovi, T., and Lonnqvist, J. (2003). Childhood central nervous system viral infections and adult schizophrenia. *Am. J. Psychiatry* 160, 1183–1185. doi: 10.1176/appi.ajp.160.6.1183
- Tabor-Godwin, J. M., Ruller, C. M., Bagalzo, N., An, N., Pagarigan, R. R., Harkins, S., et al. (2010). A novel population of myeloid cells responding to coxsackievirus infection assists in the dissemination of virus within the neonatal CNS. *J. Neurosci.* 30, 8676–8691. doi: 10.1523/JNEUROSCI.1860-10.2010
- Tam, P. E., and Messner, R. P. (1999). Molecular mechanisms of coxsackievirus persistence in chronic inflammatory myopathy: viral RNA persists through formation of a double-stranded complex without associated genomic mutations or evolution. *J. Virol.* 73, 10113–10121. doi: 10.1128/jvi.73.12.10113-10121.1999
- Tan, C. W., Sam, I. C., Lee, V. S., Wong, H. V., and Chan, Y. F. (2017). VP1 residues around the five-fold axis of Enterovirus A71 mediate heparan sulfate interaction. *Virology* 501, 79–87. doi: 10.1016/j.virol.2016.11.009
- Tan, S. H., Ong, K. C., and Wong, K. T. (2014). Enterovirus 71 can directly infect the brainstem via cranial nerves and infection can be ameliorated by passive immunization. *J. Neuropathol. Exp. Neurol.* 73, 999–1008. doi: 10.1097/NEN.0000000000000122
- Tapparel, C., Siegrist, F., Petty, T. J., and Kaiser, L. (2013). Picornavirus and Enterovirus diversity with associated human diseases. *Infect. Genet. Evol.* 14, 282–293. doi: 10.1016/j.meegid.2012.10.016
- Too, I. H., Yeo, H., Sessions, O. M., Yan, B., Libau, E. A., Howe, J. L., et al. (2016). Enterovirus 71 infection of motor neuron-like NSC-34 cells undergoes a non-lytic exit pathway. *Sci. Rep.* 6:36983. doi: 10.1038/srep36983
- Tsueng, G., Tabor-Godwin, J. M., Gopal, A., Ruller, C. M., Deline, S., An, N., et al. (2011). Coxsackievirus preferentially replicates and induces cytopathic effects in undifferentiated neural progenitor cells. *J. Virol.* 85, 5718–5732. doi: 10.1128/JVI.02261-10
- van der Schaar, H. M., Dorobantu, C. M., Albulescu, L., Strating, J., and Van Kuppeveld, F. J. M. (2016). Fat(al) attraction: picornaviruses usurp lipid transfer at membrane contact sites to create replication organelles. *Trends Microbiol.* 24, 535–546. doi: 10.1016/j.tim.2016.02.017
- Verboon-Macielek, M. A., Groenendaal, F., Cowan, F., Govaert, P., Van Loon, A. M., and De Vries, L. S. (2006). White matter damage in neonatal Enterovirus meningoencephalitis. *Neurology* 66, 1267–1269. doi: 10.1212/01.wnl.0000208429.69676.23
- Wasserstrom, R., Mamourian, A. C., Mcgary, C. T., and Miller, G. (1992). Bulbar poliomyelitis: MR findings with pathologic correlation. *AJNR Am. J. Neuroradiol.* 13, 371–373.
- Werk, D., Schubert, S., Lindig, V., Grunert, H. P., Zeichhardt, H., Erdmann, V. A., et al. (2005). Developing an effective RNA interference strategy against a plus-strand RNA virus: silencing of coxsackievirus B3 and its cognate coxsackievirus-adenovirus receptor. *Biol. Chem.* 386, 857–863.
- Wessely, R., Klingel, K., Knowlton, K. U., and Kandolf, R. (2001). Cardioselective infection with coxsackievirus B3 requires intact type I interferon signaling: implications for mortality and early viral replication. *Circulation* 103, 756–761. doi: 10.1161/01.cir.103.5.756

- Włodarczyk, A., Holtman, I. R., Krueger, M., Yogev, N., Bruttger, J., Khorrooshi, R., et al. (2017). A novel microglial subset plays a key role in myelinogenesis in developing brain. *EMBO J.* 36, 3292–3308. doi: 10.15252/embj.201696056
- Woodall, C. J., Riding, M. H., Graham, D. I., and Clements, G. B. (1994). Sequences specific for Enterovirus detected in spinal cord from patients with motor neurone disease. *BMJ* 308, 1541–1543. doi: 10.1136/bmj.308.6943.1541
- Wu, T., Fan, X. P., Wang, W. Y., and Yuan, T. M. (2014). Enterovirus infections are associated with white matter damage in neonates. *J. Paediatr. Child Health* 50, 817–822. doi: 10.1111/jpc.12656
- Xu, R., and Crowell, R. L. (1996). Expression and distribution of the receptors for coxsackievirus B3 during fetal development of the Balb/c mouse and of their brain cells in culture. *Virus Res.* 46, 157–170. doi: 10.1016/s0168-1702(96)01398-6
- Xu, W., Liu, C. F., Yan, L., Li, J. J., Wang, L. J., Qi, Y., et al. (2012). Distribution of Enteroviruses in hospitalized children with hand, foot and mouth disease and relationship between pathogens and nervous system complications. *Virology* 438, 9–18. doi: 10.1016/j.virusres.2012.07.014
- Yamayoshi, S., Fujii, K., and Koike, S. (2014). Receptors for Enterovirus 71. *Emerg. Microbes Infect.* 3:e53. doi: 10.1038/emi.2014.49
- Yan, J. J., Wang, J. R., Liu, C. C., Yang, H. B., and Su, I. J. (2000). An outbreak of Enterovirus 71 infection in Taiwan 1998: a comprehensive pathological, virological, and molecular study on a case of fulminant encephalitis. *J. Clin. Virol.* 17, 13–22. doi: 10.1016/s1386-6532(00)00067-6
- Yanagiya, A., Ohka, S., Hashida, N., Okamura, M., Taya, C., Kamoshita, N., et al. (2003). Tissue-specific replicating capacity of a chimeric poliovirus that carries the internal ribosome entry site of hepatitis C virus in a new mouse model transgenic for the human poliovirus receptor. *J. Virol.* 77, 10479–10487. doi: 10.1128/jvi.77.19.10479-10487.2003
- Yang, K. D., Yang, M. Y., Li, C. C., Lin, S. F., Chong, M. C., Wang, C. L., et al. (2001). Altered cellular but not humoral reactions in children with complicated Enterovirus 71 infections in Taiwan. *J. Infect. Dis.* 183, 850–856. doi: 10.1086/319255
- Yang, W. X., Terasaki, T., Shiroki, K., Ohka, S., Aoki, J., Tanabe, S., et al. (1997). Efficient delivery of circulating poliovirus to the central nervous system independently of poliovirus receptor. *Virology* 229, 421–428. doi: 10.1006/viro.1997.8450
- Yang, Y., Salayandia, V. M., Thompson, J. F., Yang, L. Y., Estrada, E. Y., and Yang, Y. (2015). Attenuation of acute stroke injury in rat brain by minocycline promotes blood-brain barrier remodeling and alternative microglia/macrophage activation during recovery. *J. Neuroinflammation* 12:26. doi: 10.1186/s12974-015-0245-4
- Yao, P. P., Qian, L., Xia, Y., Xu, F., Yang, Z. N., Xie, R. H., et al. (2012). Enterovirus 71-induced neurological disorders in young gerbils, *Meriones unguiculatus*: development and application of a neurological disease model. *PLoS One* 7:e51996. doi: 10.1371/journal.pone.0051996
- Yeh, M. T., Wang, S. W., Yu, C. K., Lin, K. H., Lei, H. Y., Su, I. J., et al. (2011). A single nucleotide in stem loop II of 5'-untranslated region contributes to virulence of Enterovirus 71 in mice. *PLoS One* 6:e27082. doi: 10.1371/journal.pone.0027082
- Yeung, M. L., Jia, L., Yip, C. C. Y., Chan, J. F. W., Teng, J. L. L., Chan, K. H., et al. (2018). Human tryptophanyl-tRNA synthetase is an IFN-gamma-inducible entry factor for Enterovirus. *J. Clin. Invest.* 128, 5163–5177. doi: 10.1172/JCI99411
- Yu, J., Zhang, L., Ren, P., Zhong, T., Li, Z., Wang, Z., et al. (2015). Enterovirus 71 mediates cell cycle arrest in S phase through non-structural protein 3D. *Cell Cycle* 14, 425–436. doi: 10.4161/15384101.2014.980631
- Zaini, Z., and McMin, P. (2012). A single mutation in capsid protein VP1 (Q145E) of a genogroup C4 strain of human Enterovirus 71 generates a mouse-virulent phenotype. *J. Gen. Virol.* 93, 1935–1940. doi: 10.1099/vir.0.043893-0
- Zoll, J., Heus, H. A., Van Kuppeveld, F. J., and Melchers, W. J. (2009). The structure-function relationship of the Enterovirus 3'-UTR. *Virus Res.* 139, 209–216. doi: 10.1016/j.virusres.2008.07.014
- Zonta, M., Angulo, M. C., Gobbo, S., Rosengarten, B., Hossmann, K. A., Pozzan, T., et al. (2003). Neuron-to-astrocyte signaling is central to the dynamic control of brain microcirculation. *Nat. Neurosci.* 6, 43–50. doi: 10.1038/nn980

**Conflict of Interest:** The authors declare that the research was conducted in the absence of any commercial or financial relationships that could be construed as a potential conflict of interest.

Copyright © 2020 Chen, Lee, Lee, Gong and Shih. This is an open-access article distributed under the terms of the Creative Commons Attribution License (CC BY). The use, distribution or reproduction in other forums is permitted, provided the original author(s) and the copyright owner(s) are credited and that the original publication in this journal is cited, in accordance with accepted academic practice. No use, distribution or reproduction is permitted which does not comply with these terms.



# The Mechanism of the Zika Virus Crossing the Placental Barrier and the Blood-Brain Barrier

Chi-Fen Chiu<sup>1†</sup>, Li-Wei Chu<sup>1†</sup>, I-Chen Liao<sup>1</sup>, Yogy Simanjuntak<sup>2</sup>, Yi-Ling Lin<sup>2</sup>, Chi-Chang Juan<sup>3</sup> and Yueh-Hsin Ping<sup>1,4\*</sup>

<sup>1</sup> Department and Institute of Pharmacology, National Yang-Ming University, Taipei, Taiwan, <sup>2</sup> Institute of Biomedical Sciences, Academia Sinica, Taipei, Taiwan, <sup>3</sup> Department and Institute of Physiology, National Yang-Ming University, Taipei, Taiwan, <sup>4</sup> Institute of Biophotonics, National Yang-Ming University, Taipei, Taiwan

## OPEN ACCESS

### Edited by:

Mei-Ling Li,  
Rutgers, The State University  
of New Jersey, United States

### Reviewed by:

Hsing-I Huang,  
Chang Gung University, Taiwan  
Cheng-Wen Lin,  
China Medical University, Taiwan

### \*Correspondence:

Yueh-Hsin Ping  
yhp@ym.edu.tw

<sup>†</sup> These authors have contributed  
equally to this work

### Specialty section:

This article was submitted to  
Virology,  
a section of the journal  
Frontiers in Microbiology

Received: 15 November 2019

Accepted: 30 January 2020

Published: 20 February 2020

### Citation:

Chiu C-F, Chu L-W, Liao I-C,  
Simanjuntak Y, Lin Y-L, Juan C-C and  
Ping Y-H (2020) The Mechanism  
of the Zika Virus Crossing  
the Placental Barrier  
and the Blood-Brain Barrier.  
Front. Microbiol. 11:214.  
doi: 10.3389/fmicb.2020.00214

Zika virus (ZIKV) infection causes severe neurological symptoms in adults and fetal microcephaly and the virus is detected in the brain of microcephaly and meningoencephalitis patient. However, the mechanism of ZIKV crossing the physiological barrier to the central nervous systems (CNS) remains elusive. The placental barrier and the blood brain barrier (BBB) protect the fetus from pathogens and ensure healthy brain development during pregnancy. In this study, we used human placenta trophoblasts cells (JEG-3) and human brain-derived endothelial cells (hCMEC/D3) as *in vitro* models of the physiological barriers. Results showed that ZIKV could infect JEG-3 cells effectively and reduce the amounts of ZO-1 and occludin between adjacent cells by the proteasomal degradation pathway, suggesting that the permeability of the barrier differentially changed in response to ZIKV infection, allowing the virus particle to cross the host barrier. In contrast, ZIKV could infect hCMEC/D3 cells without disrupting the BBB barrier permeability and tight junction protein expression. Although no disruption to the BBB was observed during ZIKV infection, ZIKV particles were released on the basal side of the BBB model and infected underlying cells. In addition, we observed that fluorescence-labeled ZIKV particles could cross the *in vitro* placenta barrier and BBB model by transcytosis and the action of transcytosis could be blocked by either low temperature or pharmacological inhibitors of endocytosis. In summary, the ZIKV uses a cell-type specific paracellular pathway to cross the placenta monolayer barrier by disrupting cellular tight junction. In addition, the ZIKV can also cross both the placenta barrier and the BBB by transcytosis. Our study provided new insights into on the mechanism of the cellular barrier penetration of ZIKV particles.

**Keywords:** Zika virus, placental barrier, blood-brain barrier, tight junction, transcytosis, single-virus imaging, ZO-1, Occludin

## INTRODUCTION

The Zika virus (ZIKV), first isolated from the rhesus monkey in 1947 in Uganda (Dick et al., 1952), is a re-emerging arthropod-borne RNA virus belonging to the *Flaviviridae* family, which also include the dengue virus (DENV), the West Nile virus (WNV), the Japanese encephalitis viruses (JEV) and the yellow fever virus (YFV). Until 2015, most ZIKV infections were deemed as a mild illness with some common symptoms including headache, fever, arthralgia, rash, myalgia, edema, arthritis, vomiting, and non-purulent conjunctivitis (Petersen et al., 2016). However, based

on recent epidemics, ZIKV infection in adult is associated with the Guillain-Barre' syndrome and encephalitis (Brasil et al., 2016; Dos Santos et al., 2016; Soares et al., 2016). Moreover, vertical transmission of ZIKV from mother to fetus is linked to the elevating incidences of the congenital Zika syndrome on fetuses including microcephaly, congenital malformation, and fetal demise (Cordeiro et al., 2016; Coyne and Lazear, 2016; Hoen et al., 2018). For those infants born with a normal head, congenital ZIKV infection may also cause developed postnatal-onset microcephaly, joint disorders, sensorineural hearing loss, and eye abnormalities (Fitzgerald et al., 2018). These studies revealed a wide-spectrum of effects that congenital ZIKV infection has on fetuses, strongly suggesting the importance of understanding the mechanisms of vertical transmission.

To reach the fetus brain from the infected mother, ZIKV needs to pass two major physiological barriers, the placenta and the blood-brain barrier (BBB). The placenta, a highly specialized organ formed only during pregnancy, supports the growth and development of the fetus and is precisely regulated and coordinated to ensure the maximal efficiency of the exchange of nutrients and waste products between the maternal and fetal circulatory systems (Gude et al., 2004). Its principal function is to supply the fetal brain, with oxygen and nutrients (Burton and Fowden, 2015). Moreover, the placenta barrier serves as an essential physiological barrier that protects the fetus from certain toxic molecules, maternal diseases, and pathogenic infections, such as viruses (Gude et al., 2004; Delorme-Axford et al., 2014). The main functional unit of the placenta is the chorionic villi that is composed of specialized epithelial cells known as trophoblasts derived from the outer trophoblast layer. Trophoblasts construct the epithelial covering of the placenta and also generate a subpopulation of invasive extravillous trophoblast cells within which fetal blood is separated by the placental membrane from the maternal blood (Gude et al., 2004; Burton and Fowden, 2015). To serve as the initial line of defense against any pathogens attempting to breach the placental barrier, trophoblasts constitute a tight polarized epithelial monolayer comprising tight junctions preventing lateral and paracellular diffusion of substrates. However, at the present time, our knowledge regarding virus-host interactions at the maternal-fetal interface during pregnancy is limited.

While the placenta serves as the first checkpoint to protect the fetus and support its normal growth and development of the fetus, the BBB provides the second checkpoint critical to protect the fetal brain and ensure healthy brain development (Coyne and Lazear, 2016). The BBB is a boundary that separates the circulating blood from the brain and the extracellular fluid in the central nervous system (CNS) (Daneman and Prat, 2015). The BBB is made up of endothelial cells of the vasculature forming cell-to-cell tight junctions to limit the passage of circulating molecules, cells, and pathogens to the CNS (Stamatovic et al., 2008). Tight junctions containing more than 40 proteins with both transmembrane and cytoplasmic domains generate a continuous, circumferential, belt-like structure at the luminal end of the intercellular space, where it serves as a gatekeeper of the paracellular pathway (Mateo et al., 2015). Three major transmembrane proteins, claudin, occluding, and

junctional adhesion molecule (JAM), interact with cytoplasmic proteins including ZO-1, cingulin, afadin and  $\alpha$ -catenin, which anchor strands to the cytoskeleton, resulting in the formation of cellular tight junctions (Hartsock and Nelson, 2008). Disruption of the BBB enhances permeability of endothelial cell and is a hallmark of CNS infection (Daniels and Klein, 2015). However, recent studies reported that no barrier disruption was observed when ZIKV gained access to the CNS (Papa et al., 2017; Alimonti et al., 2018), suggesting that the endocytic transport system is required for the ZIKV to cross the BBB barrier. Given the existence of endosomal sorting pathways in different cell types, it is possible for the BBB cells to employ a similar process of endosomal transportation (Ayloo and Gu, 2019). However, there is no investigation on these pathways in BBB endothelial cells, particularly in the condition under viral infection.

The placental barrier and the BBB protect the fetal brain development during human pregnancy by forming cellular tight junctions to limit pathogen paracellular movement under the normal condition. However, the ZIKV could be detected in the brains of microcephalic infants, suggesting that the ZIKV can penetrate the CNS in fetus (Calvet et al., 2016; Mlakar et al., 2016). There are two possible routes for the viruses to cross the physiological barriers. One is to disrupt the barrier integrity. The Rubella virus, cytomegalovirus (CMV), the Human immunodeficiency virus type 1 (HIV-1), the West Nile virus (WNV), the Japanese encephalitis virus (JEV), and herpes viruses are known to breach the placental barriers to reach the CNS (Roe et al., 2012, 2014; Coyne and Lazear, 2016; Al-Obaidi et al., 2017; Leibrand et al., 2017; Mittal et al., 2017). The other is through transcytosis. The hepatitis B virus (HBV) has been reported to penetrate the placenta barrier by transcytosis in the first trimester (Bhat and Anderson, 2007). The JEV has also been found to cross the endothelial cells and pericytes in the BBB in endocytic vesicles (Liou and Hsu, 1998). These findings indicate that viruses may cross the barrier not only through the paracellular pathway but also through transcytosis. Although the ZIKV is detected in both the amniotic fluid of pregnant women and in microcephalic fetal brain tissues (Calvet et al., 2016; Mlakar et al., 2016), and is thus capable of penetrating the CNS from mother to fetus, the mechanism of such remains unknown. In this study, we would like to combine the *in vitro* Transwell barrier assay and a single-virus tracking (SVT) approach to elucidate the mechanism that the ZIKV employs to cross the placental and the BBB barriers.

## MATERIALS AND METHODS

### Cell Culture

The choriocarcinoma cell lines (JEG-3, ATCC® HTB-36™) and African green monkey kidney epithelial cells (Vero, ATCC® CCL-81™) were cultured in a minimum essential medium (MEM, Gibco) supplemented with 10% fetal bovine serum (FBS, HyClone), 1% L-glutamine and 1% penicillin/streptomycin (P/S, Gibco). The immortalized human brain capillary endothelial cell line hCMEC/D3 (SCC066, Merck) was cultured in the EndoGRO™-MV Complete Media Kit (Merck). The Vero E6 cell line was cultured in Dulbecco's modified Eagle's medium

(DMEM, Gibco) supplemented with 10% fetal bovine serum and 1% penicillin/streptomycin. All cells were incubated at 37°C with 5% CO<sub>2</sub>.

## ZIKV Amplification

The ZIKV strain PRVABC59 (2015 Puerto Rico strain, GenBank accession: KU501215) kindly provided by the Centers for Disease Control, Taiwan, was propagated in Vero E6 cells. Cells were exposed to ZIKV with multiplicity of infection (MOI) of 0.02 in a serum free DMEM medium and were incubated at 37°C with 5% CO<sub>2</sub> for 2 h. Afterward, infected cells were replaced in a low serum DMEM medium containing 2% FBS, 1% P/S for virus production. At 4th and 7th days post-infection, the culture medium was collected and cell debris was removed by centrifugation at 1500 × g for 15 min at 4°C. Finally, the ZIKV-containing supernatant was stored at -80°C.

## Immunofluorescence Microscopy Imaging

For ZIKV infection assays, JEG-3 and hCMEC/D3 cells were seeded on 3.5 cm dishes and incubated overnight until cells grown to 80% confluent monolayer, and cells were then infected with different MOIs of the ZIKV. After 24 h post-infection, cells were fixed by 4% paraformaldehyde, and permeabilized by 0.1% Triton X-100 in PBS. The expression of the ZIKV E protein was recognized by a 1:100 diluted rabbit anti-ZIKV E antibody (GeneTex, GTX133314) and Alexa-488 conjugated goat anti-rabbit IgG. Nuclear DNA was stained with 4,6-diamidino-2-phenylindole, dihydrochloride (DAPI; Sigma-Aldrich). Fluorescence images were captured by an Olympus IX70 microscope equipped with a 20 × objective lens. The percentage of ZIKV-infected cells was calculated by (ZIKV E positive cells/total cells) × 100%. The average percentages in ZIKV-infected cells were collected from three independent experiments. For tight junction protein expression assays, JEG-3 cells were seeded on a 3.5 cm glass-bottom plate (Mettek) until cells grown to 100% confluent monolayer, and then incubated with/without the ZIKV. After 24 h post-infection, the cells were fixed by 4% paraformaldehyde and incubated with ZO-1 (Invitrogen) or occludin (Abcam) antibodies. Afterward, cells were recognized by the Alexa-488 conjugated secondary antibody, and nuclear DNA was stained with DAPI (Sigma-Aldrich). Fluorescence images were captured by a FluoView 1000 confocal microscope (Olympus) equipped with a 60 × oil immersion objective with a numerical aperture (N.A.) of 1.4.

## Cell Viability Assays

To determine cell viability in the presence of various inhibitors or drugs, a sulforhodamine beta (SRB) assay was performed. JEG-3 and hCMEC/D3 cells were seeded on 96-well plates. After a 24-h treatment, cells were fixed with 10% trichloroacetic acid at 4°C for 1 h. Cells were washed with water prior to incubation of 100 μl of 0.5% sulforhodamine beta in 1% acetic acid for 30 min at RT. Plates were washed four times with 1% acetic acid and air-dried. SRB was dissolved in 50 μl of 10 mM Tris solution and absorbance was measured at 510 nm using an ELISA reader.

## In vitro Transwell Barrier Assay

To assess the ability of the ZIKV crossing the barrier *in vitro*, the virus was added to the media in the apical Transwell insert (translucent polyethylene terephthalate [PET], 0.4 μm pore size). The inoculum was left on the cells for 24 h except for the experiment in which the inoculum was removed after 2 h and replaced with complete endothelial medium for additional 24 h. The inserts were placed in on a 24-well companion plate containing Vero cells growing at the bottom of the well. After 24 h post-infection, Vero cells were washed with PBS, and recognized by an anti-ZIKV E protein antibody and ALEXA488 conjugated goat anti-rabbit IgG, sequentially. Nuclear DNA was stained with DAPI (Sigma-Aldrich). The percentage of ZIKV-infected cells was calculated by (ZIKV E positive cells/total cells) × 100%.

## In vitro Transwell Permeability Assays

To test whether the permeability of the physiological barrier was affected by the ZIKV, FITC-dextran was added to the media in the apical Transwell insert after the barrier cells were exposed to the ZIKV for 24 h. The cells were seeded on the membrane insert in the Transwell chamber, as previously described. Before FITC-dextran was added to the media in the apical insert, the inserts were washed twice with a pre-warmed Krebs-HEPES buffer (99 mM NaCl, 4.7 mM KCl, 1.2 mM MgSO<sub>4</sub>, 1.0 mM KH<sub>2</sub>PO<sub>4</sub>, 19.6 mM NaHCO<sub>3</sub>, 11.2 mM glucose, 20 mM Na-HEPES, and 2.5 mM CaCl<sub>2</sub>, pH 7.4) to remove the residual medium. The inserts were then placed onto companion plates containing 500 μl of Krebs-HEPES buffer. Afterward, dextran conjugated with FITC (FITC-dextran 1 mg/ml) was added to the apical insert and incubated at 37°C for 1 h. The insert was removed and the solution in the plate well (lower chamber) was collected and measured for fluorescence intensity of FITC-dextran using a fluorescent plate reader (excitation 492 nm and excitation 518 nm).

## Western Blotting

Infected cells were lysed in RIPA buffer (20 mM Tris-HCl pH 7.5, 150 mM NaCl, 1 mM Na<sub>2</sub>EDTA, 1 mM EGTA, 1% NP-40, 1% sodium deoxycholate, 2.5 mM sodium pyrophosphate, 1 mM beta-glycerophosphate, 1 mM Na<sub>3</sub>VO<sub>4</sub>, 1 μg/ml leupeptin, and 1 mM PMSF). Proteins were separated by 10% SDS-PAGE and transferred to polyvinylidene fluoride membranes which were blocked with a blocking buffer (5% skim milk in TBS with 0.05% Tween 20) and incubated with primary antibodies in the blocking buffer. Herein, the rabbit polyclonal anti-ZO-1 (Invitrogen), the rabbit polyclonal anti-Zika virus E protein (GeneTex, GTX133314), the rabbit monoclonal anti-Occludin antibody (Abcam), and the rabbit polyclonal anti-GAPDH were utilized, respectively. After being washed three times with a blocking buffer, the membrane was probed with a horseradish peroxidase-conjugated secondary antibody and developed with an Immobilon chemiluminescent HRP substrate (Millipore). Blots were imaged on an Amersham Imager 680.

## RT-qPCR Analysis

Total RNA was extracted using a TRIzol reagent (Invitrogen, Thermo Scientific-Technologies). cDNA was synthesized from total RNA (5 µg) using RevertAid™ reverse transcriptase (Thermo Fisher Scientific). Real-time PCR amplification was performed using the KAPA SYBR™ FAST qPCR Kits on Biosystems™ Real-Time PCR Instruments. Specific primers for individual genes used for RT-qPCR are: ZO-1 (Forward: 5'-CACCTTTTGATAATCAGCACTCTCA-3'; Reverse: 5'-CTCTAGGTGCCTGTTTCGTAACGT-3'), Occludin (Forward: 5'-TCAGGGAATATCCACCTATCACTTCAG-3'; Reverse: 5'-CATCAGCAGCAGCCATGTACTCTTCAC-3'), ZIKV E protein (Forward: 5'-AAGTACACATACCAAAACAAAGTGGT-3'; Reverse: 5'-TCCGCTCCCCCTTTGGTCTTG-3'), and GAPDH (Forward: 5'-AAGGTCATCCCTGAGCTGAA-3'; Reverse: 5'-TTCTAGACGGCAGGTCAGGT-3'). Amplification of cDNA was initiated with 3 min at 95°C, followed by 50 cycles of 3 s at 95°C and 30 s at 60°C.

## Preparation of Fluorescence-Labeled ZIKV Particles

The procedure of virus labeling was performed as previously described with minor modifications (Chu et al., 2014, 2019). ZIKV particles were pelleted from a ZIKV-containing supernatant by ultra-centrifugation at 47,000 rpm in a Beckman 50.2Ti rotor for 3.5 h. Virus pellets were resuspended in a HNE buffer (5 mM HEPES, 150 mM NaCl, and 0.1 mM EDTA, pH 7.4) and further concentrated by ultrafiltration spin columns (GE healthcare). Concentrated ZIKV particles were labeled with Atto647N-NHS ester (Sigma-Aldrich), with maximum absorption at 646 nm and maximum emission at 664 nm. Briefly,  $1 \times 10^7$  pfu/ml of ZIKV were mixed with 2 nmol of Atto 647N NHS ester in an HNE buffer for 45 min at room temperature. The unincorporated dye was separated from fluorescence-labeled ZIKV particles by a Sephadex G-25 column (GE Healthcare). The fractions containing Atto647N-labeling ZIKV were detected by a multimode microplate reader (TECAN 200/200Pro) and stored at  $-80^{\circ}\text{C}$ .

## Plaque Assay

Vero E6 cells were seeded in a 12-well plate with a density of  $1.5 \times 10^5$  and incubated at  $37^{\circ}\text{C}$  with 5%  $\text{CO}_2$  overnight. After the cells reached 80–90% confluent, they were washed with PBS and were infected with 10-fold serial dilutions of the ZIKV at  $37^{\circ}\text{C}$  with 5%  $\text{CO}_2$  for 2 h. Afterward, ZIKV-infected cells were overlaid with a 1:1 mixture of 2% agarose gel and two-fold DMEM medium containing 4% FBS and 1% P/S, and then incubated at  $37^{\circ}\text{C}$  with 5%  $\text{CO}_2$ . At 4 days post-infection, the cells were fixed by 10% formaldehyde, and the gels were removed. Finally, the cells were stained with 1% crystal violet to visualize plaque formation. The virus titer was quantified by counting the plaque numbers.

## In vitro Barrier Transcytosis Assays

Cells were seeded to 24-well PET cell culture inserts, 0.4-µm pore size for 7 days, in a two-chambered system. In this system, barrier

cells form a polarized monolayer with tight junctions between cells, allowing access to both apical and basolateral domains. Cells were incubated for 30 min with various transcytosis inhibitors in different concentration, including 10 µM of nystatin (Sigma), 10 µM of chlorpromazine hydrochloride (CPZ, Sigma), 20 µM of dimethyl amiloride (DMA, Sigma), and 10 µM of colchicine (Sigma). Drugs were administered to the cells in both apical and basolateral chambers at identical concentrations. Thereafter, 100 µl of Atto647-ZIKV ( $2 \times 10^6$  copies  $\text{ml}^{-1}$  of virus) was added into the upper chamber. After 4 h incubation with cells, all of the basolateral supernatant was collected. Percent transcytosis was determined by measuring the fluorescence intensity of Atto647N through using a fluorescent plate reader.

## Statistics Analysis

The student *t*-test was used for statistical analyses in this study. The repeat times for each experiment are described in the figure legends or main text. The software Prism 6 (GraphPad) was used to perform statistical analysis. Statistical significance is defined as, n.s., not significant, \**p* < 0.05, \*\**p* < 0.01, \*\*\**p* < 0.001, \*\*\*\**p* < 0.0001.

## RESULTS

### ZIKV Infects Both JEG-3 Cells and hCMEC/D3 Cells With No Effect on Cell Viability

To investigate the mechanism of the ZIKV crossing the placental barrier and the BBB, we infected JEG-3 cells, which are derived from trophoblast cells of the placenta and commonly used in placental barrier studies, and hCMEC/D3 cells, which are the immortalized human brain capillary endothelial cell lines frequently employed in studies of the BBB (Vu et al., 2009; Rothbauer et al., 2017). To first clarify the infectivity of the ZIKV in JEG-3 and hCMEC/D3 cells, the viral envelop (E) protein was detected by immunofluorescence staining with an anti-ZIKV E protein antibody at 24 h post-infection. Apparently, the ZIKV E protein was detected in both cell lines in a dosage-dependent manner (Figure 1A). Results of the quantitative analysis revealed that the percentage of infected cells could be elevated as MOI increased (Figure 1B). The ZIKV infected more than 80% cells at a MOI of 1 and 10 in JEG-3 and hCMEC/D3 cells, respectively (Figure 1B). Importantly, there was no cytotoxicity in cell viability of both cell lines among indicated MOI at 24 h post-infection (Figure 1C).

### ZIKV Crosses an *in vitro* Human Physiological Barrier Model

Next, we established an *in vitro* Transwell barrier assay to investigate whether the ZIKV can cross barrier cells. As shown in Figure 2A, JEG-3 and hCMEC/D3 cells were, respectively, seeded on the apical chamber of the inserts, which contained a permeable membrane, of a 24-well Transwell plate. The inserts were then placed on a 24-well companion plate containing pre-seed adherent Vero cells in the basal chamber. ZIKV

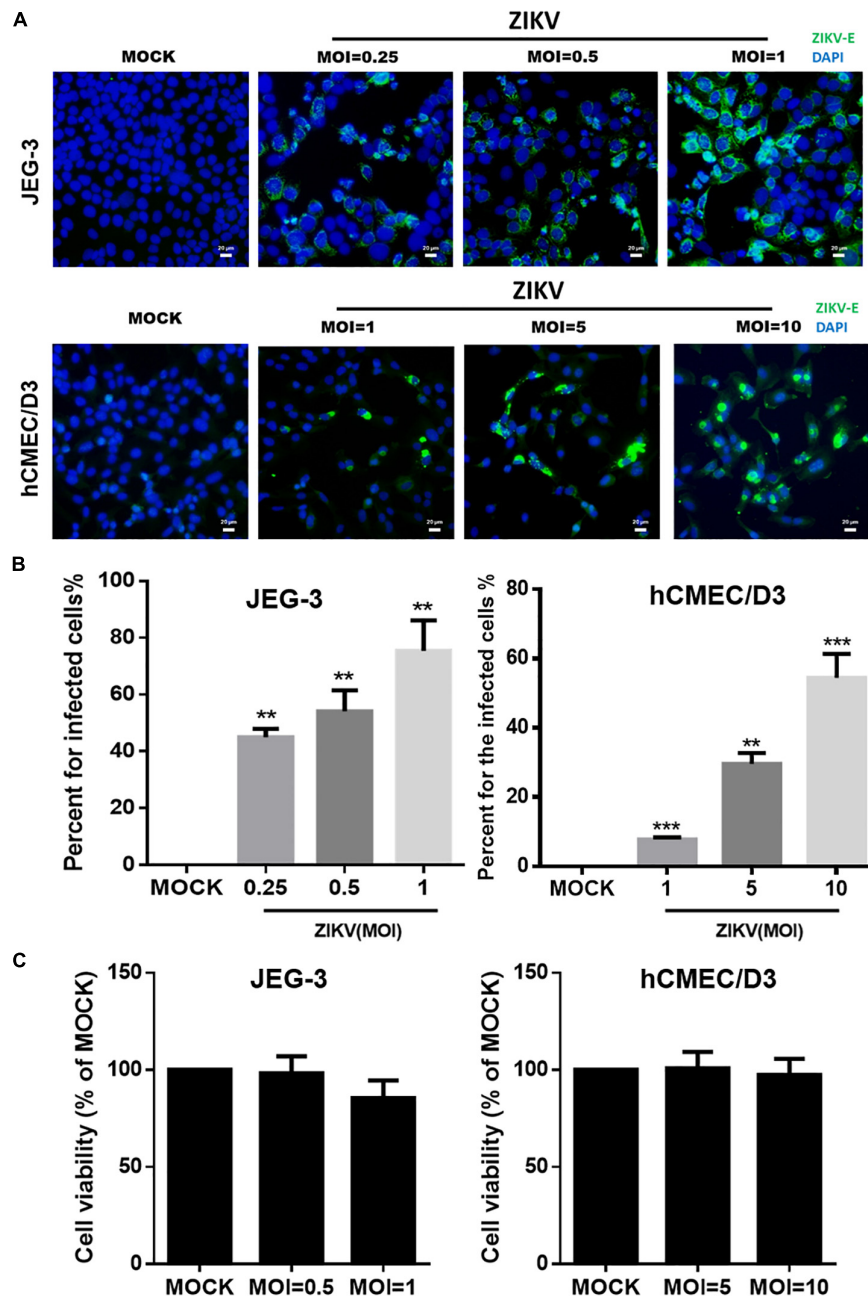
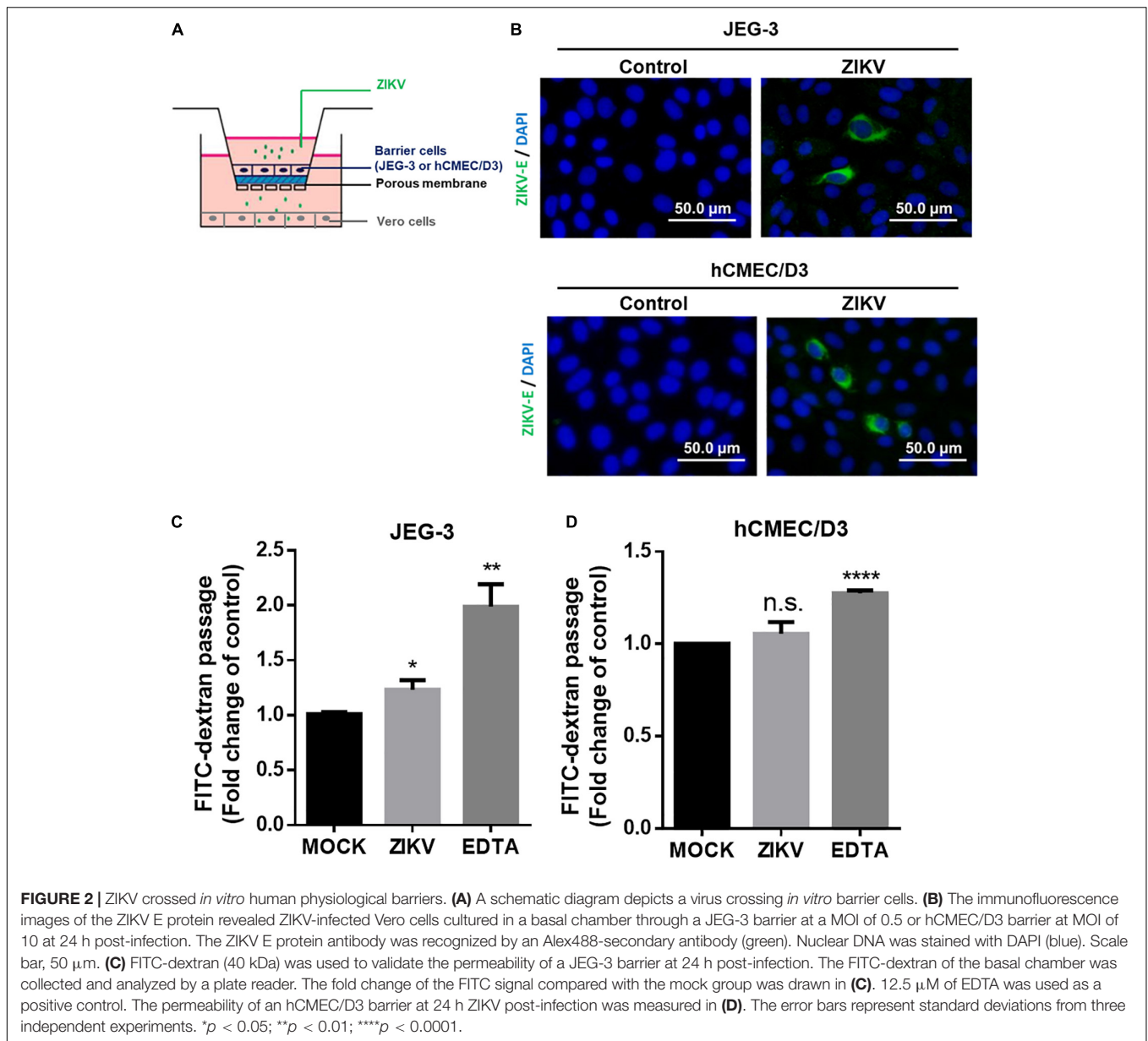


**FIGURE 1 |** The infectivity and virulence of ZIKV in JEG-3 and hCMEC/D3 cells. **(A)** The immunofluorescence images of ZIKV E protein revealed the population of ZIKV-infected cells in JEG-3 (MOI of 0.25 to 1) and hCMEC/D3 cells (MOI of 1 to 10) at 24 h post-infection. The ZIKV E protein antibody was recognized by an Alex488-secondary antibody (green). Nuclear DNA was stained with DAPI (blue). Scale bar, 20  $\mu\text{m}$ . **(B)** The percentage of infected cells was quantified from **(A)**. **(C)** JEG-3 cells were infected ZIKV at MOI of 0.5 to 1, and hCMEC/D3 cells were infected ZIKV at MOI of 5 to 10 during 24 h. The virulence of ZIKV in JEG-3 and hCMEC/D3 was measured by a cell viability assay. The error bars represent standard deviations from three independent experiments. Statistical differences were obtained through *t*-tests. \*\* $p < 0.01$ ; \*\*\* $p < 0.001$ .

was added on the top of the inserts at a MOI of 0.5. If ZIKV particles could cross barrier cells, they would exist in the basal chamber and infect into Vero cells. The existence of the ZIKV in Vero cells was detected by immunostaining using an anti-ZIKV E protein antibody. The results showed clearly that the ZIKV E protein could be detected in Vero

cells in either JEG-3 and hCMEC/D3 cells as barrier cells (**Figure 2B**). These results indicated that the ZIKV could cross the human physiological barrier cells. It is possible for the ZIKV to cross barrier cells by altering the permeability of barrier cells. To investigate this possibility, the permeability of the cells was examined by using FITC-dextran as an indicator



in the *in vitro* Transwell barrier assay. FITC-dextran was added in the apical chamber after 24 h post-infection. If ZIKV infection could alter cell permeability, the signal of FITC-dextran should be detected in the basal chamber. Compared with the mock group, ZIKV infection did increase FITC-dextran signal significantly when JEG-3 cells were used as barrier cells (Figure 2C). In contrast, there was no significant change of the FITC-dextran signal between the mock group and the ZIKV-infected group when hCMEC/D3 cells were used as barrier cells (Figure 2D). Ethylenediaminetetraacetic acid disodium salt (EDTA) that can increase cell permeability was used as a positive control. These results suggested that the ZIKV may cross the placenta barrier by changing the permeability of the barrier cells. In contrast, the ZIKV crosses the BBB barrier cells but does not change the permeability of the BBB barrier cells

(Figures 2B,C), suggesting no barrier leakage when the ZIKV crossed the BBB.

### ZIKV Down-Regulated the Expression of Tight Junction Protein Through a Proteasomal Degradation Pathway

Given that the leakage of FITC-dextran was increased by ZIKV infection in the *in vitro* placenta barrier model but not in the BBB barrier model (Figures 2C,D), it raised a possibility that the disruption of the tight junction of JEG-3 is associated with the barrier leakage because the tight junctions of trophoblasts epithelial cells bear critical barrier functions for protection against a paracellular spread of various pathogens, including viruses (Delorme-Axford et al., 2014). To investigate

this hypothesis, the expression of two tight junction proteins, ZO-1 and occludin were examined in JEG-3 as well as hCMEC/D3. The results of the western blotting assay clearly depicted a decreasing expression of ZO-1 and occludin in JEG-3 cells in the presence of ZIKV infection compared to that in the mock control group (**Figure 3A**). In contrast, there was no significantly different expression of ZO-1 and occludin between the ZIKV-infected group and the mock control group in hCMEC/D3 cells (**Figure 3B**). To further confirm the disruption of tight junction by ZIKV infection in JEG-3 cells, the distribution of ZO-1 and occludin were detected by an immunofluorescence assay. Confocal imaging revealed that tight junctions formed continuous seals between adjacent cells in the absence of ZIKV infection (**Figure 3C**). In contrast, ZIKV infection disrupted the continuity of occludin and ZO-1 in JEG-3 cells (white arrows in **Figure 3C**, left panel). The integrity of junctional ZO-1 and occludin of JEG-3 cells was quantified by measuring the branch length of segments. The results demonstrated that ZIKV infection declined the integrity of tight junction of JEG-3 cells (**Figure 3C**, right panel).

To further investigate the regulatory mechanism of ZIKV-induced decreased of ZO-1 and occludin expression, mRNA levels of these two proteins isolated from JEG-3 and hCMEC/D3 cells in the absence or presence of ZIKV infection were determined by RT-qPCR. The results of RT-qPCR depicted no significant change of mRNA level of ZO-1 and occludin in both JEG-3 and hCMEC/D3 cells regardless of ZIKV infection (**Figures 4A,B**). These data suggested that the down regulation of ZO-1 and occludin expression in JEG-3 cells might be regulated at the post-transcription level. To confirm this speculation, prior to ZIKV infection, JEG-3 cells were treated individually by a series of pharmacological inhibitors including bafilomycin (BFA), MG132, and chloroquine (CQ), which target either autophagic or proteasomal degradation pathways, the two major cellular pathways mediating protein degradation. As shown in **Figure 4C**, the expression of ZO-1 and occludin repressed by ZIKV infection could be notably rescued only by MG132, a proteasome inhibitor, but not by either BFA, an inhibitor for both V-ATPase-dependent acidification and autophagosome-lysosome fusion or CQ, an inhibitor for fusion of autophagosomes and lysosomes. Taken together, these results demonstrated that ZIKV infection causes the leakage of the placenta barrier through the disruption of cellular tight junction via the proteasomal degradation pathway.

## Visualization of Transcytosis of ZIKV

It has been reported that transcytosis, a series action to transport macromolecules intracellularly through the vesicular system, is a common strategy for molecules crossing impermeable barriers under normal physiological condition (Tuma and Hubbard, 2003). Therefore, we would like to conduct a single-virus imaging analysis to investigate whether ZIKV particle can also cross barrier cells by transcytosis in *in vitro* Transwell barrier models. To visualize single ZIKV particles directly, ZIKV particles were labeled with a fluorescence dye, atto647N, by conjugating atto647N-NHS ester with the amino group of the viral envelope protein. The atto647N-labeled ZIKV particles were purified through a Sephadex G-25 size-exclusion column. Compared to

the fractions containing the 40 nm fluorosphere (**Figure 5A**, solid circles), the fluorescent signals of atto647N existent from Fraction 6 to Fraction 10 (**Figure 5A**, solid squares) indicated atto647N-labeled ZIKV particles (atto647N-ZIKV) because the diameter of a single ZIKV particle is approximately 50 nm (Sirohi et al., 2016; Sevvana et al., 2018). No fluorescence signal was detected within the same range of fractions from the Dye-free ZIKV group (**Figure 5A**, solid triangles). These results confirmed a successful conjugation of ZIKV particles with atto647N. The infectivity of atto647N-ZIKV particles was then measured by a plaque assay. Both dye-free ZIKV and atto647N-ZIKV presented similar virus titers, suggesting no significant influence on ZIKV infectivity by the atto647N labeling procedure (**Figure 5B**).

Given that transcytosis is a characteristic pathway of intracellular trafficking that allows a selective and rapid transcellular transport from the apical side to the basolateral side within a cell, and the intracellular transport is a temperature-dependent process that can be inhibited at 4°C, in contrast to the paracellular transport (Morad et al., 2019), we speculated that the energy-dependent intracellular transport of virus particles should be inhibited at 4°C. Therefore, using an *in vitro* Transwell barrier assay, we would like to investigate whether the ZIKV can penetrate a monolayer of barrier cells at 4°C and 37°C by directly measuring the fluorescence intensity of atto647N signals in the basal chamber of a Transwell plate. In both JEG-3 and hCMEC/D3 cells, atto647N-ZIKV particles were significantly decreased in the basal chamber at 4°C condition, compared to that at 37°C (**Figure 5C**). In contrast to atto647N-ZIKV particles, there was no difference of FITC-dextran in the basal chamber of Transwell plate at both 4°C and 37°C (**Figure 5D**). These results implied that the ZIKV can cross monolayers of either JEG-3 or hCMEC/D3 cells through a temperature-dependent transcytosis. To directly visualize the transcytosis of ZIKV particle across a monolayer of barrier cells, we infected a monolayer of JEG-3 cells on a 3.5 cm glass-bottom plate with Atto647N-ZIKV and acquired confocal imaging at 0, 30, and 60 min post-infection. JEG-3 cells were stained with DAPI and WGA488 to indicate the positions of nucleus and cell membrane, respectively. As shown in **Figure 6A**, Atto647N-ZIKV particles were only detected on the surface of the JEG-3 monolayer at the initial time point (0 min). Apparently, Atto647N-ZIKV particles were internalized into cytoplasm and moved from the apical side to the basal side of the cells at 30- and 60-min post-infection (**Figure 6A**). The similar results also can be observed in hCMEC/D3 monolayers (**Figure 6B**). These results elucidated that ZIKV particles might be directly transported across the monolayer of barrier cells by transcytosis without undergoing the viral replication process.

## ZIKV Transport Can Be Blocked by Endocytosis and Microtubule Inhibitors

Endocytosis recognized as the responsible mechanism of molecule transcytosis inside the cells contains various pathways including caveolae-dependent endocytosis, clathrin-coated vesicle-mediated endocytosis and macropinocytosis. To further examine endocytic pathways for ZIKV entrance into barrier cells, we pretreated barrier cells with pharmacological

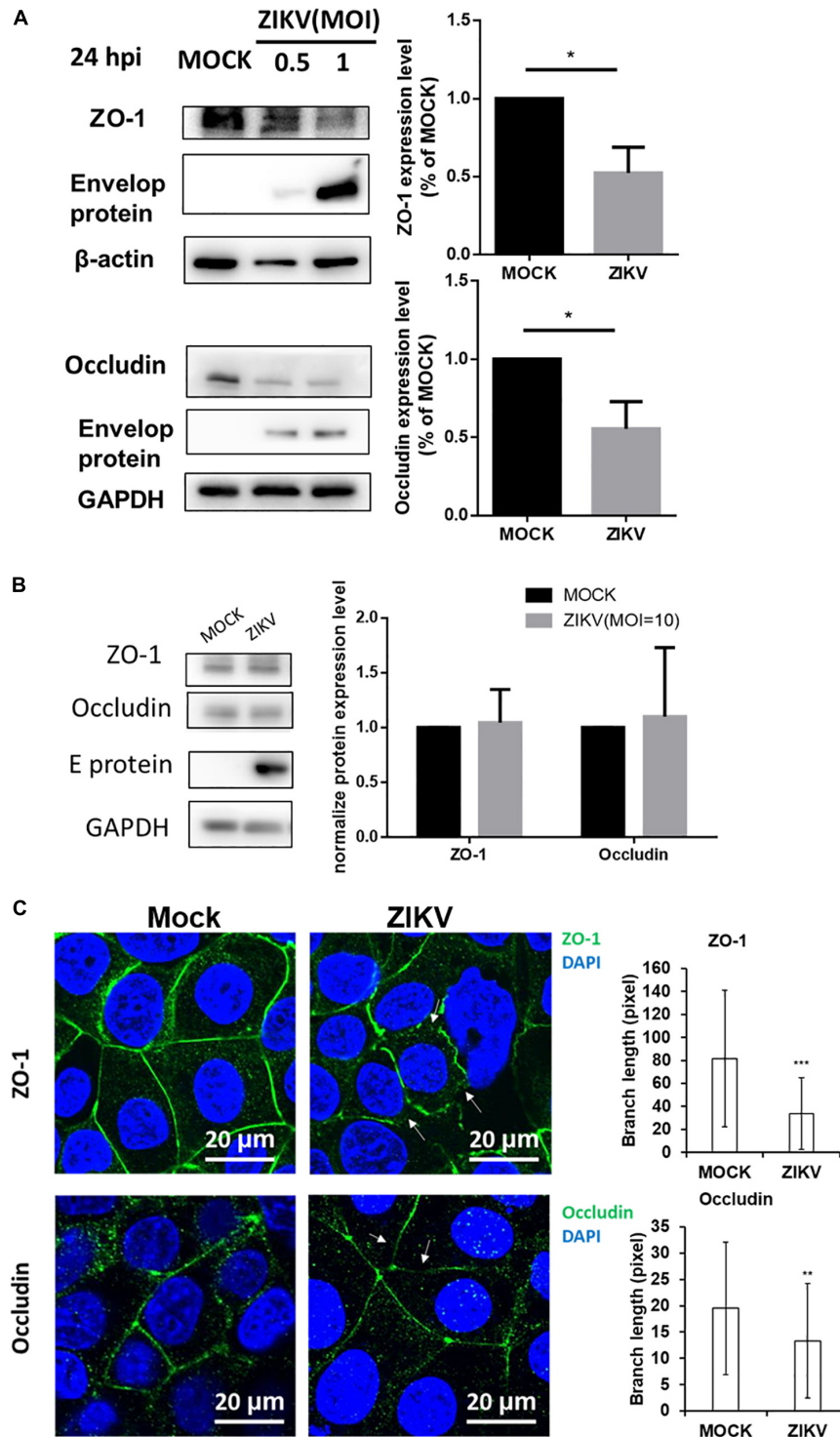


**FIGURE 3 |** ZIKV infection decreased expression of the tight junction protein ZO-1 and Occludin in JEG-3 but not hCMEC/D3. **(A)** Western blotting depicted that the amount of ZO-1 and Occludin decreased in JEG-3 cells at 24 h post-infection. The amount of ZO-1 and Occludin was normalized by  $\beta$ -actin and GAPDH, respectively. Comparison with the mock group was quantified in the right panel. Statistical differences were obtained through *t*-tests.  $**p < 0.05$ . **(B)** Western blotting depicted that the expression of ZO-1 and Occludin were not affected in hCMEC/D3 cells with ZIKV infection. The amount of ZO-1 and Occludin was normalized by GAPDH, and quantified in the right panel. **(C)** The distribution of ZO-1 and Occludin in JEG-3 cells with/without ZIKV infection were imaged by confocal microscopy. The white arrows indicate the disruption of ZO-1 and Occludin. Scale bar, 20  $\mu$ m. The tight junction integrity of ZO-1 and occludin were measured by the Skeletonize plug-in of ImageJ software. The length of segments in each group ( $n = 50$ ) were measured and quantified as right histograms.  $**p < 0.01$ ,  $***p < 0.001$ .

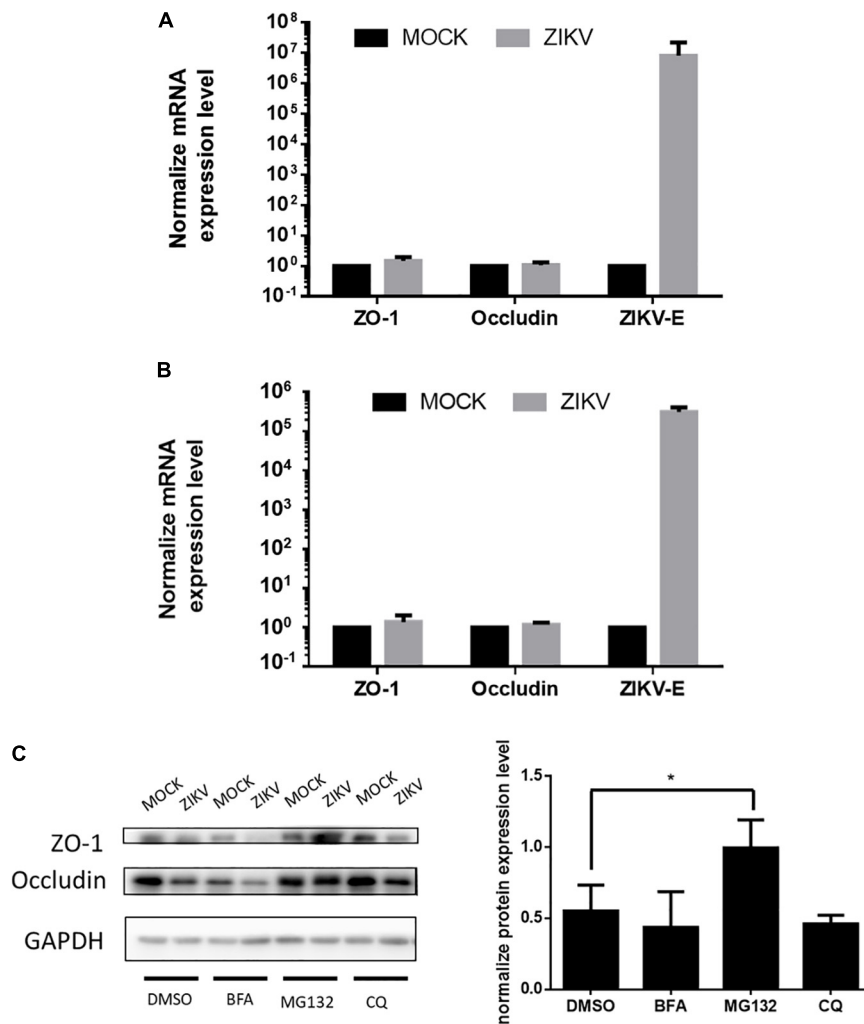


**FIGURE 4 |** ZIKV infection decreased the accumulation of tight junction proteins through post-transcription regulation. **(A)** The mRNA levels of ZO-1, Occludin and ZIKV-E in JEG-3 cells upon ZIKV infection were quantified by RT-qPCR. Data were normalized by GAPDH. The fold changes of mRNA were compared with the mock group. The mRNA levels of ZO-1, Occludin and ZIKV-E in hCMEC/D3 upon ZIKV infection are shown in **(B)**. The error bars represent standard deviations from three independent experiments. **(C)** Western blotting depicts the accumulation of ZO-1 and Occludin in JEG-3 cells with various inhibitors treatments upon ZIKV infection. The amount of ZO-1 and Occludin was normalized by GAPDH. The fold changes of protein expression compared with the mock group in each term were quantified in the right panel. The error bars represent standard deviations from three independent experiments. \* $p < 0.05$ .

inhibitors including Nystatin, chlorpromazine (CPZ), and dimethyl amiloride (DMA), which specifically inhibit caveolae-dependent endocytosis, clathrin-dependent endocytosis, and micropinocytosis, respectively. Colchicine, an inhibitor to prevent microtubule polymerization was used to disrupt intracellular trafficking. The concentration of inhibitors used in the current study did not cause cytotoxicity or increase cellular permeability in both JEG-3 and hCMEC/D3 cells (**Figures 7A,B**). Compared to the control group, the treatment of the three pharmacological inhibitors of endocytosis decreased the intensity of atto647N signals in the basal chamber of a Transwell plate (**Figure 7C**), suggesting that endocytosis might be essential for the ZIKV to cross the monolayer of barrier cells. In addition, the treatment of colchicine also reduced atto647N intensity in the basal chamber (**Figure 7C**), which indicated the requirement

of microtubule polymerization for intracellular trafficking of the ZIKV. To further quantify the effect of inhibitors on the ZIKV crossing barrier cells, the titers of ZIKV isolated from the basal chamber 3 h post-infection were determined by a plaque assay. The results depicted that all four inhibitors reduced viral titers in the basal chamber, compared to that in the control group (**Figure 7D**). Taken together, these results suggested that transcytosis may be an important pathway for the ZIKV to cross the placental barrier and the BBB.

## DISCUSSION

In this study we investigated the pathways for the ZIKV crossing the endothelial cell monolayer of both the placenta

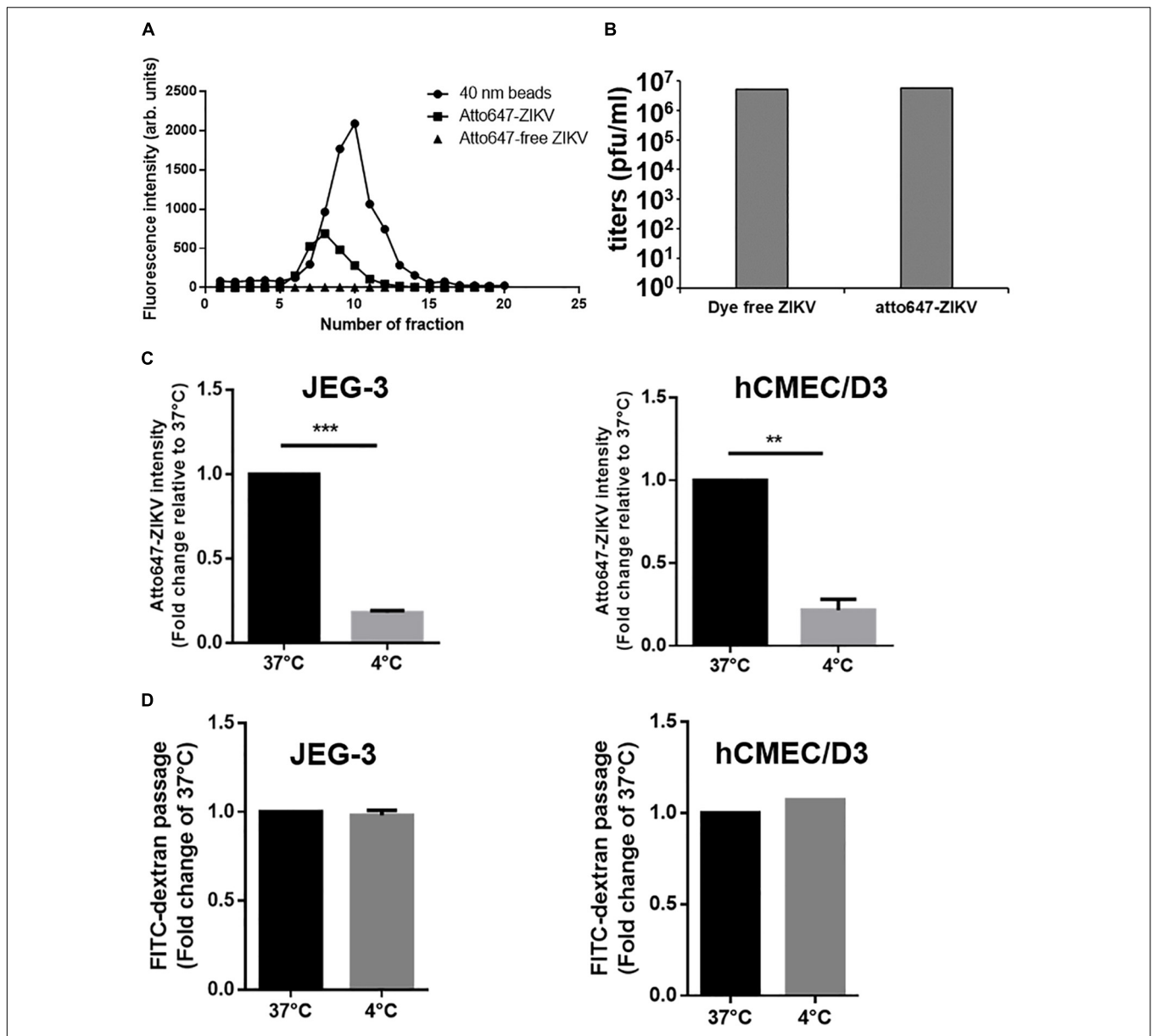
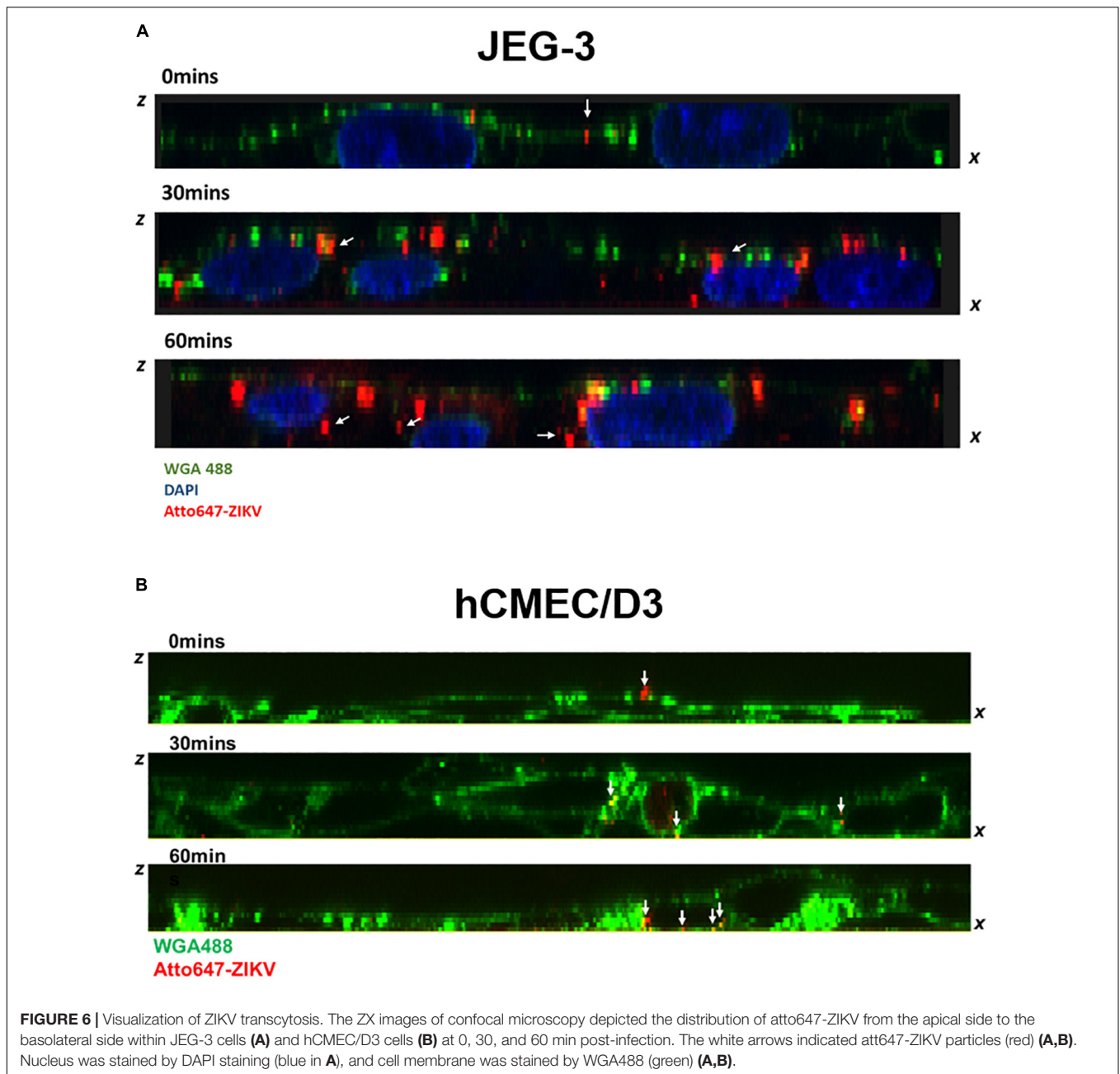


**FIGURE 5 |** Detection of ZIKV transcytosis. **(A)** Fluorescence intensity profiles of elution from a Sephadex G-25 size-exclusion column is shown. An Atto647N-ZIKV particle was purified within the fraction layer 6 to 10 from gel filtration (solid squares). No fluorescence signal was detected in Atto647N-free ZIKV (solid triangles) within the same fraction layers. The 40 nm fluorescence microspheres were used as a size marker (solid circles). **(B)** Plaque assays were performed to determine the infectivity of the Atto647N-ZIKV. Dye-free ZIKV was used as a control. Both virus samples were purified from the same fractions of the Sephadex G-25 column. **(C)** Atto647N-ZIKV was used to validate virus crossing efficiency in JEG-3 and hCMEC/D3 barriers at 37 or 4 °C. **(D)** FITC-dextran was used to validate the permeability of JEG-3 and hCMEC/D3 barriers in **(C)** condition. The error bars represent standard deviations from three independent experiments. \*\* $p < 0.01$ , \*\*\* $p < 0.001$ .

barrier and the BBB. Using fluorescence-tagged dextran as an indicator, our results revealed that ZIKV infection enhanced cellular permeability in JEG-3 cells but not in hCMEC/D3 cells. Moreover, in JEG-3 cells, ZIKV infection reduces the amount of tight junction proteins, ZO-1 and occludin, through the proteasomal degradation pathway, resulting in disruption of tight junction. In contrast, using fluorescence-labeled ZIKV particles and pharmacological inhibitors of endocytosis, we demonstrated

transcytosis as an additional pathway for the ZIKV crossing the monolayer of JEG-3 and hCMEC/D3. As summarized in **Figure 8**, our current study elucidated that the ZIKV uses a cell-type specific paracellular pathway to cross the placenta monolayer barrier by disrupting cellular tight junction. In addition, the ZIKV can also cross both the placenta barrier and the BBB by transcytosis (**Figure 6**). The present study provides new insights on cellular barrier penetration of ZIKV



particles, which may facilitate the development of anti-ZIKV agents in the future.

Several lines of evidence showed the existence of ZIKV antigens in the chronic villi of a human placenta from a mother who gave birth to an infant with microcephaly (Calvet et al., 2016), and isolation of ZIKV RNA from placental tissue of mice infected with the ZIKV (Caine et al., 2018), suggesting that the ZIKV may penetrate the placental barrier to infect the infant brain. Recent studies reported that the ZIKV is able to infect and replicate in Hofbauer cells that are primary human placental macrophages and in cytotrophoblasts, suggesting a route of intrauterine transmission that the ZIKV crosses the fetal

compartment by directly infecting the placental cells (Quicke et al., 2016). In this study, we revealed that the ZIKV could cross the placenta barrier with both paracellular and transcytosis (Figures 2, 5–7). Normally, microorganisms spreading through epithelial tissues are blocked by tight junctions and adherent junctions present on apical and basolateral surfaces, respectively (Mateo et al., 2015). However, our data revealed that ZIKV infection causes leakage of the placental barrier by disrupting the integrity of the tight junction of the barrier cells (Figures 2, 3). Further investigation elucidated that the breakdown of the tight junction in the placental barrier cells is due to a decrease in the amounts of ZO-1 and occludin, two essential

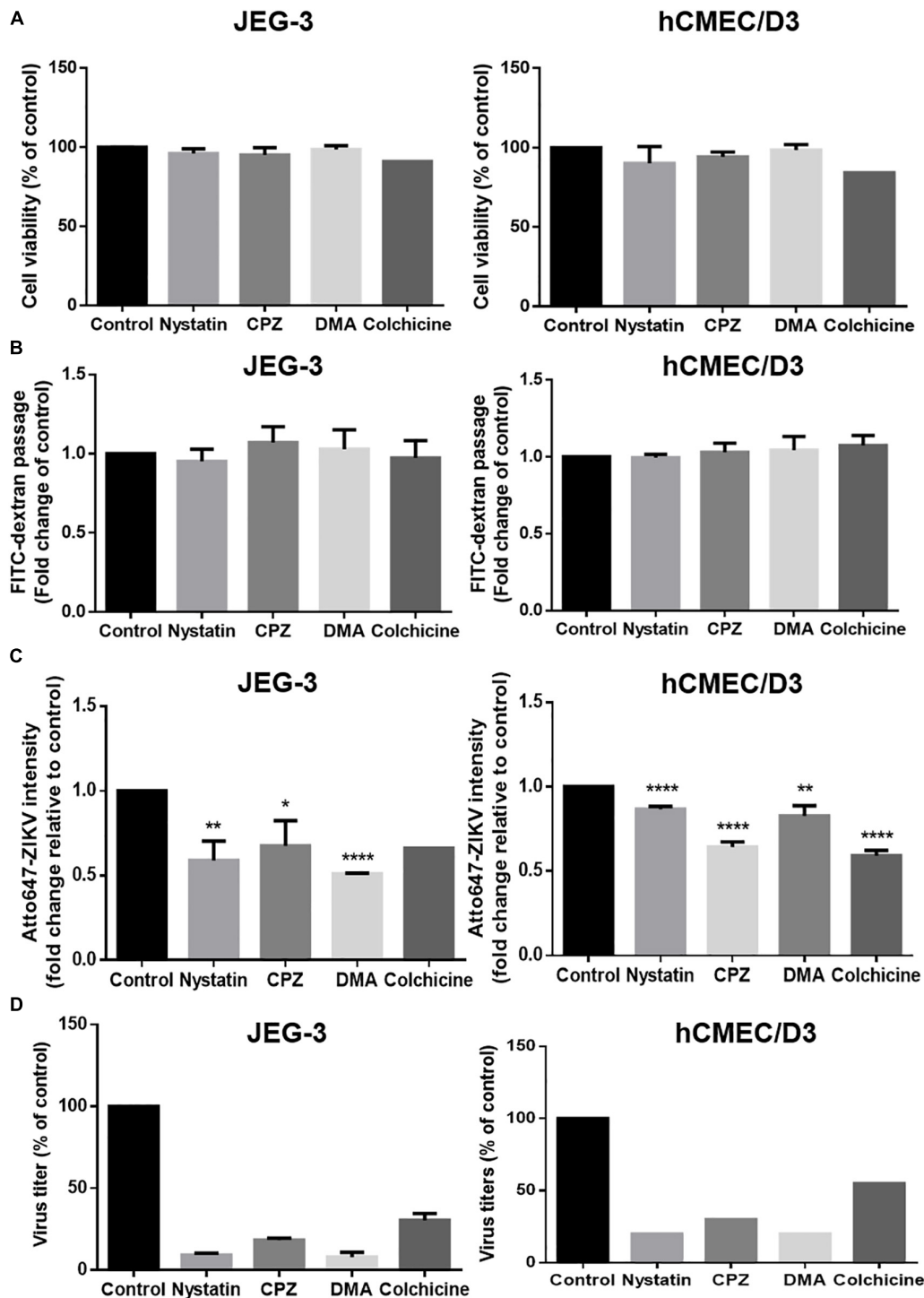
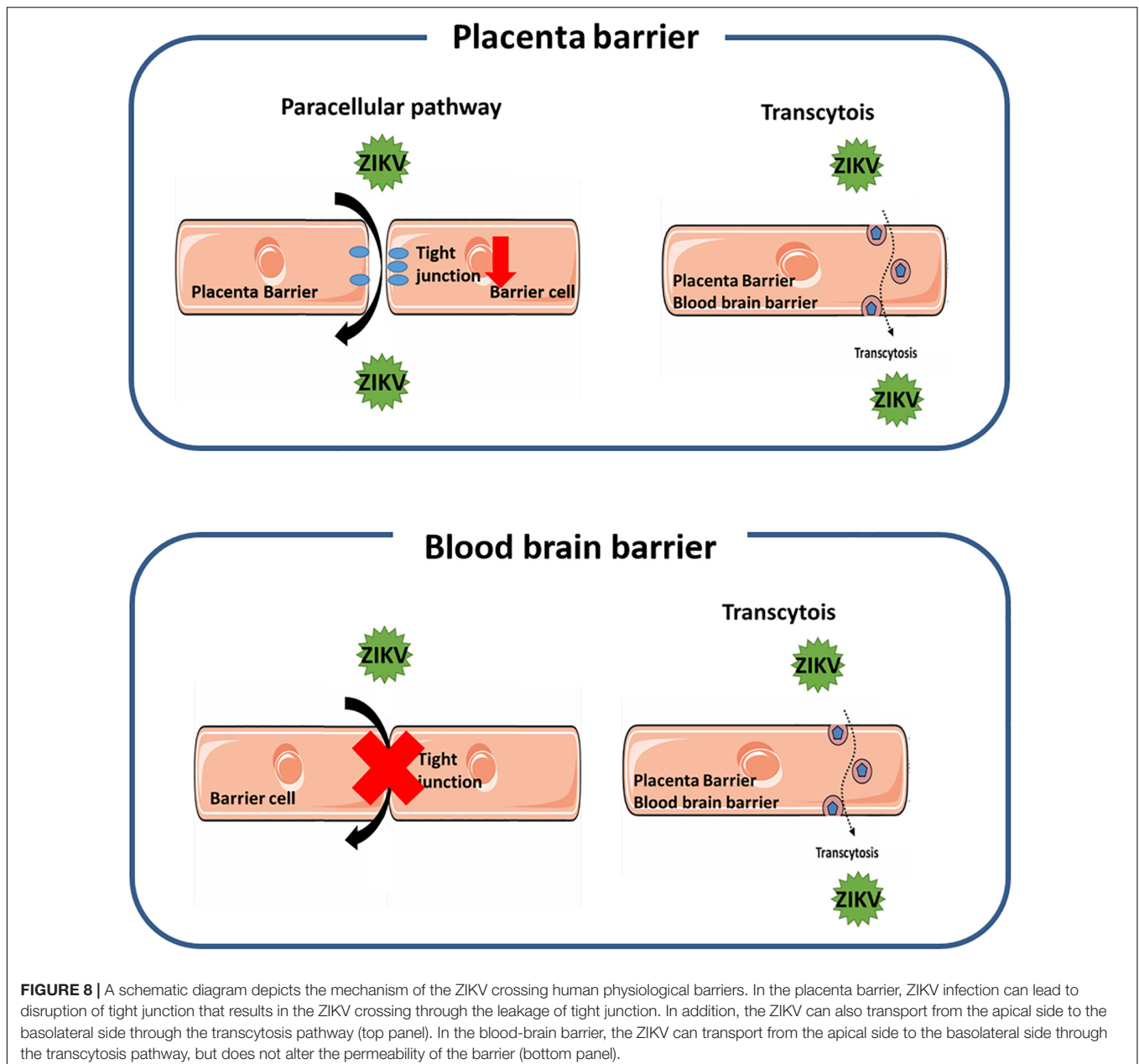


**FIGURE 7 |** ZIKV transcytosis across JEG-3 and hCMEC/D3 barriers can be reduced by endocytosis and microtubule inhibitors. **(A)** The cell viabilities of JEG-3 and hCMEC/D3 with/without various inhibitors treatment were analyzed by a SRB assay. **(B)** The permeability of JEG-3 and hCMEC/D3 barriers with/without various inhibitors treatment were validated by detecting FITC-dextran across cell barriers. **(C)** Atto647-ZIKV was used to validate virus crossing efficiency in JEG-3 and hCMEC/D3 barriers with/without inhibitors treatment. **(D)** A plaque assay was used to measure the virus titers across JEG-3 and hCMEC/D3 barriers with/without various inhibitor treatments. All results are depicted as fold changes compared to the non-treatment control. The error bars represent standard deviations from three independent experiments. \* $p < 0.05$ ; \*\* $p < 0.01$ ; \*\*\*\* $p < 0.0001$ .



tight junction proteins, through the proteasomal degradation pathway (Figure 4). In contrast to the direct infection pathway (Quicke et al., 2016), our results proposed a paracellular pathway for the ZIKV crossing the placental barrier by disrupting the cellular tight junction of the barrier cells through degradation of ZO-1 and occludin. The activation mechanism of the proteasomal degradation pathway by ZIKV infection remains to be further investigated.

Using a SVT approach, we provided evidence to elucidate that the ZIKV can cross the *in vitro* placenta model through transcytosis (Figure 6A). Maternal-fetal transmission of a number of viruses by transcytosis in the placenta has been proposed previously (Bhat and Anderson, 2007). Given that

transport of maternal IgG across the placenta is minimal during the first trimester and rises dramatically between 22 and 26 weeks of gestation (Simister and Story, 1997; Palmeira et al., 2012), Matthew et al. showed that DENV cross-reactive mAbs bound to the ZIKV undergo FcRn-mediated transcytosis across the placenta to productively infect human placental macrophages (Zimmerman et al., 2018). In the current study, the ZIKV crossing the placenta barrier cells was directly visualized by using Atto647N-ZIKV particles (Figure 6A). These results provide strong evidence demonstrating the straight passing of viral particles across the placental barrier rather than a release of newly produced viral particles after replication. Moreover,

the action of ZIKV transcytosis could be inhibited by treatments with endocytosis inhibitors and colchicine (Figure 7). Taken together, we demonstrated that both the paracellular pathway and the transcytosis pathway are utilized by ZIKV to cross the placenta barrier (Figure 8, top panel). Further studies will be needed in order to illustrate how ZIKV particles select a pathway to cross the placenta barrier and whether they require a specific receptor for ZIKV to interact with.

In addition to the placenta barrier, the BBB is the other important barrier that protect the fetal brain development during pregnancy (Goasdoue et al., 2017). A number of neurotropic viruses enter the CNS by using various pathways including direct transport from peripheral nerves, transinfection and transcytosis (Mustafa et al., 2019). In the current study, the ZIKV can cross brain endothelial cells and release of infectious virus particles, without an increase of endothelial monolayer permeability and no significant cytotoxicity *in vitro* (Figures 1, 2, 7). This is in agreement with previous studies showing the ZIKV crosses the BBB monolayer without the BBB barrier disruption (Papa et al., 2017; Alimonti et al., 2018). However, our studies showed that there were infectious atto647N-labeled virus particles that crossed the monolayer of BBB barrier cells in the presence of the treatment of endocytic inhibitors (Figures 7C,D), suggesting that we still cannot exclude the possibility that some viral particles selectively modulate tight junctions and cross the bottom chamber via paracellular diapedesis without overtly disrupting the BBB permeability. Furthermore, although *in vivo* experiment models proposed that the ZIKV crosses the BBB with no severe disruption, barrier breakdown was detected at a later post-infection time (Papa et al., 2017). Because ZIKV infection may recruit leukocyte to the brain and induce neuron lesion and death (Jurado et al., 2018; Mustafa et al., 2019), it is possible that later BBB disruption may be triggered by inflammatory response rather than ZIKV-induced proteasomal degradation.

Understanding the pathways for ZIKV passing through physiological barriers, the placental barrier and the BBB, furthers our understanding of the pathophysiology of the ZIKV and provides a basis for developing anti-ZIKV drugs in a relevant cell type. Given that the activation of the proteasome degradation pathway to disrupt tight junction protein participates in a paracellular pathway for the maternal-fetal transmission of the ZIKV by disrupting tight junction proteins (Figures 2–4), it may lead to a new anti-ZIKV approach to maintain the integrity

of tight junction and inhibit the process of viral extravasation in the placental by blocking degradation of the tight junction protein. In addition, our findings offer evidence that transcytosis may be a common strategy for the ZIKV to cross both the placental barrier and the BBB (Figures 5–7). Since transcytosis is a critical pathway to transport macromolecules intracellularly through the vesicular system (Tuma and Hubbard, 2003), it may not be a good druggable target to treat ZIKV infection. Therefore, further studies to reveal whether there is a specific interaction of the ZIKV with the transcytosis machine will facilitate the development of new anti-ZIKV agents.

## DATA AVAILABILITY STATEMENT

The datasets generated for this study are available on request to the corresponding author.

## AUTHOR CONTRIBUTIONS

C-FC, L-WC, C-CJ, and Y-HP designed the research, analyzed the data, and wrote the manuscript. C-FC, L-WC, and I-CL performed the research. C-CJ, YS, and Y-LL provided the critical reagents and assisted virus study.

## FUNDING

This work was supported by the Higher Education Sprout Project by the Ministry of Education (MOE) in Taiwan (107AC-D101 and 107AC-D962) to Y-HP, the research grants from the Ministry of Science and Technology, Taiwan (MOST 106-2320-B-010-014 and MOST 108-2320-B-010-031 to Y-HP), and the grant from the National Yang-Ming University – Far Eastern Memorial Hospital Joint Research Program (108DN01) to Y-HP.

## ACKNOWLEDGMENTS

We are thankful to Taiwan CDC for Zika virus (PRVABC59 strains). We also thank Dr. Janice Fon for critically reading and editing this article.

## REFERENCES

- Alimonti, J. B., Ribocco-Lutkiewicz, M., Sodja, C., Jezierski, A., Stanimirovic, D. B., Liu, Q., et al. (2018). Zika virus crosses an *in vitro* human blood brain barrier model. *Fluids Barriers CNS* 15:15. doi: 10.1186/s12987-018-0100-y
- Al-Obaidi, M. M. J., Bahadoran, A., Har, L. S., Mui, W. S., Rajarajeswaran, J., Zandi, K., et al. (2017). Japanese encephalitis virus disrupts blood-brain barrier and modulates apoptosis proteins in THBMEC cells. *Virus Res.* 233, 17–28. doi: 10.1016/j.virusres.2017.02.012
- Ayloo, S., and Gu, C. (2019). Transcytosis at the blood-brain barrier. *Curr. Opin. Neurobiol.* 57, 32–38. doi: 10.1016/0006-8993(87)90236-8
- Bhat, P., and Anderson, D. A. (2007). Hepatitis B virus translocates across a trophoblastic barrier. *J. Virol.* 81, 7200–7207. doi: 10.1128/jvi.02371-06
- Brasil, P., Sequeira, P. C., Freitas, A. D., Zogbi, H. E., Calvet, G. A., De Souza, R. V., et al. (2016). Guillain-Barre syndrome associated with Zika virus infection. *Lancet* 387:1482.
- Burton, G. J., and Fowden, A. L. (2015). The placenta: a multifaceted, transient organ. *Philos. Trans. R. Soc. Lond. B Biol. Sci.* 370:20140066. doi: 10.1098/rstb.2014.0066
- Caine, E. A., Jagger, B. W., and Diamond, M. S. (2018). Animal models of zika virus infection during pregnancy. *Viruses* 10:E598.
- Calvet, G., Aguiar, R. S., Melo, A. S. O., Sampaio, S. A., De Filippis, I., Fabri, A., et al. (2016). Detection and sequencing of Zika virus from amniotic fluid of fetuses with microcephaly in Brazil: a case study. *Lancet Infect. Dis.* 16, 653–660. doi: 10.1016/S1473-3099(16)00095-5
- Chu, L. W., Huang, Y. L., Lee, J. H., Huang, L. Y., Chen, W. J., Lin, Y. H., et al. (2014). Single-virus tracking approach to reveal the interaction of Dengue virus

- with autophagy during the early stage of infection. *J. Biomed. Opt.* 19:011018. doi: 10.1117/1.JBO.19.1.011018
- Chu, L. W., Yang, C. J., Peng, K. J., Chen, P. L., Wang, S. J., and Ping, Y. H. (2019). TIM-1 as a signal receptor triggers dengue virus-induced autophagy. *Int. J. Mol. Sci.* 20:4893. doi: 10.3390/ijms20194893
- Cordeiro, M. T., Pena, L. J., Brito, C. A., Gil, L. H., and Marques, E. T. (2016). Positive IgM for Zika virus in the cerebrospinal fluid of 30 neonates with microcephaly in Brazil. *Lancet* 387, 1811–1812. doi: 10.1016/s0140-6736(16)30253-7
- Coyne, C. B., and Lazear, H. M. (2016). Zika virus - reigniting the TORCH. *Nat. Rev. Microbiol.* 14, 707–715. doi: 10.1038/nrmicro.2016.125
- Daneman, R., and Prat, A. (2015). The blood-brain barrier. *Cold Spring Harb. Perspect. Biol.* 7:a020412. doi: 10.1101/cshperspect.a020412
- Daniels, B. P., and Klein, R. S. (2015). Viral sensing at the blood-brain barrier: new roles for innate immunity at the CNS vasculature. *Clin. Pharmacol. Ther.* 97, 372–379. doi: 10.1002/cpt.75
- Delorme-Axford, E., Sadovsky, Y., and Coyne, C. B. (2014). The Placenta as a barrier to viral infections. *Annu. Rev. Virol.* 1, 133–146. doi: 10.1146/annurev-virology-031413-085524
- Dick, G. W., Kitchen, S. F., and Haddow, A. J. (1952). Zika virus. i. isolations and serological specificity. *Trans. R. Soc. Trop. Med. Hyg.* 46, 509–520. doi: 10.1016/0035-9203(52)90042-4
- Dos Santos, T., Rodriguez, A., Almiron, M., Sanhueza, A., Ramon, P., De Oliveira, W. K., et al. (2016). Zika virus and the guillain-barre syndrome - case series from seven countries. *N. Engl. J. Med.* 375, 1598–1601.
- Fitzgerald, B., Boyle, C., and Honein, M. A. (2018). Birth defects potentially related to zika virus infection during pregnancy in the united states. *JAMA* 319, 1195–1196.
- Goasdoue, K., Miller, S. M., Colditz, P. B., and Bjorkman, S. T. (2017). Review: the blood-brain barrier; protecting the developing fetal brain. *Placenta* 54, 111–116. doi: 10.1016/j.placenta.2016.12.005
- Gude, N. M., Roberts, C. T., Kalonias, B., and King, R. G. (2004). Growth and function of the normal human placenta. *Thromb. Res.* 114, 397–407. doi: 10.1016/j.thromres.2004.06.038
- Hartsock, A., and Nelson, W. J. (2008). Adherens and tight junctions: structure, function and connections to the actin cytoskeleton. *Biochim. Biophys. Acta* 1778, 660–669. doi: 10.1016/j.bbame.2007.07.012
- Hoen, B., Schaub, B., Funk, A. L., Ardillon, V., Boullard, M., Cabie, A., et al. (2018). Pregnancy outcomes after ZIKV infection in french territories in the americas. *N. Engl. J. Med.* 378, 985–994. doi: 10.1056/NEJMoa1709481
- Jurado, K. A., Yockey, L. J., Wong, P. W., Lee, S., Huttner, A. J., and Iwasaki, A. (2018). Antiviral CD8 T cells induce Zika-virus-associated paralysis in mice. *Nat. Microbiol.* 3, 141–147. doi: 10.1038/s41564-017-0060-z
- Leibrand, C. R., Paris, J. J., Ghandour, M. S., Knapp, P. E., Kim, W.-K., Hauser, K. F., et al. (2017). HIV-1 Tat disrupts blood-brain barrier integrity and increases phagocytic perivascular macrophages and microglia in the dorsal striatum of transgenic mice. *Neurosci. Lett.* 640, 136–143. doi: 10.1016/j.neulet.2016.12.073
- Liou, M. L., and Hsu, C. Y. (1998). Japanese encephalitis virus is transported across the cerebral blood vessels by endocytosis in mouse brain. *Cell Tissue Res.* 293, 389–394.
- Mateo, M., Generous, A., Sinn, P. L., and Cattaneo, R. (2015). Connections matter—how viruses use cell-cell adhesion components. *J. Cell Sci.* 128, 431–439. doi: 10.1242/jcs.159400
- Mittal, R., Nguyen, D., Debs, L. H., Patel, A. P., Liu, G., Jhaveri, V. M., et al. (2017). Zika virus: an emerging global health threat. *Front. Cell Infect. Microbiol.* 7:486. doi: 10.3389/fcimb.2017.00486
- Mlakar, J., Korva, M., Tul, N., Popovic, M., Poljsak-Prijatelj, M., Mraz, J., et al. (2016). Zika virus associated with microcephaly. *N. Engl. J. Med.* 374, 951–958. doi: 10.1056/NEJMoa1600651
- Morad, G., Carman, C. V., Hagedorn, E. J., Perlin, J. R., Zon, L. I., Mustafaoglu, N., et al. (2019). Tumor-derived extracellular vesicles breach the intact blood-brain barrier via transcytosis. *ACS Nano* 13, 13853–13865. doi: 10.1021/acsnano.9b04397
- Mustafa, Y. M., Meuren, L. M., Coelho, S. V. A., and De Arruda, L. B. (2019). Pathways exploited by flaviviruses to counteract the blood-brain barrier and invade the central nervous system. *Front. Microbiol.* 10:525. doi: 10.3389/fmicb.2019.00525
- Palmeira, P., Quinello, C., Silveira-Lessa, A. L., Zago, C. A., and Carneiro-Sampaio, M. (2012). IgG placental transfer in healthy and pathological pregnancies. *Clin. Dev. Immunol.* 2012:985646. doi: 10.1155/2012/985646
- Papa, M. P., Meuren, L. M., Coelho, S. V. A., Lucas, C. G. O., Mustafa, Y. M., Lemos Matassoli, F., et al. (2017). Zika virus infects, activates, and crosses brain microvascular endothelial cells, without barrier disruption. *Front. Microbiol.* 8:2557. doi: 10.3389/fmicb.2017.02557
- Petersen, L. R., Jamieson, D. J., Powers, A. M., and Honein, M. A. (2016). Zika virus. *N. Engl. J. Med.* 374, 1552–1563.
- Quicke, K. M., Bowen, J. R., Johnson, E. L., McDonald, C. E., Ma, H., O'Neal, J. T., et al. (2016). Zika virus infects human placental macrophages. *Cell Host Microbe* 20, 83–90. doi: 10.1016/j.chom.2016.05.015
- Roe, K., Kumar, M., Lum, S., Orillo, B., Nerurkar, V. R., and Verma, S. (2012). West Nile virus-induced disruption of the blood-brain barrier in mice is characterized by the degradation of the junctional complex proteins and increase in multiple matrix metalloproteinases. *J. Gen. Virol.* 93, 1193–1203. doi: 10.1099/vir.0.040899-0
- Roe, K., Orillo, B., and Verma, S. (2014). West Nile virus-induced cell adhesion molecules on human brain microvascular endothelial cells regulate leukocyte adhesion and modulate permeability of the in vitro blood-brain barrier model. *PLoS One* 9:e102598. doi: 10.1371/journal.pone.0102598
- Rothbauer, M., Patel, N., Gondola, H., Siwetz, M., Huppertz, B., and Ertl, P. (2017). A comparative study of five physiological key parameters between four different human trophoblast-derived cell lines. *Sci. Rep.* 7:5892. doi: 10.1038/s41598-017-06364-z
- Sevvana, M., Long, F., Miller, A. S., Klose, T., Buda, G., Sun, L., et al. (2018). Refinement and analysis of the mature zika virus cryo-em structure at 3.1 Å resolution. *Structure* 26, 1169–1177.e3. doi: 10.1016/j.str.2018.05.006
- Simister, N. E., and Story, C. M. (1997). Human placental Fc receptors and the transmission of antibodies from mother to fetus. *J. Reprod. Immunol.* 37, 1–23. doi: 10.1016/s0165-0378(97)00068-5
- Sirohi, D., Chen, Z., Sun, L., Klose, T., Pierson, T. C., Rossmann, M. G., et al. (2016). The 3.8 Å resolution cryo-EM structure of Zika virus. *Science* 352, 467–470. doi: 10.1126/science.aaf5316
- Soares, C. N., Brasil, P., Carrera, R. M., Sequeira, P., De Filippis, A. B., Borges, V. A., et al. (2016). Fatal encephalitis associated with Zika virus infection in an adult. *J. Clin. Virol.* 83, 63–65. doi: 10.1016/j.jcv.2016.08.297
- Stamatovic, S. M., Keep, R. F., and Andjelkovic, A. V. (2008). Brain endothelial cell-cell junctions: how to "open" the blood brain barrier. *Curr. Neuropharmacol.* 6, 179–192. doi: 10.2174/157015908785777210
- Tuma, P., and Hubbard, A. L. (2003). Transcytosis: crossing cellular barriers. *Physiol. Rev.* 83, 871–932. doi: 10.1152/physrev.00001.2003
- Vu, K., Weksler, B., Romero, I., Couraud, P. O., and Gelli, A. (2009). Immortalized human brain endothelial cell line HCMEC/D3 as a model of the blood-brain barrier facilitates in vitro studies of central nervous system infection by *Cryptococcus neoformans*. *Eukaryot. Cell* 8, 1803–1807. doi: 10.1128/EC.00240-09
- Zimmerman, M. G., Quicke, K. M., O'Neal, J. T., Arora, N., Machiah, D., Priyamvada, L., et al. (2018). Cross-reactive dengue virus antibodies augment zika virus infection of human placental macrophages. *Cell Host Microbe* 24, 731–742.e6. doi: 10.1016/j.chom.2018.10.008

**Conflict of Interest:** The authors declare that the research was conducted in the absence of any commercial or financial relationships that could be construed as a potential conflict of interest.

Copyright © 2020 Chiu, Chu, Liao, Simanjuntak, Lin, Juan and Ping. This is an open-access article distributed under the terms of the Creative Commons Attribution License (CC BY). The use, distribution or reproduction in other forums is permitted, provided the original author(s) and the copyright owner(s) are credited and that the original publication in this journal is cited, in accordance with accepted academic practice. No use, distribution or reproduction is permitted which does not comply with these terms.



# RIPK3 Promotes JEV Replication in Neurons *via* Downregulation of IFI44L

Peiyu Bian<sup>1</sup>, Chuantao Ye<sup>1</sup>, Xuyang Zheng<sup>1</sup>, Chuanyu Luo<sup>2</sup>, Jiali Yang<sup>3</sup>, Mengyuan Li<sup>1</sup>, Yuan Wang<sup>4</sup>, Jing Yang<sup>4</sup>, Yun Zhou<sup>1</sup>, Fanglin Zhang<sup>4</sup>, Jianqi Lian<sup>1</sup>, Ying Zhang<sup>1</sup>, Zhansheng Jia<sup>1\*</sup> and Yingfeng Lei<sup>4\*</sup>

<sup>1</sup> Department of Infectious Diseases, Tangdu Hospital, Air Force Medical University, Xi'an, China, <sup>2</sup> Pathogenic Biology, Medical College of Yan'an University, Yan'an, China, <sup>3</sup> Key Laboratory of Resource Biology and Biotechnology in Western China, Ministry of Education, College of Life Sciences, Northwest University, Xi'an, China, <sup>4</sup> Department of Microbiology, School of Preclinical Medicine, Air Force Medical University, Xi'an, China

## OPEN ACCESS

### Edited by:

Mei-Ling Li,  
Rutgers, The State University  
of New Jersey, United States

### Reviewed by:

Kallol Dutta,  
University of Ottawa, Canada  
Satoko Yamaoka,  
Mayo Clinic, United States

### \*Correspondence:

Zhansheng Jia  
jjazsh@fmmu.edu.cn  
Yingfeng Lei  
yfllei@fmmu.edu.cn

### Specialty section:

This article was submitted to  
Virology,  
a section of the journal  
Frontiers in Microbiology

Received: 26 November 2019

Accepted: 19 February 2020

Published: 24 March 2020

### Citation:

Bian P, Ye C, Zheng X, Luo C,  
Yang J, Li M, Wang Y, Yang J, Zhou Y,  
Zhang F, Lian J, Zhang Y, Jia Z and  
Lei Y (2020) RIPK3 Promotes JEV  
Replication in Neurons *via*  
Downregulation of IFI44L.  
Front. Microbiol. 11:368.  
doi: 10.3389/fmicb.2020.00368

Japanese encephalitis virus (JEV), the leading cause of viral encephalitis in Asia, is neurovirulent and neuroinvasive. Neurons are the main target of JEV infection and propagation. Receptor interacting serine/threonine-protein kinase 3 (RIPK3) has been reported to contribute to neuroinflammation and neuronal death in many central nervous system diseases. In this study, we found that the progression of JE was alleviated in RIPK3-knockout (RIPK3<sup>-/-</sup>) mice in both peripheral and intracerebral infection. RIPK3-knockdown (RIPK3-RNAi) neuro2a cells showed higher cell viability during JEV infection. Moreover, the JEV load was significantly decreased in RIPK3<sup>-/-</sup> mouse-derived primary neurons and RIPK3-RNAi neuro2a cells compared with wild-type neurons, but this was not observed in microglia. Furthermore, RNA sequencing of brain tissues showed that the level of the interferon (IFN)-induced protein 44-like gene (IFI44L) was significantly increased in JEV-infected RIPK3<sup>-/-</sup> mouse brains, RIPK3<sup>-/-</sup> neurons, and RIPK3-RNAi-neuro2a cells. Then, it was demonstrated that the propagation of JEV was inhibited in IFI44L-overexpressing neuro2a cells and enhanced in IFI44L and RIPK3 double knockdown neuro2a cells. Taken together, our results showed that the increased expression of RIPK3 following JEV infection played complicated roles. On the one hand, RIPK3 participated in neuroinflammation and neuronal death during JEV infection. On the other hand, RIPK3 inhibited the expression of IFI44L to some extent, leading to the propagation of JEV in neurons, which might be a strategy for JEV to evade the cellular innate immune response.

**Keywords:** Japanese encephalitis virus (JEV), receptor interacting serine/threonine-protein kinase 3 (RIPK3), interferon-induced protein 44-like gene (IFI44L), neurons, cellular innate immune response

## INTRODUCTION

Japanese encephalitis virus (JEV) is a positive-sense, single-stranded RNA virus belonging to the genus *Flavivirus* in the family *Flaviviridae*. JEV is both neurovirulent and neuroinvasive and can lead to severe encephalitis (Lannes et al., 2017). Glycoprotein E mediates JEV entry through attachment and endocytosis, followed by membrane fusion

and uncoating (Wang et al., 2017; Yun and Lee, 2018). Pattern recognition receptors (PRRs), such as retinoic acid-inducible gene 1-like receptors (RIG-I) and Toll-like receptor 3 (TLR3), in infected cells can recognize viral components and induce the production of interferons (IFNs), which then drive the expression of various IFN-stimulated genes (ISGs) through the IFN receptor (IFNR)/Janus kinase (Jak1)/tyrosine kinase (Tyk2)/signal transducer and activator of transcription (STAT)1/STAT2 pathway to fight against virus invasion (Liu et al., 2013; Han et al., 2014). As a result of such interactions, JEV has developed many strategies to counteract the host innate immune response (Ye et al., 2017; Zhou et al., 2018).

Receptor interacting serine/threonine-protein kinase 3 (RIPK3) has been shown to participate in several biological or pathological processes and play complicated and even controversial roles in different host cells during various viral infections (He and Wang, 2018). The activation of RIPK3 and subsequent mixed lineage kinase domain-like pseudokinase (MLKL) phosphorylation can lead to cellular necroptosis and damage-associated molecular pattern (DAMP) production (Pasparakis and Vandenabeele, 2015). It has been reported that RIPK3-mediated necroptosis destroys host cells and limits the propagation of viruses such as herpes simplex virus (HSV), influenza virus (IAV), and vaccinia virus (VV) (Wang et al., 2014; Huang et al., 2015; Nogusa et al., 2016; Koehler et al., 2017). RIPK3 also promoted or inhibited the propagation of virus in a cell death-independent manner during coxsackievirus B3 (CVB), IAV, and Zika virus (ZIKV) infections (Harris et al., 2015; Downey et al., 2017; Daniels et al., 2019). Additionally, it has been reported that RIPK3 contributes to the production of chemokines CXCL10 and CCL2 in West Nile virus (WNV)-infected neurons to recruit T lymphocytes and inflammatory myeloid cells to the central nervous system (CNS) (Daniels et al., 2017). In a previous study, we found that JEV infection induced the expression of MLKL, leading to necroptosis of neurons and neuroinflammation, which was shown to be alleviated in JEV-infected MLKL-knockout mice (Bian et al., 2017). However, the role of RIPK3 in JEV infection is unknown.

In this study, we found that the survival rate of RIPK3-knockout (RIPK3<sup>-/-</sup>) mice was significantly increased after JEV infection compared to that of wild-type (WT) mice. The expression of RIPK3 in neurons was increased after JEV infection, and cell viability was improved after RIPK3 knockdown. We also found that the replication of JEV in RIPK3<sup>-/-</sup> mice and neurons was inhibited to some extent. Comparison of the RNA-sequencing results in JEV-infected brain tissues between WT and RIPK3<sup>-/-</sup> mice showed that a series of IFN-stimulated genes (ISGs) were upregulated in RIPK3<sup>-/-</sup> mice, especially the IFN-induced protein 44-like gene (IFI44L). Then, it was demonstrated that IFI44L inhibited JEV propagation in neuronal cells, and the increased expression of IFI44L contributed to the inhibition of JEV in RIPK3<sup>-/-</sup> neuronal cells. Thus, we speculated that the slightly increased RIPK3 might be a strategy for JEV to evade cellular immunity in neurons.

## MATERIALS AND METHODS

### Ethics Statement

All animal experiments were reviewed and approved by the Animal Care and Use Committee of the Laboratory Animal Center, Air Force Medical University. The number of Animal Experimental Ethical Inspection is 20160112. And all experiments were carried out complying with the recommendations in the Guide for the Care and Use of Laboratory Animals.

### Receptor Interacting Serine/Threonine-Protein Kinase 3-Knockout Mice

The RIPK3<sup>±</sup> C57BL/6 mice were a gift from the lab of Dr. Yazhou Wang (Department of Neurobiology and Collaborative Innovation Center for Brain Science, School of Basic Medicine, Air Force Medical University) and were kept in a specific pathogen-free (SPF) facility. Toe DNA from newborn mice was extracted and amplified with PrimeStar (Takara, Japan). Then, the products were analyzed by agarose gel electrophoresis to screen WT, RIPK3<sup>±</sup>, RIPK3<sup>-/-</sup> descendants. WT and RIPK3<sup>-/-</sup> mice (6–8 weeks) were infected with  $5 \times 10^6$  JEV plaque-forming units (PFUs) in 20  $\mu$ l phosphate-buffered saline (PBS) by footpad injection or 100 PFU in 2  $\mu$ l *via* intracerebral injection. The weight, behavior score, and death cases of each group were recorded twice a day at 8:00–9:00 and 16:00–17:00 for 20 days until all the groups were totally stable. The scoring criteria were as follows: 0: no significant abnormal behaviors, piloerection, restriction of movement, body stiffening, or hind limb paralysis; 1: piloerection, no restriction of movement, body stiffening, or hind limb paralysis; 2: piloerection, restriction of movement, no body stiffening or hind limb paralysis; 3: piloerection, restriction of movement, body stiffening, no hind limb paralysis; 4: piloerection, restriction of movement, body stiffening, and hind limb paralysis; 5: piloerection, restriction of movement, body stiffening, hind limb paralysis, sometimes tremor and even death.

### Cells and Virus

The JEV-P3 strain was propagated in the brains of 3-day-old inbred BALB/C suckling mice and titrated by conventional plaque assay.

The neuroblast cell line Neuro2a, baby hamster kidney (BHK) cells, and HEK 293T cells [purchased from American Type Culture Collection (ATCC)] were cultured in Dulbecco's modified Eagle's medium (DMEM; Gibco, Grand Island, NY, United States) containing 10% fetal bovine serum (FBS; Gibco, Grand Island, NY, United States) and 1% penicillin streptomycin combination (PS). The microglia cell line N9 (purchased from ATCC) was cultured in DMEM with 5% FBS and 1% PS.

### Immunohistochemical Staining

Mice were administered propidium iodide (PI; 4 mg/ml, Sigma, in 0.9% NaCl) intraperitoneally (100  $\mu$ l/20 g weight) and euthanized 1 h later. Brains were harvested and protected from

light. Brain sections of 10  $\mu\text{m}$  were prepared with a vibratome. The slides were incubated with primary anti-RIPK3 antibody (Abcam, Cambridge, MA, United States) in PBS containing 0.1% Triton X-100 and 1% bovine serum albumin (BSA) at 4°C for 16 h. After washing, the sections were incubated with the secondary antibodies for 1 h at room temperature. The nuclei were counterstained with 4',6-diamidino-2-phenylindole (DAPI), and coverslips were placed on the samples with 50% glycerol in PBS.

## RNA Sequencing Analysis

Wild-type and RIPK3<sup>-/-</sup> mice (4–6 weeks) were injected intracerebrally with PBS or 100 PFU JEV in 2  $\mu\text{l}$ . Brains were harvested at 3 days post infection (dpi) and washed with 4°C PBS three times and then stored in liquid nitrogen. Then, the total RNA was extracted for RNA sequencing. The expression values [reads per kilobase million (RPKM)] were normalized per gene over all samples, the mean and standard deviation (SD) of expression over all samples were calculated for each gene, and the expression value was linearly transformed using the formula (RPKM-mean)/SD. The results were analyzed using the Dr. Tom network platform of BGI<sup>1</sup> and GraphPad Prism 7.

## DNA Construction

To inhibit the expression of RIPK3, the shRNA targeting mouse RIPK3 (5'-GCTGGAGTTTGTGGGTAAAGG-3') was constructed. The mouse IFI44L gene segment with sites for the restriction endonucleases *Bgl*II and *Mlu*I was generated through PCR (primer sequence in **Supplementary Table S1**) with Q5 High-Fidelity DNA Polymerase (NEB, United States) and cloned into the Lenti-GFP-zeocin plasmid (pLenti-GZ) (*via Bam*HI and *Mlu*I restriction digests). The plasmids from positive clones were extracted and sequenced. Then, the recombinant IFI44L overexpression plasmid was obtained. Three oligos targeting IFI44L (sequences in **Supplementary Table S1**) with the restriction endonucleases *Age*I and *Eco*RI were annealed and inserted into the pLKO.1-puro plasmid. The plasmids from positive clones were extracted and sequenced to obtain the correct recombinant interfering plasmid.

## Generation and Purification of Recombinant Lentiviral Particles

Lentiviral pseudoparticles were generated by cotransfecting 293T cells in T75 flasks with the plasmids pLenti-IFI44L-GFP-zeocin, pLenti-shRNAi-RIPK3-puro, or pLenti-shRNAi-IFI44L-puro (1, 2, and 3) proviral DNA (12  $\mu\text{g}$ ); envelope plasmid (pMD2. G, 6  $\mu\text{g}$ ); and packing plasmid (psPAX2, 9  $\mu\text{g}$ ). Before transfection, 9 ml DMEM was added to each T75 flask. For each transfection, 108  $\mu\text{l}$  transfection reagent LipoFectMAX (ABP Biosciences, United States) was mixed with 27  $\mu\text{g}$  total DNA in 2 ml DMEM for 30 min and then added to the T75 flask. The cells were maintained at 37°C for 6 h, after which the medium was changed to DMEM with 2% FBS. The supernatants were harvested at 48 and 72 h. The cell debris was removed by

centrifugation at 1,000  $\times g$  for 10 min and then 10,000  $\times g$  for 35 min. Subsequently, the viral suspension was concentrated at 165,000  $\times g$  for 4 h at 4°C, and the virus particles were harvested in 500  $\mu\text{l}$  DMEM and stored at -80°C.

## Lentivirus Infection and Positive Cell Screening

Neuro2a cells and N9 cells were seeded into six-well plates at  $4 \times 10^5$  overnight. The supernatant was removed, and RIPK3-shRNA lentiviral particles mixed with polybrene (1  $\mu\text{g}/\text{ml}$ ) were added. After infection for 4 h, 1 ml DMEM with 10% FBS was added. Then, 48 h later, DMEM containing puromycin was added to neuro2a cells (2  $\mu\text{g}/\text{ml}$ ) and N9 cells (10  $\mu\text{g}/\text{ml}$ ) to screen the positive cells. Neuro2a cells with IFI44L overexpression or downregulation by shRNA were also constructed as described above.

## Plasmid Transfection

Neuro2a cells and RIPK3-RNAi neuro2a cells were plated in six-well plates at  $4 \times 10^5$  overnight. The supernatant was discarded, and the mixture of pCMV-GFPspark or pCMV-RIPK3-OFPSpark (Sino Biological, China) (2  $\mu\text{g}$ ) with LipoFectMAX (6  $\mu\text{l}$ ) in 1 ml DMEM was added to each well. After incubation for 6 h, the medium was changed to 10% FBS-containing DMEM. Then, 24 h after transduction, the cells were infected with JEV-p3 at a multiplicity of infection (MOI) of 0.1. At 12 and 24 h post infection (hpi), cells and supernatant were harvested for qRT-PCR and conventional plaque assay.

## Cellular Viability Assay

Neuro2a cells were inoculated into opaque-walled 96-well plates at 10,000/well and maintained overnight. After JEV infection, viability was tested with a CellTiter-Glo Assay kit (Promega, United States). According to the protocol, the substrate and buffer were mixed thoroughly to obtain the detection reagent, and the plates were equilibrated at room temperature for approximately 30 min before the experiments. Then, 100  $\mu\text{l}$  of detection reagent was added to the plates containing 100  $\mu\text{l}$  of medium and mixed on an orbital shaker for 2 min to induce cell lysis. Then, the plates were incubated at room temperature for 10 min. The luminescence signal was recorded with a Bio-Tek Synergy HT Multi-Detection Microplate Reader and analyzed with GraphPad Prism 7.

## Isolation and Culture of Primary Neurons

Mice pregnant for 16–17 days were sacrificed, and the embryos were excised. The embryonic brains were harvested, and the meninges were removed completely. Then, the cerebral cortices were dissected and treated with papain (2 mg/ml) for 15 min, and 2 ml FBS was added to terminate the digestion. The liquid was removed, and the tissues were gently dissociated in DMEM with 10% FBS by pipetting. Then, the tissue suspension was filtered through a 70- $\mu\text{m}$  cell strainer (Falcon, BD, United States). The isolated cells were seeded onto poly-L-lysine (100  $\mu\text{g}/\text{ml}$ ; Sigma, United States)-coated 60-mm plates and cultured in a humidified atmosphere at 37°C. After 24 h,

<sup>1</sup><http://report.bgi.com>

the medium was changed to serum-free neurobasal medium (Gibco, United States) containing B27 (Gibco, United States) and L-glutamine (Gibco, United States).

## Virus Infection

Neuro2a cells or modified neuro2a cells were seeded in six-well or 96-well plates at a density of  $2 \times 10^5$ /well or 10,000/well overnight. Then, the cells were infected with JEV (MOI = 0.1). After incubation for 1 h, the virus suspension was removed, and fresh DMEM was added. The cells and supernatant were harvested at different time points (24, 48, 72 h after infection) for qRT-PCR, Western blotting (WB), and conventional plaque assay.

N9 cells and RIPK3-shRNA N9 cells were seeded in six-well plates at a density of  $4 \times 10^5$ /well overnight. Then, the cells were infected with JEV (MOI = 1). After incubation for 1 h, the virus suspension was removed, and fresh DMEM was added. The cells and supernatant were harvested at different time points (24, 48, 72 h after infection) for qRT-PCR, WB, and conventional plaque assay.

## qRT-PCR

WT and RIPK3<sup>-/-</sup> mice were euthanized and perfused with PBS, and then the whole brain of each mouse was harvested and stored at  $-80^\circ\text{C}$ . Total RNA from mouse brains and cells was extracted with RNeasy RNeasy spin columns (PIONEER, China). cDNA was prepared by reverse transcription with total RNA as the template using the PrimeScript RT reagent Kit (TaKaRa, Japan). qRT-PCR experiments were carried out using SYBR Green Real-Time PCR Master Mix (TaKaRa, Japan) according to the manufacturer's instructions (for the primers used in this study, see **Supplementary Table S1**). The mRNA expression was normalized to  $\beta$ -actin expression, and the data are shown as the relative change to the corresponding reference for each group.

## Western Blotting

Total protein from the brain of each mouse or from cells was extracted with radioimmunoprecipitation assay (RIPA) buffer containing phenylmethanesulfonyl fluoride (PMSF) and phosphatase inhibitors and then quantified using a Protein Reagent Assay BCA Kit (Thermo, Waltham, MA, United States). Thirty micrograms of protein from each sample was loaded and electrophoresed using 12% sodium dodecyl sulfate-polyacrylamide gel electrophoresis (SDS-PAGE) gels and then transferred onto polyvinylidene difluoride (PVDF) membranes (Millipore, Billerica, MA, United States). After being blocked with 3% BSA at room temperature for 60 min, the membranes were incubated with primary antibodies (see **Supplementary Table S1**) overnight at  $4^\circ\text{C}$ . Then, the blots were incubated with the corresponding DyLight 800/700-labeled secondary antibodies for 2 h at room temperature. The blots were visualized using an infrared imaging system (Odyssey, LI-COR, Lincoln, NE, United States).

## Plaque Assay

BHK cells were seeded in six-well plates at  $4 \times 10^5$ /well overnight. The supernatant of the cells was removed, and the cells were

washed with  $1 \times$  PBS twice. Then, serial 10-fold diluted samples with DMEM were added and incubated at  $37^\circ\text{C}$  for 2 h. The viral supernatant was replaced with 4 ml overlay media (25 ml  $4 \times$  DMEM, 50 ml 4% methylcellulose, 2 ml FBS, 23 ml ddH<sub>2</sub>O) for 5 days. The overlay medium was washed off with  $1 \times$  PBS, and the cells were fixed with 4% paraformaldehyde (PFA) for 30 min. Crystal violet dye was added at 2 ml per well for 15 min and washed off with running tap water. Finally, the plaques were counted.

## Statistical Analysis

All statistical analyses were performed using GraphPad Prism version 7.01 software. Statistical differences were determined using Student's *t*-test or two-way analysis of variance (ANOVA). *P*-values < 0.05 were considered significant.

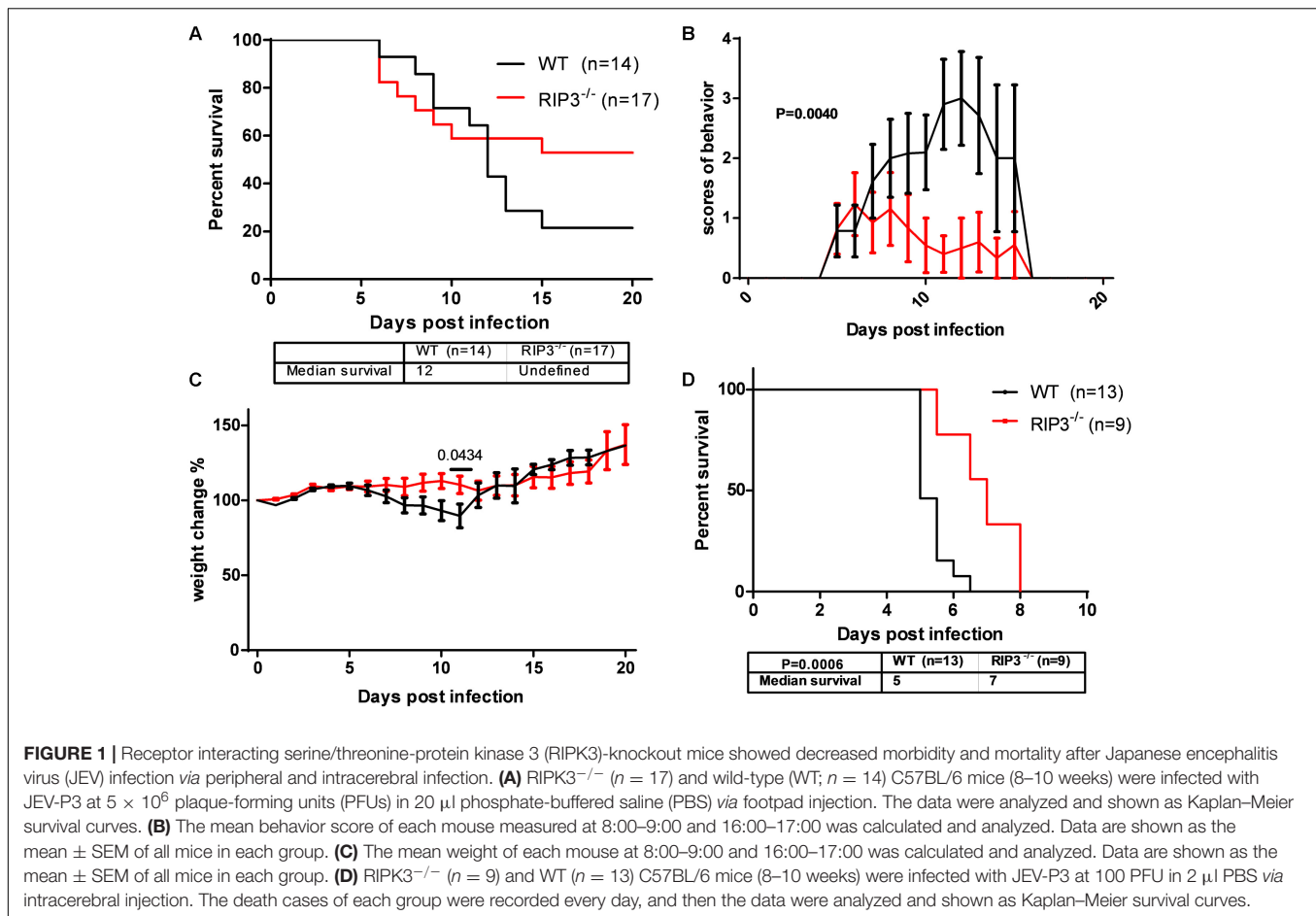
## RESULTS

### Receptor Interacting Serine/Threonine-Protein Kinase 3-Knockout Mice Showed Decreased Morbidity and Mortality After Japanese Encephalitis Virus Infection

In our previous study, MLKL<sup>-/-</sup> mice showed alleviated JE progression compared to WT mice to some extent. RIPK3, as the upstream signaling molecule of MLKL phosphorylation in classical necroptosis, has more complicated roles in apoptosis, inflammation, cytokine, and IFN production and the immunometabolic state (He and Wang, 2018). To determine the role of RIPK3 in JEV infection, RIPK3<sup>-/-</sup> mice were infected with JEV by footpad injection and monitored daily for survival, weight, and behavioral score. The results showed that RIPK3<sup>-/-</sup> mice had an increased survival rate compared with WT mice after JEV infection (**Figure 1A**). The average behavior score of RIPK3<sup>-/-</sup> mice was lower than that of WT mice (**Figure 1B**). The weight in RIPK3<sup>-/-</sup> mice was more stable (**Figure 1C**). Generally, RIPK3 deficiency led to decreased morbidity and mortality during JEV infection *in vivo*. In the early phase of infection, RIPK3<sup>-/-</sup> mice showed more aggressive onset of JE than WT mice. We speculated that RIPK3<sup>-/-</sup> monocytes and dendritic cells contributed to the propagation of JEV in the peripheral organs. Then, the RIPK3<sup>-/-</sup> and WT mice were infected with JEV by intracerebral (IC) injection to avoid the peripheral immune system. The RIPK3<sup>-/-</sup> mice were also more resistant to JEV infection than the WT mice (**Figure 1D**). Thus, the absence of RIPK3 in the CNS alleviated JE progression.

### Japanese Encephalitis Virus Infection Induced Receptor Interacting Serine/Threonine-Protein Kinase 3 Expression Which Contributed to Neuronal Death

To explore the changes in RIPK3 during JEV infection *in vivo* and *in vitro*, the expression of RIPK3 was detected. After



JEV infection, the expression of RIPK3 was increased in the CNS (**Figure 2A**). Moreover, the expression of RIPK3 was also increased in neurons and neuro2a cells following JEV infection (**Figures 2B,C**). The phosphorylation of RIPK3 led to classical MLKL-mediated necroptosis. In the JEV-infected mouse brains, PI-labeled necrotic cells were found to have increased expression of RIPK3 (**Supplementary Figure S1**). To identify the role of RIPK3 in neuronal survival, RIPK3-RNAi-neuro2a cells were constructed (**Figure 2D**). Knockdown of RIPK3 increased the survival rate of neuro2a cells after JEV infection with different PFUs and infection times (**Figures 2E,F**). Thus, the expression of RIPK3 in neuro2a cells contributed to JEV-induced neuronal death.

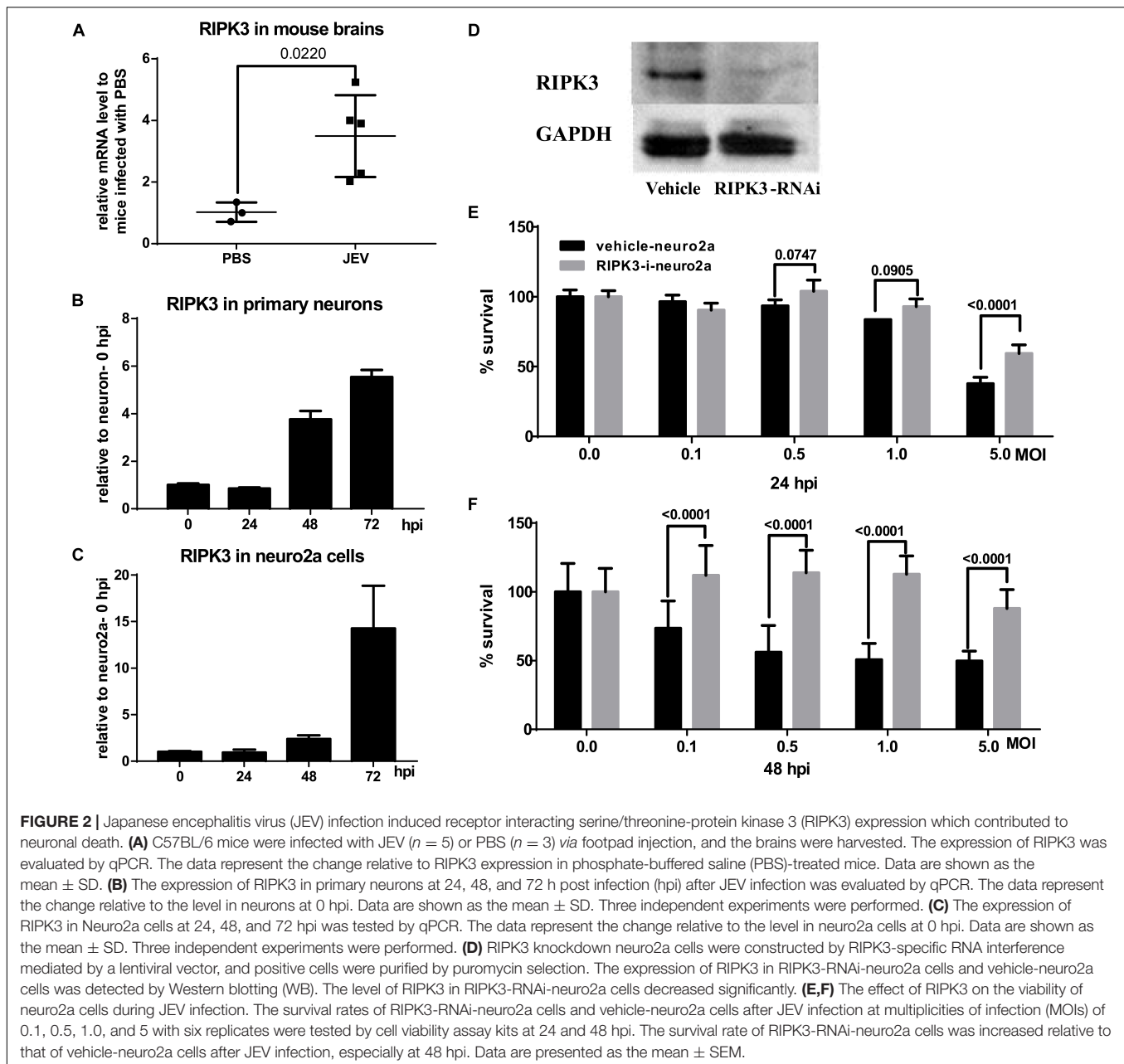
### Viral Loads Were Lower in the Brains of Receptor Interacting Serine/Threonine-Protein Kinase 3-Knockout Mice After Japanese Encephalitis Virus Infection *via* Intracerebral Injection

RIPK3 participated in the regulation of inflammation and cell survival, which directly or indirectly affected the propagation of virus during virus infection. To determine the role of RIPK3 in JEV propagation in the CNS, we tested the viral loads in the

brains after JEV infection *via* IC injection at 3, 4, and 5 days. Surprisingly, the JEV RNA copy number in RIPK3<sup>-/-</sup> mice was significantly less than that in WT mice at 3 and 4 dpi (**Figures 3A,B**). At 5 dpi, the viral load in most of the RIPK3<sup>-/-</sup> mice was still lower than that in the WT mice (**Figure 3C**). This result was different from the infections with ZIKV and WNV, in which the viral load was increased in the CNS of RIPK3<sup>-/-</sup> mice after virus infection because of the changed immunometabolism or decreased expression of chemokines in the neurons (Daniels et al., 2017, 2019).

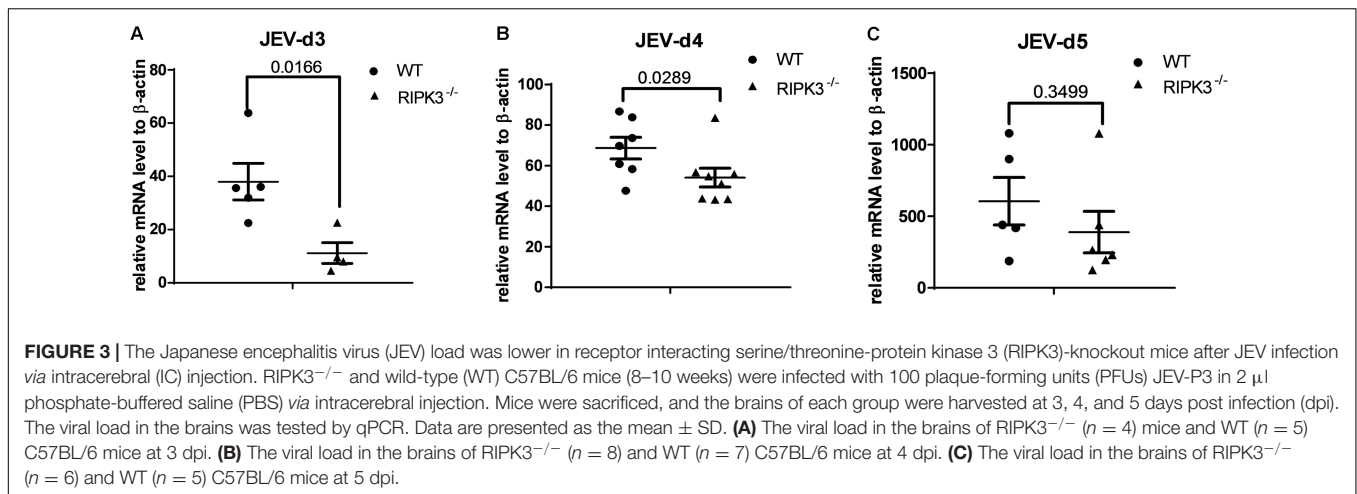
### Receptor Interacting Serine/Threonine-Protein Kinase 3 (RIPK3) Promoted the Propagation of Japanese Encephalitis Virus in Neurons

Neurons are the main target cells of JEV infection in the CNS. To observe the effect of RIPK3 on JEV propagation in neurons, we infected neuro2a cells and RIPK3-RNAi-neuro2a cells with JEV at an MOI of 0.1 and detected the viral load using qPCR and WB. The mRNA levels of JEV decreased significantly in RIPK3-RNAi-neuro2a cells compared to vehicle neuro2a cells at different times of infection (**Figure 4A**), which was consistent with the JEV-E protein levels (**Figure 4B**). Then, the viral particles in the



supernatants from different infection groups were assessed by plaque assay at a dilution of 1:100 (**Figure 4C**). There were many more infectious JEV particles in the supernatant from vehicle neuro2a cells than in the supernatant from RIPK3-RNAi-neuro2a cells. The results were further confirmed in primary neurons isolated from RIPK3<sup>-/-</sup> and WT prenatal mice. The viral RNA levels (**Supplementary Figure S2A**), viral protein levels (**Supplementary Figure S2B**), and number of particles in the supernatant (**Supplementary Figure S2C**) from the RIPK3<sup>-/-</sup> neurons were decreased compared with those from WT neurons. Thus, the propagation of JEV in RIPK3-deleted neurons was inhibited. Furthermore, to identify the role of RIPK3 in JEV replication, transient overexpression of RIPK3 in neuro2a cells

and RIPK3-RNAi-neuro2a cells was conducted. The expression of RIPK3 in neuro2a cells was increased (**Supplementary Figure S3A**), and the cells were infected with JEV at 24 h after plasmid transduction. The viral copy number was increased in the RIPK3-overexpressing neuro2a cells (**Figure 4D**) as well as the infectious viral particles in the supernatant, as determined by plaque assay (**Figure 4E**) at 12 and 24 hpi. Moreover, RIPK3 supplementation in RIPK3-RNAi-neuro2a cells was performed (**Supplementary Figure S3B**), and viral copy numbers (**Figure 4F**) and infectious particles (**Figure 4G**) were also increased in RIPK3-RNAi-neuro2a cells complemented with RIPK3. In total, RIPK3 promoted the propagation of JEV in neuro2a cells.



## Receptor Interacting Serine/Threonine-Protein Kinase 3 Knockdown Had a Limited Effect on Japanese Encephalitis Virus Replication but Inhibited the Activation of Microglia

Microglia, as the main resident immune defensive cells in the CNS, play important roles during JEV infection (Thongtan et al., 2012). After being exposed to JEV, microglia can be activated as innate immune cells and release a series of cytokines to recruit immune cells that contribute to immune defense as well as neuroinflammation. To explore whether knockdown of RIPK3 affected the level of JEV replication in microglia, RIPK3-RNAi-N9 cells were constructed. The expression of RIPK3 was decreased significantly in RIPK3-RNAi-N9 cells compared to the vehicle control cells (Figure 5A). Then, the viral load was detected at 24 and 48 h after JEV infection by qPCR and WB (Figures 5B,D). There was no significant difference in viral expression between RIPK3-RNAi-N9 and vehicle-N9 cells at 24 h. However, the expression of JEV RNA and protein was increased slightly in RIPK3-RNAi-N9 cells at 48 h. The amount of infectious JEV particles in the supernatant of RIPK3-RNAi-N9 cells was comparable to that of vehicle N9 cells (Figure 5C). Thus, RIPK3 had little effect on the propagation of JEV in N9 cells. Furthermore, the level of activated caspase-1 (Figure 5D) and the production of IL-1 $\beta$  after JEV infection (Figure 5E) in RIPK3-RNAi-N9 cells were demonstrated to decrease. Thus, the activation of microglia during JEV infection was inhibited in the absence of RIPK3, which was consistent with reports that RIPK3 participated in the formation of the inflammasome in microglia (Lawlor et al., 2015).

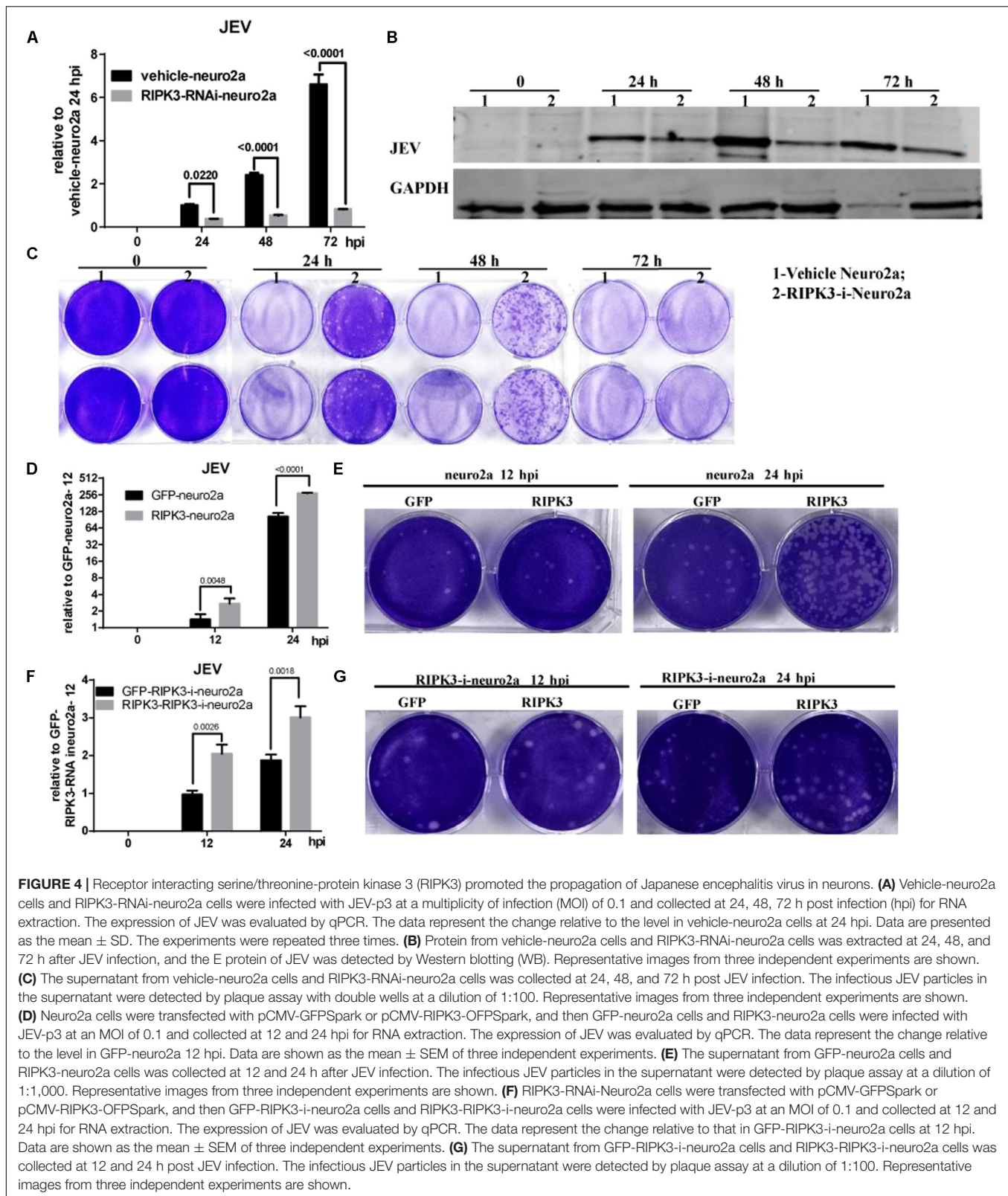
## Interferon (IFN)-Stimulated Genes, Especially IFN-Induced Protein 44-Like Gene, Were Upregulated in RIPK3<sup>-/-</sup> Mouse Brains and Neurons After Japanese Encephalitis Virus Infection

In contrast with previous reports that RIPK3 mediated the suppression of viruses in the CNS and neurons, the propagation

of JEV in the CNS of RIPK3<sup>-/-</sup> mice and RIPK3<sup>-/-</sup> neurons was inhibited. To explore the mechanism involved, RNA-sequencing of brain tissues from RIPK3<sup>-/-</sup> mice and WT mice treated with JEV or PBS via IC injection at 3 dpi was performed. According to the volcano plots of differentially expressed genes, ifi44l was the most significantly upregulated gene in RIPK3<sup>-/-</sup> mouse brains compared to WT mouse brains after JEV infection (Figure 6A). Moreover, a number of ISGs in the brains also increased between RIPK3<sup>-/-</sup> and WT mice after JEV infection and were more significant in RIPK3<sup>-/-</sup> mice (Figure 6B). To clarify the expression of IFI44L mRNA, WT and RIPK3<sup>-/-</sup> mice were injected with JEV via IC injection again. Brains were harvested at 3 dpi, and the levels of JEV RNA and IFI44L mRNA were evaluated by qPCR. Consistent with the above results, the level of JEV was relatively lower in RIPK3<sup>-/-</sup> mice than in WT mice (Figure 6C), and the mRNA level of IFI44L increased significantly in RIPK3<sup>-/-</sup> mice compared with WT mice (Figure 6D). Furthermore, the expression of IFI44L in WT and RIPK3<sup>-/-</sup> primary neurons was detected by qPCR. The level of IFI44L increased significantly in RIPK3<sup>-/-</sup> neurons after JEV infection (Figure 6E) as well as in RIPK3 knockdown neuro2a cells (Figure 6F). Thus, the absence of RIPK3 promoted the expression of IFI44L in neurons and inhibited viral replication during JEV infection.

## The Increase of Interferon-Induced Protein 44-Like Gene Was Independent of the Phosphorylation of Receptor Interacting Serine/Threonine-Protein Kinase 3 or Mixed Lineage Kinase Domain-Like Pseudokinase

The phosphorylation of RIPK3 and subsequent MLKL activation are key to the classical necroptosis pathway (Weinlich et al., 2017). To explore whether the inhibition of IFI44L was dependent on the phosphorylation of RIPK3 or MLKL, Neuro2a cells were treated with inhibitors of RIPK3 or MLKL phosphorylation (Supplementary Figure S4). The expression of



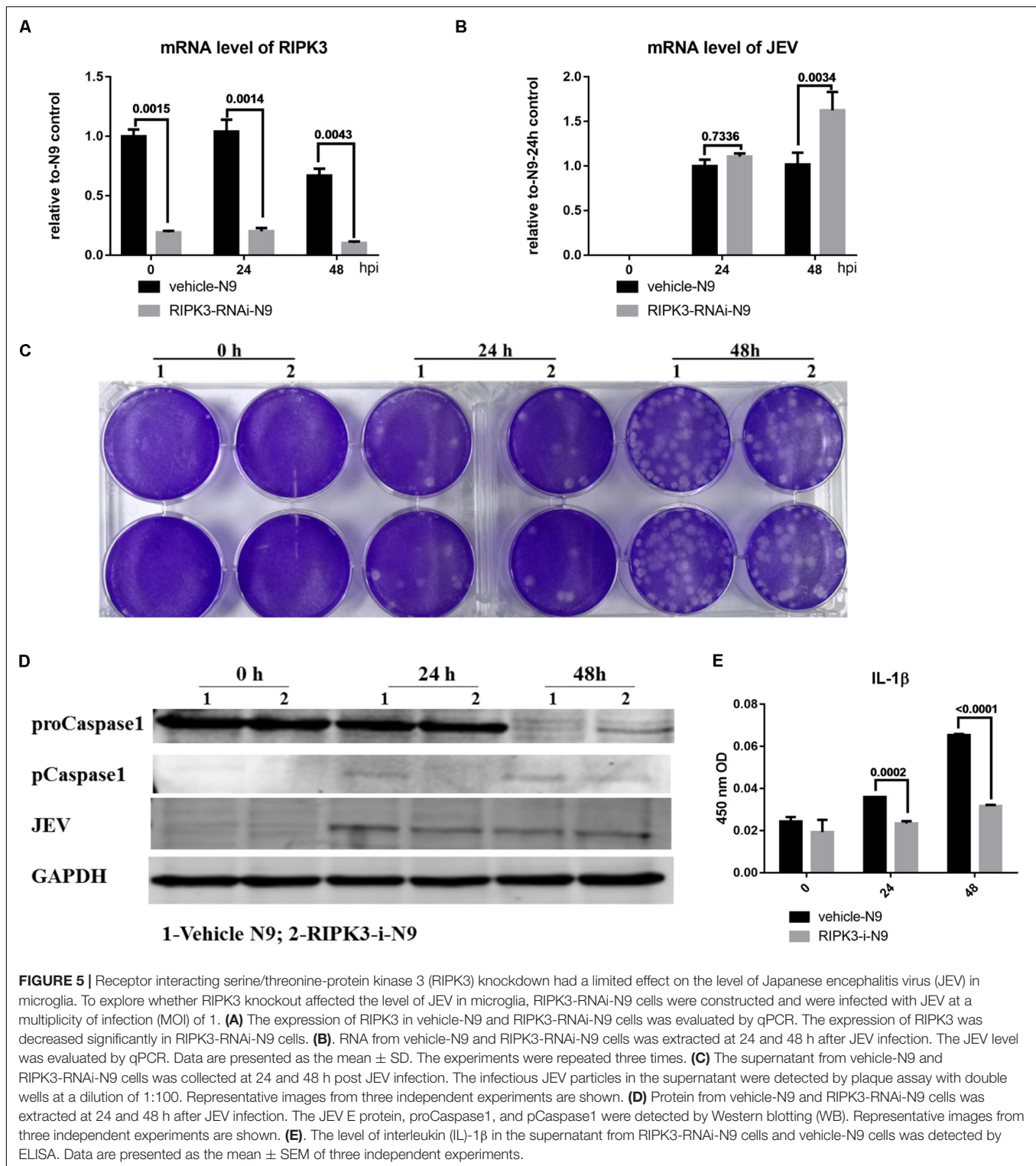
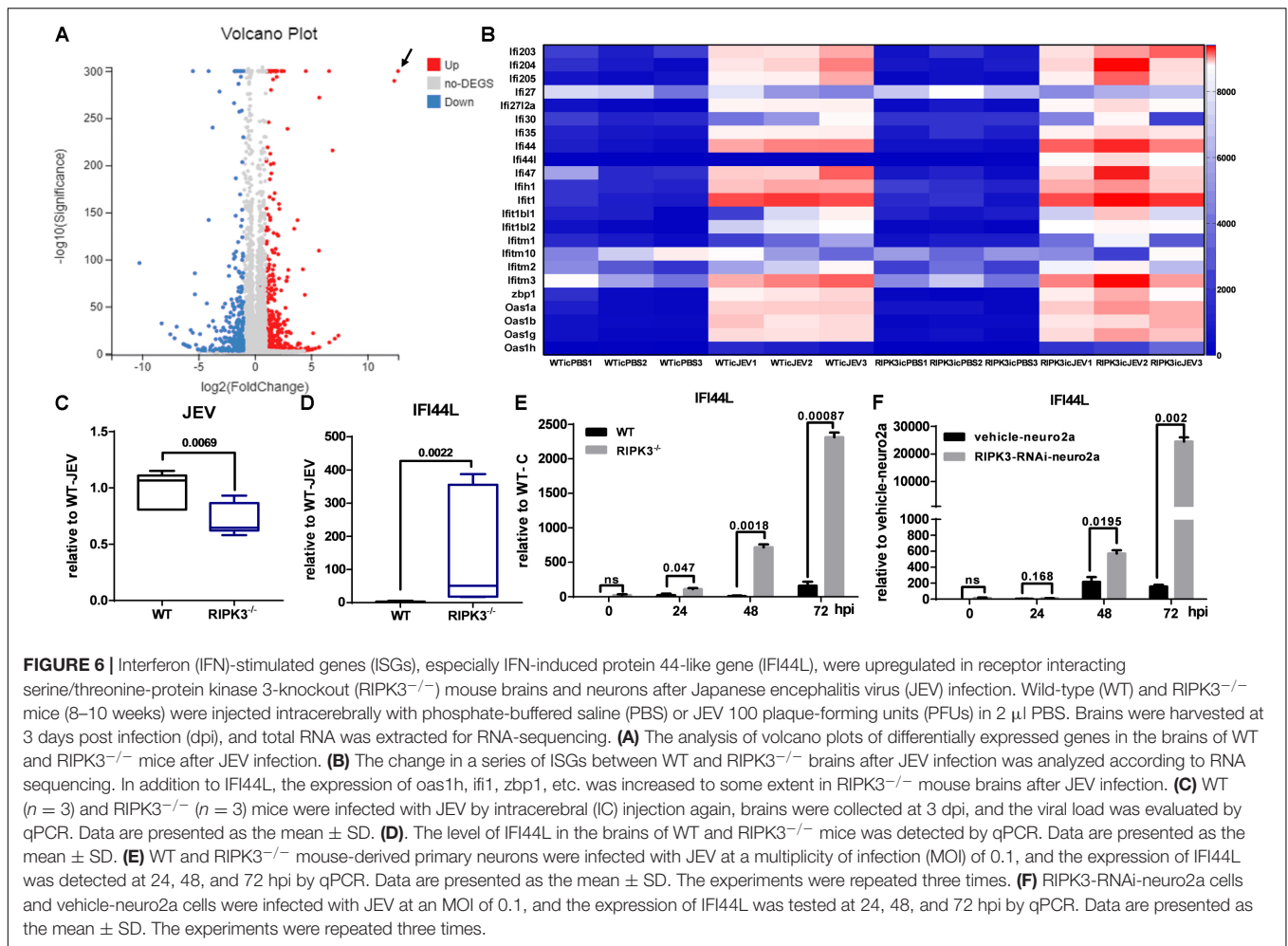


**FIGURE 5** | Receptor interacting serine/threonine-protein kinase 3 (RIPK3) knockdown had a limited effect on the level of Japanese encephalitis virus (JEV) in microglia. To explore whether RIPK3 knockout affected the level of JEV in microglia, RIPK3-RNAi-N9 cells were constructed and were infected with JEV at a multiplicity of infection (MOI) of 1. **(A)** The expression of RIPK3 in vehicle-N9 and RIPK3-RNAi-N9 cells was evaluated by qPCR. The expression of RIPK3 was decreased significantly in RIPK3-RNAi-N9 cells. **(B)** RNA from vehicle-N9 and RIPK3-RNAi-N9 cells was extracted at 24 and 48 h after JEV infection. The JEV level was evaluated by qPCR. Data are presented as the mean  $\pm$  SD. The experiments were repeated three times. **(C)** The supernatant from vehicle-N9 and RIPK3-RNAi-N9 cells was collected at 24 and 48 h post JEV infection. The infectious JEV particles in the supernatant were detected by plaque assay with double wells at a dilution of 1:100. Representative images from three independent experiments are shown. **(D)** Protein from vehicle-N9 and RIPK3-RNAi-N9 cells was extracted at 24 and 48 h after JEV infection. The JEV E protein, proCaspase1, and pCaspase1 were detected by Western blotting (WB). Representative images from three independent experiments are shown. **(E)** The level of interleukin (IL)-1 $\beta$  in the supernatant from RIPK3-RNAi-N9 cells and vehicle-N9 cells was detected by ELISA. Data are presented as the mean  $\pm$  SEM of three independent experiments.

IFI44L was tested by qPCR at 24 and 48 hpi. The level of IFI44L mRNA increased significantly in RIPK3-RNAi-neuro2a cells but not in inhibitor-treated groups (Figure 7A). Furthermore, the viral loads tested by qPCR and WB were decreased in RIPK3-RNAi-neuro2a cells (Figures 7B,C), while virus replication was

increased slightly after treatment with inhibitors, especially in pMLKL inhibitor-treated neuro2a cells, at 48 h. Moreover, the infectious viral particles in the RIPK3-RNAi-neuro2a cells were decreased but not in the neuro2a cells treated with inhibitors (Figure 7D). Thus, the inhibition of JEV replication in



RIPK3-RNAi-neuro2a cells did not rely on the phosphorylation of RIPK3 or MLKL.

### Interferon-Induced Protein 44-Like Gene (IFI44L) Inhibited Japanese Encephalitis Virus Propagation in RIPK3-RNAi Neuro2a Cells

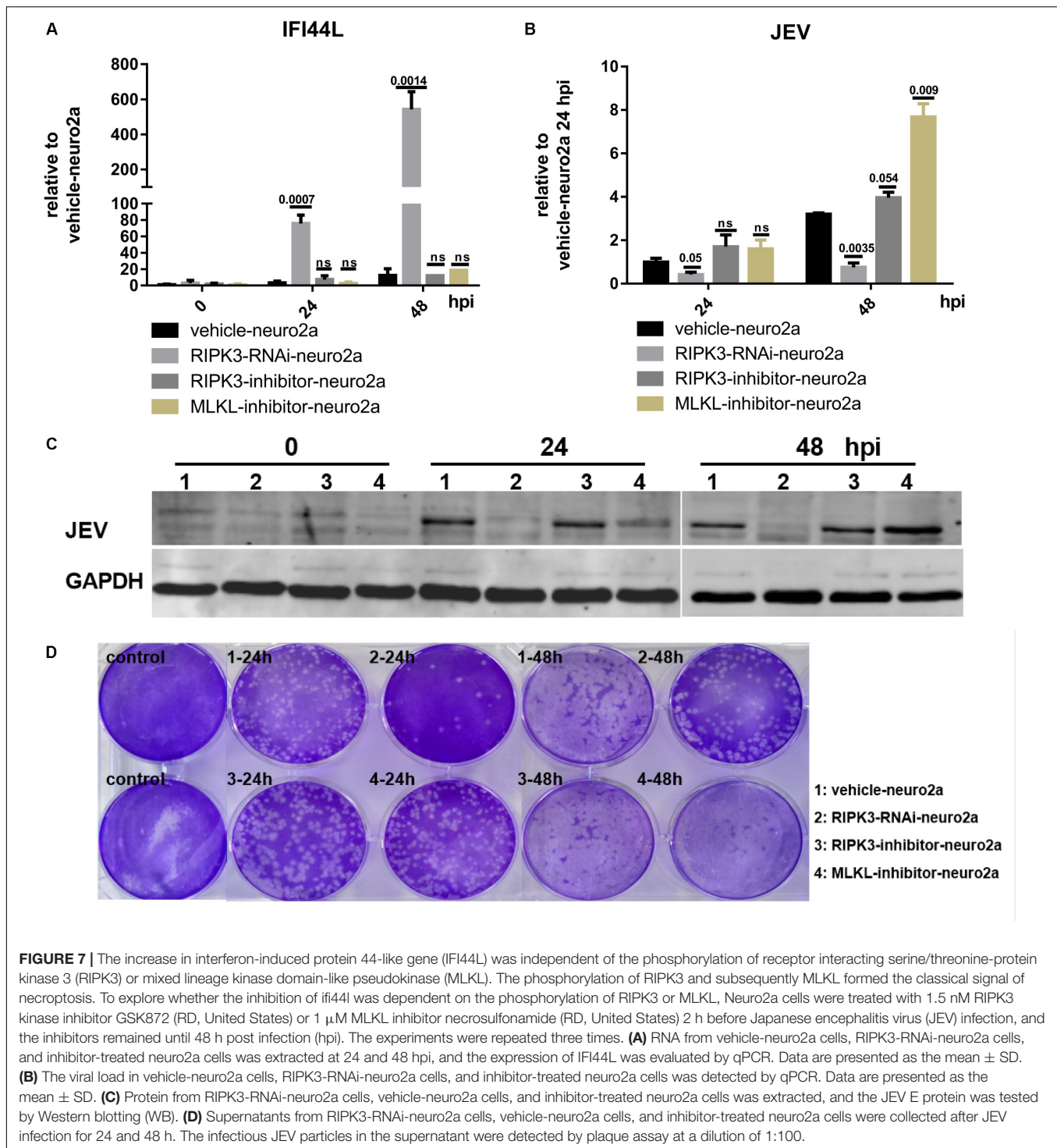
To identify the effect of IFI44L on JEV propagation, IFI44L-overexpressing neuro2a cells (IFI44L-neuro2a) were constructed. The mRNA level of IFI44L increased significantly in IFI44L-neuro2a cells (Figure 8A). The viral RNA level decreased significantly in IFI44L-neuro2a cells compared with GZ-neuro2a cells after JEV infection at 24 and 48 h (Figure 8B). The expression of IFI44L was slightly increased in neuro2a cells at 48 hpi (Figure 8C). Then, IFI44L was downregulated in neuro2a cells at 48 hpi using three IFI44L-targeting shRNAs (Figure 8D and Supplementary Figure S5A). Viral RNA copy numbers increased in IFI44L-RNAi neuro2a cells compared to vehicle neuro2a cells (Figure 8E). This result indicated that IFI44L in neuro2a cells inhibited JEV propagation. Furthermore, IFI44L in RIPK3-i-neuro2a cells was downregulated *via* shRNAs (Figure 8F and Supplementary Figure S5B). The viral RNA

level increased in IFI44L/RIPK3 double knockdown neuro2a cells compared with RIPK3-RNAi-neuro2a cells after JEV infection (Figure 8G). Thus, the upregulation of IFI44L in RIPK3-RNAi-neuro2a cells contributed to the inhibition of JEV propagation.

### DISCUSSION

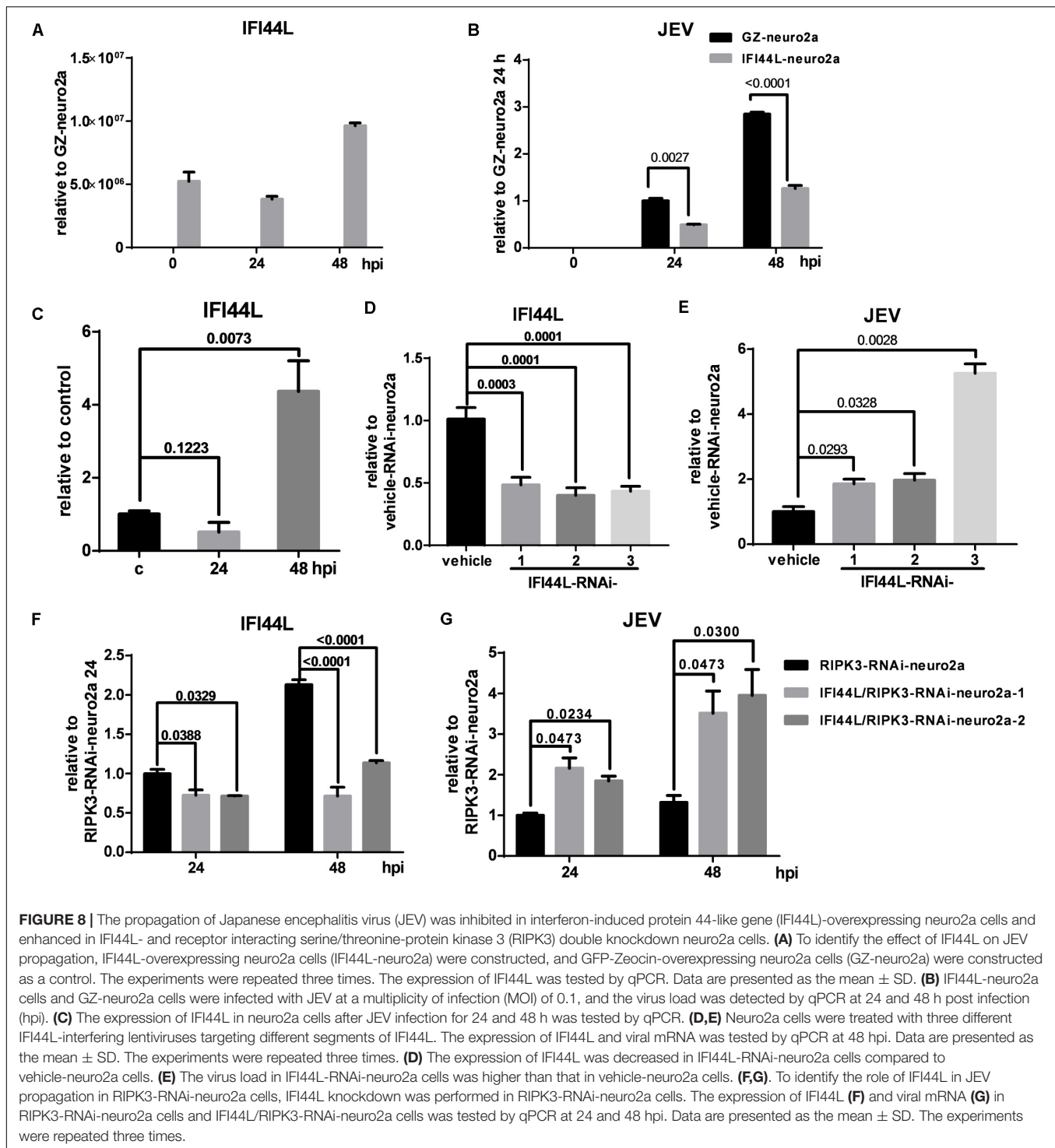
Recently, a number of studies found that RIPK3 mediated complicated roles in cell death, inflammation, and immune defense during virus infection depending on different host cells and viruses (Orozco and Oberst, 2017). In this study, we found that RIPK3<sup>-/-</sup> mice were more resistant to JEV infection during peripheral and intracerebral infection than WT mice. The expression of RIPK3 was increased in neuronal cells following JEV infection, and the increased RIPK3 promoted JEV propagation. Moreover, the viral load was decreased in RIPK3-deleted neuronal cells because of the increased expression of IFI44L. Thus, we speculated that the induced expression of RIPK3 in virus-infected neurons might be a strategy for JEV to evade cellular innate immunity.

The phosphorylation of RIPK1, RIPK3, and subsequently MLKL induces canonical necroptosis followed by DAMP



production and inflammation (Pasparakis and Vandenabeele, 2015). In our previous study, we demonstrated that MLKL-mediated necroptosis accelerated JEV-induced neuroinflammation in mice and that MLKL<sup>-/-</sup> mice showed alleviated JE progression. In this study, we found that morbidity and mortality were decreased in RIPK3<sup>-/-</sup> mice compared to WT mice after peripheral JEV infection,

and JE progression was alleviated in RIPK3<sup>-/-</sup> mice after intracerebral infection. Thus, RIPK3 accelerated JE progression in mice. The expression of RIPK3 was increased in neurons after JEV infection. RIPK3-silenced neuro2a cells showed increased cell viability during JEV infection compared with vehicle neuro2a cells. Thus, RIPK3 promoted neuronal death during JEV infection.



It has been shown that RIPK3/MLKL-mediated necroptosis has antiviral function in fibroblast and epithelial cells during lytic virus infection by destroying viral reservoirs (Nogusa et al., 2016). Additionally, RIPK3 has been demonstrated to play complicated roles in virus propagation in cell death-independent ways. During IAV infection in macrophages, on the one hand, the virus induced RIPK3 accumulation in mitochondria and interfered

with RIPK1/MAVS interactions to decrease IFN- $\beta$  expression, which might be an immune evasion strategy adopted by IAV. On the other hand, the increased RIPK3 could activate protein kinase R (PKR), which stabilized IFN- $\beta$  mRNA, leading to the increased protein level of IFN- $\beta$ , which might be the response of the host cells to counteract viral evasion (Downey et al., 2017). During CVB infection in intestinal epithelial cells (IECs),

RIPK3 promoted CVB infection *via* the positive regulation of autophagic flux (Harris et al., 2015). In neurons, the tug-of-war between cellular immune defense and viral evasion is more complex. Daniels et al. (2019) found that the activation of RIPK1 and RIPK3 in neurons induced the upregulation of IRG1 and the metabolite itaconate to restrict viral replication through an immune-metabolism mechanism during ZIKV infection. In our study, the propagation of JEV was inhibited in RIPK3-deleted neurons and was promoted in RIPK3-overexpressing neuro2a cells. The differences might be explained by the fact that RIPK3 exerts different functions depending on the virus and the host cell. Moreover, we speculated that the increased expression of RIPK3 following JEV infection might be a strategy for JEV to evade cellular innate immunity. The components of JEV particles will be explored in subsequent studies to identify the exact mechanism by which JEV infection promotes RIPK3 expression in neuronal cells.

ISGs are the cellular factors induced by type I IFN in host cells to suppress viral replication. Hundreds of ISGs have been identified, some of which are broad-spectrum antivirals, while others are specific for viruses and cells. Moreover, the antiviral activity of ISGs can be enhanced through synergistic effects (Schoggins, 2019). IFI44L has been found to inhibit the replication of HCV, ZIKV, and DENV. It has been reported that IFI44L inhibited the replication of HCV in Huh-7 cells (Schoggins et al., 2011). In addition, the low levels of IFI44L, IFI27, and STAT1 contributed to the high viral load because of the impaired IFN production caused by HCV NS3-4A protease in HCV patients (Bellocave et al., 2010). Recently, Robinson et al. (2018) also showed that the failure to induce IFI44L contributed to the long-term propagation of ZIKV in germ cells. The expression of ISGs, including IFI44L, OAS1, and IFIT3, was downregulated by the NS4B protein of dengue virus (DENV) in human cells and thus resulted in high viral replication, which was an immune evasion strategy for DENV (Bui et al., 2018). In this study, a series of ISGs were increased in RIPK3<sup>-/-</sup> mouse brains after JEV infection, among which IFI44L was increased most significantly compared with that in the WT. The antiviral role of IFI44L in neuronal cells during JEV infection was demonstrated by both the overexpression and knockdown of IFI44L. However, IFI44L did not completely inhibit JEV replication in RIPK3<sup>-/-</sup> neurons. This did not rule out the role of other molecules. In addition to IFI44L, other ISGs, such as ZBP1, OAS1, and Gbp2b, were also upregulated in RIPK3 knockout mice and neuronal cells and might defend against JEV synergistically.

Neurons were the main host cells of JEV propagation. The expression of IFI44L was higher in RIPK3<sup>-/-</sup> neurons during JEV infection. However, the relationship between IFI44L expression and RIPK3 was unclear. We further compared the levels of the main cytokines in WT and RIPK3<sup>-/-</sup> primary neurons after JEV infection. The mRNA level of CXCL10 increased significantly in WT neurons upon JEV infection compared to RIPK3<sup>-/-</sup> neurons, which was consistent with previous reports that the production of CXCL10 was impaired in RIPK3<sup>-/-</sup> neurons during WNV infection (**Supplementary Figure S6A**). The level of tumor necrosis factor (TNF) $\alpha$  was also higher in WT neurons than RIPK3<sup>-/-</sup> neurons after

JEV infection, which might be the result of different viral loads (**Supplementary Figure S6B**). Then, we detected the levels of IFNs, including IFN $\alpha$ , IFN $\beta$ , and IFN $\gamma$ . Compared to those in WT neurons without JEV infection, IFNs in both WT and RIPK3<sup>-/-</sup> neurons increased after JEV stimulation (**Supplementary Figures S6C–E**). Overall, the total expression levels of IFN $\alpha$  in WT neurons were higher during JEV infection than those in RIPK3<sup>-/-</sup> neurons, while the expression of IFN $\beta$  and IFN $\gamma$  were comparable. In terms of relative changes, the increase in magnitude of IFN $\alpha$  relative to that in the corresponding control neurons was comparable between WT and RIPK3<sup>-/-</sup> neurons, but the increase in magnitude of IFN $\beta$  and IFN $\gamma$  was higher in RIPK3<sup>-/-</sup> neurons (**Supplementary Figures S6F–H**). Taken together, these results indicated that the baseline IFN expression in RIPK3<sup>-/-</sup> neurons was lower than that in WT neurons. Upon JEV stimulation, the higher increase in the magnitude of IFN in RIPK3<sup>-/-</sup> neurons might partly contribute to the production of IFI44L. However, more studies are needed to explore the mechanism by which RIPK3 regulates ifi44l expression.

In summary, RIPK3 has complicated roles in neuroinflammation and virus propagation during viral infection. In our study, we found a novel role of RIPK3 in JEV propagation in neurons, which is different from the role of RIPK3 in CNS infected with WNV of the same genus *Flavivirus*. Our findings further reinforce the intricate and subtle nature of the game between host and virus. We believe that RIPK3 may be a new therapeutic target for the development of virus replication inhibitors to treat JEV-induced encephalitis.

## DATA AVAILABILITY STATEMENT

All datasets generated for this study are included in the article/**Supplementary Material**.

## ETHICS STATEMENT

The animal study was reviewed and approved by the Animal Care and Use Committee of the Laboratory Animal Center, Air Force Medical University. The number of Animal Experimental Ethical Inspection is 20160112.

## AUTHOR CONTRIBUTIONS

PB contributed to the conception and design, data collection and assembly, data analysis and interpretation, and manuscript writing. CY contributed to the data collection and assembly. XZ contributed to the data analysis and manuscript writing. CL, JiaY, ML, YW, JinY, and YuZ contributed to the data collection. FZ, JL, and YiZ contributed to the administrative support and provision of study material. ZJ contributed to the conception and design, administrative support, and final approval of the manuscript. YL contributed to the conception and design, financial support, and manuscript writing.

## FUNDING

This work was supported by the National Natural Science Foundation of China (No. 81871697).

## ACKNOWLEDGMENTS

We would like to thank Dr. Yazhou Wang (Department of Neurobiology and Collaborative Innovation Center for Brain Science, School of Basic Medicine, Air Force Medical University) for providing the reagents for this study.

## SUPPLEMENTARY MATERIAL

The Supplementary Material for this article can be found online at: <https://www.frontiersin.org/articles/10.3389/fmicb.2020.00368/full#supplementary-material>

**FIGURE S1** | The colocalization of PI and RIPK3 in the brains of JEV-infected mice. WT C57BL/6 mice infected with JEV via footpad injection were administered PI intraperitoneally at 5 dpi and euthanized 1 h later. The expression of RIPK3 (green) was detected, and the colocalization of RIPK3 and PI (red) was recorded. Cells with both RIPK3 and PI positivity (white row) and RIPK3 positivity without PI (blue row) were all detected.

**FIGURE S2** | The propagation of JEV was inhibited in RIPK3<sup>-/-</sup> primary neurons. Primary neurons from WT and RIPK3<sup>-/-</sup> mice were isolated and cultured for 1 week and then infected with JEV at an MOI of 0.1. Data are presented as the mean ± SD. The experiments were repeated three times. **(A)** RNA was extracted at 24, 48, and 72 h after JEV infection, and the level of JEV was detected by qPCR. The expression of JEV mRNA in each group was normalized to actin-β expression. Then, the relative fold change in each group was calculated based on the normalized mean expression of WT at 24 h. **(B)** Protein from WT and RIPK3<sup>-/-</sup> neurons was extracted at 24, 48, and 72 h after JEV infection, and the E protein of JEV was tested by WB. **(C)** Supernatants from WT and RIPK3<sup>-/-</sup>

neurons were collected at 24, 48, and 72 h post JEV infection. The infectious JEV particles in the supernatant were detected by plaque assay with double wells at a dilution of 1:1000.

**FIGURE S3** | The expression of RIPK3 after pCMV-GFPspark or pCMV-RIPK3-OFPSpark transfection. **(A)** Neuro2a cells were transfected with pCMV-GFPspark or pCMV-RIPK3-OFPSpark, and then GFP-neuro2a cells and RIPK3-neuro2a cells were infected with JEV-p3 at an MOI of 0.1 and collected at 12 and 24 hpi for RNA extraction. The expression of RIPK3 was tested by qPCR. **(B)** RIPK3-RNAi-Neuro2a cells were transfected with pCMV-GFPspark or pCMV-RIPK3-OFPSpark, and then GFP-RIPK3-i-neuro2a cells and RIPK3-RIPK3-i-neuro2a cells were infected with JEV-p3, MOI = 0.1 and collected at 12 and 24 hpi for RNA extraction. The expression of RIPK3 was tested by qPCR.

**FIGURE S4** | The expression of pRIPK3 and pMLKL in each group. Vehicle-neuro2a cells, RIPK3-RNAi-neuro2a cells, and inhibitor-treated neuro2a cells were collected for protein extraction at 48 hpi. The protein levels of pRIPK3 and pMLKL were detected by WB.

**FIGURE S5** | The expression of IFI44L in each group. **(A)** Neuro2a cells were treated with three different IFI44L interfering lentiviruses targeting different segments of IFI44L. The expression of IFI44L was evaluated by WB at 48 hpi. **(B)** To identify the role of IFI44L in JEV propagation in RIPK3-RNAi neuro2a cells, IFI44L knockdown was performed in RIPK3-RNAi-neuro2a cells. The expression of IFI44L in RIPK3-RNAi-neuro2a cells and IFI44L/RIPK3-RNAi-neuro2a cells was evaluated by WB at 24 and 48 hpi.

**FIGURE S6** | The expression of IFNs in primary neurons after JEV infection. WT and RIPK3<sup>-/-</sup> mouse-derived primary neurons were infected with JEV; MOI = 0.1. RNA was extracted, and the expression of CXCL10, TNFα and IFNs was evaluated by qPCR at 24, 48, and 72 hpi. **(A)** The expression of CXCL10 in neurons was increased after JEV infection and was higher in WT neurons than RIPK3<sup>-/-</sup> neurons. **(B)** The expression of TNFα in WT and RIPK3<sup>-/-</sup> neurons. **(C–E)** Changes in the expression of IFNα, IFNβ and IFNγ in WT and RIPK3<sup>-/-</sup> neurons after JEV infection relative to the WT control at 24, 48, and 72 hpi. **(F–H)** Changes in the expression of IFNα, IFNβ, and IFNγ in neurons after JEV infection relative to those in WT or RIPK3<sup>-/-</sup> control neurons, respectively.

**TABLE S1** | shRNA targeting sequences, PCR primers and antibodies used in this study.

## REFERENCES

- Bellecave, P., Sarasin-Filipowicz, M., Donze, O., Kennel, A., Gouttenoire, J., Meylan, E., et al. (2010). Cleavage of mitochondrial antiviral signaling protein in the liver of patients with chronic hepatitis C correlates with a reduced activation of the endogenous interferon system. *Hepatology* 51, 1127–1136. doi: 10.1002/hep.23426
- Bian, P., Zheng, X., Wei, L., Ye, C., Fan, H., Cai, Y., et al. (2017). MLKL mediated necroptosis accelerates JEV-induced neuroinflammation in mice. *Front. Microbiol.* 8:303. doi: 10.3389/fmicb.2017.00303
- Bui, T. T., Moi, M. L., Nabeshima, T., Takemura, T., Nguyen, T. T., Nguyen, L. N., et al. (2018). A single amino acid substitution in the NS4B protein of Dengue virus confers enhanced virus growth and fitness in human cells *in vitro* through IFN-dependent host response. *J. Gen. Virol.* 99, 1044–1057. doi: 10.1099/jgv.0.001092
- Daniels, B. P., Kofman, S. B., Smith, J. R., Norris, G. T., Snyder, A. G., Kolb, J. P., et al. (2019). The nucleotide sensor ZBP1 and kinase RIPK3 induce the enzyme IRG1 to promote an antiviral metabolic state in neurons. *Immunity* 50, 64–76. doi: 10.1016/j.immuni.2018.11.017
- Daniels, B. P., Snyder, A. G., Olsen, T. M., Orozco, S., Oguin, T. R., Tait, S., et al. (2017). RIPK3 restricts viral pathogenesis via cell death-independent neuroinflammation. *Cell* 169, 301–313. doi: 10.1016/j.cell.2017.03.011
- Downey, J., Pernet, E., Coulombe, F., Allard, B., Meunier, I., Jaworska, J., et al. (2017). RIPK3 interacts with MAVS to regulate type I IFN-mediated immunity to influenza A virus infection. *PLoS Pathog.* 13:e1006326. doi: 10.1371/journal.ppat.1006326
- Han, Y. W., Choi, J. Y., Uyangaa, E., Kim, S. B., Kim, J. H., Kim, B. S., et al. (2014). Distinct dictation of Japanese encephalitis virus-induced neuroinflammation and lethality via triggering TLR3 and TLR4 signal pathways. *PLoS Pathog.* 10:e1004319. doi: 10.1371/journal.ppat.1004319
- Harris, K. G., Morosky, S. A., Drummond, C. G., Patel, M., Kim, C., Stolz, D. B., et al. (2015). RIP3 regulates autophagy and promotes coxsackievirus B3 infection of intestinal epithelial cells. *Cell Host Microbe* 18, 221–232. doi: 10.1016/j.chom.2015.07.007
- He, S., and Wang, X. (2018). RIP kinases as modulators of inflammation and immunity. *Nat. Immunol.* 19, 912–922. doi: 10.1038/s41590-018-0188-x
- Huang, Z., Wu, S. Q., Liang, Y., Zhou, X., Chen, W., Li, L., et al. (2015). RIP1/RIP3 binding to HSV-1 ICP6 initiates necroptosis to restrict virus propagation in mice. *Cell Host Microbe* 17, 229–242. doi: 10.1016/j.chom.2015.01.002
- Koehler, H., Cotsmire, S., Langland, J., Kibler, K. V., Kalman, D., Upton, J. W., et al. (2017). Inhibition of DAI-dependent necroptosis by the Z-DNA binding domain of the vaccinia virus innate immune evasion protein. *E3. Proc. Natl. Acad. Sci. U.S.A.* 114, 11506–11511. doi: 10.1073/pnas.1700999114
- Lannes, N., Summerfield, A., and Filgueira, L. (2017). Regulation of inflammation in Japanese encephalitis. *J. Neuroinflamm.* 14:158. doi: 10.1186/s12974-017-0931-5
- Lawlor, K. E., Khan, N., Mildenhall, A., Gerlic, M., Croker, B. A., D’Cruz, A. A., et al. (2015). RIPK3 promotes cell death and NLRP3 inflammasome activation in the absence of MLKL. *Nat. Commun.* 6:6282. doi: 10.1038/ncomms7282

- Liu, K., Liao, X., Zhou, B., Yao, H., Fan, S., Chen, P., et al. (2013). Porcine alpha interferon inhibit Japanese encephalitis virus replication by different ISGs in vitro. *Res. Vet. Sci.* 95, 950–956. doi: 10.1016/j.rvsc.2013.08.008
- Nogusa, S., Thapa, R. J., Dillon, C. P., Liedmann, S., Oguin, T. R., Ingram, J. P., et al. (2016). RIPK3 activates parallel pathways of MLKL-driven necroptosis and FADD-mediated apoptosis to protect against influenza A virus. *Cell Host Microbe* 20, 13–24. doi: 10.1016/j.chom.2016.05.011
- Orozco, S., and Oberst, A. (2017). RIPK3 in cell death and inflammation: the good, the bad, and the ugly. *Immunol. Rev.* 277, 102–112. doi: 10.1111/imr.12536
- Pasparakis, M., and Vandenabeele, P. (2015). Necroptosis and its role in inflammation. *Nature* 517, 311–320. doi: 10.1038/nature14191
- Robinson, C. L., Chong, A. C. N., Ashbrook, A. W., Jeng, G., Jin, J., Chen, H., et al. (2018). Male germ cells support long-term propagation of Zika virus. *Nat. Commun.* 9:2090. doi: 10.1038/s41467-018-04444-w
- Schoggins, J. W. (2019). Interferon-stimulated genes: what do they all do? *Annu. Rev. Virol.* 6, 567–584. doi: 10.1146/annurev-virology-092818-015756
- Schoggins, J. W., Wilson, S. J., Panis, M., Murphy, M. Y., Jones, C. T., Bieniasz, P., et al. (2011). A diverse range of gene products are effectors of the type I interferon antiviral response. *Nature* 472, 481–485. doi: 10.1038/nature09907
- Thongtan, T., Thepparit, C., and Smith, D. R. (2012). The involvement of microglial cells in Japanese encephalitis infections. *Clin. Dev. Immunol.* 2012:890586. doi: 10.1155/2012/890586
- Wang, X., Li, S. H., Zhu, L., Nian, Q. G., Yuan, S., Gao, Q., et al. (2017). Near-atomic structure of Japanese encephalitis virus reveals critical determinants of virulence and stability. *Nat. Commun.* 8:14. doi: 10.1038/s41467-017-00024-6
- Wang, X., Li, Y., Liu, S., Yu, X., Li, L., Shi, C., et al. (2014). Direct activation of RIP3/MLKL-dependent necrosis by herpes simplex virus 1 (HSV-1) protein ICP6 triggers host antiviral defense. *Proc. Natl. Acad. Sci. U.S.A.* 111, 15438–15443. doi: 10.1073/pnas.1412767111
- Weinlich, R., Oberst, A., Beere, H. M., and Green, D. R. (2017). Necroptosis in development, inflammation and disease. *Nat. Rev. Mol. Cell Biol.* 18, 127–136.
- Ye, J., Chen, Z., Li, Y., Zhao, Z., He, W., Zohaib, A., et al. (2017). Japanese encephalitis virus NS5 inhibits type I interferon (IFN) production by blocking the nuclear translocation of IFN regulatory factor 3 and NF-kappaB. *J. Virol.* 91, e00039-17. doi: 10.1128/JVI.00039-17
- Yun, S. I., and Lee, Y. M. (2018). Early events in Japanese encephalitis virus infection: viral entry. *Pathogens* 7:68.
- Zhou, D., Jia, F., Li, Q., Zhang, L., Chen, Z., Zhao, Z., et al. (2018). Japanese encephalitis virus NS1' protein antagonizes interferon beta production. *Virology* 511, 515–523. doi: 10.1007/s12250-018-0067-5

**Conflict of Interest:** The authors declare that the research was conducted in the absence of any commercial or financial relationships that could be construed as a potential conflict of interest.

Copyright © 2020 Bian, Ye, Zheng, Luo, Yang, Li, Wang, Yang, Zhou, Zhang, Lian, Zhang, Jia and Lei. This is an open-access article distributed under the terms of the Creative Commons Attribution License (CC BY). The use, distribution or reproduction in other forums is permitted, provided the original author(s) and the copyright owner(s) are credited and that the original publication in this journal is cited, in accordance with accepted academic practice. No use, distribution or reproduction is permitted which does not comply with these terms.



# Molecular Pathogenicity of Enteroviruses Causing Neurological Disease

Anna Majer<sup>1\*</sup>, Alan McGreevy<sup>1,2,3</sup> and Timothy F. Booth<sup>1,2</sup>

<sup>1</sup> Viral Diseases Division, National Microbiology Laboratory, Winnipeg, MB, Canada, <sup>2</sup> Department of Medical Microbiology and Infectious Diseases, University of Manitoba, Winnipeg, MB, Canada, <sup>3</sup> Department of Biology, University of Winnipeg, Winnipeg, MB, Canada

## OPEN ACCESS

### Edited by:

Mei-Ling Li,  
Rutgers, The State University  
of New Jersey, United States

### Reviewed by:

Yong Zhang,  
National Institute for Viral Disease  
Control and Prevention, China  
Edson Elias Da Silva,  
Oswaldo Cruz Foundation (Fiocruz),  
Brazil

### \*Correspondence:

Anna Majer  
anna.majer@canada.ca

### Specialty section:

This article was submitted to  
Virology,  
a section of the journal  
Frontiers in Microbiology

**Received:** 26 November 2019

**Accepted:** 12 March 2020

**Published:** 09 April 2020

### Citation:

Majer A, McGreevy A and  
Booth TF (2020) Molecular  
Pathogenicity of Enteroviruses  
Causing Neurological Disease.  
*Front. Microbiol.* 11:540.  
doi: 10.3389/fmicb.2020.00540

Enteroviruses are single-stranded positive-sense RNA viruses that primarily cause self-limiting gastrointestinal or respiratory illness. In some cases, these viruses can invade the central nervous system, causing life-threatening neurological diseases including encephalitis, meningitis and acute flaccid paralysis (AFP). As we near the global eradication of poliovirus, formerly the major cause of AFP, the number of AFP cases have not diminished implying a non-poliovirus etiology. As the number of enteroviruses linked with neurological disease is expanding, of which many had previously little clinical significance, these viruses are becoming increasingly important to public health. Our current understanding of these non-polio enteroviruses is limited, especially with regards to their neurovirulence. Elucidating the molecular pathogenesis of these viruses is paramount for the development of effective therapeutic strategies. This review summarizes the clinical diseases associated with neurotropic enteroviruses and discusses recent advances in the understanding of viral invasion of the central nervous system, cell tropism and molecular pathogenesis as it correlates with host responses.

**Keywords:** enterovirus, host factor, pathogenesis, central nervous system, neurological disease

## INTRODUCTION

Enteroviruses (EVs) are single-stranded positive-sense RNA viruses of the family *Picornaviridae* (Ehrenfeld et al., 2010). There are 106 enterovirus types known to infect humans, belonging to the four species *Enterovirus A* through *Enterovirus D*. Polio is caused by three strains within the species *Enterovirus C* and the remaining types are non-polio enteroviruses that includes 21 coxsackievirus A types, 6 coxsackievirus B types, 28 echoviruses and 48 numbered enteroviruses (Simmonds et al., 2020). Three rhinovirus species, *Rhinovirus A* through *Rhinovirus C*, are also classified under the genus *Enterovirus* and include 169 rhinoviruses. Although most EVs cause self-limiting gastrointestinal or respiratory illnesses, a growing number have been found to possess the ability to invade the central nervous system and cause potentially fatal neurological symptoms including encephalitis, meningitis and paralysis. The exact number of EV-associated neurological disease

cases remains unknown, but 80% of aseptic meningitis (Morens and Pallansch, 1995) and up to 11% encephalitis cases (Koskiniemi et al., 2001) are speculated to be due to EV infection. Poliovirus is the most widely known EV and is the etiological agent of poliomyelitis that primarily affects infants and children, resulting in lifelong disability or death (Howard, 2005). As we near the global eradication of all 3 poliovirus strains, the incidence of poliomyelitis has plummeted drastically (Jorba et al., 2018). Nevertheless, the emergence of poliomyelitis-like neurological disease called acute flaccid myelitis (AFM) since 2014 clearly indicates a non-poliovirus cause. Recent epidemiological and animal work evidence suggests a strong causal link between AFM cases and EV-D68 outbreaks, a virus which previously had little, if any, clinical significance. As the number of EV species capable of invading the central nervous system and linked to neurological symptoms is growing, these viruses are increasingly being considered as re-emerging pathogens of significant importance to public health.

Our current understanding of these non-polio enteroviruses is limited, especially with regards to their neurovirulence. Without an effective treatment strategy to combat or prevent non-polio EV infections of the central nervous system, better understanding of the neuropathogenic process of neurotropic EVs is highly warranted. Elucidating the molecular pathogenesis of these viruses is paramount for the development of effective therapeutic strategies. This review summarizes clinical diseases associated with some of the most common neurotropic enteroviruses and discusses recent understanding of viral invasion into the central nervous system, cell tropism and molecular pathogenesis as it correlates with host responses during neurotropic enterovirus infections.

## NEUROLOGICAL MANIFESTATION OF ENTEROVIRUS INFECTIONS

Numerous EVs are linked to debilitating and potentially deadly neurological diseases including aseptic meningitis, encephalitis and AFM. In certain instances, EV infections are associated with the development of neurological sequelae years after the onset of acute disease, as is suspected for post-polio syndrome (Ramlow et al., 1992) and Guillain-Barré syndrome (Ooi et al., 2010). Here we will briefly describe these disorders and highlight which non-polio EVs are primarily associated with these neuropathies (Table 1).

### Enterovirus-Associated Meningitis and Encephalitis

Enterovirus infections are the most common cause of both meningitis and encephalitis in children 17 years of age and younger (Hasbun et al., 2019). Meningitis represents inflammation of the membrane lining the brain and spinal cord, known as meninges while encephalitis depicts inflammation of the brain parenchyma. Infants are highly susceptible, experiencing mortality rates as high as 10% (Rhoades et al., 2011). Diagnosis is made by several factors including clinical symptoms, neuroimaging and lumbar puncture to assess the

**TABLE 1** | Enteroviruses associated with neurological illness.

Neurological Disease	Enterovirus	Reference	
Acute flaccid myelitis	<b>EV-A71</b>	Chonmaitree et al., 1981; Lin et al., 2003	
	<b>EV-D68</b>	Kreuter et al., 2011; Yea et al., 2017; Dyda et al., 2018	
	EV-D70	Bharucha et al., 1972	
	EV-B93	Junttila et al., 2007	
	EV-D94	Junttila et al., 2007	
	Echovirus 33	Grimwood et al., 2003	
	Encephalitis	<b>CVA2</b>	Chiang et al., 2019
		<b>CVA9</b>	Zhang et al., 2013
		CVB1	Zhang et al., 2013
		<b>CVB4</b>	Geller and Condie, 1995; Zhang et al., 2013
<b>CVB5</b>		Ramelli et al., 2004; Papa et al., 2006	
<b>Echovirus 4</b>		McIntyre and Keen, 1993; Logotheti et al., 2009; Zhang et al., 2013	
<b>Echovirus 5</b>		Dumaidi et al., 2006	
<b>Echovirus 6</b>		Siafakas et al., 2004; Zhang et al., 2013	
<b>Echovirus 9</b>		Dalwai et al., 2009; Zhang et al., 2013	
<b>Echovirus 11</b>		Moline et al., 2018; Lopez et al., 2019	
Meningitis	Echovirus 17	Hart and Miller, 1973	
	Echovirus 19	Kumar et al., 2011; Singh et al., 2016	
	Echovirus 21	Singh et al., 2016	
	<b>Echovirus 30</b>	Siafakas et al., 2004; Zhang et al., 2013	
	<b>EV-A71</b>	Chonmaitree et al., 1981; Lin et al., 2003	
	<b>EV-D68</b>	Kreuter et al., 2011; Yea et al., 2017; Dyda et al., 2018	
	EV-B75	Avellón et al., 2006; Lewthwaite et al., 2010	
	EV-A76	Pallansch et al., 2013	
	EV-A89	Pallansch et al., 2013	
	<b>CVA2</b>	Chiang et al., 2019	
Poliomyelitis	<b>CVA9</b>	Zhang et al., 2013	
	CVA16	Goto et al., 2009	
	CVA5	Pallansch et al., 2013	
	CVA7	Ranzenhofer et al., 1958; Yamayoshi et al., 2012	
	<b>CVB4</b>	Geller and Condie, 1995; Zhang et al., 2013	
	<b>CVB5</b>	Ramelli et al., 2004; Papa et al., 2006	
	<b>Echovirus 4</b>	McIntyre and Keen, 1993; Logotheti et al., 2009; Zhang et al., 2013	
	<b>Echovirus 5</b>	Dumaidi et al., 2006	
	<b>Echovirus 6</b>	Siafakas et al., 2004; Zhang et al., 2013	
	<b>Echovirus 9</b>	Dalwai et al., 2009; Zhang et al., 2013	
<b>Echovirus 11</b>	Moline et al., 2018; Lopez et al., 2019		
Poliomyelitis	Echovirus 14	Chen et al., 2017	
	Echovirus 16	Baron et al., 1982	
	Echovirus 25	Zhang et al., 2013	
	<b>Echovirus 30</b>	Siafakas et al., 2004; Zhang et al., 2013	
	Echovirus 31	Kelen et al., 1964	
	<b>EV-A71</b>	Chonmaitree et al., 1981; Lin et al., 2003	
	<b>EV-D68</b>	Kreuter et al., 2011; Yea et al., 2017; Dyda et al., 2018	
	Poliovirus	Horstmann, 1949	

*Bolded enteroviruses have been linked to cause multiple neurological diseases.*

cerebral spinal fluid (CSF) for infectious agents (Venkatesan et al., 2013). Enterovirus-specific PCR of CSF specimens is highly recommended although is insufficient for diagnosis when used alone (Venkatesan et al., 2013) due to low yield of positive results (Pérez-Vélez et al., 2007; Lopez et al., 2019). Testing additional sites (i.e., throat and gastrointestinal tract) where virus shedding is prolonged (Han et al., 2010) is recommended but may still result in EV negative status if sample collection is delayed. It is therefore possible that the etiology of meningitis and encephalitis cases due to EV infection are much higher than reported.

Numerous EVs have been detected in cases of encephalitis, aseptic meningitis or meningoencephalitis – inflammation of both meninges and the brain. The wide diversity of enteroviruses associated with encephalitis or meningitis highlights their collective neuropathogenic potential and speaks to their unique tropism. Specifically, poliovirus, CV (A2, A9, B5), echoviruses (6, 9, 11, 30) and EV-A71 are commonly implicated in causing both encephalitis and aseptic meningitis (Jain et al., 2014; Pons-Salort et al., 2015; Rudolph et al., 2016). However, EV-A71 was also linked to cause outbreaks of brainstem encephalitis or AFM (Lee, 2016). CV (A5, A7, A16, B2, B3, B4) and echoviruses (14, 16, 25, 31) are all implicated in cases of meningitis, while CV (A2, B1), echoviruses (4, 5, 17, 19, 21) and EV (75, 76, 89) are implicated in cases of encephalitis (Jain et al., 2014; Pons-Salort et al., 2015; Rudolph et al., 2016).

## Acute Flaccid Paralysis and Acute Flaccid Myelitis

Acute flaccid paralysis (AFP) is a WHO reportable disease in children under the age of 15. AFP is clinically defined as acute onset of flaccid paralysis of one or more limbs due to an infectious cause (The United Kingdom Acute Flaccid Paralysis AFP Task Force, 2019). The disease may damage different parts of the body including spinal cord, peripheral nerves, neuromuscular junctions and muscles. Poliovirus was the primary etiology of infectious AFP cases causing poliomyelitis. With current near-universal vaccination strategies designed to eradicate poliovirus, the total number of AFP cases attributed to poliovirus around the world have decreased drastically (Suresh et al., 2018).

A subset of AFP called acute flaccid myelitis (AFM) represents a disease where paralysis and limb weakness typically occurs within a week of respiratory symptoms or fever caused by a non-polio viral infection. In addition to the acute limb weakness, a lesion in the spinal cord gray matter that spans at least one vertebra and often elevated leukocyte counts within the CSF is a classic diagnostic feature (Dyda et al., 2018; Centers for Disease Control and Prevention, 2019; Fatemi and Chakraborty, 2019). Symptoms result from inflammation followed by the loss of motor neurons within the brain stem and spinal cord without any signs of generalized encephalitis (Maloney et al., 2015; Hovden and Pfeiffer, 2015). AFM cases have been associated with several viral pathogens including enteroviruses and echoviruses (Gilsdorf, 2019). EV-D68 is the most consistent enterovirus linked with AFM (Kreuter et al., 2011), accounting for up to 50% of all confirmed AFM cases (Lopez et al., 2019), but other enteroviruses such as EV-A71 (Chumakov et al., 1979;

Lopez et al., 2019; Lee et al., 2014), CVs (Cho et al., 2017; Lopez et al., 2019), EV-D70 (Bharucha et al., 1972), EV-B93 and EV-D94 (Junttila et al., 2007), echovirus 33 (Grimwood et al., 2003) and echovirus 11 (Moline et al., 2018; Lopez et al., 2019) have also been identified but at a much lower frequency. Although AFM is rare, affecting more than 500 confirmed cases worldwide since 2012 (Helfferich et al., 2019), the prognosis is poor with less than 20% of children fully regaining neurological function within 6 months (Sejvar et al., 2016; Yea et al., 2017; Helfferich et al., 2019). No treatment strategy currently exists for AFM patients but physical rehabilitation which, when implemented during the acute phase of the illness, slightly helps improve long-term neurological outcomes (Van Haren et al., 2015). Latest nerve transfer procedures also show promise in restoring partial function to paralyzed limbs in AFM patients (Pino et al., 2019).

Recent epidemiological criteria using the Bradford-Hill analyses showed strong support that AFM is primarily caused by EV-D68 (Dyda et al., 2018; Messacar et al., 2018). The particular cyclical and biennial patterns of EV-D68 infections correlated well with outbreaks of AFM in children occurring in 2014, 2016, and 2018 (Dyda et al., 2018; Kramer et al., 2018). However, detecting the virus from clinical samples remains a challenge and contributed to skepticism surrounding EV-D68 as a cause of AFM. During 2018, the active surveillance network in the USA confirmed approximately 230 AFM cases of which approximately 44% of respiratory, 13% of stool and 3% of CSF specimens were EV-D68 positive (Lopez et al., 2019). Recent animal models that mimicked human disease and satisfied Koch's postulates helped solidify the link between EV-D68 infection and subsequent AFM complications. Intraperitoneal inoculation of EV-D68 into neonatal mice recapitulated clinical AFM symptoms including paralysis due to motor neuron loss in the anterior horn cells of the spinal cord (Hixon et al., 2017). Virus isolated from spinal cord lysates of paralyzed mice resulted in cell death in cultured cells and caused paralysis when injected into mice (Hixon et al., 2017). Similarly, intraperitoneal infection of EV-D68 into neonatal BALB/c mice induced both interstitial pneumonia and AFM (Sun et al., 2019). Studies within these types of animal models will help unravel the molecular mechanisms used by EV-D68 to cause AFM.

## Chronic Neurological Diseases Associated With Enterovirus Infections

Some poliovirus infected patients develop a condition called post-polio syndrome (PPS) that is characterized by muscle weakness and atrophy several decades following acute infection but, in contrast to poliomyelitis, these sequelae tend to be transient and progressive (Huang and Shih, 2015). It is commonly a diagnosis of exclusion once other possible medical or surgical causes of gradual onset weakness are discounted, occurring on average 30–35 years after acute poliomyelitis (Boyer et al., 2010). The disease is more common in patients who had severe initial poliovirus infections and subsequently developed permanent impairment (Ramlow et al., 1992). Studies vary widely in the estimated prevalence of PPS, ranging from 31% (Ragonese et al., 2005) to 85% (Takemura et al., 2004) of polio infected individuals. A case

reported in 2017 described a post-polio-like symptom several decades following a severe infection with EV-70, suggesting that polio may not be the only enterovirus capable of inducing this syndrome (Suzuki et al., 2017).

The precise mechanism of PPS is unknown and treatment is limited to supportive measures (Lin and Lim, 2005). Muscle weakness in PPS is asymmetrical and is more likely, but not exclusive to muscles that were originally affected by poliomyelitis (Lin and Lim, 2005). One proposed mechanism of PPS stems from the properties that peripheral neurons are capable of axonal regrowth and/or sprouting. For muscle weakness to be clinically apparent, more than 50% of spinal anterior horn neurons that innervate the muscle must be lost (Lin and Lim, 2005). Denervation of muscle can stimulate terminal axons of surviving neighboring neurons to sprout, re-innervating muscle fibers that lost neuronal connection with the spinal cord (Boyer et al., 2010). As denervation can be caused by neuronal cell death, this proposed mechanism helps explain the restoration of function following acute poliomyelitis in PPS patients (Boyer et al., 2010). In support of this proposed mechanism, the rate of residual disability following poliomyelitis was lower in patients with PPS (Klingman et al., 1988). However, the sprouting re-innervation of terminal axons does not appear to be stable and intense muscle use may accelerate deterioration of the terminal axon sprouts (Boyer et al., 2010). Therefore, the benefits of strength training exercises in PPS patients remains controversial where some find benefits (Chan et al., 2003) while others suggest that muscle exhaustion leads to accelerated weakness (Pastuszak et al., 2017).

Guillain-Barré syndrome (GBS) is an inflammatory immune disorder characterized by rapid-onset muscle weakness due to damage to the peripheral nervous system (PNS). The initial symptoms of GBS are often changes in sensation or pain in the extremities that develop over hours to weeks. In some cases, weakness of breathing muscles during the acute phase of the syndrome requires mechanical ventilation but, if the patient survives this phase, complete recovery is likely (Gear, 1984). Despite being classified as a single syndrome, GBS appears to result from one of two related but distinct etiologies: (1) a viral infection of CNS tissue, possibly of Schwann cells, that induces inflammation of the myelin sheaths and leads to their degradation; or (2) an autoimmune reaction to the myelin sheaths initiated in response to an infection elsewhere in the body, vaccination or drug reaction (Gear, 1984). The distinction between these two etiologies is largely made on patient history and whether virus can be detected from the CSF. Recent cases of AFM caused by EV-D68 can be distinguished from GBS via MRI, as GBS tends to be systemic and descending while AFM more commonly presents as asymmetric weakness (Gill et al., 2018). However, the overlapping clinical symptoms of muscle weakness and myelitis make it entirely possible that some GBS cases are due to enterovirus infections in which the virus is not successfully isolated, or that enterovirus infections may precipitate a GBS attack (Pallansch et al., 2013). In fact, EV-A71 outbreaks have linked the virus to GBS (Ooi et al., 2010) and one case study identified GBS with peripheral nerve demyelination following hand foot and mouth disease (HFMD), though the specific enterovirus that caused the HFMD was

not identified (Mori et al., 2000). It still remains largely unclear how often and in what capacity enteroviruses contribute to the development of GBS.

## ROUTES OF ENTEROVIRUS NEUROINVASION

Viral pathogens employ a variety of strategies to gain entry into the CNS (Kim, 2008) and uncovering these routes of neuroinvasion could reveal potential avenues that can be targeted to prevent EV-induced neurological disease. EVs replicate in either the gastrointestinal tract (i.e., poliovirus, most numbered enteroviruses and echoviruses) or the lungs (i.e., EV-D68) during early disease. Poliovirus is an excellent example of a gastrointestinal enterovirus which uses retrograde axonal transport within motor neurons to enter the CNS. Poliovirus primarily infects gastrointestinal epithelia by binding to poliovirus-specific receptor CD155, and thereby gains entry into the lymphatic and circulatory systems (reviewed in Gilsdorf, 2019). The virus then spreads within the circulatory system (i.e., viremia) and disseminates to infect peripheral tissues such as muscles. At neuromuscular junctions, poliovirus enters motor neurons by using receptor-mediated endocytosis allowing the virus to travel from the terminal to the cell body within the endosome by retrograde axonal transport (Racaniello and Ren, 1994; Gromeier and Wimmer, 1998; Mueller et al., 2002; Ohka et al., 2004). Physiologically, the virus moves from the muscle to the sciatic nerve, enters the spinal cord and eventually reaches the brain (Ren and Racaniello, 1992; Ohka et al., 1998). In support, surgically severing nerves in mice prior to poliovirus infection prevented the spread of the virus to the spinal cord (Gromeier and Wimmer, 1998). Interestingly, retrograde axonal transport of poliovirus is fairly inefficient, which could explain the low incidence of neurological complications seen in patients (Lancaster and Pfeiffer, 2010). However, local muscle injury significantly enhanced poliovirus neuroinvasiveness, allowing for 3-fold more virus to enter the CNS (Lancaster and Pfeiffer, 2010). Retrograde axonal transport was demonstrated for several non-polio enterovirus such as EV-A71 (Chen C.S. et al., 2007) and EV-D68 (Hixon et al., 2019a).

The ability of enteroviruses to infect immune cells is another potential mechanism for their neuroinvasion. Numerous EVs were found to infect circulating immune cells which can serve as a Trojan Horse to deliver the virus into the CNS tissue. For example, the myeloid-like Mac3<sup>+</sup> peripheral blood mononuclear cells (PBMCs) were found to be highly susceptible to CVB3 infection (Tabor-Godwin et al., 2010). In a neonatal mouse model these cells were recruited to the CNS via the choroid plexus, allowing for the virus to gain unrestricted entry into the brain (Tabor-Godwin et al., 2010). Infection of mice by CVB3 showed that B cells were susceptible to viral infection and also helped disseminate the virus during early infection to the brain and other tissues throughout the body (Mena et al., 1999). CVB3 was shown to replicate in several *in vitro* cell lines including Raji (B cell), Jurkat (T cell) and U-937 (monocyte) (Hwang et al., 2012) implicating these cell types to possibly serve as viral shuttles into

the CNS. Poliovirus was shown to infect monocytes (Freistadt et al., 1993; Freistadt and Eberle, 1996), EV71 was able to replicate in CD14+ cells (Wang J. et al., 2013), dendritic cells (Lin et al., 2009) and PBMCs (Wongsa et al., 2019) while echoviruses (1, 7, 8, and 9) replicated in mature dendritic cells isolated from PBMCs but not monocytes (Kramer et al., 2007). Although a wide range of circulating immune cells are susceptible to diverse enteroviruses, further studies are needed to assess the extent of viral invasion into the CNS by utilizing immune cells as shuttles.

Another possible mechanism of neuroinvasion is through the direct infection of natural barriers that encase the brain and spinal cord. The blood-brain barrier (BBB) functions to restrict entry of large molecules as well as cells and pathogens into the brain from the circulatory system. Similarly, the choroid plexus found in each of the four ventricles of the brain controls the production of CSF and serves as the blood-cerebrospinal fluid barrier (BCSFB), preventing passage of most pathogens into the brain while permitting the delivery of nutrients and removal of metabolic wastes. The BCSFB is a site of CNS immune surveillance, providing a more permissive barrier for immune cells to traverse, while the BBB is more resistant to the movement of both host cells and invasive pathogens (Ransohoff and Engelhardt, 2012). Some pathogens appear to be limited to crossing only the BBB, while others are able to traverse both the BBB and BCSFB by using various mechanisms (Dahm et al., 2016). Both CVB3 (Puccini et al., 2014) and echovirus 30 (Schneider et al., 2012) are able to directly infect the BCSFB. Intracranial infection of CVB3 into newborn mice revealed the presence of viral RNA in the choroid plexus (Feuer et al., 2003). Similarly, echovirus 30 was found to directly infect BCSFB cells from both the apical and basolateral membranes without compromising barrier integrity as demonstrated using human choroid plexus papilloma cells *in vitro* (Schneider et al., 2012). However, echovirus 30 infection of the barrier did not stimulate T cell migration into the CSF which is typically observed during enteroviral meningitis (Lucht et al., 1992) indicating that other factors are required to initiate this immune response. In turn, poliovirus can infect human brain microvascular endothelial cells, an *in vitro* model of the BBB, which would permit the shed of progeny virus into the brain and/or damage the barrier by lysing the endothelia (Coyné et al., 2007). Overall, these studies demonstrate that once EV virions are found within the blood they can induce lytic and non-lytic mechanisms by which to cross these barriers to reach the CNS.

One important factor in CNS invasion is the generation of genetic variants, otherwise known as quasispecies, which are produced during viral replication (Rhoades et al., 2011). Enteroviruses have a relatively low fidelity RNA-dependent RNA polymerase compared to eukaryotic hosts or DNA viruses (Ward and Flanagan, 1992) and high-fidelity polymerase has been correlated with decreased poliovirus fitness under selective pressure (Pfeiffer and Kirkegaard, 2005). The production of viral quasispecies was shown to be an important component for poliovirus neuroinvasion. This was demonstrated by infecting mice with a poliovirus isolate (G64S) containing a high-fidelity polymerase which made the isolate less neuroinvasive than its wild-type counterpart (Vignuzzi et al., 2006). The

neurotropism and pathogenesis of the G64S poliovirus isolate was restored when chemical mutagenesis was employed to create quasispecies before inoculating into the animal model (Vignuzzi et al., 2006). This data showed that genetic diversity produced during enterovirus replication seems to induce neuroinvasive capabilities. However, selective pressures within the host plus potential bottlenecks naturally restrict viral spread throughout the body. To identify potential bottlenecks, four restriction-enzyme tagged poliovirus strains of equivalent fitness were inoculated into mice. The authors found only a subset of these strains within mouse brain, suggesting the existence of a bottleneck between the site of inoculation and brain tissue (Pfeiffer and Kirkegaard, 2006). This bottleneck was overcome by inoculating with high viral titers, indicating that the bottleneck is not a physical barrier but an immunological one. The authors suggested that once the founder virus reached the brain an antiviral state was initiated resulting in a “burned-bridge” phenomenon that limited subsequent virus strains from entering the CNS (Pfeiffer and Kirkegaard, 2006). This phenomenon was recently observed in clinical isolates of EV-A71 infected specimens where diverse number of quasispecies was detected in the respiratory and digestive samples while a dominant haplotype mutation in the VP1 region emerged in isolates collected from the CNS (Huang et al., 2017). This haplotype conferred enhanced growth and fitness in human neuronal cells (Huang et al., 2017). Further characterization of quasispecies generated at different biological sites during mild and severe cases of neurological disease would be valuable to identify the EV haplotypes that confers neuroinvasion.

## ENTEROVIRUS TROPISM WITHIN THE NERVOUS SYSTEM

Clinical observations and animal models have revealed lesions within the CNS that indicate unique tissue tropisms for different enteroviruses. Poliovirus primarily affects the anterior horns of gray matter in the spinal cord, which are composed of motor neurons innervating skeletal muscle (Jubelt et al., 1980; Brown et al., 1987). Poliovirus receptors are highly expressed in synaptosomes and the neuromuscular junctions provide the most accessible sites outside the CNS for poliovirus binding (Brown et al., 1987). Similarly, EV-D68 damages motor neurons of the anterior horn in the spinal cord and brain stem leading to lesions visible on the MRI within these structures (Knoester et al., 2019). EV-D68-induced paralytic myelitis animal model further revealed that virus was present within motor neurons of the anterior horn of the spinal cord segments that corresponded to the paralyzed limbs (Hixon et al., 2017). In contrast, EV-A71 is associated with extensive lesions that were previously detected within the brainstem, pons, medulla, cerebellum, cortex, thalamus, dentate nuclei and cerebrum (Shieh et al., 2001; Nagata et al., 2002; Kao et al., 2004; Yu et al., 2014). The reason for such diverse tropism by EV-A71 remains largely unknown. However, encephalitis of the midbrain, pons and medulla occurs in 62% of patients with neurological complications during EV-A71 infection (Wang et al., 1999) and, due to the role of the brainstem

in autonomic regulation, encephalitis of this anatomical region is typically associated with pulmonary edema and fluctuating blood pressure (Liao et al., 2015). In terms of CVs, a mouse model designed to imitate neonatal CVB3 infections found lesions in the hippocampus and cortex, although viral RNA was detected throughout the brain (Wang et al., 2014). The choroid plexus and subventricular zone, a site of neurogenesis, were found to contain CVB3 viral proteins in another animal model; a pathology that is further supported by *in vitro* studies showing susceptibility of neural progenitor cells to CVB3 (Puccini et al., 2014). Infection of these neuroprogenitor cells may represent developmental abnormalities seen as a result of CV infection (Feuer et al., 2005). A neonatal mouse model of CVB5 revealed the presence of viral antigen and necrosis of neurons within the cerebral cortex and the entire spinal cord in addition to necrosis of hindlimb muscles and cardiomyocytes (Mao et al., 2018). These studies highlight the diverse neurotropism exhibited by enteroviruses which help explain some of the neurological symptoms.

## CNS CELL TYPES SUSCEPTIBLE TO ENTEROVIRUSES

The interplay between EV infected cells and host response is crucial to understand the progression of neurological disease. As each cell type within the CNS would invoke a slightly different response upon infection, identifying which cell type is susceptible to which EV species will provide additional clues as to the progression of CNS disease development. To date, numerous studies using animal models and *in vitro* cultures not only confirmed the neurotropic ability of numerous enteroviruses but also revealed that these viruses readily infect neuronal progenitors, mature neurons and glia cells such as astrocytes. For example, both EV-A71 and CVB3 were detected in undifferentiated neuronal progenitor cells after intraperitoneal inoculation of virus into a neonatal animal model (Huang et al., 2014; Puccini et al., 2014). In tissue culture models, EV-A71 and CVA16 infected human mature neuroblastoma cell line (SK-N-SH) and caused necrosis (Yogarajah et al., 2017b; Yu et al., 2017). Similarly, neurotropic EV-D68 strains post 2014 outbreak were able to infect and replicate in the human neuroblastoma cell line (SH-SY5Y) and human postnatal cortical neuron cultures as compared to the non-neurotropic strains (Brown et al., 2018). The authors found that only a single round of viral replication occurred from transfecting pre-2014 outbreak viral RNA into neuroblastoma cells suggesting that viral entry into the cell was the primary neurotropic factor (Brown et al., 2018). In support of this observation, a recent study using chimeras revealed that cellular and tissue tropism of EVs as well as acid sensitivity is dependent on the viral capsid protein (Royston et al., 2018). Specifically, the authors used EV-D68 (respiratory isolate) that was unable to replicate in human neuroblastoma cells (SH-SY5Y) or neuronal tissues and EV-D94 (gastrointestinal isolate) which was able to replicate in both models to high titers. When the authors generated an enteroviral chimera that expressed the capsid protein of EV-D68 and the rest of the virus was derived from EV-D94, the ability to infect neuronal cells and tissues

was abrogated and the chimeric virus exhibited the same acid sensitivity and cellular tropism as EV-D68 (Royston et al., 2018). It is therefore not surprising that primary mouse hippocampal neurons expressing the human CD155 receptor were susceptible to poliovirus infection (Daley et al., 2005). A recent study found that EV-D68 strains from pre and post 2014 outbreak infected and replicated in spinal motor neurons differentiated from human-derived induced-pluripotent stem cells (iPSC) (Hixon et al., 2019a). Interestingly, infection of motor neuron-like mouse cells (NSC-34) by EV-A71 produced a strain-dependent, non-lytic infection that released viable viral particles from the cell via autophagy (Too et al., 2016). These studies reinforce the diverse neurological manifestation observed in EV infections.

Additional host factors are likely important for mediating neuropathogenicity based on a recent study showing that not all post-2014 outbreak EV strains caused neurological disease in mice (Hixon et al., 2017). This premise is further supported by recent work using mouse organotypic brain slice cultures. Both pre- and post-2014 outbreak EV-D68 strains were able to infect and replicate within these cultures, suggesting that the neurotropic potential was not a recently acquired phenotype (Rosenfeld et al., 2019). Instead, the authors propose that the immune response is responsible for modulating neuroinvasive properties of EV-D68 (Rosenfeld et al., 2019). Recently, EV-A71 infected adult mice containing a humanized immune system where not only susceptible to a clinical isolate of EV-A71 but recapitulated clinical symptoms and histopathology of disease such that the viral antigen was detected throughout the spinal cord and several regions within the CNS (Ke et al., 2019). As wild-type mice were resistant to EV-A71 infection, this study further reinforces the critical role the immune response plays in establishing neurological disease.

Astrocytes are the most abundant cell type within the human brain (Volterra and Meldolesi, 2005) and perform numerous diverse roles. These cells support the function of endothelial cells that make up the BBB, provide nutrients and metabolize neurotransmitters for use by neurons and play a role in CNS repair after injury (Pascual et al., 2005). In terms of EV infections, tissue culture models of astrocytes are permissive to numerous enterovirus strains including EV-A71, CVA9, CVB3, CVB4 and EV-D68 (Kwon et al., 2004; Tung et al., 2010; Haolong et al., 2013; Zeng et al., 2013; Du et al., 2014; Wang C. et al., 2015; Rosenfeld et al., 2019). In fatal cases of EV-A71, the viral antigen was detected by histology within neurons and astrocytes (Yan et al., 2000; Yu et al., 2014). Similarly, post-mortem brain tissues from patients with confirmed EV-A71 infection and brain tissue from a non-human primate model of EV-A71 revealed that more than 80% of EV-A71 antigen was detected in astrocytes (Feng et al., 2016). As EV-D68 infected hiPSC derived astrocytes produced 2x more virus within 24 h post infection than 3 days post infection in neurons (Rosenfeld et al., 2019), it suggests that glia may be important for rapid viral propagation within the CNS. Further *in vitro* functional studies identified that EV-A71 infected astrocyte cultures released pro-inflammatory cytokine IL-6 which increased secretion of excitatory neurotransmitters in bystander neurons that could have profound consequences on neuronal function (Feng et al., 2016) and immune response within

the CNS. Collectively, this data highlights the important role astrocytes play in the development of neurological complications observed during EV infection. Additional studies are highly warranted to assess the impact of enterovirus-infected glial cells on neurological disease.

## RECEPTORS FOR NEUROTROPIC ENTEROVIRUSES

One important determinant of viral tropism is the expression of the viral-specific receptor(s) on the cell surface. Ever since CD155 was first identified in 1989 as the poliovirus receptor (Mendelsohn et al., 1989), the extracellular receptors for many different enteroviruses have been uncovered. These studies made clear that enteroviruses can use a wide array of receptors and attachment factors for cell entry (Table 2). For example, EV-A71 is known to bind to 2 receptors and several potential attachment factors, which reflects its ability to infect different cell types. Scavenger receptor B2 (SCARB2) (Yamayoshi et al., 2009) is expressed in human neurons and glial cells (Jiao et al., 2014) and EV-A71 infection of a transgenic mouse model expressing human SCARB2 caused ataxia, paralysis and death of the animals (Fujii et al., 2013). Another EV-A71 receptor called human P-selectin glycoprotein ligand-1 (PSGL-1) is expressed primarily on leukocytes and is bound by select EV-A71 strains (Nishimura et al., 2009). Additional attachment molecules that enhance viral infectivity and contribute to viral dissemination and neurotropism include heparan sulfate glycosaminoglycans (HS) (Tan et al., 2013), sialic acid (Yang et al., 2009), annexin II (Yang et al., 2011), nucleolin (Su et al., 2015), vimentin (Du et al., 2014) and heat shock protein 70 (Xu et al., 2019) among others (reviewed in Owino and Chu, 2019). Other receptors utilized by enteroviruses for cell entry that may contribute to neuropathogenicity include the decay-accelerating factor (DAF or CD55, part of the complement cascade) used by CVA21, echovirus 6 and echovirus 11 (Shafren et al., 1997; Lea et al., 1998; Renois et al., 2011) or Coxsackievirus and Adenovirus Receptor (CAR), which is the main entry receptor for Coxsackie B viruses (Martino et al., 2000). Significantly, CD55 is expressed on neurons within the gastrointestinal system and glia within the CNS tissue (Gelderman et al., 2004), while CAR is abundantly expressed in the brain, with highest expression levels observed in newborn mice (Honda et al., 2000). Specifically within the motor neuron cell line NSC-34, infection by EV-A71 was found to rely on the surface expressed Prohibitin (PHB), suggesting that the virus uses this protein as a receptor for entry into motor neurons (Too et al., 2018). Additional studies are necessary to determine if this is a cell type and viral strain specific receptor. In turn, EV-D68 was primarily found to depend on sialic acid for entry which allowed subsequent viral uncoating (Liu et al., 2015) and facilitated genome release into the cytoplasm. Sialic acid-mediated viral entry was also documented for other enteroviruses such as EV-D70 (Alexander and Dimock, 2002; Nokhbeh et al., 2005), EV-A71 (Yang et al., 2009; Su et al., 2012) and CVA24 (Nilsson et al., 2008). Recent neuronal-specific

**TABLE 2 |** Receptors used by neurotropic enteroviruses for cell entry.

Virus	Receptor	Reference
CVA16	PSGL-1; SCARB2	Yamayoshi et al., 2009, 2012; Nishimura and Shimizu, 2012
CVA21	CD55; ICAM-1	Shafren et al., 1997
CVA7	SCARB2	Yamayoshi et al., 2012
CVA9	$\alpha$ V $\beta$ 3, $\alpha$ V $\beta$ 6 integrins	Harvala et al., 2003
CVB1 to CVB6	CAR	Bergelson et al., 1997; Carson et al., 1997
CVB1 and CVB5	CD55	Shafren et al., 1995
Echovirus 5	Heparan sulfate; FcRn	Israelsson et al., 2010; Morosky et al., 2019
Echovirus 6	CD55; Heparan sulfate; FcRn	Goodfellow et al., 2001; Renois et al., 2011; Morosky et al., 2019
Echovirus 9	$\alpha$ V $\beta$ 3 integrin, FcRn	Ylipaasto et al., 2010; Morosky et al., 2019
Echovirus 11	CD55; FcRn	Lea et al., 1998
EV-A71	PSGL-1; SCARB2; sialic acid	Yamayoshi et al., 2009; Su et al., 2012
EV-D68	ICAM-5	Wei et al., 2016
Poliovirus	CD155	Mendelsohn et al., 1989; He et al., 2000

studies revealed that cleavage of the sialic acid receptor prevented infection of human motor neurons derived from iPSCs by only the pre-2014 outbreak EV-D68 strains while post-2014 strains were unimpeded, suggesting that contemporary EV-D68 strains used another neuronal-specific receptor for cell entry (Hixon et al., 2019a).

The intracellular adhesion molecule 5 (ICAM-5) was identified to facilitate infection by contemporary EV-D68 in otherwise non-permissive Vero cells following a sialic-acid independent mechanism (Wei et al., 2016). Although this receptor is abundantly expressed in neurons (Gahmberg et al., 2008) and shows promise for neuronal-specific tropism of neurotropic enteroviruses, the pattern of EV-D68 infection in brain slice models and microfluidic chamber motor neuron cultures does not correspond to the distribution or expression of ICAM-5 (Hixon et al., 2019a). In fact, ICAM-5 expression in human iPSC-derived motor neuron-like cells was observed within the soma and dendrites while EV-D68 viral particles were observed on the axon terminals (Hixon et al., 2019b). Furthermore, ICAM-5 was not detected in neonatal mouse spinal cords where EV-D68 is preferentially found (Hixon et al., 2019b). It is possible that a homolog to ICAM-5 is the true neuronal-specific receptor for EV-D68 (Hixon et al., 2019b).

An important factor to consider in neuropathogenicity is that EVs can gain the use of additional receptors through adaptation during replication. Receptor adaptation has been well documented for numerous enteroviruses (reviewed in Cagno et al., 2019), highlighting their inherent potential for invading the CNS as a result of adaptation. For example, a non-synonymous single amino acid change within the VP1 region of EV-A71 was identified in isolates obtained from the blood and CSF samples of an immunocompromised host as compared to respiratory

specimens (Cordey et al., 2012). This mutation improved viral growth in neuroblastoma cells (SH-SY5Y) (Cordey et al., 2012; Tseligka et al., 2018) due to the virus gaining the ability to bind to HS on the cell surface (Tseligka et al., 2018). Similarly, EV-D68 infection of RD cells resulted in mutations located within the VP1 and VP2 regions that allowed the virus to not only bind the sialic acid receptor but also sulfated glycosaminoglycans for entry (Baggen et al., 2019). Despite our knowledge of these receptors and attachment factors, it is still unclear why neurotropic EVs localize more commonly to certain regions of the CNS (Lee, 2016).

## CELLULAR MECHANISMS OF ENTEROVIRUS NEUROPATHOGENICITY

The extensive phenotypic diversity of enteroviruses has prevented the development of a universal vaccine or therapeutic to combat these diseases. Identification of possible common cellular mechanisms that are involved in EV infection, specifically within the nervous system, would provide unprecedented strides into devising a potential pantropic antiviral therapeutic strategy. In several studies, EV replication within neurons reached lower viral titers over a longer incubation period than in non-neuronal cells, implicating intrinsic cell-specific host factors that contribute to viral pathogenicity (Daley et al., 2005; Yogarajah et al., 2017b). Here we will briefly highlight some of the main host-virus interactions identified for neurotropic enteroviruses and their potential impact on neuropathogenicity. Examples of host factors involved in viral entry and replication, immune response and cell death will be further discussed.

### Host Factors Involved in Enterovirus Entry and Replication

Viral entry and replication rely heavily on numerous host factors and are fundamental processes dictating the success of a viral infection (Figure 1). Many studies have identified host factors that are critical for EV propagation (reviewed in Owino and Chu, 2019). However, much of this work was performed on non-neuronal cell types which have shown little overlap between the deregulated host proteins identified during EV infected motor neurons (Too et al., 2018), reinforcing the need to verify the role of these host factors in CNS relevant models.

Once the EV invades the host cell, the viral genome needs to escape from the endosome prior to degradation in a process called uncoating. The EV genome is released from the endosome by the formation of pores within the membrane which allow the genome to be translocated into the cytoplasm (Strauss et al., 2013; Panjwani et al., 2014). This process is typically initiated in the presence of either low pH within the endosome or triggered by viral binding to a receptor. For example, poliovirus and CVB3 require binding to their receptors for uncoating while EV-A71 also needs an acidic endosome (Hussain et al., 2011). This uncoating process promotes the conversion of the viral genome into an alternate state which favors membrane interaction (Tuthill et al., 2006) and expedites viral replication and protein translation. One host factor implicated in viral

uncoating is a lipid modifying enzyme called PLA2G16. The importance of this host factor was demonstrated when HeLa cells expressing enzymatically inactive PLA2G16 were resistant to EV infection and mice deficient in this gene were largely resistant to developing paralysis and succumbing to infection by CVA4 or CVA10 (Staring et al., 2017). The authors found that during viral entry, the pore-activated process which results in the degradation of the viral particles also initiates recruitment of the phospholipase PLA2G16 that allows for the release of the viral genome into the cytoplasm (Staring et al., 2017). This host factor was recently found to have pan-enteroviral properties for EVs that bind to sialic acid receptors for entry (Baggen et al., 2019). However, certain EVs using the sulfated glycosaminoglycans (sGAGs) for viral entry can be independent of PLA2G16 (Baggen et al., 2019).

As the positive-sense RNA genome enters the cytoplasm, replication primarily occurs on rearranged membranous structures termed replication organelles (ROs) that originate at the endoplasmic reticulum and then the *trans*-Golgi network as observed for CVB3 infection of Vero E6 cells (Melia et al., 2019). However, infection of motor neurons by EV-A71 showed that viral replication occurred on the mitochondrial membrane (Too et al., 2018) and further studies are warranted to identify if this is a neuronal-specific mechanism. In general, enteroviruses enrich these membranes with both lipids and cholesterol to facilitate the formation of ROs, which are essential for viral replication (Hsu et al., 2010; van der Schaar et al., 2013; Arita, 2014; Roulin et al., 2014; Strating et al., 2015). This is mediated by the viral protein 3A indirectly recruiting host factor PI4KB (Greninger et al., 2012). In fact, the 3A proteins of several enteroviral species including EV-A, -B, -C and -D recruit the host factor ACBD3 that serves to not only recruit PI4KB but also scaffolds other viral and host proteins for proper RO formation (Lyoo et al., 2019). However, biogenesis of ROs are not essential to the initiation of viral replication since viral replication still occurred in cells when RO formation was delayed (Melia et al., 2017). Another host factor critical for viral RNA replication is the methyltransferase SET domain containing 3 (SETD3) (Diep et al., 2019). The authors showed that the cytosolic form of the actin histidine methyltransferase SETD3 interacts with the viral 2A protease from multiple enteroviral species including EV-D68, EV-A71 and CVA10 and this interaction was important for viral RNA replication (Diep et al., 2019). Animals with *Setd3*<sup>-/-</sup> were completely resistant to EV viral infection when injected intracranially or intramuscularly (Diep et al., 2019), supporting the necessity of usurping these mechanisms by EVs within the CNS.

Another major phase of viral replication is viral protein translation. Several host factors are important in mediating translation of the viral polyprotein by associating with the internal ribosome entry site (IRES) located within the 5' untranslated region (5' UTR) of the viral genome. Mutations within the 5' UTR were shown to modulate neurovirulence of poliovirus (De Jesus et al., 2005), EV-A71 (Yeh et al., 2011) and CVA16 (Li et al., 2016). A recent study using transcriptomic analysis showed that CVA16 but not EV-A71 infected neuroblastoma cell line SK-N-SH induced the expression

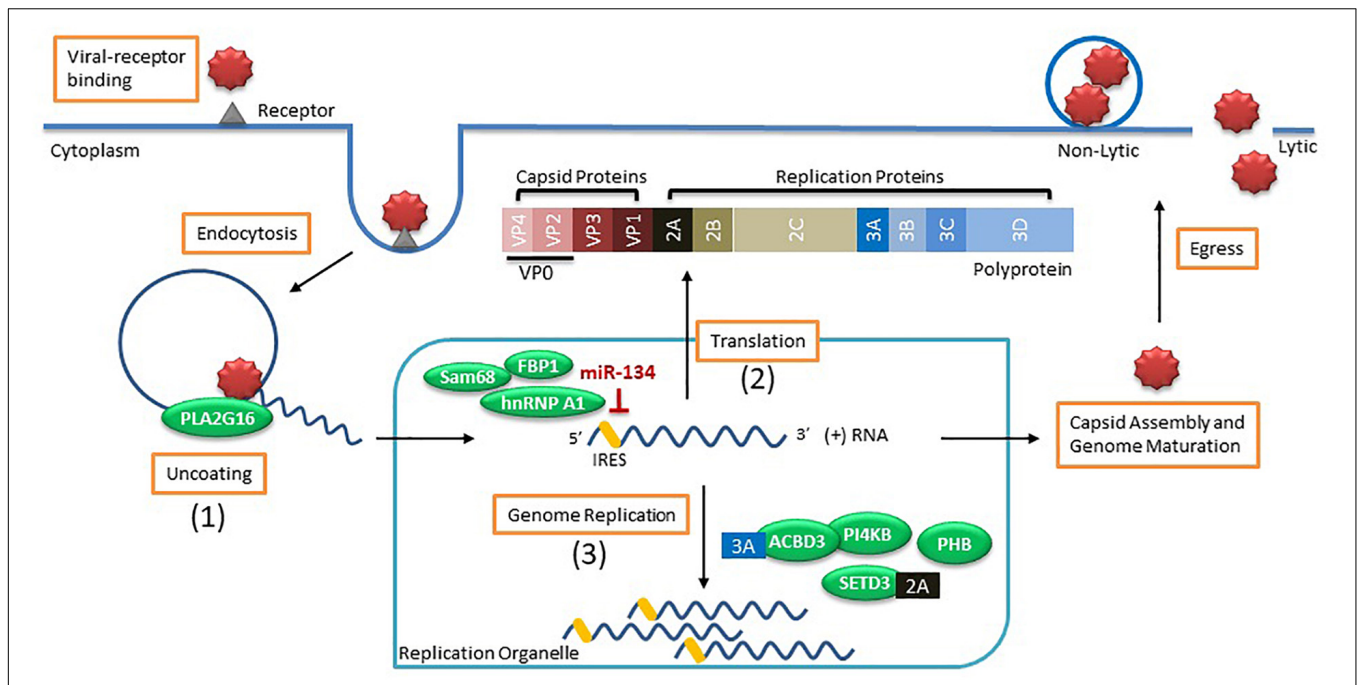


**FIGURE 1 |** Enterovirus life cycle and the host factors involved in viral entry and replication. Viral entry occurs by binding to the receptor (i.e., sialic acid) on the cell surface to induce endocytosis. Once virus is within an endosome, the host factor **(1)** PLA2G16 is recruited during pore formation and mediates viral uncoating allowing the positive sense (+) viral RNA genome to enter the cytoplasm. The viral genome associates with a replication organelle where **(2)** several host factors (i.e., Sam68, hnRNP A1, and FBP1) are recruited and bind to the IRES to promote translation of the viral genome using the cap-independent process while miR-134 binding to IRES inhibits protein translation. The generated polyprotein is cleaved into capsid proteins and replication proteins. Viral replication takes place on the membranes of replication organelles where several **(3)** host factors (i.e., ACBD3, PI4KB, SETD3, and PHB) along with viral proteins (i.e., 2A and 3A) are involved in genome replication. Capsid proteins self-assemble and genome maturation occurs which leads to viral egress using either lytic or non-lytic methods processes.

of an interferon stimulated gene (ISG) called RSAD2 (Yogarajah et al., 2018). The authors found that differences within the 5' UTR structures were the reason for this neuronal-specific modulation of RSAD2 (Yogarajah et al., 2018). Certain host proteins function as internal ribosome entry sites transacting factors (ITAFs) that help recruit ribosomes to the IRES. The heterogenous nuclear ribonucleoprotein (hnRNP) A1 was found to bind to the IRES of EV-A71 (Levengood et al., 2013) and induce a conformational change that enhanced viral protein translation (Tolbert et al., 2017). Similar positive effects by other ITAFs such as FBP2 (Huang et al., 2011) and Sam68 (Zhang et al., 2015) were observed in EV-A71 protein translation. In turn, some host factors were identified to inhibit viral protein translation. A recent study found that miR-134 binds to the IRES of Sabin 1 but not Sabin 2 poliovirus, causing degradation and modest inhibition of viral titer (Bakre et al., 2017). This miRNA binding site was conserved across other enteroviruses, such as EV-A71, indicating a universal regulation of viral replication within the host cell (Bakre et al., 2017). MiRNA expression is highly tissue-specific where miR-134 is readily expressed in the brain (Huang et al., 2015) and tissue tropism effects, such as viral inhibition or propagation, due to miRNAs were reported for numerous viruses (Orr-Burks et al., 2017). During viral infection, even modest effects may provide the necessary edge required for inhibited viral dissemination, prevention of fatal infections or providing sufficient restriction

on viral replication for effective viral clearance by the immune response. However, the tropism of enteroviruses is not dictated solely by the IRES-5'UTR sequence. A study using recombinant human adenoviruses to express IRES of wild-type and Sabin 3 polioviruses as well as CVB3 revealed that infecting animals with these viral constructs resulted in viral protein translation in many organs, including sites where wild-type virus was unable to normally replicate (Kauder and Racaniello, 2004). The authors concluded that tropism of enteroviruses is likely not directly related to potential attenuation of IRES-mediated translation but rather occurs either upstream or downstream of this process (Kauder and Racaniello, 2004). Additional studies are needed to identify these tropism factors.

A recent publication identified a neuronal-specific host factor that was implicated in modulating EV-A71 neuropathogenesis in animals. The host factor prohibitin (PHB) was upregulated during EV-A71 infection of the motor neuron cell culture NSC-34 and found to contribute to not only binding of virions for cell entry but mediating viral scaffold formation on mitochondria (Too et al., 2018). Inhibiting PHB after viral infection using an anti-cancer drug Roc-A induced mitochondrial destabilization and reduced intracellular ATP which, in turn, hindered viral replication (Too et al., 2018). Inhibiting PHB in an animal model of EV-A71 neuropathogenesis caused a delay in the development of neurological symptoms, prolonged death of these animals and decreased viral load within the spinal cord and brain

(Too et al., 2018), highlighting the pro-viral role of the host factor PHB in neurons.

As Enteroviruses hijack the host cell they are able to manipulate the cell cycle progression to generate a favorable cellular environment for viral replication. EV-A71 and CVA16 infected RD cells stopped cell cycle in the S phase, mediated by the non-structural 3D viral protein (Yu et al., 2015). In contrast, both EV-D68 and CVA6 induces cell cycle arrest in the G0/G1 phase due to expression of non-structural 3C and 3D viral proteins and subsequent modulation of cyclins and cyclin-dependent kinases (Wang Z. Y. et al., 2017; Wang Z. et al., 2018). Interestingly, recent data suggests that the CVB3 viral capsid protein, VP1, induces cell cycle arrest in G1 phase by increasing the expression of heat shock protein 70 (Wang Y. et al., 2019). These studies revealed the diverse preference EVs have for a particular stage of the cell cycle but the reason for this preference remains elusive. In terms of the CNS, mature neurons stay in post-mitotic senescence (G0) but can re-enter the cell cycle under certain circumstances. However, these neurons induce a cell cycle checkpoint arrest at G1/S phase and slowly die: a process called “abortive cell cycle re-entry” (Frade and Ovejero-Benito, 2015). The restrictive growth conditions within neurons likely contributes to the observed tissue tropism of EVs where EV-D68 can replicate in mature neurons but shows hindered viral growth (Rosenfeld et al., 2019) while EV-A71 was preferentially detected within astrocytes (Feng et al., 2016).

## Immunological Mechanisms Evoked by Enterovirus During CNS Infection

The immune response is an essential defense mechanism that combats viral infections through initiating innate and adaptive immune responses. Tight control over the immune response within the CNS tissue is especially critical in mitigating deleterious “bystander” effects while combating the viral infection. Contrarily, enteroviruses need to possess effective immune countermeasures to successfully reach the CNS and cause disease. Numerous studies describe the host immune response to EV infection and subsequent viral evasion mechanisms (reviewed in Lei et al., 2016; Jin et al., 2018). The majority of this work investigated innate immune response using non-CNS *in vitro* cells and evaluation of these mechanisms within the CNS tissue remains to be thoroughly explored. However, local immune cells of the CNS, such as astrocytes and microglia, were found to be important in mediating protective immune responses as a result of viral infection (Hwang and Bergmann, 2018). Here we will discuss these host-virus interactions during activation of innate and adaptive immune responses in light of their relevance within the CNS.

### Innate Immune Response and Enterovirus Countermeasures

The innate immune response is the first line of defense against invading pathogens and numerous mechanisms are in place to detect and respond to such threats. All cells are equipped with unique proteins that function as sensors called pattern-recognition receptors (PRRs) which detect conserved parts of pathogens, termed Pathogen-Associated Molecular Patterns

(PAMPs), or molecules that are released by damaged cells called Damage-Associated Molecular Patterns (DAMPs) (reviewed in Amarante-Mendes et al., 2018). There are several classes of PRRs including Toll-like receptors (TLRs), retinoic acid-inducible gene I (RIG-I)-like receptors (RLRs) and NOD-like receptors (NLRs) that are stimulated during viral infections (Akira et al., 2006). Activation of these PRRs initiates a signaling cascade that induces secretion of type I IFNs and stimulates an antiviral environment within the infected and neighboring cells (Müller et al., 1994). The importance of type I IFNs in EV infection was observed when mice pretreated with type I IFN were protected from a fatal infection by EV-A71 and CVA16 (Yang et al., 2015; Sun et al., 2016). As the immune response contains numerous redundancies to effectively combat pathogens, the virus needs to circumvent these mechanisms to establish an effective CNS infection. Uncovering these immune evasion mechanisms is the first step to identify effective strategies that could protect the CNS from EV-induced neuropathogenicity.

Once the viral genome is released from the viral particle it is detected by membrane bound TLR3 (detects dsRNA) and TLR7 (detects ssRNA) sensors (Mohanty and Deshpande, 2013). A signaling cascade is initiated, activating the interferon regulator transcription factors IRF3 and IRF7 that subsequently induce expression of type I IFNs (i.e., IFN- $\alpha$ , IFN- $\beta$ ). This signaling cascade is transmitted through TIR domain-containing adaptor inducible beta interferon (TRIF) for TLR3 and mediated by MyD88 for TLR7. Type I IFN response is both virus and cell-type specific; for example, mice deficient in TLR3-TRIF had decreased survival after CVA16 infection and TRIF-mediated immunity was found to be indispensable for preventing viral entry and replication within the nervous system (Yang et al., 2015). In contrast to CVA16 infection, the TLR3-TRIF pathway had no effect on poliovirus entry into the spinal cord or brain tissue (Oshiumi et al., 2011; Abe et al., 2012) perhaps due to the mechanism that poliovirus uses for CNS invasion. Furthermore, TLR activation varied between poliovirus strains within the same neuroblastoma cell culture. Specifically, wild-type poliovirus infection of human neuroblastoma cells (SK-N-SH) delayed the innate immune response by decreasing expression of TLR3 and MDA5 for 8 h post infection (Mohanty and Deshpande, 2013). However, infection of SK-N-SH by vaccine attenuated Sabin poliovirus strain was adequately controlled by TLR7 mediated type I IFN response (Mohanty and Deshpande, 2013). These stark differences clearly contribute to enteroviral neuropathogenicity and require further study. Other enteroviruses including CVB1, CVB5, EV-A71 and CVA16 induced type I IFNs through activation of TLR7 (Chehadah and Alkhabbaz, 2013; Song et al., 2018). Further study of CVB3 infection revealed the upregulation of TRIM21, an intracellular protein that directs virions for degradation, which was necessary in mediating type I IFN (IFN- $\beta$ ) antiviral response through IRF3 (Liu et al., 2018). Viral spread to other tissues was observed in TRIM21 deficient mice, but the importance of this in terms of neuroinvasion remains unexplored (Liu et al., 2018). Enteroviruses were also found to induce an antiviral state in neighboring, non-infected cells. Induction of an antiviral immune state in non-infected cells is mediated by TLR9 detection of released DAMPs from virally infected cells. This was

observed for EV-A71 where an immune response was evoked in uninfected neighboring cells (Hsiao et al., 2014) as a mechanism to prevent viral spread and tissue damage. To circumvent these immune responses, EVs can influence the cell to induce autophagy which degrades the membrane bound TLR7 sensor (Song et al., 2018). Additionally, EV-A71 and EV-D68 cleave IRF7 by the viral protein 3C<sup>Pro</sup> (Lei et al., 2013; Xiang et al., 2016), which is also used by CVA16, CVA6 and EV-D68 to inhibit TLR3 mediated type I IFN signaling (Rui et al., 2017). Furthermore, EV-A71 expressed 2A protease downregulates the TLR3 (Chen et al., 2018) and subverts the type I IFN immune response.

Additional dsRNA sensors called RIG-I and MDA5, a member of RLR, can also detect diverse dsRNA molecules produced during viral replication and cause the induction of type I IFN stimulated genes (Kato et al., 2006). Once dsRNA is detected, these cytoplasmic sensors undergo a conformation change allowing them to associate with other proteins, including mitochondrial-associated signaling adaptor proteins (MAVS), which are required to trigger the expression of type I IFN and other inflammatory cytokines (Chen et al., 2018). Additionally, Lys 63-linked (K63-linked) polyubiquitination is required for RIG-I and MAD5 activation (reviewed in Cao, 2016; Lang et al., 2017). Poliovirus, CVB3, EV-A71, EV-D68, CVA16 and CVA6 can disrupt this host response using several redundant and sometimes common mechanisms. For instance, poliovirus, CVB3 and EV-A71 induces proteolytic degradation of MDA5 and MAVS through the viral 2A<sup>Pro</sup> while RIG-I cleavage occurs via 3C<sup>Pro</sup> (Lei et al., 2010; Wang B. et al., 2013; Feng et al., 2014). Significantly, animal studies revealed that MDA5 was important for preventing early CVB3 replication, but was not essential for inducing type I IFNs (Hühn et al., 2010). Additionally, the 3C<sup>Pro</sup> of CVB3 cleaved MAVS and TRIF further suppressing type I IFN response (Mukherjee et al., 2011). For EV-A71, tissue culture studies revealed that the viral RNA-dependent RNA-polymerase (3D<sup>Pol</sup>) and viral 3C<sup>Pro</sup> interacts with MDA5 and antagonizes the antiviral immune response (Kuo et al., 2013, 2019; Rui et al., 2017) in addition to inhibiting RIG-I ubiquitination by 3C<sup>Pro</sup> (Chen et al., 2016). These host-virus interactions were largely dependent on the type of virus, cell type and genetic background of the host (Francisco et al., 2019), further underlying the adaptive capabilities of enteroviruses and the need to study these viruses within CNS-relevant cells to better understand the development of neurological disease.

The production of NF- $\kappa$ B is an essential antiviral host defense important for stimulating numerous proinflammatory cytokines and chemokines (reviewed in Rahman and McFadden, 2011). Primary human astrocytes infected with CVB3 or CVB4 induced the expression of NF- $\kappa$ B and AP-1 transcription factors, which upregulates IL-8 and MCP-1 chemokine expression (Kwon et al., 2004). As these chemokines are potent chemoattractants, they may contribute to directing neutrophils and monocytes/macrophages to the site of infection within the CNS. Similarly, infection of astrocytoma cells by EV-A71 and CVA9 induced production of VCAM-1, IL-6 and IL-8 (Zhang et al., 2013), while IL-6 and IL-8 were upregulated in EV-A71 infected mouse primary astrocytes and human glioma cells (Wang H. et al., 2019). These studies suggest that EV

may evoke common proinflammatory mechanisms to signal cell mediated immunity to converge within the virally infected CNS. In fact, consistently elevated IL-6 levels were observed in an EV-A71 infection neonatal mouse model resulting in severe damage to numerous organs including the brain (Khong et al., 2012) pointing to EV infected astrocytes as contributors to CNS damage. Indeed, previous studies found elevated levels of IL-6 and IL-8 in CSF of EV-A71 positive patients with encephalitis or meningoencephalitis (Li et al., 2015; Liu et al., 2018) and expression of these cytokines may be due to viral infected astrocytes. In one study, CVB3 infection of astrocytoma cells resulted in a productive but non-cytopathic infection (Zhang et al., 2013) that could contribute to viral persistence *in vivo* within the CNS. To subvert chemokine and cytokine production, EV-A71 encoded 3C<sup>Pro</sup> cleaves the TAK1/TAB1/TAB2/TAB3 complex upstream of NF- $\kappa$ B activation (Lei et al., 2014) while the viral 2C<sup>Pro</sup> protein suppresses formation of the NK- $\kappa$ B heterodimer (Du et al., 2015). The 3C<sup>Pro</sup> viral protein expressed by CVA16, CVA6 and EV-D68 also abrogates production of NF- $\kappa$ B (Rui et al., 2017). As with other immune evasion strategies, enteroviruses are equipped with a multitude of redundant processes to inhibit immune function.

Once virus is detected by the host cell and type I IFNs are stimulated, these molecules phosphorylate STAT1 and STAT2 via the JAK-STAT pathway (Horvath, 2004). The phosphate forms of STAT1 and STAT2 interact and translocate into the cell nucleus where they bind to IFN-stimulated response elements (ISRE) and induce expression of IFN-stimulated genes (ISGs), initiating an antiviral state within the host cell (reviewed in Schindler et al., 2007). Recently, EV-A71 infected mouse primary astrocytes and human glioma cells induced expression of STAT3 which interfered with STAT1 entry into the nucleus, inhibiting the production of ISGs and thereby the type I IFN-mediated antiviral response (Wang H. et al., 2019). In non-neuronal cells, this process was inhibited via blocking nuclear entry of phosphorylated STAT1/2 by degrading the nuclear transport receptor for STAT1/2 called KPNA1 (Wang C. et al., 2017). This downregulation was mediated via caspase-3 induced degradation (Wang C. et al., 2017), which was similarly observed in EV-A71 infected primary mouse astrocytes with identification of an additional layer of type I IFN regulation. The authors found that not only did EV-A71 degrade the importin required for STAT1 translocation into the nucleus by upregulating caspase-3, but the upregulated STAT3 competed with STAT1 for KPNA1 (Wang H. et al., 2019). Furthermore, EV-A71 reduced the levels of interferon receptor 1 (IFNAR1) via the viral 2A protease activity which in turn blocked IFN-mediated phosphorylation of STAT1, STAT2, Jak1 and Tyk2 (Lu et al., 2012).

Type II IFN (IFN- $\gamma$ ) and Type III IFN (IFN lambda) responses are also important to combat EV infections. An initial *in vitro* study found that poliovirus titers were decreased within neuronal cultures after IFN- $\gamma$  induced a modest increase in Nitric Oxide (NO) production 3 days post treatment suggesting that IFN- $\gamma$  does have protective, albeit slight, antiviral effects in neurons (Komatsu et al., 1996). Similarly, protective effects of IFN- $\gamma$  were observed in an animal model challenged with a lethal strain of CVB3, where expression of IFN- $\gamma$  decreased

viral load, viral spread and tissue destruction (Henke et al., 2003). Similarly, IFN- $\gamma$  is needed to inhibit severe EV-A71 infection in mice (Wang L. C. et al., 2015). To counteract this immune response, EV-A71 encoded viral proteins 2A and 3D decreased phosphorylation of STAT1 at 2 different sites and thereby inhibited IRF1 transactivation of IFN- $\gamma$  (Wang L. C. et al., 2015). Type III IFN response (IFN lambda) was recently identified to play an important antiviral role on mucosal endothelial membranes. At the intestinal mucosa, type III IFN disrupted replication of CVB3 in primary human pancreatic endocrine cells (Lind et al., 2013), hepatocytes (Lind et al., 2014) and goblet cells from primary human intestinal epithelial monolayers (Good et al., 2019). However, the 2A<sup>pro</sup> viral protein encoded by CVB3 degraded TRIF and MAVS, inhibiting production of type III IFN (Lind et al., 2016). It remains to be determined if the same host-virus interactions occur at the endothelial barriers surrounding the brain and spinal cord.

### Adaptive Immune Response

The adaptive immune response is involved in clearing EVs by generating neutralizing antibodies and cell mediated responses while building a memory to protect the host from secondary exposure. However, little is known about the cellular adaptive immune response to most EVs, particularly regarding infection of the CNS tissue. We will briefly describe the main contributors of immunity which includes neutralizing antibodies, T cells and microglia and how these responses relate to EV infection of the CNS.

Neutralizing antibodies produced by B cells during EV infection help control viremia and therefore prevent viral dissemination to other organs and protect the host from subsequent infections. This process was well documented in patients who suffer from agammaglobulinemia and cannot produce antibodies. These individuals were found to have heightened susceptibility to EV infection and CNS invasion that caused chronic neuropathies (reviewed in Misbah et al., 1992). As infants and young children do not have fully developed immune systems, the lack of neutralizing antibodies is a proposed explanation for their enhanced susceptibility to enterovirus infections and subsequent complications (Wells and Coyne, 2019). Similarly, mice deficient in B cells were unable to clear the CVB3 viral infection (Mena et al., 1999). In certain circumstances, neutralizing antibodies against CV were found to exacerbate disease in part by mediating CV infection of monocytes/macrophages and lymphocytes and thereby aiding in dissemination of the virus throughout the body (Mena et al., 1999; Jarasch et al., 2007) in a process called antibody dependent enhancement (ADE) (reviewed by Sauter and Hober, 2009). Indeed, adult mice that were inoculated twice by CVB4 showed enhanced viral load in numerous organs including the brain and spinal cord (Elmastour et al., 2017).

Cellular immunity determines the outcome of an EV infection since no difference in neutralizing antibodies was observed between mild, severe and fatal cases of HFMD (Chang et al., 2007). The T cell response is important for effective

EV clearance from the host but causes damage to the CNS during invasion. To date, only a few studies investigated the adaptive immune response to EV infection. B cells, CD4+ and CD8+ T cells were detected within the CNS tissue of EV-A71 infected patient and mice (Lin et al., 2009). Although these cells were detected within the CNS, they did not cause damage to uninfected tissue but rather helped combat the infection (Lin et al., 2009). This contradicts the suspected contribution of lymphocytes detected within CSF/CNS tissue and the development of neuropathology in patients with fatal EV infections (Lum et al., 1998; Wang et al., 1999; Yan et al., 2000) warranting additional studies.

A neonatal mouse model of CVB3 infection revealed that microglia/macrophages were activated during the acute phase of infection in the CNS and were detected in the hippocampus, cortex, subventricular zones, lateral ventricles and meninges (Feuer et al., 2009). These cells were found to engulf virally infected cells within the CNS (Feuer et al., 2009). Furthermore, they can serve as antigen presenting cells that can stimulate activation of cellular immunity. However, infection by CVB3 almost completely inhibits the antigen presentation by the MHC class I pathway, effectively evading the CD8+ T cell immunity (Kemball et al., 2009). Additional studies are required to dissect the role of microglia during EV-induced CNS disease.

### Mechanisms of Neuronal Cell Death

Neuronal cell death can be triggered by viral replication or the host self-destruct mechanisms to minimize damage from viral infections. Most studies point to EV-induced cell death following either pyroptosis, apoptosis or autophagy pathways. Further work into the mechanism of cell death within CNS relevant models will help identify key pathways that EVs use to induce neuronal cell death and subsequent tissue damage.

#### Pyroptosis

Pyroptosis is a programmed cell death mechanism that is characterized by caspase-1 activation, followed by DNA breakages without laddering, cell swelling, plasma membrane rupture and release of intracellular pro-inflammatory cytokines from the cell (Adamczak et al., 2014; Cai et al., 2014). This form of cell death is evoked by intracellular pathogens, mainly bacteria, as a means of escaping the inflammatory response of the host (Fink and Cookson, 2006; Cunha and Zamboni, 2013). Pyroptosis has been observed in EV-A71 infected neuroblastoma cell lines (Yogarajah et al., 2017a; Zhu et al., 2018). The mechanism of EV induced pyroptosis was found to involve upregulation of a major inflammasome gene called AIM2, along with several AIM2-mediated pyroptosis-associated genes including caspase-1 causing a decrease in EV-A71 replication within neurons (Yogarajah et al., 2017a). Furthermore, authors confirmed increased AIM2 expression in neurons within the spinal cord and medulla from EV-A71 positive autopsy specimens (Yogarajah et al., 2017a). However, CVA16 infection of SK-N-SH cells did not induce AIM2-mediated pyroptosis but rather increased expression of radical S-adenosylmethionine containing domain 2 (RSAD2) which in turn decreased viral replication (Yogarajah et al., 2018). EVs are clearly able to trigger different

mechanisms of neuronal cell death that can have profound effects on disease progression.

### Apoptosis

Apoptosis is a non-lytic cell death pathway that is largely immunologically silent and can be used to limit viral replication with minimal activation of inflammatory responses. Apoptosis can be triggered within the cell via the intrinsic pathway as a result of cell stress or extrinsic due to external signals from other cells. Intrinsic activation of apoptosis is mediated by mitochondria releasing pro-caspase-9, which is cleaved into caspase-9 and then activates caspase-3 (Brentnall et al., 2013). Extrinsic apoptosis is induced through receptor binding of tumor necrosis factor, activating caspase-8 which then activates caspase-3 (Würstle et al., 2010). In either case, activated caspase-3 interferes with many cellular processes, including DNA repair, triggering apoptotic characteristics of nuclear condensation, cell shrinking and membrane blebbing (Chan et al., 2015). *In vitro* studies showed cleaved caspase-9 in neuroblastoma SK-N-SH and SH-SY5Y cells infected with EV-A71 and CVA-A16 (Chen T.C. et al., 2007; Chan et al., 2015; Bai et al., 2019). Apoptosis was also observed in CVB3 infected rat cortical neuron cultures (Joo et al., 2002).

### Autophagy

The process of autophagy is a conserved pathway for intracellular degradation, typically in the context of maintaining homeostasis for a multicellular organism. Macroautophagy is one of three distinct forms of autophagy and is used to degrade cytosolic proteins, damaged or superfluous organelles and intracellular pathogens (Nikoletopoulou et al., 2015). As microautophagy is the only form associated with enterovirus infection, all following references to autophagy specifically refer to macroautophagy. It can function as part of either an innate or an adaptive immune response to limit intracellular pathogen replication, such as by robbing an invading virus of cellular machinery. Some viruses have evolved mechanisms to inhibit autophagy pathways, while others have found ways to exploit the acidic lysosomal vesicles that cells use to denature and degrade proteins (Lai et al., 2016). In the context of enterovirus infection, autophagy is the process of virus-mediated cell death (Lai et al., 2016).

Autophagy is initiated through a double-walled isolation membrane called a phagophore that, when closed into a sealed vesicle, is referred to as an autophagosome (Nikoletopoulou et al., 2015). The autophagosome sometimes also fuses with an endosome, producing an amphisome. The autophagosome or amphisome then fuses with a lysosome, resulting in an autolysosome that hydrolyzes the contents of the inner membrane. Autophagy can be initiated through a range of mechanisms including starvation, oxidative stress, hypoxia, infection and organelle damage and can be highly cargo-selective (Johansen and Lamark, 2011). Autophagy serves as a tool to address a specific threat or damage including misfolded protein aggregates, mitochondrial damage or intracellular pathogens. Within the context of virus infection, autophagy is considered an antiviral mechanism to selectively degrade virions or

virus-coopted machinery in autolysosomes (Mohamud and Luo, 2019). Enteroviruses initiate infection through receptor-mediated endocytosis and subsequent escape from the endosome, amphisome or autophagosome (Mohamud and Luo, 2019). The receptors vary, as do the exact mechanisms of endocytosis, but the pathways of endocytosis and autophagy overlap through their shared use of amphisomes (Mohamud and Luo, 2019). One study found that single gene knockdown of any of several autophagy related-genes (Beclin-1, Atg12, Atg14, ATC16 or LC3) inhibited echovirus 7 viral RNA release following receptor binding but had no inhibition on CVB3 (Kim and Bergelson, 2014). While echovirus 7 internalization does not appear to rely on autophagosomes or amphisomes, broader pathways regulating membrane trafficking may be responsible for this difference (Kim and Bergelson, 2014). Notably, echovirus 7 uses clathrin-dependent endocytosis while CVB3 uses caveolin-dependent endocytosis, which can indicate why disruption of host autophagy proteins may impact viral escape from internalized vesicles (Mohamud and Luo, 2019).

The role of autophagic machinery in viral replication was evidenced by the increase in autophagosome production following infection and viral replication was inhibited when genes associated with autophagosome formation or maturation were deleted (Wong et al., 2008; Huang et al., 2009; Corona et al., 2018). However, much of this work was done using single gene deletion experiments which confounded the results as some autophagy proteins are known to have other functions that may impact viral replication through other pathways (Mohamud and Luo, 2019). For example, knockdown of autophagy proteins ATG13 and RB1CC1/FIP200 enhanced replication of EV-A71, CVA21 and CVB3, while deletion of other autophagy components that make up the ULK1/2 complex did not affect viral replication (Mauthe et al., 2016).

The exact mechanisms enteroviruses use to enhance cellular autophagy are unknown (Mohamud and Luo, 2019). The signaling cascade of starvation-induced autophagy uses AMP activated protein kinase (AMPK) and mTORC1 to activate autophagy initiating complexes, such as ULK1/2. Poliovirus-induced autophagy is independent of the ULK1 complex and mTORC1 activity and phosphorylation does not change during poliovirus infection (Corona Velazquez et al., 2018). Enteroviruses appear to employ multiple strategies to initiate autophagy independent of the traditional nutrient-sensing AMPKs. Enterovirus-infected cells show an accumulation of autophagosomes resulting from some combination of increased autophagosome synthesis and decreased autolysosome fusion (Mohamud and Luo, 2019). The rate of autophagy degradation is difficult to measure with confidence because the virus can impact host protein expression and degradation, either directly, such as through viral proteases, or indirectly by affecting host transcription and translation or disrupting degradation pathways (Mohamud and Luo, 2019).

Attempts to study autophagy flux by monitoring the cargo receptor SQSTM1/p62 have been undermined through the discovery that it is cleaved by viral protease 2A during poliovirus, EV-D68, CVB3 and human rhinovirus 1A (Corona et al., 2018).

SQSTM1/p62 and CALCOCO2/NDP52 bind enterovirus capsid protein VP1 to initiate autosome degradation of virions, the first-identified virophagy receptor (Mohamud et al., 2019). VP1 was demonstrated to undergo ubiquitination, possibly leading to ubiquitin-dependent degradation as a means of virophagy (Mohamud et al., 2019). Supporting the observation that CVB3 protease 2A cleaves SQSTM1/p62 to inhibit virophagy (Corona et al., 2018), CVB3 showed enhanced viral growth in SQSTM1/p62 knockdown HeLa cells while reduction of host CALCOCO2 inhibited viral growth (Mohamud et al., 2019). CVB3 protease 2A cleavage of SWSTM1 inhibits its ability to bind viral capsid while CALCOCO2, whether full length or cleaved by viral protease 3C, are functional at suppressing host type I IFN antiviral response by promoting autophagy of host MAVS (Mohamud et al., 2019). The role of autophagy in innate or adaptive immunity has been well described as autophagy can be triggered by PAMPs and DAMPs (Deretic et al., 2013). These responses are often activated in concert with endosomal TLRs to stimulate other responses, such as type I IFN (Deretic et al., 2013). Autophagy is also used to degrade pro-inflammatory signaling factors, which suggests that autophagy contributes to controlling inflammatory responses after pathogens are eliminated; if autophagic clearance is insufficient to address the threat then inflammation can trigger a systemic response (Deretic et al., 2013). Cleverly, enteroviruses are able to use autophagy machinery to propagate within cytoplasmic vesicles, which can conceal them from adaptive immune surveillance and be used as vehicles for non-lytic release from the cell (Corona et al., 2018). EV-D68 is able to manipulate soluble *N*-ethylmaleimide-sensitive factor attachment receptor (SNARE) proteins to inhibit autophagosome-lysosome fusion, diverting vesicles from degradative autophagy to secretory autophagy, leading to exocytosis and vesicle fusion with the plasma membrane (Corona et al., 2018).

Autophagy is a transcriptionally regulated process (Di Malta et al., 2019) and is sensitive to the transcriptional dysregulation and inhibition caused by enterovirus infection. Post-translational regulation through autophagy proteins provides finer control of these mechanisms but some of these proteins, such as SQSTM1/p62 and CALCOCO2/NDP52, have been shown to interact with enterovirus proteins or to be targeted by enterovirus proteases (Mohamud et al., 2019). Because autophagy functions as a housekeeper in neurons, there is a basal level of autophagy in healthy cells and increases or decreases in autophagy flux correlate with neurodegeneration (Lee, 2012). As a result, EV-induced dysregulation of host autophagy can have a directly deleterious effect on cells due to the loss of autophagy's normal protective functions (Xi et al., 2013). Neurons are post-mitotic cells that are more prone to the accumulation of toxic metabolic byproducts than dividing cells, which experience higher regeneration of cytoplasm and organelles (Lee, 2012; Meng et al., 2019). Because of the high energy demands of the brain, neurons are sensitive to starvation, which is known to initiate autophagy through the mammalian target of rapamycin (mTOR) pathway (Heras-Sandoval et al., 2019). Conversely, inhibition of autophagy has been shown to cause neurodegeneration in mice (Komatsu et al., 2006) while knockout

of autophagy genes in mice showed a range of neurodefective phenotypes; autophagy was also impaired in glial cells but the role of autophagy in glia and the effects of its impairment have not been explored sufficiently at this time to draw any conclusions (Nikoletopoulou et al., 2015).

## CONCLUDING REMARKS

A growing number of Enteroviruses are associated with life-threatening neurological diseases including encephalitis, meningitis and AFM. The lack of an effective treatment for non-polio enteroviruses underscores the vital need for better understanding of their neuropathogenesis.

Despite extensive studies that have uncovered many important aspects of EV infection of the CNS and resulting pathogenesis, much still remains to be learned with respect to mechanisms of EV neuroinvasion, neurotropism and molecular pathogenicity upon viral entry into the CNS. For example, neurotropic EVs can recognize a diverse range of receptors and attachment factors for cell entry, however, the location of these receptors within CNS tissue are yet to be correlated with observed pathology and clinical symptom manifestation. Although molecular mechanisms of viral-host interaction in terms of innate immunity are well documented, the extent of this interaction in CNS relevant cell-types are mainly understudied. Recent studies have implicated the immune response to be an essential component of EV neuropathogenicity, further emphasizing the need to characterize these immune-specific mechanisms. In terms of viral neurotropism, all tested neurotropic EVs were capable of infecting neurons and/or glia cells but viral propagation was found to be largely dependent on viral strain, cell type and genetics of the host. Further studies are therefore needed to delineate these parameters and identify intrinsic host factors that are key for viral entry and replication within CNS-relevant cell-types. Considering that viral life-cycle is dependent on a multitude of host factors, identifying and characterizing these essential elements will provide inroads into designing novel treatments to abrogate EV infection of the CNS.

## AUTHOR CONTRIBUTIONS

AnM and AIM conceptualized the review, performed the literature search, and prepared the manuscript. TB provided the critical input and revisions for the manuscript.

## FUNDING

This work was supported by the Public Health Agency of Canada.

## ACKNOWLEDGMENTS

We would like to thank Elsie Grudeski for her helpful discussion and useful suggestions.

## REFERENCES

- Abe, Y., Fujii, K., Nagata, N., Takeuchi, O., Akira, S., Oshiumi, H., et al. (2012). The toll-like receptor 3-mediated antiviral response is important for protection against poliovirus infection in poliovirus receptor transgenic mice. *J. Virol.* 86, 185–194. doi: 10.1128/JVI.05245-5211
- Adamczak, S. E., de Rivero Vaccari, J. P., Dale, G., Brand, F. J., Nonner, D., Bullock, M. R., et al. (2014). Pyroptotic neuronal cell death mediated by the AIM2 inflammasome. *J. Cereb. Blood Flow Metab.* 34, 621–629. doi: 10.1038/jcbfm.2013.236
- Akira, S., Uematsu, S., and Takeuchi, O. (2006). Pathogen recognition and innate immunity. *Cell* 124, 783–801. doi: 10.1016/j.cell.2006.02.015
- Alexander, D. A., and Dimock, K. (2002). Sialic acid functions in enterovirus 70 binding and infection. *J. Virol.* 76, 11265–11272. doi: 10.1128/jvi.76.22.11265-11272.2002
- Amarante-Mendes, G. P., Adjemian, S., Branco, L. M., Zanetti, L. C., Weinlich, R., and Bortoluci, K. R. (2018). Pattern recognition receptors and the host cell death molecular machinery. *Front. Immunol.* 9:2379. doi: 10.3389/fimmu.2018.02379
- Arita, M. (2014). Phosphatidylinositol-4 kinase III beta and oxysterol-binding protein accumulate unesterified cholesterol on poliovirus-induced membrane structure. *Microbiol. Immunol.* 58, 239–256. doi: 10.1111/1348-0421.12144
- Avellón, A., Rubio, G., Palacios, G., Casas, I., Rabella, N., Reina, G., et al. (2006). Enterovirus 75 and aseptic meningitis, Spain, 2005. *Emerg. Infect. Dis.* 12, 1609–1611. doi: 10.3201/eid1210.060353
- Baggen, J., Liu, Y., Lyoo, H., van Vliet, A. L. W., Wahedi, M., de Bruin, J. W., et al. (2019). Bypassing pan-enterovirus host factor PLA2G16. *Nat. Commun.* 10:3171. doi: 10.1038/s41467-019-11256-z
- Bai, J., Chen, X., Liu, Q., Zhou, X., and Long, J. E. (2019). Characteristics of enterovirus 71-induced cell death and genome scanning to identify viral genes involved in virus-induced cell apoptosis. *Virus Res.* 265, 104–114. doi: 10.1016/j.virusres.2019.03.017
- Bakre, A. A., Shim, B. S., and Tripp, R. A. (2017). MicroRNA-134 regulates poliovirus replication by IRES targeting. *Sci. Rep.* 7:12664. doi: 10.1038/s41598-017-12860-z
- Baron, R. C., Hatch, M. H., Kleeman, K., and MacCormack, J. N. (1982). Aseptic meningitis among members of a high school football team. An outbreak associated with echovirus 16 infection. *JAMA* 248, 1724–1727. doi: 10.1001/jama.248.14.1724
- Bergelson, J. M., Cunningham, J. A., Droguett, G., Kurt-Jones, E. A., Krithivas, A., Hong, J. S., et al. (1997). Isolation of a common receptor for Coxsackie B viruses and adenoviruses 2 and 5. *Science* 275, 1320–1323. doi: 10.1126/science.275.5304.1320
- Bharucha, E. P., Mondkar, V. P., Wardia, N. H., Irani, P. F., and Katrak, S. M. (1972). Neurological complications of a new conjunctivitis. *Lancet* 2, 970–971. doi: 10.1016/s0140-6736(72)92492-92490
- Boyer, F. C., Tiffreau, V., Rapin, A., Laffont, I., Percebois-Macadré, L., Supper, C., et al. (2010). Post-polio syndrome: pathophysiological hypotheses, diagnosis criteria, drug therapy. *Ann. Phys. Rehabil. Med.* 53, 34–41. doi: 10.1016/j.rehab.2009.12.003
- Brentnall, M., Rodriguez-Menocal, L., De Guevara, R. L., Cepero, E., and Boise, L. H. (2013). Caspase-9, caspase-3 and caspase-7 have distinct roles during intrinsic apoptosis. *BMC Cell Biol.* 14:32. doi: 10.1186/1471-2121-14-32
- Brown, D. M., Hixon, A. M., Oldfield, L. M., Zhang, Y., Novotny, M., Wang, W., et al. (2018). Contemporary circulating enterovirus D68 strains have acquired the capacity for viral entry and replication in human neuronal cells. *mBio* 9:e01954-18. doi: 10.1128/mBio.01954-18
- Brown, R. H., Johnson, D., Ogonowski, M., and Weiner, H. L. (1987). Type 1 human poliovirus binds to human synaptosomes. *Ann. Neurol.* 21, 64–70. doi: 10.1002/ana.410210112
- Cagno, V., Tseligka, E. D., Jones, S. T., and Tapparel, C. (2019). Heparan sulfate proteoglycans and viral attachment: true receptors or adaptation bias. *Viruses* 11:E596. doi: 10.3390/v11070596
- Cai, Z., Jitkaew, S., Zhao, J., Chiang, H. C., Choksi, S., Liu, J., et al. (2014). Plasma membrane translocation of trimerized MLKL protein is required for TNF-induced necroptosis. *Nat. Cell Biol.* 16, 55–65. doi: 10.1038/ncb2883
- Cao, X. (2016). Self-regulation and cross-regulation of pattern-recognition receptor signalling in health and disease. *Nat. Rev. Immunol.* 16, 35–50. doi: 10.1038/nri.2015.8
- Carson, S. D., Chapman, N. N., and Tracy, S. M. (1997). Purification of the putative coxsackievirus B receptor from HeLa cells. *Biochem. Biophys. Res. Commun.* 233, 325–328. doi: 10.1006/bbrc.1997.6449
- Centers for Disease Control and Prevention, (2019). *Acute Flaccid Myelitis (AFM) 2018 Case Definition*. Available at: <https://www.cdc.gov/nndss/conditions/acute-flaccid-myelitis/case-definition/2018/> (accessed November 15, 2019).
- Chan, K. P., Goh, K. T., Chong, C. Y., Teo, E. S., Lau, G., and Ling, A. E. (2003). Epidemic hand, foot and mouth disease caused by human enterovirus 71, Singapore. *Emerg. Infect. Dis.* 9, 78–85. doi: 10.3201/eid0901.020112
- Chan, S. Y., Sam, I. C., Lai, J. K., and Chan, Y. F. (2015). Cellular proteome alterations in response to enterovirus 71 and coxsackievirus A16 infections in neuronal and intestinal cell lines. *J. Proteomics* 125, 121–130. doi: 10.1016/j.jpro.2015.05.016
- Chang, L. Y., Huang, L. M., Gau, S. S., Wu, Y. Y., Hsia, S. H., Fan, T. Y., et al. (2007). Neurodevelopment and cognition in children after enterovirus 71 infection. *N. Engl. J. Med.* 356, 1226–1234. doi: 10.1056/NEJMoa065954
- Chehadeh, W., and Alkhabbaz, M. (2013). Differential TLR7-mediated expression of proinflammatory and antiviral cytokines in response to laboratory and clinical enterovirus strains. *Virus Res.* 174, 88–94. doi: 10.1016/j.virusres.2013.03.006
- Chen, C. S., Yao, Y. C., Lin, S. C., Lee, Y. P., Wang, Y. F., Wang, J. R., et al. (2007). Retrograde axonal transport: a major transmission route of enterovirus 71 in mice. *J. Virol.* 81, 8996–9003. doi: 10.1128/JVI.00236-2007
- Chen, K. R., Yu, C. K., Kung, S. H., Chen, S. H., Chang, C. F., Ho, T. C., et al. (2018). Toll-like receptor 3 is involved in detection of enterovirus A71 infection and targeted by viral 2A protease. *Viruses* 10:E689. doi: 10.3390/v10120689
- Chen, N., Li, X., Li, P., Pan, Z., Ding, Y., Zou, D., et al. (2016). Enterovirus 71 inhibits cellular type I interferon signaling by inhibiting host RIG-I ubiquitination. *Microb. Pathog.* 100, 84–89. doi: 10.1016/j.micpath.2016.09.001
- Chen, P., Li, Y., Tao, Z., Wang, H., Lin, X., Liu, Y., et al. (2017). Evolutionary phylogeography and transmission pattern of echovirus 14: an exploration of spatiotemporal dynamics based on the 26-year acute flaccid paralysis surveillance in Shandong, China. *BMC Genomics* 18:48. doi: 10.1186/s12864-016-3418-3413
- Chen, T. C., Lai, Y. K., Yu, C. K., and Juang, J. L. (2007). Enterovirus 71 triggering of neuronal apoptosis through activation of Abl-Cdk5 signalling. *Cell. Microbiol.* 9, 2676–2688. doi: 10.1111/j.1462-5822.2007.00988.x
- Chiang, K. L., Wei, S. H., Fan, H. C., Chou, Y. K., and Yang, J. Y. (2019). Outbreak of recombinant coxsackievirus A2 infection and polio-like paralysis of children, Taiwan, 2014. *Pediatr. Neonatol.* 60, 95–99. doi: 10.1016/j.pedneo.2018.02.003
- Cho, S. M., MacDonald, S., and Frontera, J. A. (2017). Coxsackie B3/B4-related acute flaccid myelitis. *Neurocrit. Care* 27, 259–260. doi: 10.1007/s12028-017-0377-378
- Chonmaitree, T., Menegus, M. A., Schervish-Swierkosz, E. M., and Schwalenstocker, E. (1981). Enterovirus 71 infection: report of an outbreak with two cases of paralysis and a review of the literature. *Pediatrics* 67, 489–493.
- Chumakov, M., Voroshilova, M., Shindarov, L., Lavrova, I., Gracheva, L., Koroleva, G., et al. (1979). Enterovirus 71 isolated from cases of epidemic poliomyelitis-like disease in Bulgaria. *Arch. Virol.* 60, 329–340. doi: 10.1007/bf01317504
- Cordey, S., Petty, T. J., Schibler, M., Martinez, Y., Gerlach, D., van Belle, S., et al. (2012). Identification of site-specific adaptations conferring increased neural cell tropism during human enterovirus 71 infection. *PLoS Pathog.* 8:e1002826. doi: 10.1371/journal.ppat.1002826
- Corona, A. K., Saulsbery, H. M., Corona Velazquez, A. F., and Jackson, W. T. (2018). Enteroviruses remodel autophagic trafficking through regulation of host SNARE proteins to promote virus replication and cell exit. *Cell Rep.* 22, 3304–3314. doi: 10.1016/j.celrep.2018.03.003
- Corona Velazquez, A., Corona, A. K., Klein, K. A., and Jackson, W. T. (2018). Poliovirus induces autophagic signaling independent of the ULK1 complex. *Autophagy* 14, 1201–1213. doi: 10.1080/15548627.2018.1458805
- Coyne, C. B., Kim, K. S., and Bergelson, J. M. (2007). Poliovirus entry into human brain microvascular cells requires receptor-induced activation of SHP-2. *EMBO J.* 26, 4016–4028. doi: 10.1038/sj.emboj.7601831
- Cunha, L. D., and Zamboni, D. S. (2013). Subversion of inflammasome activation and pyroptosis by pathogenic bacteria. *Front. Cell Infect. Microbiol.* 3:76. doi: 10.3389/fcimb.2013.00076

- Dahm, T., Rudolph, H., Schwerk, C., Schrotten, H., and Tenenbaum, T. (2016). Neuroinvasion and inflammation in viral central nervous system infections. *Mediators Inflamm.* 2016:8562805. doi: 10.1155/2016/8562805
- Daley, J. K., Gechman, L. A., Skipworth, J., and Rall, G. F. (2005). Poliovirus replication and spread in primary neuron cultures. *Virology* 340, 10–20. doi: 10.1016/j.virol.2005.05.032
- Dalwai, A., Ahmad, S., Pacsa, A., and Al-Nakib, W. (2009). Echovirus type 9 is an important cause of viral encephalitis among infants and young children in Kuwait. *J. Clin. Virol.* 44, 48–51. doi: 10.1016/j.jcv.2008.10.007
- De Jesus, N., Franco, D., Paul, A., Wimmer, E., and Cello, J. (2005). Mutation of a single conserved nucleotide between the cloverleaf and internal ribosome entry site attenuates poliovirus neurovirulence. *J. Virol.* 79, 14235–14243. doi: 10.1128/JVI.79.22.14235-14243.2005
- Deretic, V., Saitoh, T., and Akira, S. (2013). Autophagy in infection, inflammation and immunity. *Nat. Rev. Immunol.* 13, 722–737. doi: 10.1038/nri3532
- Di Malta, C., Cinque, L., and Settembre, C. (2019). Transcriptional regulation of autophagy: mechanisms and diseases. *Front. Cell. Dev. Biol.* 7:114. doi: 10.3389/fcell.2019.00114
- Diep, J., Ooi, Y. S., Wilkinson, A. W., Peters, C. E., Foy, E., Johnson, J. R., et al. (2019). Enterovirus pathogenesis requires the host methyltransferase SETD3. *Nat. Microbiol.* 4, 2523–2537. doi: 10.1038/s41564-019-0551-551
- Du, H., Yin, P., Yang, X., Zhang, L., Jin, Q., and Zhu, G. (2015). Enterovirus 71 2C protein inhibits NF- $\kappa$ B activation by binding to RelA(p65). *Sci. Rep.* 5:14302. doi: 10.1038/srep14302
- Du, N., Cong, H., Tian, H., Zhang, H., Zhang, W., Song, L., et al. (2014). Cell surface vimentin is an attachment receptor for enterovirus 71. *J. Virol.* 88, 5816–5833. doi: 10.1128/JVI.03826-3813
- Dumaidi, K., Frantzidou, F., Papa, A., Diza, E., and Antoniadis, A. (2006). Enterovirus meningitis in Greece from 2003–2005: diagnosis, CSF laboratory findings, and clinical manifestations. *J. Clin. Lab. Anal.* 20, 177–183. doi: 10.1002/jcla.20129
- Dyda, A., Stelzer-Braid, S., Adam, D., Chughtai, A. A., and MacIntyre, C. R. (2018). The association between acute flaccid myelitis (AFM) and Enterovirus D68 (EV-D68) - what is the evidence for causation. *Euro Surveill.* 23:17-00310. doi: 10.2807/1560-7917.ES.2018.23.3.17-00310
- Ehrenfeld, E., Domingo, E., and Roos, R. P. (2010). *The Picornaviruses*. Washington, DC: ASM Press.
- Elmastour, F., Jaïdane, H., Benkahla, M., Aguech-Oueslati, L., Sane, F., Halouani, A., et al. (2017). Anti-coxsackievirus B4 (CV-B4) enhancing activity of serum associated with increased viral load and pathology in mice reinfected with CV-B4. *Virulence* 8, 908–923. doi: 10.1080/21505594.2016.1252018
- Fatemi, Y., and Chakraborty, R. (2019). Acute flaccid myelitis: a clinical overview for 2019. *Mayo Clin. Proc.* 94, 875–881. doi: 10.1016/j.mayocp.2019.03.011
- Feng, M., Guo, S., Fan, S., Zeng, X., Zhang, Y., Liao, Y., et al. (2016). The preferential infection of astrocytes by enterovirus 71 plays a key role in the viral neurogenic pathogenesis. *Front. Cell. Infect. Microbiol.* 6:192. doi: 10.3389/fcimb.2016.00192
- Feng, Q., Langereis, M. A., Lork, M., Nguyen, M., Hato, S. V., Lanke, K., et al. (2014). Enterovirus 2Apro targets MDA5 and MAVS in infected cells. *J. Virol.* 88, 3369–3378. doi: 10.1128/JVI.02712-2713
- Feuer, R., Mena, I., Pagarigan, R. R., Harkins, S., Hassett, D. E., and Whitton, J. L. (2003). Coxsackievirus B3 and the neonatal CNS: the roles of stem cells, developing neurons, and apoptosis in infection, viral dissemination, and disease. *Am. J. Pathol.* 163, 1379–1393. doi: 10.1016/S0002-9440(10)63496-63497
- Feuer, R., Pagarigan, R. R., Harkins, S., Liu, F., Hunziker, I. P., and Whitton, J. L. (2005). Coxsackievirus targets proliferating neuronal progenitor cells in the neonatal CNS. *J. Neurosci.* 25, 2434–2444. doi: 10.1523/JNEUROSCI.4517-04.2005
- Feuer, R., Ruller, C. M., An, N., Tabor-Godwin, J. M., Rhoades, R. E., Maciejewski, S., et al. (2009). Viral persistence and chronic immunopathology in the adult central nervous system following Coxsackievirus infection during the neonatal period. *J. Virol.* 83, 9356–9369. doi: 10.1128/JVI.02382-2387
- Fink, S. L., and Cookson, B. T. (2006). Caspase-1-dependent pore formation during pyroptosis leads to osmotic lysis of infected host macrophages. *Cell. Microbiol.* 8, 1812–1825. doi: 10.1111/j.1462-5822.2006.00751.x
- Frade, J. M., and Ovejero-Benito, M. C. (2015). Neuronal cell cycle: the neuron itself and its circumstances. *Cell Cycle* 14, 712–720. doi: 10.1080/15384101.2015.1004937
- Francisco, E., Suthar, M., Gale, M., Rosenfeld, A. B., and Racaniello, V. R. (2019). Cell-type specificity and functional redundancy of RIG-I-like receptors in innate immune sensing of Coxsackievirus B3 and encephalomyocarditis virus. *Virology* 528, 7–18. doi: 10.1016/j.virol.2018.12.003
- Freistadt, M. S., and Eberle, K. E. (1996). Correlation between poliovirus type 1 Mahoney replication in blood cells and neurovirulence. *J. Virol.* 70, 6486–6492. doi: 10.1128/jvi.70.9.6486-6492.1996
- Freistadt, M. S., Fleit, H. B., and Wimmer, E. (1993). Poliovirus receptor on human blood cells: a possible extraneural site of poliovirus replication. *Virology* 195, 798–803. doi: 10.1006/viro.1993.1433
- Fujii, K., Nagata, N., Sato, Y., Ong, K. C., Wong, K. T., Yamayoshi, S., et al. (2013). Transgenic mouse model for the study of enterovirus 71 neuropathogenesis. *Proc. Natl. Acad. Sci. U.S.A.* 110, 14753–14758. doi: 10.1073/pnas.1217563110
- Gahmberg, C. G., Tian, L., Ning, L., and Nyman-Huttunen, H. (2008). ICAM-5—a novel two-faceted adhesion molecule in the mammalian brain. *Immunol. Lett.* 117, 131–135. doi: 10.1016/j.imlet.2008.02.004
- Gear, J. H. (1984). Nonpolio causes of polio-like paralytic syndromes. *Rev. Infect. Dis.* 6(Suppl. 2), S379–S384. doi: 10.1093/clinids/6.supplement\_2.s379
- Gelderman, K. A., Zijlmans, H. J., Vonk, M. J., and Gorter, A. (2004). CD55 expression patterns on intestinal neuronal tissue are divergent from the brain. *Gut* 53, 507–513. doi: 10.1136/gut.2003.026773
- Geller, T. J., and Condie, D. (1995). A case of protracted coxsackie virus meningoencephalitis in a marginally immunodeficient child treated successfully with intravenous immunoglobulin. *J. Neurol. Sci.* 129, 131–133. doi: 10.1016/0022-510x(94)00261-1
- Gill, P. J., Bitnun, A., and Yeh, E. A. (2018). Acute flaccid myelitis. *CMAJ* 190:E1418. doi: 10.1503/cmaj.181442
- Gilsdorf, J. R. (2019). Acute flaccid myelitis: lessons from polio. *J. Pediatr. Infect. Dis. Soc.* 8, 550–553. doi: 10.1093/jpids/piz017
- Good, C., Wells, A. I., and Coyne, C. B. (2019). Type III interferon signaling restricts enterovirus 71 infection of goblet cells. *Sci. Adv.* 5:eau4255. doi: 10.1126/sciadv.aau4255
- Goodfellow, I. G., Siofay, A. B., Powell, R. M., and Evans, D. J. (2001). Echoviruses bind heparan sulfate at the cell surface. *J. Virol.* 75, 4918–4921. doi: 10.1128/JVI.75.10.4918-4921.2001
- Goto, K., Sanefuji, M., Kusuhara, K., Nishimura, Y., Shimizu, H., Kira, R., et al. (2009). Rhombencephalitis and coxsackievirus A16. *Emerg. Infect. Dis.* 15, 1689–1691. doi: 10.3201/eid1510.090594
- Greninger, A. L., Knudsen, G. M., Betegon, M., Burlingame, A. L., and Derisi, J. L. (2012). The 3A protein from multiple picornaviruses utilizes the golgi adaptor protein ACBD3 to recruit PI4KIII $\beta$ . *J. Virol.* 86, 3605–3616. doi: 10.1128/JVI.06778-6711
- Grimwood, K., Huang, Q. S., Sadleir, L. G., Nix, W. A., Kilpatrick, D. R., Oberste, M. S., et al. (2003). Acute flaccid paralysis from echovirus type 33 infection. *J. Clin. Microbiol.* 41, 2230–2232. doi: 10.1128/jcm.41.5.2230-2232.2003
- Gromeier, M., and Wimmer, E. (1998). Mechanism of injury-provoked poliomyelitis. *J. Virol.* 72, 5056–5060. doi: 10.1128/jvi.72.6.5056-5060.1998
- Han, J., Ma, X. J., Wan, J. F., Liu, Y. H., Han, Y. L., Chen, C., et al. (2010). Long persistence of EV71 specific nucleotides in respiratory and feces samples of the patients with Hand-Foot-Mouth Disease after recovery. *BMC Infect. Dis.* 10:178. doi: 10.1186/1471-2334-10-178
- Haolong, C., Du, N., Hongchao, T., Yang, Y., Wei, Z., Hua, Z., et al. (2013). Enterovirus 71 VP1 activates calmodulin-dependent protein kinase II and results in the rearrangement of vimentin in human astrocyte cells. *PLoS One* 8:e73900. doi: 10.1371/journal.pone.0073900
- Hart, R. J., and Miller, D. L. (1973). Echovirus-17 infections in Britain 1969–71. *Lancet* 2, 661–664. doi: 10.1016/s0140-6736(73)92491-92494
- Harvala, H., Kalimo, H., Stanway, G., and Hyypä, T. (2003). Pathogenesis of coxsackievirus A9 in mice: role of the viral arginine-glycine-aspartic acid motif. *J. Gen. Virol.* 84, 2375–2379. doi: 10.1099/vir.0.19246-19240
- Hasbun, R., Wootton, S. H., Rosenthal, N., Balada-Llasat, J. M., Chung, J., Duff, S., et al. (2019). Epidemiology of meningitis and encephalitis in infants and children in the United States, 2011–2014. *Pediatr. Infect. Dis. J.* 38, 37–41. doi: 10.1097/INF.0000000000002081

- He, Y., Bowman, V. D., Mueller, S., Bator, C. M., Bella, J., Peng, X., et al. (2000). Interaction of the poliovirus receptor with poliovirus. *Proc. Natl. Acad. Sci. U.S.A.* 97, 79–84. doi: 10.1073/pnas.97.1.79
- Helfferich, J., Knoester, M., Van Leer-Buter, C. C., Neuteboom, R. F., Meiners, L. C., Niesters, H. G., et al. (2019). Acute flaccid myelitis and enterovirus D68: lessons from the past and present. *Eur. J. Pediatr.* 178, 1305–1315. doi: 10.1007/s00431-019-03435-3433
- Henke, A., Zell, R., Martin, U., and Stelzner, A. (2003). Direct interferon-gamma-mediated protection caused by a recombinant coxsackievirus B3. *Virology* 315, 335–344. doi: 10.1016/s0042-6822(03)00538-535
- Heras-Sandoval, D., Pérez-Rojas, J. M., and Pedraza-Chaverri, J. (2019). Novel compounds for the modulation of mTOR and autophagy to treat neurodegenerative diseases. *Cell. Signal.* 65:109442. doi: 10.1016/j.cellsig.2019.109442
- Hixon, A. M., Clarke, P., and Tyler, K. L. (2019a). Contemporary circulating enterovirus D68 strains infect and undergo retrograde axonal transport in spinal motor neurons independent of sialic acid. *J. Virol.* 93:e00578-19. doi: 10.1128/JVI.00578-19
- Hixon, A. M., Frost, J., Rudy, M. J., Messacar, K., Clarke, P., and Tyler, K. L. (2019b). Understanding enterovirus D68-induced neurologic disease: a basic science review. *Viruses* 11:E821. doi: 10.3390/v11090821
- Hixon, A. M., Yu, G., Leser, J. S., Yagi, S., Clarke, P., Chiu, C. Y., et al. (2017). A mouse model of paralytic myelitis caused by enterovirus D68. *PLoS Pathog.* 13:e1006199. doi: 10.1371/journal.ppat.1006199
- Honda, T., Saitoh, H., Masuko, M., Katagiri-Abe, T., Tominaga, K., Kozakai, I., et al. (2000). The coxsackievirus-adenovirus receptor protein as a cell adhesion molecule in the developing mouse brain. *Brain Res. Mol. Brain Res.* 77, 19–28. doi: 10.1016/s0169-328x(00)00036-x
- Horstmann, D. M. (1949). Clinical aspects of acute poliomyelitis. *Am. J. Med.* 6, 592–605. doi: 10.1016/0002-9343(49)90132-1
- Horvath, C. M. (2004). The Jak-STAT pathway stimulated by interferon alpha or interferon beta. *Sci. STKE* 2004:tr10. doi: 10.1126/stke.2602004tr10
- Hovden, I. A., and Pfeiffer, H. C. (2015). Electrodiagnostic findings in acute flaccid myelitis related to enterovirus D68. *Muscle Nerve* 52, 909–910. doi: 10.1002/mus.24738
- Howard, R. S. (2005). Poliomyelitis and the postpolio syndrome. *BMJ* 330, 1314–1318. doi: 10.1136/bmj.330.7503.1314
- Hsiao, H. B., Chou, A. H., Lin, S. I., Chen, I. H., Lien, S. P., Liu, C. C., et al. (2014). Toll-like receptor 9-mediated protection of enterovirus 71 infection in mice is due to the release of danger-associated molecular patterns. *J. Virol.* 88, 11658–11670. doi: 10.1128/JVI.00867-14
- Hsu, N. Y., Ilnytska, O., Belov, G., Santiana, M., Chen, Y. H., Takvorian, P. M., et al. (2010). Viral reorganization of the secretory pathway generates distinct organelles for RNA replication. *Cell* 141, 799–811. doi: 10.1016/j.cell.2010.03.050
- Huang, H. I., Lin, J. Y., Chen, H. H., Yeh, S. B., Kuo, R. L., Weng, K. F., et al. (2014). Enterovirus 71 infects brain-derived neural progenitor cells. *Virology* 468–470, 592–600. doi: 10.1016/j.virol.2014.09.017
- Huang, H. I., and Shih, S. R. (2015). Neurotropic enterovirus infections in the central nervous system. *Viruses* 7, 6051–6066. doi: 10.3390/v7112920
- Huang, P. N., Lin, J. Y., Locker, N., Kung, Y. A., Hung, C. T., Lin, J. Y., et al. (2011). Far upstream element binding protein 1 binds the internal ribosomal entry site of enterovirus 71 and enhances viral translation and viral growth. *Nucleic Acids Res.* 39, 9633–9648. doi: 10.1093/nar/gkr682
- Huang, S. C., Chang, C. L., Wang, P. S., Tsai, Y., and Liu, H. S. (2009). Enterovirus 71-induced autophagy detected in vitro and in vivo promotes viral replication. *J. Med. Virol.* 81, 1241–1252. doi: 10.1002/jmv.21502
- Huang, S. W., Huang, Y. H., Tsai, H. P., Kuo, P. H., Wang, S. M., Liu, C. C., et al. (2017). A selective bottleneck shapes the evolutionary mutant spectra of enterovirus A71 during viral dissemination in humans. *J. Virol.* 91:e01062-17. doi: 10.1128/JVI.01062-17
- Huang, W., Liu, X., Cao, J., Meng, F., Li, M., Chen, B., et al. (2015). miR-134 regulates ischemia/reperfusion injury-induced neuronal cell death by regulating CREB signaling. *J. Mol. Neurosci.* 55, 821–829. doi: 10.1007/s12031-014-0434-4340
- Hühn, M. H., McCartney, S. A., Lind, K., Svedin, E., Colonna, M., and Flodström-Tullberg, M. (2010). Melanoma differentiation-associated protein-5 (MDA-5) limits early viral replication but is not essential for the induction of type 1 interferons after Coxsackievirus infection. *Virology* 401, 42–48. doi: 10.1016/j.virol.2010.02.010
- Hussain, K. M., Leong, K. L., Ng, M. M., and Chu, J. J. (2011). The essential role of clathrin-mediated endocytosis in the infectious entry of human enterovirus 71. *J. Biol. Chem.* 286, 309–321. doi: 10.1074/jbc.M110.168468
- Hwang, J. Y., Jun, E. J., Seo, I., Won, M., Ahn, J., Kim, Y. K., et al. (2012). Characterization of infections of human leukocytes by non-polio enteroviruses. *Intervirology* 55, 333–341. doi: 10.1159/000329987
- Hwang, M., and Bergmann, C. C. (2018). Alpha/Beta interferon (IFN- $\alpha/\beta$ ) signaling in astrocytes mediates protection against viral encephalomyelitis and regulates IFN- $\gamma$ -dependent responses. *J. Virol.* 92, e1901–e1917. doi: 10.1128/JVI.01901-1917
- Israelsson, S., Gullberg, M., Jonsson, N., Roivainen, M., Edman, K., and Lindberg, A. M. (2010). Studies of echovirus 5 interactions with the cell surface: heparan sulfate mediates attachment to the host cell. *Virus Res.* 151, 170–176. doi: 10.1016/j.virusres.2010.05.001
- Jain, S., Patel, B., and Bhatt, G. C. (2014). Enteroviral encephalitis in children: clinical features, pathophysiology, and treatment advances. *Pathog. Glob. Health* 108, 216–222. doi: 10.1179/204773214Y.0000000145
- Jarasch, N., Martin, U., Zell, R., Wutzler, P., and Henke, A. (2007). Influence of pan-caspase inhibitors on coxsackievirus B3-infected CD19+ B lymphocytes. *Apoptosis* 12, 1633–1643. doi: 10.1007/s10495-007-0084-86
- Jiao, X. Y., Guo, L., Huang, D. Y., Chang, X. L., and Qiu, Q. C. (2014). Distribution of EV71 receptors SCARB2 and PSGL-1 in human tissues. *Virus Res.* 190, 40–52. doi: 10.1016/j.virusres.2014.05.007
- Jin, Y., Zhang, R., Wu, W., and Duan, G. (2018). Innate immunity evasion by enteroviruses linked to epidemic hand-foot-mouth disease. *Front. Microbiol.* 9:2422. doi: 10.3389/fmicb.2018.02422
- Johansen, T., and Lamark, T. (2011). Selective autophagy mediated by autophagic adapter proteins. *Autophagy* 7, 279–296. doi: 10.4161/auto.7.3.14487
- Joo, C. H., Kim, Y. K., Lee, H., Hong, H., Yoon, S. Y., and Kim, D. (2002). Coxsackievirus B4-induced neuronal apoptosis in rat cortical cultures. *Neurosci. Lett.* 326, 175–178. doi: 10.1016/s0304-3940(02)00340-343
- Jorba, J., Diop, O. M., Iber, J., Henderson, E., Zhao, K., Sutter, R. W., et al. (2018). Update on Vaccine-Derived Polioviruses - Worldwide, January 2017–June 2018. *MMWR Morb. Mortal. Wkly. Rep.* 67, 1189–1194. doi: 10.15585/mmwr.mm6742a5
- Jubelt, B., Gallez-Hawkins, G., Narayan, O., and Johnson, R. T. (1980). Pathogenesis of human poliovirus infection in mice. I. Clinical and pathological studies. *J. Neuropathol. Exp. Neurol.* 39, 138–148. doi: 10.1097/00005072-198003000-198003003
- Juntilla, N., Lévesque, N., Kabue, J. P., Cartet, G., Mushiya, F., Muyembe-Tamfum, J. J., et al. (2007). New enteroviruses, EV-93 and EV-94, associated with acute flaccid paralysis in the Democratic Republic of the Congo. *J. Med. Virol.* 79, 393–400. doi: 10.1002/jmv.20825
- Kao, S. J., Yang, F. L., Hsu, Y. H., and Chen, H. I. (2004). Mechanism of fulminant pulmonary edema caused by enterovirus 71. *Clin. Infect. Dis.* 38, 1784–1788. doi: 10.1086/421021
- Kato, H., Takeuchi, O., Sato, S., Yoneyama, M., Yamamoto, M., Matsui, K., et al. (2006). Differential roles of MDA5 and RIG-I helicases in the recognition of RNA viruses. *Nature* 441, 101–105. doi: 10.1038/nature04734
- Kauder, S. E., and Racaniello, V. R. (2004). Poliovirus tropism and attenuation are determined after internal ribosome entry. *J. Clin. Invest.* 113, 1743–1753. doi: 10.1172/JCI21323
- Ke, Y., Liu, W. N., Her, Z., Liu, M., Tan, S. Y., Tan, Y. W., et al. (2019). Enterovirus A71 infection activates human immune responses and induces pathological changes in humanized mice. *J. Virol.* 93:e01066-18. doi: 10.1128/JVI.01066-18
- Kelen, A. E., Lesiak, J. M., and Labzoffsky, N. A. (1964). sporadic occurrence of echo virus types 27 and 31 associated with aseptic meningitis in Ontario. *Can. Med. Assoc. J.* 91, 1266–1268.
- Kemball, C. C., Harkins, S., Whitmire, J. K., Flynn, C. T., Feuer, R., and Whitton, J. L. (2009). Coxsackievirus B3 inhibits antigen presentation in vivo, exerting a profound and selective effect on the MHC class I pathway. *PLoS Pathog.* 5:e1000618. doi: 10.1371/journal.ppat.1000618
- Khong, W. X., Yan, B., Yeo, H., Tan, E. L., Lee, J. J., Ng, J. K., et al. (2012). A non-mouse-adapted enterovirus 71 (EV71) strain exhibits neurotropism, causing

- neurological manifestations in a novel mouse model of EV71 infection. *J. Virol.* 86, 2121–2131. doi: 10.1128/JVI.06103-6111
- Kim, C., and Bergelson, J. M. (2014). Echovirus 7 entry into polarized caco-2 intestinal epithelial cells involves core components of the autophagy machinery. *J. Virol.* 88, 434–443. doi: 10.1128/JVI.02706-2713
- Kim, K. S. (2008). Mechanisms of microbial traversal of the blood-brain barrier. *Nat. Rev. Microbiol.* 6, 625–634. doi: 10.1038/nrmicro1952
- Klingman, J., Chui, H., Corgiat, M., and Perry, J. (1988). Functional recovery. A major risk factor for the development of postpoliomyelitis muscular atrophy. *Arch. Neurol.* 45, 645–647. doi: 10.1001/archneur.1988.00520300065020
- Knoester, M., Helfferich, J., Poelman, R., Van Leer-Buter, C., Brouwer, O. F., Niesters, H. G. M., et al. (2019). Twenty-nine cases of enterovirus-D68-associated acute flaccid myelitis in Europe 2016: a case series and epidemiologic overview. *Pediatr. Infect. Dis. J.* 38, 16–21. doi: 10.1097/INF.0000000000002188
- Komatsu, M., Waguri, S., Chiba, T., Murata, S., Iwata, J., Tanida, I., et al. (2006). Loss of autophagy in the central nervous system causes neurodegeneration in mice. *Nature* 441, 880–884. doi: 10.1038/nature04723
- Komatsu, T., Bi, Z., and Reiss, C. S. (1996). Interferon-gamma induced type I nitric oxide synthase activity inhibits viral replication in neurons. *J. Neuroimmunol.* 68, 101–108. doi: 10.1016/0165-5728(96)00083-85
- Koskineniemi, M., Rantalaiho, T., Piiparinen, H., von Bonsdorff, C. H., Färkkilä, M., Järvinen, A., et al. (2001). Infections of the central nervous system of suspected viral origin: a collaborative study from Finland. *J. Neurovirol.* 7, 400–408. doi: 10.1080/135502801753170255
- Kramer, M., Schulte, B. M., Toonen, L. W., de Bruijini, M. A., Galama, J. M., Adema, G. J., et al. (2007). Echovirus infection causes rapid loss-of-function and cell death in human dendritic cells. *Cell. Microbiol.* 9, 1507–1518. doi: 10.1111/j.1462-5822.2007.00888.x
- Kramer, R., Sabatier, M., Wirth, T., Pichon, M., Lina, B., Schuffenecker, I., et al. (2018). Molecular diversity and biennial circulation of enterovirus D68: a systematic screening study in Lyon, France, 2010 to 2016. *Euro Surveill.* 23:1700711. doi: 10.2807/1560-7917.ES.2018.23.37.1700711
- Kreuter, J. D., Barnes, A., McCarthy, J. E., Schwartzman, J. D., Oberste, M. S., Rhodes, C. H., et al. (2011). A fatal central nervous system enterovirus 68 infection. *Arch. Pathol. Lab. Med.* 135, 793–796. doi: 10.1043/2010-0174-CR.1
- Kumar, A., Shukla, D., Kumar, R., Idris, M. Z., Misra, U. K., and Dhole, T. N. (2011). An epidemic of encephalitis associated with human enterovirus B in Uttar Pradesh, India, 2008. *J. Clin. Virol.* 51, 142–145. doi: 10.1016/j.jcv.2011.02.011
- Kuo, R. L., Chen, C. J., Wang, R. Y. L., Huang, H. I., Lin, Y. H., Tam, E. H., et al. (2019). Role of enteroviral RNA-dependent RNA polymerase in regulation of MDA5-mediated beta interferon activation. *J. Virol.* 93:e00132-19. doi: 10.1128/JVI.00132-19
- Kuo, R. L., Kao, L. T., Lin, S. J., Wang, R. Y., and Shih, S. R. (2013). MDA5 plays a crucial role in enterovirus 71 RNA-mediated IRF3 activation. *PLoS One* 8:e63431. doi: 10.1371/journal.pone.0063431
- Kwon, D., Fuller, A. C., Palma, J. P., Choi, I. H., and Kim, B. S. (2004). Induction of chemokines in human astrocytes by picornavirus infection requires activation of both AP-1 and NF-kappa B. *Glia* 45, 287–296. doi: 10.1002/glia.10331
- Lai, J. K., Sam, I. C., and Chan, Y. F. (2016). The autophagic machinery in enterovirus infection. *Viruses* 8:E32. doi: 10.3390/v8020032
- Lancaster, K. Z., and Pfeiffer, J. K. (2010). Limited trafficking of a neurotropic virus through inefficient retrograde axonal transport and the type I interferon response. *PLoS Pathog.* 6:e1000791. doi: 10.1371/journal.ppat.1000791
- Lang, X., Tang, T., Jin, T., Ding, C., Zhou, R., and Jiang, W. (2017). TRIM65-catalyzed ubiquitination is essential for MDA5-mediated antiviral innate immunity. *J. Exp. Med.* 214, 459–473. doi: 10.1084/jem.20160592
- Lea, S. M., Powell, R. M., McKee, T., Evans, D. J., Brown, D., Stuart, D. I., et al. (1998). Determination of the affinity and kinetic constants for the interaction between the human virus echovirus 11 and its cellular receptor, CD55. *J. Biol. Chem.* 273, 30443–30447. doi: 10.1074/jbc.273.46.30443
- Lee, J. A. (2012). Neuronal autophagy: a housekeeper or a fighter in neuronal cell survival. *Exp. Neurobiol.* 21, 1–8. doi: 10.5607/en.2012.21.1.1
- Lee, K. Y. (2016). Enterovirus 71 infection and neurological complications. *Korean J. Pediatr.* 59, 395–401. doi: 10.3345/kjp.2016.59.10.395
- Lee, K. Y., Lee, Y. J., Kim, T. H., Cheon, D. S., and Nam, S. O. (2014). Clinicoradiological spectrum in enterovirus 71 infection involving the central nervous system in children. *J. Clin. Neurosci.* 21, 416–420. doi: 10.1016/j.jocn.2013.04.032
- Lei, X., Han, N., Xiao, X., Jin, Q., He, B., and Wang, J. (2014). Enterovirus 71 3C inhibits cytokine expression through cleavage of the TAK1/TAB1/TAB2/TAB3 complex. *J. Virol.* 88, 9830–9841. doi: 10.1128/JVI.01425-1414
- Lei, X., Liu, X., Ma, Y., Sun, Z., Yang, Y., Jin, Q., et al. (2010). The 3C protein of enterovirus 71 inhibits retinoid acid-inducible gene I-mediated interferon regulatory factor 3 activation and type I interferon responses. *J. Virol.* 84, 8051–8061. doi: 10.1128/JVI.02491-2499
- Lei, X., Xiao, X., and Wang, J. (2016). Innate immunity evasion by enteroviruses: insights into virus-host interaction. *Viruses* 8:E22. doi: 10.3390/v8010022
- Lei, X., Xiao, X., Xue, Q., Jin, Q., He, B., and Wang, J. (2013). Cleavage of interferon regulatory factor 7 by enterovirus 71 3C suppresses cellular responses. *J. Virol.* 87, 1690–1698. doi: 10.1128/JVI.01855-1812
- Levengood, J. D., Tolbert, M., Li, M. L., and Tolbert, B. S. (2013). High-affinity interaction of hnRNP A1 with conserved RNA structural elements is required for translation and replication of enterovirus 71. *RNA Biol.* 10, 1136–1145. doi: 10.4161/rna.25107
- Lewthwaite, P., Perera, D., Ooi, M. H., Last, A., Kumar, R., Desai, A., et al. (2010). Enterovirus 75 encephalitis in children, southern India. *Emerg. Infect. Dis.* 16, 1780–1782. doi: 10.3201/eid1611.100672
- Li, H., Li, S., Zheng, J., Cai, C., Ye, B., Yang, J., et al. (2015). Cerebrospinal fluid Th1/Th2 cytokine profiles in children with enterovirus 71-associated meningoencephalitis. *Microbiol. Immunol.* 59, 152–159. doi: 10.1111/1348-0421.12227
- Li, Z., Liu, X., Wang, S., Li, J., Hou, M., Liu, G., et al. (2016). Identification of a nucleotide in 5' untranslated region contributing to virus replication and virulence of Coxsackievirus A16. *Sci. Rep.* 6:20839. doi: 10.1038/srep20839
- Liao, Y. T., Wang, S. M., Wang, J. R., Yu, C. K., and Liu, C. C. (2015). Norepinephrine and epinephrine enhanced the infectivity of enterovirus 71. *PLoS One* 10:e0135154. doi: 10.1371/journal.pone.0135154
- Lin, K. H., and Lim, Y. W. (2005). Post-poliomyelitis syndrome: case report and review of the literature. *Ann. Acad. Med. Singap.* 34, 447–449.
- Lin, T. Y., Twu, S. J., Ho, M. S., Chang, L. Y., and Lee, C. Y. (2003). Enterovirus 71 outbreaks, Taiwan: occurrence and recognition. *Emerg. Infect. Dis.* 9, 291–293. doi: 10.3201/eid0903.020285
- Lin, Y. W., Wang, S. W., Tung, Y. Y., and Chen, S. H. (2009). Enterovirus 71 infection of human dendritic cells. *Exp. Biol. Med.* 234, 1166–1173. doi: 10.3181/0903-RM-116
- Lind, K., Richardson, S. J., Leete, P., Morgan, N. G., Korsgren, O., and Flodström-Tullberg, M. (2013). Induction of an antiviral state and attenuated coxsackievirus replication in type III interferon-treated primary human pancreatic islets. *J. Virol.* 87, 7646–7654. doi: 10.1128/JVI.03431-3412
- Lind, K., Svedin, E., Domsgen, E., Kapell, S., Laitinen, O. H., Moll, M., et al. (2016). Coxsackievirus counters the host innate immune response by blocking type III interferon expression. *J. Gen. Virol.* 97, 1368–1380. doi: 10.1099/jgv.0.000443
- Lind, K., Svedin, E., Utorova, R., Stone, V. M., and Flodström-Tullberg, M. (2014). Type III interferons are expressed by Coxsackievirus-infected human primary hepatocytes and regulate hepatocyte permissiveness to infection. *Clin. Exp. Immunol.* 177, 687–695. doi: 10.1111/cei.12368
- Liu, H., Li, M., Song, Y., and Xu, W. (2018). TRIM21 restricts coxsackievirus B3 replication, cardiac and pancreatic injury via interacting with MAVS and positively regulating IRF3-mediated Type-I interferon production. *Front. Immunol.* 9:2479. doi: 10.3389/fimmu.2018.02479
- Liu, Y., Sheng, J., Baggen, J., Meng, G., Xiao, C., Thibaut, H. J., et al. (2015). Sialic acid-dependent cell entry of human enterovirus D68. *Nat. Commun.* 6:8865. doi: 10.1038/ncomms9865
- Logotheti, M., Pogka, V., Horefti, E., Papadacos, K., Giannaki, M., Pangalis, A., et al. (2009). Laboratory investigation and phylogenetic analysis of enteroviruses involved in an aseptic meningitis outbreak in Greece during the summer of 2007. *J. Clin. Virol.* 46, 270–274. doi: 10.1016/j.jcv.2009.07.019
- Lopez, A., Lee, A., Guo, A., Konopka-Anstadt, J. L., Nisler, A., Rogers, S. L., et al. (2019). Vital signs: surveillance for acute flaccid myelitis - United States, 2018. *MMWR Morb. Mortal. Wkly. Rep.* 68, 608–614. doi: 10.15585/mmwr.mm6827e1
- Lu, J., Yi, L., Zhao, J., Yu, J., Chen, Y., Lin, M. C., et al. (2012). Enterovirus 71 disrupts interferon signaling by reducing the level of interferon receptor 1. *J. Virol.* 86, 3767–3776. doi: 10.1128/JVI.06687-6611

- Lucht, F., Cordier, G., Pozzetto, B., Frésard, A., and Revillard, J. P. (1992). Evidence for T-cell involvement during the acute phase of echovirus meningitis. *J. Med. Virol.* 38, 92–96. doi: 10.1002/jmv.1890380204
- Lum, L. C., Wong, K. T., Lam, S. K., Chua, K. B., Goh, A. Y., Lim, W. L., et al. (1998). Fatal enterovirus 71 encephalomyelitis. *J. Pediatr.* 133, 795–798. doi: 10.1016/s0022-3476(98)70155-70156
- Lyoo, H., van der Schaar, H. M., Dorobantu, C. M., Rabouw, H. H., Strating, J. R. P. M., and van Kuppeveld, F. J. M. (2019). ACBD3 is an essential pan-enterovirus host factor that mediates the interaction between viral 3A protein and cellular protein PI4KB. *mBio* 10:e02742-18. doi: 10.1128/mBio.02742-2718
- Maloney, J. A., Mirsky, D. M., Messacar, K., Dominguez, S. R., Schreiner, T., and Stence, N. V. (2015). MRI findings in children with acute flaccid paralysis and cranial nerve dysfunction occurring during the 2014 enterovirus D68 outbreak. *AJNR Am. J. Neuroradiol.* 36, 245–250. doi: 10.3174/ajnr.A4188
- Mao, Q., Hao, X., Hu, Y., Du, R., Lang, S., Bian, L., et al. (2018). A neonatal mouse model of central nervous system infections caused by Coxsackievirus B5. *Emerg. Microbes Infect.* 7:185. doi: 10.1038/s41426-018-0186-y
- Martino, T. A., Petric, M., Weingartl, H., Bergelson, J. M., Opavsky, M. A., Richardson, C. D., et al. (2000). The coxsackie-adenovirus receptor (CAR) is used by reference strains and clinical isolates representing all six serotypes of coxsackievirus group B and by swine vesicular disease virus. *Virology* 271, 99–108. doi: 10.1006/viro.2000.0324
- Mauthe, M., Langereis, M., Jung, J., Zhou, X., Jones, A., Omta, W., et al. (2016). An siRNA screen for ATG protein depletion reveals the extent of the unconventional functions of the autophagy proteome in virus replication. *J. Cell Biol.* 214, 619–635. doi: 10.1083/jcb.201602046
- McIntyre, J. P., and Keen, G. A. (1993). Laboratory surveillance of viral meningitis by examination of cerebrospinal fluid in Cape Town, 1981–9. *Epidemiol. Infect.* 111, 357–371. doi: 10.1017/s095026880005706x
- Melia, C. E., Peddie, C. J., de Jong, A. W. M., Snijder, E. J., Collinson, L. M., Koster, A. J., et al. (2019). Origins of enterovirus replication organelles established by whole-cell electron microscopy. *mBio* 10:e00951-19. doi: 10.1128/mBio.00951-19
- Melia, C. E., van der Schaar, H. M., Lyoo, H., Limpens, R. W. A. L., Feng, Q., Wahedi, M., et al. (2017). Escaping host factor PI4KB inhibition: enterovirus genomic RNA replication in the absence of replication organelles. *Cell Rep.* 21, 587–599. doi: 10.1016/j.celrep.2017.09.068
- Mena, I., Perry, C. M., Harkins, S., Rodriguez, F., Gebhard, J., and Whitton, J. L. (1999). The role of B lymphocytes in coxsackievirus B3 infection. *Am. J. Pathol.* 155, 1205–1215. doi: 10.1016/S0002-9440(10)65223-65226
- Mendelsohn, C. L., Wimmer, E., and Racaniello, V. R. (1989). Cellular receptor for poliovirus: molecular cloning, nucleotide sequence, and expression of a new member of the immunoglobulin superfamily. *Cell* 56, 855–865. doi: 10.1016/0092-8674(89)90690-90699
- Meng, T., Lin, S., Zhuang, H., Huang, H., He, Z., Hu, Y., et al. (2019). Recent progress in the role of autophagy in neurological diseases. *Cell Stress* 3, 141–161. doi: 10.15698/cst2019.05.186
- Messacar, K., Asturias, E. J., Hixon, A. M., Van Leer-Buter, C., Niesters, H. G. M., Tyler, K. L., et al. (2018). Enterovirus D68 and acute flaccid myelitis-evaluating the evidence for causality. *Lancet Infect. Dis.* 18, e239–e247. doi: 10.1016/S1473-3099(18)30094-X
- Misbah, S. A., Spickett, G. P., Ryba, P. C., Hockaday, J. M., Kroll, J. S., Sherwood, C., et al. (1992). Chronic enteroviral meningoencephalitis in agammaglobulinemia: case report and literature review. *J. Clin. Immunol.* 12, 266–270. doi: 10.1007/bf00918150
- Mohamad, Y., and Luo, H. (2019). The intertwined life cycles of enterovirus and autophagy. *Virulence* 10, 470–480. doi: 10.1080/21505594.2018.1551010
- Mohamad, Y., Qu, J., Xue, Y. C., Liu, H., Deng, H., and Luo, H. (2019). CALCOCO2/NDP52 and SQSTM1/p62 differentially regulate coxsackievirus B3 propagation. *Cell Death Differ.* 26, 1062–1076. doi: 10.1038/s41418-018-0185-185
- Mohanty, M. C., and Deshpande, J. M. (2013). Differential induction of Toll-like receptors & type 1 interferons by Sabin attenuated & wild type 1 polioviruses in human neuronal cells. *Indian J. Med. Res.* 138, 209–218.
- Moline, H. L., Karachunski, P. I., Strain, A., Griffith, J., Kenyon, C., and Schleiss, M. R. (2018). Acute transverse myelitis caused by echovirus 11 in a pediatric patient: case report and review of the current literature. *Child Neurol. Open* 5:2329048X17751526. doi: 10.1177/2329048X17751526
- Morens, D. M., and Pallansch, M. A. (1995). “Epidemiology,” in *Human Enterovirus Infections*, ed. H. A. Rotbart, (Washington, DC: ASM Press).
- Mori, M., Takagi, K., Kuwabara, S., Hattori, T., and Kojima, S. (2000). Guillain-Barré syndrome following hand-foot-and-mouth disease. *Intern. Med.* 39, 503–505. doi: 10.2169/internalmedicine.39.503
- Morosky, S., Wells, A. I., Lemon, K., Evans, A. S., Schamus, S., Bakkenist, C. J., et al. (2019). The neonatal Fc receptor is a pan-enterovirus receptor. *Proc. Natl. Acad. Sci. U.S.A.* 116, 3758–3763. doi: 10.1073/pnas.1817341116
- Mueller, S., Cao, X., Welker, R., and Wimmer, E. (2002). Interaction of the poliovirus receptor CD155 with the dynein light chain Tctex-1 and its implication for poliovirus pathogenesis. *J. Biol. Chem.* 277, 7897–7904. doi: 10.1074/jbc.M111937200
- Mukherjee, A., Morosky, S. A., Delorme-Axford, E., Dybdahl-Sissoko, N., Oberste, M. S., Wang, T., et al. (2011). The coxsackievirus B 3C protease cleaves MAVS and TRIF to attenuate host type I interferon and apoptotic signaling. *PLoS Pathog.* 7:e1001311. doi: 10.1371/journal.ppat.1001311
- Müller, U., Steinhoff, U., Reis, L. F., Hemmi, S., Pavlovic, J., Zinkernagel, R. M., et al. (1994). Functional role of type I and type II interferons in antiviral defense. *Science* 264, 1918–1921. doi: 10.1126/science.8009221
- Nagata, N., Shimizu, H., Ami, Y., Tano, Y., Harashima, A., Suzuki, Y., et al. (2002). Pyramidal and extrapyramidal involvement in experimental infection of cynomolgus monkeys with enterovirus 71. *J. Med. Virol.* 67, 207–216. doi: 10.1002/jmv.2209
- Nikoletopoulou, V., Papandreou, M. E., and Tavernarakis, N. (2015). Autophagy in the physiology and pathology of the central nervous system. *Cell Death. Differ* 22, 398–407. doi: 10.1038/cdd.2014.204
- Nilsson, E. C., Jamshidi, F., Johansson, S. M., Oberste, M. S., and Arnberg, N. (2008). Sialic acid is a cellular receptor for coxsackievirus A24 variant, an emerging virus with pandemic potential. *J. Virol.* 82, 3061–3068. doi: 10.1128/JVI.02470-2477
- Nishimura, Y., and Shimizu, H. (2012). Cellular receptors for human enterovirus species a. *Front. Microbiol.* 3:105. doi: 10.3389/fmicb.2012.00105
- Nishimura, Y., Shimozima, M., Tano, Y., Miyamura, T., Wakita, T., and Shimizu, H. (2009). Human P-selectin glycoprotein ligand-1 is a functional receptor for enterovirus 71. *Nat. Med.* 15, 794–797. doi: 10.1038/nm.1961
- Nokhbeh, M. R., Hazra, S., Alexander, D. A., Khan, A., McAllister, M., Suuronen, E. J., et al. (2005). Enterovirus 70 binds to different glycoconjugates containing alpha2,3-linked sialic acid on different cell lines. *J. Virol.* 79, 7087–7094. doi: 10.1128/JVI.79.11.7087-7094.2005
- Ohka, S., Matsuda, N., Tohyama, K., Oda, T., Morikawa, M., Kuge, S., et al. (2004). Receptor (CD155)-dependent endocytosis of poliovirus and retrograde axonal transport of the endosome. *J. Virol.* 78, 7186–7198. doi: 10.1128/JVI.78.13.7186-7198.2004
- Ohka, S., Yang, W. X., Terada, E., Iwasaki, K., and Nomoto, A. (1998). Retrograde transport of intact poliovirus through the axon via the fast transport system. *Virology* 250, 67–75. doi: 10.1006/viro.1998.9360
- Ooi, M. H., Wong, S. C., Lewthwaite, P., Cardoso, M. J., and Solomon, T. (2010). Clinical features, diagnosis, and management of enterovirus 71. *Lancet Neurol.* 9, 1097–1105. doi: 10.1016/S1474-4422(10)70209-X
- Orr-Burks, N. L., Shim, B. S., Wu, W., Bakre, A. A., Karpilow, J., and Tripp, R. A. (2017). MicroRNA screening identifies miR-134 as a regulator of poliovirus and enterovirus 71 infection. *Sci. Data* 4:170023. doi: 10.1038/sdata.2017.23
- Oshiumi, H., Okamoto, M., Fujii, K., Kawanishi, T., Matsumoto, M., Koike, S., et al. (2011). The TLR3/TICAM-1 pathway is mandatory for innate immune responses to poliovirus infection. *J. Immunol.* 187, 5320–5327. doi: 10.4049/jimmunol.1101503
- Owino, C. O., and Chu, J. J. H. (2019). Recent advances on the role of host factors during non-poliovirus enteroviral infections. *J. Biomed. Sci.* 26:47. doi: 10.1186/s12929-019-0540-y
- Pallansch, M. A., Oberste, M. S., and Whitton, J. L. (2013). “Enteroviruses: polioviruses, coxsackieviruses, echoviruses and newer enteroviruses,” in *Fields Virology*, eds D. M. Knipe, and P. M. Howley, (Philadelphia: Wolters Kluwer Health/Lippincott Williams & Wilkins), 490–530.
- Panjwani, A., Strauss, M., Gold, S., Wenham, H., Jackson, T., Chou, J. J., et al. (2014). Capsid protein VP4 of human rhinovirus induces membrane permeability by the formation of a size-selective multimeric pore. *PLoS Pathog.* 10:e1004294. doi: 10.1371/journal.ppat.1004294

- Papa, A., Dumaidi, K., Franzidou, F., and Antoniadis, A. (2006). Genetic variation of coxsackie virus B5 strains associated with aseptic meningitis in Greece. *Clin. Microbiol. Infect.* 12, 688–691. doi: 10.1111/j.1469-0691.2006.01476.x
- Pascual, O., Casper, K. B., Kubera, C., Zhang, J., Revilla-Sanchez, R., Sul, J. Y., et al. (2005). Astrocytic purinergic signaling coordinates synaptic networks. *Science* 310, 113–116. doi: 10.1126/science.1116916
- Pastuszak, Z., Stępień, A., Tomczykiewicz, K., Piusińska-Macoch, R., Galbarczyk, D., and Rolewska, A. (2017). Post-polio syndrome. Cases report and review of literature. *Neurol. Neurochir. Pol.* 51, 140–145. doi: 10.1016/j.pjnns.2017.01.009
- Pérez-Vélez, C. M., Anderson, M. S., Robinson, C. C., McFarland, E. J., Nix, W. A., Pallansch, M. A., et al. (2007). Outbreak of neurologic enterovirus type 71 disease: a diagnostic challenge. *Clin. Infect. Dis.* 45, 950–957. doi: 10.1086/521895
- Pfeiffer, J. K., and Kirkegaard, K. (2005). Increased fidelity reduces poliovirus fitness and virulence under selective pressure in mice. *PLoS Pathog.* 1:e11. doi: 10.1371/journal.ppat.0010011
- Pfeiffer, J. K., and Kirkegaard, K. (2006). Bottleneck-mediated quasispecies restriction during spread of an RNA virus from inoculation site to brain. *Proc. Natl. Acad. Sci. U.S.A.* 103, 5520–5525. doi: 10.1073/pnas.0600834103
- Pino, P. A., Intravia, J., Kozin, S. H., and Zlotolow, D. A. (2019). Early results of nerve transfers for restoring function in severe cases of acute flaccid myelitis. *Ann. Neurol.* 86, 607–615. doi: 10.1002/ana.25558
- Pons-Salort, M., Parker, E. P., and Grassly, N. C. (2015). The epidemiology of non-polio enteroviruses: recent advances and outstanding questions. *Curr. Opin. Infect. Dis.* 28, 479–487. doi: 10.1097/QCO.0000000000000187
- Puccini, J. M., Ruller, C. M., Robinson, S. M., Knopp, K. A., Buchmeier, M. J., Doran, K. S., et al. (2014). Distinct neural stem cell tropism, early immune activation, and choroid plexus pathology following coxsackievirus infection in the neonatal central nervous system. *Lab. Invest.* 94, 161–181. doi: 10.1038/labinvest.2013.138
- Racaniello, V. R., and Ren, R. (1994). Transgenic mice and the pathogenesis of poliomyelitis. *Arch. Virol. Suppl.* 9, 79–86. doi: 10.1007/978-3-7091-9326-6\_9
- Ragonese, P., Fierro, B., Salemi, G., Randisi, G., Buffa, D., D'Amelio, M., et al. (2005). Prevalence and risk factors of post-polio syndrome in a cohort of polio survivors. *J. Neurol. Sci.* 236, 31–35. doi: 10.1016/j.jns.2005.04.012
- Rahman, M. M., and McFadden, G. (2011). Modulation of NF- $\kappa$ B signalling by microbial pathogens. *Nat. Rev. Microbiol.* 9, 291–306. doi: 10.1038/nrmicro2539
- Ramelli, G. P., Simonetti, G. D., Gorgievski-Hrisoho, M., Aebi, C., and Bianchetti, M. G. (2004). Outbreak of coxsackie B5 virus meningitis in a Scout camp. *Pediatr. Infect. Dis. J.* 23, 86–87. doi: 10.1097/01.inf.0000107294.96717.d5
- Ramlow, J., Alexander, M., LaPorte, R., Kaufmann, C., and Kuller, L. (1992). Epidemiology of the post-polio syndrome. *Am. J. Epidemiol.* 136, 769–786. doi: 10.1093/aje/136.7.769
- Ransohoff, R. M., and Engelhardt, B. (2012). The anatomical and cellular basis of immune surveillance in the central nervous system. *Nat. Rev. Immunol.* 12, 623–635. doi: 10.1038/nri3265
- Ranzenhofer, E. R., Dizon, F. C., Lipton, M. M., and Steigman, A. J. (1958). Clinical paralytic poliomyelitis due to Coxsackie virus group A, type 7. *N. Engl. J. Med.* 259:182. doi: 10.1056/NEJM195807242590408
- Ren, R., and Racaniello, V. R. (1992). Poliovirus spreads from muscle to the central nervous system by neural pathways. *J. Infect. Dis.* 166, 747–752. doi: 10.1093/infdis/166.4.747
- Renois, F., Hong, S. S., Le Naour, R., Gafa, V., Talmud, D., Andréoletti, L., et al. (2011). Development of a recombinant CHO cell model for the investigation of CAR and DAF role during early steps of echovirus 6 infection. *Virus Res.* 158, 46–54. doi: 10.1016/j.virusres.2011.03.009
- Rhoades, R. E., Tabor-Godwin, J. M., Tsueng, G., and Feuer, R. (2011). Enterovirus infections of the central nervous system. *Virology* 411, 288–305. doi: 10.1016/j.virology.2010.12.014
- Rosenfeld, A. B., Warren, A. L., and Racaniello, V. R. (2019). Neurotropism of enterovirus D68 isolates is independent of sialic acid and is not a recently acquired phenotype. *mBio* 10:e02370-19. doi: 10.1128/mBio.02370-2019
- Roulin, P. S., Lötzerich, M., Torta, F., Tanner, L. B., van Kuppeveld, F. J., Wenk, M. R., et al. (2014). Rhinovirus uses a phosphatidylinositol 4-phosphate/cholesterol counter-current for the formation of replication compartments at the ER-Golgi interface. *Cell Host Microbe* 16, 677–690. doi: 10.1016/j.chom.2014.10.003
- Royston, L., Essaïdi-Laziosi, M., Pérez-Rodríguez, F. J., Piuz, I., Geiser, J., Krause, K. H., et al. (2018). Viral chimeras decrypt the role of enterovirus capsid proteins in viral tropism, acid sensitivity and optimal growth temperature. *PLoS Pathog.* 14:e1006962. doi: 10.1371/journal.ppat.1006962
- Rudolph, H., Schrotten, H., and Tenenbaum, T. (2016). Enterovirus infections of the central nervous system in children: an update. *Pediatr. Infect. Dis. J.* 35, 567–569. doi: 10.1097/INF.0000000000001090
- Rui, Y., Su, J., Wang, H., Chang, J., Wang, S., Zheng, W., et al. (2017). Disruption of MDA5-mediated innate immune responses by the 3C proteins of coxsackievirus A16, coxsackievirus A6, and enterovirus D68. *J. Virol.* 91:e00546-17. doi: 10.1128/JVI.00546-17
- Sauter, P., and Hober, D. (2009). Mechanisms and results of the antibody-dependent enhancement of viral infections and role in the pathogenesis of coxsackievirus B-induced diseases. *Microbes Infect.* 11, 443–451. doi: 10.1016/j.micinf.2009.01.005
- Schindler, C., Levy, D. E., and Decker, T. (2007). JAK-STAT signaling: from interferons to cytokines. *J. Biol. Chem.* 282, 20059–20063. doi: 10.1074/jbc.R700016200
- Schneider, H., Weber, C. E., Schoeller, J., Steinmann, U., Borkowski, J., Ishikawa, H., et al. (2012). Chemotaxis of T-cells after infection of human choroid plexus papilloma cells with Echovirus 30 in an in vitro model of the blood-cerebrospinal fluid barrier. *Virus Res.* 170, 66–74. doi: 10.1016/j.virusres.2012.08.019
- Sejvar, J. J., Lopez, A. S., Cortese, M. M., Leshem, E., Pastula, D. M., Miller, L., et al. (2016). Acute flaccid myelitis in the United States, August–December 2014: results of nationwide surveillance. *Clin. Infect. Dis.* 63, 737–745. doi: 10.1093/cid/ciw372
- Shafren, D. R., Bates, R. C., Agrez, M. V., Herd, R. L., Burns, G. F., and Barry, R. D. (1995). Coxsackieviruses B1, B3, and B5 use decay accelerating factor as a receptor for cell attachment. *J. Virol.* 69, 3873–3877. doi: 10.1128/jvi.69.6.3873-3877.1995
- Shafren, D. R., Dorahy, D. J., Ingham, R. A., Burns, G. F., and Barry, R. D. (1997). Coxsackievirus A21 binds to decay-accelerating factor but requires intercellular adhesion molecule 1 for cell entry. *J. Virol.* 71, 4736–4743. doi: 10.1128/jvi.71.6.4736-4743.1997
- Shieh, W. J., Jung, S. M., Hsueh, C., Kuo, T. T., Mounts, A., Parashar, U., et al. (2001). Pathologic studies of fatal cases in outbreak of hand, foot, and mouth disease, Taiwan. *Emerg. Infect. Dis.* 7, 146–148. doi: 10.3201/eid0701.700146
- Siafakas, N., Markoulatos, P., and Levidiotou-Stefanou, S. (2004). Molecular identification of enteroviruses responsible for an outbreak of aseptic meningitis; implications in clinical practice and epidemiology. *Mol. Cell. Probes* 18, 389–398. doi: 10.1016/j.mcp.2004.06.005
- Simmonds, P., Gorbalenya, A. E., Harvala, H., Hovi, T., Knowles, N. J., Lindberg, A. M., et al. (2020). Recommendations for the nomenclature of enteroviruses and rhinoviruses. *Arch. Virol.* 165, 793–797. doi: 10.1007/s00705-019-04520-6
- Singh, D. V., Kumar, A., Kumar, P., Baluni, M., Ghildiyal, S., Kumar, R., et al. (2016). An outbreak of encephalitis associated with echovirus 19 in Uttar Pradesh, India, in 2011. *Arch. Virol.* 161, 967–970. doi: 10.1007/s00705-015-2714-2716
- Song, J., Hu, Y., Li, J., Zheng, H., Wang, J., Guo, L., et al. (2018). Suppression of the toll-like receptor 7-dependent type I interferon production pathway by autophagy resulting from enterovirus 71 and coxsackievirus A16 infections facilitates their replication. *Arch. Virol.* 163, 135–144. doi: 10.1007/s00705-017-3592-x
- Staring, J., von Castelmuur, E., Blomen, V. A., van den Hengel, L. G., Brockmann, M., Baggen, J., et al. (2017). PLA2G16 represents a switch between entry and clearance of Picornaviridae. *Nature* 541, 412–416. doi: 10.1038/nature21032
- Strating, J. R., van der Linden, L., Albulescu, L., Bigay, J., Arita, M., Delang, L., et al. (2015). Itraconazole inhibits enterovirus replication by targeting the oxysterol-binding protein. *Cell Rep.* 10, 600–615. doi: 10.1016/j.celrep.2014.12.054
- Strauss, M., Levy, H. C., Bostina, M., Filman, D. J., and Hogle, J. M. (2013). RNA transfer from poliovirus 135S particles across membranes is mediated by long umbilical connectors. *J. Virol.* 87, 3903–3914. doi: 10.1128/JVI.03209-312
- Su, P. Y., Liu, Y. T., Chang, H. Y., Huang, S. W., Wang, Y. F., Yu, C. K., et al. (2012). Cell surface sialylation affects binding of enterovirus 71 to rhabdomyosarcoma

- and neuroblastoma cells. *BMC Microbiol.* 12:162. doi: 10.1186/1471-2180-12-162
- Su, P. Y., Wang, Y. F., Huang, S. W., Lo, Y. C., Wang, Y. H., Wu, S. R., et al. (2015). Cell surface nucleolin facilitates enterovirus 71 binding and infection. *J. Virol.* 89, 4527–4538. doi: 10.1128/JVI.03498-3414
- Sun, J., Ennis, J., Turner, J. D., and Chu, J. J. (2016). Single dose of an adenovirus vectored mouse interferon- $\alpha$  protects mice from lethal EV71 challenge. *Antiviral Res.* 134, 207–215. doi: 10.1016/j.antiviral.2016.09.003
- Sun, S., Bian, L., Gao, F., Du, R., Hu, Y., Fu, Y., et al. (2019). A neonatal mouse model of Enterovirus D68 infection induces both interstitial pneumonia and acute flaccid myelitis. *Antiviral Res.* 161, 108–115. doi: 10.1016/j.antiviral.2018.11.013
- Suresh, S., Forgie, S., and Robinson, J. (2018). Non-polio Enterovirus detection with acute flaccid paralysis: a systematic review. *J. Med. Virol.* 90, 3–7. doi: 10.1002/jmv.24933
- Suzuki, S., Misawa, S., Ota, T., Li, Y., Kuwabara, S., and Ikusaka, M. (2017). Post-polio-like syndrome. *Am. J. Med.* 130, e491–e492. doi: 10.1016/j.amjmed.2017.05.024
- Tabor-Godwin, J. M., Ruller, C. M., Bagalzo, N., An, N., Pagarigan, R. R., Harkins, S., et al. (2010). A novel population of myeloid cells responding to coxsackievirus infection assists in the dissemination of virus within the neonatal CNS. *J. Neurosci.* 30, 8676–8691. doi: 10.1523/JNEUROSCI.1860-10.2010
- Takemura, J., Saeki, S., Hachisuka, K., and Aritome, K. (2004). Prevalence of post-polio syndrome based on a cross-sectional survey in Kitakyushu, Japan. *J. Rehabil. Med.* 36, 1–3. doi: 10.1080/16501970310017423
- Tan, C. W., Poh, C. L., Sam, I. C., and Chan, Y. F. (2013). Enterovirus 71 uses cell surface heparan sulfate glycosaminoglycan as an attachment receptor. *J. Virol.* 87, 611–620. doi: 10.1128/JVI.02226-2212
- Tolbert, M., Morgan, C. E., Pollum, M., Crespo-Hernández, C. E., Li, M. L., Brewer, G., et al. (2017). HnRNP A1 alters the structure of a conserved enterovirus IRES domain to stimulate viral translation. *J. Mol. Biol.* 429, 2841–2858. doi: 10.1016/j.jmb.2017.06.007
- Too, I. H., Yeo, H., Sessions, O. M., Yan, B., Libau, E. A., Howe, J. L., et al. (2016). Enterovirus 71 infection of motor neuron-like NSC-34 cells undergoes a non-lytic exit pathway. *Sci. Rep.* 6:36983. doi: 10.1038/srep36983
- Too, I. H. K., Bonne, I., Tan, E. L., Chu, J. J. H., and Alonso, S. (2018). Prohibitin plays a critical role in Enterovirus 71 neuropathogenesis. *PLoS Pathog.* 14:e1006778. doi: 10.1371/journal.ppat.1006778
- Tseligka, E. D., Sobo, K., Stoppini, L., Cagno, V., Abdul, F., Piuz, I., et al. (2018). A VP1 mutation acquired during an enterovirus 71 disseminated infection confers heparan sulfate binding ability and modulates ex vivo tropism. *PLoS Pathog.* 14:e1007190. doi: 10.1371/journal.ppat.1007190
- Tung, W. H., Lee, I. T., Hsieh, H. L., and Yang, C. M. (2010). EV71 induces COX-2 expression via c-Src/PDGFR/PI3K/Akt/p42/p44 MAPK/AP-1 and NF- $\kappa$ B in rat brain astrocytes. *J. Cell. Physiol.* 224, 376–386. doi: 10.1002/jcp.22133
- Tuthill, T. J., Bubeck, D., Rowlands, D. J., and Hogle, J. M. (2006). Characterization of early steps in the poliovirus infection process: receptor-decorated liposomes induce conversion of the virus to membrane-anchored entry-intermediate particles. *J. Virol.* 80, 172–180. doi: 10.1128/JVI.80.1.172-180.2006
- van der Schaar, H. M., Leyssen, P., Thibaut, H. J., de Palma, A., van der Linden, L., Lanke, K. H., et al. (2013). A novel, broad-spectrum inhibitor of enterovirus replication that targets host cell factor phosphatidylinositol 4-kinase III $\beta$ . *Antimicrob. Agents Chemother.* 57, 4971–4981. doi: 10.1128/AAC.01175-1113
- Van Haren, K., Ayscue, P., Waubant, E., Clayton, A., Sheriff, H., Yagi, S., et al. (2015). Acute flaccid myelitis of unknown etiology in California, 2012–2015. *JAMA* 314, 2663–2671. doi: 10.1001/jama.2015.17275
- Venkatesan, A., Tunkel, A. R., Bloch, K. C., Lauring, A. S., Sejvar, J., Bitnun, A., et al. (2013). Case definitions, diagnostic algorithms, and priorities in encephalitis: consensus statement of the international encephalitis consortium. *Clin. Infect. Dis.* 57, 1114–1128. doi: 10.1093/cid/cit458
- Vignuzzi, M., Stone, J. K., Arnold, J. J., Cameron, C. E., and Andino, R. (2006). Quasispecies diversity determines pathogenesis through cooperative interactions in a viral population. *Nature* 439, 344–348. doi: 10.1038/nature04388
- Volterra, A., and Meldolesi, J. (2005). Astrocytes, from brain glue to communication elements: the revolution continues. *Nat. Rev. Neurosci.* 6, 626–640. doi: 10.1038/nrn1722
- Wang, B., Xi, X., Lei, X., Zhang, X., Cui, S., Wang, J., et al. (2013). Enterovirus 71 protease 2Apro targets MAVS to inhibit anti-viral type I interferon responses. *PLoS Pathog.* 9:e1003231. doi: 10.1371/journal.ppat.1003231
- Wang, C., Sun, M., Yuan, X., Ji, L., Jin, Y., Cardona, C. J., et al. (2017). Enterovirus 71 suppresses interferon responses by blocking Janus kinase (JAK)/signal transducer and activator of transcription (STAT) signaling through inducing karyopherin- $\alpha$ 1 degradation. *J. Biol. Chem.* 292, 10262–10274. doi: 10.1074/jbc.M116.745729
- Wang, C., Zhou, R., Zhang, Z., Jin, Y., Cardona, C. J., and Xing, Z. (2015). Intrinsic apoptosis and proinflammatory cytokines regulated in human astrocytes infected with enterovirus 71. *J. Gen. Virol.* 96, 3010–3022. doi: 10.1099/jgv.0.000235
- Wang, H., Yuan, M., Wang, S., Zhang, L., Zhang, R., Zou, X., et al. (2019). STAT3 Regulates the Type I IFN-Mediated Antiviral Response by Interfering with the Nuclear Entry of STAT1. *Int. J. Mol. Sci.* 20:E4870. doi: 10.3390/ijms20194870
- Wang, J., Pu, J., Huang, H., Zhang, Y., Liu, L., Yang, E., et al. (2013). EV71-infected CD14(+) cells modulate the immune activity of T lymphocytes in rhesus monkeys. *Emerg. Microbes Infect.* 2:e44. doi: 10.1038/emi.2013.44
- Wang, L., Dong, C., Chen, D. E., and Song, Z. (2014). Coxsackievirus-induced acute neonatal central nervous system disease model. *Int. J. Clin. Exp. Pathol.* 7, 858–869.
- Wang, L. C., Chen, S. O., Chang, S. P., Lee, Y. P., Yu, C. K., Chen, C. L., et al. (2015). Enterovirus 71 proteins 2A and 3D antagonize the antiviral activity of gamma interferon via signaling attenuation. *J. Virol.* 89, 7028–7037. doi: 10.1128/JVI.00205-215
- Wang, S. M., Liu, C. C., Tseng, H. W., Wang, J. R., Huang, C. C., Chen, Y. J., et al. (1999). Clinical spectrum of enterovirus 71 infection in children in southern Taiwan, with an emphasis on neurological complications. *Clin. Infect. Dis.* 29, 184–190. doi: 10.1086/520149
- Wang, Y., Zhao, S., Chen, Y., Wang, T., Dong, C., Wo, X., et al. (2019). The capsid protein VP1 of coxsackievirus B induces cell cycle arrest by up-regulating heat shock protein 70. *Front. Microbiol.* 10:1633. doi: 10.3389/fmicb.2019.01633
- Wang, Z., Wang, Y., Wang, S., Meng, X., Song, F., Huo, W., et al. (2018). Coxsackievirus A6 induces cell cycle arrest in G0/G1 phase for viral production. *Front. Cell. Infect. Microbiol.* 8:279. doi: 10.3389/fcimb.2018.00279
- Wang, Z. Y., Zhong, T., Wang, Y., Song, F. M., Yu, X. F., Xing, L. P., et al. (2017). Human enterovirus 68 interferes with the host cell cycle to facilitate viral production. *Front. Cell Infect. Microbiol.* 7:29. doi: 10.3389/fcimb.2017.00029
- Ward, C. D., and Flanagan, J. B. (1992). Determination of the poliovirus RNA polymerase error frequency at eight sites in the viral genome. *J. Virol.* 66, 3784–3793. doi: 10.1128/jvi.66.6.3784-3793.1992
- Wei, W., Guo, H., Chang, J., Yu, Y., Liu, G., Zhang, N., et al. (2016). ICAM-5/telencephalin is a functional entry receptor for enterovirus D68. *Cell Host Microbe* 20, 631–641. doi: 10.1016/j.chom.2016.09.013
- Wells, A. I., and Coyne, C. B. (2019). Enteroviruses: a gut-wrenching game of entry, detection, and evasion. *Viruses* 11:E460. doi: 10.3390/v11050460
- Wong, J., Zhang, J., Si, X., Gao, G., Mao, I., McManus, B. M., et al. (2008). Autophagosome supports coxsackievirus B3 replication in host cells. *J. Virol.* 82, 9143–9153. doi: 10.1128/JVI.00641-648
- Wongsa, A., Noulstri, E., Phawong, C., Puthavathana, P., and Tassaneeritthep, B. (2019). Replication and cytokine profiles of different subgenotypes of enterovirus 71 isolated from Thai patients in peripheral blood mononuclear cells. *Microb. Pathog.* 132, 215–221. doi: 10.1016/j.micpath.2019.05.008
- Würstle, M. L., Laussmann, M. A., and Rehm, M. (2010). The caspase-8 dimerization/dissociation balance is a highly potent regulator of caspase-8, -3, -6 signaling. *J. Biol. Chem.* 285, 33209–33218. doi: 10.1074/jbc.M110.113860
- Xi, X., Zhang, X., Wang, B., Wang, T., Wang, J., Huang, H., et al. (2013). The interplays between autophagy and apoptosis induced by enterovirus 71. *PLoS One* 8:e56966. doi: 10.1371/journal.pone.0056966
- Xiang, Z., Liu, L., Lei, X., Zhou, Z., He, B., and Wang, J. (2016). 3C protease of enterovirus D68 inhibits cellular defense mediated by interferon regulatory factor 7. *J. Virol.* 90, 1613–1621. doi: 10.1128/JVI.02395-2315
- Xu, T., Lin, Z., Wang, C., Li, Y., Xia, Y., Zhao, M., et al. (2019). Heat shock protein 70 as a supplementary receptor facilitates enterovirus 71 infections *in vitro*. *Microb. Pathog.* 128, 106–111. doi: 10.1016/j.micpath.2018.12.032
- Yamayoshi, S., Iizuka, S., Yamashita, T., Minagawa, H., Mizuta, K., Okamoto, M., et al. (2012). Human SCARB2-dependent infection by coxsackievirus A7, A14, and A16 and enterovirus 71. *J. Virol.* 86, 5686–5696. doi: 10.1128/JVI.00020-12

- Yamayoshi, S., Yamashita, Y., Li, J., Hanagata, N., Minowa, T., Takemura, T., et al. (2009). Scavenger receptor B2 is a cellular receptor for enterovirus 71. *Nat. Med.* 15, 798–801. doi: 10.1038/nm.1992
- Yan, J. J., Wang, J. R., Liu, C. C., Yang, H. B., and Su, I. J. (2000). An outbreak of enterovirus 71 infection in Taiwan 1998: a comprehensive pathological, virological, and molecular study on a case of fulminant encephalitis. *J. Clin. Virol.* 17, 13–22. doi: 10.1016/s1386-6532(00)00067-66
- Yang, B., Chuang, H., and Yang, K. D. (2009). Sialylated glycans as receptor and inhibitor of enterovirus 71 infection to DLD-1 intestinal cells. *Virol. J.* 6:141. doi: 10.1186/1743-422X-6-141
- Yang, J., Yang, C., Guo, N., Zhu, K., Luo, K., Zhang, N., et al. (2015). Type I interferons triggered through the toll-like receptor 3-TRIF pathway control coxsackievirus A16 infection in young mice. *J. Virol.* 89, 10860–10867. doi: 10.1128/JVI.01627-1615
- Yang, S. L., Chou, Y. T., Wu, C. N., and Ho, M. S. (2011). Annexin II binds to capsid protein VP1 of enterovirus 71 and enhances viral infectivity. *J. Virol.* 85, 11809–11820. doi: 10.1128/JVI.00297-211
- Yea, C., Bitnun, A., Robinson, J., Mineyko, A., Barton, M., Mah, J. K., et al. (2017). Longitudinal outcomes in the 2014 acute flaccid paralysis cluster in Canada. *J. Child Neurol.* 32, 301–307. doi: 10.1177/0883073816680770
- Yeh, M. T., Wang, S. W., Yu, C. K., Lin, K. H., Lei, H. Y., Su, I. J., et al. (2011). A single nucleotide in stem loop II of 5'-untranslated region contributes to virulence of enterovirus 71 in mice. *PLoS One* 6:e27082. doi: 10.1371/journal.pone.0027082
- Ylipaasto, P., Eskelinen, M., Salmela, K., Hovi, T., and Roivainen, M. (2010). Vitronectin receptors, alpha v integrins, are recognized by several non-RGD-containing echoviruses in a continuous laboratory cell line and also in primary human Langerhans' islets and endothelial cells. *J. Gen. Virol.* 91, 155–165. doi: 10.1099/vir.0.012450-12450
- Yogarajah, T., Ong, K. C., Perera, D., and Wong, K. T. (2017a). AIM2 inflammasome-mediated pyroptosis in enterovirus A71-infected neuronal cells restricts viral replication. *Sci. Rep.* 7:5845. doi: 10.1038/s41598-017-05589-5582
- Yogarajah, T., Ong, K. C., Perera, D., and Wong, K. T. (2017b). Enterovirus A71 and coxsackievirus A16 show different replication kinetics in human neuronal and non-neuronal cell lines. *Arch. Virol.* 162, 727–737. doi: 10.1007/s00705-016-3157-3154
- Yogarajah, T., Ong, K. C., Perera, D., and Wong, K. T. (2018). RSAD2 and AIM2 modulate coxsackievirus A16 and enterovirus A71 replication in neuronal cells in different ways that may be associated with their 5' nontranslated regions. *J. Virol.* 92, e1914–e1917. doi: 10.1128/JVI.01914-1917
- Yu, J., Zhang, L., Ren, P., Zhong, T., Li, Z., Wang, Z., et al. (2015). Enterovirus 71 mediates cell cycle arrest in S phase through non-structural protein 3D. *Cell Cycle* 14, 425–436. doi: 10.4161/15384101.2014.980631
- Yu, P., Bao, L., Xu, L., Li, F., Lv, Q., Deng, W., et al. (2017). Neurotropism *in vitro* and mouse models of severe and mild infection with clinical strains of Enterovirus 71. *Viruses* 9:E351. doi: 10.3390/v9110351
- Yu, P., Gao, Z., Zong, Y., Bao, L., Xu, L., Deng, W., et al. (2014). Histopathological features and distribution of EV71 antigens and SCARB2 in human fatal cases and a mouse model of enterovirus 71 infection. *Virus Res.* 189, 121–132. doi: 10.1016/j.virusres.2014.05.006
- Zeng, J., Wang, G., Li, W., Zhang, D., Chen, X., Xin, G., et al. (2013). Induction of cytopathic effect and cytokines in coxsackievirus B3-infected murine astrocytes. *Virol. J.* 10:157. doi: 10.1186/1743-422X-10-157
- Zhang, H., Song, L., Cong, H., and Tien, P. (2015). Nuclear protein Sam68 interacts with the enterovirus 71 internal ribosome entry site and positively regulates viral protein translation. *J. Virol.* 89, 10031–10043. doi: 10.1128/JVI.01677-1615
- Zhang, L., Yan, J., Ojcius, D. M., Lv, H., Miao, Z., Chen, Y., et al. (2013). Novel and predominant pathogen responsible for the enterovirus-associated encephalitis in eastern China. *PLoS One* 8:e85023. doi: 10.1371/journal.pone.0085023
- Zhu, X., Wu, T., Chi, Y., Ge, Y., Wu, B., Zhou, M., et al. (2018). Pyroptosis induced by enterovirus A71 infection in cultured human neuroblastoma cells. *Virology* 521, 69–76. doi: 10.1016/j.virol.2018.05.025

**Conflict of Interest:** The authors declare that the research was conducted in the absence of any commercial or financial relationships that could be construed as a potential conflict of interest.

Copyright © 2020 Majer, McGreevy and Booth. This is an open-access article distributed under the terms of the Creative Commons Attribution License (CC BY). The use, distribution or reproduction in other forums is permitted, provided the original author(s) and the copyright owner(s) are credited and that the original publication in this journal is cited, in accordance with accepted academic practice. No use, distribution or reproduction is permitted which does not comply with these terms.



# A Large-Scale Outbreak of Echovirus 30 in Gansu Province of China in 2015 and Its Phylodynamic Characterization

Jianhua Chen<sup>1†</sup>, Zhenzhi Han<sup>2†</sup>, Haizhuo Wu<sup>1</sup>, Wenbo Xu<sup>2,3</sup>, Deshan Yu<sup>1\*</sup> and Yong Zhang<sup>2,3\*</sup>

<sup>1</sup> Key Laboratory of Infectious Diseases in Gansu Province, Gansu Center for Disease Control and Prevention, Lanzhou, China, <sup>2</sup> WHO WPRO Regional Polio Reference Laboratory and National Health Commission Key Laboratory of Biosafety, National Institute for Viral Disease Control and Prevention, Chinese Center for Disease Control and Prevention, Beijing, China, <sup>3</sup> Center for Biosafety Mega-Science, Chinese Academy of Sciences, Wuhan, China

## OPEN ACCESS

### Edited by:

Mei-Ling Li,  
Rutgers, The State University  
of New Jersey, United States

### Reviewed by:

Mojtaba Rasti,  
Ahvaz Jundishapur University  
of Medical Sciences, Iran  
Peng Chen,  
Shandong University, China

### \*Correspondence:

Deshan Yu  
gscdc123@sina.com  
Yong Zhang  
yongzhang75@sina.com

†These authors have contributed  
equally to this work

### Specialty section:

This article was submitted to  
Virology,  
a section of the journal  
Frontiers in Microbiology

Received: 22 October 2019

Accepted: 05 May 2020

Published: 10 June 2020

### Citation:

Chen J, Han Z, Wu H, Xu W, Yu D  
and Zhang Y (2020) A Large-Scale  
Outbreak of Echovirus 30 in Gansu  
Province of China in 2015 and Its  
Phylodynamic Characterization.  
*Front. Microbiol.* 11:1137.  
doi: 10.3389/fmicb.2020.01137

**Background:** Echovirus 30 (E-30) has been investigated and reported worldwide and is closely associated with several infectious diseases, including encephalitis; myocarditis; and hand, foot, and mouth disease. Although many E-30 outbreaks associated with encephalitis have been reported around the world, it was not reported in northwest China until 2015.

**Methods:** The clinical samples, including the feces, serum, throat swabs, and cerebrospinal fluid, were collected for this study and were analyzed for diagnosis. E-30 was isolated and processed according to the standard procedures. The epidemiological and phylogenetic analysis were performed to indicate the characteristics of E-30 outbreaks and phylodynamics of E-30 in China.

**Results:** The E-30 outbreaks affected nine towns of Gansu Province in 2015, starting at a school of Nancha town and spreading to other towns within 1 month. The epidemiological features showed that children aged 6–15 years were more susceptible to E-30 infection. The genotypes B and C cocirculated in the world, whereas the latter dominated the circulation of E-30 in China. The genome sequences of this outbreak present 99.3–100% similarity among these strains, indicating a genetic-linked aggregate outbreak of E-30 in this study. Two larger genetic diversity expansions and three small fluctuations of E-30 were observed from 1987 to 2016 in China, which revealed the oscillating patterns of E-30 in China. In addition, the coastal provinces of China, such as Zhejiang, Fujian, and Shandong, were initially infected, followed by other parts of the country. The E-30 strains isolated from mainland of China may have originated from Taiwan of China in the last century.

**Conclusion:** The highly similar E-30 genomes in this outbreak showed an aggregate outbreak of E-30, with nine towns affected. Our results suggested that, although the genetic diversity of E-30 oscillates, the dominant lineages of E-30 in China has complex

genetic transmission. The coastal provinces played an important role in E-30 spread, which implied further development of effective countermeasures. This study provides a further insight into the E-30 outbreak and transmission and illustrates the importance of valuable surveillance in the future.

**Keywords:** echovirus 30 (E-30), phylogenetic analysis, molecular epidemiology, phylodynamics, encephalitis

## INTRODUCTION

Enteroviruses belong to the genus *Enterovirus* of the *Picornaviridae* family, which now consists of 15 species designated as *Enterovirus* A–L and *Rhinovirus* A–C (Zell et al., 2017). *Enterovirus* A–D (EV-A, EV-B, EV-C, and EV-D) are closely associated with human diseases and were studied for the purpose of public health. The genomic length of enterovirus is ~7.5 kb, which contained a long open reading frame (ORF), with 5'-untranslated region (UTR) and 3'-UTR. The polyprotein could be cleaved into *P1*, *P2*, and *P3* protein precursors, followed by the further cleavage into *VPI–VP4*, *2A–2C*, and *3A–3D*, respectively. The *VPI* coding region of enterovirus contained the major antigenic neutralization sites responsible to immunoreaction. The molecular typing approach, which primarily based on the *VPI* coding region of enterovirus, was accepted as the major method for serotyping (Rohll et al., 1995; Bergamini et al., 2000). With the development of molecular typing technologies, there are more and more new serotypes of enteroviruses have been found, with the *VPI* coding region and partial *VPI* coding region targeted (Oberste et al., 2005; Yozwiak et al., 2010; Tokarz et al., 2013; Zhang Y. et al., 2014; Han et al., 2018). This method has become the gold standard for enterovirus typing and detection and allows for greater convenience than serotyping (Oberste et al., 1999a,b). EV-B consists of 63 serotypes, including coxsackievirus (CV)-A9, CV-B group (serotypes 1–6), echovirus (serotypes 1–7, 9, 11–21, 24–27, 29–33), and newly identified enteroviruses (serotypes 69, 73–75, 77–88, 93, 97–98, 100–101, 106–107, 110–113) (Adams et al., 2017). These serotypes of enteroviruses are usually associated with a series of diseases, such as encephalitis; myocarditis; hand, foot, and mouth disease (HFMD); acute flaccid paralysis (AFP); and other diseases. For example, CV-B3 has been linked to myocarditis and encephalitis, whereas it could also cause outbreaks of HFMD as reported recently (Tao et al., 2012; Wu et al., 2013; Han et al., 2019). CV-B5 is an important pathogen that caused the outbreaks of encephalitis and HFMD (Han et al., 2012; Chen et al., 2013).

Echovirus 30 (E-30), which was classified as a member of *Enterovirus* species B, has caused several diseases, including encephalitis, HFMD, myocarditis, and other mild clinical manifestations, such as fever and headache (Tapparel et al., 2013; Adams et al., 2017; Rasti et al., 2019). Several E-30 outbreaks in the world have been reported and analyzed to confirm the epidemiological characteristics and evolutionary patterns, which have provided valuable information for disease control (Milia et al., 2013; Wiczorek et al., 2016; Chen et al., 2017). The first molecular epidemiological study of E-30 was reported in 1999, which revealed the temporal dynamics and genetic diversity in

the world, whereas the prototype was sampled in 1958 (Oberste et al., 1999b; Palacios et al., 2002). There were several reports of encephalitis caused by E-30 worldwide (Wang et al., 2002; Cabrerizo et al., 2008; dos Santos et al., 2011; Kim et al., 2012; Milia et al., 2013), and the E-30 isolates were frequently detected from cases of encephalitis, indicating epidemiological relationship between E-30 and encephalitis. In rare cases, it can cause cute myalgia, rhabdomyolysis, and acute flaccid paralysis in immunosuppressed transplant recipients (Mauri et al., 2019; Sousa et al., 2019).

In 2001, an outbreak of encephalitis occurred in Taiwan, China. One thousand one hundred thirty cases of enterovirus infection were reported, and the detection rate of E-30 was 16.6% (Wang et al., 2002). In Jiangsu Province of China in 2003, 1,681 patients with encephalitis were reported, and E-30 was confirmed as the etiologic agent of this outbreak (Zhao et al., 2005). Similar incidences of E-30 outbreaks were reported in Shandong Province of China, showing that E-30 was a major pathogen in encephalitis patients (Tao et al., 2014). The outbreaks of E-30, which were closely associated with encephalitis, were also frequently reported in other parts of the world, including Italy, Bulgaria, France, United Kingdom, Spain, Brazil, and Korea (Cabrerizo et al., 2008; Yang et al., 2013; Mladenova et al., 2014; Holmes et al., 2016). Surprisingly, a recent report showed that E-30 was detected in an outbreak of acute myalgia and rhabdomyolysis, indicating that E-30 possibly caused severe non-neuropathic diseases and that E-30 could cause a variety of clinical symptoms (Sousa et al., 2019).

In this study, we have described a large-scale outbreak of E-30 associated with viral meningitis, fever, headache, nausea, and vomiting symptoms, which led to aggregated cases in Gansu province of China in 2015. The clinical features, molecular epidemiological characteristics, and evolutionary dynamics of this outbreak were analyzed. Furthermore, the detailed transmission patterns were tracked to illustrate the prevalence scope and extent of occurrence of E-30 in China. This is the first report about encephalitis caused by E-30 in the northwest region of China. The investigation provides further insight into the epidemiological patterns and evolutionary history of E-30 in China.

## MATERIALS AND METHODS

### Case Definition and Investigation

The probable cases were reported, and samples of patients were referred to the laboratories for pathogen detection. The local Centers for Disease Control and Prevention (CDC)

staffs collected the clinical samples in several local hospitals that have patients with viral encephalitis; the use of their clinical samples was explained to the guardians of children, and written consent was signed by guardians of children for permitting analysis of their clinical samples. Patients were classified as having viral encephalitis infection in Gansu province between June 27 and August 5 of 2015 if they had encephalitis, high fever ( $\geq 38^{\circ}\text{C}$ ), nausea, vomit, and other neurological symptoms, such as seizures, unconsciousness, and autonomic nervous system dysregulation (**Figure 1**). Following this outbreak, 101 suspected cases were recognized by HFMD surveillance system. A total of 95 patients met the clinical diagnostic criteria of encephalitis according to their clinical manifestations (**Table 1**). The representative clinical samples from the 74 probable patients were collected for lab detection (**Figure 1**). We have excluded the common infections of Japanese encephalitis virus, adenovirus, mumps virus, and human herpesvirus hominis using ELISA immunoglobulin M

(IgM) method and real-time quantitative reverse transcription polymerase chain reaction (qRT-PCR).

### Sample Collection and Viral Isolation

For the purpose of public health under the investigation of the National Health Commission of the People's Republic of China, we collected the feces ( $n = 27$ , 20.5%), serum ( $n = 66$ , 50%), throat swab ( $n = 25$ , 18.9%), and cerebrospinal fluid ( $n = 14$ , 10.6%). Real-time RT-PCR method was used to directly detect the enterovirus genome in clinical samples, with public probe and primers used (Cui et al., 2013; Zhang S. et al., 2014). We defined a laboratory-confirmed patient with laboratory evidence of enteroviruses infection. The positive samples were cultured and processed according to the standard procedures described before and were then inoculated into human rhabdomyosarcoma (RD) cells and human laryngeal epidermoid carcinoma (HEp-2) cells, provided by the WHO Global Poliovirus Specialized Laboratory for viral isolation. Infected cell cultures were harvested once

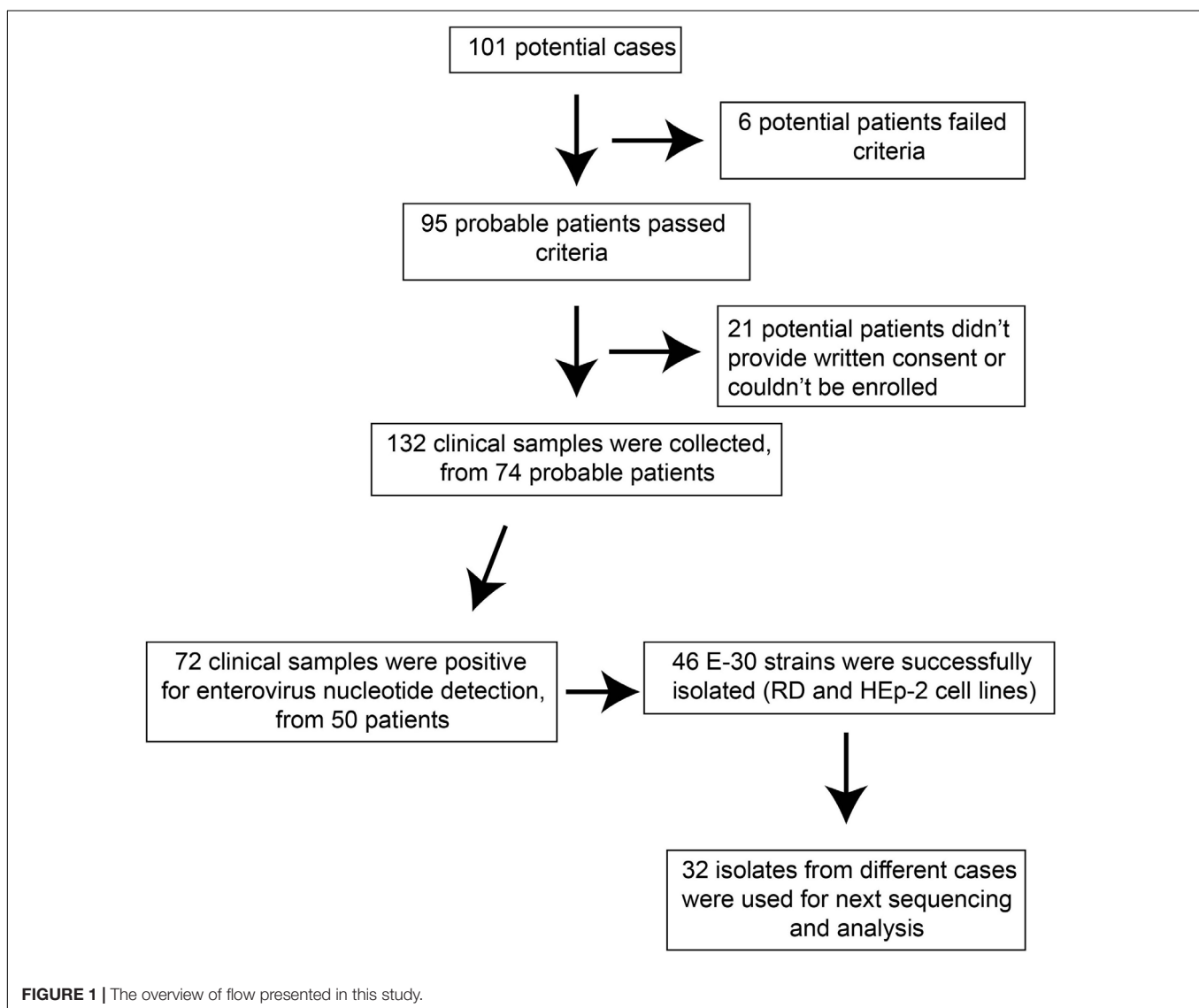


**TABLE 1** | The demographic characteristics of probable cases and laboratory-confirmed cases from the encephalitis outbreak in Gansu, 2015.

	Probable cases	Laboratory-confirmed cases
<b>Age group (n,%)</b>		
≤5	10 (10.5%)	9 (18%)
6–10	49 (51.6%)	22 (44%)
11–15	27 (28.4%)	12 (24%)
≥16	9 (9.5%)	7 (14%)
<b>Symptoms (n,%)</b>		
High fever (≥ 38°C)	95 (100%)	48 (96%)
Headache	28 (29.5%)	12 (24%)
Nausea and vomit	58 (61.1%)	34 (68%)
Neurological symptoms (listlessness and unconsciousness)	59 (62.1%)	30 (60%)
<b>Sex (n,%)</b>		
Male	62 (65.3%)	34 (68%)
Female	33 (34.7%)	16 (32%)
<b>Region (town)</b>		
Nancha	43 (45.3%)	21 (42%)
Guangzhi	24 (25.3%)	17 (34%)
Other	28 (29.5%)	12 (24%)
<b>Total</b>	95	50

complete EV-like cytopathic effect (CPE) was observed. All experimental protocols were carried out in accordance with the approved guidelines by WHO, as were reported before (Yan et al., 2010; Zhang et al., 2010b; Burns et al., 2013; Luo et al., 2013). As a result, 46 E-30 strains were harvested, with complete EV-like CPE. Subsequently, we randomly selected 32 isolates sampled from different patients for sequencing and phylogenetic analysis (Figure 1).

## Sequencing and Molecular Typing

Viral RNA was extracted from the cell cultures using the QIAamp Viral RNA Mini Kit (Qiagen, Germany). Reverse transcription PCR was performed to amplify the entire *VP1* coding region using the PrimeScript One-Step RT-PCR Kit, Ver.2 (TakaraBio, Dalian, China) using primers 490–493 as described before (Oberste et al., 2006). The entire *VP1* region of the amplicons was sequenced using ABI 3130 Genetic Analyzer (Applied Biosystems, Foster City, CA, United States). Using the BLAST server and the EV Genotyping Tool, the *VP1* sequences were analyzed to determine the serotypes (Kroneman et al., 2011). The genome sequence of the entire *VP1* region has been deposited in the GenBank database under accession number MN590241–MN590272.

## Phylogenetic Analysis

For molecular epidemiology study of E-30, the entire *VP1* sequences of E-30 from GenBank database were downloaded (~1,400 sequences available until April 2019). First, based on the entire *VP1* coding region of E-30, we constructed the maximum likelihood phylogenetic tree and randomly selected the representative strains of E-30 from each branch of phylogenetic tree. In addition, the representative sequences should cover

more regions to obtain higher geographical representation and cover each cluster of phylogenetic trees for obtaining higher phylogenetic representation. Second, the datasets were filtered by discarding the low-quality sequences and incomplete genome sequences. At last, we randomly selected 36 representative entire *VP1* sequences for genotyping, including an E-21 sequence as an outgroup. To assess the mean genetic distance among different genotypes, we calculated the mean genetic distance between genotypes and within each genotype using the Kimura two-parameter model.

In general, 25% of the genome difference of enterovirus is used as the criteria for serotyping, while 15% of the genome difference is used as the criteria for genotyping; this is widely accepted for serotyping and genotyping of enterovirus, such as EV-A71, CV-A16, and CV-A6 (Brown et al., 1999; Oberste et al., 1999a,b; Mizuta et al., 2005; Zhang et al., 2010a, 2013; Song et al., 2017). We refer to the published genotyping criteria of EV-A71, CV-A16, and CV-A6 and combined with the latest research progress of E-30 (Lema et al., 2019; Maruo et al., 2019; Mauri et al., 2019; Sousa et al., 2019). In addition to being able to better represent the E-30 sequences in the world, we also avoid the redundancy sequences of E-30 for genotyping, which leads to the confusion and divergence of enterovirus genotyping.

A total of 446 entire *VP1* genome sequences acquired from China (until April 2019), which were extracted from ~1,400 entire *VP1* genome sequence pools with known sampling dates and locations in the world, were used to analyze the phylodynamic in China (Supplementary Table S1). Genome sequences were aligned using the Muscle method implemented in MEGA software (version 7.0) (Kumar et al., 2016). The topology of maximum likelihood phylogenetic tree was assessed using the RaxML software (version 8.0) (Stamatakis, 2014).

Using Bayesian inference method implemented in BEAST software (version 1.8.4), the maximum clade credibility (MCC) tree and the coalescent-based Gaussian Markov random field (GMRF) skyride plots were inferred, with the genome substitution model of GTR + I +  $\Gamma$  supported by the ModelGenerator (version 0.85) (Drummond et al., 2012). The randomization tests in R package (version 3.5.0) using the TipDatingBeast package were performed to determine the temporal signal in the data (Rieux and Khatchikian, 2017). Sufficient temporal signals of datasets are confirmed when 95% credibility intervals of rate estimation of real datasets do not fall into the 95% credibility intervals of rate estimation from date randomized replicates (Supplementary Figure S1). Sampling times of the sequences available were used to calibrate the molecular clock. A total of 15 dataset analyses was run combined with one genome substitution model, three different clock models, and five different Coalescent tree priors. The path sampling (PS) and stepping stone sampling (SS) analysis, which showed the marginal likelihood estimation results, were implemented in BEAST to choose the best parameters of Bayesian phylogenetic models (Supplementary Figure S2) (Baele et al., 2012). We checked the convergence and effective sample size (>200) of the parameters with Tracer software (version 1.7) (Rambaut et al., 2018). The output trees were summarized using the maximum clade credibility (MCC) topology from

TreeAnnotator software (version 1.8.4), with a burn-in of the first 10% of sampled trees. To assess demographic dynamics of E-30 in mainland of China, the GMRF method with time-aware smoothing parameter was used to investigate the past population dynamics. The GMRF skyride plots were summarized and visualized using Tracer software (version 1.7.1) (Rambaut et al., 2018). The ggtree (version 1.16.3) was used to manipulate the phylogenetic tree for best performance (Yu et al., 2017).

## Ethics Statement

Written informed consent for the use of their clinical samples was obtained from all individuals or their guardians included in the study. The study was also supported by the Second Ethics Review Committee of the National Institute for Viral Diseases Control and Prevention, Chinese Center for Diseases Control and Prevention.

## RESULTS

### Demographic and Clinical Characteristics of Large-Scale Outbreak Associated With E-30

A large-scale encephalitis outbreak caused by E-30 was confirmed through clinical characteristics, epidemiological evidences, and laboratory diagnosis. We defined the potential probable patients ( $n = 101$ ), probable cases ( $n = 95$ ), and laboratory-confirmed cases ( $n = 50$ ) during epidemiological investigation (Figure 1 and Table 1). Among the probable cases ( $n = 95$ ), male outnumbered female patients, with the ratio of male to female being 188% (Table 1). All cases had high fever ( $\geq 38^\circ\text{C}$ ), and headache accounted for 29.5% of all suspected cases. Of all the probable cases ( $n = 95$ ), 61.1 and 62.1% had nausea, vomiting, and neurological appearance (listlessness and unconsciousness), respectively. Of the total number of probable cases ( $n = 95$ ), 10.5% were children aged  $\leq 5$ . Children aged 6–10 years accounted for the highest percentage at 51.6%, followed by children 11–15 years of age (28.4%). Children aged  $\geq 16$  only accounted for 9.5%. Several probable cases ( $n = 82$ , 86.3%) were school students, while other 13 cases were from different professions, including farmers (Table 1 not shown). From the geographical distribution angle, the Nancha town and Guangzhi town constituted 45.3 and 25.3% within the probable cases ( $n = 95$ ), respectively, whereas seven other towns only accounted for 29.5% within the probable cases. A total of 60% (9/15) towns of this prefecture were attacked by the large-scale infectious disease outbreak.

Among the laboratory-confirmed cases ( $n = 50$ ), the male outnumbered female patients, with a proportion of 210% (Figure 1 and Table 1). The ratios of demographic characteristics between probable cases and lab-confirmed cases were similar (Table 1). The collective outbreak, which presented similar symptoms for all patients and showed rapid diffusion in a short timescale, exhibited the increasing transmission ability of E-30 (Figure 2). The major period of E-30 transmission, which caused the most infection and outbreak, is July. A total of 91 probable cases were reported in July and August, constituting

95.8% (91/95) of total probable cases ( $n = 95$ ). It is consistent with the detected proportion of laboratory-confirmed cases and E-30 isolation. From the opening phase of E-30 transmission, E-30 spread to nine towns using only 1-month timescale, indicating the rapid transmission ability.

### The Detection and Isolation Results of E-30 Outbreak

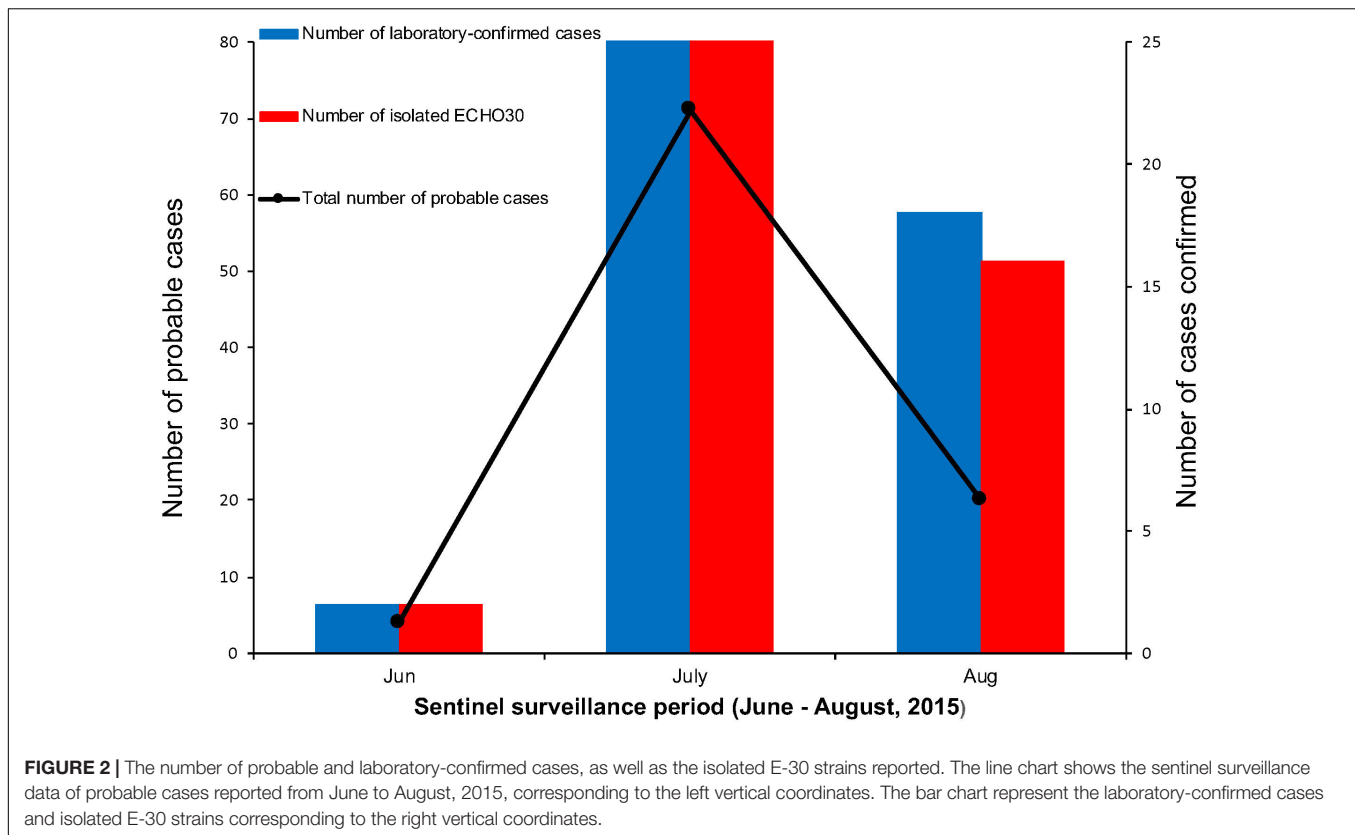
In these clinical samples, 54.5% (72/132) were positive for EV genome detection (Table 2). The positive number of EV genome detection for feces, serum, throat swab, and cerebrospinal fluid are 22 (81.5%), 15 (22.7%), 24 (96%), and 11 (78.6%), respectively. We tried to inoculate RD and HEp-2 cell lines with all positive samples of enterovirus nucleic acid and showed different proportions of isolation of E-30 with total viral isolation ratio of 63.9% (46/72); 12 feces samples (44.4%), 0 serum samples (0%), 24 throat swabs (96%), and 10 cerebrospinal fluid samples (71.4%) were successfully used to isolate E-30 strains. About 10 randomly selected serum samples were subjected to ELISA IgM test, out of which 50% (5/10) serum samples tested positive for CV IgM.

### The Genotype Identification of the E-30 Outbreak

We used 36 entire *VPI* coding region sequences, including one E-21 genome sequence as an outgroup for genotyping (see section “Materials and Methods”). The neighbor-joining phylogenetic tree, based on the 36 entire *VPI* genome sequences with 1,000 bootstrap replicates, was constructed. According to the criteria of difference of at least 15% genetic distance over the entire *VPI* sequence, the genotype of E-30 are segregated into three distinct genotypes designated as genotype A, B, and C (Figure 3). The outgroup of E-21 strain and E-30 prototype strain isolated from America in 1958 formed a single genotype, respectively, and differed from other genotypes by 19.2–21.5%. The genotype B, which consisted of several strains isolated from many regions between 1979 and 2010, such as France, Netherlands, United States, Taiwan of China, and other regions, showed 16–21.5% genetic distance compared with other genotypes. The genotype C, which revealed the genetic differences between 16 and 19.2% among different genotypes, primarily was composed of Chinese isolates ranging from 2003 to 2016, besides two strains of E-30 from Russia. The mean genetic divergence within the genotype B and C showed 7 and 10.1%, respectively.

### Molecular Epidemiological Characteristics of E-30 in China

The midpoint-rooted maximum likelihood phylogenetic tree showed that two lineages (lineage 1–2) circulated in China (Figure 4B). The mean genetic distance between the two lineages, which was calculated using the Kimura two-parameter model, is 18.1% and is larger than the mean genetic distance within these two lineages (7.3 and 9.6%), indicating the reliability of lineages division. The lineage 1, which circulated in the mainland of China and Taiwan of China earlier, consisted of fewer E-30 isolates recently and was infrequently detected in China. The



strains of lineage 1 seemed to be disappearing in recent years, indicating that the E-30 evolved in nearly 20 years. However, the lineage 2, which circulated in China from 2003 till present, comprised mostly E-30 strains isolated from the mainland of China, including the encephalitis outbreak isolates of this study (Figure 4A, colored in red). The *VPI* genome sequences of these strains isolated from this study showed high similarity, with 99.3–100% identity among these *VPI* sequences. The close phylogenetic relationship, as shown in the maximum likelihood tree, also confirmed the occurrence of collective outbreak.

## Evolutionary Characteristics of E-30 in China

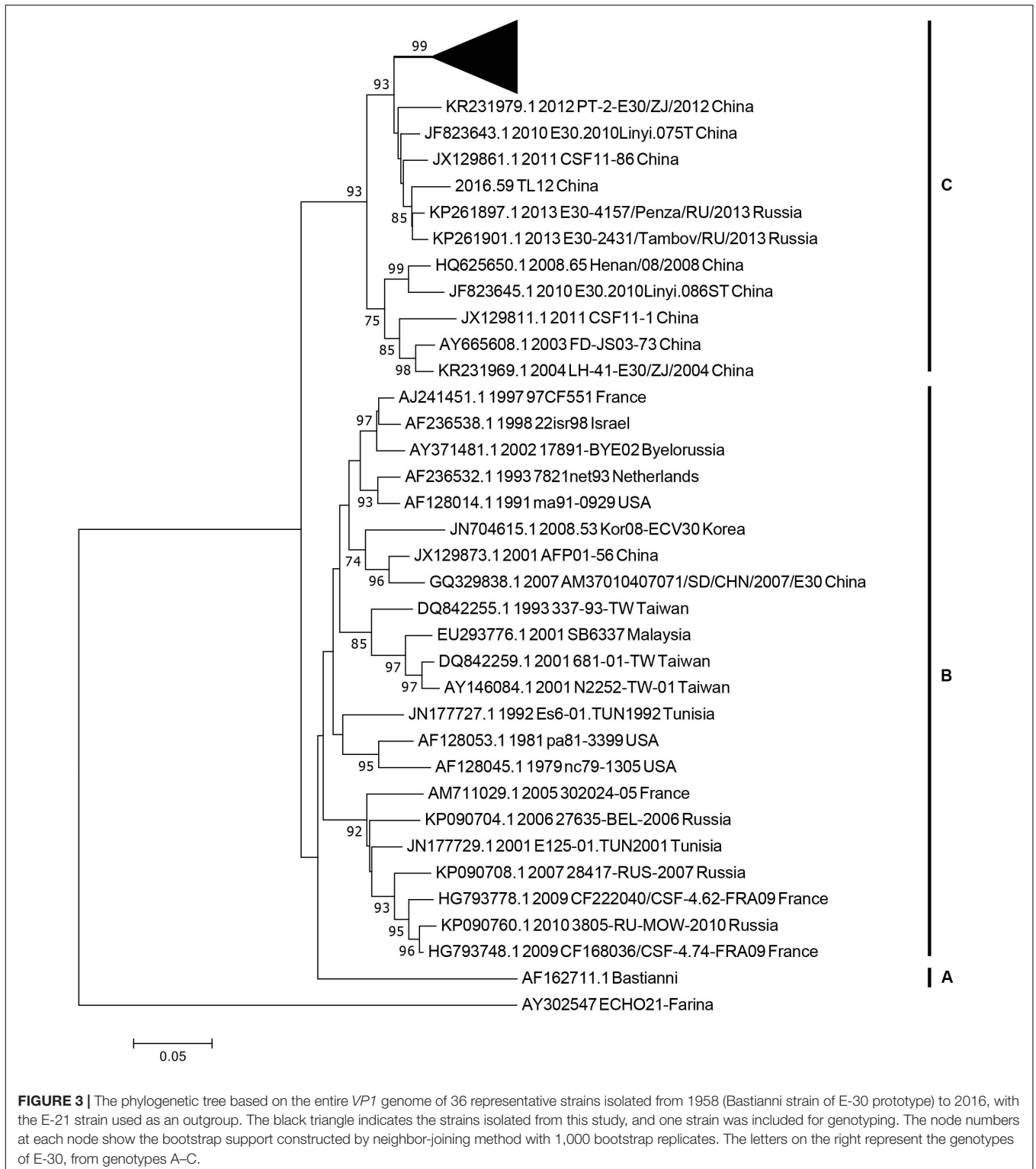
The MCC phylogenetic tree of 446 entire *VPI* coding region sequences of E-30, sampled from 1988 to 2016 in China, formed a ladder-like phylogenetic tree topology colored by

locations of isolation. The MCC phylogenetic tree classified all E-30 strains into two lineages (lineage 1–2), consistent with the maximum likelihood phylogenetic tree described above (Figure 5B). The Bayesian phylogenetic analysis show that lineage 2 still dominated in China, whereas lineage 1 seemed to be disappearing. As shown in Figure 5, each clade did not locate in only one province, illustrating that E-30 transmitted and spread in several regions. Sporadic importing and exporting of cases among provinces of China were monitored, showing a certain level of genetic flow of E-30 among different regions. The clades of MCC phylogenetic tree, covering several provinces, showed a more complex distribution phenomenon compared with CV-B3 geographical distribution reported before (Han et al., 2019). For example, the strains isolated from Yunnan province almost located at each clade of MCC phylogenetic tree, indicating that the E-30 spread widely in China (Figure 5B, colored in light green).

The evolutionary dynamics of E-30 in China was estimated using a Bayesian method with relaxed molecular clock, including their evolutionary rate, tMRCA, and phylodynamic. The substitution rate for the *VPI* coding region of E-30 is  $6.54 \times 10^{-3}$  substitutions per site per year [95% highest posterior density (HPD),  $5.76 \times 10^{-3}$ – $7.33 \times 10^{-3}$ ], which is lower than the *VPI* evolutionary rate of EV-A71 and CV-A6 reported by others (McWilliam Leitch et al., 2012; Anh et al., 2018). However, the median value of substitutions rate of *VPI* sequences is slightly larger than that of CV-B3, indicating that the E-30 relatively evolved compared with CV-B3, whereas 95% HPD

**TABLE 2 |** Genome detection and viral isolation results of the encephalitis outbreak in Gansu Province, 2015.

Species	Numbers	Positive number of EV	Number of isolated E-30*
Feces	27	22 (81.5%)	12 (44.4%)
Serum	66	15 (22.7%)	0 (0%)
Throat swab	25	24 (96%)	24 (96%)
Cerebrospinal fluid	14	11 (78.6%)	10 (71.4%)
Total	132	72 (54.5%)	46 (34.9%)



values of CV-B3 cover the threshold value of E-30 (Han et al., 2019). According to the estimated molecular clock, the common ancestor of lineage 1 was dated to about July of 1986 (95% HPD, November 1985–February 1987), whereas the strains of E-30 were isolated first in Taiwan of China in 1988. The isolates

of lineage 2, which was estimated for tMRCA of April 2001 (95% HPD, June 2000–November 2001), emerged in Jiangsu and Shandong Province first in 2003. The results showed that E-30 had transmitted in China for approximately 2 years before it was detected in China.

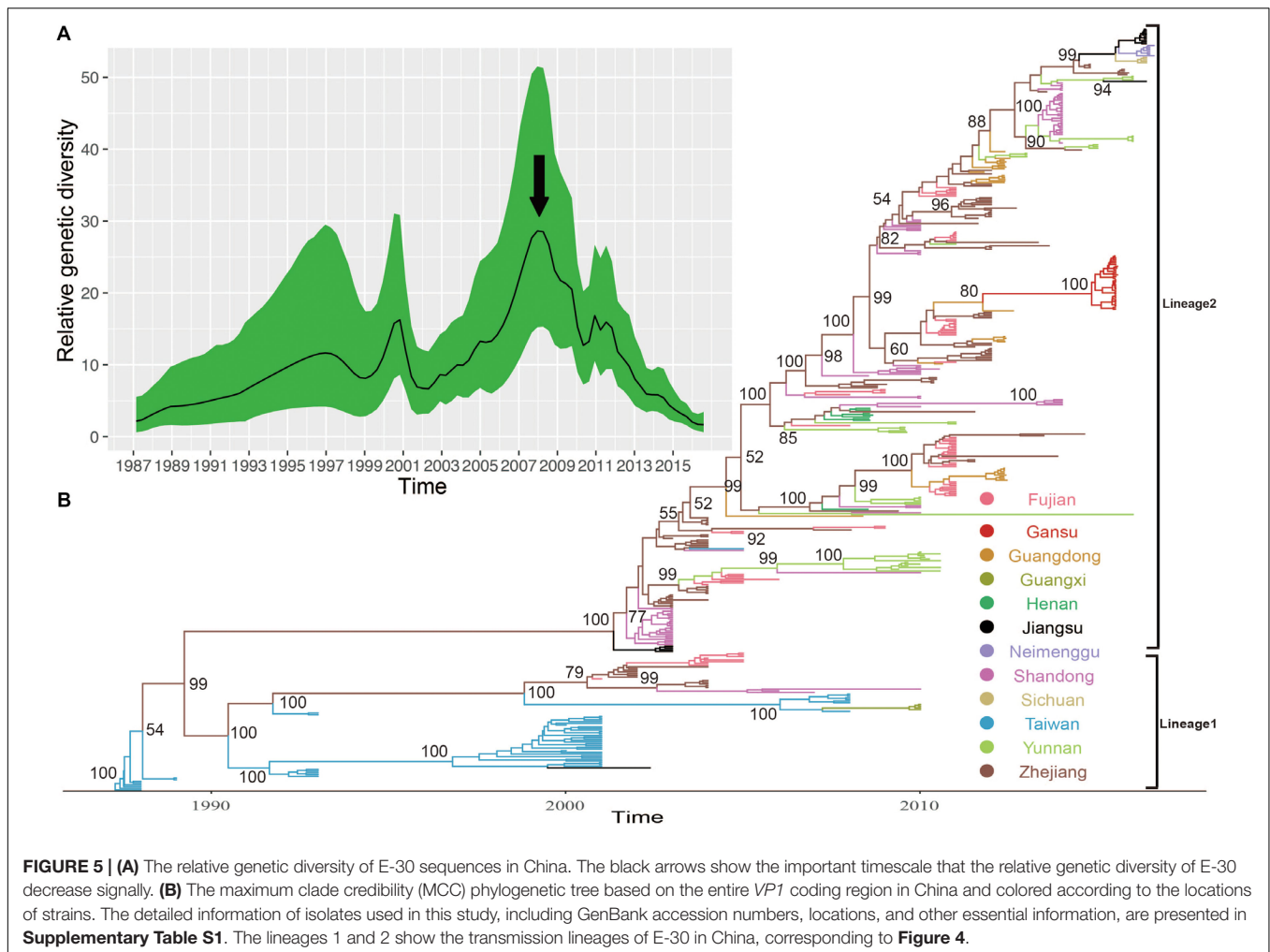


Based on the *VP1* coding region, the coalescent reconstruction revealed the oscillating patterns on the genetic diversity of Chinese E-30 from 1996 onward (Figure 5A). The results showed that the genetic diversity of E-30 in China experienced two large expansions besides three small increases. In 2000 and 2008 nearby, the genetic diversity of E-30 arrived at the top and subsequently decreased dramatically. The increases of genetic diversity in 2000 were primarily associated with E-30 outbreaks in Taiwan of China, with 16.6% detection ratios of E-30 in 1130 enterovirus-infected patients with encephalitis (Wang et al., 2002). The E-30 strains isolated from Zhejiang, Fujian, Shandong, and Jiangsu Provinces closely clustered with the isolates from Taiwan of China (Zhao et al., 2005; Wang et al., 2006). With the decrease in relative genetic diversity of E-30 after 2008, it was coincided with the construction of hand, foot, and mouth pathogen surveillance net of China in 2008. The genetic diversity also showed a dynamic fluctuation between 2009 and 2012, especially the small-scale epidemics in 2011, revealing the transmission activities of E-30 among provinces. From 2012 till present, the population dynamics of E-30 showed weaker

fluctuations over time, whereas it locally caused a large-scale outbreak in Gansu Province in 2015.

## DISCUSSION

Although E-30 outbreaks were recorded in China, the deep evolutionary characteristics of E-30 remained unclear (Zhao et al., 2005; Tao et al., 2014; Chen et al., 2017, 2018). To assess the phylogenetic dynamic of E-30 in China and provide insight of E-30 evolution, we performed deep analysis for revealing the epidemiological features and transmission models. Our analysis revealed that this outbreak affected nine towns of the prefecture of Gansu Province and caused a severe infectious disease transmission. The Nancha town of Gansu Province has the most infected patients. The outbreak of E-30 started at a school in Nancha town in June and gradually spread to other towns in July, with a strong transmission ability. The cases reported presented common clinical symptoms, including high fever ( $\geq 38^{\circ}\text{C}$ ), nausea, vomiting, and neurological appearance



(listlessness and unconsciousness), indicating a major clinical characteristics of E-30 surveillance. Males comprise higher ratio, with 65.3 and 68% cases in probable cases panel and laboratory-confirmed cases panel, respectively. Children aged between 0 and 15 accounted for 90.5 and 86% in probable cases panel and laboratory-confirmed cases panel, respectively. The results show that children are more easily attacked by E-30 infection, which is consistent with other enterovirus infections (Xing et al., 2014; Huang et al., 2018). However, the age group between 6 and 15 constituted the highest ratio. In the process of laboratory test, the throat swabs, cerebrospinal fluids, and feces presented high detection ratios, with the proportion of 96, 78.6, and 81.5%, respectively. However, the serum samples are not good samples for viral isolation compared with other clinical samples; therefore, when collecting clinical samples during E-30 outbreak, investigators do not collect serum for virus isolation.

The analysis of entire *VP1* sequences of chosen strains have shown that genotypes B and C have been cocirculating in the world and are responsible for many E-30 outbreaks (Wang et al., 2002; Kim et al., 2012; Yang et al., 2013; Maruo et al., 2019). Genotype C plays a leading role in the transmission of

E-30 in China, including the strains of E-30 outbreak reported in this study. It is now evolving and spreading in different provinces of China. Two lineages (lineage 1–2) were formed in China, which have played an causal role in encephalitis outbreaks (Wang et al., 2002; Zhao et al., 2005; Yang et al., 2013; Tao et al., 2014; Chen et al., 2017). The strains of lineage 2 have been isolated from many provinces of China, such as Zhejiang, Guangdong, Shandong, Henan, Fujian, and Sichuan provinces. This lineage, diffusing in many provinces of China, evolved rapidly and caused several encephalitis outbreaks. For example, 1,681 encephalitis patients were reported in Jiangsu Province in 2003, and E-30 was confirmed as an etiologic agent of the outbreak (Zhao et al., 2005). It was also reported as a major pathogen of encephalitis cases in Shandong Province of China between 2006 and 2012 (Tao et al., 2014). From the maximum likelihood phylogenetic tree, spatial transmission events of E-30 were confirmed, and many sublineages cocirculated in several different regions of China. For example, the strains (GenBank accession number JX129864) isolated from Fujian Province cluster with the strains from Guangdong Province (GenBank accession number KC867102) (**Figure 4A**). This phenomenon was also observed in several other regions of China. The strain

of 45R (GenBank accession number LC201508), which was isolated from Yunnan province in 2016, was encompassed by the strains (GenBank accession number KY048011-KY048043) isolated from Shandong Province. The 99.3–100% genome similarity based on the *VPI* genome of this study confirmed the occurrence of collective outbreak, although the strains were isolated from different towns of Gansu province.

Using the Bayesian phylogenetic inference method, the evolutionary dynamics of E-30 were analyzed. Sporadic importing and exporting of cases were observed in several provinces of China, indicating that E-30 transmitted through different regions and that the gene flow of E-30 among different provinces was apparent. The substitution rate of *VPI* coding region of E-30 is higher than that of CV-B3, indicating the relatively faster evolution extent of E-30 as compared to CV-B3 (Han et al., 2019). The low substitution rate, compared with EV-A71 and CV-A6, revealed relatively slower evolutionary levels, implying less possibility of outbreaks (McWilliam Leitch et al., 2012; Geoghegan et al., 2015; Anh et al., 2018). The timespan for the emergence of lineages 1 and 2 was 15 years, indicating chronic transmission and evolution. Two larger expansions of relative genetic diversity in China were observed, whereas three small-scale fluctuations were confirmed. From 1996 onward, the oscillating patterns of E-30 presented a complicated phenomenon. With the increase in genetic diversity, the outbreak possibility of E-30 increased, as the genetic diversity provided the breeding grounds for subsequent outbreaks. For example, the genetic diversity of E-30 isolated in Taiwan of China increased remarkably in 2000, followed by a large outbreak of E-30 in Taiwan of China in 2001. Based on the evidence from our data, the E-30 strains isolated from mainland of China possibly originated from Taiwan of China through population movement in last century. The coastal provinces, such as Zhejiang, Fujian, and Shandong, were primary regions infected, followed by spreading to the nationwide regions.

It is important to mention here that the results of this study, which is based on the molecular epidemiological data currently available, including the *VPI* genome sequences of China, could change slightly in the future when more information will become available. The perfect HFMD pathogen surveillance system was significant for preventing infections, as was supported by the relative genetic diversity reduction after the surveillance net was built. The E-30 surveillance system has not been built yet in several countries of the world, which hinders the formulation of countermeasures for E-30 associated with encephalitis outbreaks. The basic research efforts and current surveillance should be strengthened to help understand and develop effective medical countermeasures (Gao, 2018).

## REFERENCES

Adams, M. J., Lefkowitz, E. J., King, A. M. Q., Harrach, B., Harrison, R. L., Knowles, N. J., et al. (2017). Changes to taxonomy and the international code of virus classification and nomenclature ratified by the international committee on taxonomy of viruses (2017). *Arch. Virol.* 162, 2505–2538.

## DATA AVAILABILITY STATEMENT

The datasets generated for this study can be found in the GenBank database, MN590241–MN590272.

## ETHICS STATEMENT

The studies involving human participants were reviewed and approved by the Second Ethics Review Committee of the National Institute for Viral Diseases Control and Prevention, Chinese Center for Diseases Control and Prevention. Written informed consent to participate in this study was provided by the participants' legal guardian/next of kin.

## AUTHOR CONTRIBUTIONS

DY and YZ conceived and designed the experiments. JC and ZH performed the experiments. ZH, HW, and WX analyzed the data. JC and ZH wrote the main manuscript. ZH prepared all the tables and figures. All authors reviewed the manuscript.

## FUNDING

This study was supported by the National Key Technology R&D Program of China (Project Nos. 2017ZX10104001, 2017ZX10103006, and 2018ZX10711001). We thank the funding received from Key Technologies R&D Program of the National Ministry of Science (Project Nos. 2018ZX10713002 and 2018ZX10713001-003). The funding body was not involved in the design of the study, clinical sample collection, data analysis and interpretation, or writing of the manuscript.

## ACKNOWLEDGMENTS

We would like to acknowledge the staffs of the Guazhou County Center for Disease Control and Prevention in Gansu Province for collecting the clinical samples and conducting the epidemiological investigations.

## SUPPLEMENTARY MATERIAL

The Supplementary Material for this article can be found online at: <https://www.frontiersin.org/articles/10.3389/fmicb.2020.01137/full#supplementary-material>

Anh, N. T., Nhu, L. N. T., Van, H. M. T., Hong, N. T. T., Thanh, T. T., Hang, V. T. T., et al. (2018). Emerging coxsackievirus A6 causing hand, foot and mouth disease, vietnam. *Emerg. Infect. Dis.* 24, 654–662.

Baele, G., Lemey, P., Bedford, T., Rambaut, A., Suchard, M. A., and Alekseyenko, A. V. (2012). Improving the accuracy of demographic and molecular clock model comparison while accommodating phylogenetic uncertainty. *Mol. Biol. Evol.* 29, 2157–2167. doi: 10.1093/molbev/mss084

- Bergamini, G., Preiss, T., and Hentze, M. W. (2000). Picornavirus IRESes and the poly(A) tail jointly promote cap-independent translation in a mammalian cell-free system. *RNA* 6, 1781–1790. doi: 10.1017/s1355838200001679
- Brown, B. A., Oberste, M. S., Alexander, J. P. Jr., Kennett, M. L., and Pallansch, M. A. (1999). Molecular epidemiology and evolution of enterovirus 71 strains isolated from 1970 to 1998. *J. Virol.* 73, 9969–9975. doi: 10.1128/jvi.73.12.9969-9975.1999
- Burns, C. C., Shaw, J., Jorba, J., Bukbuk, D., Adu, F., Gumedé, N., et al. (2013). Multiple independent emergences of type 2 vaccine-derived polioviruses during a large outbreak in northern Nigeria. *J. Virol.* 87, 4907–4922. doi: 10.1128/jvi.02954-12
- Cabrerizo, M., Echevarria, J. E., Gonzalez, I., De Miguel, T., and Trallero, G. (2008). Molecular epidemiological study of HEV-B enteroviruses involved in the increase in meningitis cases occurred in Spain during 2006. *J. Med. Virol.* 80, 1018–1024. doi: 10.1002/jmv.21197
- Chen, P., Lin, X., Liu, G., Wang, S., Song, L., Tao, Z., et al. (2018). Analysis of enterovirus types in patients with symptoms of aseptic meningitis in 2014 in Shandong, China. *Virology* 516, 196–201. doi: 10.1016/j.virol.2018.01.022
- Chen, P., Tao, Z., Song, Y., Liu, G., Wang, H., Liu, Y., et al. (2013). A coxsackievirus B5-associated aseptic meningitis outbreak in Shandong province, China in 2009. *J. Med. Virol.* 85, 483–489. doi: 10.1002/jmv.23478
- Chen, Y., Sun, Y., Yan, J., Miao, Z., Xu, C., Zhang, Y., et al. (2017). Molecular Epidemiology and prevalence of echovirus 30 in Zhejiang Province, China, from 2002 to 2015. *J. Microbiol. Biotechnol.* 27, 2221–2227. doi: 10.4014/jmb.1707.07016
- Cui, A., Xu, C., Tan, X., Zhang, Y., Zhu, Z., Mao, N., et al. (2013). The development and application of the two real-time RT-PCR assays to detect the pathogen of HFMD. *PLoS One* 8:e61451. doi: 10.1371/journal.pone.0061451
- dos Santos, G. P., Da Costa, E. V., Tavares, F. N., Da Costa, L. J., and Da Silva, E. E. (2011). Genetic diversity of Echovirus 30 involved in aseptic meningitis cases in Brazil (1998–2008). *J. Med. Virol.* 83, 2164–2171. doi: 10.1002/jmv.22235
- Drummond, A. J., Suchard, M. A., Xie, D., and Rambaut, A. (2012). Bayesian phylogenetics with BEAUti and the BEAST 1.7. *Mol. Biol. Evol.* 29, 1969–1973. doi: 10.1093/molbev/mss075
- Gao, G. F. (2018). From “A”IV to “Z”IKV: attacks from emerging and Re-emerging pathogens. *Cell* 172, 1157–1159. doi: 10.1016/j.cell.2018.02.025
- Geoghegan, J. L., Tan Le, V., Kuhnert, D., Halpin, R. A., Lin, X., Simenauer, A., et al. (2015). Phylodynamics of enterovirus A71-associated hand, foot, and mouth disease in viet nam. *J. Virol.* 89, 8871–8879.
- Han, J. F., Jiang, T., Fan, X. L., Yang, L. M., Yu, M., Cao, R. Y., et al. (2012). Recombination of human coxsackievirus B5 in hand, foot, and mouth disease patients, China. *Emerg. Infect. Dis.* 18, 351–353. doi: 10.3201/eid1802.111524
- Han, Z., Zhang, Y., Huang, K., Cui, H., Hong, M., Tang, H., et al. (2018). Genetic characterization and molecular epidemiological analysis of novel enterovirus EV-B80 in China. *Emerg. Microb. Infect.* 7:193.
- Han, Z., Zhang, Y., Huang, K., Wang, J., Tian, H., Song, Y., et al. (2019). Two Coxsackievirus B3 outbreaks associated with hand, foot, and mouth disease in China and the evolutionary history worldwide. *BMC Infect. Dis.* 19:466. doi: 10.1186/s12879-019-4107-z
- Holmes, C. W., Koo, S. S., Osman, H., Wilson, S., Xerry, J., Gallimore, C. I., et al. (2016). Predominance of enterovirus B and echovirus 30 as cause of viral meningitis in a UK population. *J. Clin. Virol.* 81, 90–93. doi: 10.1016/j.jcv.2016.06.007
- Huang, J., Liao, Q., Ooi, M. H., Cowling, B. J., Chang, Z., Wu, P., et al. (2018). Epidemiology of recurrent hand, foot and mouth disease, China, 2008–2015. *Emerg. Infect. Dis.* 24, 432–442.
- Kim, H. J., Kang, B., Hwang, S., Hong, J., Kim, K., and Cheon, D. S. (2012). Epidemics of viral meningitis caused by echovirus 6 and 30 in Korea in 2008. *Virology* 438, 38–43. doi: 10.1016/j.virol.2012.03.038
- Kroneman, A., Vennema, H., Deforche, K., Avoort, H., Penaranda, S., Oberste, M. S., et al. (2011). An automated genotyping tool for enteroviruses and noroviruses. *J. Clin. Virol.* 51, 121–125. doi: 10.1016/j.jcv.2011.03.006
- Kumar, S., Stecher, G., and Tamura, K. (2016). MEGA7: molecular evolutionary genetics analysis version 7.0 for bigger datasets. *Mol. Biol. Evol.* 33, 1870–1874. doi: 10.1093/molbev/msw054
- Lema, C., Torres, C., Van Der Sanden, S., Cisterna, D., Freire, M. C., and Gomez, R. M. (2019). Global phylodynamics of echovirus 30 revealed differential behavior among viral lineages. *Virology* 531, 79–92. doi: 10.1016/j.virol.2019.02.012
- Luo, H. M., Zhang, Y., Wang, X. Q., Yu, W. Z., Wen, N., Yan, D. M., et al. (2013). Identification and control of a poliomyelitis outbreak in Xinjiang, China. *N. Engl. J. Med.* 369, 1981–1990.
- Maruo, Y., Nakanishi, M., Suzuki, Y., Kaneshi, Y., Terashita, Y., Narugami, M., et al. (2019). Outbreak of aseptic meningitis caused by echovirus 30 in Kushiro, Japan in 2017. *J. Clin. Virol.* 116, 34–38. doi: 10.1016/j.jcv.2019.05.001
- Mauri, E., Mastrangelo, A., Testa, S., Pellegriani, L., Pariani, E., Binda, S., et al. (2019). Acute flaccid paralysis due to Echovirus 30 in an immunosuppressed transplant recipient. *J. Neurovirol.* doi: 10.1007/s13365-019-00812-4
- McWilliam Leitch, E. C., Cabrerizo, M., Cardosa, J., Harvala, H., Ivanova, O. E., Koike, S., et al. (2012). The association of recombination events in the founding and emergence of subgenogroup evolutionary lineages of human enterovirus 71. *J. Virol.* 86, 2676–2685. doi: 10.1128/jvi.06065-11
- Milia, M. G., Cerutti, F., Gregori, G., Burdino, E., Allice, T., Ruggiero, T., et al. (2013). Recent outbreak of aseptic meningitis in Italy due to Echovirus 30 and phylogenetic relationship with other European circulating strains. *J. Clin. Virol.* 58, 579–583. doi: 10.1016/j.jcv.2013.08.023
- Mizuta, K., Abiko, C., Murata, T., Matsuzaki, Y., Itagaki, T., Sanjoh, K., et al. (2005). Frequent importation of enterovirus 71 from surrounding countries into the local community of Yamagata, Japan, between 1998 and 2003. *J. Clin. Microbiol.* 43, 6171–6175. doi: 10.1128/jcm.43.12.6171-6175.2005
- Mladenova, Z., Buttinelli, G., Dikova, A., Stoyanova, A., Troyancheva, M., Komitova, R., et al. (2014). Aseptic meningitis outbreak caused by echovirus 30 in two regions in Bulgaria, May–August 2012. *Epidemiol. Infect.* 142, 2159–2165. doi: 10.1017/s0950268813003221
- Oberste, M. S., Maher, K., Kilpatrick, D. R., Flemister, M. R., Brown, B. A., and Pallansch, M. A. (1999a). Typing of human enteroviruses by partial sequencing of VP1. *J. Clin. Microbiol.* 37, 1288–1293. doi: 10.1128/jcm.37.5.1288-1293.1999
- Oberste, M. S., Maher, K., Kilpatrick, D. R., and Pallansch, M. A. (1999b). Molecular evolution of the human enteroviruses: correlation of serotype with VP1 sequence and application to picornavirus classification. *J. Virol.* 73, 1941–1948. doi: 10.1128/jvi.73.3.1941-1948.1999
- Oberste, M. S., Maher, K., Michele, S. M., Belliot, G., Uddin, M., and Pallansch, M. A. (2005). Enteroviruses 76, 89, 90 and 91 represent a novel group within the species human enterovirus A. *J. Gen. Virol.* 86, 445–451. doi: 10.1099/vir.0.80475-0
- Oberste, M. S., Maher, K., Williams, A. J., Dybdahl-Sissoko, N., Brown, B. A., Gookin, M. S., et al. (2006). Species-specific RT-PCR amplification of human enteroviruses: a tool for rapid species identification of uncharacterized enteroviruses. *J. Gen. Virol.* 87, 119–128. doi: 10.1099/vir.0.81179-0
- Palacios, G., Casas, I., Cisterna, D., Trallero, G., Tenorio, A., and Freire, C. (2002). Molecular epidemiology of echovirus 30: temporal circulation and prevalence of single lineages. *J. Virol.* 76, 4940–4949. doi: 10.1128/jvi.76.10.4940-4949.2002
- Rambaut, A., Drummond, A. J., Xie, D., Baele, G., and Suchard, M. A. (2018). Posterior summarization in bayesian phylogenetics using tracer 1.7. *Syst. Biol.* 67, 901–904. doi: 10.1093/sysbio/syy032
- Rasti, M., Rastegarvand, N., Makvandi, M., Teimoori, A., and Azaran, A. (2019). Co-circulation of echovirus 6 and 30 with coxsackievirus A6 among children with hand, foot, and mouth disease in Ahvaz, Southwest Iran. *Arch. Clin. Infect. Dis.* 14:e83522.
- Rieux, A., and Khatchikian, C. E. (2017). tipdatingbeast: an R package to assist the implementation of phylogenetic tip-dating tests using beast. *Mol. Ecol. Resour.* 17, 608–613. doi: 10.1111/1755-0998.12603
- Rohll, J. B., Moon, D. H., Evans, D. J., and Almond, J. W. (1995). The 3' untranslated region of picornavirus RNA: features required for efficient genome replication. *J. Virol.* 69, 7835–7844. doi: 10.1128/jvi.69.12.7835-7844.1995
- Song, Y., Zhang, Y., Ji, T., Gu, X., Yang, Q., Zhu, S., et al. (2017). Persistent circulation of Coxsackievirus A6 of genotype D3 in mainland of China between 2008 and 2015. *Sci. Rep.* 7:5491.
- Sousa, I. P. Jr., Burlandy, F. M., Lima, S. T. S., Maximo, A. C. B., and Figueiredo, M. A. A. (2019). Echovirus 30 detection in an outbreak of acute myalgia and rhabdomyolysis, Brazil 2016–2017. *Clin. Microbiol. Infect.* 25:e255.
- Stamatidis, A. (2014). RAXML version 8: a tool for phylogenetic analysis and post-analysis of large phylogenies. *Bioinformatics* 30, 1312–1313. doi: 10.1093/bioinformatics/btu033
- Tao, Z., Song, Y., Li, Y., Liu, Y., Jiang, P., Lin, X., et al. (2012). Coxsackievirus B3, shandong province, China, 1990–2010. *Emerg. Infect. Dis.* 18, 1865–1867. doi: 10.3201/eid1811.120090

- Tao, Z., Wang, H., Li, Y., Liu, G., Xu, A., Lin, X., et al. (2014). Molecular epidemiology of human enterovirus associated with aseptic meningitis in shandong province, China, 2006-2012. *PLoS One* 9:e89766. doi: 10.1371/journal.pone.0089766
- Tapparel, C., Siegrist, F., Petty, T. J., and Kaiser, L. (2013). Picornavirus and enterovirus diversity with associated human diseases. *Infect. Genet. Evol.* 14, 282–293. doi: 10.1016/j.meegid.2012.10.016
- Tokarz, R., Haq, S., Sameroff, S., Howie, S. R., and Lipkin, W. I. (2013). Genomic analysis of coxsackieviruses A1, A19, A22, enteroviruses 113 and 104: viruses representing two clades with distinct tropism within enterovirus C. *J. Gen. Virol.* 94, 1995–2004. doi: 10.1099/vir.0.053462-0
- Wang, H. Y., Xu, A. Q., Zhu, Z., Li, Y., Ji, F., Zhang, Y., et al. (2006). The genetic characterization and molecular evolution of echovirus 30 during outbreaks of aseptic meningitis. *Zhonghua Liu Xing Bing Xue Za Zhi* 27, 793–797.
- Wang, J. R., Tsai, H. P., Huang, S. W., Kuo, P. H., Kiang, D., and Liu, C. C. (2002). Laboratory diagnosis and genetic analysis of an echovirus 30-associated outbreak of aseptic meningitis in Taiwan in 2001. *J. Clin. Microbiol.* 40, 4439–4444. doi: 10.1128/jcm.40.12.4439-4444.2002
- Wieczorek, M., Krzyszczek, A., and Figas, A. (2016). Molecular characterization of echovirus 30 isolates from Poland, 1995–2015. *Virus Genes* 52, 400–404. doi: 10.1007/s11262-016-1310-5
- Wu, Z., Du, J., Zhang, T., Xue, Y., Yang, F., and Jin, Q. (2013). Recombinant human coxsackievirus B3 from children with acute myocarditis in China. *J. Clin. Microbiol.* 51, 3083–3086. doi: 10.1128/jcm.00270-13
- Xing, W., Liao, Q., Viboud, C., Zhang, J., Sun, J., Wu, J. T., et al. (2014). Hand, foot, and mouth disease in China, 2008–12: an epidemiological study. *Lancet Infect. Dis.* 14, 308–318.
- Yan, D., Li, L., Zhu, S., Zhang, Y., An, J., Wang, D., et al. (2010). Emergence and localized circulation of a vaccine-derived poliovirus in an isolated mountain community in Guangxi, China. *J. Clin. Microbiol.* 48, 3274–3280. doi: 10.1128/jcm.00712-10
- Yang, X. H., Yan, Y. S., Weng, Y. W., He, A. H., Zhang, H. R., Chen, W., et al. (2013). Molecular epidemiology of Echovirus 30 in Fujian, China between 2001 and 2011. *J. Med. Virol.* 85, 696–702. doi: 10.1002/jmv.23503
- Yozwiak, N. L., Skewes-Cox, P., Gordon, A., Saborio, S., Kuan, G., Balmaseda, A., et al. (2010). Human enterovirus 109: a novel interspecies recombinant enterovirus isolated from a case of acute pediatric respiratory illness in Nicaragua. *J. Virol.* 84, 9047–9058. doi: 10.1128/jvi.00698-10
- Yu, G., Smith, D. K., Zhu, H., Guan, Y., Lam, T. T.-Y., and McInerney, G. (2017). ggtree: anrpackage for visualization and annotation of phylogenetic trees with their covariates and other associated data. *Methods Ecol. Evol.* 8, 28–36. doi: 10.1111/2041-210x.12628
- Zell, R., Delwart, E., Gorbalenya, A. E., Hovi, T., King, A. M. Q., Knowles, N. J., et al. (2017). ICTV virus taxonomy profile: picornaviridae. *J. Gen. Virol.* 98, 2421–2422. doi: 10.1099/jgv.0.000911
- Zhang, S., Wang, J., Yan, Q., He, S., Zhou, W., Ge, S., et al. (2014). A one-step, triplex, real-time RT-PCR assay for the simultaneous detection of enterovirus 71, coxsackie A16 and pan-enterovirus in a single tube. *PLoS One* 9:e102724. doi: 10.1371/journal.pone.0010274
- Zhang, Y., Hong, M., Sun, Q., Zhu, S., Li, X., Yan, D., et al. (2014). Molecular typing and characterization of a new serotype of human enterovirus (EV-B111) identified in China. *Virus Res.* 183, 75–80. doi: 10.1016/j.virusres.2014.01.002
- Zhang, Y., Tan, X., Cui, A., Mao, N., Xu, S., Zhu, Z., et al. (2013). Complete genome analysis of the C4 subgenotype strains of enterovirus 71: predominant recombination C4 viruses persistently circulating in China for 14 years. *PLoS One* 8:e56341. doi: 10.1371/journal.pone.0056341
- Zhang, Y., Wang, D., Yan, D., Zhu, S., Liu, J., Wang, H., et al. (2010a). Molecular evidence of persistent epidemic and evolution of subgenotype B1 coxsackievirus A16-associated hand, foot, and mouth disease in China. *J. Clin. Microbiol.* 48, 619–622. doi: 10.1128/jcm.02338-09
- Zhang, Y., Yan, D., Zhu, S., Wen, N., Li, L., Wang, H., et al. (2010b). Type 2 vaccine-derived poliovirus from patients with acute flaccid paralysis in china: current immunization strategy effectively prevented its sustained transmission. *J. Infect. Dis.* 202, 1780–1788. doi: 10.1086/657410
- Zhao, Y. N., Jiang, Q. W., Jiang, R. J., Chen, L., and Perlin, D. S. (2005). Echovirus 30, jiangsu province, China. *Emerg. Infect. Dis.* 11, 562–567. doi: 10.3201/eid1104.040995

**Conflict of Interest:** The authors declare that the research was conducted in the absence of any commercial or financial relationships that could be construed as a potential conflict of interest.

Copyright © 2020 Chen, Han, Wu, Xu, Yu and Zhang. This is an open-access article distributed under the terms of the Creative Commons Attribution License (CC BY). The use, distribution or reproduction in other forums is permitted, provided the original author(s) and the copyright owner(s) are credited and that the original publication in this journal is cited, in accordance with accepted academic practice. No use, distribution or reproduction is permitted which does not comply with these terms.



# Establishment of a Fosmid Library for Pseudorabies Virus SC Strain and Application in Viral Neuronal Tracing

Hansong Qi<sup>\*†</sup>, Hongxia Wu<sup>†</sup>, Muhammad Abid<sup>†</sup>, Hua-Ji Qiu<sup>\*</sup> and Yuan Sun<sup>\*</sup>

State Key Laboratory of Veterinary Biotechnology, Harbin Veterinary Research Institute, Chinese Academy of Agricultural Sciences, Harbin, China

## OPEN ACCESS

### Edited by:

Mei-Ling Li,  
Rutgers, The State University  
of New Jersey, United States

### Reviewed by:

Sylvie Lecollinet,  
Agence Nationale de Sécurité  
Sanitaire de l'Alimentation,  
de l'Environnement et du Travail  
(ANSES), France  
Hong-bing Xiang,  
Huazhong University of Science  
and Technology, China

### \*Correspondence:

Hansong Qi  
qih9510@163.com  
Hua-Ji Qiu  
qiuhuaji@caas.cn  
Yuan Sun  
sunyuan@caas.cn

<sup>†</sup>These authors have contributed  
equally to this work

### Specialty section:

This article was submitted to  
Virology,  
a section of the journal  
Frontiers in Microbiology

Received: 21 October 2019

Accepted: 07 May 2020

Published: 11 June 2020

### Citation:

Qi H, Wu H, Abid M, Qiu H-J  
and Sun Y (2020) Establishment of a  
Fosmid Library for Pseudorabies Virus  
SC Strain and Application in Viral  
Neuronal Tracing.  
*Front. Microbiol.* 11:1168.  
doi: 10.3389/fmicb.2020.01168

Pseudorabies virus (PRV) is a member of *Alphaherpesvirinae* subfamily, its neurotropism and latency infection attract the attention of many scientists. PRV tagged with a fluorescent reporter gene as a tracker has been used to analyze neuronal circuits, including anterograde and retrograde. In this study, we used fosmid library to construct a rapid and efficient platform to generate recombinant PRV. Firstly, the highly purified PRV ShuangCheng (SC) genomic DNA was sheared randomly into approximately 30–49-kb DNA fragments. After end-blunting and phosphorylation, the DNA fragments were cloned into the fosmid vector and transformed into *Escherichia coli*. A total of 200 fosmids that cover the complete genome of PRV SC was sequenced. Thirteen fosmid combinations in five groups were transfected into Vero cells, respectively, and each group can successfully rescue PRV strain SC. There was no significant difference between wild type and recombinant in both morphology and growth kinetics. In the next step, an enhanced green fluorescent protein (EGFP) was fused into the amino-terminal of UL36 protein by Red/ET recombination technology, and recombinant rPRV SC-UL36-EGFP was rescued successfully. At last, the single viral particles with green fluorescent were monitored retrograde moving in the axon with an average velocity of  $0.71 \pm 0.43 \mu\text{m/s}$  at 0.5–2 h post infection (hpi) and anterograde moving with an average velocity of  $0.75 \pm 0.49 \mu\text{m/s}$  at eight hpi. Integration of fosmid library and Red/ET recombination technology in our work was highly efficient and stable for constructing PRV recombinants. This study will accelerate understanding the biology of PRV and the development of novel vaccines.

**Keywords:** pseudorabies virus, fosmid library, UL36, neuron, transport

## INTRODUCTION

Pseudorabies virus (PRV) is a neurotropic herpesvirus, a member of *Alphaherpesvirinae* subfamily (Kramer et al., 2011). PRV invades the axon-endings distributed in the epithelial tissue after infection and replication at the epithelial cells. In detail, membrane fusion initiated between PRV envelope membrane and nerve cell membrane facilitates PRV to enter into neurons. Immediately, PRV virions undergo axonal retrograde transport from the axon to soma side and replicate in the nucleus. Subsequently, progeny virions are assembled and transported through the nervous system. Meanwhile, latency can also develop at the cell body in the neuron (Koyuncu et al., 2013).

Due to the latent infection, it is very difficult to eradicate PRV. The direct contact between diseased animals and healthy animals is the main transmission route for this disease (Pomeranz et al., 2017). Clinical symptoms of PRV-infected pigs vary by age. Fattening pigs mainly suffer from respiratory disorders, while nursery pigs and younger piglets die from central nervous system (CNS) disorders (Pomeranz et al., 2005).

After PRV particle binding to axonal terminal, viral envelopes of PRV fuse with the plasma membrane of host cells. Then, viral particles enter into the axon where most tegument proteins are released into the cytoplasm. However, the inner tegument proteins such as UL37, UL36, UL21, UL16, UL14, US3, and ICP0 remain associated with capsids, and this capsid tegument complexes are transported toward nucleus where progeny viral genome is replicated (Luxton et al., 2005; Radtke et al., 2010). Several tegument proteins such as UL36, UL37, and UL21 play an essential role in recruiting motors for viral capsid tegument complexes for retrograde transport (Douglas et al., 2004; Luxton et al., 2006). UL36 and UL37 proteins interact with each other to form a physical complex (Roberts et al., 2009); on one hand, UL36 is the critical protein that directly binds to the dynein motor subunit p150 and p50, on the other hand, UL37 renders PRV neuroinvasion and retrograde axonal transport (Richards et al., 2017). Viral particles are unable to retrograde transport when UL36 is deleted. The deletion of UL37 does not show the same result as the UL36; UL37-deleted PRV is defective for secondary envelopment, which reduces capsid transport (Schipke et al., 2012). UL21 is another protein associated with neuroinvasion. It can promote PRV retrograde transport through interaction with cytoplasmic dynein light chain Roadblock-1 (Yan et al., 2019); however, UL21 mutation causes a delay in the spread to presynaptic neurons and reduces infectious particle production (Curanovic et al., 2009).

US9 is the key factor for recruiting KIF1A to promote anterograde transport which also needs gE and gI as helper proteins. Additionally, UL36 and US11, as candidates of PRV viral proteins, could recruit kinesin motors to envelop viral particles for anterograde transport. So UL36 interacts with motor proteins of opposite polarity and transport viral particles in both the anterograde and retrograde directions (Diefenbach et al., 2002). Fundamentally, the visualization of axonal transportation is the most convincing strategy to access this process, and the possible idealized marker locus is UL36 due to its direct interaction with molecular motor dynein (Zaichick et al., 2013).

For neurotropic herpesvirus, viral particles tagged with fluorescent protein have proven to be a powerful tool to visualize virus replication cycle and transport in long-distance of neurons (Kramer et al., 2012; Hogue et al., 2014). Since PRV is a linear, double-stranded DNA virus of about 143 kb, it is not easy to alter such a big genome. At present, several genetic manipulation methods have been used to modify the genome of PRV, including homologous recombination, bacterial artificial chromosome (BAC), and CRISPR/Cas9 (Lerma et al., 2016; Hubner et al., 2018). These methods were time-consuming and labor-intensive due to a series of plaque purification or were genetically unstable. Recently, the fosmid library for PRV TJ strain has been established by Zhou et al. (2018) and successfully

constructed the rPRV TJ-VP26-EGFP. It was easily operated and highly efficient (Zhou et al., 2018). Therefore, the fosmid library is relatively dynamic at present due to the high recombination efficiency and the needlessness of purification (Zhou et al., 2018).

Extensive vaccination with Bartha-K61 vaccine strain has controlled PRV epidemics in China. Nevertheless, the disease still continues to circulate in China, especially after the emergence of variant PRV (An et al., 2013). All known full-length PRV sequences from the GenBank were divided into two clades according to ML phylogenetic tree analysis, and all the strains isolated from China were grouped in one clade (He et al., 2019). For the variant strain PRV TJ as an example, sequence comparison revealed that about 62 of total 67 viral proteins displayed variations compared with the previous isolates, and there are 43 viral proteins different compared with PRV ShuangCheng (SC) (Luo et al., 2014). To explore the characteristics of PRV, a convenient and efficient gene manipulation platform for PRVs is essential, especially for studying the evolution of PRV. Fosmid library is a convenient tool with numerous advantages.

In this study, a fosmid library for PRV SC was constructed. Using the fosmid library as well as Red/ET-mediated recombination, a recombinant rPRV SC-UL36-EGFP with EGFP fused into the amino-terminal of UL36 was successfully generated. It can help to visualize both anterograde and retrograde transport in neural circuits without affecting virus replication. This work will accelerate the progress of the PRV study and the development of novel vaccines.

## MATERIALS AND METHODS

### Cells and Virus

The PRV SC strain (GenBank accession number: KT809429.1) is a virulent strain isolated in China in 1980, which is a reference challenge virus to evaluate the efficacy of the Bartha-K61 vaccine in China (Yuan et al., 1987). Porcine Kidney 15 cell (PK-15, ATCC CCL-33) and Vero cell lines were maintained in Dulbecco's modified minimum essential medium (DMEM) (Gibco, Grand Island, NY, United States) containing 10% fetal bovine serum (FBS), 100 U/ml penicillin, and 100 µg/ml streptomycin.

### Extraction of Pseudorabies Virus Genomic DNA

The method of extraction of PRV full-length genomic DNA has been described previously (Smith and Enquist, 1999). PK-15 cells in 10 75-cm<sup>2</sup> flask were infected with PRV SC strain at a multiplicity of infection (MOI) of 5 and cultured for 12–15 h at 37°C with 5% CO<sub>2</sub>. When all the cells show cytopathic effects (CPEs), the cells were collected, then washed with phosphate-buffered saline (PBS) twice. The cell pellet was lysed with 10 ml of LCM buffer [130 mM KCl, 30 mM Tris (pH 7.4), 5 mM MgCl<sub>2</sub>, 0.5 mM EDTA, 0.5% Nonidet P-40 (NP-40), and 0.043% 2-mercaptoethanol] to release viral capsids. Capsids were extracted with Freon twice and separated by ultracentrifugation through glycerol step gradients (8 ml of 5% glycerol and 16 ml of 45%

glycerol) at 28,000 rpm for 2.5 h at 4°C. The genomic DNA was released by 10% sodium dodecyl sulfate (SDS) treatment. Then the DNA deposits were washed with 75% ethanol twice and dissolved in ultrapure water. The concentration of DNA was detected by the NanoDrop™ 2000 (Thermo Scientific, Carlsbad, CA, United States) and *gI* gene was amplified using the primers listed in the **Table 1** for sequencing. To check the infection activity, the genomic DNA was transfected into Vero cells using X-treme GENE HP DNA transfection reagent (Roche, Mannheim, Germany) according to manufacturer's instructions.

## Construction of a Fosmid Library

Twenty micrograms of highly infective genomic DNA of PRV SC was pipetted using 200 µl tip to shear the DNA. The sheared genomic DNA was end-repaired using the End-Repairing Enzyme Mix to generate 5' phosphorylated DNA. The DNA fragment was analyzed on a 1% gold agarose gel by pulsed-field gel electrophoresis (PFGE), a Lambda DNA Mono Cut Mix (New England BioLabs, Beijing, United Kingdom) as a size marker. DNA fragments ranging from 33 to 49 kb were excised from the gel, recovered using GELase (Epicentre, Madison, United States) and ligated into the pCC1FOS cloning-ready vector at room temperature for 4 h. The ligation mixture was packaged using MaxPlax Lambda Packaging Extracts and transformed into EPI300-T1<sup>R</sup> cells. Except genomic DNA, all the materials and protocol as mentioned above were supplied by the Copy Control™ Fosmid Library Production Kit (Epicentre, Madison, WI, United States). Two hundred clones were picked randomly and cultured overnight in 5 ml of LB liquid medium containing 12.5 µg/ml chloramphenicol and 50 µl of auto-induction solution (Epicentre). The fosmids were extracted using ZR BAC DNA Miniprep Kit (Zymo Research, United States), and the terminal of DNA fragment in the fosmids was sequenced based on pCC1FOS sequencing primers. The whole genomic DNA of PRV SC was assembled according to the terminal sequence of DNA fragment.

**TABLE 1** | Primers for construction and identification of rPRV SC-UL36-EGFP.

Names	Sequences (5'-3')	Target gene
UL36-rpsI-F	CGTGTCCAATAAAAAGATTTTTCCCCAC	rpsLneo
	GCGCGTGTGTTATTTAGCCGCGCCTGGTGA	
	TGATGGCGGGATCG	
UL36-rpsI-R	TCGGGGTCATACTGATTACGATAGCCGACG	rpsLneo/EGFP
	ACCACCGCGTCGGCCGTCATTAGAAAGAA	
	CTCGTCAAGAAGCGCGTGTCCAATAAAAAGATTTTTCCCCAC	
UL36-EGFP-F	GCGCGTGTGTTATTTAGCCATGGTGA	EGFP
	AGGCGAGGAGCTG	
	TCGGGGTCATACTGATTACGATAGCCGACG	
UL36-EGFP-R	ACCACCGCGTCGGCCGTCATTCTAGATCCG	rpsLneo/EGFP
	GTGGATCCCGGGCC	
JC-UL36-F	CGGCGAGCGTCAACGTGCGCGA	rpsLneo/EGFP
JC-UL36-R	AGTCGCTGATGGCGCACATG	
gI-F	ATGATGGTGGCGCGACGTGA	gI
gI-R	TTATTGTTCTTCTGCGATGGTG	

## Rescue of the Recombinant Pseudorabies Virus ShuangCheng

Thirteen fosmids that cover the whole genome of PRV SC in five groups (**Tables 2, 3**) were transfected into Vero cells cultured in 10-cm plates. Five fosmids (2 µg each) in each group were gently mixed together with 30 µl X-treme GENE HP DNA transfection reagent in 1 ml DMEM, incubated for 30 min at room temperature, and added into Vero cells. Before transfection, Vero cells were washed twice with PBS, 10 µg genomic DNA of PRV SC was transfected using the same way as a positive control, and non-transfected cells served as a negative control. CPEs in the Vero cells were observed at 5–7 days post-transfection, and cell supernatants were collected and stored for further identification of the recombinant viruses.

## Electron Microscopy

The second generation (F2) of rPRV SC from the five fosmid groups and wild-type PRV SC were negatively stained with 2% phosphotungstic acid, and the morphologies of both Res-PRV SC and its parental virus PRV SC were observed under the electron microscope.

## Immunofluorescence Assay

After infection, the cells were fixed with ethanol at -20°C for 30 min, then washed with PBS three times. The fixed cells were incubated with swine anti-PRV sera (1:200 dilution) for 2 h at 37°C and then incubated with Alexa 488-conjugated goat anti-pig IgG (Thermo Fisher Scientific) (1:1,000 dilution) for 1 h at

**TABLE 2** | Fosmids that cover the whole genome of PRV SC.

Fosmid	Location in genome(nt)	Size(bp)
60	1-33361	33361
142	1-31701	31701
22	1-31943	31943
50	29470-63289	33819
147	24017-61243	37226
78	29619-60993	31374
38	59987-92335	32348
66	50966-83734	32768
21	50301-99259	48958
24	80390-114445	34055
20	74192-109646	35454
65	111583-142825	31242
82	106487-142825	36338

**TABLE 3** | Fosmid groups that cover the genome of PRV SC.

Group	Combinations	CPE
1	60 + 50 + 38 + 24 + 65	+
2	142 + 147 + 66 + 20 + 82	+
3	22 + 78 + 66 + 24 + 65	+
4	60 + 147 + 21 + 24 + 65	+
5	22 + 50 + 38 + 24 + 65	+

37°C. After incubation, the cells were washed three times. The images were captured using an Olympus CK40 microscope.

## Restriction Fragment Length Polymorphism Analysis

PRV SC genomic DNA was purified as described by Smith and Enquist (1999). For RFLP analysis, the genomes of the viruses were digested with *Bam*HI (Thermo Fisher Scientific) in reaction mixtures containing 2 µg DNA, 10 × reaction buffer, 10 U restriction enzyme, and ddH<sub>2</sub>O in a total volume of 50 µl, and the reaction was performed at 37°C for 4 h. The digested samples were resolved in 0.8% agarose gel containing 0.2 µg/ml ethidium bromide and 1 × TAE buffer at 2 V/cm for 4 h at room temperature.

## One-Step Growth Curve and Plaque Size Determination

One-step growth curve was performed to compare the growth kinetics of the rPRV SC and parental virus PRV SC. PK-15 cells (or Vero cells) cultured in 24-well plate were infected with each virus at an MOI of five, then the supernatants and cells from three wells were harvested at 4, 8, 12, 24, 36, 48, 60, 72 h post infection (hpi) and stored at -80°C. The viral titers were determined by 50% tissue culture infectious dose (TCID<sub>50</sub>). To compare the plaque size of the rPRV SC and parental virus PRV SC, PK-15 cells (or Vero cells) were infected with each virus diluted serially in 10-fold and incubated for 1 h, then the medium was removed, and the cells were overlaid with 1% low-melting-point agarose diluted in DMEM. For each virus, 30 plaques were randomly selected, and their size was determined by ImageJ software.

## Red/ET-Mediated Recombination

The fosmid 50 (containing UL36 gene) was modified using the Red/ET-mediated recombination Counter Selection BAC Modification Kit (Gene Bridges, Berkeley, CA, United States) according to the manufacturer's instructions. At first, the fosmid 50 and the Red/ET expression plasmid (pRed/ET) were co-transformed into competent *E. coli* DH10B cells by electroporation, naming with *E. coli* DH10B-fos50-Red/ET. Then the selection antibiotic cassette (*rpsL*-neo) flanked by 50 bp homology arms was transformed into competent *E. coli* DH10B-fos50-Red/ET to get *E. coli* DH10B-fos50-UL36-*rpsL*-Red/ET in which the *rpsL*-neo gene was fused to the amino-terminal of the UL36 gene. Finally, the EGFP flanked by 50-bp homology arms was transformed into competent *E. coli* DH10B-fos50-UL36-*rpsL*-Red/ET to get *E. coli* DH10B-fos50-UL36-EGFP in which the *rpsL*-neo gene fused to the amino-terminal of UL36 gene was replaced by EGFP. The modified UL36 ORFs were amplified and sequenced. The modified fosmid 50-UL36-EGFP was extracted from *E. coli* DH10B-fos50-UL36-EGFP and transfected into Vero cells with other fosmids to rescue the virus rPRV SC-UL36-EGFP. All the primers used in this experiment were listed in **Table 1**.

## PCR and Real-Time PCR

The genomic DNA was extracted from the cells and tissues infected with PRV as the template of PCR and real-time PCR

amplification. The genomic DNA of PRV SC strain was used as the positive control and water as the negative control. The EGFP gene of rPRV SC-UL36-EGFP was amplified using forward primer EGFP-F and reverse primer EGFP-R, and gI genes of PRV SC, rPRV SC, and rPRV SC-UL36-EGFP were amplified by forward primer gI-F and reverse primer gI-R (listed in **Table 1**). The reaction mixture and condition were performed according to the manufacturer's instruction of LA Taq<sup>TM</sup> with GC Buffer (TaKaRa, Japan). Additionally, gI gene also was detected using forward primer gI-F and reverse primer gI-R and the Taq Man probe FAM-PRV-Cla (FAM-50-CGC GTG CAC CAC GAG GCC TT-30-BHQ1) in a real-time PCR as Meng et al. (2016) reported.

## Western Blot

PK-15 cell monolayers infected with rPRV-SC were gently washed with PBS and lysed by NP40 lysis buffer containing 1% PMSF (Solarbio, Beijing, China) for 1 h at 4°C. The lysates were mixed with 5× sample loading buffer, incubated in boiling water baths for 10 min, and cleared by centrifugation at 10,000 × *g* for 5 min at 4°C. A total of 30-µl sample was separated by SDS-polyacrylamide gel electrophoresis (PAGE) and transferred onto nitrocellulose membranes. After blocking with 5% skim milk for 2 h at 37°C, the membranes were incubated at room temperature for 2 h with specific mouse anti-gI polyclonal antibody (a gift from Jin Tian, State Key Laboratory of Veterinary Biotechnology, Harbin Veterinary Research Institute, Chinese Academy of Agricultural Sciences, Harbin, China), mouse anti-gB monoclonal antibody (a gift from Jing Zhao, State Key Laboratory of Veterinary Biotechnology, Harbin Veterinary Research Institute, Chinese Academy of Agricultural Sciences, Harbin, China), and anti-EGFP polyclonal antibody (Solarbio, Beijing, China). After washing membranes using PBST (PBS with 5% Tween 20) buffer, the membranes were incubated with DyLight 800 goat anti-mouse IgG (1:8,000; Thermo Fisher Scientific) at 37°C for 45 min, the membranes were washed three times in PBST, then visualized and analyzed with an Odyssey infrared imaging system (LI-COR Biosciences, Lincoln, NE, United States).

## Primary Neuronal Culture and Microfluidic Chambers

Dorsal root ganglia (DRG) from the spine of new-born BALB/c mice less than 3 days were collected, washed, and digested by Collagenase/Dispase (Roche) at 37°C in the CO<sub>2</sub> incubator for 45–60 min. The neurons were separated from each other sufficiently, filtered, washed, and cultured in Neurobasal Medium (Gibco) supplemented with 100 ng/ml nerve growth factor 2.5S (Invitrogen), 2% B27 (Gibco), and 1% penicillin and streptomycin with 2 mM glutamine (Invitrogen). Before the neuron was planted in one side of the microfluidic chamber, the coverslips were treated with Poly-DL-ornithine hydrobromide (Sigma) for one night and laminin (Invitrogen) for at least 6 h and washed with Hanks' balanced salt solution (HBSS) buffer two times, dried completely, then covered with microfluidic device, neurons were added in one well of microfluidic device, flowed

into the chamber connected with two adjacent wells, after 3 days culturing, the axons grow to another chamber along the chamber microgrooves (see illustration). Infection was performed by replacing the Neurobasal Medium in the distal wells and changed with  $10^7$  TCID<sub>50</sub> rPRV SC-UL36-EGFP. Time-lapse imaging was achieved by automated sequential capture.

## Pseudorabies Virus Infection of Mice

Thirty-five 6-week-old specific pathogen-free (SPF) BALB/c mice were randomly divided into seven groups, five mice in each group. Groups 1–3 were each intramuscularly injected with 100  $\mu$ l of different titer ( $10^2$ – $10^4$  TCID<sub>50</sub>) of PRV SC strain at left hind limb, and groups 4–6 were inoculated with rPRV SC-UL36-EGFP strain at the same way, viral titer, and position; group seven as control was injected with 100  $\mu$ l DMEM. The clinical signs were recorded every day until 7 days post infection (dpi), and the 50% lethal doses (LD<sub>50</sub>) of PRV SC and rPRV SC-UL36-EGFP strains in mice were calculated. The tissue samples from brain, spinal cord, sciatic nerve, leg, and foot of mice infected with  $10^4$  TCID<sub>50</sub> of PRV SC or rPRV SC-UL36-EGFP were collected to detect the level of PRV genome using real-time PCR following the method of Meng et al. (2016).

## Ethics Statement

The Animal Ethics Committee approval number is Heilongjiang-SYXK-2006-032. All the experiments were operated in the Biosafety Level II laboratory following strict biosecurity measures according to instructions of the Harbin Veterinary Research Institute. Fertilized BALB/c mice for DRG collection were bred.

## Statistical Analysis

All experiments were performed at least three times. Data were statistically analyzed by unpaired t-tests and a one-way ANOVA in Prism 7.0 software (GraphPad Software, La Jolla, CA, United States). Differences were considered significant if there was an unadjusted *P*-value less than 0.05. The instantaneous velocity and direction were analyzed by Imaris  $\times$  64 9.3.1 software (Imaris Software, Oxford Instruments, United Kingdom), and the data were analyzed by Statistical Product and Service Solutions (SPSS) 13.0 software (SPSS Software, IBM, United States).

## RESULTS

### Construction of the Fosmid Library for Pseudorabies Virus ShuangCheng

After end-blunting and phosphorylation, the DNA fragments were cloned into the fosmid vectors and transformed into *E. coli*. A total of 200 clones were randomly picked from the fosmid library for end-sequencing. As a result, there are 165 clones match for PRV SC genome according to the two terminal sequences of each DNA fragment, and a majority of which contains insert of 30–49 kb. Moreover, the fosmid library can cover the complete genome of PRV SC. There are three DNA fragments including 5' terminal sequence, two DNA fragments including 3' terminal

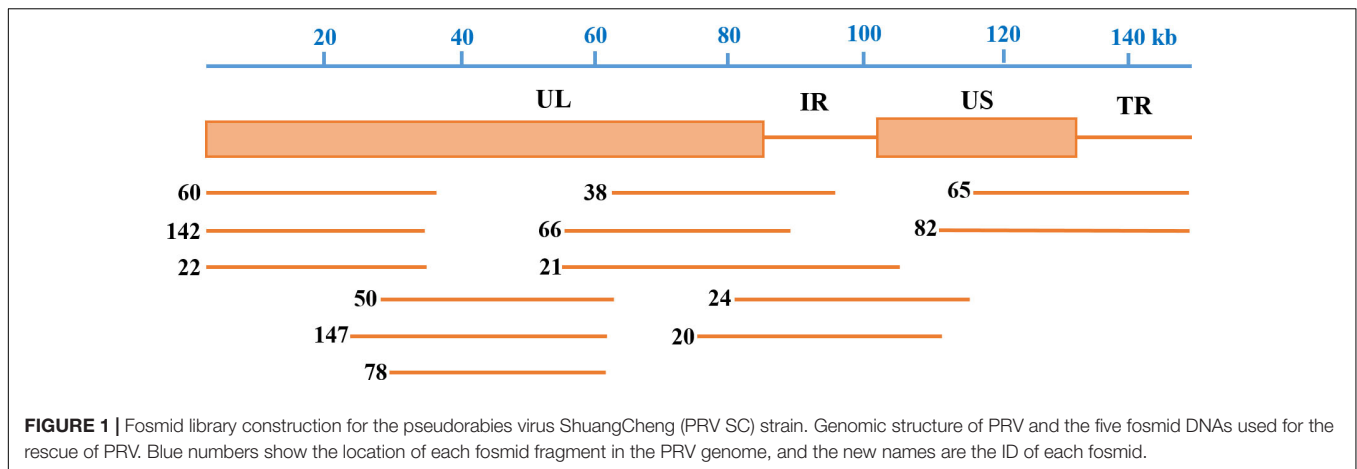
sequence, most DNA fragments including the middle part of genome, and some fragments including incomplete terminal genome. At last, 13 fosmids were selected for generating the fosmid combinations that cover the complete genome of PRV SC (Table 2). Five sets of overlapping fosmid combinations were prepared to rescue the recombinant PRV SC (rPRV SC); each group consisting of five overlapping fosmids (Figure 1 and Table 3).

### Rescue and Characterization of Recombinant Pseudorabies Virus ShuangCheng Based on Overlapping Fosmids

Five sets of fosmid plasmids were transfected into Vero cells to rescue rPRV SC; non-transfected Vero cells served as the negative control. CPEs of five transfection groups were observed at 5–7 dpi, while no CPEs in the negative control during the progress. This suggested that all the CPEs were caused by the rPRV SC, not by contaminated PRV or other viruses. Then Vero cells and PK-15 cells were infected with the first generation of rPRV SC. After culturing for 48 h, CPE and immunofluorescence assay (IFA) were performed, and the results were consistent with the first-generation virus (Figure 2A). To check the morphology of recombinant viral particles, under the electron microscope, the rPRV SC particles showed similar to that of the parental virus with an apparently external envelope (Figure 2B). To further identify the genome of rPRV SC, we performed PCR using the specific primer for gI gene. As a result, the gI genes of PRV SC was successfully amplified from the genomic DNA of every rPRV SC and wild PRV SC (Figure 2D). To further confirm rPRV SC, the genome of rPRV SC from group five was digested with *Bam*HI, the result of restriction fragment length polymorphism (RFLP) showed no significant difference from parental PRV SC (Figure 2C). Moreover, the comparison of the replication kinetics and plaque morphology of rPRV SC with parental PRV SC showed no significant difference in the PK-15 cells (Figures 2E,F). So, the results demonstrated that rPRV SC could be rescued successfully using the five sets of fosmid plasmids.

### Generation and Identification of Recombinant Pseudorabies Virus ShuangCheng-UL36-Enhanced Green Fluorescent Protein

UL36, a large tegument protein, attaches to the capsid during axonal retrograde transport. Previous studies have shown that UL36 directly interacts with dynein subunit p150 and p50 to mediate PRV retrograde transport (Zaichick et al., 2013). Consequently, UL36 is a possible ideal reporter target for visualization axonal retrograde kinetics. To rescue rPRV SC-UL36-EGFP, EGFP was fused into the amino-terminal of UL36. Fosmid 50 (29470-63289) that harbors UL36 gene was modified by the Red/ET-mediated recombination (Figure 3A). The modified fosmid 50 (fosmid 50-UL36-EGFP) and other fosmid plasmids in group five were transfected into Vero cells.



After 5 days' incubation, CPEs with green fluorescence were observed, and the supernatant was inoculated into PK-15 cells. The images of CPEs with green fluorescence were captured at 12 and 24 hpi in rPRV SC-UL36-EGFP-infected cells, and only CPEs were observed in the PRV SC-infected cells (**Figure 3B**). The gI and EGFP gene were amplified from the genomic DNA of the rPRV SC-UL36-EGFP and PRV SC strains, and the EGFP gene could be amplified only from the rPRV SC-UL36-EGFP genome but not from PRV SC (**Figure 3C**). To further identify rPRV SC-UL36-EGFP, the expression of gB, gI, and EGFP proteins were identified by Western blotting. The result showed the same bands of gB and gI presented in the samples of rPRV SC-UL36-EGFP-, rPRV SC-, and PRV SC-infected groups, and UL36-EGFP was detected only in rPRV SC-UL36-EGFP-infected group (**Figure 3D**). In addition, rPRV SC-UL36-EGFP and PRV SC showed similar growth kinetics in both PK-15 and Vero cells (**Figures 3E,F**), and the plaque size of rPRV SC-UL36-EGFP was also the same as that of PRV SC (**Figure 3G**).

### Pathogenicity of Recombinant Pseudorabies Virus ShuangCheng-UL36-Enhanced Green Fluorescent Protein Strain in Mice

To check the pathogenicity of rPRV SC-UL36-EGFP strain compared with the wild strain PRV SC, mice were infected with same titer of rPRV SC-UL36-EGFP as PRV SC simultaneously. All the mice in the control group remained healthy during the experiments. The mice infected with  $10^4$  TCID<sub>50</sub> of both rPRV SC-UL36-EGFP and PRV SC strain showed serious itching at 2 dpi; the skin around of injected position was scratched and bitten interally at the beginning, more and more frequently, until the mice could not move and died as Brittle et al. (2004) described. The itching symptoms of mice infected with  $10^3$  TCID<sub>50</sub> started at 3 dpi. The depression and rough hair could be observed in most of the mice infected with  $10^2$  TCID<sub>50</sub>. When the mice suffered from itching, they would die at 10–12 h later. So the average time point of itching onset was earlier about half a day than the average mortality time point as shown in **Table 4**. The LD<sub>50</sub> of rPRV SC-UL36-EGFP ( $1.48 \times 10^3$

TCID<sub>50</sub>) was lower than that of wild PRV SC strain ( $2.09 \times 10^3$  TCID<sub>50</sub>), but there was no statistically significant difference. So the pathogenicity of rPRV SC-UL36-EGFP was the same as that of its parental virus PRV SC.

The genomes of both PRV SC and rPRV SC-UL36-EGFP strains were detected by real-time PCR to compare the viral replication in the injection point and nervous system. As a result, the viral genomic DNA was positive in the sciatic nerve ( $1.6 \times 10^7$  and  $1.6 \times 10^7$  copies) (**Figure 4C**), spinal cord ( $1.7 \times 10^9$  and  $1.3 \times 10^9$  copies) (**Figure 4B**), and brain ( $8.5 \times 10^5$  and  $4.4 \times 10^5$  copies) (**Figure 4A**) where particles of PRV were retrograde transported and replicated. Moreover, the highest viral copies were in the lumbar spine, the peripheral nerve center near the injection point. Although all the mice infected with  $10^4$  TCID<sub>50</sub> of PRV SC and rPRV SC-UL36-EGFP strain died before 4 dpi, the virus titers were lower in the brain compared to the spinal cord and sciatic nerves. There were also high copies of viral genomic DNA in the legs ( $7.0 \times 10^7$  and  $7.6 \times 10^7$  copies) (**Figure 4D**) and the feet ( $8.4 \times 10^7$  and  $8.7 \times 10^7$  copies) (**Figure 4E**) where PRV particles were anterograde transported to the nerve endings. The viral loads in the tissue of mice infected with rPRV SC-UL36-EGFP strain were not statistically different from that of the PRV SC strain. In conclusion, the EGFP fused with UL36 gene of PRV SC strain did not affect viral replication and spread in the nervous system of mouse.

### Visualization of the Enhanced Green Fluorescent Protein-Tagged Viral Particle Transport in Neuron

Next, we checked whether the EGFP-tagged reporter virus rPRV SC-UL36-EGFP could be used to track the trajectory of PRV particle transport in the neuron and analyzed the velocity kinetics, direction, and displacement of transport. The rPRV SC-UL36-EGFP was added into two wells of the microfluidics and flowed into the chamber in the axonal side. In the first 10–20 min, the green particles randomly distributed in the medium; only a minority of viral particles that attached to the axon terminals were captured in the same focal length with the axons. At this time, viral particles were quiet at the vision of microscope as

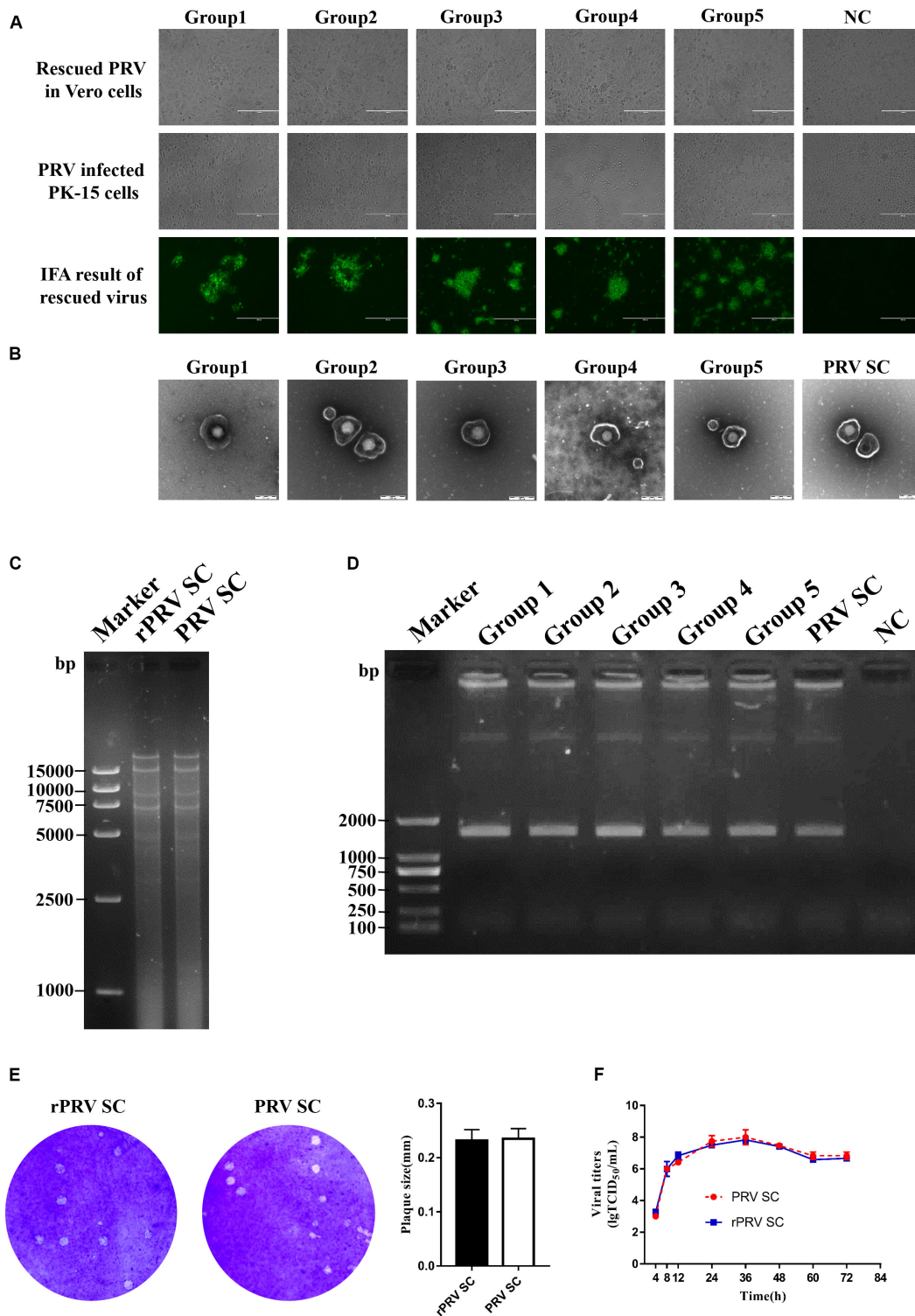


**FIGURE 2 |** Identification of recombinant pseudorabies virus ShuangCheng (rPRV SC). **(A)** The first row represents the cytopathic effects (CPEs) of Vero cells, which is infected with the first generation of rPRV SC, and no infection as negative control (NC). The second row represents the CPEs of PK-15 cells infected with the first generation of rPRV SC from different groups in the second line. The third row represents the immunofluorescence assay (IFA) of PK-15 cells infected with rPRV SC using an anti-PRV serum. The images were captured using EVOS Cell Imaging Systems under 10 × magnification. **(B)** Transmission electron of PRV SC and rPRV SC. The virus particles were 25,000 times magnified. **(C)** The restriction fragment length polymorphism analysis of the rescued and the parent PRV in 0.8% agarose. The genome of the rescued and the parent PRV was digested with *Bam*HI. **(D)** PCR amplification of the gI gene from the genome of PRV SC and rPRV SC. **(E)** Plaque of PRV SC and rPRV SC in the PK-15 cells. The diameter of plaques was averaged from three independent experiments. **(F)** One-step growth curve of PRV SC and rPRV SC in the PK-15 cells.

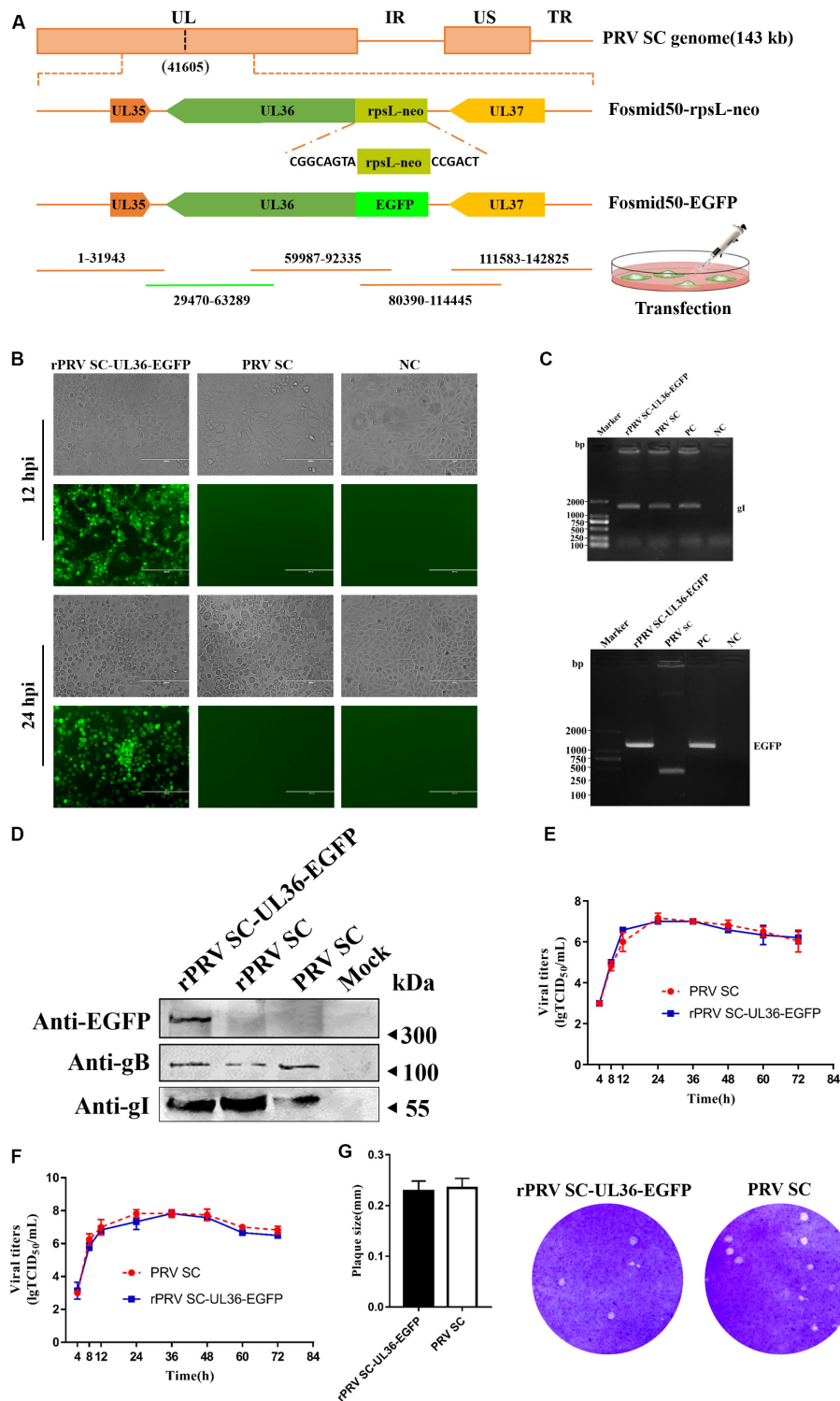


**FIGURE 3 |** Rescue and identification of recombinant pseudorabies virus ShuangCheng (rPRV SC)-UL36-enhanced green fluorescent protein (EGFP). **(A)** Schematic for rPRV SC-UL36-EGFP design. Finally, Fosmid 22(1-31943), 38(59987-92335), 24(80390-114445), 65(111583-142825), and Fosmid 50-EGFP were transfected into Vero cells to rescue rPRV SC-UL36-EGFP. **(B)** The green fluorescence and cytopathic effects (CPEs) in the PK-15 cells infected with rPRV SC-UL36-EGFP or PRV SC at 12, 24 h post infection (hpi). **(C)** The viral gene gI and EGFP from rPRV SC-UL36-EGFP and PRV SC were identified by PCR. Plasmid pflag-gI and pok-UL36-EGFP act as a positive control. **(D)** The expression of gB, gI, and EGFP in the rPRV SC-UL36-EGFP- and PRV SC-infected cells were identified by Western blot at 12 hpi. **(E)** One-step growth curves of rPRV SC-UL36-EGFP and PRV SC in Vero cells. **(F)** One-step growth curves of rPRV SC-UL36-EGFP and PRV SC in PK-15 cells. **(G)** Plaque size of rPRV SC-UL36-EGFP and PRV SC. The diameter of 30 pots was measured.

**TABLE 4** | Result of mouse infected with PRV SC and rPRVSC-UL36-EGFP strain.

Groups	Amounts	Dose (TCID <sub>50</sub> )	Clinical signs	Morbidity (mean days of itch onset)	Mortality (mean days to death)
PRVSC	5	10 <sup>4</sup>	+++	5/5 (2.6)	5/5 (3.1)
	5	10 <sup>3</sup>	++	3/5 (3.25)	3/5 (3.75)
	5	10 <sup>2</sup>	+	0/5	0/5
rPRVSC-UL36-EGFP	5	10 <sup>4</sup>	+++	5/5 (3.1)	5/5 (3.7)
	5	10 <sup>3</sup>	++	3/5 (3.3)	3/5 (3.9)
	5	10 <sup>2</sup>	+	1 (4.5)	1/5 (5)
DMEM	5	100 μL	/	0/5	0/5

Mean time to itch onset and death was calculated for five mice of each group after intramuscular injection with different dose of viruses shown in the table. Clinical symptoms were scored in four degrees: +++, severe; ++, moderate; +, mild; /, none.

shown in **Figure 5A**. A little of the particles had entered into the axon, and maybe part of viral particles just attached to the upper axon not the end.

After membrane fusion, capsid–tegument complexes were started moving along the axon. There is more than one mode of movement after penetration of viral particles into the axon. Some viral particles in the terminal axon were moving toward the cell body (retrograde movement), here, the movement of one EGFP-tagged capsid was observed during 0–32 s (**Figure 5B**), but some capsids stopped halfway to the cell center (stationary). Other viral particles just moved back at one stage (anterograde movement) and forward at the next stage. The percentages of capsids in the three states including anterograde movement, retrograde movement, and stationary state were calculated as shown in **Figure 5F**. In detail, 57.3% of total capsids moved through the retrograde at 0.5 hpi, 27.4% of capsids moved through anterograde, and 15.3% remained in stationary state. So, majority of viral capsids moved toward the cell body after entering into the axon. The instantaneous velocity of retrograde movement varied from 0 to 2.22 μm/s, and the average velocity was  $0.71 \pm 0.43$  μm/s (**Figure 5E**).

The green fluorescence particles retrograde transport intermittently only happened at the first 0.5 to 2 h. The time duration varied based on the length and number of axons. Another continual particle movement can be observed until 8 hpi; the virus run away from the cell body (anterograde) reverse to the first 2 h observed, the movement of one particle from 0–13.2 s was shown in **Figure 5C**. The capsids also perform three states at this time, including anterograde movement, retrograde movement, and stationary state. The percentages of each state were 50.9%, 30.4%, and 18.7%. So half of them moved far away from the cell body. The instantaneous velocity of anterograde movement varied from 0 to 2.35 μm/s, and the average velocity was  $0.75 \pm 0.49$  μm/s (**Figure 5D**).

Overview of the speed distribution of anterograde and retrograde shows that the forward velocity is widely distributed between 0 and 1.5 μm/s, while the reverse velocity tends to the normal distribution curve (**Figures 5D,E**). Subsequently, the distribution of virus particles' state in the axon shows that the viral particles mainly conduct retrograde transport at 0.5–2 hpi and mainly conduct anterograde transport at about eight hpi (**Figure 5F**). Those results indicate that rPRV SC-UL36-EGFP was

suitable for tracing PRV behavior between cell body and axon in the neuron.

## DISCUSSION

The technology for constructing recombination PRV develops quickly in recent years. CRISPR/Cas9 is applied, which leads to the gene deletion mutation easier than before, but the method cannot be used in the gene insertion mutation, especially specific site mutation and seamless insert (Xu et al., 2015; Tang et al., 2016). Meanwhile, plaque purification of recombination PRVs from parental viruses always takes more than 1 month. Infectious BAC of PRV, another genetic manipulation technology, is efficient for gene insertion and deletion using Red/ET technology in *E. coli* (Osterrieder et al., 2003; Wang et al., 2018). However, it takes several months to construct BAC clones, but the genetic and phenotypic change occurs in the recombinant virus due to the unstable large genome of PRV in *E. coli*. Fosmid library is a powerful platform for rescuing DNA viruses and has been used in genomic manipulation of DNA viruses to generate a duck enteritis virus vaccine strain (Chen et al., 2013). The first fosmid library for pseudorabies variant strain PRV TJ has been reported in 2018 by our group (Zhou et al., 2018). In this study, a fosmid library for pseudorabies strain PRV SC was established using the same method. In this study, we got 200 fosmid DNAs that cover the whole genome of PRV SC. Most of the DNA segments are between 30 and 49 kb, and each fragment was cloned into pCC1FOS vector hosted in the *E. coli* strain separately. The positive percentage of most of the fragments was more than 90%. We selected 13 plasmids separated into five groups, five plasmids in one group, and all the groups can rescue the virus successfully. Further, we rescued the rPRV SC-UL36-EGFP strains. There is no significant difference between rPRV SC and PRV SC in growth kinetics, restriction profiles, plaque size, and morphology of virus particles, so the fosmid groups are highly efficient for recovering recombination PRV SC.

The capsid protein VP26 was fused usually with fluorescent protein such as EGFP, Red, or mCherry as a tool for tracing PRV in neural circuits, but the amino-terminal of VP26 fused with EGFP would reduce virus replication by nearly 10-fold (Douglas et al., 2004; Krautwald et al., 2008). The recombinant virus with mCherry fusion to VP26 carboxy-terminal expresses more VP26 fusion protein in infected cells and incorporates

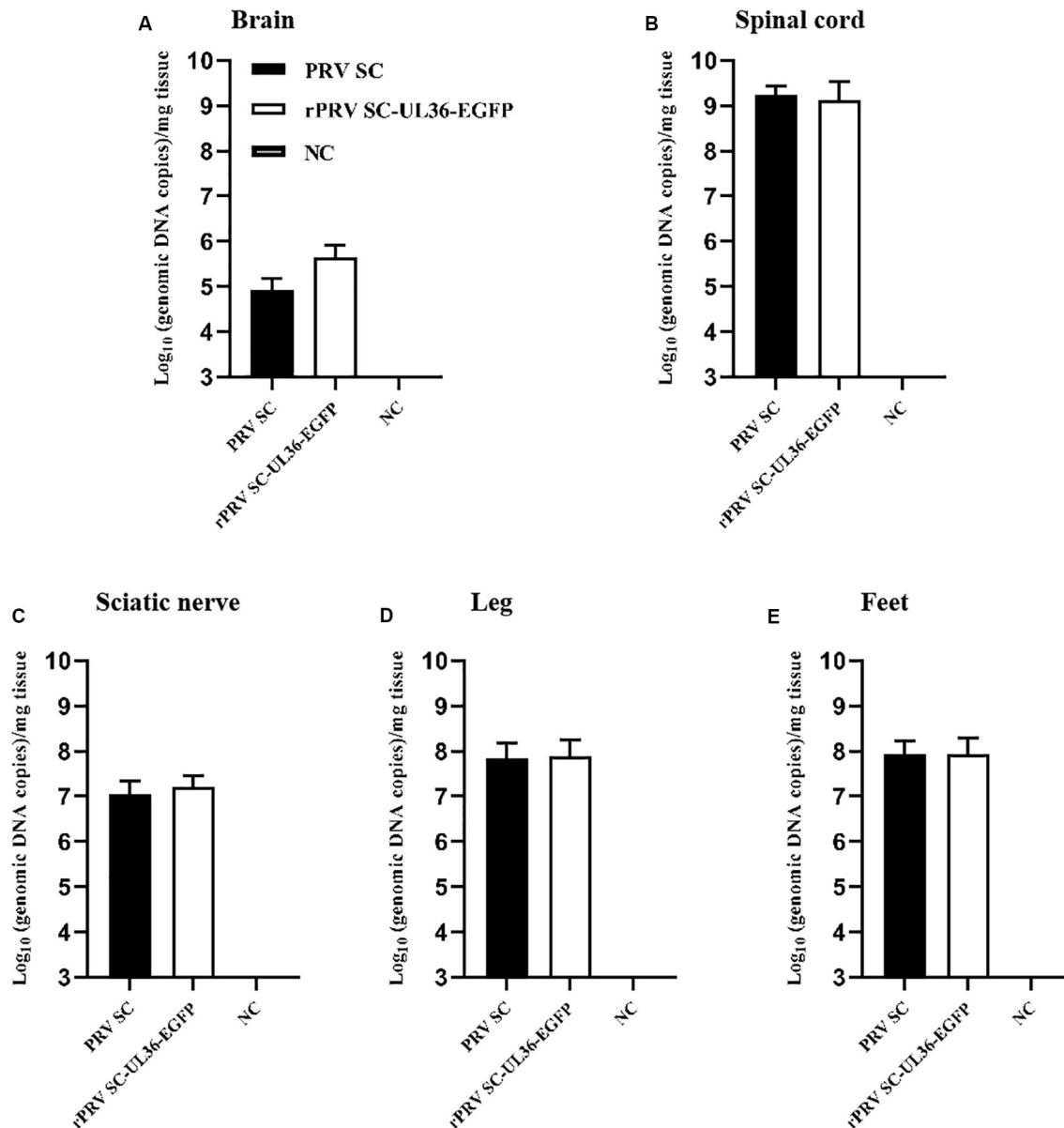
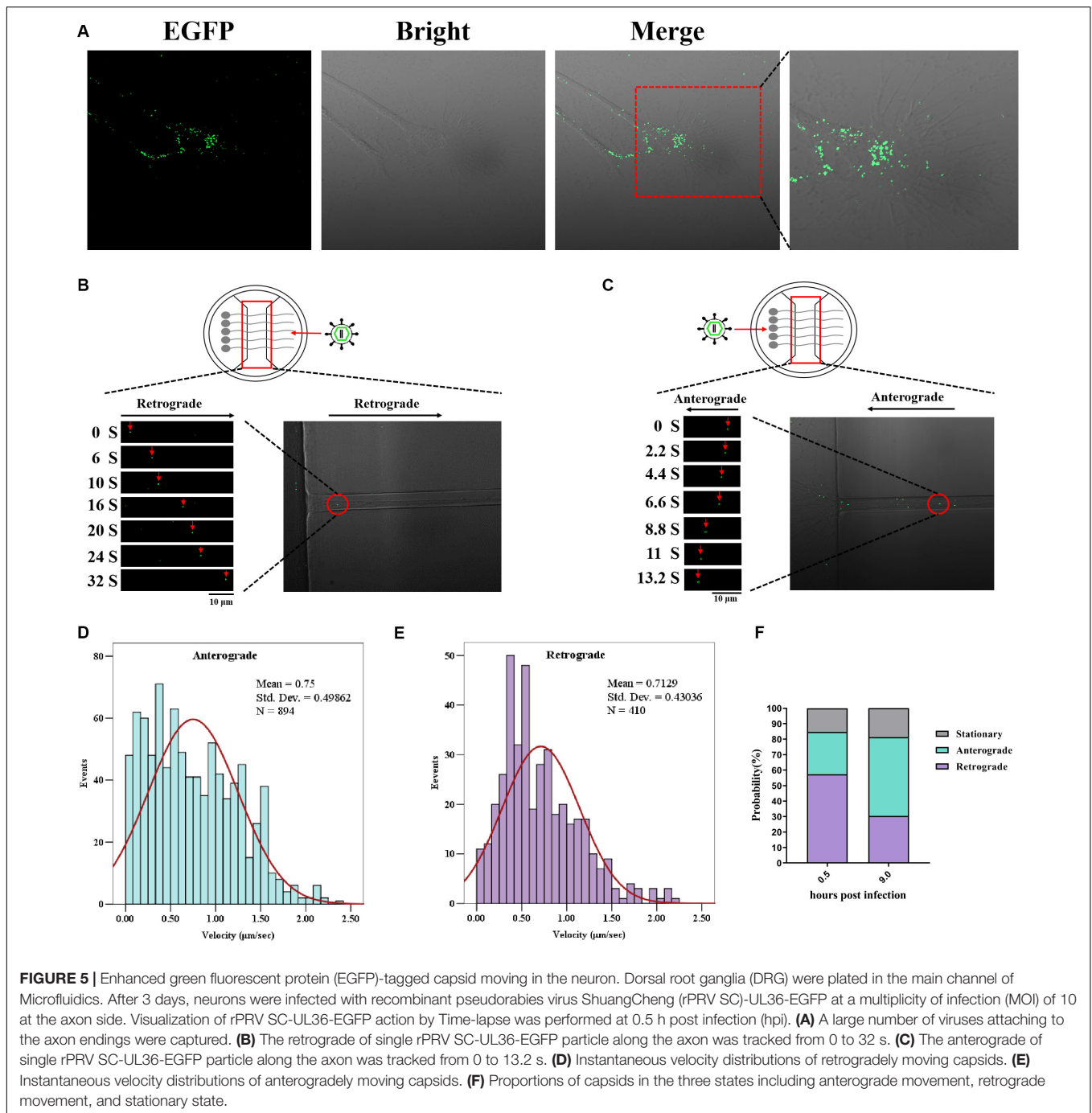


**FIGURE 4 |** Viral loads in the tissue of mice infected with pseudorabies virus ShuangCheng (PRV SC) and recombinant PRV SC (rPRV SC)-UL36-enhanced green fluorescent protein (EGFP) strains. The indicated tissues of mice that were mock infected or infected with  $10^4$  TCID<sub>50</sub> PRV SC or rPRV SC-UL36-EGFP strains, the *gI* gene was detected by real-time PCR to quantify genomic DNA of both two PRV strains. The data represent average copies + SE (error bars) for five samples per group. Samples of 100 mg brain (A), 100 mg lumbar spine (B), and the sciatic nerves (C), 100 mg leg muscles (D), and feet (E) on the inoculated side were harvested from each mouse after they died of infections.

more VP26 fusion protein into virus particles. Individual virus particle exhibits brighter red fluorescence compared to the amino-terminal mCherry-VP26 fusion virus (Hogue et al., 2018). However, the fluorescent protein fusion to VP26 of herpes simplex virus (HSV) is also reported to cause a reduction of the neurovirulence in mice (Krautwald et al., 2008).

UL36 is the critical protein that links PRV capsid with the dynein of the neuron. UL36 and UL37 form viral capsid-tegment complexes for retrograde transport *via* an amino-terminal domain. The carboxy-terminal of UL36 comprises a

proline/alanine-rich region that plays an essential role in PRV replication (Bottcher et al., 2006). In this work, EGFP protein was fused to the amino-terminal of UL36 protein, and rPRV SC-UL36-EGFP performs the same morphology, growth kinetics, and plaque sizes with the parental virus; all these show EGFP protein fused at the amino-terminal of UL36 protein did not affect viral replication and also did not affect the pathogenicity to mouse. The green fluorescent-labeled capsid moving along the axon of neuron both anterograde and retrograde was monitored step by step, and the average velocities of retrograde and



anterograde movements were  $0.71 \pm 0.43$  and  $0.75 \pm 0.49 \mu\text{m/s}$ . This is close to  $0.62 \pm 0.18 \mu\text{m/s}$  of HSV anterograde movement in cortical neuron axons by the same statistical analysis method (Dong et al., 2020). However, The average of PRV movement speed was  $1.2 \mu\text{m/s}$  in the research by Hogue et al. (2018), while the events less than  $0.5 \mu\text{m/s}$  were deleted in the data of Gaussian distribution. The velocity changed at different times post-infection (Dong et al., 2020). Moreover, the virus strain, the kind of neuron, and statistical analysis method may all affect the reported average speed of capsid transport

in axon retrograde. So EGFP fusion to the amino-terminal of UL36 did not affect capsid–tegument complexes transport along the axon of neuron *in vitro*. Our result demonstrated that the rPRV SC-UL36-EGFP could be used for tracking PRV movement in the neuron.

In summary, this fosmid library was efficient and flexible for rescuing recombination PRV SC. The fosmid library and Red/ET technology would be applied in other PRV strains and other DNA virus research. We successfully rescue the rPRV SC-UL36-EGFP using this method. Moreover, we found that the EGFP fusion to

the amino-terminal of UL36 did not affect viral replication and could also work as a tool for tracing PRV in neural circuits.

## DATA AVAILABILITY STATEMENT

All datasets generated for this study are included in the article/supplementary material.

## ETHICS STATEMENT

The animal study was reviewed and approved by The Animal Ethics Committee approval number is Heilongjiang-SYXK-2006-032.

## REFERENCES

- An, T. Q., Peng, J. M., Tian, Z. J., Zhao, H. Y., Li, N., Liu, Y. M., et al. (2013). Pseudorabies virus variant in Bartha-K61-vaccinated pigs, China, 2012. *Emerg. Infect. Dis.* 19, 1749–1755. doi: 10.3201/eid1911.130177
- Bottcher, S., Klupp, B. G., Granzow, H., Fuchs, W., Michael, K., and Mettenleiter, T. C. (2006). Identification of a 709-amino-acid internal nonessential region within the essential conserved tegument protein (p)UL36 of pseudorabies virus. *J. Virol.* 80, 9910–9915. doi: 10.1128/jvi.01247-06
- Brittle, E. E., Reynolds, A. E., and Enquist, L. W. (2004). Two modes of pseudorabies virus neuroinvasion and lethality in mice. *J. Virol.* 78, 12951–12963. doi: 10.1128/JVI.78.23.12951-12963.2004
- Chen, L., Yu, B., Hua, J., Ye, W., Ni, Z., Yun, T., et al. (2013). Construction of a full-length infectious bacterial artificial chromosome clone of duck enteritis virus vaccine strain. *Virol. J.* 10:328. doi: 10.1186/1743-422x-10-328
- Curanovic, D., Lyman, M. G., Bou-Abboud, C., Card, J. P., and Enquist, L. W. (2009). Repair of the UL21 locus in pseudorabies virus Bartha enhances the kinetics of retrograde, transneuronal infection in vitro and in vivo. *J. Virol.* 83, 1173–1183. doi: 10.1128/jvi.02102-08
- Diefenbach, R. J., Miranda-Saksena, M., Diefenbach, E., Holland, D. J., Boadle, R. A., Armati, P. J., et al. (2002). Herpes simplex virus tegument protein US11 interacts with conventional kinesin heavy chain. *J. Virol.* 76, 3282–3291. doi: 10.1128/jvi.76.7.3282-3291.2002
- Dong, X., Zhou, J., Qin, H. B., Xin, B., Huang, Z. L., Li, Y. Y., et al. (2020). Anterograde viral tracer herpes simplex virus 1 strain H129 transports primarily as capsids in cortical neuron axons. *J. Virol.* 94:e01957-19. doi: 10.1128/JVI.01957-19
- Douglas, M. W., Diefenbach, R. J., Homa, F. L., Miranda-Saksena, M., Rixon, F. J., Vittone, V., et al. (2004). Herpes simplex virus type 1 capsid protein VP26 interacts with dynein light chains RP3 and Tctex1 and plays a role in retrograde cellular transport. *J. Biol. Chem.* 279, 28522–28530. doi: 10.1074/jbc.m311671200
- He, W., Auclert, L. Z., Zhai, X., Wong, G., Zhang, C., Zhu, H., et al. (2019). Interspecies transmission, genetic diversity, and evolutionary dynamics of pseudorabies virus. *J. Infect. Dis.* 219, 1705–1715. doi: 10.1093/infdis/jiy731
- Hogue, I. B., Bosse, J. B., Hu, J. R., Thiberge, S. Y., and Enquist, L. W. (2014). Cellular mechanisms of alpha herpesvirus egress: live cell fluorescence microscopy of pseudorabies virus exocytosis. *PLoS Pathog.* 10:e1004535. doi: 10.1371/journal.ppat.1004535
- Hogue, I. B., Jean, J., Esteves, A. D., Tanneti, N. S., Scherer, J., and Enquist, L. W. (2018). Functional carboxy-terminal fluorescent protein fusion to pseudorabies virus small capsid protein VP26. *J. Virol.* 92:e01193-17.
- Hubner, A., Keil, G. M., Kabuuka, T., Mettenleiter, T. C., and Fuchs, W. (2018). Efficient transgene insertion in a pseudorabies virus vector by CRISPR/Cas9 and marker rescue-enforced recombination. *J. Virol. Methods* 262, 38–47.
- Koyuncu, O. O., Hogue, I. B., and Enquist, L. W. (2013). Virus infections in the nervous system. *Cell Host Microbe* 13, 379–393.

## AUTHOR CONTRIBUTIONS

YS and H-JQ designed the research. HQ and MA performed the experiments. HW wrote the manuscript. All authors reviewed the manuscript.

## FUNDING

This work was supported by the National Key Research and Development Program of China (No. 2016YFD0500105), the National Natural Science Foundation of China (Nos. 31870152 and 31702279), and the Heilongjiang Natural Science Foundation (No. C2018067).

- Kramer, T., Greco, T. M., Enquist, L. W., and Cristea, I. M. (2011). Proteomic characterization of pseudorabies virus extracellular virions. *J. Virol.* 85, 6427–6441. doi: 10.1128/jvi.02253-10
- Kramer, T., Greco, T. M., Taylor, M. P., Ambrosini, A. E., Cristea, I. M., and Enquist, L. W. (2012). Kinesin-3 mediates axonal sorting and directional transport of alphaherpesvirus particles in neurons. *Cell Host Microbe* 12, 806–814. doi: 10.1016/j.chom.2012.10.013
- Krautwald, M., Maresch, C., Klupp, B. G., Fuchs, W., and Mettenleiter, T. C. (2008). Deletion or green fluorescent protein tagging of the pUL35 capsid component of pseudorabies virus impairs virus replication in cell culture and neuroinvasion in mice. *J. Gen. Virol.* 89, 1346–1351. doi: 10.1099/vir.0.83652-0
- Lerma, L., Munoz, A. L., Wagner, S., Dinu, M., Martin, B., and Tabares, E. (2016). Construction of recombinant pseudorabies viruses by using PRV BACs deficient in IE180 or pac sequences: application of vBAC90D recombinant virus to production of PRV amplicons. *Virus Res.* 213, 274–282. doi: 10.1016/j.virusres.2015.11.028
- Luo, Y., Li, N., Cong, X., Wang, C. H., Du, M., Li, L., et al. (2014). Pathogenicity and genomic characterization of a pseudorabies virus variant isolated from Bartha-K61-vaccinated swine population in China. *Vet. Microbiol.* 174, 107–115. doi: 10.1016/j.vetmic.2014.09.003
- Luxton, G. W., Haverlock, S., Collier, K. E., Antinone, S. E., Pincetic, A., and Smith, G. A. (2005). Targeting of herpesvirus capsid transport in axons is coupled to association with specific sets of tegument proteins. *Proc. Natl. Acad. Sci. U.S.A.* 102, 5832–5837. doi: 10.1073/pnas.0500803102
- Luxton, G. W., Lee, J. I., Haverlock-Moyns, S., Schober, J. M., and Smith, G. A. (2006). The pseudorabies virus VP1/2 tegument protein is required for intracellular capsid transport. *J. Virol.* 80, 201–209. doi: 10.1128/jvi.80.1.201-209.2006
- Meng, X. Y., Luo, Y., Liu, Y., Shao, L., Sun, Y., Li, Y., et al. (2016). A triplex real-time PCR for differential detection of classical, variant and Bartha-K61 vaccine strains of pseudorabies virus. *Arch. Virol.* 161, 2425–2430. doi: 10.1007/s00705-016-2925-5
- Osterrieder, N., Schumacher, D., Trapp, S., Beer, M., Von Einem, J., and Tischer, K. (2003). [Establishment and use of infectious bacterial artificial chromosome (BAC) DNA clones of animal herpesviruses]. *Berl. Munch Tierarztl. Wochenschr* 116, 373–380.
- Pomeranz, L. E., Ekstrand, M. I., Latcha, K. N., Smith, G. A., Enquist, L. W., and Friedman, J. M. (2017). Gene expression profiling with cre-conditional pseudorabies virus reveals a subset of midbrain neurons that participate in reward circuitry. *J. Neurosci.* 37, 4128–4144. doi: 10.1523/jneurosci.3193-16.2017
- Pomeranz, L. E., Reynolds, A. E., and Hengartner, C. J. (2005). Molecular biology of pseudorabies virus: impact on neurovirology and veterinary medicine. *Microbiol. Mol. Biol. Rev.* 69, 462–500. doi: 10.1128/mmbr.69.3.462-500.2005
- Radtke, K., Kieneke, D., Wolfstein, A., Michael, K., Steffen, W., Scholz, T., et al. (2010). Plus- and minus-end directed microtubule motors bind simultaneously to herpes simplex virus capsids using different inner tegument structures. *PLoS Pathog.* 6:e1000991. doi: 10.1371/journal.ppat.1000991

- Richards, A. L., Sollars, P. J., Pitts, J. D., Stults, A. M., Heldwein, E. E., Pickard, G. E., et al. (2017). The pUL37 tegument protein guides alpha-herpesvirus retrograde axonal transport to promote neuroinvasion. *PLoS Pathog.* 13:e1006741. doi: 10.1371/journal.ppat.1006741
- Roberts, A. P., Abaitua, F., O'hare, P., McNab, D., Rixon, F. J., and Pasdeloup, D. (2009). Differing roles of inner tegument proteins pUL36 and pUL37 during entry of herpes simplex virus type 1. *J. Virol.* 83, 105–116. doi: 10.1128/jvi.01032-08
- Schipke, J., Pohlmann, A., Diestel, R., Binz, A., Rudolph, K., Nagel, C. H., et al. (2012). The C terminus of the large tegument protein pUL36 contains multiple capsid binding sites that function differently during assembly and cell entry of herpes simplex virus. *J. Virol.* 86, 3682–3700. doi: 10.1128/jvi.06432-11
- Smith, G. A., and Enquist, L. W. (1999). Construction and transposon mutagenesis in *Escherichia coli* of a full-length infectious clone of pseudorabies virus, an alphaherpesvirus. *J. Virol.* 73, 6405–6414. doi: 10.1128/jvi.73.8.6405-6414.1999
- Tang, Y. D., Liu, J. T., Wang, T. Y., An, T. Q., Sun, M. X., Wang, S. J., et al. (2016). Live attenuated pseudorabies virus developed using the CRISPR/Cas9 system. *Virus Res.* 225, 33–39. doi: 10.1016/j.virusres.2016.09.004
- Wang, T., Tong, W., Ye, C., Yu, Z., Chen, J., Gao, F., et al. (2018). Construction of an infectious bacterial artificial chromosome clone of a pseudorabies virus variant: reconstituted virus exhibited wild-type properties *in vitro* and *in vivo*. *J. Virol. Methods* 259, 106–115. doi: 10.1016/j.jviromet.2018.06.004
- Xu, A., Qin, C., Lang, Y., Wang, M., Lin, M., Li, C., et al. (2015). A simple and rapid approach to manipulate pseudorabies virus genome by CRISPR/Cas9 system. *Biotechnol. Lett.* 37, 1265–1272. doi: 10.1007/s10529-015-1796-2
- Yan, K., Liu, J., Guan, X., Yin, Y. X., Peng, H., Chen, H. C., et al. (2019). The carboxyl terminus of tegument protein pUL21 contributes to pseudorabies virus neuroinvasion. *J. Virol.* 93:e02052-18.
- Yuan, Q. Z., Li, Z. R., Nan, X., Wu, Y. X., and Li, Y. X. (1987). Isolation and identification of pseudorabies virus. *Chin. J. Prev. Vet. Med.* 3, 10–11.
- Zaichick, S. V., Bohannon, K. P., Hughes, A., Sollars, P. J., Pickard, G. E., and Smith, G. A. (2013). The herpesvirus VP1/2 protein is an effector of dynein-mediated capsid transport and neuroinvasion. *Cell Host Microbe* 13, 193–203. doi: 10.1016/j.chom.2013.01.009
- Zhou, M., Abid, M., Yin, H., Wu, H., Teklue, T., Qiu, H. J., et al. (2018). Establishment of an efficient and flexible genetic manipulation platform based on a fosmid library for rapid generation of recombinant pseudorabies virus. *Front. Microbiol.* 9:2132. doi: 10.3389/fmicb.2018.02132

**Conflict of Interest:** The authors declare that the research was conducted in the absence of any commercial or financial relationships that could be construed as a potential conflict of interest.

Copyright © 2020 Qi, Wu, Abid, Qiu and Sun. This is an open-access article distributed under the terms of the Creative Commons Attribution License (CC BY). The use, distribution or reproduction in other forums is permitted, provided the original author(s) and the copyright owner(s) are credited and that the original publication in this journal is cited, in accordance with accepted academic practice. No use, distribution or reproduction is permitted which does not comply with these terms.



# Polymerase Spiral Reaction Assay for Rapid and Real Time Detection of West Nile Virus From Clinical Samples

Priyanka Singh Tomar<sup>1</sup>, Jyoti S. Kumar<sup>1\*</sup>, Sapan Patel<sup>2</sup> and Shashi Sharma<sup>1</sup>

<sup>1</sup> Division of Virology, Defence Research and Development Establishment, Gwalior, India, <sup>2</sup> School of Studies in Botany, Jiwaji University, Gwalior, India

## OPEN ACCESS

### Edited by:

Bo-Shiun Chen,  
Augusta University, United States

### Reviewed by:

Luiz Tadeu Figueiredo,  
University of São Paulo, Brazil  
Wei-Hua Wu,  
United States Food and Drug  
Administration, United States

### \*Correspondence:

Jyoti S. Kumar  
jyotishukla2@drde.drdo.in

### Specialty section:

This article was submitted to  
Clinical Microbiology,  
a section of the journal  
Frontiers in Cellular and Infection  
Microbiology

**Received:** 13 November 2019

**Accepted:** 13 July 2020

**Published:** 27 August 2020

### Citation:

Tomar PS, Kumar JS, Patel S and  
Sharma S (2020) Polymerase Spiral  
Reaction Assay for Rapid and Real  
Time Detection of West Nile Virus  
From Clinical Samples.  
Front. Cell. Infect. Microbiol. 10:426.  
doi: 10.3389/fcimb.2020.00426

West Nile virus (WNV) is a mosquito-borne virus of public health importance. Currently, there is no FDA approved vaccine available against WNV infection in humans. Therefore, the early diagnosis of the WNV infection is important for epidemiologic control and timely clinical management in areas where multiple Flaviviruses are endemic. The present study aimed to develop reverse transcription polymerase spiral reaction (RT-PSR) assay that rapidly and accurately detects the envelope (env) gene of WNV. RT-PSR assay was optimized at 63°C for 60 min using real-time turbidimeter or visual detection by the addition of SYBR Green I dye. The standard curve for RT-PSR assay was generated using the 10-fold serial dilutions of *in vitro* transcribed WNV RNA. To determine the detection limit of RT-PSR assay, an amplified product of conventional RT-PCR was *in vitro* transcribed as per standard protocol. The detection limit of the newly developed RT-PSR assay was compared with that of conventional RT-PCR and CDC reported TaqMan real-time RT-PCR using a serial 10-fold dilution of IVT WNV RNA. The detection limit of RT-PSR was found to be 1 RNA copy, which is 100-fold higher than that of conventional RT-PCR (100 copies). This suggests that RT-PSR assay is a valuable diagnostic tool for rapid and real-time detection of WNV in acute-phase serum samples. The assay was validated with a panel of 107 WNV suspected human clinical samples with signs of acute posterior uveitis and onset of febrile illness. Out of 107 samples, 30 were found positive by RT-PSR assay. The specificities of the selected primer sets were established by the absence of cross-reactivity with other closely related members viruses of the Flaviviruses, Alphaviruses, and Morbilliviruses groups. No cross-reactivity was observed with other viruses. To best of our knowledge, this is the first report describing the RT-PSR assay for the detection of RNA virus (WNV) in clinical samples. RT-PSR is a high throughput method and more than 30 reactions can be run at once in real-time turbidimeter. PSR assay has potential to be used for a rapid screening of large number of clinical samples in endemic areas during an outbreak.

**Keywords:** WNV, PSR, env, rapid diagnosis, Flaviviruses

## INTRODUCTION

West Nile virus (WNV) causes numerous outbreaks worldwide and major cases were reported in New York, in 1999 (Lanciotti et al., 1999). It was first isolated from the West Nile region of Uganda in 1937 and has become an important cause of humans and animal disease worldwide (Anderson et al., 1999; Chancey et al., 2015). During outbreaks of emerging infectious viruses, accurate and rapid diagnosis is important for reducing further spread through timely implementation of appropriate antiviral treatments, vaccines and controlling measures (Petersen and Roehrig, 2001; Mukhopadhyay et al., 2003; Solomon et al., 2003; Dauphin and Zientara, 2007; Michaelis et al., 2009; Lim et al., 2011; Zengguo et al., 2016). Outbreaks of WN viral disease in human beings have been reported in Africa, the Middle East, Europe, West and South Asia, Australia, and North America (Lanciotti et al., 1999; Vazquez et al., 2010; Caren et al., 2015; European Centre for Disease Prevention Control (ECDC), 2017). WNV can now be found in many avian and mosquito species throughout North America. From 1999 to 2010, more than 2.5 million people were infected with over 12,000 reported cases of encephalitis or meningitis and over 1,300 deaths (Komar, 2000; Marfin and Gubler, 2001; Kilpatrick, 2011; Jolanta et al., 2018). The outbreak of WNV has been recently reported from south Indian states including TamilNadu and Kerala in 2011 (Anukumar et al., 2011; Kumar et al., 2011; Shukla et al., 2012). WNV is a neurotropic pathogen that is the causative agent of West Nile fever and encephalitis in humans and horses. It is a member of the Japanese encephalitis (JE) virus serocomplex, which includes JEV, Murray Valley encephalitis virus (MVEV) and Saint Louis encephalitis virus (SLEV). WNV is classified within the family *Flaviviridae* and genus *Flavivirus*. WNV is maintained in an enzootic cycle between mosquitoes and birds but can also infect and cause disease in horses and other vertebrate animals (Indenbach, 2001; Knipe and Howley, 2001; Faggioni et al., 2014).

The genome is composed of an 11 kb single open reading frame without a polyadenylation tail (Khromykh et al., 2001; Friebe and Harris, 2010; Colpitts et al., 2012; Mehul et al., 2013). The RNA of WNV is translated into a single polyprotein that is post-translationally cleaved by host and viral proteases into three structural (capsid, envelope, and premembrane) and seven non-structural (NS1, NS2A, NS2B, NS3, NS4A, NS4B, and NS5) proteins. The structural proteins are encoded by the 5' end of the genome, which are essential for viral entry, fusion and encapsidation of the viral genome during assembly, and envelope protein (53 kDa) is the major protein on the surface of Flavivirus.

WNV infection is diagnosed by serological tests and hemagglutination inhibition test commonly used for demonstration of a 4-fold increase or decrease of antibody titer in serum samples. MAC (IgM-antibody capture) ELISA is routinely used for the acute WNV infection diagnosis in humans (Sambri et al., 2013). The commercially available WNV specific monoclonal antibody (MicroBix Biosystem INC, Canada) used for the detection of the WNV in antibody capture ELISA (Johnson et al., 2000; Martin et al., 2000; Hunt et al.,

2002). Plaque reduction neutralization (PRNT) test is very important in confirmation of virus isolates (Martin et al., 2000). Additionally, various molecular based diagnostic methods have been applied for the diagnosis of WNV including traditional RT-PCR (Shi et al., 2001), real-time PCR-based assays, such as TaqMan RT-PCR (Lanciotti and Kerst, 2001; Centers for Disease Control and Prevention, 2002) and nucleic acid sequence-based amplification (NASBA) (Compton, 1991; Kumar et al., 2018). Gold standard method for virus detection is isolation; but it is time consuming and tedious method. Most acceptable method for routine diagnosis of WNV infection is CDC reported TaqMan real-time RT-PCR, which is consider as gold standard method for detection of WNV infection. However, all of these nucleic acid amplification methods have some drawbacks of requiring either a sophisticated instrument for amplification or a complicated method for amplified product detection (Leone et al., 1998). Owing to the problems associated with the current screening systems, it is widely accepted that test results should be confirmed by more than one type of assay. More techniques are therefore needed to complement those already existing techniques.

A number of isothermal gene amplification techniques such as loop-mediated isothermal amplification (LAMP) (Notomi et al., 2000), helicase-dependent amplification (HDA), nucleic-acid-sequence-based amplification (NASBA) (Shi et al., 2001), cross-priming amplification (CPA) (Meng et al., 2016), and self-sustained sequence replication reaction (3SR) (Muller et al., 1997) have been reported during past decades (Gupta et al., 2017). These techniques have their own limitations with respect to optimizing the reaction conditions. LAMP assay comprises 6 sets of primers for amplification, HDA require additional enzymes, such as DNA helicase for achieving denaturation of double-stranded DNA and it takes 90 min for completion of the reaction, CPA requires complexity in primer designing and 3SR requires different incubation temperature for completion of the reaction.

In the present study, we have developed the RT-PSR isothermal gene amplification technique for the detection of WNV. The PSR assay was originally described by (Liu et al., 2015) which uses only one set of primers and one enzyme. The PSR method has the advantages of high specificity, sensitivity and rapidity under isothermal conditions over other established gene amplification methods. Until now, the PSR technique has been developed for bacteria (Liu et al., 2015, 2018) yeast (*Candida albicans*) and DNA viruses (canine parvovirus and Bovine herpesvirus-1) (Xiaoqun et al., 2016). PSR approach is based on strand displacement activity of *Bst* DNA polymerase enzyme, isolated from *Bacillus stearothermophilus*.

However, no reports are available on application of the PSR method for detection of RNA viruses. In the present study, we have developed an RT-PSR assay for rapid and real-time detection of WNV where amplification is achieved by incubating with buffer and other components with viral RNA in the presence of *Bst* DNA polymerase at a constant temperature of 63°C for 1 h. Results were interpreted by real-time monitoring in a turbidimeter and visually detected using SYBR Green I dye.

## MATERIALS AND METHODS

### Cells and Virus Strains

Vero cells (African Green Monkey Kidney epithelial cells) were obtained from National Center for Cell Science (NCCS) Pune, India. The cells were maintained in Eagle Dulbecco's minimum essential medium (Sigma, USA) supplemented with 10% fetal bovine serum (Sigma, USA), Trypsin-EDTA solution (Himedia, India) and antibiotic-antimycotic solution (Conc. 100 mg/ml penicillin and 100 mg/ml streptomycin) (Sigma, USA) at 37°C in humidified atmosphere with 5% CO<sub>2</sub> incubator. The WNV (Eg101 strain) used in the present study was obtained from the Institute of Tropical Medicine, Nagasaki, Japan. WNV was propagated by regular passaging in *Aedes albopictus* C6/36 cell lines. The virus was titrated by plaque assay in Vero cells in accordance with the standard protocol (Igarashi, 1978). The viruses utilized in the present study were WNV, JE, SLE, Yellow fever, Dengue, Chikungunya, Ross River, Measles, Mumps, and Rubella.

### Clinical Samples

The serum and plasma samples ( $n = 107$ ) used in this study were collected from the Department of Microbiology, Aravind Eye Hospital, Madurai (TamilNadu) India, from patients with signs of acute posterior uveitis and onset of febrile illness symptoms suspected to have WNV infections during December 2012. The acute phase serum samples collected between days 1 and 9 after the onset of symptoms were used for evaluation. The other clinical symptoms of the patients include fever, ocular manifestation muscle weakness, and poliomyelitis-like flaccid paralysis (Shukla et al., 2012). The patient study was approved by the institutional ethics committee of Aravind Eye Hospital, Madurai, India.

### RNA Extraction

The genomic viral RNA was extracted from 140  $\mu$ l of WNV infected cell culture supernatant and patient serum and plasma samples using QIAamp Viral RNA Mini Kit (Qiagen, Germany), according to the manufacturer's protocol. The RNA was eluted in 50  $\mu$ l of elution buffer using QIA spin columns and stored at -80°C until further use.

### Primer Design

WNV specific RT-PSR primers were designed using the DNA STAR software program. Primers were designed using the nucleotide sequence of the env gene of WNV (Accession no. AF260968) with 20–22-bases oligonucleotide sequence was added at the 5' end to primers. High-performance liquid chromatography (HPLC) grade primers were procured from Chromous Biotech Ltd, Bangalore, India. The details of the oligonucleotide primers used for amplification of the env gene of WNV are given in Table 1.

### In vitro Transcription (IVT)

To determine the detection limit of RT-PSR, IVT was carried out. Briefly, full length cloned env gene in PET 28a+ vector was used for IVT. The plasmid was extracted from an overnight grown culture of kanamycin resistant recombinant clone using the plasmid extraction kit (Qiagen, Germany). Plasmid was confirmed using env gene specific primer set by conventional

RT-PCR. RT-PCR amplified product was used as the template for IVT. *In-vitro* RNA was synthesized using the Megascript-T7 transcription kit (Invitrogen, USA) according to the manufacturer's protocol. Finally, the RNA pellet was resuspended in nuclease free water. Copy number was determined using the following formula-

$$Y \text{ molecules}/\mu\text{l} = \left( X \text{ g}/\mu\text{l RNA} / \left[ \text{transcript length in nucleotides} \times 340 \right] \right) \times 6.022 \times 10^{23}$$

WNV RNA was quantified using a Nanodrop ND-1000 spectrophotometer (Thermo Scientific, Germany). Further 10-fold serial dilutions of the RNA transcript were used for detection of sensitivity and construction of standard curve using the Tp values obtained against the known concentration of serially diluted RNA.

### Reverse Transcription Polymerase Spiral Reaction (RT-PSR Assay)

The RT-PSR assay was carried out at 63°C for 60 min using a real-time turbidimeter instrument (LA-200, Teramecs, Japan). The RT-PSR reaction was performed in 25  $\mu$ l reaction volume using 2.5  $\mu$ l 10  $\times$  ThermolPol reaction buffer (New England Biolabs, USA) (containing 20 mM Tris-HCl, 10 mM (NH<sub>4</sub>)<sub>2</sub>SO<sub>4</sub>, 2 mM MgSO<sub>4</sub>, 10 mM KCl, 0.1% Tween 20) 0.8 M Betaine (Sigma, USA), 6 mM MgSO<sub>4</sub> (Sigma, USA), 1.0  $\mu$ l *Bst* DNA polymerase large fragment (New England Biolabs, USA), 1.4 mM each deoxynucleotide triphosphate (Sigma, USA), 4.0  $\mu$ M for both forward and reverse primer and 2.5  $\mu$ l (40 ng) of template. The RT-PSR assay was also optimized the effect of different primer and template concentrations. The effect of higher concentrations of RNA templates in the RT-PSR reaction was also observed by real-time monitoring.

### Reverse-Transcription Polymerase Chain Reaction (RT-PCR)

To compare the clinical sensitivity of the RT-PSR method, RT-PCR was performed using env gene specific reported primers for WNV [Forward: 5'TGGATTTGGTTCTCGAAGG3' genome position (1,228–1,046) and reverse: 5'GCTCAGCACGTTTGT CATT3' genome position (1,228–1,210)] (Parida et al., 2004). The amplification was carried out in total reaction volume of 25  $\mu$ l using a one-step RT-PCR kit (Qiagen, Germany) with 20 nM of forward and reverse primers and 2.5  $\mu$ l (40 ng) of RNA. The thermal profile of RT-PCR reaction was as follows: RT-step at

**TABLE 1** | Details of RT-PSR Primer set designed for rapid detection of WNV.

Name of primers	Genome position accession no. [AF260968]	Primer sequences
WNV PSR-forward primer	1,268–1,288	5' acgattcgtacatagaagtata-gAGATACAGCTTGGGACTTTG 3'
WNV PSR-reverse primer	1,340–1,359	5' gatatgaagatacatgcttag-caCAACTGCGAGAACGTGAG 3'

50°C for 30 min, denaturation at 94°C for 10 min, followed by 35 cycles of 94°C for 1 min, 55°C for 1 min, 72°C for 1 min and final extension cycle at 72°C for 10 min.

The amplified product was analyzed by agarose gel electrophoresis on a 2% agarose gel (Sigma, USA). The DNA was visualized by ethidium bromide staining and imaged using gel Doc system (Bio-Rad, USA).

### TaqMan Real-Time RT-PCR

For comparative evaluation of the RT-PSR assay, TaqMan real-time RT-PCR was performed using WN-3'NC gene primers WN-3'NC Forward: CAGACCACGCTACGGCG (genome position (10,668–10,684), WN-3'NC reverse: CTAGG GCCGCGTGG (genome position (10,770–10,756) and a WN 3'NC-probe: TCTGCGGAGAGTGCAGTCTGCGAT (genome position 10,691–10,714). The amplification was carried out with total reaction volume of 25 µl using Ag Path-ID one-step RT-PCR reagents (Thermo Fisher, USA) performed in real-time instrument (AB Biosystems USA) with 20 nM of forward and reverse primers along with 50 nM probe and 2.5 µl (40 ng) of RNA according to the manufacturer's protocol. The thermal profile of TaqMan real-time RT-PCR consists 1 cycle of reverse transcription reaction 50°C for 30 min and 95°C for 10 min and 40 cycles of 95°C for 15 s and 60°C for 1 min.

### Analysis of RT-PSR Product

The RT-PSR amplified products detected by two methods either by real-time turbidity monitoring or direct visual detection under UV light using SYBR Green I dye.

### Real-Time Monitoring of RT-PSR

RT-PSR reaction was carried out in the Real-time turbidimeter that measures the optical density through spectrophotometric analysis at 400 nm every 6 s. The turbidimeter determined results in terms of time of positivity ( $T_p$ ; in minutes). The processing of the sample having  $T_p$  values of 60 min or less and threshold value above the  $>0.1$  was considered positive while the threshold values that remained fixed at  $\geq 0.1$  were considered negative.

### Naked-Eye Visualization

RT-PSR amplified product was visualized by addition of SYBR Green I dye (Invitrogen, USA). A positive reaction emits bright green fluorescence under ultraviolet (UV) light (302 nm) while negative samples remained orange.

### Statistical Analysis

The clinical sensitivity and specificity of the RT-PSR assay were determined and compared to the conventional RT-PCR. The standard deviation among samples was also calculated. Each experiment repeated three times.

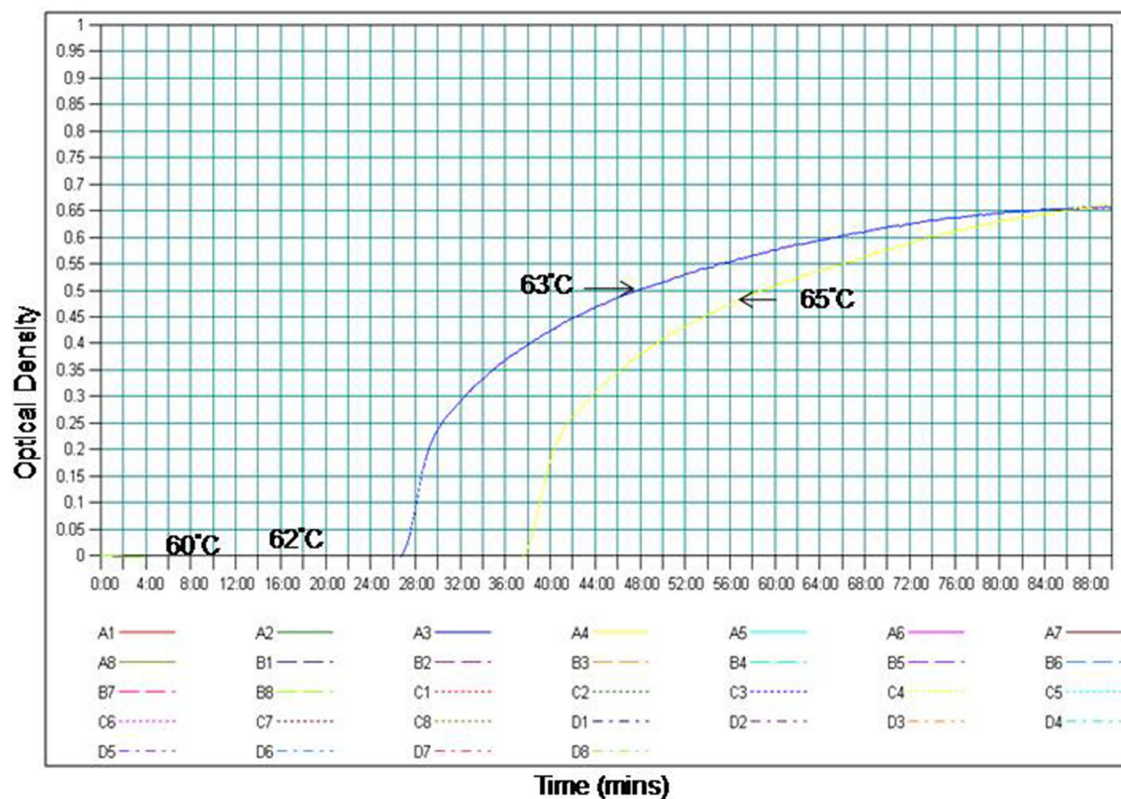


**FIGURE 1** | Effect of temperature on the time kinetics of the RT-PSR amplification reaction of WNV Eg101 strain as monitored in real time turbidimeter.

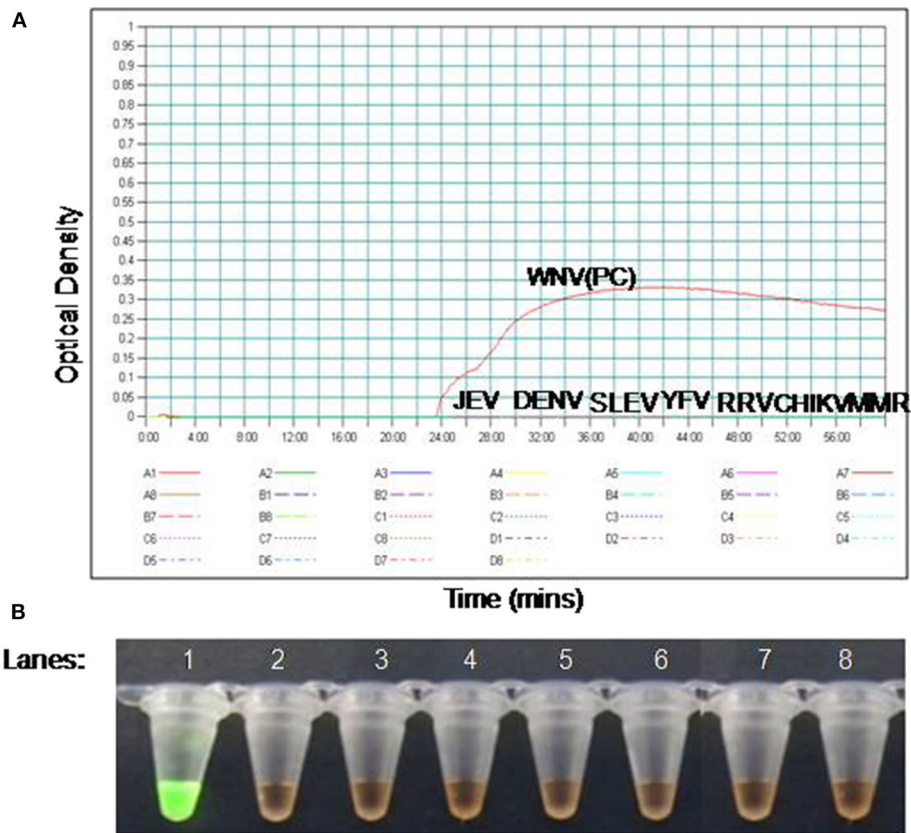


**FIGURE 2 |** The RT-PSR assay specificity for WNV detection. **(A)** Evaluation by real-time turbidimeter for real time monitoring, **(B)** evaluation by SYBR Green I dye naked eye visualization. Lane 1. West Nile virus (WNV); lane 2. Japanese Encephalitis virus (JEV); lane 3. Dengue virus (DENV); lane 4. Saint Louis encephalitis virus (SLE), lane 5. Yellow Fever virus (YFV), lane 6. Ross River fever virus (RRV); lane 7. Chikungunya virus (CHIKV); lane 8. Measles, Mumps, and Rubella virus (MMR).

## RESULTS

### Temperature Optimization

The temperature for RT-PSR assay was optimized using the gradient range from 60 to 65°C (60, 62, 63, 64, and 65°C) for 60 min. At 63°C amplification was observed within 30 min as compared to 65°C where amplification was obtained within 39 min. Therefore, 63°C temperature was selected for the RT-PSR assay to perform further experiments (Figure 1).

### Specificity of RT-PSR

The specificity of the PSR assay was established by ruling out the cross-reactivity with other viruses. The Eg101 strain of WNV was used as positive control. No cross-reactivity was observed with other Flaviviruses, Alphaviruses and Morbillivirus including WNV, JEV, SLEV, YFV, DENV, CHIKV, RRV, and MMR (Figure 2).

### Comparative Sensitivities of RT-PSR and RT-PCR Assay

To compare the sensitivity of the RT-PSR assay with conventional RT-PCR, 10-fold serial dilutions ranging from  $10^5$  to 1 copy were tested in triplicates. The detection limit of RT-PSR assay was found to be 1 RNA copy. The comparative sensitivity revealed that RT-PSR is 100 times more sensitive than the conventional

RT-PCR, which detected 100 RNA copies (Figure 3). The standard curve generated from 10-fold serial dilutions of IVT WNV RNA showed a linear curve with the coefficient of correlation  $R^2 = 0.979$  (Figure 4).

### Comparative Evaluation of RT-PSR With Conventional RT-PCR and TaqMan Real-Time RT-PCR Assay

To determine the clinical applicability of the RT-PSR method, 107 WNV suspected serum and plasma samples were screened, in addition with a panel of positive serum samples of chikungunya ( $n = 12$ ) and healthy volunteers ( $n = 20$ ), included as negative control (Figure 5).

From the 107 samples, 30 were positive in both RT-PSR and TaqMan real-time RT-PCR, while only 28 were positive by conventional RT-PCR (Table 2). Comparative evaluation between RT-PSR and conventional RT-PCR revealed 98.13% concordance with a sensitivity and specificity of 93.75 and 100%, respectively (Figure 6).

## DISCUSSION

In India, the presence of antibodies against WNV in humans was first reported in Bombay, in 1952 Banker (1952), and have been reported in other cities more recently (Paramasivan et al.,

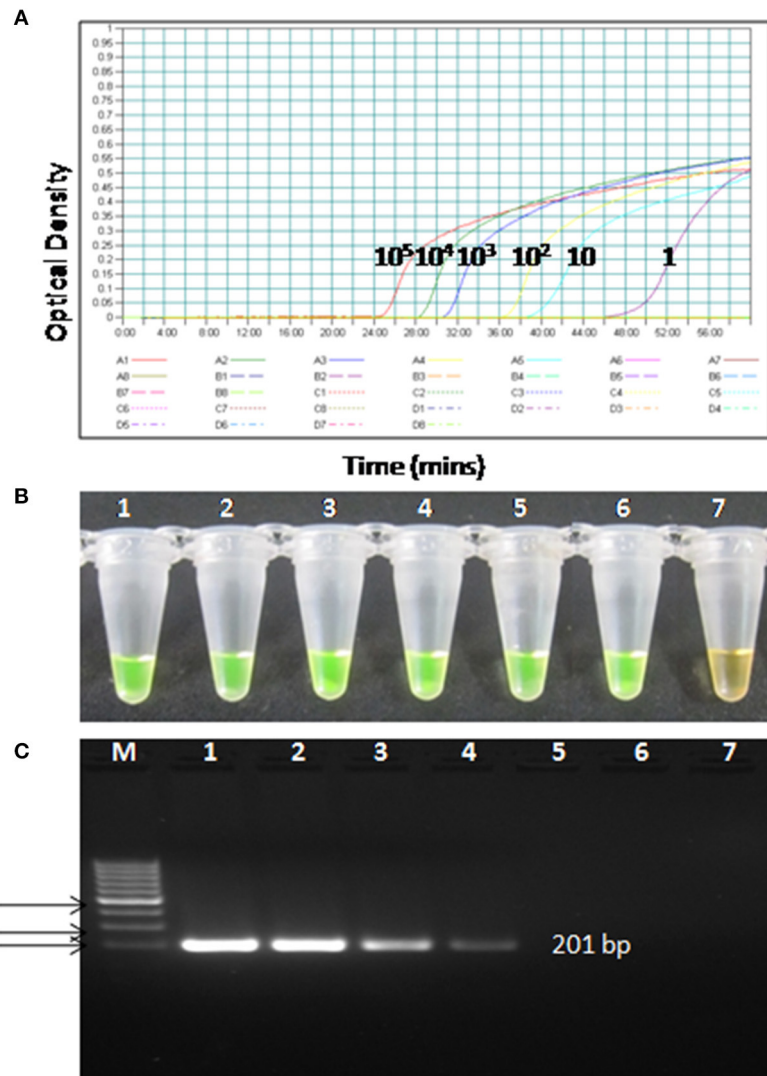


**FIGURE 3** | Comparison between sensitivity of RT-PSR and conventional RT-PCR (A) real-time kinetics of WNV RT-PSR amplification of the env gene showing the amplification curve with serial 10-fold dilutions of the WNV IVT RNA ( $10^5$  to 1 copy no.), (B) naked eye visualization through SYBR Green I dye, (C) RT-PCR performed as the same serial dilution used for RT-PSR and amplified products were stained with ethidium bromide dye. M, 100 bp marker; Lane 1–6, IVT serial dilution ( $10^5$  to 1 copy no.) Lane 7, Negative (without template) control.

2003). WNV neutralizing antibodies have been also reported in human serum samples collected from Andhra Pradesh, Orissa, Rajasthan, Madhya Pradesh, Maharashtra, Tamil Nadu, and Karnataka. Similarly, during 1977, 1978, and 1981 WNV seropositive cases were reported from Vellore and Kollar district (Paramasivan et al., 2003). A number of different laboratory based diagnostic methods is used for detection of WNV in clinical samples. Several nucleic acid amplification techniques such as RT-PCR (Higuchi et al., 1993; Shi et al., 2001), TaqMan real-time RT-PCR (Lanciotti and Kerst, 2001) and SYBR Green real-time RT-PCR (Papain et al., 2004) have been reported for rapid detection of WNV. In spite of the high degree of nucleic acid amplification, these PCR-based methods are expensive and require trained personnel to perform the reaction. In addition, these methods are often complex to adapt for use in clinics with

resource limited settings. Therefore, a rapid, sensitive and cost-effective detection method is necessary for proper surveillance of new WNV circulating strains.

TaqMan real-time RT-PCR assay has been reported for detection of WNV from various samples including serum, cerebrospinal fluid (CSF), brain tissue samples from human, field-collected mosquitoes and birds tissue samples (Lanciotti and Kerst, 2001). The real-time PCR based assays have many advantages over conventional RT-PCR methods, presenting rapidity, lower contamination rate, higher sensitivity, quantitative measurement and higher specificity (Heid et al., 1996). These assays are easy to perform, but can be afforded only by referral laboratories with good financial supports. The development of fluorogenic PCR utilizing 5'-3' nuclease activity of *Taq* DNA polymerase facilitated the removal of post-PCR

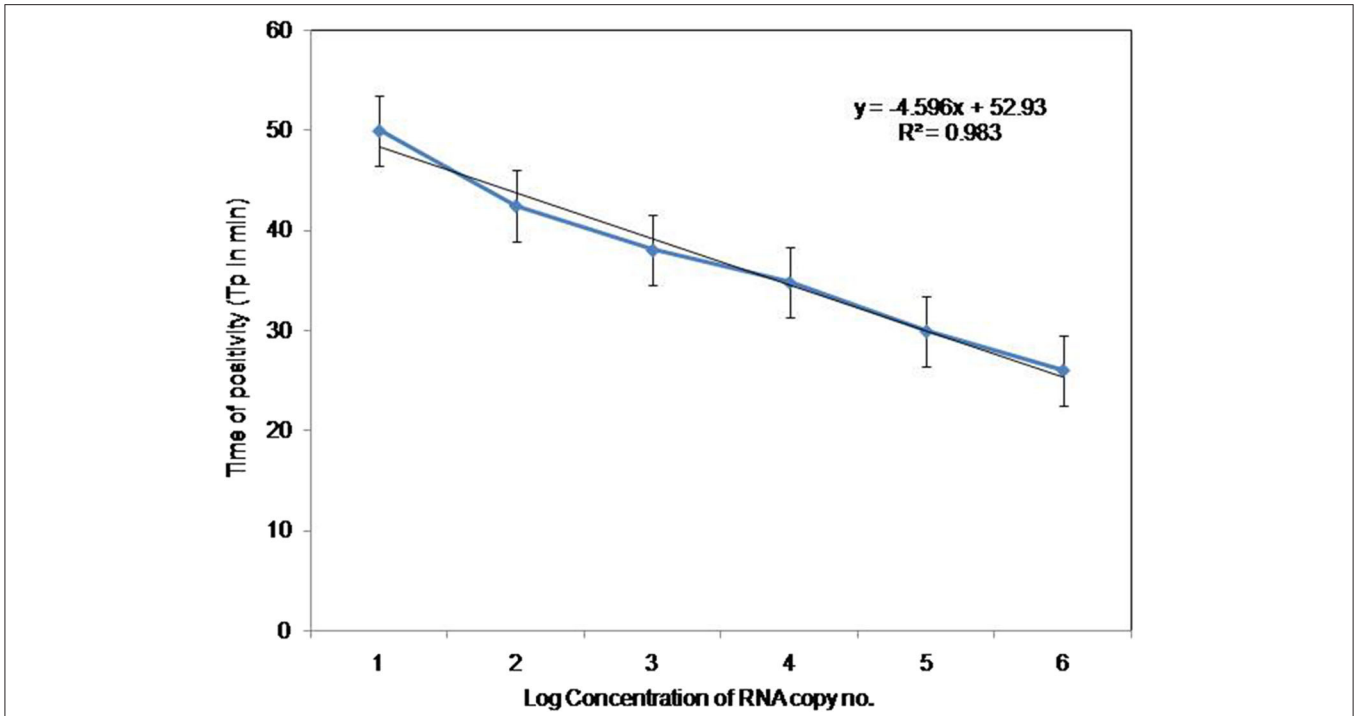


**FIGURE 4 |** Standard curve for RT-PSR Assay. Env RT-PSR specific standard curve as generated from the amplification plot between different copy number of the template (serial 10-fold dilution from  $10^5$  to 1 copy number) and Tp. The Tp value shown here is the average of triplicates run for each concentration.

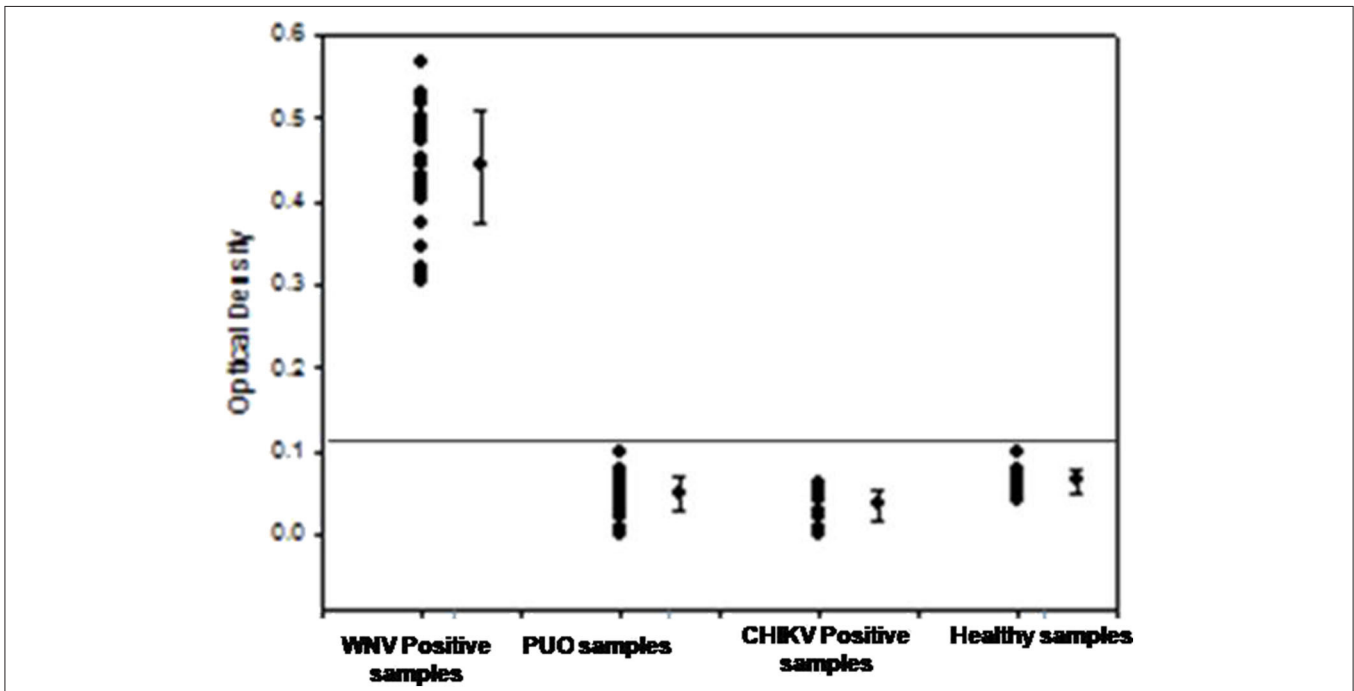


**FIGURE 5 |** The optical density profile of different patient samples including WNV positive samples, PUO (pyrexia of unknown origin), Chikungunya positive along with samples from healthy volunteers as obtained through the West Nile-specific RT-PSR assay.

processing agarose gel electrophoresis (Del et al., 2013). However, all these nucleic acid amplification methods have several drawbacks of requiring either a high precision instrument for amplification or complicated post-PCR processing method for the endpoint detection of amplified products.

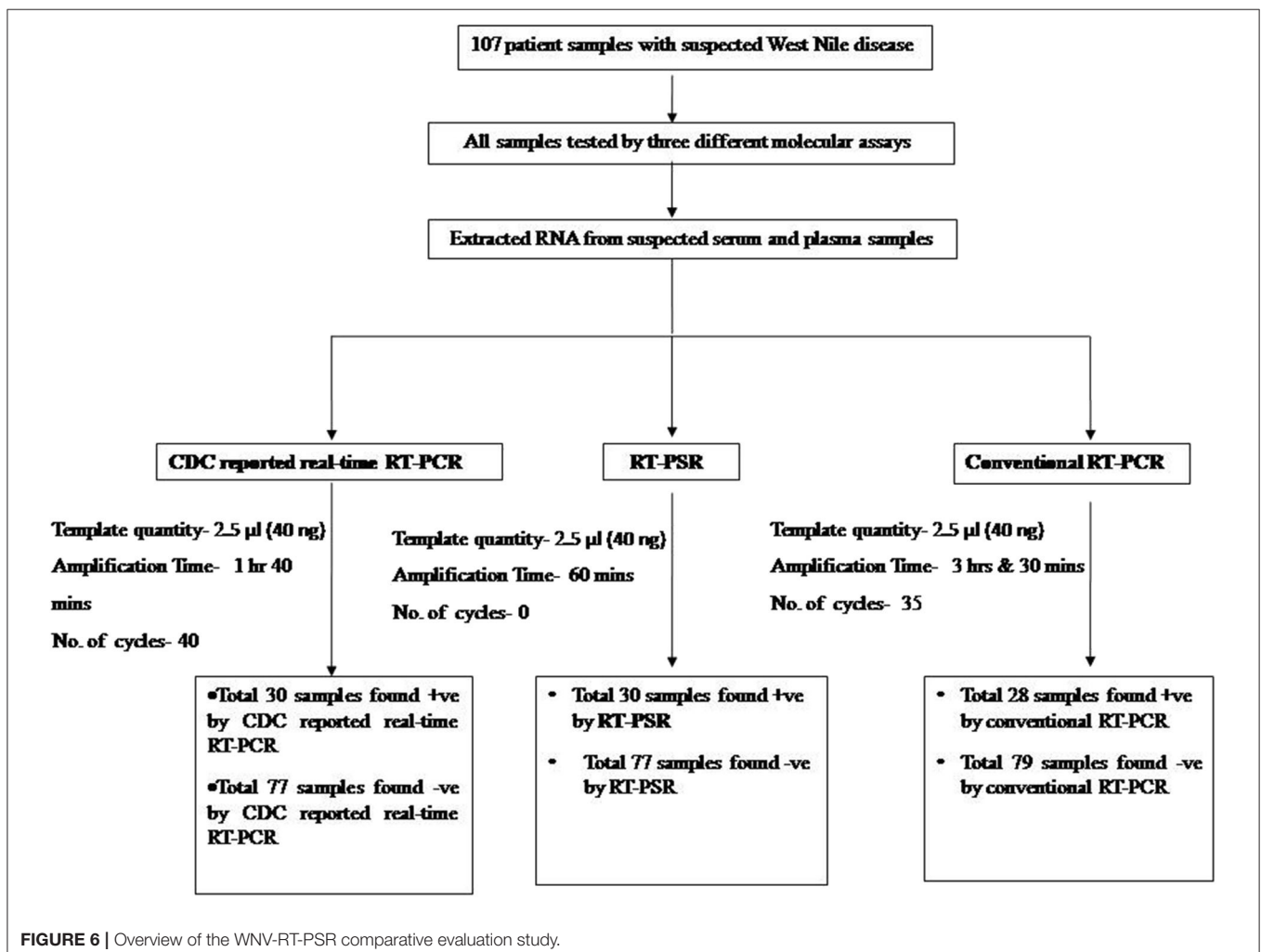
These rapid molecular tests might not be the ideal method in basic clinical settings or field based situations. Therefore, it is important to develop simple and rapid molecular tests to overcome the limitations within existing techniques. The present study aimed to develop a RT-PSR assay for a rapid detection of WNV.

The RT-PSR assay is a simple diagnostic tool in which the reaction is performed in a single tube by mixing thermopol buffer, primers and DNA polymerase followed by incubation at 63°C for 60 min. Since the reaction is performed at a constant temperature, an energy intensive thermal cycler is not needed. Moreover, the positive results could be determined through a visual color change. The sensitivity of RT-PSR was 1 RNA copy when compared to 100 RNA copies in conventional RT-PCR. The assay was evaluated on 107 clinical samples. No cross-reactivity was observed with any of the Flaviviruses, Alphaviruses and Morbilliviruses tested. Comparative sensitivity of RT-PSR and RT-PCR revealed 98.13% concordance. PSR has so far been used for detection of a recombinant plasmid containing a blaNDM-1 gene in *E. coli* BL21 bacteria (Liu et al., 2015; Wei et al., 2015, 2018), yeast *Candida albicans* (Xiaoqun et al., 2016), canine

**TABLE 2** | Comparative evaluation of RT-PSR assay with conventional RT-PCR and real-time RT-PCR assay for the detection of the Env gene of WNV in suspected human-patient serum-plasma samples.

RT-PSR	Conventional RT-PCR	Real-time RT-PCR	No. of samples
+	+	+	28
-	-	-	77
+	-	+	2
-	+	-	0

+, positive; -, negative; Total no. of samples: 107. 28 Samples: Total samples +ve by all three methods. 77 Samples: Total samples -ve by all three methods. 2 Samples: -ve by Conventional RT-PCR methods but +ve by CDC reported Real-Time RT-PCR and RT-PSR methods. 0 Sample: No sample found +ve in Conventional RT-PCR which were -ve by CDC reported Real-Time RT-PCR and RT-PSR methods.



parvovirus and Bovine Herpesvirus 1 (Gupta et al., 2017; Javed et al., 2018). One important characteristic of this isothermal gene amplification technique is the field based application, by using SYBR Green I dye-mediated naked eye visualization.

This is low cost, rapid, simple, and sensitive technique, since gene amplification can be performed in a heating block/water bath, and visualization of the green fluorescence light can be performed by using a simple UV hand-held torch (Parida et al., 2011). Currently, the cost of a RT-PSR reaction is estimated to be 47.46 Rupees per sample test. The light green fluorescence can be observed by using a simple UV hand-held torch. The test is rapid and amplification can be achieved within 60 min as compared to the 3–4 h required by conventional gene amplification techniques. The method is sensitive, specific and enables to detect low copy number of virus, mostly in some cases that would be missed by conventional RT-PCR techniques. These findings suggest that the env gene-specific RT-PSR assay is an important diagnostic tool for rapid and real-time detection of WNV.

## CONCLUSION

RT-PSR is a rapid, sensitive and specific method to detect the RNA virus WNV in clinical samples with comparison to the RT-PCR method. The method is simple, low cost and rapid, performed under isothermal conditions over 1 h and can be both quantified through turbidity or through UV color change, making it an attractive option for use in the field.

RT-PSR has a short performance time, which is a desirable characteristic amenable for samples testing in limited infrastructure settings in endemic rural areas during an outbreak. We believe it will enable early detection of the WNV infection and help controlling its spread among humans.

## REFERENCES

- Anderson, J. F., Andreadis, T. G., Vossbrinck, C. R., Tirrell, S., Wakem, E. M., French, R. A., et al. (1999). Isolation of West Nile virus from mosquitoes, crows and a Cooper's hawk in Connecticut. *Science* 286, 2331–2333. doi: 10.1126/science.286.5448.2331
- Anukumar, B., Sakpal, G. N., Tandale, B. V., Balasubramaniam, R., and Gangale, D. (2011). West Nile Encephalitis outbreak in Kerala, India. *J. Clin. Virol.* 61, 152–155. doi: 10.1016/j.jcv.2014.06.003
- Banker, D. (1952). Preliminary observation on antibody patterns against certain viruses among inhabitants of Bombay City. *Indian J. Med. Res.* 6, 733–746.
- Caren, C., Andriyan, G., and Evgeniya, V. (2015). The global ecology and epidemiology of West Nile Virus. *Biomed. Res. Int.* 2015:376230.
- Centers for Disease Control and Prevention (2002). Laboratory acquired West Nile virus infections-United States. *M.M.W.R. Morb. Mortal. Wkly. Rep.* 51, 1133–1135.
- Chancey, C., Grinev, A., Volkova, E., and Rios, M. (2015). NASBA and other transcription-based amplification methods for research and diagnostic microbiology. *Biomed. Res. Int.* 10, 185–196.
- Colpitts, T. M., Conway, M. J., Montgomery, R. R., and Fikrig, E. (2012). West Nile virus: biology, transmission, and human infection. *Clin. Microbiol. Rev.* 25, 635–648. doi: 10.1128/CMR.00045-12
- Compton, J. (1991). Nucleic acid sequence-based amplification. *Nature* 350, 91–102. doi: 10.1038/350091a0
- Dauphin, G., and Zientara, S. (2007). West Nile virus: recent trends in diagnosis and vaccine development. *Vaccine* 25, 5563–5576. doi: 10.1016/j.vaccine.2006.12.005

## DATA AVAILABILITY STATEMENT

The datasets generated for this study can be found in NCBI, accession numbers JN591727 to JN591753.

## ETHICS STATEMENT

The studies involving human participants were reviewed and approved by Aravind Eye Hospital, Madurai, India. The patients/participants provided their written informed consent to participate in this study.

## AUTHOR CONTRIBUTIONS

JK: conceptualization, data analysis, review, and supervision of MS. PT: standardization, evaluation of the assay, data analysis, and manuscript writing. SP: review and editing of MS writing. SS: review of MS. All authors: read and approved the final manuscript.

## FUNDING

This work was supported by Defence Research and Development Organization (DRDO) research funds.

## ACKNOWLEDGMENTS

Authors would like express their gratitude to Dr. D.K. Dubey, Director, Defence Research and Development Establishment (DRDE), Ministry of Defence, Government of India, for constant inspiration, support, and providing facilities required for this study. This manuscript is assigned DRDE accession no. DRDE/VIRO/34/2019.

- Del, A. J., Sotelo, E., Fernandez, P. J., Gallardo, C., Llorente, F., Agüero, M., et al. (2013). A novel quantitative multiplex real-time Rt- Pcr for the simultaneous detection and differentiation of West Nile virus Lineages1and 2 and of Usutu virus. *J. Virol. Methods* 189, 321–327. doi: 10.1016/j.jviromet.2013.02.019
- European Centre for Disease Prevention and Control (ECDC). (2017). *West Nile Fever in Europe in 2017 and Previous Transmission Seasons*. Stockholm: ECDC. Available online at: <https://ecdc.europa.eu/en/publications-data/west-nile-fever-europe-2017> (accessed December 14, 2017).
- Faggioni, G., Santis, D., Pomponi, A., Fantini, M., Savini, G., Monaco, F., et al. (2014). Rapid molecular detection and genotyping of West Nile Virus lineages and by real time PCR and melting curve analysis. *J. Virol. Methods* 207, 54–59. doi: 10.1016/j.jviromet.2014.06.020
- Friebe, P., and Harris, E. (2010). Interplay of RNA elements in the dengue virus 5' and 3' ends required for viral RNA replication. *J. Virol.* 84, 6103–6118. doi: 10.1128/JVI.02042-09
- Gupta, V., Soumendu, C., Chander, V., Sourabh, M., Shabir, A. B., Vivek, K. G., et al. (2017). Polymerase spiral reaction (PSR): a novel, visual isothermal amplification method for detection of canine parvovirus 2 genomic DNA. *Arch. Virol.* 20, 189–196. doi: 10.1007/s00705-017-3321-5
- Heid, C. A., Stevens, J., Livak, K. J., and Williams, P. M. (1996). Real time quantitative PCR. *Genome. Res.* 6, 986–994. doi: 10.1101/gr.6.10.986
- Higuchi, R., Fockler, C., Dollinger, G., and Watson, R. (1993). Kinetic PCR analysis: real-time monitoring of DNA amplification reaction. *Nat. Biotechnol.* 11, 1026–1030. doi: 10.1038/nbt0993-1026

- Hunt, A. R., Hall, R. A., Kerst, A. J., Nasci, R. S., Savage, H. M., Panella, N. A., et al. (2002). Detection of West Nile virus antigen in mosquitoes and avian tissues by a monoclonal antibody based capture enzyme immunoassay. *J. Clin. Microbiol.* 40, 2023–2030. doi: 10.1128/JCM.40.6.2023-2030.2002
- Igarashi, A. (1978). Isolation of a Singh's *Aedes albopictus* cell clone sensitive to Dengue and Chikungunya viruses. *J. Gen. Virol.* 40, 531–544. doi: 10.1099/0022-1317-40-3-531
- Indenbach, B. D. (2001). "Flaviviridae: the viruses and their replication," in *Fields Virology*, eds D. M. Knipe and P. M. Howley (Philadelphia, PA: Lippincott Williams and Wilkins), 991–1041.
- Javed, M. A., Chakravarti, S., Gupta, V., Chander, V., Sharma, G. K., Nandi, S., et al. (2018). Novel polymerase spiral reaction (PSR) for rapid visual detection of Bovine Herpesvirus 1 genomic DNA from aborted bovine fetus and semen. *Gene* 25, 222–231. doi: 10.1016/j.gene.2018.11.004
- Johnson, A. J., Martin, D. A., Karabatsos, N., and Roehrig, J. T. (2000). Detection of anti-arboviral immunoglobulin G by using a monoclonal antibody-based capture enzyme-linked immunosorbent assay. *J. Clin. Microbiol.* 38, 1827–1831. doi: 10.1128/JCM.38.5.1827-1831.2000
- Jolanta, K., Jungbauer, C., Stephan, W., and Aberle. (2018). Integrated analysis of human-animal-vector surveillance: West Nile virus infections in Austria, 2015–2016. *Emerg. Microbes Infect.* 32, 334–345. doi: 10.1038/s41426-018-0021-5
- Khromykh, A. A., Meka, H., Guyatt, K. J., Westaway, E. G. (2001). Essential role of cyclization sequences in *Flavivirus* RNA replication. *J. Virol.* 75, 6719–6728. doi: 10.1128/JVI.75.14.6719-6728.2001d
- Kilpatrick, A. M. (2011). Globalization, land use, and the invasion of West Nile virus. *Science* 334, 323–327. doi: 10.1126/science.12011010
- Knipe, D. M., and Howley, P. M. (eds.). (2001). "Flaviviridae: the viruses and their replication," in *Fields virology*, 4th Edn. (Philadelphia, PA: Lippincott Williams and Wilkins), 991–1041.
- Komar, N. (2000). West Nile viral encephalitis. *Rev. Sci. Tech.* 19, 166–176. doi: 10.20506/rst.19.1.1201
- Kumar, J. S., Parida, M. M., and Rao, P. V. L. (2011). Monoclonal antibody-based antigen capture immunoassay for detection of circulating non-structural protein NS1: implications for early diagnosis of Japanese encephalitis virus infection. *J. Med. Virol.* 83, 1063–70. doi: 10.1002/jmv.22097
- Kumar, J. S., Saxena, D., Parida, M. M., and Rathinam, S. (2018). Evaluation of real-time reverse-transcription loop-mediated isothermal amplification assay for clinical diagnosis of West Nile virus in patients. *Indian J. Med. Res.* 147, 293–298. doi: 10.4103/0971-5916.234607
- Lanciotti, R. S., and Kerst, A. J. (2001). Nucleic acid sequence based amplification assays for rapid detection of West Nile and St. Louis encephalitis viruses. *J. Clin. Microbiol.* 39, 4506–4513. doi: 10.1128/JCM.39.12.4506-4513.2001
- Lanciotti, R. S., Roehrig, J. T., Deubel, V., Smith, J., Parker, M., Steele, K., et al. (1999). Origin of the West Nile virus responsible for an outbreak of encephalitis in the northeastern United States. *Science* 286, 2333–2337. doi: 10.1126/science.286.5448.2333
- Leone, G., Schijndel, H. V., Gemen, B. V., Kramer, F. R., and Schoen, C. D. (1998). Molecular beacon probes combined with amplification by NASBA enable homogeneous, real-time detection of RNA. *Nucl. Acids Res.* 26, 2150–2155. doi: 10.1093/nar/26.9.2150
- Lim, S. M., Koraka, P., Osterhaus, A. D., and Martina, B. E. (2011). West Nile virus: immunity and pathogenesis. *Viruses* 3, 811–828. doi: 10.3390/v3060811
- Liu, W., Dong, D., Yang, Z., Zou, D., Chen, Z., Yuan, J., et al. (2015). Polymerase spiral reaction (PSR): a novel isothermal nucleic acid amplification method. *Sci. Rep.* 5:12723. doi: 10.1038/srep12723
- Liu, W., Zou, D., He, X., Yang, Z., Huang, S., Zhao, Q., et al. (2018). Development and application of a rapid *Mycobacterium tuberculosis* detection technique using polymerase spiral reaction. *Sci. Rep.* 8. doi: 10.1038/s41598-018-21376-z
- Marfin, A. A., and Gubler, D. J. (2001). West Nile encephalitis: an emerging disease in the United States. *Clin. Infect. Dis.* 33, 1713–1719. doi: 10.1086/322700
- Martin, D. A., Muth, D. A., Brown, T., Johnson, A. J., Karabatsos, N., and Roehrig, J. T. (2000). Standardization of immunoglobulin M capture enzyme linked immunosorbent assays for routine diagnosis of arboviral infections. *J. Clin. Microbiol.* 38, 1823–1826. doi: 10.1128/JCM.38.5.1823-1826.2000
- Mehul, S. S., Michael, S. D., and Michael, G. Jr. (2013). West Nile virus infection and immunity. *Nature Rev.* 11, 115–128. doi: 10.1038/nrmicro2950
- Meng, S., Wang, Y., and Ye, C. (2016). Rapid and sensitive detection of *Plesiomonas shigelloides* by cross-priming amplification of the *hugA* gene. *Mol. Med. Rep.* 14, 5443–5450. doi: 10.3892/mmr.2016.5937
- Michaelis, M., Doerr, H. W., and Cinatl, J. (2009). Novel swine-origin influenza A virus in humans: another pandemic knocking at the door. *Med. Microbiol. Immunol.* 198, 175–183. doi: 10.1007/s00430-009-0118-5
- Mukhopadhyay, S., Kim, B. S., Chipman, P. R., Rossmann, M. G., and Kuhn, R. J. (2003). Structure of West Nile virus. *Science* 302:248. doi: 10.1126/science.1089316
- Muller, J. D., Putz, B., and Hofler, H. (1997). Self-sustained sequence replication (3SR): an alternative to PCR. *Sci. Rep.* 108, 431–437. doi: 10.1007/s004180050183
- Notomi, T., Okayama, H., Masubuchi, H., Yonekawa, T., Watanabe, K., Amino, N., et al. (2000). Loop-mediated isothermal amplification of DNA. *Nucl. Acids Res.* 28, 1–8. doi: 10.1093/nar/28.12.e63
- Papain, F. J., Vahrson, W., and Dittmer, P. D. (2004). SYBR green-based real-time quantitative PCR assay for detection of West Nile virus circumvents false-negative results due to strain variability. *J. Clin. Microbiol.* 42, 1511–1518. doi: 10.1128/JCM.42.4.1511-1518.2004
- Paramasivan, R., Mishra, A. C., and Mourya, D. T. (2003). West Nile virus: the Indian scenario. *IJMR.* 118, 101–108.
- Parida, M. M., Posadas, G., Inoue, S., Hasebe, F., and Morita, K. (2004). Real-time reverse transcription loop-mediated isothermal amplification for rapid detection of West Nile virus. *J. Clin. Microbiol.* 42, 257–263. doi: 10.1128/JCM.42.1.257-263.2004
- Parida, M. M., Shukla, S., Sharma, S., Santosh, S. R., Rao, P. V. L., Ratho, R. K., et al. (2011). Development and evaluation of reverse transcription loop-mediated isothermal amplification assay for rapid and real-time detection of the swine-origin influenza A H1N1 virus. *J. Mol. Diagn.* 13, 100–107. doi: 10.1016/j.jmoldx.2010.11.003
- Petersen, L. R., and Roehrig, J. T. (2001). West Nile virus: a reemerging global pathogen. *Emerg. Infect. Dis.* 7, 611–614. doi: 10.3201/eid0704.017401
- Sambri, V., Capobianchi, M. R., Cavrini, F., Charrel, R., Escadafal, C., Franco, L., et al. (2013). Diagnosis of West Nile virus human infections: overview and proposal of diagnostic protocols considering the results of external quality assessment studies. *Viruses* 5, 2329–2348. doi: 10.3390/v5102329
- Shi, P., Kauffman, E. B., Ren, A., Felton, T., Tai, J. H., Alan, P. D., et al. (2001). High-throughput detection of West Nile virus RNA. *J. Clin. Microbiol.* 39, 1264–1271. doi: 10.1128/JCM.39.4.1264-1271.2001
- Shukla, J., Saxena, D., Rathinam, S., Lalitha, P., Josesh, C. R., Sharma, S., et al. (2012). Molecular detection and characterization of WNV associated with multifocal retinitis in patients from Southern India. *Int. J. Infect. Dis.* 16, 53–59. doi: 10.1016/j.ijid.2011.09.020
- Solomon, T., Ooi, M. H., Beasley, D. W., and Mallewa, M. (2003). West Nile encephalitis. *BMJ.* 326, 865–869. doi: 10.1136/bmj.326.7394.865
- Vazquez, A., Sanchez, M. P., Ruiz, S., Molero, F., Hernandez, L., Moreno, J., et al. (2010). Putative new lineage of West Nile virus, Spain. *Emerg. Infect. Dis.* 16, 549–552. doi: 10.3201/eid1603.091033
- Wei, L., Dayang, Z., Xiaoming, H., Da, A., Yuxin, S., Zhan, Y., et al. (2018). Development and application of a rapid *Mycobacterium tuberculosis* detection technique using polymerase spiral reaction. *Sci. Rep.* 65, 343–352.
- Wei, L., Derong, D., Zhan, Y., Zeliang, C., Jing, Y., Liuyu, H., et al. (2015). Polymerase Spiral Reaction (PSR): a novel isothermal nucleic acid amplification method. *Sci. Rep.* 34, 123–131.
- Xiaoqun, J., Dong, D., Bian, L., Zou, D., He, X., Huang, L., et al. (2016). Rapid detection of *Candida albicans* by polymerase spiral reaction assay in clinical blood samples. *Front. in Microbiol.* 7:916. doi: 10.3389/fmicb.2016.00916
- Zengguo, C., Wang, H., Lina, W., Ling, L., Hongli, J., Changping, X., et al. (2016). Visual detection of West Nile virus using reverse transcription loop-mediated isothermal amplification combined with a vertical flow visualization strip. *Front. Microbiol.* 7:554. doi: 10.3389/fmicb.2016.00554

**Conflict of Interest:** The authors declare that the research was conducted in the absence of any commercial or financial relationships that could be construed as a potential conflict of interest.

Copyright © 2020 Tomar, Kumar, Patel and Sharma. This is an open-access article distributed under the terms of the Creative Commons Attribution License (CC BY). The use, distribution or reproduction in other forums is permitted, provided the original author(s) and the copyright owner(s) are credited and that the original publication in this journal is cited, in accordance with accepted academic practice. No use, distribution or reproduction is permitted which does not comply with these terms.

# Advantages of publishing in Frontiers



## OPEN ACCESS

Articles are free to read for greatest visibility and readership



## FAST PUBLICATION

Around 90 days from submission to decision



## HIGH QUALITY PEER-REVIEW

Rigorous, collaborative, and constructive peer-review



## TRANSPARENT PEER-REVIEW

Editors and reviewers acknowledged by name on published articles

## Frontiers

Avenue du Tribunal-Fédéral 34  
1005 Lausanne | Switzerland

Visit us: [www.frontiersin.org](http://www.frontiersin.org)

Contact us: [info@frontiersin.org](mailto:info@frontiersin.org) | +41 21 510 17 00



## REPRODUCIBILITY OF RESEARCH

Support open data and methods to enhance research reproducibility



## DIGITAL PUBLISHING

Articles designed for optimal readership across devices



## FOLLOW US

[@frontiersin](https://www.instagram.com/frontiersin)



## IMPACT METRICS

Advanced article metrics track visibility across digital media



## EXTENSIVE PROMOTION

Marketing and promotion of impactful research



## LOOP RESEARCH NETWORK

Our network increases your article's readership